Wireless Device-to-Device Communications and Networks

Lingyang Song, Dusit Niyato, Zhu Han, and Ekram Hossain

Wireless Device-to-Device Communications and Networks

Covering the fundamental theory together with the state of the art in research and development, this practical guide provides the techniques needed to design, analyze, and optimize device-to-device (D2D) communications in wireless networking.

With an ever-increasing demand for higher-data-rate wireless access, D2D communication is set to become a key feature supported by next-generation cellular networks. This book introduces D2D-based wireless communications from the physical-, MAC-, network-, and application-layer perspectives, providing all the key background information before moving on to discuss real-world applications as well as potential future developments. Key topics are discussed in detail, such as dynamic resource sharing (e.g., of spectrum and power) between cellular and ad-hoc D2D communications to accommodate larger volumes of traffic and provide better service to users. Readers will understand the practical challenges of resource management, optimization, security, standardization, and network topology, and learn how the design principles are applied in practice.

Lingyang Song is Professor of Wireless Communications at Peking University, China, where he has worked since 2009. His main research interests include cooperative and cognitive communications, physical-layer security, smart grids, and mobile social networks. He is the recipient of the 2012 IEEE Asia Pacific Young Researcher Award and the 2012 NSFC Outstanding Young Investigator Award.

Dusit Niyato is an Associate Professor in the School of Computer Engineering at the Nanyang Technological University (NTU), Singapore. He has won international awards including the IEEE Communications Society Asia Pacific Young Researcher Award and the 2011 IEEE Communications Society Fred W. Ellersick Prize. He works in various research areas, including cognitive radio, mobile cloud computing,

machine-to-machine communications, performance analysis, and optimization of wireless networks.

Zhu Han is an Associate Professor in the Electrical and Computer Engineering Department at the University of Houston, Texas. He received an NSF CAREER award in 2010 and the IEEE Fred W. Ellersick Prize in 2011. He co-authored papers that won the best paper award at the IEEE International Conference on Communications 2009, the 7th International Symposium on Modeling and Optimization in Mobile, Ad Hoc, and Wireless Networks (WiOpt09), and the IEEE Wireless Communication and Networking Conference, 2012. He is an IEEE Fellow.

Ekram Hossain is a Professor in the Department of Electrical and Computer Engineering at the University of Manitoba, Canada, where his current research interests include the design, analysis, and optimization of wireless/mobile communications networks, cognitive radio systems, and network economics. He has received several awards, including the 2010 and the 2014 University of Manitoba Merit Award (for Research and Scholarly Activities), the 2011 IEEE Communications Society Fred W. Ellersick Prize Paper Award, and the IEEE Wireless Communications and Networking Conference 2012 Best Paper Award.

Wireless Device-to-Device Communications and Networks

LINGYANG SONG
Peking University, Beijing

DUSIT NIYATO
Nanyang Technological University, Singapore

ZHU HAN
University of Houston, Texas

EKRAM HOSSAIN
University of Manitoba, Canada

CAMBRIDGE
UNIVERSITY PRESS

CAMBRIDGE
UNIVERSITY PRESS

University Printing House, Cambridge CB2 8BS, United Kingdom

Cambridge University Press is part of the University of Cambridge.

It furthers the University's mission by disseminating knowledge in the pursuit of education, learning and research at the highest international levels of excellence.

www.cambridge.org
Information on this title: www.cambridge.org/9781107063570

First published 2015

Printed in the United Kingdom by TJ International Ltd., Padstow, Cornwall

A catalogue record for this publication is available from the British Library

Library of Congress Cataloguing in Publication data
Song, Lingyang.
Wireless device-to-device communications and networks / Lingyang Song,
Peking University, Beijing, Dusit Niyato, Nanyang Technical University, Singapore,
Zhu Han, University of Houston, Texas, Ekram Hossain, University of Manitoba, Canada.
pages cm
Includes bibliographical references and index.
ISBN 978-1-107-06357-0
1. Machine-to-machine communications. I. Title.
TK5105.67.S66 2015
004.6′1–dc23

2014035056

ISBN 978-1-107-06357-0 Hardback

Dedications
To my family, Zhu Han
To Suprova Hossain and Nirvoy Lalon, Ekram Hossain

Contents

Part III Resource management, cross-layer design, and security for D2D communications

4 Mode selection and resource allocation for D2D communications underlaying cellular networks

Preface

Now that more and more new mobile multimedia-rich services are becoming available to mobile users, there is an ever-increasing demand for higher-data-rate wireless access. Therefore, new wireless technologies such as Long Term Evolution Advanced (LTE-A) and WiMAX have been introduced, which are capable of providing high-speed, large-capacity, and guaranteed-quality-of-service (QoS) mobile services. Apart from the new technologies, new techniques such as small-cell networks and heterogeneous networks (HetNets) have also been developed, which are able to improve network capacity by reducing cell size and effectively controlling the interference. However, all these attempts still rely on a centralized network topology, which entails mobile devices communicating with a base station or access point. Such a centralized network topology is inherently limited by the capabilities of the base station and access point, which could be congested due to the presence of a large number of communicating devices. Also, the base station and access point might not have complete information about transmission parameters among devices, which is required in order to achieve the optimal network performance. To mitigate this problem, the concept of device-to-device (D2D) communications has been introduced to allow local peer-to-peer transmission among mobile devices offloading traffic from the base station and access point. Also, it is crucial to increase the wireless network capacity to accommodate the bandwidth-consuming mobile applications and services. Device-to-device communications is a promising concept to improve user experience and resource utilization in cellular networks, operating in both licensed and unlicensed spectrum bands.

The D2D communications can underlay or overlay a cellular network, using the same resources to improve the system throughput. Specifically, besides cellular operation, where user equipment (UE) is served by the

network via the evolved NodeBs (eNBs) in the LTE architecture, UEs may communicate with each other directly over the D2D links. The UE in D2D connections still has to be loosely controlled by the eNBs in a network-controlled manner, thus continuing cellular operation. The eNBs can control the resources used for the cellular and D2D links. The eNBs can also set constraints on the transmission parameters (e.g., transmit power and communication duration) of D2D transmitters to limit the interference experienced at the cellular receivers.

Numerous researchers and wireless engineers have postulated that D2D communications will become a key feature supported by next-generation cellular networks. D2D communication has the following advantages. One can

- extend coverage,
- offload in cellular networks,
- improve energy efficiency,
- increase throughput and spectrum efficiency, and
- create new services such as social/vehicular ad-hoc networking services, etc.

The design, analysis, and optimization of D2D communications and networking require multidisciplinary knowledge, namely knowledge of wireless communications and networking, signal processing, artificial intelligence (e.g., for learning), decision theory, optimization, and economic theory. Therefore, a book containing the basic concepts/theories for addressing the research advances that enable D2D communications in cellular networks as well as the state of the art of research and development and related information will be very useful for researchers and engineers.

This book summarizes the state of the art of research on D2D communications coexisting with cellular networks from physical-, MAC-, network-, and application-layer perspectives. The key features of this book are as follows:

- a unified view of D2D communications and networking,

- a comprehensive review of the state-of-the-art research and key technologies for D2D communications networks,
- coverage of a wide range of techniques for design, analysis, optimization, and applications of D2D communications networks,
- outlining the key research issues related to D2D communications and networking, and
- Standardization activities on D2D communications.

This book is divided into five parts: Part I (Introduction), Part II (Techniques for modeling and analysis of D2D communications), Part III (Resource management, cross-layer design, and security for D2D communications), Part IV (Applications of D2D communications), and Part V (Standardization of D2D communications). Part I contains Chapter 1, which provides an introduction to D2D communications. The topics include the different methods for configuration or access, device synchronization and discovery, spectrum sharing and resource management, power control, and D2D local area networks. Also, a simulation scenario for D2D communications is described.

In Part II, which consists of Chapters 2 and 3, different techniques that can be applied to the problem of design, analysis, and optimization of D2D communications are introduced. In particular, the optimization techniques which are useful to obtain the optimal resource-management schemes for D2D communications are discussed in Chapter 2. Major variations of optimization techniques (e.g., unconstrained and constrained optimization, nonlinear optimization, combinatorial optimization) are presented. Also, stochastic optimization based on dynamic programming, the Markov decision process (MDP), and stochastic programming are discussed. In Chapter 3, the game-theory techniques are discussed. The basics of different game-theoretic models, namely noncooperative game, repeated game, cooperative game (i.e., bargaining game, coalition game), and evolutionary game models as well as the basics of matching theory and auction theory are presented.

Part III, which consists of Chapters 4–8, deals with radio-resource management, cross-layer design, and security for D2D communications.

Chapter 4 presents a framework for mode selection for D2D communications that is based on a coalitional game. Also, a model for joint mode selection and resource allocation is developed. Chapter 5 focuses on interference coordination for D2D communications. A network-assisted power control scheme that considers both interference reduction and power saving is proposed. Chapter 6 introduces methods for subcarrier allocation and time-domain scheduling for D2D communications. Chapter 7 provides an overview of cross-layer design concepts and discusses the challenges in adopting these concepts to develop new protocols. Several examples of cross-layer design are also illustrated. Chapter 8 studies the security issues that arise during the neighbor-discovery phase and data-transmission phase of D2D communications. The concept of physical-layer security is discussed as a method for secure D2D communications.

Part IV, which consists of Chapters 9–11, deals with several application scenarios of D2D communications. In particular, applications of D2D communications in the context of vehicular ad-hoc networks (VANETs) are discussed in Chapter 9. In Chapter 10, application of D2D communications for cooperative content delivery in mobile social networks is discussed. Chapter 11 deals with the paradigm of machine-to-machine (M2M) communications, noting that D2D communications can be considered as a type of M2M communication when the D2D users are in close mutual proximity.

Part V consists of Chapter 12, which introduces the motivation, requirements, and application scenarios for using D2D communications over LTE/LTE-A networks. Also, this chapter introduces the key methods and system parameters to evaluate the performance of D2D communications (at both link and system levels) by computer simulations.

Since each chapter in this book is quite independent, skipping any chapter in this book will not affect your ability to follow the rest of the book.

The authors would like to acknowledge the research support from the National Science Foundation (NSF), USA, and the Natural Sciences and Engineering Research Council of Canada (NSERC) during the course of this book project.

Lingyang Song
Dusit Niyato
Zhu Han
Ekram Hossain

Part I

Introduction

1 Basics of D2D communications

As one of the next-generation wireless communication systems, the Third Generation Partnership Project (3GPP) Long Term Evolution (LTE) is committed to providing technologies for high data rates and system capacity. Further, LTE-Advanced (LTE-A) was defined to support new components for LTE to meet higher communication demands [1]. In particular, the performance and quality of service (QoS) of local area services need to be improved significantly by reusing the spectrum resources. However, reuse of the unlicensed spectrum might not provide a stable controlled environment [2]. Therefore, the approach of exploiting the licensed spectrum for local area services has attracted much attention. In this chapter, we present the basic concepts of device-to-device (D2D) communications in the licensed spectrum bands. We first provide an overview of D2D communications underlaying the cellular network. We then discuss access methods, device synchronization, and discovery mechanisms. Next, mode selection, spectrum sharing, power control, and multiple-input–multiple-output (MIMO) techniques are briefly introduced. The concepts of D2D direct and D2D local area networks (LANs) are proposed, a simulation scenario for D2D direct is given as an example, and, finally, the issues and challenges in D2D communications are outlined.

1.1 Overview of D2D communications

The term D2D communications commonly refers to the techniques that enable devices to communicate directly without an infrastructure of access points or base stations. D2D communications amount to a technology component for LTE-A, where user equipments (UEs) transmit data signals to

each other over a direct link/connection using the cellular resources instead of through the eNB (i.e., a base station). As an underlay to the cellular network, D2D communications allow one to increase the spectral efficiency [1, 3, 4, 5, 6, 7, 8, 9]. While D2D communications is considered as an add-on component in the 4G systems, it is expected to be a native feature supported by the next-generation (e.g., fifth-generation [5G]) cellular networks.

D2D communications may be of three types, as shown in Figure 1.1.

- Peer-to-peer communication: This is point-to-point communication, and most studies on D2D communication consider this type of transmission.
- Cooperative communication: This uses mobiles as relays to extend coverage, and exploits cooperative diversity through multiple collaborative mobiles to obtain space diversity.
- Multiple-hop (multihop) communication: This is similar to mobile ad-hoc network and mesh network, which may include complex data superposition, and data routing, e.g., wireless network coding.

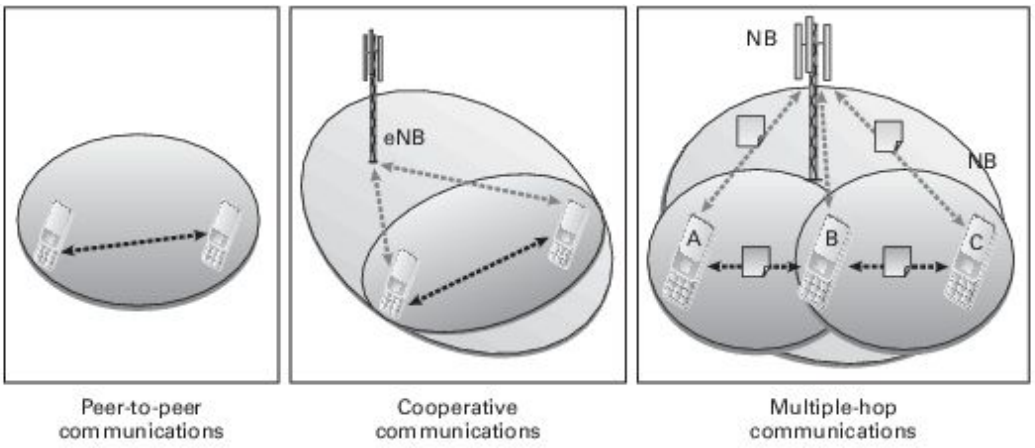

Figure 1.1. Device-to-device signal transmissions.

Although the use of D2D communications brings an improvement in spectral efficiency and has large benefits in terms of system capacity, it also causes interference with the cellular network as a result of spectrum sharing. Thus, an efficient interference coordination must be formulated to guarantee

a target performance level of the cellular communication. There exist several works about the use of D2D UEs for restricting co-channel interference [1, 3, 10, 11]. The authors in [12] utilize MIMO transmission schemes to avoid interference from the cellular downlink to D2D receivers sharing the same resources, with the aim of guaranteeing the required performance for the D2D communications. Interference management both from cellular to D2D communications and from D2D to cellular networks is considered in [13]. To further improve the gain from intra-cell spectrum reuse, properly pairing the cellular and D2D users for sharing the same resources has been studied [14, 15]. The authors in [15] propose an alternative greedy heuristic algorithm to lessen interference with the primary cellular networks using channel state information (CSI). The scheme is easy to operate yet cannot avoid signaling overhead. In [16], the resource-allocation scheme avoids the harmful interference by tracking the near–far interference, identifies the interfering cellular users, and ensures that the uplink (UL) frequency bands are efficiently used. Additionally, the goal is to prevent interference from cellular to D2D communication. In [17], the authors provide an analysis on optimal resource allocation and power control between the cellular and D2D connections that share the same resources for different resource-sharing modes, and evaluate the performance of the D2D underlay system both in a single-cell scenario and in the Manhattan grid environment. Then, the schemes are applied to further optimize the resource usage among users sharing the same resources.

The existing works in the literature show that by proper resource management, D2D communications can effectively improve the system throughput with the interference between cellular networks and D2D transmissions being minimized. However, the problem of allocating cellular resources to D2D transmissions is not trivial. In the later parts of the book, we will discuss different resource-management methods for D2D communications.

1.2 Key technologies for D2D communications

1.2.1 Configuration of D2D communications

The D2D networks can be configured in the following three ways to allow or restrict their usage by certain users.

- Network-controlled D2D: In this scenario, the communication signaling setup and thereafter resource allocation for both cellular and D2D users are controlled by the base station (BS) and the core network. This centralized configuration benefits from efficient interference avoidance and resource management. However, when the number of D2D links becomes large, this scheme incurs a large amount of control signaling, which can increase the overhead and reduce the spectrum efficiency. Therefore, this fully network-controlled approach is particularly useful for scenarios with small numbers of D2D links.
- Self-organized D2D: In this scenario, D2D users themselves realize the communication in a self-organizing way by finding the empty spectrum hole. This configuration is similar to cognitive radio, which allows D2D users to sense a surrounding environment, thereby obtaining CSI, interference, and cellular system information. This distributed method can effectively avoid the controlling signaling overhead, and the time delay, but the self-organized nature of this method may cause communication chaos and instability due to lack of control by the operators in the licensed spectrum.
- Network-assisted D2D: The D2D users operate in a self-organized way, and, for resource management, exchange with the cellular system a limited amount of controlling information. The cellular network can use the status of D2D communications for better control purposes. This approach has the merits of the first two approaches.

1.2.2 Device synchronization and discovery

For D2D communications, synchronization between cellular networks and D2D users and among D2D users themselves will be necessary to minimize multiple-access interference and for proper handoff. The approaches in IEEE 802.11 or in LTE can be adopted to enable the synchronization among mobiles. Typically, device synchronization and discovery are realized in a joint way.

The fundamental problem of device discovery is that two devices have to meet in space, time, and frequency without any coordination. This can be made possible via some randomized procedure, and one of the peers assumes the responsibility of sending the beacon. For traditional peer discovery, both in the ad-hoc case and in the cellular case, the discovery is made possible by one party transmitting a known synchronization or reference signal sequence (the beacon). Depending on whether or not there are responses from the discovering UEs, the discovery approaches can be classified into two categories: beacon-based discovery and request-based discovery. According to whether there is network participation in the detection, the discovery procedure could be categorized into two types: network-assisted detection and non-network-assisted detection.

In the case of network-assisted D2D, the network can mediate in the discovery process by recognizing D2D candidates, coordinating the time and frequency allocations for sending/scanning for beacons, and thereby making the pairing process more energy efficient and less time consuming. A typical procedure is as follows.

- Use direct signal to discover a peer.
- Set the transmission power so that UEs within a certain distance can hear the broadcast.
- Whoever receives the broadcast confirms that with the eNB.

1.2.3 Mode selection

In a D2D underlay communications system, one of the most challenging problems is to decide whether communicating devices should use cellular or direct communication mode. In the D2D mode, data is directly transmitted to the receiver while the cellular communication mode requires the source device to transmit to the eNB and then the destination device receives from the eNB on downlink (DL). Here, three different mode selection criteria are considered.

(i) *Cellular:* All devices are in cellular mode.

(ii) *Force D2D:* D2D mode is always selected for all the communicating devices.

(iii) *Path-loss D2D:* D2D mode is selected if any of the path losses between a source device and its serving eNB, or a destination device and its serving eNB, is greater than the path loss in the direct link between the source node and the destination node.

1.2.4 Spectrum sharing and resource management

Spectrum-sharing methods for D2D communications can be categorized as follows.

- *Overlay D2D communications:* The D2D users occupy the vacant cellular spectrum for communication. This approach can completely eliminate cross-tier interference by dividing the licensed spectrum into two parts (i.e., orthogonal channel assignment). That is, one fraction of the subchannels will be used by the cellular users while another fraction would be used by the D2D networks. Although it is optimal from a cross-tier interference standpoint, this approach is inefficient in terms of spectrum reuse.
- *Underlay D2D communications:* In this spectrum-sharing scheme, multiple D2D users are allowed to work as an underlay with cellular users, and thus improve the spectrum efficiency. Co-channel assignment of the cellular and D2D users will be more efficient and profitable for operators, although this is far more intricate than the overlay scheme from the technical point of view.

The overlay approach is easy to realize, but might not be spectrally efficient. While the underlay method incurs a relatively greater signaling overhead, it can achieve a better overall system performance. To optimize the system performance over spectrum sharing of both D2D and cellular modes, radio resource management is important. Radio resource management can be performed in either a noncooperative or a cooperative manner. In a noncooperative solution, each D2D user can manage its spectrum so as to maximize the throughput and quality of service (QoS). By

contrast, in a cooperative approach, the D2D users can gather partial information about spectrum usage and perform spectrum allocation taking into account the effect that it would have on its co-channel neighbors. In this way, the average cellular and D2D users' throughput and QoS, as well as their performances, can be locally optimized.

1.2.5 Power control

Power control is an important and effective way to coordinate the co-channel interference. Power control can be performed by two methods.

- Self-organized power control: The D2D users make power changes in a self-organized way according to a predefined signal-to-interference-plus-noise ratio (SINR) threshold in order to meet the QoS without affecting the cellular users.
- Network-managed power control: Both cellular and D2D users adaptively adjust their transmit power according to the SINR report. Typically, the D2D users can control the transmit power first, and then the cellular users make changes afterward. This iterative process terminates when all the users have satisfied their SINR requirements.

Obviously, the first method is not going to change the behaviors of cellular users since the D2D users are treated invisibly. This method is simple, but less efficient than the second method, which allows all of the users to adjust their transmit powers. However, the network-controlled approach requires some information exchange among cellular users, D2D users, and the eNB.

1.2.6 Uplink and downlink transmission with MIMO

The use of multiple-input and multiple-output (MIMO) antennas can improve system capacity by multiplexing signals in the spatial domain and increase robustness by exploiting space diversity. Specifically, by performing transmit or receive beamforming, the use of multiple antennas at the eNB and the UE can reduce the co-channel interference to other users and thus improve spectrum efficiency.

The different MIMO-based methods are as follows.

- *eNB beamforming:* This type of multi-user MIMO-like approach can be performed at the cellular downlink to reduce interference to the D2D users so that D2D communications can be allowed.
- *D2D beamforming:* This avoids any harmful interference being caused by the D2D transmissions to the cellular and other D2D users.
- *Virtual D2D beamforming:* This borrows the ideas of cooperation among mobile nodes such that multiple D2D users collaboratively form the beamforming matrices to improve the system performance.

1.3 Device-to-device local area networks

D2D communications can be classified into two main categories: *D2D direct* and *D2D local area networks* (D2D LANs). Specifically, D2D direct simply refers to conventional one-hop communication [1]. In multihop D2D LAN, the network-controlled smart devices can realize cluster-wise communications in an ad-hoc manner, and meanwhile work in the license band to achieve maximal flexibility and performance. Figure 1.2 shows a typical single-cell scenario with multiple users consisting of conventional cellular communications, one-hop D2D direct transmission, and D2D LAN for group communication.

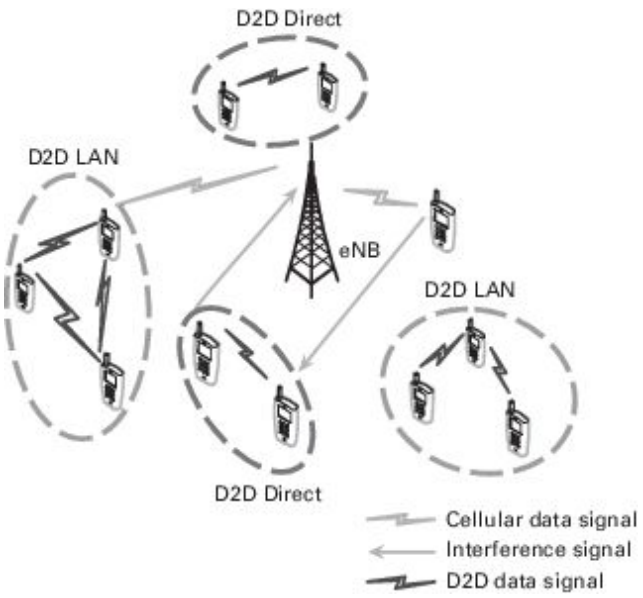

Figure 1.2. D2D communications underlaying cellular networks, including cellular communication, D2D direct, and D2D LAN.

With regard to D2D LAN, the network-controlled mobiles can form group communications, and thus provide various functionalities for specific application purposes. Similarly to D2D direct, these mobiles in the LAN can also work as an underlay to cellular networks for spectrum reuse, which makes the resource-allocation problems even more challenging. The representative scenarios for D2D LANs are as follows.

- *Group communications:* When large numbers of similar requests are received by the eNB, the LAN can be used to efficiently offload data. For example, in stadium or concert networks, when many mobiles ask for the content, some "*seed*" UEs can be first selected to obtain the complete information from the eNB, and then these seeds can share data with the remaining mobiles to reduce the eNB's effort.
- *Multihop relay communications:* When some smart devices are out of the coverage of the eNB, the mobiles in the D2D LAN can serve as relays for completing the file delivery among mobiles. This is particularly useful for disaster situations as well as suburb areas.
- *Collaborative smartphone sensing:* Since smartphones have the capability of environment sensing, which is similar to wireless sensor networks, the data can be collaboratively aggregated to some "sink" UEs and then transmitted to the eNB.

One representative example of an application of D2D LAN is mobile social networks, where social interests play a major role in enhancing the smartphone transmission in D2D LAN, and a contract game can be used to model utilities of the social-related individuals.

1.4 D2D direct: a simulation scenario

A single-cell scenario is considered as illustrated in Figure 1.3. For simplicity, just one cellular user (UE1) and one D2D pair (UE2 and UE3), which is in D2D mode, are located in the cell. Three users share the same radio resources at the same time. As a result, co-channel interference should

be considered. The position of UE2 is fixed as long as the distance from BS to it is D. The position of the other D2D user UE3 is uniformly distributed inside a region of radius *L* from UE2. As in a traditional cellular system, UE1 is free to be anywhere inside the cell, following a uniform distribution. In the simulation, the locations of three users are updated in each iteration.

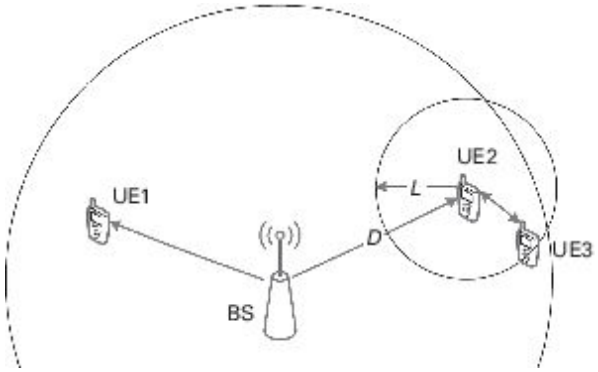

Figure 1.3. The scenario of underlay D2D communications.

According to Figure 1.3, three communicating users are in the system. UE2 and UE3 are in D2D mode, and UE1 is a cellular user. We set the maximum distance between UE2 and UE3 to be 25 meters. Actually, as much as 100 meters distance between them can be effective. The results presented here give only a representative scenario. Table 1.1 shows the main simulation parameters.

Table 1.1. Main simulation parameters

Parameter	Value
Cellular	Isolated cell, one-sector
System area	User devices are distributed within a range of 500 m from the BS
Noise spectral density	−174 dBm/Hz
System bandwidth	5 MHz
Noise figure	5dB at BS/9 dB at device

Antenna gains and patterns	BS: 14 dBi; device: omnidirectional 0 dBi
Cluster radius	5 m, 10 m, 15 m, 20 m, 25 m
Transmit power	BS: 46 dBm; device: 24 dBm (without power control)

The wireless propagation is modeled according to WINNER II channel models, and the D2D channel is based on an office/indoor scenario while the cellular channel is based on an urban macrocell scenario. Table 1.2 gives path-loss models. d is the link distance in meters, and n_{walls} is the number of walls penetrated in the link. $d'_{\text{BP}} = 4h'_{\text{BS}}h'_{\text{MS}}f_c/c$, where f_c is the center frequency in Hz, $c = 3.0 \times 10^8$ m/s is the propagation velocity in free space, and h'_{BS} and h'_{MS} are the effective antenna heights at the BS and the MS, respectively. The effective antenna heights h'_{BS} and h'_{MS} are computed as follows: $h'_{\text{BS}} = h_{\text{BS}} - 1.0m$, and $h'_{\text{MS}} = h_{\text{MS}} - 1.0$ m, where h_{BS} and h_{MS} are the actual antenna heights, and the effective environment height in urban environments is assumed to be 1.0 m. The LOS probability is given in Table 1.3.

Table 1.2. Path-loss models [18]

Scenario	Path loss (dB)	Shadow fading (dB)
D2D (LOS)	$18.7 \log_{10} d + 46.8$	3
D2D (NLOS)	$36.8 \log_{10} d + 43.8 + 5(n_{\text{walls}} - 1)$	4
Cellular (LOS)	$26 \log_{10} d + 39$ $40.0 \log_{10} d + 13.47 - 14.0 \log_{10} h'_{\text{BS}} - 14.0 \log_{10} h'_{\text{MS}}$	4 for $10\text{m} < d < d_{\text{BP}}$ 6 for $d'_{\text{BP}} < d < 5\text{km}$, $h_{\text{BS}} = 25\text{m}$, $h_{\text{MS}} = 1.5\text{m}$
Cellular (NLOS)	$(44.9 - 6.55 \log_{10} h_{\text{BS}}) \cdot \log_{10} d + 34.46 + 5.83 \log_{10} h_{\text{BS}}$	8 for $50\text{m} < d < 5\,\text{km}$,

		$h_{BS} = 25\text{m}$, $h_{MS} = 1.5\text{m}$
D2D user-Cellular user	$\text{PL} = \text{PL}_b + \text{PL}_{tw} + \text{PL}_{in}$ $\text{PL}_b = \text{PL}_{B1}(d_{out} + d_{in})$ $\text{PL}_{tw} = 14 + 15(1 - \cos\theta)^2$ $\text{PL}_{in} = 0.5 d_{in}$	7

Table 1.3. LOS probability [18]

Scenario	LOS probability
D2D	$P_{\text{LOS}} = \begin{cases} 1, & d \le 2.5 \\ 1 - 0.9\left(1 - (1.24 - 0.61\log_{10} d)^3\right)^{1/3}, & d > 2.5 \end{cases}$
Cellular	$P_{\text{LOS}} = \min(18/d, 1) \cdot (1 - \exp(-d/63)) + \exp(-d/63)$

Next, D2D and cellular SINR distribution with power control are investigated. The LTE uplink open-loop-fraction power-control scheme (OFPC) is given as [19]

$$P = \min\left\{P_{\max}, P_0 + 10 \cdot \log_{10} M + \alpha \cdot L\right\}. \tag{1.1}$$

The parameters for the power-control scheme are given in Table 1.4.

Table 1.4. OFPC parameters

Parameter	Value
$P_{\max}$	24 dBm
P_0	-78 dBm
α	0.8
L	Path loss between two UEs in a pair

M 1

In this scenario, the interference between D2D and cellular users due to UL resource sharing has been taken into account. When the distance between D2D and co-channel cellular users is not larger than the maximum distance of D2D communications, the interference channel can be based on an indoor/office scenario. However, when co-channel interference comes from a more distant location, the D2D channel model is not suitable. In accord with WINNER II channel models, we choose an indoor-to-outdoor/outdoor-to-indoor scenario to simulate the long-distance interference channel.

Table 1.2 also shows the interference channel model. $\mathrm{PL}_{\mathrm{B1}}$ is the path loss of the urban microcell scenario (see p . 44 in [18] for parameter detail), d_{out} is the distance between the outdoor terminal and the point on the wall that is nearest to the indoor terminal, d_{in} is the distance from the wall to the indoor terminal, θ is the angle between the outdoor path and the normal of the wall. For simplicity, we assume $\theta = 0$ so that $d_{\mathrm{out}} + d_{\mathrm{in}} = d$ in the simulation.

Consider a scenario of 19 cells, each of which is shown in Figure 1.3. For simplicity, a model with one cellular user and one D2D pair is considered. We update the locations of three users in each simulation iteration. Moreover, co-channel interference is taken into account. Neighbor cell interference is also from D2D, cellular users (UL), and BS (DL). Figures 1.4 and 1.5 give the SINR distribution of D2D communications without a power-control (PC) mechanism in the downlink (DL) and uplink (UL) periods, respectively.

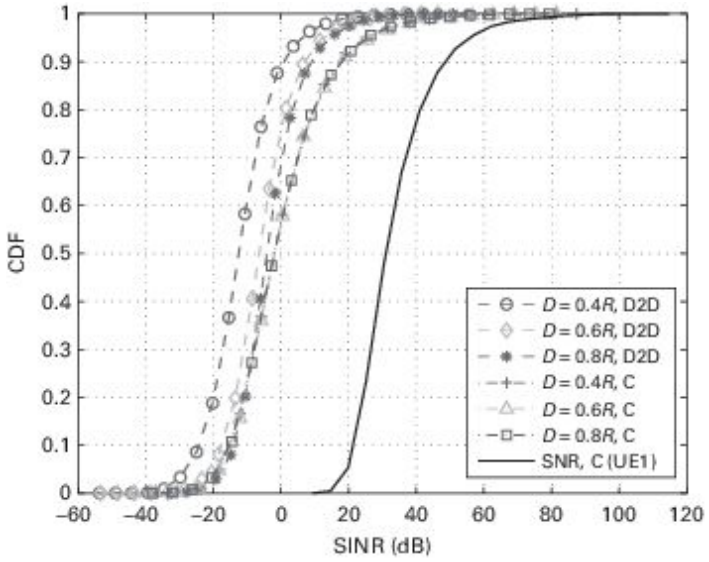

Figure 1.4. SINR distribution of D2D underlay communications with L = 25 m (DL). C, cellular.

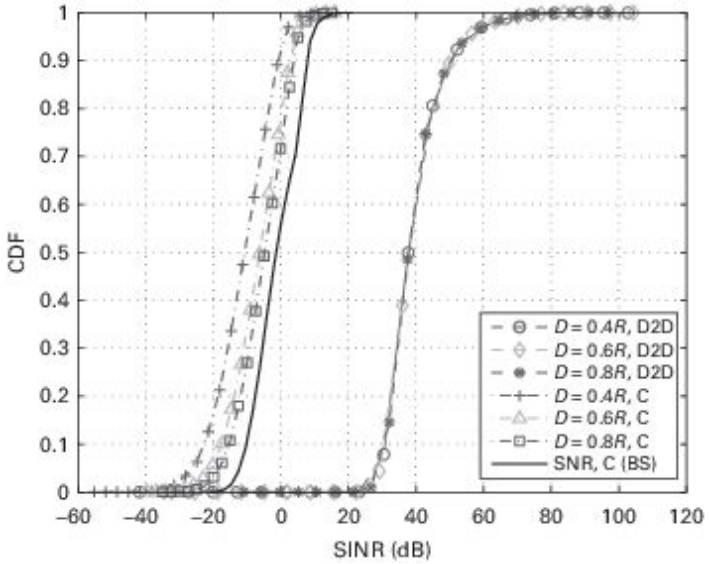

Figure 1.5. SINR distribution of D2D underlay communications with L = 25 m (UL). C, cellular.

When D2D users share cellular DL resources without PC, D2D SINR is better when the pair is farther away from BS. Cellular (UE1) SINR is less sensitive to the location of D2D users. The UE1 SINR is higher than D2D SINR. When sharing DL resources, the interference to D2D is from BS. The position of the pair has direct influence on the strength of the interference.

For a cellular user, the strength of interference depends not only on the position of D2D users, but also on the position of the cellular user. Since both are randomly distributed, the position of the D2D pair does not significantly affect the results. The UE transmit power is smaller than that of BS. As a result, the interference from BS is higher than that from D2D. As a result, the D2D SINR is clearly worse than that of UE1.

When D2D users share cellular UL resources without PC, the D2D SINR remains almost unchanged as the distance from BS to the pair changes. The BS SINR is better when the D2D pair is farther away from the BS. The D2D SINR is better than the BS SINR. In UL resource sharing, the strength of D2D interference depends not only on the positions of D2D users, but also on the positions of cellular users. Since both are randomly distributed, the position of the D2D pair does not significantly affect the results. For the BS, the interference is from D2D users. The position of the pair has direct influence on the strength of the interference. UE3 is 0–25 m from UE2 and UE1 is 0–500 m away from the BS, which is likely to make the D2D receive power larger than the BS receive power.

Figures 1.6 and 1.7 show the SINR distribution of D2D communications under power control in DL and UL periods, respectively. When D2D users share cellular DL resources with power control, the D2D SINR has decreased. The UE1 SINR has increased. When D2D users share cellular UL resources with power control, the D2D SINR has decreased. The BS SINR has increased. Figure 1.8 shows a comparison of SINR distribution between D2D communications with and without power control. With power control, the D2D SINR has decreased about 30 dB. The D2D SINR with power control gives a smaller dynamic range.

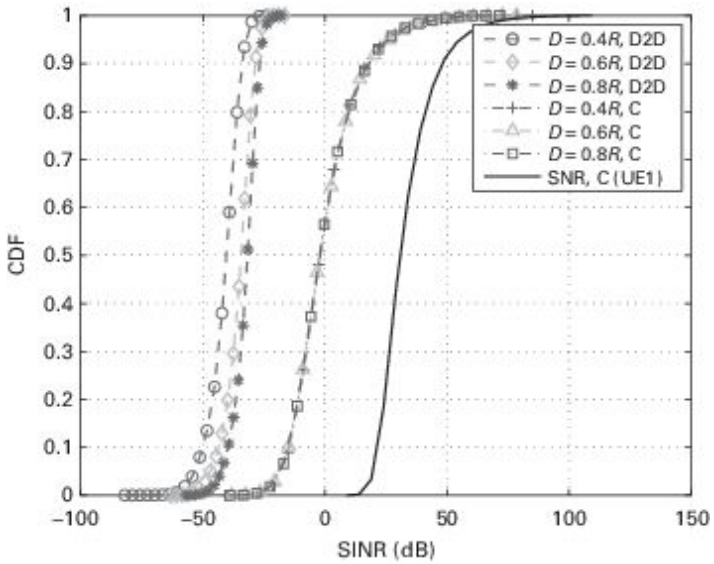

Figure 1.6. SINR distribution of D2D underlay communications under PC with L = 25 m (DL). C, cellular.

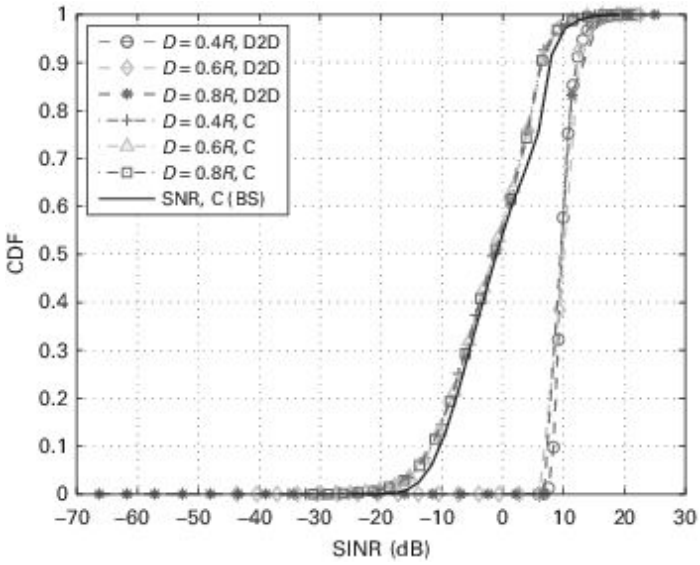

Figure 1.7. SINR distribution of D2D underlay communications under PC with L = 25m (UL). C, cellular.

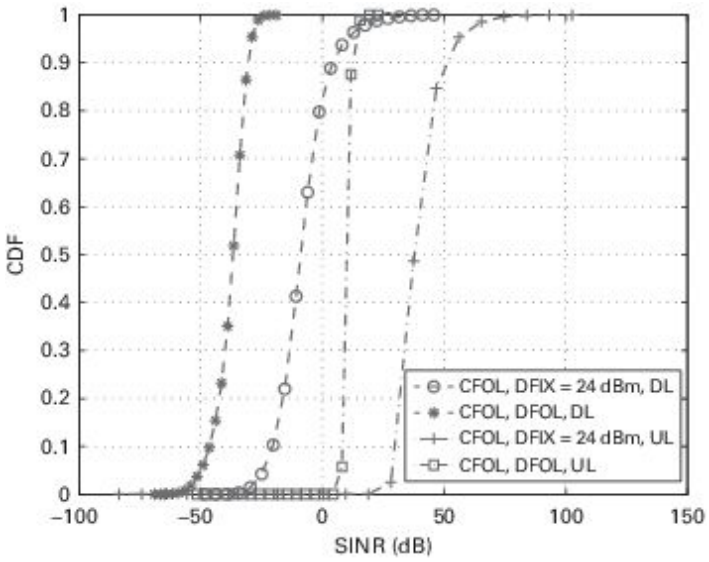

Figure 1.8. The SINR distribution of D2D underlay communications under PC with L = 25 m, $D = 0.5R$. CFOL, Cellular fraction open-loop PC; DFIX, D2D fixed power; DFOL, D2D fraction open-loop PC.

The OFPC scheme limits the transmit power of D2D users, which results in D2D SINR degradation. Because the D2D transmit power drops, the interference to cellular user and BS decreases. Owing to the path-loss compensation in the OFPC scheme, the D2D SINR obtains a more concentrated distribution.

1.5 Issues and challenges in D2D communications

For D2D direct, several key challenges are as follows.

- Scaling law and capacity analysis.
- Channel measurement and modeling, and interference analysis.
- Proximity-based applications, such as context-aware networks, and offload in concert and stadium networks.
- Mobility measurement, modeling, and management.
- Reduction of signaling overhead.
- Limited-backhaul issues for cross-cell D2D transmission

One of the major difficulties hindering D2D communications is the need to develop efficient data spreading in the D2D networks without causing severe disturbance of the original cellular networks. Power control, cooperative transmission, and multiple-access methods need to be carefully researched. The use of wireless network coding has been recognized as an efficient way to improve the network performance in terms of spectrum efficiency, and thus the question of how to adopt this technique has to be studied carefully.

For multihop D2D communications, which is particularly useful for coverage extension, it would be desirable to incentivize intermediate nodes to participate in a relaying process. In this case, a rewarding system regarding proper payment must be developed.

Radio resource management in MIMO and orthogonal frequency-division multiple-access (OFDMA)-based underlay D2D networks is particularly challenging. In these networks, the problem of how to effectively coordinate space, time, frequency, power, and device becomes interesting. Energy harvesting (e.g., from the ambient radio environment) for short-range D2D communications is another emerging research topic. Other challenges include identification of services for which D2D communication is useful, cognitive and self-organizing D2D links, proximity-based offloading, and capacity and performance evaluation of D2D communications. Finally, many applications, such as mobile social networks, vehicular ad-hoc networks, and even machine-type communications, which exploit D2D communications, deserve intensive studies.

1.6 Chapter summary

D2D communications will be a main feature supported by future wireless communications networks. D2D communication in the licensed spectrum bands is more controllable for communication operators than that in the unlicensed spectrum. By reusing cellular spectrum resources, D2D communications can improve the spectrum efficiency and thus contribute to a relatively high system capacity.

In this chapter, we have introduced some basic concepts and technologies for D2D communications. First, we have provided an overview of D2D communications. The term D2D communications commonly refers to the technology that enables devices to communicate directly without an infrastructure of access points or base stations. It can be classified into three categories involving peer-to-peer communication, cooperative communication, and multiple-hop communication. We have discussed the D2D configuration methods, device synchronization, and discovery mechanisms. Then, we have briefly introduced mode selection, spectrum resource sharing, power control, and MIMO techniques. A simple simulation scenario has been described, along with some simulation results. Furthermore, we have proposed the concept of D2D LANs, in which the network-controlled mobile devices can perform group communications and realize various functionalities for specific applications. We have finally discussed a few challenges in D2D communications.

Part II

Techniques for modeling and analysis of D2D communications

2 Optimization

In this chapter, we discuss how to formulate resource allocation problems in a communication network. Specifically, we study what the resources are, what the parameters are, what the practical constraints are, and what the optimized performances across the different layers are. The tradeoffs between the different optimization goals and different users' interests are also investigated. The goal is to provide the reader with a new perspective from the optimization point of view for wireless networking and resource allocation problems.

2.1 Constrained optimization

Many resource-allocation problems can be formulated as constrained optimization problems. The general formulation can be written as

$$\min_{\mathbf{x}\in\Omega} f(\mathbf{x}) \quad \text{s.t.} \begin{cases} g_i(\mathbf{x}) \le 0, & \text{for } i = 1, \ldots, m, \\ h_j(\mathbf{x}) = 0, & \text{for } j = 1, \ldots, l, \end{cases} \tag{2.1}$$

where $\mathbf{x}$ is the parameter vector for optimizing the resource allocation, Ω is the feasible range for the parameter vector, and $f(\mathbf{x})$ is the optimization goal matrix, objective goal, or utility function that represents the performance or cost. Here, $g_i(\mathbf{x})$ and $h_j(\mathbf{x})$ are the inequality and equality constraints for the parameter vector, respectively. The optimization process finds the solution

$\bar{\mathbf{x}} \in \Omega$ that satisfies all inequality and equality constraints. For optimal solution, $f(\bar{\mathbf{x}}) \leq f(\mathbf{x}), \forall \mathbf{x} \in \Omega$.

2.1.1 Basic definition

If the optimization goal, the inequality constraints, and the equality constraints are all linear functions of the parameter function $\mathbf{x}$, then the problem in (2.1) is called a *linear program*. One important characteristic of a linear-program problem is that there is a global optimal point that is very easy to obtain by linear programming. By contrast, one major drawback of linear programs is that most of the practical problems in wireless networking and resource allocation are nonlinear. Therefore, it is hard to model these practical problems as linear programs. If either the optimization goal or the constraints functions are nonlinear, the problem in (2.1) is called a *nonlinear program*. In general, there are multiple local optima in a nonlinear program, and finding the global optimum is not an easy task. Furthermore, if the feasible set Ω contains some integer sets, the problem in (2.1) is called an *integer program*. Most integer programs are nondeterministic polynomial-time hard (NP-hard) problems that cannot be solved in polynomial time.

One special kind of nonlinear program is a *convex optimization* problem in which the feasible set Ω is a convex set, and the optimization goal and the constraints are convex/concave/linear functions. A convex set is defined as follows.

DEFINITION 1. *A set* Ω *is* convex *if for any* $\mathbf{x}_1, \mathbf{x}_2 \in \Omega$ *and any* θ *with* $0 \leq \theta \leq 1$, *we have*

$$\theta \mathbf{x}_1 + (1 - \theta)\mathbf{x}_2 \in \Omega.$$

A convex function f is defined as follows.

DEFINITION 2. *A function* f *is* convex *over* $\mathbf{x}$ *if the feasible range* Ω *of the parameter vector* $\mathbf{x}$ *is a convex set, and if, for all* $\mathbf{x}_1, \mathbf{x}_2 \in \Omega$ *and* $0 \leq \theta \leq 1$,

$$f(\theta \mathbf{x}_1 + (1-\theta)\mathbf{x}_2) \leq \theta f(\mathbf{x}_1) + (1-\theta) f(\mathbf{x}_2).$$

A function is strictly convex if the strict inequality holds whenever $\mathbf{x}_1 \neq \mathbf{x}_2$ *and* $0 < \theta < 1$. *A function is called concave if* $-f$ *is convex.*

In Figure 2.1, we show examples of a convex set and a nonconvex set. In Figure 2.2, we show the example of a convex function. If the function is differentiable, and if either of the following two conditions holds, the function is a convex function.

$$\text{First-order condition: } f(\mathbf{x}_2) \geq f(\mathbf{x}_1) + \nabla f(\mathbf{x}_1)^\top (\mathbf{x}_2 - \mathbf{x}_1). \tag{2.2}$$

$$\text{Second-order condition: } \nabla^2 f(\mathbf{x}) \succeq 0. \tag{2.3}$$

One important application of the convex function is Jensen's inequality. Suppose function f is convex and the parameter $\mathbf{x}$ has any arbitrary random distribution over Ω. Then the following equality holds:

$$f(E[\mathbf{x}]) \leq Ef(\mathbf{x}), \tag{2.4}$$

where E denotes expectation.

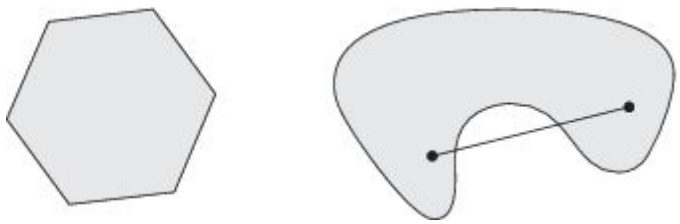

Figure 2.1. A convex set and a nonconvex set.

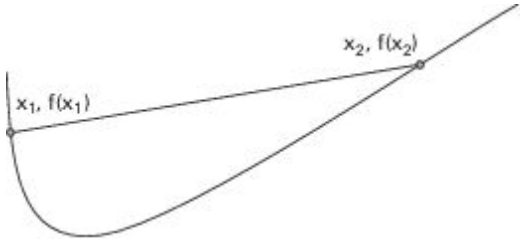

Figure 2.2. An example of a convex function.

The advantages of convex optimization are as follows.

- It has a variety of applications such as automatic control systems, estimation and signal processing, communications and networks, electronic-circuit design, data analysis and modeling, statistics, and finance.
- The computation time is usually of quadratic order. The problems can then be solved, very reliably and efficiently, using interior-point methods or other special methods for convex optimization.
- Solution methods are reliable enough to be embedded in a computer-aided design or analysis tool, or even a real-time reactive or automatic control system.
- There are also theoretical or conceptual advantages of formulating a problem as a convex optimization problem.

The challenges of the convex optimization concern how to recognize and model the problem as a convex optimization. Moreover, there are many tricks for transforming problems into convex forms.

We have discussed the basics for constrained optimization problems. Next we will see how the problem can be formulated. Resource allocation can be formulated as a constrained optimization problem with the parameters, objective functions, and constraints of the following physical meanings.

- *Examples of parameters*: Physical-layer parameters include transmitted power, modulation level, channel coding rate, and channel/code selection. MAC-layer parameters include transmission time/frequency,

service rate, and priorities for transmission. Network-layer parameters include route selection and routing cost. Application-layer parameters include source-coding rate, buffer priority, and packet arrival rate.

- *Example of objective function*: Physical layer: minimal overall power, maximal throughput, maximal rate per joule, and minimal bit error rate. MAC layer: maximal overall throughput, minimal buffer-overflow probability, and minimal delay. Network layer: minimal cost and maximal profit. Application layer: minimal distortion and minimal delay.
- *Examples of constraints*: Physical layer: maximal mobile transmitted power, available modulation constellation, available channel coding rate, and limited energy. MAC layer: contentions, limited time/frequency slot, and limited information about other mobiles. Network layer: maximal hops and security concerns. Application layer: the base-layer transmission, limited source rate, strict delay, and security.

2.1.2 The Lagrangian method

After formulating the constrained optimization problem for resource allocation, we need to find solutions. Next, we explain how to obtain the solution in closed form. One of the most important methods used to find a closed-form solution for constrained optimization is the Lagrangian method, which has the following steps.

(i) Rewrite (2.1) as a Lagrange multiplier function J as

$$J = f(\mathbf{x}) + \sum_{i=1}^{m} \lambda_i g_i(\mathbf{x}) + \sum_{j=1}^{l} \mu_j h_j(\mathbf{x}), \tag{2.5}$$

where λ_i and μ_j are Lagrange multipliers.

(ii) Differentiate J over $\mathbf{x}$ and set to zero as

$$\frac{\partial J}{\partial \mathbf{x}} = 0. \tag{2.6}$$

(iii) From (2.6), solve for λ_i and μ_j.

(iv) Replace λ_i and μ_j in the constraints to get optimal $\mathbf{x}$.

Notice that the difficulty in the Lagrangian method is in steps (iii) and (iv), where the closed-form solution is obtained for the Lagrange multipliers. Some approximations and mathematical tricks are necessary to obtain the closed-form solutions.

The difficulty in obtaining the analytical results from (2.1) is because of the nonlinearity and nonconvexity of the constraints and the optimization goal. This makes the Lagrange multiplier function in (2.5) hard to differentiate and makes it hard to obtain the optimal points. If some approximations for the constraints or the optimization goal functions can be obtained under some conditions, we can solve (2.1) by differentiating (2.5) and putting the results back into the constraints to get the optimal Lagrange multiplier. There are several methods to put the above idea into practice. We classify them as follows.

(i) Parameterized approximation. In this method, the nonlinear or nonconvex function is approximated by the parameterized function. The goal is to obtain the optimal parameters such that the approximation errors can be minimized.

The most common type of approximation is *linear approximation*. Suppose the original function is $f(x)$, the linear approximation can be written as

$$\min_{a,b} \int_c^d \|f(x) - (ax + b)\|^2 dx, \tag{2.7}$$

where $[c, d]$ are the interested region where the approximation needs to be accurate.

Another type of approximation is *polynomial or Tyler expansion*. The original function can be expanded as

$$f(x) = c_0 + c_1(x - x_0) + c_2(x - x_0)^2 + \cdots, \tag{2.8}$$

where x_0 is the point where the series are expanded, and c_0, c_1, c_2, … are constant.

In general, for any convex function $f'(x; \mathbf{a})$ of x with parameter vector $\mathbf{a}$, the approximation within region $[c, d]$ can be written as

$$\min_{\mathbf{a}} \int_c^d \| f(x) - f'(x; \mathbf{a}) \|^2 dx. \tag{2.9}$$

(ii) Omitting unimportant parts. The basic idea for this type of approximation is that, even though the function itself is not convex, within a certain range, some components can be omitted. Consequently, the approximation is convex.

One good example is the channel capacity function as

$$C = W \log_2(1 + \text{SNR}), \tag{2.10}$$

where C is the capacity, W is the bandwidth, and SNR is the signal-to-noise ratio. However, when the SNR is high, i.e., $\text{SNR} \gg 1$, we can omit 1 and have

$$C' = W \log_2(\text{SNR}). \tag{2.11}$$

C' is a convex function. This approximation has been employed in some networking optimizations such as [20].

2.1.3 Optimality

In this subsection, we will discuss the optimality of the solution, i.e., how to determine whether the solution is optimal or not, and in what sense the solution is optimal. The organization of this section is as follows. First the optimality for the unconstrained problem is discussed. Then Fritz John conditions and Karush–Kuhn–Tucker (KKT) conditions are explained. Finally, second-order conditions are illustrated.

Before we discuss the unconstrained optimality, we define the global optimum and local optimum as follows.

DEFINITION 3. *Consider* $\min f(\mathbf{x})$ *over* Ω *and let* $\bar{\mathbf{x}} \in \Omega$. *If* $f(\bar{\mathbf{x}}) \leq f(\mathbf{x}), \ \forall\, \mathbf{x} \in \Omega$, *and then* $\bar{\mathbf{x}}$ *is called a global minimum. If* $f(\bar{\mathbf{x}})$ *is no more than the neighbor of* $\bar{\mathbf{x}}$, $\bar{\mathbf{x}}$ *is called a local minimum.*

Some necessary and sufficient conditions for the optimality are as follows.

- Necessary conditions

  (i) First-order necessary condition: If $f(\mathbf{x})$ is differentiable at $\bar{\mathbf{x}}$, then $\bar{\mathbf{x}}$ is a local minimum if $\nabla f(\bar{\mathbf{x}}) = 0$.

  (ii) Second-order necessary condition: If $f(\mathbf{x})$ is twice differentiable at $\bar{\mathbf{x}}$ and if $\bar{\mathbf{x}}$ is a local minimum, then $\nabla f(\bar{\mathbf{x}}) = 0$ and Hessian matrix $\mathbf{H}(\bar{\mathbf{x}})$ is positive semidefinite.

- Sufficient conditions

(i) First-order necessary and sufficient condition: If $f(\mathbf{x})$ is pseudo-convex at $\bar{\mathbf{x}}$, then $\bar{\mathbf{x}}$ is a global minimum if and only if $\nabla f(\bar{\mathbf{x}}) = 0$.

(ii) Second-order sufficient condition: If $f(\mathbf{x})$ is twice differentiable at $\bar{\mathbf{x}}$ and if $\nabla f(\bar{\mathbf{x}}) = 0$ and Hessian matrix $\mathbf{H}(\bar{\mathbf{x}})$ is positive definite, then $\bar{\mathbf{x}}$ is a strict local minimum.

It is worth mentioning that some points on the curves satisfying the necessary conditions might not be the true optimum. For example, in Figure 2.3, we show $z = x^2 - y^2$. We can see that the necessary condition of the first-order differential equal to zero is satisfied for the saddle point at $(0, 0)$. However, the saddle point is not a local optimum.

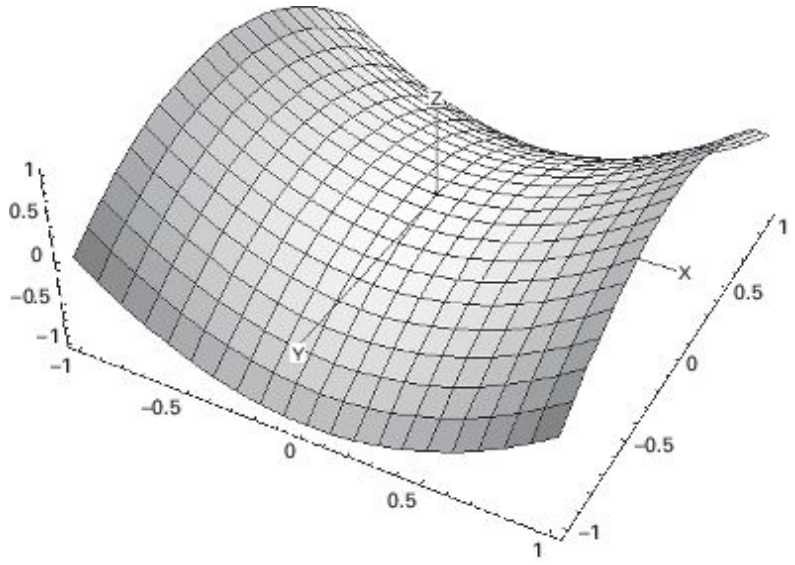

Figure 2.3. An example of a saddle point.

Next we list a few theorems for the optimality of (2.1) as follows.

- Fritz John necessary conditions. Let $\bar{\mathbf{x}}$ be a feasible solution, and let $I=\{i : g_i(\bar{\mathbf{x}})=0\}$. Suppose $g_i, i \in I$ is continuous at $\bar{\mathbf{x}}$. f and $g_i, i \in I$ are differentiable at $\bar{\mathbf{x}}$, and $h_j, \forall j$ is continuous and differentiable at $\bar{\mathbf{x}}$.

If $\bar{\mathbf{x}}$ is a local minimum, then there exist scalars u_0, u_i, for $i \in I$, and v_j for $j = 1, \ldots, l$ such that

$$u_0 \nabla f(\bar{\mathbf{x}}) + \sum_{i \in I} u_i \nabla g_i(\bar{\mathbf{x}}) + \sum_{j=1}^{l} v_j \nabla h_j(\bar{\mathbf{x}}) = \mathbf{0},$$
$$u_0, u_i \geq 0, \forall i \in I, (u_0, \mathbf{u}_I, \mathbf{v}) \neq (0, \mathbf{0}, \mathbf{0}), \tag{2.12}$$

where $\mathbf{u}_I$ is the vector whose component is u_i and $\mathbf{v} = (v_1, \ldots, v_l)^\top$.

- Fritz John sufficient conditions. Define $S = \{\mathbf{x} : g_i(\mathbf{x}) \leq 0, \text{ for } i \in I, h_j(\mathbf{x}) = 0, \text{ for } j = 1, \ldots, l\}$. If h_j for $j = 1, \ldots, l$ are affine and $\nabla h_j(\bar{\mathbf{x}})$, $j = 1, \ldots, l$, are linearly independent, and if there exists an ε-neighborhood $N_\varepsilon(\bar{\mathbf{x}})$ of $\bar{\mathbf{x}}, \varepsilon > 0$, such that f is pseudo-convex on $S \cap N_\varepsilon(\bar{\mathbf{x}})$, then $\bar{\mathbf{x}}$ is a local minimum for (2.1).
- KKT necessary conditions. Suppose f and $g_i, i \in I$, are differentiable at $\bar{\mathbf{x}}$, $g_i, i \in I$, is continuous at $\bar{\mathbf{x}}$, and $h_j, \forall j$, is continuous and differentiable at $\bar{\mathbf{x}}$. Suppose $\nabla g_i(\bar{\mathbf{x}}), \forall i \in I$, and $\nabla h_j(\bar{\mathbf{x}}), j = 1, \ldots, l$, are linearly independent. If $\bar{\mathbf{x}}$ is a local optimum, then unique scalars $u_i, i \in I$, and v_j for $j = 1, \ldots, l$ exist such that

$$\nabla f(\bar{\mathbf{x}}) + \sum_{i \in I} u_i \nabla g_i(\bar{\mathbf{x}}) + \sum_{j=1}^{l} v_j \nabla h_j(\bar{\mathbf{x}}) = \mathbf{0},$$
$$u_i \geq 0, \forall i \in I. \tag{2.13}$$

- KKT sufficient conditions. Suppose KKT conditions hold at $\bar{\mathbf{x}}$, i.e., there exist scalars $\bar{u}_i \geq 0$ for $i \in I$ and $\bar{v}_j$ for $j = 1, \ldots, l$ such that

$$\nabla f(\bar{\mathbf{x}}) + \sum_{i \in I} \bar{u}_i \nabla g_i(\bar{\mathbf{x}}) + \sum_{j=1}^{l} \bar{v}_j \nabla h_j(\bar{\mathbf{x}}) = \mathbf{0}. \tag{2.14}$$

Let $J = \{j : \bar{v}_j > 0\}$ and $K = \{j : \bar{v}_j < 0\}$. Suppose f is pseudo-convex at $\bar{\mathbf{x}}$, g_i is quasi-convex at $\bar{\mathbf{x}}$ for $i \in I$, h_j is quasi-convex at $\bar{\mathbf{x}}$ for $j \in J$, and h_j is quasi-concave at $\bar{\mathbf{x}}$ for $j \in K$. Then $\bar{\mathbf{x}}$ is a global optimal solution to (2.1). If the generalized convexity assumptions on the objective and constraint functions are restricted to a domain $N_\varepsilon(\bar{\mathbf{x}})$ for some $\varepsilon > 0$, then $\bar{\mathbf{x}}$ is a local minimum for (2.1).

- KKT second-order necessary conditions. Suppose the objective and constraints defined in (2.1) are twice differentiable, and Ω is not empty. If $\bar{\mathbf{x}}$ is a local optimum, define the restricted Lagrangian function $L(\mathbf{x})$ as

$$L(\mathbf{x}) = \phi(\mathbf{x}, \bar{\mathbf{u}}, \bar{\mathbf{v}}) = f(\mathbf{x}) + \sum_{i \in I} \bar{u}_i g_i(\mathbf{x}) + \sum_{j=1}^{l} \bar{v}_j h_j(\mathbf{x}). \tag{2.15}$$

  Denote its Hessian at $\bar{\mathbf{x}}$ by

$$\nabla^2 L(\bar{\mathbf{x}}) = \nabla^2 f(\bar{\mathbf{x}}) + \sum_{i \in I} \bar{u}_i \nabla^2 g_i(\bar{\mathbf{x}}) + \sum_{j=1}^{l} \bar{v}_j \nabla^2 h_j(\bar{\mathbf{x}}), \tag{2.16}$$

  where $\nabla^2 f(\bar{\mathbf{x}})$, $\nabla^2 g_i(\bar{\mathbf{x}})$ for $i \in I$, and $\nabla^2 h_j(\bar{\mathbf{x}})$ for $j = 1, \ldots, l$ are the Hessians of f, g_i for $i \in I$, and h_j for $j = 1, \ldots, l$, respectively. Assume that $\nabla g_i(\bar{\mathbf{x}})$ for $i \in I$ and $\nabla h_j(\bar{\mathbf{x}})$ for $j = 1, \ldots, l$ are linearly independent. Then $\bar{\mathbf{x}}$ is a KKT point and

$$\mathbf{d}^\top \nabla^2 L(\bar{\mathbf{x}}) \mathbf{d} \geq 0, \tag{2.17}$$

  for all $\mathbf{d} \in \{\mathbf{d} \neq \mathbf{0} : \nabla g_i(\bar{\mathbf{x}})^\top \mathbf{d} \leq \mathbf{0}\}$ for all $i \in I$, $\nabla h_j(\bar{\mathbf{x}})^\top \mathbf{d} = 0$ for all $j = 1, \ldots, l$.
- KKT second-order sufficient conditions. Suppose the objective and constraints defined in (2.1) are twice differentiable, and Ω is not empty. Let $\bar{\mathbf{x}}$ be a KKT point for (2.1), with Lagrange multiplier $\bar{u}$ and $\bar{v}$ associated with the inequality and equality constraints, respectively. Denote $I^+ = \{i \in I : \bar{u}_i > 0\}$ and $I^0 = \{i \in I : \bar{u}_i = 0\}$. Define the restricted Lagrangian function $L(\mathbf{x})$ and its Hessian. Define the cone

$$C = \{\mathbf{d} \neq \mathbf{0} : \begin{array}{ll} \nabla g_i(\bar{\mathbf{x}})^\top \mathbf{d} = 0\} & \text{for } i \in I^+, \\ \nabla g_i(\bar{\mathbf{x}})^\top \mathbf{d} \leq 0\} & \text{for } i \in I^0, \\ \nabla h_j(\bar{\mathbf{x}})^\top \mathbf{d} = 0\} & \text{for } j = 1, \ldots, l. \end{array} \tag{2.18}$$

  Then, if $\mathbf{d} \in \{\mathbf{d} > \mathbf{0}\}$ for all $\mathbf{d} \in C$, we have that $\bar{\mathbf{x}}$ is a strict local minimum for (2.1).

The optimality discussed in this subsection can be used for different scenarios. For example, it can prove the optimality of a certain solution, it can determine the termination criteria for the adaptive algorithm, or it can be used for convergence analysis.

2.1.4 The primal–dual algorithm

In this subsection, we define the duality concept for the constrained optimization. Under some convexity assumptions and constraints, the primal and dual problems have the same optimal objective values, so it is possible to solve the prime problem by considering the dual problem and develop very efficient algorithms. We will define the dual problem first and then introduce the duality theorem. Some properties will be discussed and then we will introduce the primal–dual algorithm.

Consider (2.1) as the primal problem. The Lagrangian dual problem of (2.1) can be defined as

$$\begin{aligned} &\max \theta(\mathbf{u}, \mathbf{v}) \\ &\text{s.t. } \mathbf{u} \geq \mathbf{0}, \end{aligned} \tag{2.19}$$

where $\theta(\mathbf{u}, \mathbf{v}) = \inf\{f(\mathbf{x}) + \sum_{i=1}^{m} u_i g_i(\mathbf{x}) + \sum_{j=1}^{l} v_j h_j(\mathbf{x}) : \ \mathbf{x} \in \Omega\}$.

For example, the primal problem for linear programming in standard form is

$$\begin{aligned} &\min_{\mathbf{x}} \mathbf{c}^{\top}\mathbf{x} \\ &\text{s.t. } \begin{cases} \mathbf{A}\mathbf{x} = \mathbf{b}, \\ \mathbf{x} \geq 0, \end{cases} \end{aligned} \tag{2.20}$$

where $\mathbf{x}$ is the optimized vector with dimension $N \times 1$, $\mathbf{c}$ and $\mathbf{b}$ are constant vectors, and $\mathbf{A}$ is a constant matrix. The dual function is

$$\theta(\mathbf{u},\mathbf{v}) = \inf_{\mathbf{x}} \left(\mathbf{c}^\top \mathbf{x} - \sum_{i=1}^{N} \lambda_i \mathbf{x}_i + \mathbf{v}^\top (\mathbf{A}\mathbf{x} - \mathbf{b}) \right)$$
$$= -\mathbf{b}^\top \mathbf{v} + \inf_{\mathbf{x}} (\mathbf{c} + \mathbf{A}^\top \mathbf{v} - \boldsymbol{\lambda})^\top \mathbf{x}, \tag{2.21}$$

where $\lambda = [\lambda_1 \ldots \lambda_N]^\top$. Since a linear function $(\mathbf{c} + \mathbf{A}^\top \mathbf{v} - \boldsymbol{\lambda})$ is unbounded below, $\theta(\mathbf{u},\mathbf{v}) = -\infty$ only when $\mathbf{c} + \mathbf{A}^\top \mathbf{v} - \boldsymbol{\lambda} = 0$. We have the dual problem as follows:

$$\max \theta(\mathbf{u},\mathbf{v}) = \begin{cases} -\mathbf{b}^\top \mathbf{v} & \mathbf{c} + \mathbf{A}^\top \mathbf{v} - \boldsymbol{\lambda} = 0, \\ -\infty & \text{otherwise}, \end{cases}$$
$$\text{s.t. } \lambda \geq \mathbf{0}. \tag{2.22}$$

One of the major applications of the dual problem is the duality theorem. The following weak duality theorem states that the objective value of any feasible solution to the dual problem is a lower bound on the objective value of any feasible solution to the primal problem.

THEOREM 1. *Weak duality theorem: If* $\boldsymbol{x}$ *is a feasible solution to the prime problem in (2.1) and* $(\boldsymbol{u},\boldsymbol{v})$ *are the feasible solution to the dual problem in (2.19), then* $f(\mathbf{x}) \geq \theta(\boldsymbol{u},\boldsymbol{v})$. *The duality gap is defined as* $f(\boldsymbol{x}) - \theta(\boldsymbol{u},\boldsymbol{v})$.

Under convexity assumptions and constraint qualification, the duality gap is zero under the following strong duality theorem.

THEOREM 2. *Strong duality theorem: Let* Ω *be a convex set, let* g_i *be convex, and let* h_j *be affine. Suppose there exists an* $\boldsymbol{x} \in \Omega$ *such that* $\boldsymbol{g}(\boldsymbol{x}) \leq \boldsymbol{0}$ *and* $\boldsymbol{h}(\boldsymbol{x}) = \boldsymbol{0}$, *and* $\boldsymbol{0}$ *is the interior point for* $\boldsymbol{h}$ *(Slater's (interiority) condition). Then the optimal point of a prime problem is the same as the optimal point of a dual problem, i.e.,*

$$\inf\{(2.1)\} = \sup\{(2.19)\}. \tag{2.23}$$

The necessary and sufficient condition for the zero duality gap is the existence of a saddle point defined as follows.

DEFINITION 4. $(\bar{\boldsymbol{x}}, \bar{\boldsymbol{u}}, \bar{\boldsymbol{v}})$ *with* $\bar{\boldsymbol{x}} \in \Omega$ *and* $\bar{\boldsymbol{u}} \geq \boldsymbol{0}$ *if and only if*

(i) $\phi(\bar{\boldsymbol{x}}, \bar{\boldsymbol{u}}, \bar{\boldsymbol{v}}) = \min(f(\boldsymbol{x}) + \sum_{i \in I} \bar{u}_i g_i(\boldsymbol{x}) + \sum_{j=1}^{l} \bar{v}_j h_j(\boldsymbol{x}))$,

(ii) $\boldsymbol{g}(\bar{\boldsymbol{x}}) \leq \boldsymbol{0}, \boldsymbol{h}(\bar{\boldsymbol{x}}) = \boldsymbol{0}$, and

(iii) $\bar{\boldsymbol{u}}^{\top} \boldsymbol{g}(\bar{\boldsymbol{x}}) = 0$.

The other similar interpretation is the complementary slackness [20].

If the primal and dual problems are equal, it is possible to solve the primal problem indirectly by solving the dual problem. For nonlinear nonconvex problems, the duality gap might not be zero. Sometimes, in practice, the dual problem will need less information to optimize, and consequently it is easier to solve. In addition, primal and dual problems can be solved iteratively to find the optimal solution. One solution is called cutting planes or the outer-linearization method with the steps as follows.

(i) Initialization.

(ii) Solve primal optimization.

(iii) Solve dual optimization.

(iv) Go back to step (i), until an optimal condition such as the KKT condition has been satisfied.

2.2 Linear programming and the simplex algorithm

Linear programming (LP) is the problem of maximizing/minimizing a linear function over a convex polyhedron. It is used extensively in engineering. An example of an engineering application is improving the network performance for different users using the same radio resources. Linear programs can be solved by using the simplex method [21, 22]. Some other algorithms will also be discussed.

A linear program is a problem that can be expressed in *standard form* as follows:

$$\begin{aligned} &\min \mathbf{c}^{\top}\mathbf{x} \\ &\text{subject to} \begin{cases} \mathbf{A}\mathbf{x} = \mathbf{b}, \\ \mathbf{x} \geq \mathbf{0}, \end{cases} \end{aligned} \tag{2.24}$$

where $\mathbf{x}$ is the vector of variables to solve, $\mathbf{A}$ is a matrix of known coefficients, and $\mathbf{c}$ and $\mathbf{b}$ are vectors of known coefficients. The expression $\mathbf{cx}$ is called the objective function, and the equations $\mathbf{Ax} = \mathbf{b}$ are called the constraints. The matrix $\mathbf{A}$ is generally not square and usually $\mathbf{A}$ has more columns than rows, and $\mathbf{Ax} = \mathbf{b}$ is therefore quite likely to be underdetermined, leaving great latitude in the choice of $\mathbf{x}$ with which to minimize $\mathbf{c}^{\top}\mathbf{x}$.

Two families of solution techniques are in wide use today. Both visit a progressively improving series of trial solutions until a solution that satisfies the conditions for an optimum is reached.

- The *simplex methods*, which were introduced by Dantzig about 50 years ago, visit "basic" solutions computed by fixing enough of the variables at their bounds to reduce the constraints $\mathbf{Ax} = \mathbf{b}$ to a square system, which can be solved for unique values of the remaining variables. Basic solutions represent extreme boundary points of the feasible region defined by $\mathbf{Ax} = \mathbf{b}, \mathbf{x} \geq \mathbf{0}$, and the simplex method can be viewed as moving from one such point to another along the edges of the boundary.

- *Barrier or interior-point methods*,[1] by contrast, visit points within the interior of the feasible region. These methods stem from techniques for nonlinear programming that were developed and popularized in the 1960s by Fiacco and McCormick, but their application to LP dates back only to Karmarkar's innovative analysis in 1984.

Whether the solution of an LP problem falls on the boundary of the feasible region is specified by the following theorem.

THEOREM 3. *Extreme-point (or simplex filter) theorem: If the maximum or minimum value of a linear function defined over a polygonal convex region exists, then it is found at the boundary of the region.*

This theorem implies that a finite number of extreme points indicates a finite number of solutions. Hence, the search is reduced to a finite set of points. However, a finite set can still be too large for practical purposes. The simplex method provides an efficient systematic search guaranteed to converge in a finite number of steps.

Linear programming problems must be converted into augmented form before being solved by the simplex algorithm. This form introduces non-negative slack variables to replace inequalities with equalities in the constraints. The problem can then be written in the following augmented form:

$$\begin{pmatrix} 1 & -\mathbf{c}^{\top} & 0 \\ \mathbf{0} & \mathbf{A} & \mathbf{I} \end{pmatrix} \begin{pmatrix} Z \\ \mathbf{x} \\ \mathbf{x}_S \end{pmatrix} = \begin{pmatrix} 0 \\ \mathbf{b} \end{pmatrix}, \tag{2.25}$$

where $\mathbf{x}$ is the variable vector from the standard form in (2.24), $\mathbf{x}_S$ is the introduced slack variable vector from the augmentation process, c contains the optimization coefficients, $\mathbf{A}$ and $\mathbf{b}$ describe the system of constraint equations, and Z is the variable to be maximized.

The system is typically under-determined, since the number of variables exceeds the number of equations. The difference between the number of variables and the number of equations gives us the number of degrees of freedom associated with the problem. Any solution, optimal or not, will therefore include a number of variables of arbitrary value. The simplex algorithm uses zero as this arbitrary value, and the number of variables with value zero equals the degrees of freedom.

Variables with non-zero values are called basic variables, and variables of zero value are called nonbasic variables in the simplex algorithm. The augmented form simplifies finding the initial basic feasible solution. The simplex method provides an efficient systematic search guaranteed to converge in a finite number of steps. The algorithm is as follows.

(i) Begin the search at an extreme point (i.e., a basic feasible solution).

(ii) Determine whether the movement to an adjacent extreme can improve on the optimization of the objective function. If not, the current solution is optimal. If, however, improvement is possible, then proceed to the next step.

(iii) Move to the adjacent extreme point which offers (or, perhaps, appears to offer) the most improvement in the objective function.

(iv) Repeat steps (ii) and (iii) until the optimal solution has been found or it can be shown that the problem is either unbounded or infeasible.

In 1972, Klee and Minty gave an example of an LP problem in which the polytope P is a distortion of an n-dimensional cube. They showed that the simplex method as formulated by Dantzig visits all 2^n vertices before arriving at the optimal vertex. This shows that the worst-case time-complexity of the algorithm is exponential. Similar examples have been found for other pivot rules. It is an open question whether there is a pivot rule with polynomial time worst-case complexity. Nevertheless, the simplex method is remarkably efficient in practice.

The importance of LP derives in part from its many applications and in part from the existence of good general-purpose techniques for finding optimal solutions. For example, Khachian [23] found an $O(x^5)$ polynomial time algorithm. A much more efficient polynomial time algorithm was found by Karmarkar [24]. This method goes through the middle of the solid (making it a so-called interior-point method), and then transforms and warps. Interior-point methods were known as early as the 1960s in the form of the barrier-function methods. These techniques take as input only a linear program in the standard form, and determine a solution without reference to any information concerning the linear program's origins or special structure. These techniques are fast and reliable over a substantial range of problem sizes and applications.

By contrast, there are some limitations of LP. In practice, the objectives and the constraints are rarely linear functions of the optimization parameters. Under nonlinear conditions, there might be many local optima and the simplex algorithm cannot then find good solutions. In the next few sections, we will discuss more generalized programming methods that deal with the more complicated problems.

2.3 Convex programming

A convex optimization problem can be defined as

$$\begin{aligned} &\min f_0(x) \\ &\text{subject to } \begin{cases} f_i(x) \leq 0, i = 1, \ldots, m, \\ \mathbf{a}_i^\top \mathbf{x} = \mathbf{b}_i, i = 1, \ldots, p, \end{cases} \end{aligned} \tag{2.26}$$

where the objective function f_0 is convex, the inequality constraint functions $f_1, \ldots, f_m$ are convex, and the equality constraint functions $g_i(\mathbf{x}) = \mathbf{a}_i^\top \mathbf{x} - \mathbf{b}_i$ are affine.

A fundamental property of convex optimization problems is that any locally optimal point is also globally optimal. Moreover, by using the duality theory studied in the previous section, the optimality conditions can be easily identified. Since linearity is a special kind of convexity, LP is a special kind of convex optimization. Some typical convex programming problems are discussed in the following subsections.

2.3.1 *Quadratic, geometric, and semidefinite programming*

A problem is called a *quadratic program* if the objective function is quadratic and the constraint functions are affine as

$$\begin{aligned} &\min \mathbf{x}^\top \mathbf{P}\mathbf{x} + 2\mathbf{q}^\top \mathbf{x} \\ &\text{subject to} \begin{cases} \mathbf{G}\mathbf{x} \leq \mathbf{h}, \\ \mathbf{A}\mathbf{x} = \mathbf{b}, \end{cases} \end{aligned} \tag{2.27}$$

where $\mathbf{P} = \mathbf{P}^\top$. If $\mathbf{P}$ is a positive semidefinite matrix, then the problem in (2.27) is a convex function. In this case, the quadratic program has a global optimal point, if there exists at least one vector $\mathbf{x}$ satisfying the constraints and the optimization goal is bounded on the feasible region. If $\mathbf{P}$ is positive definite, then the global optimal point is unique. If $\mathbf{P}$ is zero, the problem becomes a linear program. The KKT condition is sufficient when the problem is convex.

The dual of a quadratic program is also a quadratic program. For example, if we ignore the equality constraint in (2.27), the dual function is given by

$$q(\mathbf{u}) = \inf_{\mathbf{x}} \left\{ \frac{1}{2}\mathbf{x}^\top \mathbf{P}\mathbf{x} + \mathbf{q}^\top \mathbf{x} + \mathbf{u}^\top (\mathbf{G}\mathbf{x} - \mathbf{h}) \right\}. \tag{2.28}$$

The infimum is attained for $\mathbf{x} = -(\mathbf{P})^{-1}(\mathbf{q} + \mathbf{G}^\top \mathbf{u})$, and we have the dual problem as

$$\min \frac{1}{2}\mathbf{u}^\top \mathbf{G}(\mathbf{P})^{-1}\mathbf{G}^\top \mathbf{u} + (\mathbf{h}^\top + \mathbf{G}(\mathbf{P})^{-1}\mathbf{q})\mathbf{u}$$
$$\text{s.t. } \mathbf{u} \geq \mathbf{0}. \tag{2.29}$$

For positive-definite **P**, the ellipsoid method solves the problem in polynomial time [25]. If **P** is negative definite (even if **Q** has only one negative eigenvalue), then the problem is NP-hard [25].

For *geometric programming*, we need the following two definitions.

DEFINITION 5. *A function f is called monomial if*

$$f(x) = cx_1^{a_1}x_2^{a_2}\ldots x_n^{a_n}, \tag{2.30}$$

where $c \geq 0$ *and* $a_i \in \mathbf{R}$.

DEFINITION 6. *A function f is called posynomial if*

$$f(x) = \sum_{k=1}^{K} c_k x_1^{a_{1k}} x_2^{a_{2k}} \ldots x_n^{a_{nk}}, \tag{2.31}$$

where $c_k \geq 0$ *and* $a_{ik} \in \mathbf{R}$.

An optimization problem is called a geometric program if

$$\text{subject to } \begin{cases} \min f_0(x) \\ f_i(x) \leq 1, i = 1, \ldots, m, \\ h_i(x) = 1, i = 1, \ldots, p, \end{cases} \tag{2.32}$$

where $f_0, \ldots, f_m$ are posynomials and $h_1, \ldots, h_p$ are monomials. Geometric programs have numerous applications, including circuit sizing and parameter

estimation via logistic regression in statistics. The maximum likelihood estimator in logistic regression is a geometric program.

Geometric programs are not (in general) convex optimization problems, but they can be transformed to convex problems by a change of variables and a transformation of the objective and constraint functions. For example, on putting $y = \log x$, a posynomial becomes a sum of exponentials of affine functions.

The field of *semidefinite programming* (SDP) or semidefinite optimization (SDO) deals with optimization problems over symmetric positive-semidefinite matrix variables with linear cost functions and linear constraints. Popular special cases are LP and convex quadratic programming with convex quadratic constraints. An SDP problem is

$$\begin{aligned} &\min \mathbf{c}^\top \mathbf{x} \\ &\text{subject to } F(\mathbf{x}) \geq 0, \end{aligned} \tag{2.33}$$

where

$$F(\mathbf{x}) = \mathbf{F}_0 + \sum_{i=1}^{m} x_i \mathbf{F}_i, \tag{2.34}$$

and $F(\mathbf{x})$ is positive semidefinite.

The dual of a semidefinite program is given by

$$\begin{aligned} &\min \mathbf{F}_0 \mathbf{y} \\ &\text{subject to } \begin{cases} \mathbf{F}_i \mathbf{y} = 0, \ \forall i, \\ \mathbf{y} \geq 0. \end{cases} \end{aligned} \tag{2.35}$$

Many practical problems in operations research and combinatorial optimization can be modeled or approximated as semidefinite programming problems. There are two types of algorithms for solving SDPs. One is the interior-point methods, and the other one is specialized general convex optimization algorithms.

2.3.2 The gradient method, the Newton method, and their variations

One advantage of convex optimization is the fact that there are many simple methods to find the global optimum. We will discuss the solutions of unconstrained optimization first, and then we will generalize the solutions to the constrained optimizations. For the unconstrained cases, some methods are as follows.

- The gradient method finds the nearest local minimum of a function with the assumption that the gradient of the function can be computed. The method of steepest descent, also called the gradient-descent method, starts at a point $\mathbf{X}_0$ and, as many times as needed, moves from $\mathbf{X}_i$ to $\mathbf{X}_{i+1}$ by minimizing along the line extending in the direction of $-\nabla f(\mathbf{x})$, the local downhill gradient. The pseudo-code is given as follows.

  Given a feasible starting point $\mathbf{X}_0$, repeat the following steps.

  (i) Calculate the gradient $\nabla f(\mathbf{x})$.

  (ii) Line search: Choose the step size t that optimizes $f(\mathbf{x}_i - t\nabla f(\mathbf{x}_i))$.

  (iii) Update: $\mathbf{x}_{i+1} = \mathbf{x}_i - t\nabla f(\mathbf{x}_i)$.

  Continue repeating the above steps until the stopping criteria, such as the KKT condition (defined in the previous section) or the desired accuracy, are satisfied.

One example of the gradient method is shown in Figure 2.4. As can be seen, the method of steepest descent is simple and easy to apply, and each iteration is fast. It is also very stable. If minimum points exist, the method is guaranteed to locate them. But, even with all these positive characteristics, the method has one very important drawback: It generally has slow convergence. For badly scaled systems, i.e., if the eigenvalues of the Hessian matrix at the solution point are different by several orders of magnitude, the method can end up spending a long number of iterations before locating a minimum point. It starts out with a reasonable convergence, but the progress gets slower and slower.

- The Newton method is a well-known algorithm for finding roots of equations in one or more dimensions. It can also be used to find local maxima and local minima of functions by noticing that, if a real number x^* is where the first-order gradient of a function $f(x)$ is equal to zero, one can solve for x^* by applying Newton's method to $f'(x)$.

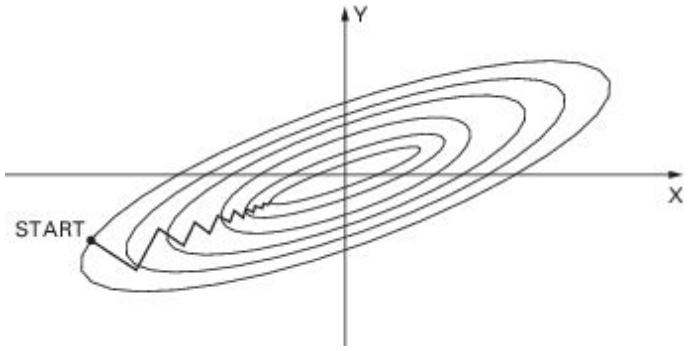

Figure 2.4. An example of the gradient-descent method.

DEFINITION 7. *Given that the second-order differential exists, theNewton step is defined as*

$$\mathbf{v}_{\mathrm{nt}} = -\nabla^2 f(\mathbf{x})^{-1} \nabla f(\mathbf{x}). \tag{2.36}$$

This can have the following interpretations:

$\mathbf{v}_{\mathrm{nt}}$ is the minimizer of the second-order approximation

$$\hat{f}(\mathbf{x}+\mathbf{v}) = f(\mathbf{x}) + \nabla f(\mathbf{x})^{\top}\mathbf{v} + \frac{1}{2}\mathbf{v}^{\top}\nabla^2 f(\mathbf{x})\mathbf{v}. \tag{2.37}$$

$\mathbf{v}_{\mathrm{nt}}$ is the steepest descent direction in Hessian norm.

$\mathbf{v}_{\mathrm{nt}}$ is the solution of a linearized optimality condition for the first-order differential $\nabla f(\mathbf{x}^*) = 0$.

The Newton step is independent of linear changes of the parameters.

DEFINITION 8. *TheNewton decrement is defined as*

$$\lambda(\mathbf{x}) = (\nabla f(\mathbf{x})^{\top}\nabla^2 f(\mathbf{x})^{-1}\nabla f(\mathbf{x}))^{\frac{1}{2}}. \tag{2.38}$$

$\lambda^2/2$ *is an estimate of* $f(\mathbf{x}) - f^*$*, based on the quadratic approximation of* f *at* $\mathbf{x}$ *[20].*

The geometric interpretation of Newton's method is that at each iteration one approximates $f(\mathbf{x})$ by a quadratic function around $\mathbf{x}$, and then takes a step towards the maximum/minimum of that quadratic function. The detailed steps are given below.

Given a feasible starting point $\mathbf{x}_0$, tolerance $\epsilon > 0$, repeat the following steps.

(i) Calculate the Newton step and decrement.

(ii) Quit if $\lambda^2/2 \leq \epsilon$.

(iii) Line search: Choose the step size t.

(iv) Update: $\mathbf{x}_{i+1} = \mathbf{x}_i + t\mathbf{v}_{\mathrm{nt}}$.

Newton's method converges much faster towards a local maximum or minimum than does the gradient-descent method. However, to use

Newton's method, one needs to know the Hessian of $f(\mathbf{x})$, which sometimes can be difficult to compute. There exist various quasi-Newton methods, where an approximation for the Hessian is used instead. Another drawback of Newton's method is that finding the inverse of the Hessian can be an expensive operation.

There are some other methods for unconstrained optimization.

- Conjugate gradients. This method is an attempt to resolve this problem by "learning" from experience. It uses conjugate directions instead of the local gradient for going downhill. The method proceeds by generating vector sequences of iterates (i.e., successive approximations to the solution), residuals corresponding to the iterates, and search directions used in updating the iterates and residuals. Although the length of these sequences can become large, only a few vectors need to be kept in memory. In every iteration of the method, two inner products are performed in order to compute update scalars that are defined to make the sequences satisfy certain orthogonality conditions. If the vicinity of the minimum has the shape of a long and narrow valley, the minimum is reached in far fewer steps than the case using the method of steepest descent.
- The secant method. For the Newton method, it can be laborious both to calculate and to invert the Hessian matrix for systems with a large number of dimensions. The idea of the secant method is not to use the Hessian matrix directly, but rather to start the procedure with an approximation to the matrix, which, as one gets closer to the solution, gradually approaches the Hessian.
- Stochastic (or "on-line") gradient descent. The true gradient is approximated by the gradient of the cost function evaluated for a single training example. The parameters are then adjusted by an amount proportional to this approximate gradient. Therefore, the parameters of the model are updated after each training example. For large data sets, on-line gradient descent can be much faster than batch gradient descent.
- The Broyden–Fletcher–Goldfarb–Shanno (BFGS) method. Quasi-Newton or variable metric methods can be used when it is difficult or time-consuming to evaluate the Hessian matrix. Instead of obtaining an estimate of the Hessian matrix at a single point, these methods

gradually build up an approximate Hessian matrix by using gradient information from some or all of the previous iterates visited by the algorithm.

In the rest of this section, we will discuss how to solve the constrained optimization. First, by using the KKT condition, sometimes we can prove that the constraints can be eliminated without affecting the final solutions. Moreover, by utilizing the dual problem, some constraints can be removed without loss of the optimality. If the constraints cannot be reduced, the following methods are the general approaches which can be employed to solve the problems.

- The projected-gradient method/Newton method. If there is no inequality constraint, we can project the gradient or search direction according to the equality constraint. Suppose the optimization problem is given by

$$\begin{aligned} &\min f(\mathbf{x}) \\ &\text{subject to } \mathbf{A}\mathbf{x} = \mathbf{b}. \end{aligned} \tag{2.39}$$

For the projected-gradient method, the project gradient $\mathbf{v}_{\text{pg}}$ can be written as

$$\begin{pmatrix} \mathbf{I} & \mathbf{A}^\top \\ \mathbf{A} & \mathbf{0} \end{pmatrix} \begin{pmatrix} \mathbf{v}_{\text{pg}} \\ \mathbf{w} \end{pmatrix} = \begin{pmatrix} -\nabla f(\mathbf{x}) \\ \mathbf{0} \end{pmatrix}, \tag{2.40}$$

where $\mathbf{w}$ is an estimate of the Lagrange multiplier.

For the projected Newton method, the projected Newton step $\mathbf{v}_{\text{nt}}$ can be expressed as

$$\begin{pmatrix} \nabla^2 f(\mathbf{x}) & \mathbf{A}^\top \\ \mathbf{A} & \mathbf{0} \end{pmatrix} \begin{pmatrix} \mathbf{v}_{\text{nt}} \\ \mathbf{w} \end{pmatrix} = \begin{pmatrix} -\nabla f(\mathbf{x}) \\ \mathbf{0} \end{pmatrix}. \tag{2.41}$$

- The interior-point method/barrier method. When the searching point approaches the boundary of the feasibility, the approach is to add the penalty to the objective so that the solution always satisfies the inequality constraints. We will discuss these approaches in detail in Section 2.4.
- The cutting planes method. The basic idea of this approach is to find a hyperplane so that the searching space for the optimal solution can be greatly reduced. We will discuss this method in Section 2.5.

2.3.3 The alternating-direction method-of-multipliers algorithm

The general form of the alternating-direction method of multipliers (ADMM) is described as follows:

$$\begin{aligned} \min_{\mathbf{x},\mathbf{z}} \quad & f(\mathbf{x}) + g(\mathbf{z}) \\ \text{subject to} \quad & \mathbf{A}\mathbf{x} + \mathbf{B}\mathbf{z} = \mathbf{c}, \end{aligned} \tag{2.42}$$

where $\mathbf{x} \in \mathbb{R}^n$, $\mathbf{z} \in \mathbb{R}^m$, and $\mathbf{c} \in \mathbb{R}^p$, with matrices $\mathbf{A} \in \mathbb{R}^{p \times n}$ and $\mathbf{B} \in \mathbb{R}^{p \times m}$. The functions f and g are closed, convex, and proper. The scaled augmented Lagrangian can be expressed as

$$\mathcal{L}_\rho(\mathbf{x},\mathbf{z},\boldsymbol{\mu}) = f(\mathbf{x}) + g(\mathbf{z}) + \frac{\rho}{2}\|\mathbf{A}\mathbf{x} + \mathbf{B}\mathbf{z} - \mathbf{c} + \boldsymbol{\mu}\|_2^2, \tag{2.43}$$

where $\rho > 0$ is the penalty parameter and $\boldsymbol{\mu}$ is the scaled dual variable. Using the scaled dual variable, $\mathbf{x}$ and $\mathbf{z}$ are updated in a Gauss–Seidel fashion. At each iteration t, the update process can be expressed as

$$\begin{aligned} \mathbf{x}^{t+1} &= \operatorname*{argmin}_{\mathbf{x}} f(\mathbf{x}) + \frac{\rho}{2}\|\mathbf{A}\mathbf{x} + \mathbf{B}\mathbf{z}^t - \mathbf{c} + \boldsymbol{\mu}^t\|_2^2, \\ \mathbf{z}^{t+1} &= \operatorname*{argmin}_{\mathbf{z}} g(\mathbf{z}) + \frac{\rho}{2}\|\mathbf{A}\mathbf{x}^{t+1} + \mathbf{B}\mathbf{z} - \mathbf{c} + \boldsymbol{\mu}^t\|_2^2. \end{aligned} \tag{2.44}$$

Finally, the scale dual variable is updated by

$$\boldsymbol{\mu}^{t+1} = \boldsymbol{\mu}^{t} + \mathbf{A}\mathbf{x}^{t+1} + \mathbf{B}\mathbf{z}^{t+1} - \mathbf{c}. \tag{2.45}$$

ADMM-based methods offer an opportunity for a general framework of distributed optimization, one canonical example of which is the sharing problem which has the form

$$\min_{\mathbf{x}_i} \sum_{i}^{N} f_i(\mathbf{x}_i) + g\left(\sum_{i}^{N} \mathbf{x}_i\right), \tag{2.46}$$

where $\mathbf{x}_i \in \mathbb{R}^n$, $i = 1, \ldots, N$, are local variables. The function f_i depicts the local cost for subsystem i, and function g is the common objective. In the sharing problem, each agent i determines its own individual variable $\mathbf{x}_i$ to optimize the local cost/payoff function f_i and the shared objective g. The sharing problem can be delicately handled by ADMM in a distributed fashion. By duplicating all the variables $\mathbf{x}_i$, the sharing problem can be rewritten as follows:

$$\begin{aligned} &\min_{\mathbf{x}_i, \mathbf{z}_i} \sum_{i}^{N} f_i(\mathbf{x}_i) + g\left(\sum_{i}^{N} \mathbf{z}_i\right) \\ &\text{subject to} \quad \mathbf{x}_i = \mathbf{z}_i, \quad \forall i. \end{aligned} \tag{2.47}$$

The scaled update process of ADMM consists of the iterations. The $\mathbf{x}_i$-update can be performed individually by each local agent $i = 1, \ldots, N$ in parallel as

$$\mathbf{x}_i^{t+1} = \operatorname*{argmin}_{\mathbf{x}_i} f_i(\mathbf{x}_i) + \frac{\rho}{2}\|\mathbf{x}_i - \mathbf{z}_i^t + \boldsymbol{\mu}_i^t\|_2^2, \tag{2.48}$$

and the variable $\mathbf{z}$ is updated after collecting all the local variables as

$$\mathbf{z}^{t+1} = \underset{\mathbf{z}}{\operatorname{argmin}}\, g\left(\sum_{i}^{N} \mathbf{z}_i\right) + \frac{\rho}{2}\|\mathbf{x}_i^{t+1} - \mathbf{z}_i + \boldsymbol{\mu}_i^t\|_2^2. \tag{2.49}$$

The scaled dual variable $\boldsymbol{\mu}_i$-update step is also performed independently in parallel as follows:

$$\boldsymbol{\mu}_i^{t+1} = \boldsymbol{\mu}_i^t + \mathbf{x}_i^{t+1} - \mathbf{z}_i^{t+1}. \tag{2.50}$$

Hence, the original sharing problem is decomposed into two parts: a **z**-update optimization problem, which requires collecting $\mathbf{x}_i$ from each agent; and N $\mathbf{x}_i$-update optimization problems, which are calculated by each individual agent from the scattered new **z**.

2.4 Nonlinear programming

A nonlinear program is a problem that can be put into the form

$$\begin{aligned} &\min F(\mathbf{x}) \\ \text{subject to } &\begin{cases} g_i(\mathbf{x}) = 0, & \text{for } i = 1, \ldots, m_1, \text{ where } m_1 \geq 0, \\ h_j(\mathbf{x}) \geq 0, & \text{for } j = m_1 + 1, \ldots, m, \text{ where } m \geq m_1, \end{cases} \end{aligned} \tag{2.51}$$

where F is a scalar-valued function of variable vector **x**. We seek to minimize F subject to one or more other such functions that serve to limit or define the values of the variable vector. F is called the "objective function," and the various other functions are called the "constraints." Since the objective function or the constraints can be nonlinear, the optimization in (2.51) is called nonlinear programming (NLP).

One of the greatest challenges in NLP is that some problems exhibit "local optima," i.e., solutions that merely satisfy the requirements on the derivatives of the functions but are not necessarily good. These situations are

similar to multiple peaks. It is difficult for an algorithm that tries to move from point to point only by climbing uphill, since the peak it achieves might not be the highest. Algorithms that have been proposed in order to overcome this difficulty are termed "global optimization." Next, we will first discuss how to find a local optimum from an initialization. Specifically, we will discuss the barrier/interior-point method. Then we will study the techniques to find the global optimum.

The idea of encoding the feasible set using a barrier and designing barrier methods was studied in the early 1960s by Fiacco, McCormick and others. These ideas were mainly developed for general NLP. Nesterov and Nemirovskii came up with a special class of such barriers that can be used to encode any convex set. They guarantee that the number of iterations of the algorithm is bounded by a polynomial in the dimension, and guarantee the accuracy of the solution.

2.4.1 The barrier/interior-point method

In constrained optimization, a barrier function is a continuous function whose value at a point increases to infinity as the point approaches the boundary of the feasible area. It is used as a penalizing term for violations of constraints. The barrier function will also be convex and smooth. The two most common types of barrier functions are inverse barrier functions and logarithmic barrier functions given as

$$I_{\text{inv}} = \begin{cases} \sum_{j=m_1}^{m} 1/h_j(\mathbf{x}) & \text{if } h_j \geq 0, j = m_1, \ldots, m, \\ +\infty & \text{otherwise}, \end{cases} \tag{2.52}$$

and

$$I_{\log} = \begin{cases} -\sum_{j=m_1}^{m} \log(h_j(\mathbf{x})) & \text{if } h_j \geq 0, j = m_1, \ldots, m \\ +\infty & \text{otherwise}, \end{cases} \tag{2.53}$$

respectively.

On adding the barrier function to the objective function $F(\mathbf{x})$, the problem in (2.51) becomes

$$\begin{aligned} &\min tF(\mathbf{x}) + I(\mathbf{x}) \\ &\text{subject to } g_i(\mathbf{x}) = 0, \quad \text{for } i = 1, \ldots, m_1. \end{aligned} \tag{2.54}$$

In the extreme case, where t is large enough, the barrier function I becomes an ideal barrier function, and the problem in (2.54) becomes the problem in (2.51).

The barrier method (path-following algorithm) tries to solve the problem in (2.51) by solving a sequence of the simplified problem in (2.54). In other words, the method computes the optimal $\mathbf{x}^*$ for a sequence of increasing values of t until the solution is close enough to the original problem. The details of the barrier method are shown in Table 2.1.

Table 2.1. The barrier method

Given a feasible initialization $\mathbf{x}_0$, tolerance $\epsilon > 0$, and $t > 0$, $\mu > 1$, repeat the following steps.

1. Calculate $\mathbf{x}^*$ in (2.54).
2. Put $\mathbf{x} = \mathbf{x}^*$.
3. If the tolerance is satisfied, return **x**.
4. Put $t = \mu t$.

There is a tradeoff in the choice of μ. If μ is small, the complexity in solving the problem in (2.54) for each iteration is small, and the iterations closely follow the central path within the feasible range which can avoid possible local optima. However, it needs more iterations. By contrast, if μ is

large, the barrier function converges fast to the ideal one, but the complexity for solving (2.54) increases and a certain possible local optimum might appear.

Interior-point methods are a certain class of algorithms used to solve linear and nonlinear convex optimization problems. These algorithms were inspired by the algorithms of Narendra Karmarkar for linear programming, which he developed in 1984. The basic elements of the method consist of a self-concordant barrier function used to encode the convex set. Mehrotra's predictor–corrector algorithm is a common implementation of an interior-point method. The primal–dual interior-point method proposed by Kojima, Mizuno, and Yoshise is also widely used. The interior-point method starts from the analytic center (which is proposed by Sonnevend and Megiddo), then follows the central path, and finally converges to an optimal solution. One example is shown in Figure 2.5.

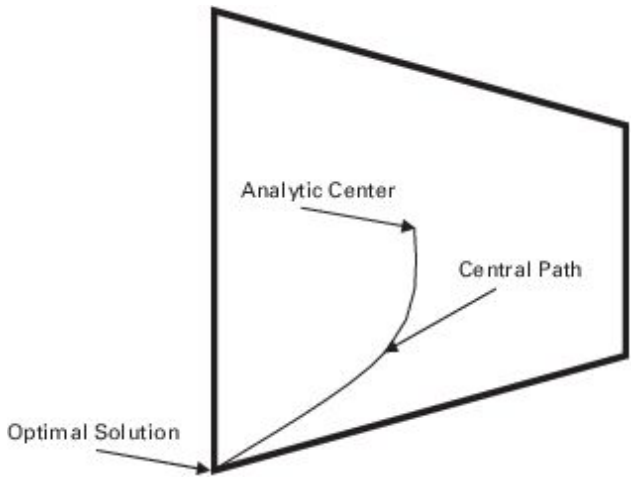

Figure 2.5. An example of the interior-point method.

To achieve the global optimum, the initial starting point for the algorithms plays an important role. One popularly used approach starts with some heuristics with good solutions, and then uses a certain algorithm to converge to a better solution. In most cases, some good solutions can be obtained. However, the global optimum is not guaranteed. In order to obtain the global optimum, some other method can be employed.

2.4.2 *The Monte Carlo method*

Monte Carlo methods are a class of computational algorithms for simulating the behavior of various physical and mathematical systems. They are distinguished from other simulation methods (such as molecular dynamics) by being stochastic, which means that they are nondeterministic in a certain manner. The algorithm usually uses random numbers (or more often pseudo-random numbers) as opposed to deterministic algorithms.

Interestingly, the Monte Carlo method does not require truly random numbers for it to be useful. Many of the most useful techniques use deterministic, pseudo-random sequences, making it easy to test and re-run simulations. The only quality usually necessary to make good simulations is for the pseudo-random sequence to appear "random enough" in a certain sense. That is, the elements must either be uniformly distributed or follow another desired distribution when a large enough number of elements of the sequence are considered. Because of the repetition of algorithms and the large number of calculations involved, the Monte Carlo method can be applied in a computer by utilizing many techniques of computer simulation.

For optimization problems, especially for problems with large dimensions, there might be a lot of local optima. To overcome the problem, we initialize the algorithm randomly within the feasible region. By comparing the local optima, the probability of finding the global optimum is increased with the number of Monte Carlo initialization points. There are some variations of Monte Carlo methods such as parallel tempering and stochastic tunneling.

2.4.3 *Simulated annealing*

Simulated annealing (SA) is a generic probabilistic meta-algorithm for the global optimization problem. It was independently invented by S. Kirkpatrick, C. D. Gelatt, and M. P. Vecchi in 1983, and by V. Cerny in 1985.

The name and inspiration come from annealing in metallurgy, a technique involving heating and controlled cooling of a material to increase the size of its crystals and reduce their defects. The heat causes the atoms to become unstuck from their initial positions (a local minimum of the internal energy) and wander randomly through states of higher energy; the slow cooling gives them more chances of finding configurations with lower internal energy than the initial one.

By analogy with this physical process, each step of the SA algorithm replaces the current solution by a random "nearby" solution. This solution is chosen with a probability that depends on the difference between the corresponding function values and on a global parameter T (called the temperature). The temperature is gradually decreased during the process. The dependence is such that the current solution changes almost randomly when T is large, but increasingly "downhill" as T goes to zero. The allowance for "uphill" moves saves the method from becoming stuck at local minima.

At each step, the SA heuristic considers a certain neighbor of the current state, and probabilistically decides between moving the system to a neighbor state or staying in the current state. The probabilities are chosen so that the system ultimately tends to move to states of lower energy. The probability is large when the temperature is high so that the algorithm will not become stuck in a certain local optimum. By contrast, the probability is low since the probability of local optima is low. When the temperature is zero, the algorithm reduces to the greedy algorithm. Typically this step is repeated until the system reaches a state that is good enough for the application, or until a given computation budget has been exhausted. It can be shown that, for any given finite problem, the probability that the simulated annealing algorithm terminates with the global optimal solution approaches 1 as the annealing schedule is extended.

2.4.4 Genetic algorithms

A genetic algorithm (GA) is a search technique used to find approximate solutions for optimization problems. Genetic algorithms are a particular class

of evolutionary algorithms that use techniques inspired by evolutionary biology such as inheritance, mutation, natural selection, and recombination (or crossover).

Genetic algorithms are typically implemented as a computer simulation in which a population of abstract representations (called chromosomes) of candidate solutions (called individuals) to an optimization problem evolves toward better solutions. Traditionally, solutions are represented in binary as strings of 0s and 1s, but different encodings are also possible. The evolution starts from a population of completely random individuals and happens in generations. In each generation, the fitness of the whole population is evaluated. Then, multiple individuals are stochastically selected from the current population (according to their fitness), and modified (mutated or recombined) to form a new population, which becomes current in the next iteration of the algorithm. The details of the algorithm are shown in Table 2.2.

Table 2.2. Genetic algorithm

Choose the population of random initializations.

Repeat the following steps.

1. Evaluate the individual performance of a certain proportion of the population.
2. Select pairs of best-ranking individuals to reproduce.
3. Apply a crossover operator, which determines the probability that the two selected individuals will be actually combined together for the offspring.
4. Apply a mutation operator, whereby a small probability of mutation is added to the offspring.

Continue to repeat the above steps until a terminating condition is attained.

2.4.5 Swarm intelligence

Swarm intelligence (SI) is the collective behavior of decentralized, self-organized systems, natural or artificial. The concept is employed in artificial intelligence. SI systems consist typically of a population of simple agents interacting locally with one another and with their environment. The inspiration often comes from nature, especially biological systems. The agents follow very simple rules, and, although there is no centralized control structure dictating how individual agents should behave, local, and, to a certain degree, random, interactions among such agents lead to the emergence of "intelligent" global behavior, unknown to the individual agents. Natural examples of SI include ant colonies, bird flocking, animal herding, bacterial growth, and fish schooling. In principle, a swarm should be a multi-agent system that has self-organized behavior and shows certain intelligent behavior. The application of swarm principles to robots is called swarm robotics, while the term SI refers to the more general set of algorithms. "Swarm prediction" has been used in the context of forecasting problems.

Examples of algorithms include, but are not limited to, altruism algorithms [25, 26], ant colony optimization [27, 28], artificial bee colony algorithms [29], artificial immune systems [30], gravitational search algorithms [31, 32], glowworm swarm optimization [33, 34], intelligent water drops [35], particle swarm optimization [36, 37, 38], river formation dynamics [39, 40, 41], self-propelled particles [42, 43, 44], stochastic diffusion search [45, 46, 47, 48, 49], and multi-swarm optimization [50, 51], which fit different scenarios. SI-based techniques can be used in a number of applications such as orbital swarms for self-assembly and interferometry, swarm technology for planetary mapping, data mining, ant-based routing, and crowd simulation.

In the following, we show an example of how to find the shortest path. Suppose that, from the source to the destination, there are multiple paths, and ants need to find the shortest path. The SI algorithm can be summarized as follows.

(i) As they move, ants deposit a pheromone.

(ii) The pheromone decays in time.

(iii) Ants follow the path with the highest pheromone concentration.

(iv) Without pheromone, the probability of choosing a short path is equal to that of choosing a long path.

A shorter path allows a higher number of passages, and therefore the pheromone level will be higher on shorter paths. Ants will increasingly tend to choose shorter paths.

2.5 Integer programming

Discrete optimization is the problem in which the decision variables assume discrete values from a specified set. Combinatorial optimization problems, on the other hand, are problems that involve choosing the best combination out of all possible combinations. Most combinatorial problems can be formulated as integer programs. Integer/combinatorial optimization problems are investigated with the efficient allocation of limited resources to meet desired objectives when the values of some or all of the variables are restricted to be integral. Constraints on basic resources, such as modulation, channel allocation, and coding rate, restrict the possible alternatives that are considered feasible. For example, channel allocation, modulation level, channel coding rate, and even power are discrete in the real-practice system. To design future wireless networks, it is of importance to study these integer optimization problems, especially from an industrial implementation point of view.

The versatility of the integer/combinatorial optimization model stems from the fact that, in many practical problems, activities and resources such as the channel, user, and time slot are indivisible. Also, many problems have only a finite number of alternative choices (such as modulation) and consequently can appropriately be formulated as combinatorial optimization problems, the word combinatorial referring to the fact that only a finite

number of alternative feasible solutions can exist. Combinatorial optimization models are often referred to as integer programming models, where programming refers to "planning" so that these are models used in planning where some or all of the decisions can take on only a finite number of alternative possibilities. Integer optimization is the process of finding one or more best (optimal) solutions in a well-defined discrete problem space. In this section, we study how to use integer optimization for wireless networking and resource-allocation problems.

The major difficulty with these problems is that we do not have any optimality conditions to check whether a given (feasible) solution is optimal or not. For example, in linear programming we do have an optimality condition: When a candidate solution is given, we'll check whether there exists an "improving feasible direction" in which to move; if there doesn't, then the solution is optimal. If we can find a direction in which to move that results in a better solution, then the solution is not optimal. There are no such global optimality conditions in discrete or combinatorial optimization problems. The means to guarantee that a given feasible solution is optimal is to "compare" with every other feasible solution. To do this explicitly amounts to total enumeration of all possible alternatives, which is computationally prohibitive due to the NP-completeness of integer programming problems. Therefore, this comparison must be done implicitly, resulting in partial enumeration of all possible alternatives.

There are at least three different approaches for solving integer programming problems, although they are frequently combined into "hybrid" solution procedures in computational practice. They are

- relaxation and decomposition techniques,
- enumeration techniques, and
- cutting planes approaches that are based on polyhedral combinatorics.

Before we study those techniques, we investigate the general problem and one simple example, namely the knapsack problem, in the following two sections.

2.5.1 *General formulation*

In this subsection, we first discuss the general problem formulation for integer optimization. Then we discuss the potential applications for wireless networking and resource allocation. We further illustrate the concerns for formulating the problem.

Most of the integer optimization research to date covers only the linear case. A survey of nonlinear integer programming approaches is given in [52]. The general problem formulation can be given by

$$\min_{\mathbf{x},\mathbf{y},\mathbf{z}} f(\mathbf{x},\mathbf{y},\mathbf{z})$$
$$\text{s.t.} \begin{cases} g_i(\mathbf{x},\mathbf{y},\mathbf{z}) \le 0, \text{ for } i = 1,\ldots,m, \\ h_j(\mathbf{x},\mathbf{y},\mathbf{z}) = 0, \text{ for } j = 1,\ldots,l, \\ \mathbf{x} \in \mathcal{R}, \mathbf{y} \in \{0,1\}, \text{ and } \mathbf{z} \in \mathcal{I}, \end{cases} \tag{2.55}$$

where the function f is the objective function, the functions g_i are the equality constraint functions, the functions h_j are the inequality constraint functions, the component of the vector x is a real-valued variable, the component of the vector y is a variable of either 0 or 1, and the component of the vector z is an integer value in a space $\mathcal{I}$. If $\mathbf{y} = \mathbf{0}$ and $\mathbf{z} = \mathbf{0}$, (2.55) becomes a nonlinear optimization case. If $\mathbf{z} = \mathbf{0}$, the problem in (2.55) is referred to as a pure 0–1 integer-programming problem; if $\mathbf{y} = \mathbf{0}$, the problem in (2.55) is called a pure-integer programming problem. Otherwise, the problem is a mixed-integer programming problem.

For wireless networking and resource allocation, there are many potential applications of integer optimization. Next, we will list some representative examples.

- **Network, routing, and graph problems**. Many optimization problems can be represented by a network, where a network (or graph) is defined by nodes and by arcs connecting those nodes. Many practical problems arise around physical networks such as

communication networks. In addition, there are many problems that can be modeled as networks even when there is no underlying physical network. For example, one can think of the assignment problem where one wishes to assign a set of users to a certain set of jobs in a way that minimizes the cost of the assignment. Here one set of nodes represents the users to be assigned, another set of nodes represents the possible jobs, and there is an arc connecting a user to a job if that user is capable of performing that job.

In addition, there are many graph-theoretic problems that examine the properties of the underlying graph or network. Such problems include the Chinese-postman problem where one wishes to find a path (a connected sequence of edges) through the graph that starts and ends at the same node, which covers every edge of the graph at least once; and has the shortest length possible. If one adds the restriction that each node must be visited exactly once and drops the requirement that each edge be traversed, the problem becomes the notoriously difficult traveling-salesman problem. Other graph problems include the vertex-coloring problem, whose object is to determine the minimum number of colors needed to color each vertex of the graph in order that no pair of adjacent nodes (nodes connected by an edge) will share the same color; the edge-coloring problem, whose object is to find a minimum total weighted collection of edges such that each node is incident to at least one edge; the maximum-clique problem, whose objective is to find the largest subgraph of the original graph such that every node is connected to every other node in the subgraph; and the minimum-cut problem, whose objective is to find a minimum weighted collection of edges that (if removed) would disconnect a set of nodes s from a set of nodes t.

Although these combinatorial optimization problems on graphs might appear, at first glance, to be interesting mathematically but to have little application to the decision making in management or engineering, their domain of applicability is extraordinarily broad. The traveling-salesman problem has applications in routing and scheduling, in large-scale circuitry design, and in strategic defense. The four-color problem (can a map be colored in four colors or fewer?) is a special case of the vertex-coloring problem. Both the

clique problem and the minimum-cut problem have important implications for the reliability of large systems.

- **The scheduling problem**. Space–time networks are often used in scheduling applications. Here one wishes to meet specific demands at different points in time. To model this problem, different nodes represent the same entity at different points in time. An example of the many scheduling problems that can be represented as a space–time network is the channel-assignment problem, which requires that one assign a specific favorable user to the channel to maximize the system performance or QoS. Each time, a channel must have one and only one user assigned to it, and a user can be assigned to a channel according to its instantaneous channel conditions as well as its transmission history or QoS.
- **The assignment problem**. The assignment problem is one of the fundamental combinatorial optimization problems in the branch of optimization or operations research in mathematics. In its most general form, the problem is as follows.

  There are a number of agents and a number of tasks. Any agent can be assigned to perform any task, incurring a certain cost that may vary depending on the assignment. It is required to perform all tasks by assigning exactly one agent to each task in such a way that the total cost of the assignment is minimized. If the numbers of agents and tasks are equal and the total cost of the assignment for all tasks is equal to the sum of the costs for each agent (or the sum of the costs for each task, which is the same thing in this case), then the problem is called a linear assignment problem. Commonly, when one speaks of an assignment problem without any additional qualification, the linear assignment problem is meant. Other kinds are the quadratic assignment problem and the bottleneck assignment problem.

  The assignment problem is a special case of another optimization problem known as the transportation problem, which is a special case of the maximal flow problem, which in turn is a special case of a linear program. While it is possible to solve any of these problems using the simplex algorithm, each problem has more efficient algorithms designed to take advantage of its special structure.

Algorithms that solve the linear assignment problem within an amount of time bounded by a polynomial expression of the number of agents are known.

The restrictions on agents, tasks, and cost in the (linear) assignment problem can be relaxed, as shown in the example below. Suppose that a taxi firm has three taxis (the agents) available, and three customers (the tasks) wishing to be picked up as soon as possible. The firm prides itself on speedy pickups, so for each taxi the "cost" of picking up a particular customer will depend on the time taken for the taxi to reach the pickup point. The solution to the assignment problem will be whichever combination of taxis and customers results in the least total cost.

However, the assignment problem can be made rather more flexible than it first appears. In the above example, suppose that there are four taxis available, but still only three customers. Then a fourth task can be invented, perhaps called "sitting still doing nothing," with a cost of 0 for the taxi assigned to it. The assignment problem can then be solved in the usual way and still give the best solution to the problem.

Similar tricks can be played in order to allow more tasks than agents, tasks to which multiple agents must be assigned (for instance, a group of more customers than will fit in one taxi), or maximizing profit rather than minimizing cost.

The formal definition of the assignment problem (or linear assignment problem) can be written as follows. Each of n tasks can be performed by any of n agents. The cost of task i being accomplished by agent j is c_{ij}. Assign one agent to each task to minimize the total cost as

$$\min \sum_{i=1}^{n} \sum_{j=1}^{n} c_{ij} x_{ij}$$

$$\text{s.t.} \begin{cases} \sum_{j=1}^{n} x_{ij} = 1, & \text{for all } i, \\ \sum_{i=1}^{n} x_{ij} = 1, & \text{for all } j, \\ x_{ij} \in \{0, 1\}. \end{cases} \tag{2.56}$$

Now we discuss the formulation considerations. The versatility of the integer programming formulation, as illustrated by the above examples, shall provide sufficient explanation for the high activity in the field of combinatorial optimization that is investigated by developing solution procedures for such problems. Since there are often different ways of mathematically representing the same problem, and since obtaining an optimal solution to a large integer-programming problem in a reasonable amount of computer time may well depend on the way it is "formulated," much recent research has been directed toward the reformulation of integer programming problems. In this regard, it is sometimes advantageous to increase (rather than decrease) the number of integer variables, the number of constraints, or both. Moreover, a certain problem may be of such a nature that it can hardly be formulated as (2.55), but (2.55) has a wide range of applications.

Once the problem has been formulated (or reformulated) into an integer programming problem, solution approaches for obtaining optimal – or at least near-optimal – solutions must be found. In the next subsection, we discuss a special case of integer programming, namely the knapsack problem, and its variety of applications.

2.5.2 The knapsack problem

In this subsection, we discuss one special case of integer programming and its applications. Then, we list different formats of the problem formulation.

Suppose one wants to fill a knapsack that can hold a total weight of c with a certain combination of items from a list of n possible items each with weight w_i and value p_i so that the value of the items packed into the knapsack is maximized. This problem has a single linear constraint (that the weight of the items in the knapsack not exceed c), a linear objective function, which sums the values of the items in the knapsack, and the added restriction that each item either be in the knapsack or not, i.e., a fractional amount of an item is not possible. Define a vector of binary variable x_j having the following meaning:

$$x_j = \begin{cases} 1, & \text{if item j is selected,} \\ 0, & \text{otherwise.} \end{cases} \tag{2.57}$$

The simplest knapsack problem is that of how to pack as many valuable items as possible, which has the following formulation:

$$\begin{aligned} &\max_{x_j} \sum_{j=1}^{n} p_j x_j \\ &\text{s.t.} \sum_{j=1}^{n} w_j x_j \leq c. \end{aligned} \tag{2.58}$$

In general the knapsack problems are NP-hard. For solution approaches specific to the knapsack problem see [53].

Although this problem might seem almost too simple to have much applicability, the knapsack problem is important to cryptographers and to those interested in protecting computer files, electronic transfers of funds, and electronic mail. These applications use a "key" to allow entry into secure information. Often the keys are based on linear combinations of a certain collection of data items that must equal a certain value. This problem is also structurally important in that most integer programming problems are generalizations of this problem (i.e., there are many knapsack constraints that together constitute the problem). Approaches for the solution of multiple knapsack problems are often based on examining each constraint separately.

Next, we will list all types of knapsack-problem formulations. For wireless networking and resource allocation, we can select the best fits for the specific problem.

- The 0–1 knapsack problem. The problem formulation is the same as (2.58). The problem itself attracts a lot of attention for three reasons. First, it can be viewed as the simplest integer optimization problem.

Second, it appears as a subproblem of many complex problems. Third, it may represent many practical situations.

- The bounded knapsack problem. The bounded knapsack problem is a generalized 0–1 knapsack problem since x_j can be a certain integer other than binary. The problem is formulated as

$$\max_{x_j} \sum_{j=1}^{n} p_j x_j$$

$$\text{s.t.} \begin{cases} \sum_{j=1}^{n} w_j x_j \le c, \\ 0 \le x_j \le b_j \text{ and integer}, j \in N = \{1, \ldots, n\}. \end{cases} \tag{2.59}$$

- The subset-sum problem. The subset-sum problem is also called the value-independent knapsack problem or stick-stacking problem. It is a particular case of the 0–1 knapsack problem with $p_j = w_j$, $\forall j$. The problem can be written as

$$\max_{x_j} \sum_{j=1}^{n} w_j x_j$$

$$\text{s.t.} \begin{cases} \sum_{j=1}^{n} w_j x_j \le c, \\ x_j = 1, \text{ if item j is selected; } x_j = 0, \text{ otherwise}. \end{cases} \tag{2.60}$$

- The change-making problem. The problem is to make changes for a fixed amount of money and minimize the number of changes. The unit for each change is denoted by w_j and the overall amount of money is c. The problem can be formulated as

$$\min_{x_j} \sum_{j=1}^{n} x_j$$

$$\text{s.t.} \begin{cases} \sum_{j=1}^{n} w_j x_j = c, \\ 0 \le x_j \text{ and is an integer}, j \in N = \{1, \ldots, n\}. \end{cases} \tag{2.61}$$

- The multiple-knapsack problem. If there is more than one knapsack, the problem is a multiple-knapsack problem. Suppose there are in total m knapsacks and n items. The 0–1 multiple-knapsack problem is given by

$$\max \sum_{i=1}^{m} \sum_{j=1}^{n} p_j x_{ij}$$

$$\text{s.t.} \begin{cases} \sum_{j=1}^{n} w_j x_{ij} \leq c_i, \ \forall i \in M = \{1, \ldots, m\}, \\ \sum_{i=1}^{m} x_{ij} \leq 1, \ \forall j \in N = \{1, \ldots, n\}, \\ x_{ij} = 1, \text{ if item } j \text{ is selected for knapsack } i; \ x_{ij} = 0, \text{ otherwise.} \end{cases} \tag{2.62}$$

- The generalized assignment problem. In the generalized assignment problem, the profit and weight are different for different knapsacks, i.e., we have p_{ij} and w_{ij}. The problem formulation is given by

$$\max \sum_{i=1}^{m} \sum_{j=1}^{n} p_{ij} x_{ij}$$

$$\text{s.t.} \begin{cases} \sum_{j=1}^{n} w_{ij} x_{ij} \leq c_i, \ \forall i \in M = \{1, \ldots, m\}, \\ \sum_{i=1}^{m} x_{ij} = 1, \ \forall j \in N = \{1, \ldots, n\}, \\ x_{ij} = 1, \text{ if item } j \text{ is selected for knapsack } i; \ x_{ij} = 0, \text{ otherwise.} \end{cases} \tag{2.63}$$

- The bin-packing problem. The bin-packing problem is that of how to select the minimal number of knapsacks with capacity c to pack all the items. Suppose $y_i = 1$ if the ith knapsack is occupied; otherwise $y_i = 0$. The problem formulation is given by

$$\min \sum_{i=1}^{n} y_i$$

$$\text{s.t.} \begin{cases} \sum_{j=1}^{n} w_j x_{ij} \leq c y_i, \ \forall i \in N = \{1, \ldots, n\}, \\ \sum_{i=1}^{m} x_{ij} = 1, \ \forall j \in N = \{1, \ldots, n\}, \\ x_{ij} = 1, \text{ if item } j \text{ is selected for knapsack } i; \ x_{ij} = 0, \text{ otherwise.} \end{cases} \tag{2.64}$$

In the next three subsections, we will discuss three different approaches to solve the integer/combinatorial problem. Examples are given to clarify the approaches.

2.5.3 *Relaxation and decomposition*

One approach to the solution to integer-programming problems is to take a set of "complicating" constraints into the objective function in a Lagrangian fashion (with fixed multipliers that are changed iteratively). This approach is known as Lagrangian relaxation. Removing the complicating constraints from the constraint set frequently makes the resulting subproblem considerably easier to solve. The latter is a necessity for the approach to work because the subproblems must be solved repetitively until optimal values for the multipliers are found. The bound found by Lagrangian relaxation can be tighter than that found by linear programming, but only at the expense of solving subproblems in integers, i.e., only if the subproblems do not have the integrality property. (A problem has the integrality property if the solution to the Lagrangian problem is unchanged when the integrality restriction is removed.) Lagrangian relaxation requires that one understands the structure of the problem being solved in order to then relax the constraints that are "complicating" it [54]. A related approach that attempts to strengthen the bounds of Lagrangian relaxation is called Lagrangian decomposition [55]. This approach consists of isolating sets of constraints so as to obtain separate, easily solved problems over each of the subsets. The dimension of the problem is increased by creating linking variables that link the subsets. All Lagrangian approaches are problem-dependent and no underlying general theory has evolved.

Suppose an example constrained combinatorial optimization as follows:

$$\max \sum_{j=1}^{n} p_j x_j$$
$$\text{s.t.} \begin{cases} \sum_{j=1}^{n} w_j x_j = c, \\ x_j = \{0, 1\}, \forall j. \end{cases} \tag{2.65}$$

The Lagrangian relaxation relaxes the complicated constraint to the objective function, which is given by

$$\max \sum_{j=1}^{n} p_j x_j + \lambda \left(c - \sum_{j=1}^{n} w_j x_j \right)$$
$$\text{s.t. } x_j = \{0, 1\}, \forall j, \tag{2.66}$$

where λ is the Lagrange multiplier. The goal is that there is a certain simple solution to solve (2.66) with fixed λ. Consequently, the complexity can be reduced a lot. By adjusting λ, the feasibility and slackness of the complicated constraints are improved. This method is called the sub-gradient method and can be implemented as follows.

(i) Begin with each λ at 0. Let the step size be a certain (problem-dependent) value k.

(ii) Solve (2.66) to get the current solution x.

(iii) For every constraint violated by x, increase the corresponding λ by k.

(iv) For every constraint with positive slack relative to x, decrease the corresponding λ by k.

(v) If m iterations have passed since the best relaxation value has decreased, cut k in half.

(vi) Go to step (ii).

Next, we give an example for Lagrangian relaxation. The integer optimization problem is

$$\max_{x_i \in \{0,1\}} 4x_1 + 5x_2 + 6x_3 + 7x_4$$
$$\text{s.t. } \begin{cases} 2x_1 + 2x_2 + 3x_3 + 4x_4 \leq 7, \\ x_1 - x_2 + x_3 - x_4 \leq 0. \end{cases} \tag{2.67}$$

The Lagrangian relaxation is given by

$$\max_{x_i \in \{0,1\}} 4x_1 + 5x_2 + 6x_3 + 7x_4 + \lambda_1(7 - 2x_1 - 2x_2 - 3x_3 - 4x_4) + \lambda_2(-x_1 + x_2 - x_3 + x_4). \tag{2.68}$$

We select the initial value as $\lambda_1 = \lambda_2 = 0$ and a step size of 0.5. The solution is $x_j = 1, \forall j$. However, it violates the first constraint. We set $\lambda_1 = 0.5$ and $\lambda_2 = 0$, and the solution and the constraint violation are the same. We set the new value until $\lambda_1 = 2$ and $\lambda_2 = 0$. There is slackness of the first constraint and the second constraint is satisfied. Since we cannot go back to $\lambda_1 = 1.5$, which causes constraint violation, we reduce the step size by setting $\lambda_1 = 1.75$ and $\lambda_2 = 0$. The process stops when $\lambda_1 = 1.83$ and $\lambda_2 = 0.33$, with optimal solution $x_1 = x_2 = x_3 = 1$ and $x_4 = 0$.

Most Lagrangian-based strategies provide approaches that deal with special row structures. Other problems may possess special column structure, such that, when some subsets of the variables are assigned specific values, the problem reduces to one that is easy to solve. Benders' decomposition algorithm fixes the complicating variables, and solves the resulting problem iteratively [56]. Using the problem's associated dual, the algorithm must then find a cutting plane (i.e., a linear inequality) that "cuts off" the current solution point but no integer feasible points. This cut is added to the collection of inequalities and the problem is re-solved.

Since each of the decomposition approaches described above provides a bound on the integer solution, it can be incorporated into a branch-and-bound algorithm (discussed in the next subsection), instead of the more commonly used linear-programming relaxation. However, these algorithms are special-purpose algorithms in that they exploit the "constraint pattern" or special structure of the problem.

2.5.4 An enumerative technique: the branch-and-bound approach

The simplest approach to solving a pure-integer-programming problem is to enumerate all the possibilities. However, due to the "combinatorial explosion" resulting from the parameter "size," only the smallest instances can be solved by such an approach. Sometimes one can implicitly eliminate many possibilities by domination or feasibility arguments. Besides straightforward or implicit enumeration, the most commonly used enumerative approach is called branch and bound, where the "branching" refers to the enumeration part of the solution technique and "bounding" refers to the fathoming of possible solutions by comparison with a known upper or lower bound on the solution value. Next, we will discuss the branch-and-bound approach in detail and some examples will also be given.

The general idea may be described in terms of finding the minimal value of a function $f(x)$ over a set of admissible values of the argument x called the feasible region. Both f and x may be of arbitrary nature. A branch-and-bound procedure requires two tools.

The first one is a smart way of covering the feasible region by several smaller feasible subregions (ideally, splitting into subregions). This is called branching, since the procedure is repeated recursively to each of the subregions and all produced subregions naturally form a tree structure, called a search tree or branch-and-bound tree or something similar. Its nodes are the constructed subregions. Another tool is bounding, which is a fast way of finding upper and lower bounds for the optimal solution within a feasible subregion.

The core of the approach is the simple observation that (for a minimization task), if the lower bound for a subregion A from the search tree is greater than the upper bound for any other (previously examined) subregion B, then A may be safely discarded from the search. This step is called pruning. It is usually implemented by maintaining a global variable m that records the minimum upper bound seen among all subregions examined so far; any node whose lower bound is greater than m can be discarded.

It may happen that the upper bound for a node matches its lower bound; that value is then the minimum of the function within the corresponding subregion. Sometimes there is a direct way of finding such a minimum. In both these cases it is said that the node is solved. Note that this node may still be pruned as the algorithm progresses.

Ideally the procedure stops when all nodes of the search tree have been either pruned or solved. At that point, all non-pruned subregions will have their upper and lower bounds equal to the global minimum of the function. In practice the procedure is often terminated after a given time; at that point, the optimal lower bound and the optimal upper bound, among all non-pruned sections, define a range of values that contains the global minimum.

The efficiency of the method depends critically on the effectiveness of the branching and bounding algorithms used; bad choices can lead to repeated branching, without any pruning, until the subregions become very small. In that case the method will be reduced to an exhaustive enumeration of the domain, which is often impractically large. There is no universal bounding algorithm that works for all problems, and there is little hope that one will ever be found; therefore the general paradigm needs to be implemented separately for each application, with branching and bounding algorithms that are specially designed for it.

In the following, we give an example of a branch-and-bound algorithm. We maximize the following constrained integer optimization:

$$\begin{aligned} &\max Z = 21x_1 + 11x_2 \\ &\text{s.t.} \begin{cases} 7x_1 + 4x_2 \le 13, \\ x_1 \ge 0, x_2 \ge 0, \\ x_1, x_2 \text{ are integers.} \end{cases} \end{aligned} \tag{2.69}$$

(i) The first step relaxes (2.69) that x_1 and x_2 are continuous variables. We have the solution $Z = 39$, $x_1 = 1.86$, and $x_2 = 0$. Then we try to branch on x_1 to steps (ii) and (iii), since it is not an integer value.

(ii) $x_1 \geq 2$. In this case, there is no feasible solution.

(iii) $0 \leq x_1 \leq 1$. The solution is $Z = 37.5$, $x_1 = 1$, and $x_2 = 1.5$. Then we try to branch on x_2 to steps (iv) and (v), since it is not an integer value.

(iv) $0 \leq x_1 \leq 1$ and $0 \leq x_2 \leq 1$. The solution is $Z = 32$, $x_1 = 1$, and $x_2 = 1$. Since all variables are integer, stop branching. Return one of the possible solutions.

(v) $0 \leq x_1 \leq 1$ and $x_2 \geq 2$. The solution is $Z = 37$, $x_1 = 0.71$, and $x_2 = 2$. Then we try to branch on x_1 to steps (vi) and (vii), since it is not an integer value.

(vi) $x_1 = 1$ and $x_2 \geq 2$. There is no feasible solution.

(vii) $x_1 = 0$ and $x_2 \geq 2$. The solution is $Z = 35.75$, $x_1 = 0$, and $x_2 = 3.25$. Then we try to branch on x_2 to steps (viii) and (ix) , since it is not an integer value.

(viii) $x_1 = 0$ and $2 \leq x_2 \leq 3$. The solution is $Z = 33$, $x_1 = 0$, and $x_2 = 3$. Since all variables are integer, stop branching. Return one of the possible solutions.

(ix) $x_1 = 0$ and $x_2 \geq 4$. There is no feasible solution.

The steps are shown in Figure 2.6. Compared with the results in steps (iv) and (viii), the optimal solution is $Z = 32$, $x_1 = 1$, and $x_2 = 1$.

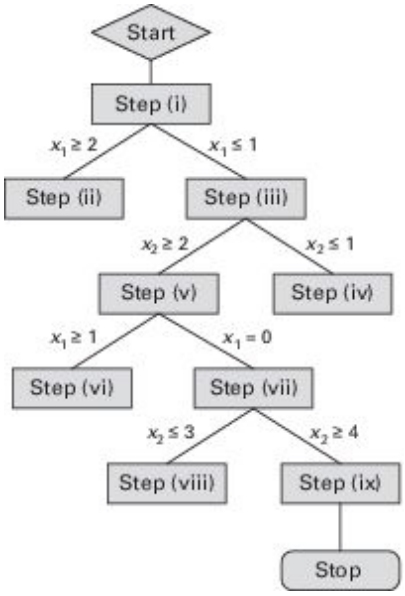

Figure 2.6. An example of a branch-and-bound algorithm.

2.5.5 Cutting planes

Significant computational advances in exact optimization have taken place. Both the size and the complexity of the problems solved were increased considerably when polyhedral theory, which has been developed over the past 25 years, was applied to numerical problem solving. The underlying idea of polyhedral combinatorics is to replace the constraint set of an integer-programming problem by an alternative convexification of the feasible points and extreme rays of the problem.

Weyl [57] established the fact that a convex polyhedron can alternatively be defined as the intersection of finitely many half-spaces or as the convex hull plus the conical hull of a certain finite number of vectors or points. If the data of the original problem formulation are rational numbers, then Weyl's theorem implies the existence of a finite system of linear inequalities whose solution set coincides with the convex hull of the mixed-integer points in S that we denote $\mathrm{conv}(S)$. Thus, if we can list the set of linear inequalities that completely define the convexification of S, then we can solve the integer-programming problem by linear programming. Gomory

[58] derived a "cutting-plane" algorithm for integer-programming problems that can be viewed as a constructive proof of Weyl's theorem, in this context.

Although Gomory's algorithm converges to an optimal solution in a finite number of steps, the convergence to an optimum is extraordinarily slow due to the fact that these algebraically derived cuts are "weak" in the sense that they frequently do not even define supporting hyperplanes to the convex hull of feasible points. Since one is interested in a linear constraint set for $\mathrm{conv}(S)$ that is as small as possible, one is led to consider minimal systems of linear inequalities such that each inequality defines a facet of the polyhedron $\mathrm{conv}(S)$. When viewed as cutting planes for the original problem, the linear inequalities that define facets of the polyhedron $\mathrm{conv}(S)$ are "best possible" cuts, i.e., they cannot be made "stronger" in any sense of the word without losing a certain feasible integer or mixed-integer solution to the problem. Considerable research activity has focused on identifying part (or all) of those linear inequalities for specific combinatorial optimization problems that are, however, derived from an underlying general theme due to Weyl's theorem that applies generally. Since for most interesting integer-programming problems the minimal number of inequalities necessary to describe this polyhedron is exponential in the number of variables, one is led to wonder whether such an approach can ever be computationally practical. It is therefore remarkable that the implementation of cutting-plane algorithms that are based on polyhedral theory has been successful in solving problems of sizes previously believed intractable. The numerical success of the approach can be explained, in part, by the fact that we are interested in proving the optimality of a single extreme point of $\mathrm{conv}(S)$. We therefore do not require the complete description of S but rather only a partial description of S in the neighborhood of the optimal solution.

Thus, a general cutting-plane approach relaxes in a first step the integrality restrictions on the variables and solves the resulting linear program over the set S. If the linear program is unbounded or infeasible, so is the integer program. If the solution to the linear program is integer, then one has solved the integer program. If not, then one solves a facet-identification problem whose objective is to find a linear inequality that "cuts off" the fractional linear-programming solution while assuring that all

feasible integer points satisfy the inequality, i.e., an inequality that "separates" the fractional point from the polyhedron $\text{conv}(S)$. The algorithm continues until (1) an integer solution has been found (we have successfully solved the problem); (2) the linear program is infeasible and therefore the integer problem is infeasible; or (3) no cut is identified by the facet-identification procedures either because a full description of the facial structure is not known or because the facet-identification procedures are inexact, i.e., one is unable to algorithmically generate cuts of a known form. If we terminate the cutting-plane procedure because of the third possibility, then, in general, the process has "tightened" the linear-programming formulation so that the resulting linear-programming solution value is much closer to the integer solution value. In general, the cutting-plane method can be described as follows.

(i) Solve the linear-programming relaxation.

(ii) If the solution to the relaxation is feasible in the integer-programming problem, STOP with optimality.

(iii) Otherwise, find one or more cutting planes that separate the optimal solution to the relaxation from the convex hull of feasible integral points, and add a subset of these constraints to the relaxation.

(iv) Return to the first step.

Typically, the first relaxation is solved using the primal simplex algorithm. After the addition of cutting planes, the current primal iterate is no longer feasible. However, the dual problem is only modified by the addition of some variables. If these extra dual variables are given the value 0, the current dual solution is still dual feasible. Therefore, subsequent relaxations are solved using the dual simplex method. Notice that the values of the relaxations provide lower bounds on the optimal value of the integer program. These lower bounds can be used to measure progress towards optimality, and to give performance guarantees on integral solutions.

Consider an example integer-programming problem as

$$\begin{aligned} &\min -2x_1 - x_2, \\ \text{s.t.} \quad &\begin{cases} x_1 + 2x_2 \le 7, \\ 2x_1 - x_2 \le 3, \\ x_1, x_2 \ge 0, \text{ integer.} \end{cases} \end{aligned} \tag{2.70}$$

The feasible integer points are indicated in Figure 2.7. The linear-programming relaxation (or LP relaxation) is obtained by ignoring the integrality restrictions; this is given by the polyhedron contained in the solid lines. The boundary of the convex hull of the feasible integer points is indicated by dashed lines.

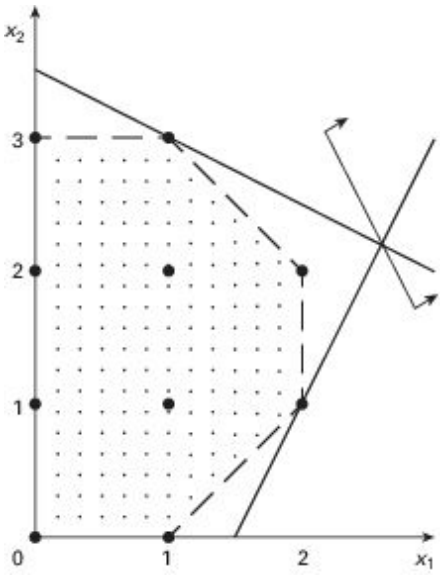

Figure 2.7. An example of a cutting plane.

If a cutting-plane algorithm were used to solve this problem, the linear programming relaxation would first be solved, giving the point $x_1 = 2.6$, $x_2 = 2.2$, which has value -7.4. The inequalities $x_1 + x_2 \le 4$ and $x_1 \le 2$ are satisfied by all the feasible integer points but they are violated by the point (2.6; 2.2). Thus, these two inequalities are valid cutting planes. These two constraints can then be added to the relaxation, and, when the

relaxation is solved again, the point $x_1 = 2, x_2 = 2$ results, with value -6. Notice that this point is feasible in the original integer program, so it must actually be optimal for that problem, since it is optimal for a relaxation of the integer program.

If, instead of adding both inequalities, just the inequality $x_1 \leq 2$ had been added, the optimal solution to the new relaxation would have been $x_1 = 2, x_2 = 2.5$, with value -6.5. The relaxation can then have been modified by adding a cutting plane that separates this point from the convex hull, for example $x_1 + x_2 \leq 4$. Solving this new relaxation will again result in the optimal solution to the integer program.

2.5.6 Benders' decomposition

Benders' decomposition [56] is a widely used algorithm to solve large-scale linear programs (as well as mixed-integer programming) with a special block structure, by dividing the large-scale complicated problems into multiple smaller problems. Then solving those smaller problems iteratively can be much more computationally efficient than directly solving a single large problem. Specifically, a master problem is solved for a subset of variables, and the remaining variables are calculated by the subproblems given the variable values calculated by the main problem. If the subproblems find the master-problem decisions are infeasible, more constraints are generated and added to the main problem. The above iteration is performed until convergence is attained.

As an example, we consider the single large-scale linear mixed-integer programming as follows:

$$\max_{\mathbf{x},\mathbf{y}} \quad z = \mathbf{c}^\top \mathbf{x} + \mathbf{h}^\top \mathbf{y}$$
$$\text{s.t.} \begin{cases} \mathbf{A}\mathbf{x} + \mathbf{G}\mathbf{y} \leq \mathbf{b}, \\ \mathbf{x} \in \mathbb{Z}_+^n, \\ \mathbf{y} \in \mathbb{R}_+^p, \end{cases} \tag{2.71}$$

where **x** and **y** are variables, and **c**, **h**, **b**, **A**, and **G** are constant vectors or matrices. When **A** is block decomposable, the resulting integer programming (the master problem) is much easier than the original problem. Here **x** is called a complicating variable, since the problem becomes significantly easier to solve if **x** is fixed.

First, we assume **x** is fixed, and we obtain the following linear-programming problem:

$$z_{\mathrm{LP}}(\mathbf{x}) = \max_{\mathbf{y}} \{\mathbf{hy} | \mathbf{Gy} \leq \mathbf{b} - \mathbf{Ax}\}, \tag{2.72}$$

which is the subproblem mentioned above, and its dual

$$\max_{\mathbf{u}} \{\mathbf{u}(\mathbf{b} - \mathbf{Ax}) | \mathbf{uG} \geq \mathbf{h}, \mathbf{u} \in \mathbb{R}_+^m\}. \tag{2.73}$$

Assuming that the dual polyhedron is nonempty and bounded, the master problem can be stated as

$$z = \max_{\mathbf{x} \in \mathbb{Z}_+^n} \left(\mathbf{cx} + \min_{i \in 1,\ldots,T} u^i(\mathbf{b} - \mathbf{Ax}) \right), \tag{2.74}$$

where $4\{u^i\}_{i=1}^T$ are the extreme points of the dual polyhedron. Then we can reformulate the master problem as

$$z = \max_{\eta} \{\eta \leq u^i(\mathbf{b} - \mathbf{Ax}), i \in 1, \ldots, T, \mathbf{x} \in \mathbb{Z}_+^n\}. \tag{2.75}$$

The above master problem and subproblem are optimized iteratively. As long as the original single large-scale linear mixed-integer program in (2.71) is a partitionable problem along with feasible, bounded-value linear-programming relaxation, after a finite number of steps, Benders' decomposition finds an optimal solution or proves that none exists.

2.6 Dynamic programming and Markov decision processes

We first study the basics of dynamic programming. Then, one major application, the Markov decision process, will be introduced and solved by use of the Bellman equation. Then for the cases where the transition probability for the Markov process is not random or not known, partially observable MDP and reinforcement learning will be investigated. Finally, two examples for wireless networks will be illustrated.

2.6.1 A general definition of dynamic programming

Basically, the dynamic-programming approach solves a high-complexity problem by combining the solutions of a series of low-complexity subproblems. Dynamic programming relies on the principle of optimality, which states that, in an optimal sequence of decisions or choices, each subsequence must also be optimal. To understand the basic problem formulation, we define the following concepts.

- State: A state is a configuration of a system and is identified by a label that indicates the properties corresponding to that state.
- Stage: A stage is a single step in the system undergoing a certain process and corresponds to the transition from one state to an adjacent state.
- Action: At each state there is a set of actions available, among which a choice must be made.
- Policy: A policy is a set of actions, one for each of a number of states. An optimal policy is the best set of actions in accordance with a given objective.
- Return: A return is something that a system generates over one stage of a process. A return is usually something like a profit, a cost, a distance, a yield, or consumption of a product.
- Value of a state: The value of a state is a function of the returns (sum) generated when the system starts in that state and a particular policy is followed. The value of a state under an optimal policy is the optimal value.

Depending on the different characteristics of the above definitions, the dynamic programming problems can be classified as those in Table 2.3. Dynamic programming usually takes one of two approaches.

- The top-down approach. The problem is broken into subproblems, and these subproblems are solved and the solutions remembered, in case they need to be solved again.
- The bottom-up approach. All subproblems that might be needed are solved in advance and then used to build up solutions to larger problems. This approach is slightly better in terms of stack space and number of function calls, but it is sometimes not intuitive to figure out all the subproblems needed for solving the given problem.

Table 2.3. Classifications of dynamic programming

Discrete	**Continuous**
Finite horizon	Infinite horizon
Deterministic	Stochastic
Constrained	Unconstrained
Perfect state information	Imperfect state information
Single objective	Multiple objective

In practice, to formulate the problem, the following steps are required.

(i) Characterize the structure of an optimal solution.

(ii) Define the value of the optimal solution recursively.

(iii) Compute the optimal solution values either top-down with caching or bottom-up in a table.

(iv) Construct an optimal solution from computed values.

Several typical applications are as follows.

- Problems which involve a sequence of decisions in time: production planning, stock control, investment decision making, and replacement policy.
- Problems in which the sequence of decisions is not directly related to time: sequential production processes, optimal-path problems, optimal-search problems.
- Allocation problems: deciding a sequence of allocations of one or more limited resources.
- Combinatorial and graph-theoretic problems: scheduling, sequencing, and set partitioning.

2.6.2 Markov decision processes

One of the major applications of dynamic programming is Markov decision processes (MDPs), which provide a mathematical framework for modeling decision making in situations where outcomes are partly random and partly under the control of the decision maker. In MDP, the Markov property is assumed, i.e., the effects of an action taken in a state depend only on that state and not on the prior history. MDPs are useful for studying a wide range of optimization problems [59].

An MDP model contains the action for time n as α_n, the state as s_n, the reward function as $R(s_n, \alpha_n)$, and the forgetting factor as β. The discounted time-average reward for infinite time scale can be expressed as

$$V = \sum_{n=1}^{\infty} \beta^n R(s_n, \alpha_n). \tag{2.76}$$

Here the action can be deterministic or stochastic. The deterministic action is $\alpha_n = \pi(s_n)$, where π is the policy. The stochastic action is characterized by $P(s'|s, \pi(s))$, which means the probability of the next state under the condition of the current state and policy.

A Bellman equation is also called an optimality equation or a dynamic-programming equation. We can omit the time n and have the Bellman equation as

$$V^{\pi}(s) = R(s) + \beta \sum_{s'} P(s'|s, \pi(s)) V^{\pi}(s'), \tag{2.77}$$

while the equation for the optimal policy is referred to as the Bellman optimality equation:

$$V^{*}(s) = R(s) + \max_{\alpha} \beta \sum_{s'} P(s'|s, \alpha) V^{*}(s'). \tag{2.78}$$

In other words, the Bellman equation calculates the action that gives the best expected return.

One major disadvantage of MDP is the *curse of dimensionality*. The state space is typically astronomically large. To overcome this, factored MDP is one approach to represent large, structured MDPs compactly, in which a state is implicitly described by an assignment to some set of state variables.

The solution above assumes that the state s is known when action is to be taken; otherwise $\pi(s)$ cannot be calculated. When this assumption is not true, the problem is called a partially observable Markov decision process (POMDP). MDPs are a special case of POMDPs in which the observations always uniquely identify the true state (i.e., the states are directly observed or can be directly deduced from the observation). In Table 2.4, we compare classical planning, MDP, and POMDP.

Table 2.4. Types of planning problems

	State	Action model

Classical planning	Observable	Deterministic
MDP	Observable	Stochastic
POMDP	Partial observable	Stochastic

Since the true state of the world cannot be uniquely identified, a POMDP reasoner must maintain a probability distribution, called the belief state, which describes the probabilities for each true state of the world. Maintenance of the belief states is Markovian, in that it requires only knowledge of the previous belief state, the action taken, and the observation seen.

Each belief is a probability distribution, thus, each value in a POMDP is a function of an entire probability distribution. This is problematic, since probability distributions are continuous. Additionally, we have to deal with the huge complexity of belief spaces. This is similar to the *curse of dimensionality* for MDP. POMDPs so far have been applied successfully only to very small state spaces with small numbers of possible observations and actions.

If the state-transition probabilities for an MDP problem are unknown, the problem is one of reinforcement learning, which is a sub-area of machine learning concerned with how an agent ought to take actions in an environment so as to maximize some notion of long-term reward. Reinforcement learning algorithms attempt to find a policy that maps states of the world to the actions the agent ought to take in those states.

Q-learning is the most popular model-free reinforcement learning technique that works by learning an action-value function that gives the expected utility of taking a given action in a given state and following a fixed policy thereafter. One strength of *Q*-learning is that it is able to compare the expected utility of the available actions without requiring a model of the environment. The core of the algorithm is a simple value iteration update. For each state s in the state set S and for each action α in the action set A, we can calculate an update to its expected discounted reward with the following expression:

$$Q_{t+1}(s_t, \alpha_t) \leftarrow Q_t(s_t, \alpha_t) + \alpha_t(s_t, \alpha_t)\left[R_t + \beta \max_{\alpha} Q_t(s_{t+1}, \alpha_{t+1}) - Q_t(s_t, \alpha_t)\right], \tag{2.79}$$

where R_t is an observed real reward at time t, $\alpha_t(s, a)$ are the learning rates such that $0 \leq \alpha_t(s, a) \leq 1$, and β is the discount factor such that $0 \leq \beta < 1$.

2.7 Stochastic programming

Stochastic optimization refers to the minimization (or maximization) of a function in the presence of randomness in the optimization process. Stochastic optimization methods are optimization algorithms that incorporate probabilistic (random) elements, either in the problem data (the objective function, the constraints, etc.) or in the algorithm itself (through random parameter values, random choices, etc.), or in both. The concept contrasts with the deterministic optimization methods, where the values of the objective function are assumed to be exact, and the computation is completely determined by the values sampled so far. While deterministic optimization problems are formulated with known parameters, real-world problems almost invariably include some unknown parameters.

When the parameters are known only within certain bounds, one approach to tackling such problems is called robust optimization. Here the goal is to find a solution that is feasible for all such data and optimal in some sense. Stochastic programming models are similar in style but take advantage of the fact that probability distributions governing the data are known or can be estimated. The goal here is to find some policy that is feasible for all (or almost all) the possible data instances and maximizes the expectation of some function of the decisions and the random variables. More generally, such models are formulated, solved analytically or numerically, and analyzed in order to provide useful information to a decision maker.

By contrast, even when the data is exact, it is sometimes beneficial to deliberately introduce randomness into the search process as a means of speeding convergence and making the algorithm less sensitive to modeling

errors (perturbation analysis). Further, the injected randomness may provide the necessary impetus to move away from a local solution when searching for a global optimum. Indeed, this randomization principle is known to be a simple and effective way to obtain algorithms with almost certain good performance uniformly across all data sets, for all sorts of problems.

In this section, we first study the general problem formulation. Then we investigate several categories of solution, such as the distribution problem, chance constraint and penalize shortage, and recourse. Simple examples are also given for clarity.

2.7.1 Problem definition

Let us start from a simple linear-programming example as follows:

$$\begin{aligned} &\min x_1 + x_2 \\ \text{s.t.} \quad &\begin{cases} w_1 x_1 + x_2 \geq 7, \\ w_2 x_1 + x_2 \geq 4, \\ x_1 \geq 0, \\ x_2 \geq 0, \end{cases} \end{aligned} \tag{2.80}$$

where w_1 is uniformly distributed from 1 to 4 (i.e., $w_1 \sim U(1, 4)$) and $w_2 \sim U(1/3, 1)$.

The problem in (2.80) is shown in Figure 2.8. The random variables w_1 and w_2 present the gradients of the constraints. The solution can be any point within the pentagonal area. However, the solution point can be optimal with a specific value of the random variable, while it cannot be optimal or even is not feasible with the other values. The question now is how to solve the problem. Or, more precisely, under what criteria should we solve the problem?

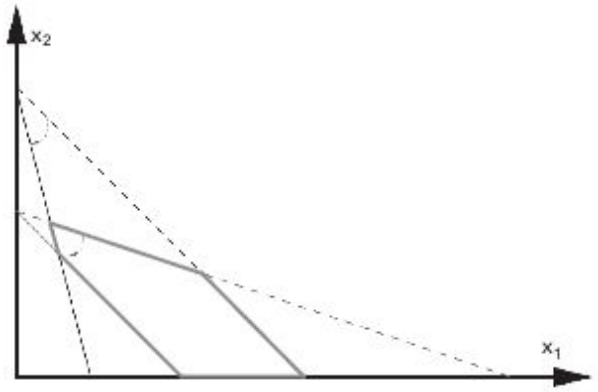

Figure 2.8. An example of random linear programming.

The general form of the problem formulation can be written as

$$\begin{aligned} &\min g_0(x,\xi) \\ \text{s.t.} &\begin{cases} g_i(x,\xi) \le 0, i = 1,\ldots,m, \\ x \in X \subset \mathbb{R}^n, \end{cases} \end{aligned} \tag{2.81}$$

where ξ is a random vector and g_i are deterministic functions.

If it is possible to decide after the observation of the random variable, we can simply solve it as the deterministic program, and we call this the *wait-and-see* approach. Unfortunately, it is not generally appropriate since we need to decide what to do without knowing the exact values of the random variables. Next, we discuss several types of solutions.

The first category of solutions tries to explore the distribution of the random variable. The simplest one is to guess the uncertainty. For the example in (2.80), we show as follows three possible guesses, each of which tells us something about the level of "risk" as follows.

(i) Unbiased: Choose mean values for each random variable. Since the mean $E(w) = (2.5, 1.5)$, we can take $w_1 = 2.5$ and $w_2 = 1.5$ into (2.80). The resulting solution is $(\hat{x}_1, \hat{x}_2) = (18/11, 32/11)$.

(ii) Pessimistic: Choose the worst-case value for random variables. The worst-case $(w_1, w_2) = (1, 1/3)$, and the resulting solution is $(\hat{x}_1, \hat{x}_2) = (0, 7)$.

(iii) Optimistic: Choose the best-case values for random variables. The best-case $(w_1, w_2) = (4, 1)$, and the resulting solution is $(\hat{x}_1, \hat{x}_2) = (4, 0)$.

The advantage of the above guessing methods is the simplicity. However, since only rough information about the randomness is utilized, the results can be very inaccurate or even infeasible.

2.7.2 Chance constraint, sampling method, and variation

To overcome the above problem, the following methods are usually employed in practice.

(i) Chance constraint: Let us enforce that the probability of a constraint holding is sufficiently large. For example, for the problem in (2.80), we can add the following two constraints:

$$P(w_1 x_1 + x_2 \geq 7) \geq \alpha_1, \tag{2.82}$$

$$P(w_1 x_1 + x_2 \geq 7) \geq \alpha_1, \tag{2.83}$$

where α_1 and α_2 are the probabilities of the constraints being satisfied.

(ii) Sampling method: First the Monte Carlo method is used to generate the sets of random variables. For each set, an optimal solution is then computed. Finally, the probability distributions of the solutions are analyzed.

(iii) Likelihood ratio method: The Monte Carlo sampling method does not work if the goal is discontinuous or if the corresponding probability distribution also depends on decision variables. Similarly to the estimation-and-detection method, a likelihood ratio can be defined to solve the problem.

(iv) Genetic algorithm: A search technique used to compute the exact or approximate solutions to optimization and search problems, which was discussed in the previous section.

(v) Simulated annealing: This is a generic probabilistic meta-algorithm for the global optimization problem, namely locating a good approximation to the global optimum of a given function in a large search space. It was also discussed in the previous section.

2.7.3 Recourse

The most widely applied and studied stochastic programming models are two-stage recourse programs. Here the decision maker takes some action in the first stage, after which a random event occurs, affecting the outcome of the first-stage decision. A recourse decision can then be made in the second stage to compensate for any bad effects that might have been experienced as a result of the first-stage decision. The optimal policy from such a model is a single first-stage policy and a collection of recourse decisions (a decision rule) defining which second-stage action should be taken in response to each random outcome.

As in the barrier method that we discussed in the section on nonlinear optimization, the infeasibility can be accepted, but with the penalty of the expected shortage. Define $x^- = \max(0, -z)$ as the negative part of z. For the constraint $w_1 x_1 + x_2 \geq 7$ in (2.80), the shortfall is $(w_1 x_1 + x_2 - 7)^-$. For each constraint, a shortfall cost q_i is assigned. So the optimization problem in (2.80) becomes

$$\min_{x \in \mathbb{R}^2_+} = \{x_1 + x_2 + q_1 E_{w_1}[(w_1 x_1 + x_2 - 7)^-] + q_2 E_{w_2}[(w_2 x_1 + x_2 - 4)^-]\}.$$

(2.84)

The above problem is convex, and it is equivalent to the following problem:

$$\min_{x\in\mathbb{R}^2_+} = \{x_1 + x_2 + Q(x_1, x_2)\}, \tag{2.85}$$

where

$$Q(x_1, x_2) = E_w \left[\min_{y\in\mathbb{R}^2_+} \{q_1 y_1 + q_2 y_2\} \right]$$
$$\text{s.t.} \begin{cases} w_1 x_1 + x_2 + y_1 = 7, \\ w_2 x_1 + x_2 + y_2 = 4. \end{cases} \tag{2.86}$$

Here $Q(x_1, x_2)$ is called the recourse function. Using the above equations, we can correct the actions by imposing the following sequence of events.

(i) First-period decision.

(ii) Nature makes a random decision.

(iii) A second-period decision that attempts to repair the havoc wrought by Nature in step (ii).

The idea of two-stage recourse can be easily extended to multistage recourse, which fits the situation where decisions are made periodically on the basis of a currently known realization of some random variable. It has some learning flavor in the multistage recourse. An *H*-stage stochastic linear program with fixed recourse can be written as

$$\min c^1 x^1 + E\{\min x^2(w)x^2(w) + \cdots + \min x^H(w)x^H(w)\}$$
$$\text{s.t.} \begin{cases} W^1 x^1 = h^1, \\ T^1(w)x^1 + W^2 x^2(w) = h^2(w), \\ \quad \cdots \\ T^{H-1}(w)x^{H-1} + W^H x^H(w) = h^H(w), \\ x^1 \geq 0, \ldots, x^H(w) \geq 0, \end{cases} \tag{2.87}$$

where the decision variables $x^2(w), \ldots, x^H(w)$ are allowed to depend on the random variable w. $T(w)$ and $H(w)$ are technology and recourse matrices, respectively.

One algorithm for recourse, the L-shaped method [60], is a decomposition method that is useful for solving problems that have the form of a master problem and several subproblems represented by the side model. The complete problem with both the master problem and subproblems may be very large. The L-shaped method is a process that solves a sequence of much smaller problems. The combined solution converges in a finite number of iterations to the optimum. Because the number of iterations required may be large, we can terminate the process when the lower- and upper-bound values differ by a specified minimum tolerance. Some theoretical bounds are available to analyze the L-shaped method.

2.8 Sparse optimization

In this section, we first study the sparse optimization models, and then introduce the current state of the art for techniques. Finally, we summarize how to select the algorithms for specific problems.

2.8.1 Sparse-optimization models

First, we overview a set of widely used algorithms for solving problems in the form of

$$\min_{\mathbf{x}}\{r(\mathbf{x}) : \mathbf{A}\mathbf{x} = \mathbf{b}\}, \tag{2.88a}$$

$$\min_{\mathbf{x}} r(\mathbf{x}) + \mu h(\mathbf{A}\mathbf{x} - \mathbf{b}), \tag{2.88b}$$

$$\min_{\mathbf{x}}\{r(\mathbf{x}) : \bar{h}(\mathbf{A}\mathbf{x} - \mathbf{b}) \leq \sigma\}, \tag{2.88c}$$

where $r(\mathbf{x})$, $h(\mathbf{x})$, and $\bar{h}(\mathbf{x})$ are convex functions.

The function $r(\mathbf{x})$ is a regularizer and is typically non-differentiable in sparse optimization problems; the functions $h(\mathbf{x})$ and $\bar{h}(\mathbf{x})$ are data fidelity measures, which are often differentiable, though there are exceptions such as ℓ_1 and ℓ_∞ fidelity measures (or loss functions), which are non-differentiable.

When introducing algorithms, our *first* focus is on the ℓ_1 problems

$$\min_{\mathbf{x}}\{\|\mathbf{x}\|_1 : \mathbf{A}\mathbf{x} = \mathbf{b}\}, \tag{2.89a}$$

$$\min_{\mathbf{x}} \|\mathbf{x}\|_1 + \frac{\mu}{2}\|\mathbf{A}\mathbf{x} - \mathbf{b}\|_2^2, \tag{2.89b}$$

$$\min_{\mathbf{x}}\{\|\mathbf{x}\|_1 : \|\mathbf{A}\mathbf{x} - \mathbf{b}\|_2 \leq \sigma\}. \tag{2.89c}$$

We also consider the variants in which the ℓ_1 norm of $\mathbf{x}$ is replaced by regularization functions corresponding to transform sparsity, joint sparsity, and low rankness, as well as those involving more than one regularization term. These problems are convex and non-smooth. For example, as variants of problem (2.89a), most of the algorithms in this section can be extended to solve

$$\min_{\mathbf{s}}\{\|\mathbf{s}\|_1 : \mathbf{A}\Psi\mathbf{s} = \mathbf{b}\}, \tag{2.90a}$$

$$\min_{\mathbf{x}}\{\|\Upsilon\mathbf{x}\|_1 : \mathbf{A}\mathbf{x} = \mathbf{b}\}, \tag{2.90b}$$

$$\min_{\mathbf{u}}\{\mathrm{TV}(\mathbf{u}) : \mathcal{A}(\mathbf{u}) = \mathbf{b}\}, \tag{2.90c}$$

$$\min_{\mathbf{X}}\{\|\mathbf{X}\|_{2,1} : \mathbf{A}\mathbf{X} = \mathbf{b}\}, \tag{2.90d}$$

$$\min_{\mathbf{X}}\{\|\mathbf{X}\|_* : \mathcal{A}(\mathbf{X}) = \mathbf{b}\}, \tag{2.90e}$$

where $\mathcal{A}(\cdot)$ is a given linear operator, Υ is a linear transform, $\mathrm{TV}(\mathbf{u})$ is a certain discretization of total variation $\int |\nabla \mathbf{u}(x)| dx$ (also, see [61] for a rigorous definition in the space of generalized functions of bounded variation), the $\ell_{2,1}$-norm is defined as

$$\|\mathbf{X}\|_{2,1} := \sum_{i=1}^{m} \left\| [x_{i1}\ x_{i,2} \cdots x_{in}] \right\|_2, \tag{2.91}$$

and the nuclear norm $\|\mathbf{X}\|_*$ equals the sum of singular values of $\mathbf{X}$. The models (2.90a)–(2.90e) are widely used to obtain, respectively, a vector that is sparse under Ψ, a vector that will become sparse on application of the transform Υ, a piece-wise constant signal, a matrix consisting of joint-sparse vectors, and a low-rank matrix.

Decompose $\{1, \ldots, n\} = \mathcal{G}_1 \cup \mathcal{G}_2 \cup \cdots \cup \mathcal{G}_S$, where the $\mathcal{G}_i$ are certain sets of coordinates and $\mathcal{G}_i \cap \mathcal{G}_j = \emptyset,\ \forall i \neq j$. Define the (weighted) group $\ell_{2,1}$ -norm as

$$\|\mathbf{x}\|_{\mathcal{G},2,1} = \sum_{s=1}^{S} w_s \|\mathbf{x}_{\mathcal{G}_s}\|_2,$$

where $w_s \geq 0,\ s = 1, \ldots, S$, are a given set of weights and $\mathbf{x}_{\mathcal{G}_s}$ is a subvector of $\mathbf{x}$ corresponding to the coordinates in $\mathcal{G}_s$. The model

$$\min_{\mathbf{x}}\{\|\mathbf{x}\|_{\mathcal{G},2,1} : \mathbf{A}\mathbf{x} = \mathbf{b}\} \tag{2.92}$$

tends to give solutions with all but a few non-zero subvectors $\mathbf{x}_{\mathcal{G}_s}$.

When the equality constraints of the problems in (2.90) and (2.92) do not hold for the target solutions, one can apply relaxation and penalty to the constraints like those in (2.89b) and (2.89c).

Depending on the type of noise, one may replace the ℓ_2-norm in (2.89b) and (2.89c) by other distance measures or loss functions such as the Kullback–Leibler divergence [62, 63] of two probability distributions p and q and the logistic loss function [64].

Practical problems sometimes have additional constraints such as the non-negativity constraints $\mathbf{x} \geq 0$ or bound constraints $\mathbf{l} \leq \mathbf{x} \leq \mathbf{u}$.

The $\ell_{2,1}$-norm in (2.91) is generalizable to the $\ell_{p,q}$-norm

$$\|\mathbf{X}\|_{p,q} = \left(\sum_i \left(\sum_j |x_{i,j}|^p\right)^{q/p}\right)^{1/q},$$

which is convex if $1 \leq p, q \leq \infty$. For these problems and extensions, we study their algorithms extending from those for ℓ_1 minimization.

The following model is not covered:

$$\min_{\mathbf{x}}\{\|\mathbf{A}\mathbf{x} - \mathbf{b}\|_2 : \|\mathbf{x}\|_1 \leq k\},$$

as well as its variants. Solving such models may require projection to a polyhedral set such as the ℓ_1-ball $\{\mathbf{x} \in \mathbb{R}^n : \|\mathbf{x}\|_1 \leq 1\}$, which is more expensive than solving subproblems involving minimizing the ℓ_1-norm.

However, there are efficient projection methods [65, 66, 67], as well as algorithms [68, 69] for ℓ_1-constrained sparse-optimization problems.

2.8.2 A list of sparse-optimization algorithms

We list some of the popular sparse optimization algorithms. For detailed descriptions, please refer to Chapter 4 in [70].

(i) **Classic solvers:** The convex sparse-optimization problems can be transformed into equivalent cone programs and solved by off-the-shelf algorithms. However, these algorithms are usually inefficient or even infeasible for large-scale problems.

(ii) **Shrinkage operation:** One common reason that makes many of these algorithms efficient is their use of shrinkage-like operations, which can be computed very efficiently.

(iii) **Prox-linear algorithm:** A prox-linear framework and several algorithms under this framework are based on gradient descent and take advantage of shrinkage-like operations. Duality is a very powerful tool in modern convex optimization; sparse optimization is not an exception.

(iv) **Dual algorithms:** There are a few dual models and algorithms for sparse optimization. One class of dual algorithms is very efficient and extremely versatile, being applicable to nearly all convex sparse-optimization problems; it is based on variable/operator splitting and alternating minimization, which decomposes a difficult problem into a sequence of simple steps.

(v) **(Block) coordinate minimization and gradient descent:** The (block) coordinate descent algorithm has been a popular tool for solving many convex and nonconvex problems in engineering practice. It can be integrated with prox-linear algorithms and is then especially efficient on sparse-optimization problems.

(vi) **Homotopy algorithms and parametric quadratic programming:** Unlike other algorithms, the homotopy algorithms produce not just one solution but a path of solutions; they are not only efficient at producing multiple solutions corresponding to different parameter values, but also especially fast if the solution is extremely sparse.

(vii) **Continuation, varying step sizes, and line search:** All the above algorithms can be (often significantly) accelerated by appropriately setting their step-size parameters that determine the amount of progress at each iteration.

(viii) **Nonconvex approaches for sparse optimization:** Since ℓ_q quasi-norms, $0 < q < 1$, are better approximations to the ℓ_0 "norm" than the ℓ_1-norm, solving nonconvex ℓ_q minimization problems, when the global minimizers are successfully obtained, can give more faithful recoveries than ℓ_1 minimization. That's a big "if"; it can be explained why, in problems with fast-decaying signals, certain smoothing algorithms for ℓ_q minimization can indeed find global minimizers and perform better than ℓ_1 minimization.

(ix) **Greedy algorithms:** Unlike all previous algorithms, greedy algorithms do not necessarily correspond to an optimization model; instead of systematically searching for solutions that minimize objective functions, they build sparse solutions by constructing their supports step by step in a greedy manner. They have very good performance on fast-decaying signals.

(x) **Algorithms for low-rank matrices:** Most of the algorithms and techniques can be extended from sparse-vector recovery to low-rank-matrix recovery. However, for the latter problem, there is also a class of algorithms that are based on decomposing a low-rank matrix into the product of a skinny matrix and a fat one; algorithms in this class require relatively less memory and run very efficiently.

---

[1] We will discuss barrier or interior-point methods in detail in Section 2.4.

3 Game theory

In this chapter, we will discuss the basic concepts of different types of games and illustrate simple examples. The goal is to let the reader understand the basic problems and basic approaches. Since our objective in this book is not to teach game theory, we limit the mathematical details. For the details of game theory, readers can refer to the references [71, 72, 73, 74].

3.1 Basics of game theory

In this section, we will discuss the basic concepts and elements of game theory. Then, we give an example of the prisoner's dilemma to explain the players' behaviors. Furthermore, we classify the games according to different criteria. Next, we study how to write utility functions in wireless networking and resource-allocation problems to represent distributed users' own interests.

A game can be roughly defined as each user adjusts her strategy to optimize her own utility to compete with others. Strategy and utility can be defined as follows.

DEFINITION 9. *A **strategy** r is a complete contingency plan, or a decision rule, that defines the action an agent will select in every distinguishable state* Ω *of the world.*

DEFINITION 10. *In any game, the **utility** (payoff) u represents the motivations of players. Autility function for a given player assigns a number for every*

possible outcome of the game, with the property that a higher (or lower) number implies that the outcome is more preferred.

One of the most common assumptions made in game theory is rationality. In its mildest form, rationality implies that all players are motivated by maximizing their own utilities. In a stricter sense, it implies that every player always maximizes her utility, thus being able to perfectly calculate the probabilistic result of every action. A game can be defined as follows.

DEFINITION 11. *A **game** G in the strategic form has three elements: the set of players $i \in \mathcal{I}$, which is a finite set $\{1, 2, \ldots, N\}$; the strategy space Ω_i for each player i; and a utility function u_i, which measures the outcome of the ith user for each strategy profile $\mathbf{r} = (r_1, r_2, \ldots, r_N)$. We define $\mathbf{r}_{-i}$ as the strategies of player i's opponents, i.e., $r_{-i} = (r_1, \ldots, r_{i-1}, r_{i+1}, \ldots, r_N)$. In static games, the interaction between users occurs only once, while in dynamic games the interaction occurs several times.*

One of the most commonly cited games is called the "prisoner's dilemma." The name comes from a hypothetical situation: Two criminals are arrested for committing a crime in unison, but the police do not have enough proof to convict either. Thus, the police separate the two and offer a deal: If one testifies to convict the other, he will get a reduced sentence or go free. Here the prisoners do not have information about the other's "move" as they would in chess. The payoff if they both say nothing (and thus cooperate with each other) is good, since neither can be convicted without further proof. If one of them betrays but the other remains silent, then he benefits because he goes free while the other is imprisoned because there is sufficient proof to convict the silent one. If they both betray each other, they both get a reduced sentence, which can be described as a null result. The obvious dilemma is the choice between two options, where a good decision cannot be made without information.

This decision in terms of the outcomes of the decisions of the prisoner may be assigned arbitrary point values and described with Table 3.1. The prisoner's dilemma is a two-player game. One player plays as the row player

and the other plays as the column player. Both have the strategy option of cooperating (C) or defecting (D). Thus, there are four possible outcomes to the game: $\{(C, C), (D, D), (C, D), (D, C)\}$. Under mutual cooperation, $\{(C, C)\}$, both players will receive the reward payoff, 3. Under mutual defection, $\{(D, D)\}$, both players receive the punishment of defection, 1. When one player cooperates while the other defects, $\{(C, D), (D, C)\}$, the cooperating player receives the payoff, 0, and the defecting player receives the temptation to defect, 5.

Table 3.1. The prisoner's dilemma

	Cooperate	**Defect**
Cooperate	(3, 3)	(0, 5)
Defect	(5, 0)	(1, 1)

In the "prisoner's dilemma" game, if one player cooperates, the other player will have a better payoff (5 instead of 3) if he/she defects; if one player defects, the other player will still have a better payoff (1 instead of 0) if he/she defects. Regardless of the other players' strategies, the player always selects defect and $\{(D, D)\}$ is an equilibrium. Although cooperation will give each player a better payoff of 3, greediness leads to an inefficient outcome.

Three basic distinctions can be made to classify different games, as follows.

(i) Noncooperative versus cooperative game. In a noncooperative game, an individual player acts to maximize her own payoff, while in a cooperative game, coalitions of players are formed and players have joint actions so as to make mutual benefits.

(ii) Strategic (or normal form) game and extensive (form) game. The normal form is a matrix representation of a simultaneous game. For two players, one is the "row" player, and the other is the "column" player. Each row or column represents a strategy and each box represents the payoffs to each player for every combination of strategies.

The extensive form (also called a game tree) is a graphical representation of a sequential game. It provides information about the players, payoffs, strategies, and the order of moves. The game tree consists of nodes (or vertices), which are points at which players can take actions, connected by edges, which represent the actions that may be taken at that node. An initial (or root) node represents the first decision to be made. Every set of edges from the first node through the tree eventually arrives at a terminal node, representing an end to the game. Each terminal node is labeled with the payoffs earned by each player if the game ends at that node.

(iii) Game with complete or incomplete information. A game is one of complete information if all factors of the game are common knowledge. Specifically, each player is aware of all other players, the timing of the game, and the set of strategies and payoffs for each player.

A sequential game is one of imperfect information if a player does not know exactly what actions other players took up to that point. Technically, there exists at least one information set with more than one node. If every information set contains exactly one node, the game is one of perfect information. Intuitively, if it is my turn to move, I may not know what every other player has done up to now. Therefore, I have to infer from their likely actions and from Bayes' rule which actions likely led to my current decision.

3.2 The noncooperative static game

In this section, we first define the noncooperative static game. Next we study two ways to present a game. Then we give some properties of the game, such as dominance, Nash equilibrium, Pareto optimality, and mix strategies. Some basic examples are employed for illustration. Finally, we discuss the low efficiency of the outcome for noncooperative static games applied to wireless networking and resource-allocation problems. The ideas of two methods, pricing and referee, are briefly discussed to improve the game outcomes.

DEFINITION 12. *A **noncooperative game** is one in which players are unable to make enforceable contracts outside of those specifically modeled in the game. Hence, a noncooperative game is defined not as a game in which players do not cooperate, but as games in which any cooperation must be self-enforcing.*

DEFINITION 13. *A **static game** is one in which all players make decisions (or select a strategy) simultaneously, without knowledge of the strategies that are being chosen by other players. Even though the decisions may be made at different points in time, the game is simultaneous because each player has no information about the decisions of others; thus, it is as if the decisions were made simultaneously.*

3.2.1 The normal form of a static game

Static games can be represented by the normal form defined as follows.

DEFINITION 14. *The **strategic (or normal) form** is a matrix representation of a simultaneous game. For two players, one is the "row" player, and the other is the "column" player. Each row or column represents a strategy and each box represents the payoff to each player for every combination of strategies.*

One example is the "battle of the sexes" shown in Table 3.2 with the following scenario. A husband and wife have agreed to attend a rare entertainment event in the evening. Unfortunately, neither remembers which

of the two special events in town they had agreed on: the boxing match or the opera. The husband prefers the boxing match while the wife prefers the opera; yet, both prefer being together to being apart. They must decide simultaneously and without communication which event to attend. There are two pure strategy equilibria. Different pure strategy equilibria are preferred by each player. However, either equilibrium is preferred by both players to any of the non-equilibrium outcomes.

Table 3.2. The battle of the sexes: (wife, husband)

	Boxing	**Opera**
Boxing	(1, 2)	(0, 0)
Opera	(0, 0)	(2, 1)

For each user, there are some strategy spaces. Some of the strategies are superior to the others for the user's interests. To define such superiority, we have the following two definitions.

DEFINITION 15. ***Dominant strategies****: A strategy is dominant if, regardless of what any other players do, the strategy earns a player a larger payoff than any other. Hence, a strategy is dominant if it is always better than any other strategy, regardless of what opponents may do. If a player has a dominant strategy then he or she will always play it in equilibrium. Also, if one strategy is dominant, than all others are dominated.*

DEFINITION 16. ***Dominated strategies****: A strategy is dominated if, regardless of what any other players do, the strategy earns a player a smaller payoff than a certain other strategy. Hence, a strategy is dominated if it is always better to play some other strategy, regardless of what opponents may do. A dominated strategy is never played in equilibrium.*

For example, in the prisoner's dilemma in Table 3.1, each player has a dominated strategy of cooperation and a dominant strategy of defection. This is because, no matter what other players' strategies are, for each user defection always yields a higher utility. Notice that here domination does not imply higher payoff. In this case, the dominated strategy for both players has a better payoff than that of the dominating strategy.

3.2.2 *Nash equilibrium, Pareto optimality, and mixed strategy*

To analyze the outcome of the game, one can use the Nash equilibrium, named after John Nash, which is a well-known concept that states that in the equilibrium every agent will select a utility-maximizing strategy given the strategies of every other agent.

DEFINITION 17. *Define a strategy vector* $\mathbf{r} = [r_1 \dots r_K]$ *and define the strategy vector of the* ith *player's opponents as* $\mathbf{r}_i^{-1} = [r_1 \dots r_{i-1}\ r_{i+1} \dots r_K]$, *where K is the number of users and* r_i *is the* ith *user's strategy.* U_i *is the* ith *user's utility.The* ***Nash-equilibrium*** *point* $\mathbf{r}$ *is defined as*

$$u_i(r_i, \mathbf{r}_i^{-1}) \geq u_i(\tilde{r}_i, \mathbf{r}_i^{-1}),\ \forall i,\ \forall \tilde{r}_i \in \Omega,\ \mathbf{r}_i^{-1} \in \Omega^{K-1}; \tag{3.1}$$

i.e., given the other users' strategies, no user can increase her utility alone by changing her own strategy.

In other words, a Nash equilibrium is a set of strategies, one for each player, such that no player has an incentive to unilaterally change her action. Players are in an equilibrium if a change in strategy by any one of them will lead that player to earn less than if she sticks to her current strategy.

The existence of the Nash equilibrium could sometimes be hard to prove. There are some existing theorems to show its existence. We only need to prove that the proposed game satisfies the requirements of the theorems. For example, in [71], it has been shown that a Nash-equilibrium point (NEP) exists, if $\forall i$

(i) Ω, the support domain of $u_i(\mathbf{r}_i)$, is a nonempty, convex, and compact subset of a certain Euclidean space $\Re^L$; and

(ii) $u_i(\mathbf{r}_i)$ is continuous in $\mathbf{r}_j$ and quasi-convex in $\mathbf{r}_j$.

There might be an infinite number of Nash equilibria. Among all these equilibria, we need to select the optimal one. There are many criteria by which to judge whether the equilibrium is optimal or not. Among these criteria, Pareto optimality is one of the most important ones.

DEFINITION 18. ***Pareto optimality***: *Pareto optimality, named after Vilfredo Pareto, is a measure of efficiency. An outcome of a game is Pareto optimal if there is no other outcome that makes every player at least as well off and at least one player strictly better off. That is, a Pareto-optimal outcome cannot be improved upon without hurting at least one player. Often, a Nash equilibrium is not Pareto optimal, implying that the players' payoffs can all be increased.*

Until now, we have discussed only strategy that is deterministic or pure. A pure strategy defines a specific move or action that a player will follow in every possible attainable situation in a game. Such moves need not be random, or drawn from a distribution, as in the case of mixed strategies.

DEFINITION 19. ***Mixed strategy***: *A strategy consists of possible moves and a probability distribution (collection of weights) that corresponds to how frequently each move is played. A player will use a mixed strategy only when she is indifferent about several pure strategies. Moreover, if the opponent can benefit from knowing the next move, the mixed strategy is preferred since keeping the opponent guessing is desirable.*

To illustrate the idea of Pareto optimality and mixed strategy, we give an example of the "game of chicken" shown in Table 3.3 (it is also called a hawk–dove game). The scenario is as follows. Two hooligans with something to prove drive at each other on a narrow road. The first to swerve loses face among his peers. If neither swerves, however, a terminal fate

plagues both. There are two pure strategy equilibria. A different pure strategy equilibrium is preferred by each player. Both equilibria, $(1, -1)$ and $(-1, 1)$, are Pareto optimal. A mixed-strategy equilibrium also exists, where each user plays swerve with probability 0.99 and plays stay with probability 0.01.

Table 3.3. Chicken: (driver1, driver2)

	Stay	**Swerve**
Stay	$(-100, -100)$	$(1, -1)$
Swerve	$(-1, 1)$	$(0, 0)$

A zero-sum game is a special case of a constant sum game in which all outcomes involve a sum of all players' payoffs of 0. Hence, a gain for one participant is always at the expense of another, such as in most sporting events. Therefore, one of the strategies to gain benefit for oneself is to suppress the other's play. Given the conflicting interests, the equilibrium of such games is often in mixed strategies.

One example of a zero-sum game is the game of "matching pennies" shown in Table 3.4. The scenario determines who is required to do the nightly chores. Two children first select who will be represented by "same" and who will be represented by "different." Then, each child conceals in her palm a penny either with its face up or with its face down. The two coins are revealed simultaneously. If they match (both are heads or both are tails), the child who claims "same" wins. If they are different (one heads and one tails), the child who claims "different" wins. The game is equivalent to "odds or evens" and quite similar to a three-strategy version – rock, paper, scissors. The game is zero sum. The only equilibrium is in mixed strategies. Each plays each strategy with equal probability, resulting in an expected payoff of zero for each player.

Table 3.4. Matching pennies: (different, same)

	Heads	Tails
Heads	$(-1, 1)$	$(1, -1)$
Tails	$(1, -1)$	$(-1, 1)$

Unfortunately, the Nash equilibria of noncooperative static games often have low efficiency. For example, in the prisoner's dilemma example in Table 3.1, if one player cooperates, the other player will have a better payoff, 5, than 3 if he/she defects; if one player defects, the other player will still have better payoff, 1, than 0 if he/she defects. Therefore, regardless of the other players' strategies, the player always selects defect and $\{(D, D)\}$ is a Nash equilibrium. Although cooperation will give each player a better payoff of 3, greediness leads to an inefficient outcome, so the outcome of the noncooperative static game can be less efficient. There are many schemes to overcome this low efficiency in the literature. In the following, we give two examples, namely pricing and referee-based approaches.

3.2.3 Social optimum: price of anarchy and referee

Since the individual user has no incentive to cooperate with the other users in the system and imposes harm on the other users' resources, the outcome of the game might not be optimal from the system point of view. Traditionally, the social optimum is calculated by assuming there is a genie that can tell the complete information of the networks. Then the social optimum is calculated using the optimization techniques which were discussed in the previous chapter. The resulting socially optimal solutions are compared with the game outcomes. Next, we study two techniques that can improve the game outcomes to approach the socially optimal solutions.

To approach the socially optimal solution, pricing (or taxation) has been used as an effective tool both by economists and by researchers in computer networks. The pricing technique is motivated by the following two objectives.

(i) The revenue for the system is optimized.

(ii) Cooperation for resource usage is encouraged.

An efficient pricing mechanism can make the distributed decisions compatible with the system efficiency obtained by centralized control. A pricing policy is called *incentive compatible* if pricing enforces a Nash equilibrium that achieves the system optimum. In [75, 76], a policy based on usage-based pricing is proposed, where the price a user pays for using the resources is proportional to the amount of resources consumed by the user.

Second, the basic idea for the referee-based scheme is to introduce a referee for the noncooperative game. The game may have multiple Nash equilibria. A referee is in charge of detecting these less efficient Nash equilibria and then changes the game rule to prevent the players from falling into undesirable game outcomes. It is worth mentioning that the noncooperative game is still played in a distributive way. The referee intervenes only when it is necessary. In [77, 78], the above idea is applied to a multicell orthogonal frequency-division multiple access (OFDMA) network to have an efficient distributed resource allocation.

3.3 The dynamic game

When players interact by playing a similar stage game numerous times, the game is called a dynamic, or repeated, game. Unlike in simultaneous games, players have at least some information about the strategies chosen by others and thus their play may be contingent on past moves. Cooperation among autonomous users can be encouraged by considering the long-term benefit and threat from others. In this section, we first describe how to represent a dynamic game. Then, we discuss the information available to the players. We further study the properties of the dynamic games. Next, two practical strategies, tit-for-tat and cartel maintenance, are proposed using a repeated game. Then, a special kind of game, a stochastic game (Markov game), is investigated. Finally, we discuss the concept of a differential control/game.

3.3.1 Sequential games, and games in extensive form

First, we define the concept of a sequential game as follows.

DEFINITION 20. *A **sequential game** is one in which players make decisions (or select a strategy) following a certain predefined order, and in which at least some players can observe the moves of players who preceded them. If no players observe the moves of previous players, then the game is simultaneous. If every player observes the moves of every other player who has gone before her, the game is one of perfect information. If some (but not all) players observe prior moves, while others move simultaneously, the game is one of imperfect information.*

For the information to a game, there are three concepts.

DEFINITION 21. *A game is one of **complete information** if all factors of the game are common knowledge. Specifically, each player is aware of all other players, the timing of the game, and the set of strategies and payoffs for each player.*

DEFINITION 22. *A sequential game is one of **perfect information** if only one player moves at a time and if each player knows every action of the players who moved before him at every point. Technically, every information set contains exactly one node. Intuitively, if it is my turn to move, I always know what every other player has done up to that point. All other games are of imperfect information.*

DEFINITION 23. *A sequential game is one of **imperfect information** if a player does not know exactly what actions other players took up to that point. Technically, there exists at least one information set with more than one node. If every information set contains exactly one node, the game is one of perfect information. Intuitively, if it is my turn to move, I may not know what every other player has done up to now. Therefore, I have to infer from their likely actions and from Bayes' rule which actions likely led to my current decision.*

Sequential games are represented by game trees (the extensive form).

DEFINITION 24. *A **game tree** (also called the **extensive form**) is a graphical representation of a sequential game. It provides information about the players, payoffs, strategies, and the order of moves. The game tree consists of nodes, which are points at which players can take actions, connected by vertices, which represent the actions that may be taken at that node. An initial (or root) node represents the first decision to make. Every set of vertices from the first node through the tree eventually arrives at a terminal node, representing an end to the game. Each terminal node is labeled with the payoffs earned by each player if the game ends at that node.*

To illustrate the idea, one example is shown in Figure 3.1. The game has two players: 1 and 2. The numbers by every non-terminal node indicate to which player that decision node belongs. The numbers by every terminal node represent the payoffs to the players (e.g., 2, 1 represents a payoff of 2 to player 1 and a payoff of 1 to player 2). The labels by every edge of the graph are the name of the action which that edge represents.

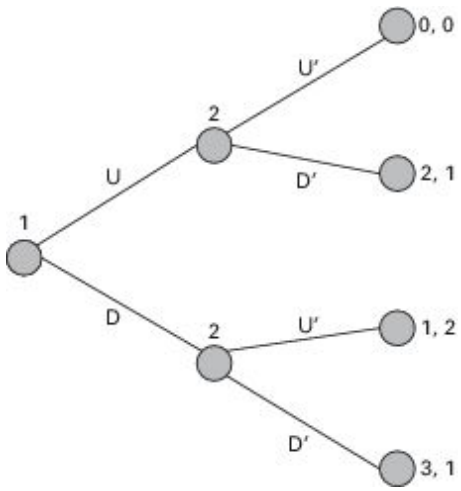

Figure 3.1. An example of a game in extensive form (game tree).

The initial node belongs to player 1, indicating that that player moves first. According to the tree, the game is played as follows: Player 1 chooses between U and D; player 2 observes player 1's choice and then chooses

between U′ and D′. The payoffs are as specified in the tree. There are four outcomes represented by the four terminal nodes of the tree: (U, U′), (U, D′), (D, U′), and (U, U′). The payoffs associated with each outcome, respectively, are as follows: (0, 0), (2, 1), (1, 2), and (3, 1).

Sequential games can be solved using the concept of subgame-perfect equilibrium.

DEFINITION 25. *A **subgame-perfect** Nash equilibrium is an equilibrium such that the players' strategies constitute a Nash equilibrium in every subgame of the original game. It may be found by backward induction, an iterative process for solving finite extensive-form or sequential games. First, one determines the optimal strategy of the player who makes the last move of the game. Then, the optimal action of the next-to-last-moving player is determined taking the last player's action as given. The process continues backwards in time until all players' actions have been determined.*

In the example shown in Figure 3.1, if player 1 plays D, player 2 will play U′ to maximize her payoff and so player 1 will receive a payoff of only 1. However, if player 1 plays U, player 2 maximizes her payoff by playing D′ and player 1 receives a payoff of 2. Player 1 prefers 2 to 1 and so will play U and player 2 will play D′. This is the subgame-perfect equilibrium.

Subgame-perfect equilibria eliminate noncredible threats. A noncredible threat is a threat made by a player in a sequential game that will not be in the best interest for the player to carry out. The hope is that the threat is believed in which case there is no need to carry it out. Even though Nash equilibria may depend on noncredible threats, backward induction eliminates them.

3.3.2 Repeated games

For repeated games, the technical definition can be written as follows.

DEFINITION 26. *Let G be a static game and let β be a discount factor. The T-period **repeated game**, denoted as $G(T, \beta)$, consists of game G repeated T*

times. The payoff for such a game is given by

$$V_i = \sum_{t=1}^{T} \beta^{t-1} \pi_i^t, \tag{3.2}$$

where π_i^t denotes the payoff to player i in period t. If T goes to infinity, then $G(\infty, \beta)$ is referred to as the infinitely repeated game. In this paper, we employ the infinitely repeated game.

From the folk theorem stated below, we know that, in an infinitely repeated game, any feasible outcome that gives each player a better payoff than the Nash equilibrium can be obtained.

THEOREM 4. *Folk theorem: Let $(e_1, \ldots, e_n)$ be the payoffs from a Nash equilibrium of G and let $(x_1, \ldots, x_n)$ be any feasible payoffs from G. If $x_i > e_i$ for every player i, then there exists an equilibrium (it is also subgame-perfect) of $G(\infty, \beta)$ that attains $(x_1, \ldots, x_n)$ as the average payoff, provided that β is sufficiently close to 1.*

Now we know that, by using the repeated game, any feasible payoffs better than the Nash equilibrium can be obtained. The reason is that, with enough patience, a player's noncooperative behavior will be punished by the future revenge from other cooperative users, or, on the other hand, a player's cooperation can be rewarded in the future by others' cooperation. The remaining problem is how to define a good rule to achieve these better payoffs by enforcing cooperation among users. In what follows, we propose two approaches, namely tit-for-tat and cartel maintenance.

Tit-for-tat is a type of trigger strategy in which a player responds in one period with the same action as that which her opponent used in the last period. Many research works have used this method [79, 80]. The advantage of tit-for-tat is that it is easy to implement. However, there are some potential problems. The best response of a user is not the same action as that of the other opponent. The information on others' actions is hard to obtain.

All these limit the possible applications for tit-for-tat. There are many less harsh and more optimal variations of trigger strategies than tit-for-tat. One of the optimal design criteria is cartel maintenance [81].

The basic idea for the cartel maintenance repeated-game framework is to provide enough of a threat to greedy users so as to prevent them from deviating from cooperation. First, the cooperative point is obtained so that all users have better performances than those corresponding to noncooperative NEPs. However, if any user deviates from cooperation while others still play cooperatively, this deviating user has a better utility, while others have relatively worse utilities. If no rule is employed, the cooperative users will also have incentives to deviate. Consequently, non-cooperation results in inefficient performances. The cartel-maintenance framework provides a mechanism so that the current defecting gains of the selfish user will be outweighed by future punishment strategies from other users. For any rational user, this threat of punishment prevents them from deviation, so the cooperation is enforced.

The proposed trigger strategy is a strategy to introduce punishment on the defecting users. In the trigger strategy, the players start with cooperation. Assume each user can observe the public information (e.g., the outcome of the game), P_t at time t. Examples of this public information can be the successful-transmission rate and network throughput. Notice that such public information is mostly imperfect or simply partial information about the users' strategies. Here we assume a larger P_t stands for a higher cooperation level, resulting in higher performances for all users. Let the cooperation strategies be $\bar{\lambda} = [\lambda_1, \lambda_2, \ldots, \lambda_N]^{\mathsf{T}}$ and the noncooperative strategies be $\bar{s} = [s_1, s_2, \ldots, s_N]^{\mathsf{T}}$, respectively. The trigger–punishment game rule is characterized by three parameters: the optimal punishment time T, the trigger threshold P^*, and the cooperation strategy $\bar{\lambda}$. The trigger–punishment strategy $(\bar{\lambda}, P^*, T)$ for distributed user i is given as follows.

(i) User i plays the strategy of the cooperation phase, $\bar{\lambda}$, in period 0.

(ii) If the cooperation phase is played in period t and $P_t > P^*$, user i plays the cooperation phase in period $t + 1$.

(iii) If the cooperation phase is played in period t and $P_t < P^*$, user i switches to a punishment phase for $T - 1$ periods, in which the players play a static Nash equilibrium $\bar{s}$ regardless of the outcomes realized. At the Tth period, the play returns to the cooperative phase.

Note that $\bar{s}$ generates the non-cooperation outcome, which is much worse than that generated by the cooperation strategy $\bar{\lambda}$. Therefore, the selfish users who deviate will have much lower utilities in the punishment phase. Moreover, the punishment time T is designed to be long enough to let all cheating gains of the selfish users be outweighed by the punishment. Therefore, users have no incentive to deviate from cooperation, since the users aim to maximize the long-run payoffs over time.

The rest of the problem is how to calculate the optimal parameters of $(\bar{\lambda}, P^*, T)$, i.e., how to construct a cartel so that the benefit is optimized and the incentive for deviation is eliminated. We define $\mathcal{P}_{\text{trig}} = \Pr(P_t < P^*)$, which is the trigger probability that the realization of public information is less than the trigger threshold. If we discuss the different future situations in (3.2), the expected payoff V_i is given as follows:

$$V_i(\bar{\lambda}, P^*, T) = \pi_i(\bar{\lambda}) + (1 - \mathcal{P}_{\text{trig}})\beta V_i(\bar{\lambda}, P^*, T) + \mathcal{P}_{\text{trig}} \left[\sum_{t=1}^{T-1} \beta^t \pi_i(\bar{s}) + \beta^T V_i(\bar{\lambda}, P^*, T) \right], \forall i, \tag{3.3}$$

where $\pi_i(\bar{\lambda})$ and $\pi_i(\bar{s})$ are the cooperation and non-cooperation payoffs, respectively. The first term at the right-hand side of (3.4) is the current expected payoff if cooperation is played; the second and third terms are the payoffs for two different results, depending on whether or not the punishment is triggered, respectively. Notice that V_i is a function not only of users' strategies $\bar{\lambda}$ but also of the game parameters P^* and T. Our objective is to maximize the expected payoff V_i for each user while the optimal strategy yields an NEP for the proposed algorithm. In order to achieve the

NEP given P^* and T, the optimal strategies of the repeated games can also be characterized by the following first-order necessary conditions:

$$\frac{\partial V_i(\lambda_i, \lambda_{-i})}{\partial \lambda_i} = 0, \forall i. \tag{3.4}$$

If all users have the same utility and the game outcome is symmetric for all users, the solution λ^* of the first-order conditions is the same for all users. This solution is also a function of parameters P^* and T. In order to obtain the optimal P^* and T for maximizing the expected payoff V_i, we have the following differential equations:

$$\frac{\partial V_i(P^*, T)}{\partial P^*} = 0, \quad \frac{\partial V_i(P^*, T)}{\partial T} = 0, \forall i. \tag{3.5}$$

In general, (3.4) and (3.5) need to be solved via numerical methods. For a certain structure of the payoff function, the closed-form optimal configuration $\{\bar{\lambda}, P^*, T\}$ may be derived.

3.3.3 Stochastic games

In game theory, a stochastic game is a dynamic, competitive game with probabilistic transitions played by one or more players. The game is played in a sequence of stages. At the beginning of each stage the game is in some state. The players select actions and each player receives a payoff that depends on the current state and the chosen actions. The game then moves to a new random state whose distribution depends on the previous state and the actions chosen by the players. The procedure is repeated at the new state and play continues for a finite or infinite number of stages. The total payoff to a player is often taken to be the discounted sum of the stage payoffs or the limit inferior of the averages of the stage payoffs. Notice that the one-state stochastic game is equal to an (infinitely) repeated game, and the one-agent stochastic game is equal to a Markov decision process (MDP). The formal definition is as follows.

DEFINITION 27. *An N-person stochastic game G consists of a finite, nonempty set of states S, N players, a finite set of actions set A_i for the players, a conditional probability distribution p on $S \times (A_1 \times A_2 \times \cdots \times A_N)$ called the law of motion, and bounded real-valued payoff functions U_i defined on the history space $H = S \times A \times S \times A \ldots$, where $A = A_1 \times A_2 \times \cdots \times A_N$. The game is called an N-player deterministic game if for all states $s \in S$ and action choices $a = (a^1, a^2, \ldots, a^N)$ there is a unique state s' such that $p(s'|s, a) = 1$.*

If there is a finite number of players and the action sets and the set of states are finite, then a stochastic game with a finite number of stages always has a Nash equilibrium. The same is true for a game with infinitely many stages if the total payoff is the discounted sum. Vieille [82] has shown that all two-person stochastic games with finite state and action spaces have approximate Nash equilibrium when the total payoff is the limit inferior of the averages of the stage payoffs. Whether such equilibria exist when there are more than two players is an open question. Shapley proposed an algorithm [83] for two-player zero-sum stochastic games using value iteration.

Stochastic games were invented by Lloyd Shapley [83] in the early 1950s. One complete reference is the book of articles edited by Neyman and Sorin [84]. The more elementary book by Filar and Vrieze [85] provides a unified rigorous treatment of the theories of MDPs and two-person stochastic games. They coin the term competitive MDPs to encompass both one- and two-player stochastic games. Stochastic games have applications in economics and evolutionary biology. In wireless networking, stochastic games have been investigated in the areas such as flow control, routing, and scheduling [86, 87].

3.3.4 *Differential control/games*

We consider a game that does not take place instantaneously but over a whole interval of time. This leads to the study of dynamic games. The study of differential games as a special class of dynamic games was initiated by

Rufus Isaacs in the early 1950s. Basically a differential game is a mathematical model designed to solve a conflicting situation that changes with time. In differential games, there is more than one player, with each player having separate objective functions that he or she is trying to maximize subject to a set of differential equations that model the dynamic nature of the system [88].

A differential game is an extension of static noncooperative game theory by adopting the methods and models developed in optimal control theory. Optimal control theory was developed to study the optimal solution of the optimization problem for a dynamic system (i.e., the state evolves over time). Therefore, optimal control can be applied to game theory to obtain the equilibrium solution for rational entities with different objective or payoff functions. One major approach employed to solve for optimal solutions in optimal control theory is dynamic programming. This approach has been adopted in differential games in which the payoff of a player depends on the state (i.e., constrained by the state), which evolves over time. The common solution concepts of differential games are Nash equilibrium and Stackelberg solution for non-hierarchical and hierarchical structures, respectively. Using techniques in optimal control theory, these solutions can be obtained [89].

The differential optimal control problem

In optimal control, each player has an optimization problem with a single objective (e.g., to maximize payoff) over a period of time. This optimization problem considers the actions of the other players to be fixed at the equilibrium.

In the standard model of control theory, the state of a system is described by a variable x. This state evolves in time, according to an ordinary differential equation (ODE) [90]:

$$\begin{aligned} \dot{x}(t) &= f(x(t), u(t)) + \rho w, \\ x(0) &= x^0, \end{aligned} \tag{3.6}$$

where w is a control function. A basic problem in optimal control is to find a control function that maximizes the payoff:

$$L[u(\cdot)] = \int_0^T g(x(t), u(t))dt + h(x(T)), \tag{3.7}$$

where h is a terminal payoff, while g accounts for a running payoff.

Differential games

Differential games are the extension of the basic optimal control problem to the situation where more than one player participates in the game, and each of them tries to maximize her own pay. The system state x evolves through time according to the following ODE:

$$\begin{aligned} \dot{x}(t) &= f(x(t), u_1(t), \ldots, u_i, \ldots, u_N), \\ x(0) &= x^0, \end{aligned} \tag{3.8}$$

where u_i is the control function of player i and N is the total number of players. Player i chooses her control function in a way that maximizes its payoff:

$$L_i[u(\cdot)] = \int_0^T g_i(x(t), u(t))dt + h_i(x(T)). \tag{3.9}$$

The analysis of differential games relies heavily on the concepts and techniques of optimal control theory. Equilibrium strategies in feedback form are best studied by looking at a Hamilton–Jacobi–Bellman (HJB) system for the value functions of the various players, derived from the principle of dynamic programming. Dynamic programming is based on the principle of optimality. With this principle, an optimal action has the property that, whatever the initial state and time are, all remaining decisions must also constitute an optimal action. To realize this principle, the solution

can be obtained backwards in time. That is, we start at all possible final states with the corresponding final times (e.g., stages). The optimal action at this final time is selected, then we proceed back one step in time and determine the optimal action again. This step is repeated until the initial time or stage is reached. The core of dynamic programming when it is applied to continuous-time optimal control is the HJB partial differential equation (PDE).

In order to derive the optimal control functions for each player using dynamic programming, first the value functions should be defined as follows:

$$v_i(x,t) = \max_{u(\cdot)} L_i[u(\cdot)], \tag{3.10}$$

and

$$v_i(x,t) = h_i(x). \tag{3.11}$$

For players to play the game, the available information is required. In differential games, there are three cases of available information.

- Open-loop information: With open-loop action, the players have common knowledge of the values of state variables at the initial time $t = 0$. At this initial state, each player chooses the control variable path by taking into account the expected behavior of all other players. All players commit themselves to their action paths before the game starts.
- Closed-loop information: With closed-loop information, players are assumed to know the values of state variables from time 0 to t, i.e., [0, t) without delay.
- Feedback information: At time t, players are assumed to know the values of state variables at time $t - \epsilon$, where ε is positive and arbitrarily small. The information set at time t can be estimated from the vector of values of state variables of all players at time $t - \epsilon$.

At this stage, a natural assumption is that the strategies adopted by players have the feedback form: $u_i = u_i^*(x^*)$; in other words, they depend only on the current state of the system, not on the past history. For a Nash noncooperative solution in feedback form, one can show that the value functions, V_i, satisfy HJB equations derived from the principle of dynamic programming.

THEOREM 5. *The optimal solutions u_i^*, $i = 1, \ldots, N$ lead to a feedback Nash-equilibrium solution to the game, and $x^*(t)$ is the corresponding state trajectory, if there exist suitably smooth functions V_i satisfying the following rectilinear parabolic partial differential equations [89]:*

$$-\frac{\partial v_i(x,t)}{\partial t} = \max_{u_i(t,x)} \left\{ \frac{\partial^2 v_i(x,t)}{\partial x^2} + \frac{\partial v_i(x,t)}{\partial x} f[t, x, U_i, U_{j\neq i}^*] + g_i[t, x, u_i, u_{j\neq i}^*] \right\}. \tag{3.12}$$

The HJB equation is usually solved backward in time, starting from $t = T$ and ending at $t = 0$. In the general case, the HJB equation does not have a classical (smooth) solution. Several notions of generalized solutions have been developed to cover such situations, including viscosity solution [91] and minimax solution [92]. For the special case of an affine-linear quadratic game, the value function has a unique solution that should satisfy a set of first-order differential equations. The closed-form solution for the optimal action can be obtained for this special case.

Stochastic differential games

A stochastic formulation for dynamic games defined in continuous time of prescribed duration involves a stochastic differential equation that describes the evolution of the state as follows:

$$\begin{aligned} \dot{x}(t) &= f(x(t), u_1(t), \ldots, u_i, \ldots, u_N) + \rho w, \\ x(0) &= x^0, \end{aligned} \tag{3.13}$$

where w represents random fluctuations modeled as Gaussian noise with zero mean and variance σ^2. The value functions of players for the stochastic scenario can be written as

$$v_i(x,t) = \max_{u_i(t)} L_i = E_w \left\{ \int_0^T g_i(t)dt + h_i[x(T)] \right\}. \tag{3.14}$$

Finally, the optimal control functions can be obtained using stochastic HJB equations as follows:

$$-\frac{\partial v_i(x,t)}{\partial t} = \max_{u_i(t)} \left\{ \frac{(\rho)^2\sigma^2}{2} \frac{\partial^2 v_i(x,t)}{\partial x^2} + \frac{\partial v_i(x,t)}{\partial x} f[t,x,u_i(t)] + g_i[t,x,u_i(t)] \right\}. \tag{3.15}$$

For the special case of a quadratic payoff function, the closed-form solutions can be derived. For this case, the standard form of the game can be written as follows [93]:

$$\begin{aligned} \dot{x} &= f[x(t), u_1(t), \ldots, u_N] + \rho w \\ &= Ax(t) + B_1 u_1(t) + B_2 u_2(t) + \cdots + B_N u_N(t) + C + \rho w. \end{aligned} \tag{3.16}$$

The affine-quadratic cost function can be rewritten as follows:

$$g_i = \frac{1}{2} Q x^2 + R {u_i}^2 + N, \tag{3.17}$$

$$h_i = \frac{1}{2} Q^f x^2. \tag{3.18}$$

Finally, for the value function, we have

$$v_i(x,t) = \max_{u_i(t)} L$$
$$= \max_{u_i(t)} E_w \left\{ \int_0^T \mu[x(t), u_i(t)(t)]dt + h[x(T)] \right\}. \tag{3.19}$$

According to [89], the value function for an affine-linear quadratic problem has a unique solution for $v_i(t)$:

$$v_i[t] = \frac{1}{2} T_i(t) X(t)^2 + x(t)\zeta_i(t) + \xi_i(t) + m_i(t), \tag{3.20}$$

where $T_i(t)$ satisfies the following Riccati differential equations:

$$\frac{dT_i}{dt} + 2T_i F_i + Q_i + \frac{T_i^2 B_i^2}{R_i} = 0, \tag{3.21}$$

$$T_i(T) = Q_i^f, \tag{3.22}$$

and

$$F_i = A - \frac{T_i {B_i}^2}{R_i}. \tag{3.23}$$

ζ_i and m_i can be obtained from the following differential equations:

$$\frac{d\zeta_i}{dt} + \frac{F_i\zeta_i + T_i\zeta_i {B_i}^2}{R_i} + T_i B_i = 0, \tag{3.24}$$

$$\zeta_i(T) = 0, \tag{3.25}$$

$$\frac{dm_i}{dt} + \alpha_i \zeta_i + \frac{\zeta_i^2 B_i^2}{2R_i} = 0, \tag{3.26}$$

$$m_i(T) = 0, \tag{3.27}$$

$$\alpha_i = C - \frac{\zeta_i B_i^2}{R_i}. \tag{3.28}$$

Finally, the ξ_i statistics are given by the equation.

$$\frac{d\xi_i}{dt} = -\frac{R_i \sigma^2 u_i}{2}. \tag{3.29}$$

The optimal control variable can be obtained as follows:

$$u_i^* = -\frac{B_i}{R_i}\frac{\partial v_i}{\partial x} = -\frac{B_i(T_i x + \zeta_i)}{R_i}. \tag{3.30}$$

The optimal control function constitutes a feedback Nash equilibrium for the stochastic differential game.

3.4 Cooperative game theory – bargaining games

A cooperative game is one in which players are able to make enforceable contracts. Hence, it is not defined as the game in which players actually do cooperate, but as games in which any cooperation is enforceable by an outside party (e.g., a judge and police). There are two major components of cooperative game theory: the bargaining solution and coalition concepts. We will discuss bargaining games in this section and coalition concepts in the next section.

The bargaining problem of cooperative game theory can be described as follows [72, 76, 94]:

DEFINITION 28. *Let* $N = \{1, 2, \ldots, N\}$ *be the set of players. Let* S *be a closed and convex subset of* $\Re^N$ *to represent the set of feasible payoff allocations that the players can get if they all work together. Let* $u^i_{\min}$ *be the minimal payoff that the* i*th player will expect; otherwise, she will not cooperate. Suppose* $\{u_i \in \mathbf{S} | u_i \geq u^i_{\min}, \forall i \in N\}$ *is a nonempty bounded set. Define* $\mathbf{u}_{\min} = (u^1_{\min}, \ldots, u^N_{\min})$*, then the pair* $(\mathbf{S}, \mathbf{u}_{\min})$ *is called an N-person bargaining problem.*

Within the feasible set **S**, we define the notion of Pareto optimality as a selection criterion for the bargaining solutions.

DEFINITION 29. *The point* $(u_1, \ldots u_N)$ *is said to be* ***Pareto optimal****, if and only if there is no other allocation* u'_i *such that* $u'_i \geq u_i, \forall i$*, and* $u'_i > u_i, \exists i$*, i.e., there exists no other allocation that leads to superior performance for some users without inferior performance for some other users.*

Next, we first discuss some bargaining solution. Then several examples are illustrated.

3.4.1 Bargaining solutions

There might be an infinite number of Pareto optimal points. We need further criteria to select a bargaining result. A possible criterion is the fairness. One commonly used fairness criterion for wireless resource allocation is max–min [95], where the performance of the user with the worst channel conditions is maximized. This criterion penalizes the users with good channels and as a result generates inferior overall system performance. Here, we first introduce the concept of fairness in the Nash bargaining solution (NBS) [72]. The intuitive idea is that, after the minimal requirements have been satisfied for all users, the rest of the resources are allocated proportionally to users according to their conditions. There exist many kinds

of bargaining solution [72]. Among them, the NBS provides a unique and fair Pareto-optimal operation point under the following conditions.

DEFINITION 30. $\bar{\mathbf{u}}$ *is said to be an NBS in* S *for* $\mathbf{u}_{\min}$, *i.e.,* $\bar{\mathbf{u}} = \phi(\mathbf{S}, \mathbf{u}_{\min})$, *if the following axioms are satisfied.*

(i) *Individual rationality:* $\bar{u}_i \geq u^i_{\min}, \forall i$.

(ii) *Feasibility:* $\bar{\mathbf{u}} \in \mathbf{S}$.

(iii) *Pareto optimality: For every* $\hat{\mathbf{u}} \in \mathbf{S}$, *if* $u_i \geq \bar{u}_i, \forall i$, *then* $\hat{u}_i = \bar{u}_i, \forall i$.

(iv) *Independence of irrelevant alternatives: If* $\bar{\mathbf{u}} \in \mathbf{S}' \subset \mathbf{S}$, $\bar{\mathbf{u}} = \phi(\mathbf{S}, \mathbf{u}_{\min})$, *then* $\bar{\mathbf{u}} = \phi(\mathbf{S}', \mathbf{u}_{\min})$.

(v) *Independence of linear transformations: For any linear scale transformation* ψ, $\psi(\phi(\mathbf{S}, \mathbf{u}_{\min})) = \phi(\psi(\mathbf{S}), \psi(\mathbf{u}_{\min}))$.

(vi) *Symmetry: If* S *is invariant under all exchanges of agents,* $\phi_j(\mathbf{S}, \mathbf{u}_{\min}) = \phi_{j'}(\mathbf{S}, \mathbf{u}_{\min}), \ \forall j, j'$.

Axioms (iv)–(vi) are called axioms of fairness. The irrelevant alternative axiom asserts that eliminating the feasible solutions that would not have been chosen shall not affect the NBS solution. Axiom (v) asserts that the bargaining solution is scale-invariant. The symmetry axiom asserts that, if the feasible ranges for all users are completely symmetric, then all users have the same solution.

The following optimization has been shown to have the NBS that satisfies the above axioms [72].

THEOREM 6. *Existence of NBS: There is a solution function* $\phi(\mathbf{S}, \mathbf{u}_{\min})$ *that satisfies all six axioms in Definition 30. This solution satisfies*

$$\phi(\mathbf{S}, \mathbf{u}_{\min}) \in \arg \max_{\bar{\mathbf{u}} \in \mathbf{S}, \bar{u}_i \geq u^i_{\min}, \forall i} \prod_{i=1}^{N} \left(\bar{u}_i - u^i_{\min}\right). \tag{3.31}$$

Two other bargaining solutions have been proposed as alternatives to the NBS – the Kalai–Smorodinsky solution (KSS) [71] and the egalitarian solution (ES). To define these solutions, we need to introduce the following definition.

DEFINITION 31. *Restricted monotonicity: If* $\mathcal{U} \subset \mathcal{V}$ *and* $H(\mathcal{U}, \mathbf{u}_{\min}) = H(\mathcal{V}, \mathbf{u}_{\min})$ *then* $\phi(\mathcal{U}, \mathbf{u}_{\min}) \geq \phi(\mathcal{V}, \mathbf{u}_{\min})$*, where* $H(\mathcal{U}, \mathbf{u}_{\min})$*, called the* utopia point*, is defined as*

$$H(\mathcal{U}, \mathbf{u}_{\min}) = \left[\max_{\mathbf{u} > \mathbf{u}_{\min}} u_1(\mathbf{u}) \quad \max_{\mathbf{u} > \mathbf{u}_{\min}} u_2(\mathbf{u})\right]. \tag{3.32}$$

DEFINITION 32. *Kalai–Smorodinsky solution: Let* Λ *be a set of points on the line containing* $\mathbf{u}_{\min}$ *and* $H(\mathcal{U}, \mathbf{u}_{\min})$*.* $\phi(\mathcal{U}, \mathbf{u}_{\min})$ *is the KSS, which can be expressed as*

$$\phi(\mathcal{U}, \mathbf{u}_{\min}) = \max \left\{\mathbf{u} > \mathbf{u}_{\min} \left| \frac{1}{\theta_1}(u_1 - u^1_{\min}) = \frac{1}{\theta_2}(u_2 - u^2_{\min}) \right.\right\}, \tag{3.33}$$

where $\theta_i = H_i(\mathcal{U}, \mathbf{u}_{\min}) - u^i_{\min}$*. The solution is in* Λ*.*

DEFINITION 33. *Egalitarian solution.* $\phi(\mathcal{U}, \mathbf{u}_{\min})$ *is the ES, which can be expressed as*

$$\phi(\mathcal{U}, \mathbf{u}_{\min}) = \max \left\{\mathbf{u} > \mathbf{u}_{\min} | u_1 - u^1_{\min} = u_2 - u^2_{\min}\right\}. \tag{3.34}$$

Next, we study the ultimatum game (sequential bargaining) in which players interact anonymously and only once. For example, for the two-player

case, the first player proposes how to divide a sum of money between themselves and the second player can either accept or reject this proposal. If the second player rejects, neither player receives anything. If the second player accepts, the money is split according to the proposal. Since the game is played only once and anonymously, reciprocation is not an issue.

For illustration, we will suppose there is a smallest division of the good available (say 1 cent). Suppose that the total amount of money available is x. The first player chooses some amount in the interval $[0, x]$. The second player chooses some function $f : [0, x] \rightarrow$ {"*accept*", "*reject*"} (i.e., the second chooses which divisions to accept and which to reject). We will represent the strategy profile as (p, f), where p is the proposal and f is the function. If $f(p) =$ "*accept* " the first receives p and the second $x - p$, otherwise both get zero. (p, f) is a Nash equilibrium of the ultimatum game if $f(p) =$ "*accept* " and there is no $y > p$ such that $f(y) =$ "*accept* " (i.e., p is the largest amount the second will accept). The first player would not want to unilaterally increase his demand since the second will reject any higher demand. The second would not want to reject the demand, since he would then get nothing.

There is another Nash equilibrium where $p = x$ and $f(y) =$ "*reject*" for all $y > 0$ (i.e., the second player rejects all demands that give the first any amount at all). Here both players get nothing, but neither could get more by unilaterally changing her strategy.

However, only one of these Nash equilibria satisfies a more restrictive equilibrium concept, subgame perfection. Suppose that the first demands a large amount that gives the second some (small) amount of money. By rejecting the demand, the second is choosing nothing rather than something. Therefore, it would be better for the second to choose to accept any demand that gives her any amount whatsoever. If the first knows this, she will give the second the smallest (non-zero) amount possible.

3.4.2 Applications of bargaining games

There are many applications of bargaining solutions in wireless networks. We list a few of them below.

- OFDMA resource allocation [96]: For multi-user single-cell OFDMA systems, the resource-allocation problem is to allocate subcarrier, rate, and power to maximize the overall system rate, under each user's maximal-power and minimal-rate constraints, while considering the fairness among users. The approach considers a new fairness criterion, which is a generalized proportional fairness based on NBSs and coalitions. First, a two-user algorithm is developed to bargain subcarrier usage between two users. Then a multi-user bargaining algorithm based on optimal coalition pairs among users is developed. The simulation results show that the proposed algorithms not only provide fair resource allocation among users, but also have comparable overall system rate to that of the scheme maximizing the total rate without considering fairness. They also have much higher rates than that of the scheme with max–min fairness. Moreover, the iterative fast implementation has a complexity for each iteration of only $O(K^2 N \log N + K^4)$, where N is the number of subcarriers and K is the number of users.
- Dynamic spectrum access [97]: Dynamic spectrum access can achieve near-optimal utilization of radio spectrum by allowing devices to sense and utilize available spectrum opportunistically. However, a naive distributed spectrum assignment can lead to significant interference between devices. A general framework is defined for the spectrum-access problem for several definitions of overall system utility. By reducing the allocation problem to a variant of the graph-coloring problem, the global optimization problem is shown to be NP-hard, and one can provide a general approximation methodology through vertex labeling. A centralized strategy, where a central server calculates an allocation assignment based on global knowledge, and a distributed approach, where devices collaborate to negotiate local channel assignments towards global optimization, are investigated. The experimental results show that the allocation algorithms can dramatically reduce interference and improve throughput (as much as 12-fold). Further simulations show that the distributed algorithms generate allocations similar in quality to those based on the centralized

algorithms using global knowledge, while incurring substantially less computational complexity in the process.

- Ad-hoc networks [98]: There is a need for new spectrum-access protocols that are opportunistic, flexible and efficient, yet fair. Game theory provides an ideal framework for analyzing spectrum access, a problem that involves complex distributed decisions by independent spectrum users. A cooperative game-theory model is developed to analyze a scenario where nodes in a multihop wireless network need to agree on a fair allocation of spectrum. In high-interference environments, the utility space of the game is shown to be nonconvex, which may make some optimal allocations unachievable with pure strategies. However, as the number of channels available increases, the utility space becomes close to convex and thus optimal allocations become achievable with pure strategies. The use of the NBS is proposed to achieve a good compromise between fairness and efficiency, using a small number of channels. Finally, a distributed algorithm is proposed for spectrum sharing and it is shown that it achieves allocations reasonably close to the NBS.
- Mesh networks [99]: A new fair scheduling scheme is proposed for OFDMA-based wireless mesh networks (WMNs), which fairly allocates subcarriers and power to mesh routers (MRs) and mesh clients to maximize the NBS fairness criterion. In WMNs, since not all the information necessary for scheduling is available at a central scheduler (e.g., MR), it is advantageous to involve the MR and as many mesh clients as possible in distributed scheduling based on the limited information that is available locally at each node. Instead of solving a single global control problem, hierarchically the subcarrier- and power-allocation problem is decoupled into two subproblems, where the MR allocates groups of subcarriers to the mesh clients, and each mesh client allocates transmit power among its subcarriers to each of its outgoing links. The two subproblems are formulated by nonlinear integer programming and nonlinear mixed-integer programming, respectively. A simple and efficient solution algorithm is developed for the MR's problem. Also, a closed-form solution is obtained by transforming the mesh client's problem into a time-division scheduling problem. The simulation results demonstrate that the proposed scheme provides fair

opportunities to the respective users (mesh clients) and a comparable overall end-to-end rate when the number of mesh clients increases.

- Multimedia transmission [100]: Multi-user multimedia applications such as enterprise streaming, surveillance, and gaming are now emerging, and they are often deployed over bandwidth-constrained network infrastructures. To ensure the quality of service (QoS) required by the delay-sensitive and bandwidth-intensive multimedia data for these applications, efficient resource (bandwidth) management becomes paramount. The well-known game-theoretic concept of bargaining is deployed to allocate the bandwidth fairly and optimally among multiple collaborative users. Specifically, two bargaining solutions are considered for the resource management problem: the NBS and the Kalai–Smorodinsky bargaining solution (KSBS). Interpretations for the two bargaining solutions investigated for multi-user resource allocation are as follows: The NBS can be used to maximize the system utility, while the KSBS ensures that all users incur the same utility penalty relative to the maximum achievable utility. The bargaining strategies and solutions are implemented in the network using a resource manager, which explicitly considers the application-specific distortion for the bandwidth allocation. These bargaining solutions exhibit important properties (axioms) that can be used for effective multimedia resource allocation. Moreover, several criteria are proposed for determining bargaining powers for these solutions, which enable one to provide additional flexibility in choosing a solution by taking into consideration the visual quality impact, the spatiotemporal resolutions deployed, etc.

3.5 Cooperative game theory – coalitional games

We have discussed how to play the cooperative game by bargaining. Other analysis tools for the game are coalition, core, Shapley function, and nucleolus. In the following, we will explain these concepts and give examples. Also, fairness issue will be discussed. Finally, a merge/split algorithm to distributively achieve the coalition will also be shown.

3.5.1 Characteristic function and core

First, we discuss how to divide the benefits among users and the properties and stability of the division by introducing the following concepts.

DEFINITION 34. *A **coalition** S is defined to be a subset of the total set of players N, $S \in N$. The users in a coalition try to cooperate with each other. The **coalition form** of a game is given by the pair (N, v), where v is a real-valued function, called the **characteristic function**. $v(S)$ is the value of the cooperation for coalition S with the following properties:*

(i) $v(\emptyset) = 0$; *and*

(ii) *(superadditivity) if S and T are disjoint coalitions ($S \bigcap T = \emptyset$), then $v(S) + v(T) \leq v(S \bigcup T)$.*

The coalition states the benefit obtained via cooperation agreement. But we still need to study how to divide the benefit among the cooperative users. One of the possible properties of an agreement on a fair division is that it is stable since no coalition shall have the incentive and power to upset the cooperative agreement. The set of such divisions of v is called the core and defined as follows.

DEFINITION 35. *A payoff vector $\mathbf{x} = (x_1, \ldots, x_N)$ is said to be **group rational** or **efficient** if $\sum_{i=1}^{N} x_i = v(N)$. A payoff vector $\mathbf{x}$ is said to be **individually rational** if the user can obtain no less benefit than when acting alone, i.e., $x_i \geq v(\{i\})$, $\forall i$. An **imputation** is a payoff vector satisfying the above two conditions.*

DEFINITION 36. *An imputation $\mathbf{x}$ is said to be unstable through a coalition S if $v(S) > \sum_{i \in S} x_i$, i.e., the users have incentives for coalition S and upset the proposed $\mathbf{x}$. The set C of a stable imputation is called the **core**, i.e.,*

$$C = \left\{ \mathbf{x} : \sum_{i \in N} x_i = v(N) \text{ and } \sum_{i \in S} x_i \geq v(S), \ \forall S \subset N \right\}. \tag{3.35}$$

The *core* gives a reasonable set of possible shares. A combination of shares is in a core if there exists no subcoalition in which its members may gain a higher total outcome than the share of concern. If the share is not in a core, some members may be frustrated and may think of leaving the whole group with some other members to form a smaller group.

To illustrate the idea of a core, we give the following example. Consider the game with the following characteristic functions:

$$\begin{aligned} v(\emptyset) = 0, v(\{1\}) = 1, v(\{2\}) = 0, v(\{3\}) = 1, \\ v(\{1,2\}) = 4, v(\{1,3\}) = 3, v(\{2,3\}) = 5, v(\{1,2,3\}) = 8. \end{aligned} \tag{3.36}$$

By using $v(\{2,3\}) = 5$, we can eliminate the payoff vector (such as $(4,3,1)$), since user 2 and user 3 can achieve better payoffs by forming a coalition themselves. Using the same analysis, the final core of the game is $(3,4,1)$, $(3,3,2)$, $(3,2,3)$, $(3,1,4)$, $(2,5,1)$, $(2,4,2)$, $(2,3,3)$, $(2,2,4)$, $(1,5,2)$, $(1,4,3)$, and $(1,3,4)$.

3.5.2 Fairness

The concept of a *core* defines the stability of an allocation of payoff. Next, we investigate how to divide the benefits among players according to different fairness criteria. First, we study each individual player's power in the coalition by defining a value called the Shapley function.

DEFINITION 37. *A Shapley function ϕ is a function that assigns to each possible characteristic function v a real number, i.e.,*

$$\phi(v) = (\phi_1(v), \phi_2(v), \ldots, \phi_N(v)), \tag{3.37}$$

where $\phi_i(v)$ represents the worth or value of player i in the game. The Shapley axioms for $\phi(v)$ are as follows.

(i) *Efficiency:* $\sum_{i \in N} \Phi_i(v) = v(N)$.

(ii) *Symmetry: If i and j are such that* $v(S \bigcup \{i\}) = v(S \bigcup \{j\})$ *for every coalition S not containing i and j, then* $\phi_i(v) = \phi_j(v)$.

(iii) *Dummy axiom: If i is such that* $v(S) = v(S \bigcup \{i\})$ *for every coalition S not containing i, then* $\phi_i(v) = 0$.

(iv) *Additivity: If u and v are characteristic functions, then* $\phi(u + v) = \phi(v + u) = \phi(u) + \phi(v)$.

It can be proved that there exists a unique function ϕ satisfying the Shapley axioms. To calculate the Shapley function, suppose we form the grand coalition by entering the players into this coalition one at a time. As each player enters the coalition, she receives the amount by which her entry increases the value of the coalition she enters. The amount that a player receives by this scheme depends on the order in which the players are entered. The Shapley value is just the average payoff to the players if the players are entered in a completely random order, i.e.,

$$\phi_i(v) = \sum_{S \subset N, i \in S} \frac{(|S| - 1)!(N - |S|)!}{N!} [v(S) - v(S - \{i\})]. \tag{3.38}$$

For the example in (3.36), it can be shown that the Shapley value is $\phi = (14/6, 17/6, 17/6)$.

Another concept for multiple cooperative games is the nucleolus. For a fixed characteristic function, an imputation **x** is found such that the worst inequity is minimized, i.e., for each coalition S and its associated dissatisfaction, an optimal imputation is calculated to minimize the maximum dissatisfaction. First we define the concept of excess which measures the dissatisfactions.

DEFINITION 38. *The measure of the inequity of an imputation* **x** *for a coalition S is defined as the* ***excess****:*

$$e(\mathbf{x}, S) = v(S) - \sum_{j \in S} x_j. \tag{3.39}$$

Obviously, any imputation **x** is in the core, if and only if all of its excesses are negative or zero.

Among all allocations, the kernel is a fair allocation, defined as follows.

DEFINITION 39. *A* ***kernel*** *of v is the set of all allocations* **x** *such that*

$$\max_{S \subseteq N-j, i \in S} e(\mathbf{x}, S) = \max_{T \subseteq N-i, j \in T} e(\mathbf{x}, T). \tag{3.40}$$

If players i and j are in the same coalition, then the highest excess that i can make in a coalition without j is equal to the highest excess that j can make in a coalition without i.

Finally, we define the nucleolus as follows.

DEFINITION 40. *The* ***nucleolus*** *is the allocation* **x** *which minimizes the maximum excess, that is,*

$$\mathbf{x} = \arg \min_{\mathbf{x}} (\max e(\mathbf{x}, S), \ \forall S). \tag{3.41}$$

The nucleolus has the following property: The nucleolus of a game in coalitional form exists and is unique. The nucleolus is group rational, individually rational, and satisfies the symmetry axiom and the dummy axiom. If the core is not empty, the nucleolus is in the core and kernel. In other words, the nucleolus is the best allocation with the min–max criteria.

3.5.3 *The merge/split algorithm*

Using the coalition-formation concepts described in the previous section, a coalition-formation algorithm for self-organization can be generated. This algorithm will be based on simple merge-and-split rules that allow one to modify a partition T of N nodes as follows [101].

- **The merge rule:** Merge any set of coalitions $\{S_1, \ldots, S_l\}$, where $\{\bigcup_{j=1}^{l} S_j\} \rhd \{S_1, \ldots, S_l\}$. Therefore, $\{S_1, \ldots, S_l\} \rightarrow \{\bigcup_{j=1}^{l} S_j\}$ (each S_i denotes a coalition).
- **The split rule:** Split any coalition $\bigcup_{j=1}^{l} S_j$, where $\{S_1, \ldots, S_l\} \rhd \{\bigcup_{j=1}^{l} S_j\}$. Thus, $\{\bigcup_{j=1}^{l} S_j\} \rightarrow \{S_1, \ldots, S_l\}$.

In brief, multiple coalitions will merge (split) if merging (splitting) yields a preferred collection based on a chosen $\rhd$. In [101] and [102] it is shown that any arbitrary iteration of merge-and-split operations *terminates*, therefore, it will be suitable to devise a coalition-formation algorithm by means of merge-and-split. The Pareto order is highly appealing as a comparison relation $\rhd$ for the merge-and-split rules. With the Pareto order, coalitions will merge only if at least one user can enhance his or her individual payoff through this merge without decreasing the other users' payoffs. Similarly, a coalition will split only if at least one user in that coalition is able to strictly improve his or her individual payoff through the split without hurting other users. A decision to merge or split is, thus, tied to the fact that all users must benefit from the merge or split, thus, any merged (or split) form is reached only if it allows all of the users involved to maintain their payoffs, with the payoff of at least one user improving. In Figure 3.2, we show an example of forming a virtual MIMO system in wireless networks using coalitional games.

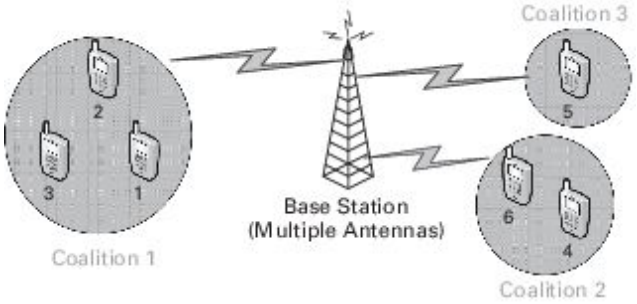

Figure 3.2. The coalitional game and merge/split algorithm for virtual MIMO.

Two important defection functions can be pinpointed [101], [103]. The first is the $\mathbb{D}_{hp}(T)$ function (denoted $\mathbb{D}_{hp}$), which associates with each partition T of N the family of all partitions of N that the players can form through merge-and-split operations applied to T. This function allows any group of players to leave the partition T of N through merge-and-split operations to create another *partition* in N. The second is the $\mathbb{D}_c(T)$ function (denoted $\mathbb{D}_c$), which associates with each partition T of N the family of all collections in N. This function allows any group of players to leave the partition T of N through *any* operation and create an arbitrary *collection* in N. Two forms of stability stem from these definitions: $\mathbb{D}_{hp}$ stability and a stronger $\mathbb{D}_c$ stability. A partition T is $\mathbb{D}_{hp}$-stable if no players in T are interested in leaving T through merge-and-split to form other partitions in N; a partition T is $\mathbb{D}_c$-stable if no players in T are interested in leaving T through *any* operation (not necessary merge or split) to form other collections in N.

3.6 Matching theory

In economics, matching theory is a mathematical framework attempting to describe the formation of mutually beneficial relationships over time [104]. It has been especially influential in labor economics, where it has been used to describe the formation of new jobs, as well as to describe other human relationships such as marriage [105, 106]. Thus, matching theory is showing itself to be a promising paradigm to model cooperation among nodes in a wireless/mobile network.

In matching theory, the main problem we try to solve is to find a stable matching between two sets of elements, given the preference lists for each element. A matching is a mapping from the elements of one set to the elements of the other set. The concept of stable matching can be described as follows. Consider that elements A and D in one set are matched with elements B and C in the other set, respectively. In this scenario, A prefers C over B, and C also prefers A over D. A and C are called a blocking pair. In other words, a stable matching means there does not exist any blocking pair (A, C) in which they are not matched together, but both are individually better off if they are matched together, as opposed to their current matching.

On the basis of the number of players in each stable matching pair, the type of matching could be divided into different catenaries. Typically, there are three types of matching: one-to-one matching, many-to-one matching, and many-to-many matching.

3.6.1 One-to-one matching

In one-to-one matching problems, each element in one set is matched with only one element from the other set. There are many problems that can be fit into the one-to-one matching model, one representative is the stable-marriage problem (SMP).

The stable-marriage problem is commonly stated as follows: Given n men and n women, where each person has ranked all members of the opposite sex with a unique number between 1 and n in order of preference, marry the men and women together such that there are no two people of opposite sex who would both rather have each other than their current partners. If there are no such people, all the marriages are "stable" [107].

To solve the one-to-one matching problem, we introduce the *Gale–Shapley (GS) algorithm* as shown in Algorithm 1, which was originally used to solve the SMP and make all marriages stable [108]. In 1962, David Gale and Lloyd Shapley proved that, for any equal number of men and women, it

is always possible to solve the SMP and make all marriages stable. They presented an algorithm to do so [107].

Algorithm 1 Gale–Shapley algorithm

1. Initialization;
Initialize all $m \in M$ and $w \in W$ to free
2. Men propose to women
while ∃ free man m who still has a woman w to propose to **do**
  $w = m$'s highest ranked such woman to whom he has not yet proposed
  if w is free **then**
    (m, w) become engaged
  else
    if w prefers m to m' **then**
      (m, w) become engaged
      m' becomes free
    else
      (m', w) remain engaged
    end if
  end if
end while
3. End of algorithm
Each man matched with the woman that they kept with.

3.6.2 Many-to-one matching

One example of many-to-one matching is the hospitals/residents problem, also known as the college-admissions problem. In this type of matching problem, players on one side (hospitals/colleges) are matched with multiple players of the other side (residents/students). But each player on the applicant side (resident/student) can match with only one player of the other side.

A publication in 1962 by Gale and Shapley noted that there always exists a stable solution when colleges are matching with students, but that it is possible to favor colleges as a group over applicants as a group (and vice versa). That is, Gale and Shapley found that there is a college-optimal stable match and an applicant-optimal stable match [108]. This phenomenon is also consistent with the results found in one-to-one matching. That is, the side of players who propose first will get better satisfaction. We can easily extend this to stable many-to-one matching, as we will propose in the following subsections.

The framework of many-to-many matching has been widely used in some famous projects such as the US National Resident Matching Program (NRMP) for medical school graduates, and public-schools recursion in Boston and NYC. Recently, it has also been adopted in the communication area [109, 110].

The many-to-one GS matching algorithm

The many-to-one GS matching algorithm can be implemented in three steps. In the first stage, all colleges and students start the initialization process by giving evaluations regarding the other students and colleges. Then the descending-order preference lists $\mathcal{CLGLIST}_i$ and $\mathcal{STDLIST}_j$ of all colleges and students are constructed. We also construct a set of unmatched students as $\mathcal{UNMATCH}$. Initially, all the students are in the $\mathcal{UNMATCH}$. Having the preference list, all students will apply to colleges in the second stage simultaneously. Since each student can be matched with only one college, students can apply to only one college each time.

Upon receiving students' applications, $\mathcal{CLG}_i$ will make decisions in the third stage according to their preference lists $\mathcal{CLGLIST}_i$. Since each college can serve a maximum number of K students simultaneously, in the case that the number of applications is larger than the limitation, the college will select only the K most preferable students so as to maximize its utility, and reject the others. Then we will remove those students that are kept by colleges from the $\mathcal{UNMATCH}$, and keep the rejected ones in the set.

If $\mathcal{UNMATCH} \neq \emptyset$, the algorithm will go back to stage 2. Otherwise, the matching process goes on, until $\mathcal{UNMATCH} = \emptyset$, i.e., all students are matched with a college. Then, the algorithm comes to the end.

In the many-to-one GS matching algorithm we proposed, both colleges and students are behaving selfishly in the matching process. Thus, the algorithm can achieve only a locally optimal result for students or colleges. The algorithm is summarized in Algorithm 2.

Algorithm 2 Many-to-one GS matching algorithm

1. Initialization

Construct the preference list of colleges, $\mathcal{CLGLIST}_i = \{STD_j\}_{j=1}^{M}$

Construct the preference list of students, $\mathcal{STDLIST}_j = \{CLG_i\}_{i=1}^{N}$

Construct the set of students who are not matched, $\mathcal{UNMATCH}$

2. Students apply to colleges

for all *student* $\in \mathcal{UNMATCH}$ **do**

Propose to Clg_i that has never rejected it before

end for

3. Colleges make decisions

for Clg_i, $i \in \mathcal{N}$

if $\sum_{j \in \mathcal{M}} x_{ij} \leq K$ **then**

Clg_i keeps all of the proposed students

Remove Std_i from the $\mathcal{UNMATCH}$

else

Clg_i keeps the most preferred K students, rejects the rest

Remove the kept student from the $\mathcal{UNMATCH}$

Add the rejected student into the $\mathcal{UNMATCH}$

end if

if $\mathcal{UNMATCH} \neq \emptyset$ **then**

Go to step 2

else

Go to step 4

end if

4. End of algorithm

Each college matched with the students that they kept with.

The cooperative matching algorithm

In many-to-one matching, since each player on one side (e.g., hospitals, colleges) serves multiple applicants simultaneously, limited resources are shared among many. A high-utility player usually receives more proposals

than do the other ones. Thus the number of matched applicants is large. Since the number of its matched applicants is large, the resources for each may decrease. As a result, the applicants who are matched with the high-utility one receive lower utility than they expect.

One example can be found in a cognitive radio network where the spectrum resources are shared among secondary users. After the many-to-one matching has attained a stable stage, for high-utility primary users (PUs), due to the large number of secondary users (SUs) they need to serve, the resources they provide to the SUs are decreased; while for low-utility PUs, which have fewer proposals in hand, the spectrum resources they can provide to their matched SUs may be greater than those for high-utility PUs.

If there is a chance that the SUs can make a second choice to find another PU that can provide them with more available resources rather than the first stable matching, resources can be better utilized and the SUs may have better satisfaction. Overall, the social welfare could increase. Next, we propose another distributed-matching algorithm that is an extension of the greedy algorithm, but can achieve better satisfaction for users and result in higher social welfare. Here, we briefly list the procedure of the cooperative matching as follows.

For the initialization stage, it is exactly the same as the greedy algorithm. In the matching process, the PUs and SUs are first matched with each other by the greedy algorithm. Then, assuming all the other SUs are fixed with their recent matchings, SU *j* will try to estimate its utility if it re-matches with the other PUs, to see whether it can obtain a higher utility by changing to another PU.

If the proposed PU i' has not achieved its highest capacity of *K*, the process can be performed fluently. But, if the $PU_{i'}$ already has *K* SUs matched, SU_j needs to check first that it is eligible to propose to $PU_{i'}$. That is, it needs to check whether $PU_{i'}$ prefers SU_j rather than its recent matched SUs (if $U_{PU_{i'}^j}$ is higher than the minimum value of $U_{PU_{i'}^j}$). Thus, we could guarantee that the PU i' will not lose any utility in this re-match process. Otherwise, even if SUs would prefer to re-match, the PUs have no incentive

to participate. If SU j could satisfy this requirement of $PU_{i'}$, SU_j will consider proposing to PU i'. After SU j has checked with all the other PUs, if there is any PU i' that can provide SU_j a higher utility, it will choose the best alternative and leave the current one. After SUs have finished re-proposing, the PUs will again make decisions just like in the Greedy algorithm. The algorithm will continue until $\mathcal{UNMATCH} = \emptyset$, i.e., all SUs are matched with a PU. Then, the algorithm comes to the end.

To guarantee that our algorithm could converge to a stable matching and provide a higher social welfare, we set up a few constraints. After all the SUs have finished estimating their re-match utility, we will form a descending ordered list of all the SUs who would like to re-propose. The SUs who could gain higher utility will have the privilege of being allowed to re-propose, whereas the rest, if their re-match would decrease the utility of high-order SUs below zero, will not be allowed to re-propose. In addition, in order to prevent SUs looping in the re-propose process between their previous and current PUs, we introduce a flag to mark their times of re-proposing. Each SU can propose to any particular PU only twice.

The algorithm is summarized in Algorithm 3.

Algorithm 3 Cooperative matching algorithm

1. Initialization

2. Matching by greedy algorithm;

for all SU $j, j = 1 : M$ **do**

Stable matched with PU_i^j

$SELECT_j = 1$

end for

3. SUs propose to PUs;

for all SU $j, j = 1 : M$ **do**

Fix the other SUs

if $k_{i'} < K, i \neq i'$ **then**

Calculate the new utility $\hat{U}_{SU_j}^{i'}$ if propose to $PU_{i'}$

else

if $U_{PU_{i'}^j} > \min U_{PU_{i'}^{j'}}$ **then**

Calculate the new utility $\hat{U}_{SU_j}^{i'}$ without $SU_{j'} = \arg\min_{j'} U_{PU_{i'}^{j'}}$

end if

end if

end for

if $\hat{U}_{SU_j}^{i'} > U_{SU_j}^{i}$ and $SELECT_j \leq 2$ **then**

Propose to the best alternative $PU_{i'}$

$SELECT_j = SELECT_j + 1$

else

Propose to the recent PU_i

$SELECT_j = SELECT_j$

end if

4. PUs make decisions

5. End of algorithm

3.6.3 Many-to-many matching

Consider a collection of firms and consultants. Each firm wishes to hire a set of consultants, and each consultant wishes to work for a set of firms. Firms have preferences over the possible sets of consultants, and consultants have preferences over the possible sets of firms. This is an example of a many-to-many matching market. A matching is an assignment of sets of consultants to firms, and of sets of firms to consultants, so that firm f is assigned to consultant w if and only if w is also assigned to f. The problem is to predict which matchings can occur.

Many-to-many matching markets are understood less well than many-to-one markets, in which firms hire many workers, but each worker works for only one firm. Even though many-to-many contracts are less common than one-to-one and many-to-one matching, most labor markets have at least a few many-to-many contracts. In the USA, 76% of total employment is in industries with 5% or more multiple jobholders [111]. It is known that, in two-sided many-to-many matching problems, pairwise stable matchings might not be immune to group deviations, unlike in many-to-one matching problems. But many-to-many matching problems still can make a big difference in some areas if they are well studied.

In the communication area, there are many areas that can be described by many-to-many matching. One application could be introduced for the new femto-cell technology. By introducing this technology, users can be matched with a specific femto cell and (or) macro cell and be served by either of them. Thus the service coverage is extended [109]. This match among multiple femto-cell access points (FAPs), multiple wireless operators (WOs) that own multiple macro-cell access points (MAPs), and multiple final users (FUs) who have subscribed to these WOs is a great application of this theory.

3.7 Auction theory

3.7.1 Auction basics

In this section, we first define the concept of an auction. Then, we present the auction in a game-theoretic model. Some basic properties are also discussed. Finally, we list several basic types of auctions, followed by a simple example.

Auctions take many forms, but always satisfy two conditions. First, they may be used to sell any item, hence they are universal; and second, the outcome of the auction does not depend on the identity of the bidders, i.e., auctions are anonymous. Most auctions have the feature that participants submit bids, or specify the amounts of money they are willing to pay. The following is the definition of an auction.

DEFINITION 41. *A market mechanism in which an object, service, or set of objects, is exchanged on the basis of bids submitted by participants. An* auction *provides a specific set of rules that will govern the sale or purchase (procurement auction) of an object to the submitter of the most favorable bid. The specific mechanisms of the auction include first-price, second-price, English, and Dutch auctions.*

A game-theoretic auction model is a mathematical game represented by a set of players, a set of actions (strategies) available to each player, and a payoff vector corresponding to each combination of strategies. Generally, the players are the buyer(s) and the seller(s). The action set of each player is a set of bid functions or reservation prices. Each bid function maps the player's value (in the case of a buyer) or cost (in the case of a seller) to a bid price. The payoff of each player under a combination of strategies is the expected utility (or expected profit) of that player under that combination of strategies.

Game-theoretic models of auctions and strategic bidding generally fall into either of the following two categories. In a private-value model, each participant (bidder) assumes that each of the competing bidders obtains a random private value from a probability distribution. For a common-value model, each participant assumes that any other participant obtains a random signal from a probability distribution common to all bidders. Usually, but not

always, a private-value model assumes that the values are independent across bidders, while a common-value model usually assumes that the values are independent up to the common parameters of the probability distribution. When it is necessary to make explicit assumptions about bidders' value distributions, most of the published research assumes symmetric bidders. This means that the probability distributions from which the bidders obtain their values (or signals) are identical across bidders. In a private-value model that assumes independence, symmetry implies that the bidders' values are independently and identically distributed (i.i.d.).

There are various properties for an auction. First, allocative efficiency means that in all these auctions the highest bidder always wins (i.e., there are no reserve prices). Second, it is desirable for an auction to be computationally efficient. Finally, to study the revenue (expected selling price) of different auctions, we have the following theorem.

THEOREM 7. *Revenue equivalence theorem: Any two auctions such that*

- *the bidder with the highest value wins,*
- *the bidder with the lowest value expects zero profit,*
- *bidders are risk-neutral,*[1] *and*
- *value distributions are strictly increasing and atomless*

have the same revenue and also the same expected profit for each bidder. The theorem can help one to find an equilibrium strategy.

It is worth mentioning the phenomenon of the winner's curse, which can occur in common-value settings when the actual values to the different bidders are unknown but correlated, and the bidders make bidding decisions that are based on estimated values. In such cases, the winner will tend to be the bidder with the highest estimate, and that winner will frequently have bid too much for the auctioned item.

There are many ways to categorize different types of auctions. For example, standard auctions require that the winner of the auction be the

participant with the highest bid. A non-standard auction does not require this (e.g., a lottery). There are traditionally four types of auctions that are used for the allocation of a single item, as follows.

DEFINITION 42. ***First-price auction:*** *An auction in which the bidder who submitted the highest bid is awarded the object being sold and pays a price equal to the amount bid. Alternately, in a procurement auction, the winner is the bidder who submits the lowest bid and is paid an amount equal to her bid. In practice, first-price auctions are either sealed-bid, in which bidders submit bids simultaneously, or Dutch. In first-price auctions, bidders shade their bids below their true value.*

DEFINITION 43. ***Second-price auction:*** *An auction in which the bidder who submitted the highest bid is awarded the object being sold and pays a price equal to the second highest amount bid. Alternately, in a procurement auction, the winner is the bidder who submits the lowest bid, and is paid an amount equal to the next lowest submitted bid. In practice, second-price auctions are either sealed-bid, in which bidders submit bids simultaneously, or English auctions, in which bidders continue to raise each other's bids until only one bidder remains. The theoretical nicety of second-price auctions, first pointed out by William Vickrey, is that bidding one's true value is a dominant strategy. Alternately, first-price auctions also award the object to the highest bidder, but the payment is equal to the amount bid.*

DEFINITION 44. ***English auction (open ascending-bid auctions)****: A type of sequential second-price auction in which an auctioneer directs participants to beat the current standing bid. New bids must increase the current bid by a predefined increment. The auction ends when no participant is willing to outbid the current standing bid. Then, the participant who placed the current bid is the winner and pays the amount bid. An English auction, in which the highest bidder pays the amount bid, is termed a second-price auction since the winning bidder need only outbid the next highest bidder by the minimum increment. Thus, the winner effectively pays an amount equal to (slightly higher than) the second highest bid.*

DEFINITION 45. ***Dutch auction (open descending-bid auctions)****: A type of first-price auction in which a "clock" initially indicates a price for the object for sale substantially higher than any bidder is likely to pay. Then, the clock gradually decreases the price until a bidder "buzzes in" or indicates his or her willingness to pay. The auction is then concluded, and the winning bidder pays the amount reflected on the clock at the time he or she stopped the process by buzzing in. These auctions are named after a common market mechanism for selling flowers in Holland, but they also reflect stores successively reducing prices on sale items.*

Most auction theory revolves around these four "standard" auction types listed above. However, other auction types have also received some academic study, such as the following.

DEFINITION 46. ***Japanese auction:*** *A type of sequential second-price auction, similar to an English auction in which an auctioneer regularly raises the current price. Participants must signal at every price level their willingness to stay in the auction and pay the current price. Thus, unlike an English auction, each participant must bid at each level to stay in the auction. The auction concludes when only one bidder indicates her willingness to stay in. This auction format is also known as the button auction.*

DEFINITION 47. ***All-pay auctions****: Bidders place their bids in sealed envelopes and simultaneously hand them to the auctioneer. The envelopes are opened, and the individual with the highest bid wins, paying a price equal to the exact amount that he or she bid. All losing bidders are also required to make a payment to the auctioneer equal to their own bid in an all-pay auction. This auction format is non-standard, but it can be used to understand things such as election campaigns (in which bids can be interpreted as campaign spending) or queuing for a scarce commodity (in which your bid is the amount of time that you are prepared to remain in the queue). The most straightforward form of an all-pay auction is a Tullock auction, sometimes called a Tullock lottery, in which everyone submits a bid but both the losers and the winners pay their submitted bids. This is instrumental in describing certain ideas in public-choice economics. The dollar auction is a two-player Tullock auction, or a multiplayer game, in*

which only the two highest bidders pay their bids. Other forms of all-pay auctions exist, such as the war of attrition, in which the highest bidder wins, but all (or both, more typically) bidders pay only the lower bid. The war of attrition is used by biologists to model conventional contests, or agonistic interactions resolved without recourse to physical aggression.

DEFINITION 48. ***Unique–bid auction**: A type of strategy game related to traditional auctions in which the winner is usually the individual with the lowest unique bid, although less commonly the auction rules may specify that the highest unique bid is the winner. Unique-bid auctions are often used as a form of competition or lottery.*

DEFINITION 49. ***Generalized second-price auction (GSP)**: A non-truthful auction mechanism for multiple items, first thought of as a natural extension of the Vickrey auction, it actually does not conserve some good properties of the Vickrey auction (such as truthfulness, for example). It is used mainly in the context of keyword auctions, in which sponsored search slots are sold on an auction basis.*

Now, we study a simple first-price auction model with two buyers who are bidding for an object. Each buyer might assume that the rival buyer's private value is drawn from the uniform distribution over the interval $[0, 1]$, with the cumulative distribution function $F(v) = v$.[2] We assume that (1) the value of the object for the seller is 0, and (2) the seller's reservation price is also 0. Each buyer's expected utility U can be written as

$$U(p) = (v - p)\Pr[p > B(v_0)], \tag{3.42}$$

where p is the bid price, $(v - p)$ is the consumer surplus that the buyer will receive conditional upon winning, and $\Pr[p > B(v_0)]$ is the likelihood that he or she is going to be the buyer with the highest bid price. That likelihood is given by the probability that this buyer's bid price p exceeds the other buyer's bid price B (expressed as a function of the other buyer's value v_0).

Assume that each buyer's equilibrium bid price is monotonically increasing in that buyer's value; this implies that the bid function B has an inverse function. Let Y be the inverse of B: $Y = B^{-1}$. Then $U(p) = (v - p)\Pr[Y(p) > v_o]$. Since v_o is distributed $F(v_o)$, we have

$$\Pr[Y(p) > v_o] = F(Y(p)) = Y(p), \tag{3.43}$$

which implies $U(p) = (v - p)Y(p)$. A bid price p maximizes U if $U'(p) = 0$. On differentiating U with respect to p and setting to zero, we have

$$U'(p) = -Y(p) + (v - p)Y'(p) = 0. \tag{3.44}$$

Since the buyers are symmetric, in equilibrium it must be the case that $p = B(v)$ or (equivalently) $Y(p) = v$. Therefore, we have

$$-Y(p) + (Y(p) - p)Y'(p) = 0. \tag{3.45}$$

A solution $\hat{Y}$ of this differential equation is an inverse Nash equilibrium strategy of this game.

At this point, we may conjecture that the (unique) solution is the linear function $\hat{Y}(p) = \alpha p$ and $\hat{Y}'(p) = \alpha$ for some real number α. On substituting into $U'(p) = 0$, we have

$$-\alpha p + (\alpha p - p)\alpha = 0. \tag{3.46}$$

Solving for α yields $\hat{\alpha} = 2$. Therefore, $\hat{Y}(p) = 2p$ satisfies $U'(p) = 0$. $\hat{Y}(p) = \hat{\alpha}p$ implies $\hat{Y}(p)/\hat{\alpha} = p$, or $v/\hat{\alpha} = \hat{B}(v)$. Thus, the (unique) Nash-equilibrium-strategy bidding function of this game is established as $\hat{B}(v) = v/2$, at least within the set of invertible bidding functions.

3.7.2 Mechanism design

A game designer tries to consider all the possible games and choose the one that best influences other players' tactics. Mechanism design is used to define the game rule so as to achieve the desired game outcome. This is different from the game analysis, in which the game rules are predefined and then the outcome is investigated. In addition, the game designer has to consider the situation in which the players may lie. Fortunately, by virtue of the revelation principle, it is necessary only to consider games in which players truthfully report their private information. In this section, we discuss mechanism design in detail.

First, we have the basic definitions for the following mechanisms.

- Outcome set: Ω.
- Players $i \in \mathcal{I}$, where $\mathcal{I}$ is the set of the players of size $|\mathcal{I}| = N$, with preference types $\theta_i \in \Theta_i$.
- Utility $u_i(o, \theta_i)$, over outcome $o \in \Omega$.
- Mechanism $M = (S, g)$ defines

  a strategy space $S^N = S_1 \times \cdots \times S_N$, s.t. player i chooses a strategy $s_i(\theta_i) \in S_i$ with $s_i : \Theta_i \rightarrow S_i$;

  an outcome function $g : S^N \rightarrow \Omega$, s.t. outcome $g(s_i(\theta_1), \ldots, s_N(\theta_N))$ is implemented given strategy profile $s = (s_1(\cdot), \ldots, s_N(\cdot))$.
- Game: The utility of player i from strategy profile s is $u_i(g(s(\theta)), \theta_i)$, which is denoted as $u_i(s, \theta_i)$.

The objective of a mechanism $M = (S, g)$ is to achieve the desired game outcome $f(\theta)$ such that

$$g(s_1^*(\theta_1), \ldots, s_N^*(\theta_N)) = f(\theta), \ \forall \theta \in \Theta^N \tag{3.47}$$

for an equilibrium strategy $(s_1^*, \ldots, s_N^*)$. The desired properties of a mechanism can be listed as follows.

- Efficiency: Select the outcome that maximizes total utility.
- Fairness: Select the outcome that achieves a certain fairness criterion in utility.
- Revenue maximization: Select the outcome that maximizes revenue to a seller (or more generally, utility to one of the players).
- Budget-balance: Implement outcomes that have balanced transfers across players.
- Pareto optimality: Implement only outcomes o^* for which for all $o' \neq o^*$, either $u_i(o';\theta_i) = u_i(o^*;\theta_i)$ for all i, or $\exists i \in \mathcal{I}$ with $u_i(o',\theta_i) < u_i(o^*,\theta_i)$.

In that which follows, we first discuss several design concepts, then we explain the revelation principle, and finally we explain the impossibility and possibility. The Groves mechanism is also studied as an example.

Equilibrium concepts

We define three equilibria concepts: Nash implementation, Bayes–Nash implementation, and dominant implementation, with increasing difficulty.

DEFINITION 50. *Nash implementation: Mechanism* $M=(S,g)$ *implements* $f(\theta)$ *in Nash equilibrium if, for all* $\theta \in \Theta$, $g(s^*(\theta))=f(\theta)$, *where* $s^*(\theta)$ *is a Nash equilibrium, i.e.,*

$$u_i(s_i^*(\theta_i), s_{-i}^*(\theta_{-i}), \theta_i) \geq u_i(s_i'(\theta_i), s'_{-i}(\theta_{-i}), \theta_i), \ \forall i, \forall \theta_i, \forall s_i' \neq s_i^*. \tag{3.48}$$

DEFINITION 51. *Bayes–Nash implementation: With common prior* $F(\theta)$, *mechanism* $M=(S,g)$ *implements* $f(\theta)$ *in Bayes–Nash equilibrium if, for all* $\theta \in \Theta$, $g(s^*(\theta)) = f(\theta)$, *where* $s^*(\theta)$ *is a Bayes–Nash equilibrium, i.e.,*

$$E_{\theta_{-i}}[u_i(s_i^*(\theta_i), s_{-i}^*(\theta_{-i}), \theta_i)] \geq E_{\theta_{-i}}[u_i(s_i'(\theta_i), s'_{-i}(\theta_{-i}), \theta_i)], \ \forall i, \forall \theta_i, \forall s_i' \neq s_i^*. \tag{3.49}$$

DEFINITION 52. *Dominant implementation: Mechanism* $M=(S,g)$ *implements* $f(\theta)$ *in a dominant-strategy equilibrium if, for all* $\theta \in \Theta$,

$g(s^*(\theta)) = f(\theta)$, *where* $s^*(\theta)$ *is a dominant-strategy equilibrium, i.e.,*

$$u_i(s_i^*(\theta_i), s_{-i}^*(\hat{\theta}_{-i}), \theta_i) \geq u_i(s_i'(\theta_i), s_{-i}'(\hat{\theta}_{-i}), \theta_i), \ \forall i, \forall \theta_i, \forall \hat{\theta}_{-i}, \forall s_i' \neq s_i^*. \tag{3.50}$$

Participation and incentive-compatibility

Next, we define three rationality concepts: ex-ante individual rationality, interim individual rationality, and ex-post individual rationality, with increasing difficulty.

Let $\bar{u}_i(\theta_i)$ denote the (expected) utility to player i with type θ_i as its outside option, and recall that $u_i(f(\theta); \theta_i)$ is the equilibrium utility of player i from the mechanism. We have the following three definitions of rationality.

- Ex-ante individual rationality: Players choose to participate before they know their own types,

$$E_{\theta \in \Theta}[u_i(f(\theta); \theta_i)] \geq E_{\theta_i \in \Theta_i}[\bar{u}_i(\theta_i)]. \tag{3.51}$$

- Interim individual rationality: Players can withdraw once they know their own type,

$$E_{\theta_{-i} \in \Theta_{-i}}[u_i(f(\theta, \theta_{-i}); \theta_i)] \geq \bar{u}_i(\theta_i). \tag{3.52}$$

- Ex-post individual rationality: Players can withdraw from the mechanism at the end,

$$u_i(f(\theta); \theta_i) \geq \bar{u}_i(\theta_i). \tag{3.53}$$

A special kind of mechanism is called the direct-revelation mechanism (DRM), which has a strategy space $S = \Theta$ and a player simply reports a type to the mechanism with outcome rule $g : \Theta \to \Omega$. For DRM, we have the following definitions for a mechanism being incentive-compatible and strategy-proof.

DEFINITION 53. *Incentive-compatible: A DRM is (Bayes–)Nash incentive-compatible if truth revelation is a (Bayes–)Nash equilibrium, i.e.,* $s_i^*(\theta_i) = \theta_i$, *for all* $\theta \in \Theta$.

DEFINITION 54. *Strategy-proof: A DRM is strategy-proof if truth revelation is a dominant-strategy equilibrium, for all* $\theta \in \Theta$.

The revelation principle

The revelation principle states that to any Bayesian Nash equilibrium there corresponds a Bayesian game with the same equilibrium outcome but in which players truthfully report type. The principle allows one to solve for a Bayesian equilibrium by assuming all players truthfully report type (subject to an incentive-compatibility constraint), which eliminates the need to consider either strategic behavior or lying. Therefore, no matter what the mechanism, a designer can confine his or her attention to equilibria in which players truthfully report type.

THEOREM 8. *For any mechanism, M, there is a direct, incentive-compatible mechanism with the same outcome.*

Proof. Consider a mechanism, $M = (S, g)$, that implements $f(\theta)$, in a dominant-strategy equilibrium. In other words, $g(s^*(\theta)) = f(\theta)$, for all $\theta \in \Theta$, where s^* is a dominant-strategy equilibrium. We construct the direct mechanism $M = (S, g)$. By contradiction, we suppose

$$\exists \theta_i' \neq \theta_i, \text{ s.t. } u_i(f(\theta_i', \theta_{-i}), \theta_i) > u_i(f(\theta_i, \theta_{-i}), \theta_i) \tag{3.54}$$

for some $\theta_i' \neq \theta_i$. But, because $f(\theta) = g(s^*(\theta))$, this implies that

$$u_i(g(s_i^*(\theta_i'), s_{-i}^*(\theta_{-i})), \theta_i) > u_i(g(s_i^*(\theta_i), s_{-i}^*(\theta_{-i})), \theta_i), \tag{3.55}$$

which contradicts the strategy-proof-ness of s^* in mechanism M. □

The practical implications are obvious for the above theorem. First, incentive-compatibility is free, i.e., any outcome implemented by mechanism M can be implemented by an incentive-compatible mechanism, M'. Second, fancy mechanisms are unnecessary, i.e., any outcome implemented by a mechanism with complex strategy space, S, can be implemented by a DRM.

Budget balance and efficiency

Before we define the budget balance, we first introduce transfers or side payments. Define the outcome space $\mathcal{O} = \mathcal{K} \times \mathbb{R}^N$, such that an outcome rule, $o = (k, t_1, \ldots, t_N)$, defines a choice, $k(s) \in \mathcal{K}$, and a transfer, $t_i(s) \in \mathbb{R}$ from player i to the mechanism, given strategy profile $s \in S$. For example, the utility can be written as

$$u_i(o, \theta_i) = v_i(k, \theta_i) - t_i, \tag{3.56}$$

where $v_i(k, \theta_i)$ is the value of player i and t_i is the payment (transfer) to the auctioneer.

DEFINITION 55. *Budget balance introduces constraints over the total transfers made from the players to the mechanism. Let $s^*(\theta)$ denote the equilibrium strategy of a mechanism. We have the following.*

(i) *Weak budget balance:*

(a) *ex post:* $\sum_t t_i(s^*(\theta)) \geq 0, \forall \theta$;

(b) *ex ante:* $E_{\theta \in \Theta}[\sum_t t_i(s^*(\theta))] \geq 0$.

(ii) *Strong budget balance:*

(a) *ex post:* $\sum_t t_i(s^*(\theta)) = 0, \forall \theta$;

(b) *ex ante:* $E_{\theta\in\Theta}[\sum_t t_i(s^*(\theta))] = 0$.

Obviously, strong budget balance is harder than weak budget balance, and ex post is harder than ex ante.

Next, we define the efficiency and discuss the tradeoff between efficiency and budget balance.

DEFINITION 56. *A choice rule,* $k^* : \Theta \to \mathcal{K}$, *is (ex post) efficient if, for all* $\theta \in \Theta$, $k^*(\theta)$ *maximizes the sum of individual value functions* $\sum_{k\in\mathcal{K}} v_i(k,\theta_i)$.

Unfortunately, according to the Green–Laffont impossibility theorem [112], if Θ allows all valuation functions from $\mathcal{K}$ to $\mathbb{R}$, then no mechanism can implement an efficient and ex-post budget-balanced dominant strategy. So we can (1) restrict the space of preferences, (2) drop budget-balance, (3) drop efficiency, or (4) drop the dominant strategy.

The Groves mechanism

Now, we discuss a special mechanism, the Groves mechanism, as an example.

DEFINITION 57. *A Groves mechanism,* $M = (\Theta, k, t_1, \ldots, t_N)$, *is defined with choice rule*

$$k^*(\hat{\theta}) = \arg\max_{k\in\mathcal{K}} \sum_i v_i(k,\hat{\theta}_i) \tag{3.57}$$

and transfer rule

$$t_i(\hat{\theta}) = h_i(\hat{\theta}_{-i}) - \sum_{j\neq i} v_j(k^*(\hat{\theta}),\hat{\theta}_j), \tag{3.58}$$

where $h_i(\cdot)$ is an (arbitrary) function that does not depend on the reported type, $\hat{\theta}_i$, of player i.

It has been proved that Groves mechanisms are strategy-proof and efficient [113]. Groves mechanisms are unique, in the sense that any mechanism that implements efficient choice, $k^*(\theta)$, in a truthful dominant strategy must implement Groves transfers.

Impossibility and possibility

For the different desired properties discussed so far, some combinations are possible, while others are impossible. We list some well-known results for impossibility and possibility as the following theorems.

THEOREM 9. The Gibbard–Satterthwaite impossibility theorem [114, 115]*: If agents have general preferences, and there are at least two agents, and at least three different optimal outcomes over the set of all agent preferences, then a social-choice function is dominant-strategy implementable if and only if it is dictatorial (i.e., one (or more) of the agents will always receive one of its most preferred alternatives).*

THEOREM 10. The Hurwicz impossibility theorem [116]: *It is impossible to implement an efficient, budget-balanced, and strategy-proof mechanism in a simple exchange economy* [3] *with quasi-linear preferences.*

THEOREM 11. The Myerson–Satterthwaite theorem [117]: *It is impossible to achieve allocative efficiency, budget balance, and (interim) individual rationality in a Bayesian–Nash incentive-compatible mechanism, even with quasi-linear utility functions.*

An interesting extension of the Groves mechanism, the dAGVA (or "expected Groves" [118, 119]) mechanism demonstrates that it is possible to achieve efficiency and budget balance in a Bayesian–Nash equilibrium, even though this is impossible in a dominant-strategy equilibrium (the Hurwicz

impossibility theorem). However, the dAGVA mechanism is not individual rational, which we should expect by virtue of the Myerson–Satterthwaite impossibility theorem.

3.7.3 VCG auctions

A Vickrey auction [120] is a type of sealed-bid auction, in which bidders (players) submit written bids without knowing the bids of the other people in the auction. The highest bidder wins, but the price paid is the second-highest bid. This type of auction was created by William Vickrey. It is strategically similar to an English auction, and it gives bidders an incentive to bid their true value.

If only a single, indivisible good is being sold, the terms Vickrey auction and second-price sealed-bid auction are equivalent, and they are used interchangeably. When multiple identical units (or a divisible good) are being sold in a single auction, the most obvious generalization is to have all winning bidders pay the amount of the highest non-winning bid. This is known as a uniform-price auction. The uniform-price auction does not, however, result in bidders bidding their true valuations as they do in a second-price auction unless each bidder has demand for only a single unit. A generalization of the Vickrey auction that maintains the incentive to bid truthfully is known as the Vickrey–Clarke–Groves (VCG) mechanism [120]. The idea here is that each player in the auction pays the opportunity cost that their presence introduces to all the other players. Next, we formally define the VCG auction and explain some of its properties.

DEFINITION 58. *The VCG mechanism implements an efficient outcome,* $k^* = \max_k \sum_j v_j(k, \hat{\theta}_j)$*, and computes transfers*

$$t_i(\hat{\theta}) = \sum_{j \neq i} v_j(k^{-i}, \hat{\theta}_j) - \sum_{j \neq i} v_j(k^*, \hat{\theta}_j), \tag{3.59}$$

where $k^{-i} = \max_k \sum_{j \neq i} v_j(k, \hat{\theta}_j)$.

In other words, the payment equals the performance loss of all other users because of including user *i*.

For example, suppose two apples are being auctioned among three bidders. Bidder A wants one apple and bids $5 for that apple. Bidder B wants one apple and is willing to pay $2 for it. Bidder C wants two apples and is willing to pay $6 to have both of them, but is uninterested in buying only one without the other. First, the outcome of the auction is determined by maximizing bids: The apples go to bidder A and bidder B. Next, to decide payments, the opportunity cost each bidder imposed on the rest of the bidders is considered. Currently, B has a utility of $2. If bidder A had not been present, C would have won, and had a utility of $6, so A pays $6–$2 = $4. For the payment of bidder B, currently A has a utility of $5 and C has a utility of 0. If bidder B had been absent, C would have won and had a utility of $6, so B pays $6–$5 = $1. The outcome is identical whether or not bidder C participates, so C does not need to pay anything.

In a Vickrey auction with independent private values (IPVs), each bidder maximizes her expected utility by bidding (revealing) her true valuation. A Vickrey auction is ex-post efficient (the winner is the bidder with the highest valuation) under the most general circumstances; it thus provides a baseline model against which the efficiency properties of other types of auctions can be compared. The auction is also strategy-proof. Owing to the above strengths, VCG auctions are widely used in wireless networking, especially in situations where it is important to prevent players from lying.

Despite the strengths of the Vickrey auction, it has the following shortcomings.

- It does not allow for price discovery – that is, discovery of the market price if the buyers are unsure of their own valuations – without sequential auctions.
- Sellers may use shill bids to increase profit.
- In iterated Vickrey auctions, the strategy of revealing true valuations is no longer dominant.

The VCG mechanism has the following additional shortcomings.

- It is vulnerable to collusion by losing bidders.
- It is vulnerable to shill bidding with respect to the buyers.
- It does not necessarily maximize seller revenues; seller revenues may even be zero in VCG auctions. If the purpose of holding the auction is to maximize profit for the seller rather than just allocate resources among buyers, then VCG may be a poor choice.
- The seller's revenues are non-monotonic with regard to the sets of bidders and offers.

3.7.4 Share auctions

A share auction [121, 122, 123] is concerned with allocating a perfectly divisible good among a set of bidders. The most commonly used example in the literature comes from the financial markets (such as the auction of treasury notes) [124, 125, 126]. Other examples include the allocation of emission permits [127] and the sale of electricity [128]. There are two basic pricing structures in a share auction. In a uniform-price auction, all the winners (typically more than one) get some portions of the good and pay the same unit price. In a discriminatory pricing auction (sometimes called pay-your-bid auction [122]), winning bids are filled at the bid price. The papers mentioned above largely focus on examining how different pricing and information structures affect the auction results, such as the final price, the seller's revenue, and the allocations of the divisible good.

Compared with the well-studied single-unit good auction, in which bidders typically submit one-dimensional bids in the auction, some share auctions allow bidders to submit multiple combinations of price and quantity as the bids (e.g., [124, 125, 127]). This significantly complicates the auction design since the bidders have large strategy spaces. When using a share auction to allocate resources such as bandwidth in communication networks, researchers typically adopt simple one-dimensional bidding rules as in [129, 130, 131, 132, 133]. The allocation is proportional to the bids. Some researchers have been focusing on developing bounds of efficiency loss in such simple bidding games: Johari and Tsitsiklis [129] show that with a

uniform-pricing scheme the Nash equilibrium (NE) of a share auction achieves at least $3/4$ of the total utility at a socially optimal solution. Yang and Hajek [130] and Maheswaran and Basar [131] advance the results further by showing that more complex pricing functions can reduce the efficiency loss to zero under certain conditions on the bidders' utility functions. Maheswaran and Basar have considered several network-resource-allocation games using share auctions, with a focus on studying the effects of coalition [132] or designing decentralized negotiation methods [133].

Let us consider how a share auction can be used in spectrum sharing. We consider the case in which there is a measurement point in the network. The aggregated interference generated by all users at the measurement point should not be larger than a threshold P, i.e., $\sum_{i=1}^{i} p_i \leq P$. Here, p_i is the allocated power for the ith user.

In a share auction, users submit one-dimensional bids b_i representing their willingness to pay, and the manager simply allocates the available resource P in proportion to the bids. The users then pay an amount proportional to their performance gain γ_i. The manager announces a non-negative reserve bid β. In contrast to the situation in which the manager submits a reserve bid to extract more revenue from the other bidders [134], here the main purpose of the reserve bid is to guarantee a unique desirable outcome of the auction. A share auction mechanism can be expressed as follows.

(i) The manager announces a reserve bid $\beta \geq 0$, and a price $\pi > 0$.

(ii) After observing β and π, user i submits a bid $b_i \geq 0$.

(iii) The resources are allocated to each user i, and its share p_i is proportional to its bid, i.e.,

$$p_i = \frac{\beta}{\sum_i b_i + \beta} P. \tag{3.60}$$

The resulting performance of user i is γ_i.

For example, if P is the overall transmitted power, for the interference case, we can have the resulting SINR for user i as

$$\gamma_i(\mathbf{p}) = \frac{p_i h_{ii}}{n_0 + \sum_{j \neq i} p_j h_{ji}}, \tag{3.61}$$

where h_{ij} is the channel gain for user i to receiver j and n_0 is the noise level.

(iv) In a share auction, user i pays $C_i = \pi \gamma_i$.

A *bidding profile* is the vector containing the users' bids $\mathbf{b} = (b_1, \ldots, b_N)$. The *bidding profile of user i's opponents* is defined as $b_{-i} = (b_1, \ldots, b_{i-1}, b_{i+1}, \ldots, b_N)$, so that $\mathbf{b} = (b_i; b_{-i})$. Typically, each user i submits a bid b_i to maximize its *surplus function*

$$S_i(b_i; b_{-i}) = U_i(\gamma_i(b_i; b_{-i})) - C_i.$$

Here, we omit the dependence on β and π. An NE of the auction is a fixed point of all users' best responses.

These auction mechanisms differ from some previously proposed auction-based network-resource-allocation schemes (e.g., [129, 131]) in that the bids here are not the same as the payments. Instead, the bids are signals of willingness to pay. The manager can, therefore, influence the NE by choosing β and π. This alleviates the typical inefficiency of the NE and in some cases allows us to achieve socially optimal solutions.

Under a properly chosen price π, the share auction can achieve fair (or efficient) allocation. In a fair allocation, users achieve their performances

satisfying some predefined fairness criteria. In an efficient allocation, the total utility of the network is maximized.

3.7.5 Double auctions

In a double auction [135], there are I buyers and N sellers. Each buyer i wants to purchase x_i items, and each seller n wants to sell y_n items. The information about x_i and y_n is available publicly. In a double auction, a buyer i reports price $p_i^{(b)}$ (i.e., bidding price), while a seller n reports price $p_n^{(s)}$ (i.e., an asking price). These prices are per unit item. Without loss of generality, we may assume $p_1^{(b)} \geq p_2^{(b)} \geq \cdots \geq p_I^{(b)}$ and $p_1^{(s)} \leq p_2^{(s)} \leq \cdots \leq p_N^{(s)}$. Note that, if two prices are equal, their indexes are interchangeable. Also, each seller or each buyer can set different prices for different items, where the seller and buyer sells and buys each item separately.

To determine the trading price in a double auction, the demand quantities from all buyers are arranged according to ascending price order. Similarly, the supply quantities from all sellers are arranged according to descending price order (Figure 3.3). At the trading point T^*, the aggregate demand and supply intersect, and hence K sellers will sell T^* items to L buyers. There are two cases to determine the trading price and the quantity traded.

- *Case 1:* The bidding and asking prices satisfy the condition $p_{i'}^{(b)} \geq p_{n'}^{(s)} \geq p_{i'+1}^{(b)}$ and aggregate demand and supply satisfy $\sum_{n=1}^{n'-1} y_n \leq \sum_{i=1}^{i'} x_i \leq \sum_{n=1}^{n'} y_n$. In this case, the sellers $n = \{1, \ldots, n'\}$ sell all their items y_n at price $p_{n'}^{(s)}$, and the buyers $i = \{1, \ldots, i'\}$ buy at price $p_{i'}^{(b)}$. Each buyer buys a quantity $\left\lfloor x_i - \left(\sum_{j=1}^{i'-1} x_j - \sum_{j=1}^{n'-1} y_j\right) / (i'-1) \right\rfloor$, where $\lfloor x \rfloor$ denotes the floor function.
- *Case 2:* The bidding and asking prices satisfy the condition $p_{n'+1}^{(s)} \geq p_{i'}^{(b)} \geq p_{i'}^{(s)}$ and aggregate demand and supply satisfy $\sum_{i=1}^{i'-1} x_i \leq \sum_{n=1}^{n'} y_n \leq \sum_{i=1}^{i'} x_i$. In this case, the buyers $i = \{1, \ldots, i'\}$ buy at price $p_{i'}^{(b)}$, and the sellers $n = \{1, \ldots, n'\}$ sell at price $p_{n'}^{(s)}$. Each seller sells with quantity $\left\lfloor y_n - \left(\sum_{j=1}^{n'-1} y_j - \sum_{j=1}^{i'-1} x_j\right) / (n'-1) \right\rfloor$.

However, when a central controller is available in this double auction, an optimization problem can be formulated to obtain the quantity of items to be traded. Let the reserved price of each buyer and seller be fixed and denoted

by $\hat{p}_i^{(b)}$ and $\hat{p}_n^{(s)}$. Let $\hat{x}_{i,n}$ and $\hat{p}_{i,n}$ be the solutions in terms of the quantity for buyer i to buy from seller n and the trading price, respectively. The utility of buyer i from a double auction can be defined as

$$U_i^{(b)} = \sum_{n=1}^{\hat{n}} (p_i^{(b)} - \hat{p}_{i,n})\hat{x}_{i,n}, \tag{3.62}$$

and that of seller n is defined as

$$U_n^{(s)} = \sum_{i=1}^{\hat{i}} (\hat{p}_{i,n} - p_n^{(s)})\hat{x}_{i,n}. \tag{3.63}$$

To maximize the utility of both seller and buyer, an optimization can be formulated as a linear-programming problem as follows:

$$\max \sum_{i=1}^{\hat{i}} \sum_{n=1}^{\hat{n}} \hat{x}_{i,n} \left(p_i^{(b)} - p_n^{(s)} \right), \tag{3.64}$$

$$\text{s.t.} \sum_{i=1}^{\hat{i}} \hat{x}_{i,n} \le y_n, \forall n, \sum_{n=1}^{\hat{n}} \hat{x}_{i,n} \le x_i, \forall i, \hat{x}_{i,n} \ge 0, \forall i, n. \tag{3.65}$$

The constraints limit the quantity of the item to be traded less than the supply and demand quantities for the seller and buyer, respectively.

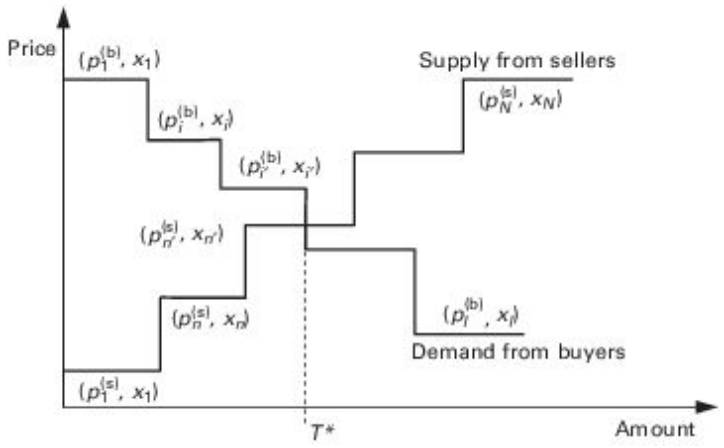

Figure 3.3. An example of ordered demand and supply in a double auction.

3.8 Contract theory

In economics, contract theory studies how economic actors can and do construct contractual arrangements, generally in the presence of asymmetric information [136]. In the field of economics, the first formal treatment of this topic was given by Kenneth Arrow in the 1960s. Recently, it has attracted more attention from researchers in communication-related areas. In the area of cognitive radio networks (CRNs), the authors of a number of works have already developed contract-theoretic techniques such as those in [137], [138], and [139].

Usually contract theory can be used to model the relationship between employer(s) and employee(s), such as a manager hiring a worker, a farmer hiring a sharecropper, or a company owner hiring a manager. In fact, besides the actors on the two sides, we also could note that there is a court between the two parties who operate in a market economy with a well-functioning legal system. The penalties for breaching the contract will be assumed to be sufficiently severe that no contracting party will ever consider the possibility of not honoring the contract.

There exist many forms of transactions in contract theory. If the transaction is a simple exchange of goods or services for money, then the

typical problems to solve in the model could be as follows. What is the price per unit the parties shall agree on? Does the contract specify rebates? Are there penalty clauses for late delivery? If so, what form do they take? The transaction could even be an insurance contract that does not involve any exchange of goods or services. In this model, we should determine how the terms vary with the underlying risk, with the risk aversion of the parties or with the private information the insuree, or the insurer, might have about the exact nature of the risk.

Basically, we can categorize contract theory by the number of contracting groups. Generally we have bilateral contracting and multilateral contracting problems. Bilateral contracting is the commonest and easiest, while multilateral contracting is more complex. An auction is a typical example of a multilateral contracting problem. In the following, we first discuss some basic concepts, and then we discuss one simple example for bilateral contracting. For a more comprehensive study of contract theory, please refer to [140].

3.8.1 Information and incentives

Even in the best possible contracting environments, it is unlikely that employees will be perfectly insured against business risks. The equilibrium price of such insurance would be too high if employers were also averse to risk. Thus, employees are likely to get only limited insurance since there need to be adequate incentives to make then work. If their pay were independent of performance and their job security were not affected by their performance, then why should they put any effort into their work? Thus, it is critical to find the tradeoff between incentives and insurance.

To find the balance between the two, we should answer the following questions. How far should employee insurance be scaled back to make way for adequate work incentives? How could adequate work incentives be structured while preserving job security as much as possible?

Having observed the activities of players, two general types of incentive problems have been distinguished. The first type is hidden-information

problems, also referred to as adverse selection, in which the employee may have private information about her inability or unwillingness to take on certain tasks. The other type is hidden-action problems, also called moral hazard, in which the information about some relevant characteristics of the employee, such as their distaste for certain tasks, how hard they work, and how careful they are, is hidden from their employer.

3.8.2 Bilateral contracting

We start to introduce the basic idea of contract theory with the simplest form of contracting: bilateral contracting. We will generally explain the idea of bilateral contracting by presenting three basic examples. We start from the simplest ideal contracting, passing thereafter to contracting with uncertainty added, which is a more general case.

Optimal contracts without uncertainty

Consider a market in which the employer gets no employee time but has all the money, and the employee has all of her time for herself but has no money before any trade. In this initial state, the employer and employee each achieves a utility of $\hat{U} = U(0, 1)$ and $\hat{u} = u(1, 0)$.

When the two start to trade, both individuals can increase their joint payoff by exchanging labor services l for money/output. Thus, the utility functions of the employer and employee can be written as $U(l, t)$ and $u(l, t)$. Both of the utility functions are strictly increasing and concave.

Thus, the highest possible utility that the employee can receive in this ideal scenario is

$$\begin{aligned} \max \quad & u(l_2, t_2), \\ \text{subject to} \quad & U(1 - l_2, 1 - t_2) \geq \hat{U}. \end{aligned} \tag{3.36}$$

The highest payoff for the employer is

$$\begin{aligned} \max \quad & U(l_1, t_1), \\ \text{subject to} \quad & u(1 - l_1, 1 - t_1) \geq \hat{u}. \end{aligned} \tag{3.37}$$

Optimal contracts under uncertainty

Pure insurance: In reality, there exists uncertainty that cannot be described by the previous example. In the contract of insurance, employees are insured against economic downturns. A question concerning these insurance schemes is how much risk should be absorbed by employers, and how much by employees. So, to enrich the previous example by introducing uncertainty, we are going to analyze the question of optimal risk allocation.

Let us consider two possible future states of nature, θ_{L} and θ_{H}. θ_{L} represents an adverse output shock, or a "recession." θ_{H} represents a good output realization, or a "boom". In a pure insurance problem without production, we disregard time endowments in the time/output bundles (l, t), and adopt the consumption bundles $(t_{\mathrm{L}}, t_{\mathrm{H}})$ instead. The state of nature influences only the value of the outputs $E(t_{\mathrm{L}}, t_{\mathrm{H}})$ for the employer and $e(t_{\mathrm{L}}, t_{\mathrm{H}})$ for the employee.

Thus, the optimization problem is

$$\max E(t_{\mathrm{L}}, t_{\mathrm{H}}) + e(t_{\mathrm{L}}, t_{\mathrm{H}}). \tag{3.68}$$

Given the first-order conditions, we could have $E_{\mathrm{L}} + e_{\mathrm{L}} = 0 = E_{\mathrm{H}} + e_{\mathrm{H}}$. Thus,

$$E_{\mathrm{L}}/E_{\mathrm{H}} = e_{\mathrm{L}}/e_{\mathrm{H}}. \tag{3.69}$$

The joint surplus maximization is achieved when the marginal rates of substitution between the states of nature θ_{L} and θ_{H} for both individuals are equalized. Pure exchange under certainty can be transposed entirely to the case with uncertainty.

Von Neumann–Morgenstern utility functions: Indeed, there are two important elements hidden in the optimal insurance contract, which are the ex-post utility once the state of nature has been realized and the probability of each state occurring.

The ex-post utility functions can be defined as $U(t)$ for the employer and $u(t)$ for the employee. $P_j \in (0, 1)$ is the probability of occurrence of any particular state of nature θ_j. Thus, the ex-ante utility function is the expectation over ex-post utility outcomes, which can be written as

$$E(t_{1\mathrm{L}}, t_{1\mathrm{H}}) = p_L U(t_{1\mathrm{L}}) + p_H U(t_{1\mathrm{H}}), \tag{3.70}$$

$$e(t_{2\mathrm{L}}, t_{2\mathrm{H}}) = p_L u(t_{2\mathrm{L}}) + p_H u(t_{2\mathrm{H}}). \tag{3.71}$$

Optimal employment contracts under uncertainty: With the framework of the von Neumann and Morgenstern utility function, we can extend to our analysis optimal employment contracts under the uncertainty problem with two goods, leisure l and a consumption good t.

First, we use $(l_{1\mathrm{L}}, t_{1\mathrm{L}})$ and $(l_{1\mathrm{H}}, t_{1\mathrm{H}})$ to represent two different state-contingent time/output bundles of the employer. Similarly, we use $(l_{2\mathrm{L}}, t_{2\mathrm{L}})$ and $(l_{2\mathrm{H}}, t_{2\mathrm{H}})$ to denote the two different state-contingent time/output bundles of the employee. In addition, (l'_{ij}, t'_{ij}) denotes the initial endowments, where $i = 1, 2; j = \mathrm{L}, \mathrm{H}$.

Thus, the optimal contracting problem for the employer is

$$\max \quad [p_{\mathrm{L}} U(l_{1\mathrm{L}}, t_{1\mathrm{L}}) + p_{\mathrm{H}} U(l_{1\mathrm{H}}, t_{1\mathrm{H}})], \tag{3.72}$$

$$\begin{aligned} \text{subject to} \quad & p_{\mathrm{L}} u(l_{2\mathrm{L}}, t_{2\mathrm{L}}) + p_{\mathrm{H}} u(l_{2\mathrm{H}}, t_{2\mathrm{H}}) \hat{u}, \\ & l_{1j} + l_{2j} l'_{1j} + l'_{2j}, \\ & t_{1j} + t_{2j} l'_{1j} + l'_{2j}, \end{aligned} \tag{3.73}$$

where $\hat{u} = p_L u(li_{2L}, l'_{2L}) + p_H u(l'_{2H}, l'_{2H})$.

3.9 Bayesian games with imperfect information

In game theory, a Bayesian game is one in which information about the characteristics of the other players (i.e., payoffs) is incomplete. Following John C. Harsanyi's framework, a Bayesian game can be modeled by introducing Nature as a player in a game. Nature assigns to each player a random variable, which could take values of types for each player, and associates probabilities or a probability density function with those types (in the course of the game, Nature randomly chooses a type for each player according to the probability distribution across each player's type space). Harsanyi's approach to modeling a Bayesian game in such a way allows games of incomplete information to become games of imperfect information (in which the history of the game is not available to all players). The type of a player determines that player's payoff function and the probability associated with the type is the probability that the player for whom the type is specified is that type. In a Bayesian game, the incompleteness of information means that at least one player is unsure of the type (and so the payoff function) of another player.

Such games are called Bayesian because of the probabilistic analysis inherent in the game. Players have initial beliefs about the type of each player (where a belief is a probability distribution over the possible types for a player) and can update their beliefs according to Bayes' rule as play takes place in the game; i.e., the belief a player holds about another player's type might change on the basis of the actions they have played. The lack of information held by players and modeling of beliefs mean that such games are also used to analyze imperfect information scenarios.

In this section, we discuss the impacts of imperfect information on the normal and extensive forms of game in the following two subsections.

3.9.1 Bayesian games in normal form

As shown in the previous section, the normal-form representation of a non-Bayesian game with perfect information is a specification of the strategy spaces and payoff functions of players. A strategy for a player is a complete plan of action that covers every contingency of the game, even if that contingency can never arise. The strategy space of a player is thus the set of all strategies available to a player. A payoff function is a function from the set of strategy profiles to the set of payoffs (normally the set of real numbers), where a strategy profile is a vector specifying a strategy for every player.

In a Bayesian game, it is necessary to specify the strategy spaces, type spaces, payoff functions, and beliefs for every player. A strategy for a player is a complete plan of actions that covers every contingency that might arise for every type that player might be. A strategy must specify not only the actions of the player given the type that she is, but also the actions that she would take if she were of another type. A type space for a player is just the set of all possible types of that player. The beliefs of a player describe the uncertainty of that player about the types of the other players. Each belief is the probability of the other players having particular types, given the type of the player with that belief (i.e., the belief is Prob(types of other players given the type of this player)). A payoff function is a two-place function of strategy profiles and types. If a player has payoff function $u(x, y)$ and he is of type t, the payoff he receives is $u(x^*, t)$, where x^* is the strategy profile played in the game (i.e., the vector of strategies played). The formal definition of a Bayesian game is given as follows.

DEFINITION 59. *A game of incomplete information is defined as follows.*

(i) *Set of players:* $i \in \{1, 2, \ldots, N\}$.

(ii) *Actions available to player i:* A_i *for* $i \in \{1, 2, \ldots, N\}$. *Let* $a_i \in A_i$ *denote a typical action for player i.*

(iii) *Sets of possible types for all players:* T_i *for* $i \in \{1, 2, \ldots, N\}$. *Let* $t_i \in T_i$ *denote a typical type of player i.*

(iv) *Let* $\mathbf{a} = (a_1, \ldots, a_N)$, $\mathbf{t} = (t_1, \ldots, t_N)$, $\mathbf{a}_{-i} = (a_1, \ldots, a_{i-1}, a_{i+1}, \ldots, a_N)$, $\mathbf{t}_{-i} = (t_1, \ldots, t_{i-1}, t_{i+1}, \ldots, t_N)$.

(v) *Nature's move:* $\mathbf{t}$ *is selected according to a joint probability distribution* $p(\mathbf{t})$ *on* $T = T_1 \times \cdots \times T_N$.

(vi) *Strategies:* $s_i : T_i \to A_i$, *for* $i \in \{1, 2, \ldots, N\}$. $s_i(t_i) \in A_i$ *is then the action that type* t_i *of player i takes.*

(vii) *Payoff:* $u_i(a_1, \ldots, a_N; t_1, \ldots, t_N)$.

The game proceeds as follows. First, Nature chooses $\mathbf{t}$ according to probability Prob($\mathbf{t}$). Then each player i observes realized type $\hat{t}_i$ and updates its belief: Each player comes up with a conditional probability on remaining types conditional on $t_i = \hat{t}_i$; denote the distribution on $\mathbf{t}_{-i}$ conditional on $\hat{t}_i$ by $p_i(\mathbf{t}_{-i}|\hat{t}_i)$. Finally, the players take actions simultaneously.

The expected payoff is calculated as follows. Given strategy s_i, type t_i of player i plays action $s_i(t_i)$. With a vector of type $\mathbf{t} = (t_1, \ldots, t_N)$ and strategies $(s_1, \ldots, s_N)$, the realized action profile is $(s_1(t_1), \ldots, s_N(t_N))$. Player i of type $\hat{t}_i$ has beliefs about types of other players given by conditional probability distribution $p_i(\mathbf{t}_{-i}|\hat{t}_i)$. The expected payoff of action s_i is

$$\sum_{\mathbf{t}:t_i=\hat{t}_i} u_i(s_i, \mathbf{s}_{-i}(\mathbf{t}_{-i}), \mathbf{t}) p_i(\mathbf{t}_{-i}|\hat{t}_i). \tag{3.74}$$

The action $s_i(\hat{t}_i)$ for player i is a best response to $\mathbf{s}_{-i}(\mathbf{t}_{-i})$ if and only if, for all $s_i' \in A_i$,

$$\sum_{\mathbf{t}:t_i=\hat{t}_i} u_i(s_i(\hat{t}_i), \mathbf{s}_{-i}(\mathbf{t}_{-i}), \mathbf{t}) p_i(\mathbf{t}_{-i}|\hat{t}_i) \geq \sum_{\mathbf{t}:t_i=\hat{t}_i} u_i(s_i', \mathbf{s}_{-i}(\mathbf{t}_{-i}), \mathbf{t}) p_i(\mathbf{t}_{-i}|\hat{t}_i). \tag{3.75}$$

Using the above equation, we introduce the solution concept of a Bayesian game, namely, Bayesian Nash equilibrium, as follows.

DEFINITION 60. *A strategy profile* $(s_1(t_1), \ldots, s_N(t_N))$ *is a Bayesian Nash equilibrium if* $s_i(t_i)$ *is a best response to* $\mathbf{s}_{-i}(\mathbf{t}_{-i})$ *for all* $t_i \in T_i$ *and for all i. In other words, the action specified by the strategy of any given player has to be optimal given the strategies of all other players and beliefs of the player.*

In a non-Bayesian game, a strategy profile is a Nash equilibrium if every strategy in that profile is a best response to every other strategy in the profile, i.e., there is no strategy that a player could play that would yield a higher payoff, given all the strategies played by the other players. In a Bayesian game (where players are modeled as risk-neutral), rational players are seeking to maximize their expected payoff, given their beliefs about the other players (in the general case, where the players may be risk-averse or risk-loving, the assumption is that the players are utility-maximizing). A Bayesian Nash equilibrium is defined as a strategy profile and beliefs specified for each player about the types of the other players that maximizes the expected payoff for each player, given their beliefs about the other players' types and given the strategies played by the other players.

Next, we give an example on Cournot competition with privately known cost. Suppose there are two firms which compete by deciding simultaneously on quantities $q1$ and $q2$. One firm has a known marginal cost of 2; the other firm may have either a high or a low cost: $t_2 = t_{\mathrm{H}} = 3$ with probability 0.5 and $t_2 = t_{\mathrm{L}} = 1$ with probability 0.5. The price as function of quantities is $P = 4 - q_1 - q_2$. The question is what is the Bayesian Nash equilibrium. Suppose $q_2^{\mathrm{H}}, q_2^{\mathrm{L}}, q_1$ is an equilibrium if

$$q_2^{\mathrm{H}} = \arg\max_{q_2^{\mathrm{H}}} (4 - q_1 - q_2^{\mathrm{H}}) q_2^{\mathrm{H}} - 3q_2^{\mathrm{H}}, \tag{3.76}$$

$$q_2^{\mathrm{L}} = \arg\max_{q_2^{\mathrm{L}}} (4 - q_1 - q_2^{\mathrm{L}}) q_2^{\mathrm{L}} - q_2^{\mathrm{L}}, \tag{3.77}$$

$$q_1 = \arg\max_{q_1} \frac{1}{2}[(4 - q_1 - q_2^{\mathrm{H}})q_1 - 2q_1] + \frac{1}{2}[(4 - q_1 - q_2^{\mathrm{L}})q_1 - 2q_1]. \tag{3.78}$$

Using the first-order condition, we can get the Bayesian Nash equilibrium solution $q_1 = \frac{2}{3}$, $q_2^{\mathrm{L}} = \frac{7}{6}$, and $q_2^{\mathrm{H}} = \frac{1}{6}$.

3.9.2 Bayesian games in extensive games

The solution concept of Bayesian Nash equilibrium yields an abundance of equilibria in dynamic games, when no further restrictions are placed on players' beliefs. This makes Bayesian Nash equilibrium an incomplete tool to analyze dynamic games of incomplete information.

Bayesian Nash equilibrium results in some implausible equilibria in dynamic games, where players take turns sequentially rather than simultaneously. Similarly, implausible equilibria might arise in the same way as implausible Nash equilibria arise in games with perfect and complete information such as incredible threats and promises. Such equilibria might be eliminated in perfect- and complete-information games by applying subgame-perfect Nash equilibrium. However, it is not always possible to use this solution concept in incomplete-information games because such games contain non-singleton information sets. Since subgames must contain complete information sets, sometimes there is only one subgame – the entire game – and so every Nash equilibrium is trivially subgame perfect. Even if a game does have more than one subgame, the inability of subgame perfection to cut through information sets can result in implausible equilibria not being eliminated.

To refine the equilibria generated by the Bayesian-Nash-solution concept or subgame perfection, one can apply the perfect-Bayesian-equilibrium (PBE) solution concept. PBE is in the spirit of subgame perfection in that it demands that subsequent play be optimal. However, it places player beliefs on decision nodes that enables moves in non-singleton information sets to be dealt with more satisfactorily.

DEFINITION 61. *A perfect Bayesian equilibrium is a strategy profile and a set of beliefs for each player,* (s^C, i^C) *such that*

(i) *at every information set* I_i*, player i's strategy maximizes its payoff, given actions of all other players and player i's beliefs;*

(ii) *at information sets reached with positive probability when* s^C *is played, beliefs are formed according to* s^C *and Bayes' rule when necessary; and*

(iii) *at information sets that are reached with probability zero when* s^C *is played, beliefs may be arbitrary but must be formed according to Bayes' rule when possible.*

So far in our discussion on Bayesian games, it has been assumed that information is perfect (or, if imperfect, play is simultaneous). In examining dynamic games, however, it might be necessary to have the means to model imperfect information. PBE affords this means: Players place beliefs on nodes occurring in their information sets, which means that the information set can be generated by Nature (in the case of incomplete information) or by other players (in the case of imperfect information).

The beliefs held by players in Bayesian games can be approached more rigorously in PBE. A belief system is an assignment of probabilities to every node in the game such that the sum of probabilities in any information set is 1. The beliefs of a player are exactly those probabilities of the nodes in all the information sets at which that player has the move (a player's belief might be specified as a function from the union of his information sets to [0,1]). A belief system is consistent for a given strategy profile if and only if the probability assigned by the system to every node is computed as the probability of that node being reached given the strategy profile, i.e., by Bayes' rule.

The notion of sequential rationality is what determines the optimality of subsequent play in PBE. A strategy profile is sequentially rational at a

particular information set for a particular belief system if and only if the expected payoff of the player whose information set it is (i.e., whose move it is at that information set) is maximal given the strategies played by all the other players. A strategy profile is sequentially rational for a particular belief system if it satisfies the above for every information set.

Next, let us consider the example shown in Figure 3.1, in which information is imperfect since player 2 does not know what player 1 does when she comes to play. If both players are rational and both know that both players are rational and everything that is known by any player is known to be known by every player (i.e., player 1 knows player 2 knows that player 1 is rational and player 2 knows this, etc.), play in the game will be as follows according to perfect Bayesian equilibrium.

Player 2 cannot observe player 1's move. Player 1 would like to fool player 2 into thinking she has played U when she has actually played D so that player 2 will play D′ and player 1 will receive 3. In fact, in the second game there is a perfect Bayesian equilibrium where player 1 plays D and player 2 plays U′, and player 2 holds the belief that player 1 will definitely play D (i.e., player 2 places a probability of 1 on the node reached if player 1 plays D). In this equilibrium, every strategy is rational given the beliefs held and every belief is consistent with the strategies played. In this case, the perfect Bayesian equilibrium is the only Nash equilibrium.

Sequential equilibrium is a refinement of Nash equilibrium for extensive-form games due to David M. Kreps and Robert Wilson [141]. A sequential equilibrium specifies not only a strategy for each of the players but also a belief for each of the players. A belief gives, for each information set of the game belonging to the player, a probability distribution on the nodes in the information set. A profile of strategies and beliefs is called an assessment for the game. Informally speaking, an assessment is a sequential equilibrium if its strategies are sensible given its beliefs and its beliefs are sensible given its strategies.

The formal definition of a strategy being sensible given a belief is straightforward; the strategy should simply maximize the expected payoff in

every information set. It is also straightforward to define what a sensible belief should be for those information sets that are reached with positive probability given the strategies; the beliefs should be the conditional probability distribution on the nodes of the information set, given that it is reached.

It is far from straightforward to define what a sensible belief should be for those information sets that are reached with probability zero, given the strategies. Indeed, this is the main conceptual contribution of Kreps and Wilson [141]. Their consistency requirement is the following: The assessment should be a limit point of a sequence of totally mixed strategy profiles and associated sensible beliefs, in the above straightforward sense.

Sequential equilibrium is a further refinement of subgame-perfect equilibrium and even perfect Bayesian equilibrium. It is itself refined by extensive-form trembling-hand perfect equilibrium. Strategies of sequential equilibria (or even extensive-form trembling-hand perfect equilibria) are not necessarily admissible. A refinement of sequential equilibrium that guarantees admissibility is a quasi-perfect equilibrium.

3.10 Other special types of games

In this section, we investigate several important special games that are widely used to model wireless networking problems.

3.10.1 Zero-sum games

First, we discuss the zero-sum game that appears widely in daily life. In game theory and economic theory, the term zero-sum describes a situation in which a participant's gain or loss is exactly balanced by the losses or gains of the other participant(s). It is so named because, when the total gains of the participants are added up, and the total losses are subtracted, they will sum to zero. "Go" is an example of a zero-sum game: It is impossible for both players to win. Zero-sum can be thought of more generally as constant-sum where the benefits and losses to all players sum to the same value of money

and pride and dignity. Cutting a cake is zero- or constant-sum because taking a larger piece reduces the amount of cake available for others. In contrast, non-zero-sum describes a situation in which the interacting parties' aggregate gains and losses are either less than or more than zero.

Situations where participants can all gain or suffer together, such as a country with an excess of bananas trading with another country for their excess of apples, where both benefit from the transaction, are referred to as non-zero-sum. Other non-zero-sum games are games in which the sum of gains and losses by the players is always more or less than what they began with. For example, a game of poker, disregarding the house's rake, played in a casino is a zero-sum game unless the pleasure of gambling or the cost of operating a casino is taken into account, making it a non-zero-sum game.

The concept was first developed in game theory and consequently zero-sum situations are often called zero-sum games, though this does not imply that the concept, or game theory itself, applies only to what are commonly referred to as games. In pure strategies, each outcome is Pareto optimal (generally, any game where all strategies are Pareto optimal is called a conflict game). Nash equilibria of two-player zero-sum games are exactly pairs of minimax strategies.

In 1944 John von Neumann and Oskar Morgenstern proved that any zero-sum game involving n players is in fact a generalized form of a zero-sum game for two players, and that any non-zero-sum game for n players can be reduced to a zero-sum game for $n+1$ players; the $(n+1)$ player representing the global profit or loss.

Next, we show an example of a zero-sum game. Consider, for example, the payoff matrix for a two-player zero-sum game as shown in Table 3.5. The order of play proceeds as follows: The first player chooses in secret one of the two actions, 1 or 2; the second player, unaware of the first player's choice, chooses in secret one of the three actions, A, B, or C. Then, the choices are revealed and each player's total number of points is affected according to the payoff for those choices. For example, player 1 chooses

action 2 and player 2 chooses action B. When the payoff is allocated, player 1 gains 20 points and player 2 loses 20 points.

Table 3.5. An example of a zero-sum game

	A	B	C
1	30, −30	−10, 10	20, −20
2	10, −10	20, −20	−20, 20

Now, in this example game both players know the payoff matrix and attempt to maximize their number of points. What should they do? Player 1 could reason as follows: “With action 2, I could lose up to 20 points and can win only 20, while with action 1, I can lose only 10 but can win up to 30, so action 1 looks a lot better.” With similar reasoning, player 2 would choose action C. If both players take these actions, player 1 will win 20 points. But what happens if player 2 anticipates player 1’s reasoning and choice of action 1, and deviously goes for action B, so as to win 10 points? Or if player 1 in turn anticipates this devious trick and goes for action 2, so as to win 20 points after all?

John von Neumann had the fundamental and surprising insight that probability provides a way out of this conundrum. Instead of deciding on a definite action to take, the two players assign probabilities to their respective actions, and then use a random device which, according to these probabilities, chooses an action for them. Each player computes the probabilities so as to minimize the maximum expected point-loss independently of the opponent’s strategy. This leads to a linear-programming problem with a unique solution for each player. This minimax method can compute provably optimal strategies for all two-player zero-sum games.

For the example given above, it turns out that player 1 should choose action 1 with probability 4/7 and action 2 with probability 3/7, while player

2 should assign the probabilities 0, 4/7, and 3/7 to the three actions A, B, and C. Player 1 will then win 20/7 points on average per game.

3.10.2 Potential games

A game in game theory is considered a potential game if the incentive of all players to change their strategies can be expressed in one global function, the potential function. The concept was proposed by Dov Monderer and Lloyd Shapley [142]. The potential function is a useful tool to analyze equilibrium properties of games, since the incentives of all players are mapped into one function, and the set of pure Nash equilibria can be found by simply locating the local optima of the potential function. Next, we will formally define the potential game as follows.

DEFINITION 62. *Let N be the number of players, A the set of action profiles over the action sets A_i of each player and u the payoff function. Then, a game $G = (N, A = A_1 \times \cdots \times A_N, u : A \to \mathcal{R}^N)$ is a (cardinal) potential game if there is an exact potential function $\Phi : A \to \mathcal{R}$ such that $\forall i$*

$$\Phi(b_i, a_{-i}) - \Phi(a_i, a_{-i}) = u_i(b_i, a_{-i}) - u_i(a_i, a_{-i}),\ \forall a_i, b_i \in A_i, \forall a \in A. \tag{3.79}$$

A game is a general (ordinal) potential game if there is an ordinal potential function $\Phi : A \to \mathcal{R}$ that

$$\text{sgn}[\Phi(b_i, a_{-i}) - \Phi(a_i, a_{-i})] = \text{sgn}[u_i(b_i, a_{-i}) - u_i(a_i, a_{-i})],\ \forall a_i, b_i \in A_i, \forall a \in A, \tag{3.80}$$

where sgn *denotes the sign function.*

In other words, in cardinal games*, the difference in individual payoffs for each player from individually changing one's strategy with other things the same has to have the same value as the difference in values for the potential function. In* ordinal games*, only the signs of the differences have to be the same.*

Next, we show a simple example of a two-player, two-strategy game with externalities. Individual players' payoffs are given by the function $u_i(s_i, s_j) = b_i s_i + w s_i s_j$, where s_i is player i's strategy, s_j is the opponent's strategy, and w is a positive externality from choosing the same strategy. The strategy choices are $+1$ and -1, as seen in the payoff matrix in Table 3.6. This game has a potential function

$$P(s_1, s_2) = b_1 s_1 + b_2 s_2 + w s_1 s_2. \tag{3.81}$$

Table 3.6. An example of a potential game

	$+1$	-1
$+1$	$(b_1 + w, b_2 + w)$	$(b_1 - w, -b_2 - w)$
-1	$(-b_1 - w, b_2 - w)$	$(-b_1 + w, -b_2 + w)$

If player 1 moves from -1 to $+1$, the payoff difference is $\Delta u_1 = u_1(+1, s_2) - u_1(-1, s_2) = 2b_1 + 2ws_2$. The change in potential is $\Delta P = P(+1, s_2) - P(-1, s_2) = (b_1 + b_2 s_2 + w s_2) - (-b_1 + b_2 s_2 - w s_2) = 2b_1 + 2ws_2 = \Delta u_1$. The solution for player 2 is equivalent.

Using numerical values $b_1 = 2, b_2 = -1$, and $w = 3$, this example transforms into a simple battle of the sexes, as shown in Table 3.7. The game has two pure Nash equilibria, $(+1, +1)$ and $(-1, -1)$. These are also the local maxima of the potential function (Table 3.8). The only stochastically stable equilibrium is $(+1, +1)$, the global maximum of the potential function.

Table 3.7. Battle of the sexes (payoffs)

	$+1$	-1

$+1$	(5, 2)	$(-1, -2)$
-1	$(-5, -4)$	(1, 4)

Table 3.8. Battle of the sexes (potentials)

	$+1$	-1
$+1$	4	0
-1	-6	2

There has been a lot of work on modeling wireless networking and resource-allocation problems (e.g., power control, waveform adaptation) using potential games such as those in [143, 144, 145, 146, 147, 148, 149, 150, 151, 152, 153].

3.10.3 Super-modular games

Super-modular games constitute an important class of games that have the nice properties of existence and convergence to Nash equilibrium. Roughly speaking, in a super-modular game, when one player takes a higher action, the others want to do the same. The game can encompass many applied models, such as a power-control game. Moreover, the super-modular game is analytically appealing, with many properties and desirable behaviors for learning algorithms.

First, we define the super-modular game as follows.

DEFINITION 63. *Let A be the action and u be the utility for an N user game. The game $G(A_1, \ldots, A_N; u_1, \ldots, u_N)$ is a super-modular game if for all i*

- *A_i is a compact subset of $\mathbb{R}$,*
- *u_i is upper semi-continuous in (A_i, A_{-i}), and*
- *u_i has increasing differences in (A_i, A_{-i}).*

The major properties of a super-modular game are explained in the following theorem and properties.

THEOREM 12. *Let $G(A, u)$ be a super-modular game. The set of strategies surviving iterated strict dominance has greatest and least elements $\overline{A}$ and $\underline{A}$, and $\overline{A}$ and $\underline{A}$ are both Nash equilibria. In other words, the following statements hold.*

- *A pure strategy of Nash equilibrium exists.*

- *The largest and smallest strategies compatible with iterated deletion, rationalizability, and Nash equilibrium are the same.*
- *If a super-modular game has a unique Nash equilibrium, then it is dominance solvable, and lots of adjustment rules will converge to it, e.g., best-response dynamics.*

PROPOSITION 1. *Suppose a super-modular game indexed by t. The largest and smallest Nash equilibria are increasing in t.*

PROPOSITION 2. *Suppose a super-modular game with positive spillovers (for all i, $u_i(A_i, A_{-i})$ is increasing in A_{-i}). Then the largest Nash equilibrium is Pareto-preferred.*

Several examples of applications for super-modular games are listed below.

(i) *An investment game: Suppose N firms simultaneously make investments $A_i \in \{0, 1\}$ and the payoffs are*

$$u_i(A_i, A_{-i}) = \begin{cases} \pi(\sum_i A_i) - k, & A_i = 1, \\ 0, & A_i = 0, \end{cases} \tag{3.82}$$

where π is increasing in aggregate investment and k is a constant.

(ii) *Bertrand competition: Suppose N firms simultaneously set prices and that*

$$D_i(p_i, p_{-i}) = a_i - b_i p_i + \sum_{j \neq i} d_{ij} p_j, \tag{3.83}$$

where $b_i, d_{ij} > 0$.

(iii) *Cournot duopoly: Super-modular if A_1 is firm 1's quantity and A_2 is the negative of firm 2's quantity.*

(iv) *Diamond search model: N agents who exert effort looking for trading partners. Let A_i denote the effort of agent i and $c(A_i)$ denote the cost of this effort, where c is increasing and continuous. The probability of finding a partner is $A_i \sum_{j \neq i} A_j$. Then*

$$u_i(A_i, A_{-i}) = A_i \sum_{j \neq i} A_j - c(A_i) \tag{3.84}$$

has increasing differences in (A_i, A_{-i}). Hence it is super-modular.

3.10.4 Correlated equilibrium

In this subsection, we investigate a special kind of equilibrium, correlated equilibrium. In 2006, a Nobel Prize was awarded to Robert J. Aumann for his proposal of the concept of correlated equilibrium [154, 155]. Unlike Nash equilibrium, in which each user considers only its own strategy, correlated equilibrium achieves better performance by allowing each user to consider the joint distribution of users' actions. In other words, each user needs to consider the others' behaviors to see whether there are mutual benefits to explore. It has been shown that the correlated equilibrium can be better than the convex hull of the Nash equilibria.

If a user will follow an action in every possible attainable situation in a game, the action is called a pure strategy, in which the probability of using action v_l, $p(r_i^n = v_l)$, has only one non-zero value 1 for all l. In the case of mixed strategies, the user will follow a probability distribution over different possible actions, i.e., different rate l. In Tables 3.9–3.12, we illustrate an example of two users with different actions. In Table 3.9, we list the utility function for two users taking actions 0 and 1. We can see that when two users take action 0, they have the best overall benefit. We can see this action as a cooperative action, or in our case the users transmit less

aggressively. However, if any user plays more aggressively using action 1 while the other still plays action 0, the aggressive user has a better utility, but the other user has a lower utility and the overall benefit is reduced. In our case, the aggressive user can achieve a higher rate. However, if both users play aggressively using action 1, both users obtain very low utilities. In Table 3.10, we show two Nash equilibria, where one of the users dominates the other. The dominating user has the utility of 6 and the dominated user has the utility of 3, which is unfair. In Table 3.11, we show the mixed Nash equilibrium where two users have the probabilities 0.75 for action 0 and 0.25 for action 1, respectively. The utility for each user is 4.5.

Table 3.9. The reward table in a two-user game

	0	**1**
0	(5, 5)	(6, 3)
1	(3, 6)	(0, 0)

Table 3.10. The Nash equilibrium in a two-user game

	0	**1**
0	0	(0 or 1)
1	(1 or 0)	0

Table 3.11. The mixed Nash equilibrium in a two-user game

	0	**1**
0	9/16	3/16
1	3/16	1/16

Table 3.12. The correlated equilibrium in a two-user game

	0	**1**
0	0.6	0.2
1	0.2	0

In Tables 3.10 and 3.11, the Nash equilibria and mixed Nash equilibria are all within the set of correlated equilibria. In Table 3.12, we show an example where the correlated equilibrium is outside the convex hull of the Nash equilibrium. Notice that the joint distribution is not the product of the two users' probability distributions, i.e., the two users' actions are not independent. Moreover, the utility for each user is 4.8, which is higher than that of the mixed strategy.

Next, we define the correlated equilibrium. Let $\mathbb{G} = \{K, (\Omega_i)_{i\in K}, (u_i)_{i\in K}\}$ be a finite K-user game in strategic form, where Ω_i is the strategy space for user i, and u_i is the utility function for user i. Define Ω_{-i} as the strategy space for user i's opponents. Let us denote the action of user i and the actions of its opponents as $\mathbf{r}_i$ and $\mathbf{r}_{-i}$, respectively. Then, the correlated equilibrium is defined as follows.

DEFINITION 64. *A probability distribution p is a correlated strategy of game $\mathbb{G}$, if and only if, for all $i \in K$, $\mathbf{r}_i \in \Omega_i$, and $\mathbf{r}_{-i} \in \Omega_{-i}$,*

$$\sum_{\mathbf{r}_{-i}\in\Omega_{-i}} p(\mathbf{r}_i, \mathbf{r}_{-i})[u_i(\mathbf{r}_i', \mathbf{r}_{-i}) - u_i(\mathbf{r}_i, \mathbf{r}_{-i})] \leq 0, \forall \mathbf{r}_i' \in \Omega_i. \tag{3.85}$$

On dividing the inequality in (3.85) by $p(\mathbf{r}_i) = \sum_{\mathbf{r}_{-i}\in\Omega_{-i}} p(\mathbf{r}_i, \mathbf{r}_{-i})$, we have

$$\sum_{\mathbf{r}_{-i}\in\Omega_{-i}} p(\mathbf{r}_{-i}|\mathbf{r}_i)[u_i(\mathbf{r}_i', \mathbf{r}_{-i}) - u_i(\mathbf{r}_i, \mathbf{r}_{-i})] \leq 0, \forall \mathbf{r}_i' \in \Omega_i. \tag{3.86}$$

The inequality in (3.86) means that, when the recommendation to user i is to choose action $\mathbf{r}_i$, then choosing action $\mathbf{r}_i'$ instead of $\mathbf{r}_i$ cannot obtain a higher expected payoff to i.

We note that the set of correlated equilibria is nonempty, closed, and convex in every finite game. Moreover, it may include the distribution that is not in the convex hull of the Nash equilibrium distributions. In fact, every Nash equilibrium is a correlated equilibrium and Nash equilibria correspond to the special case where $p(\mathbf{r}_i, \mathbf{r}_{-i})$ is a product of each individual user's probability for different actions, i.e., the play of the different players is independent [154, 155, 156]. The correlated equilibrium can be calculated via linear programming. If only the local information is available, some learning algorithms such as non-regret learning can achieve the correlated equilibrium with probability 1 [156].

3.10.5 Satisfaction equilibrium

In real-life distributed systems, agents generally do not have knowledge of their opponents' strategies. In this context, most game-theoretic solution concepts are hardly applicable. Therefore, it is necessary to define equilibrium concepts that do not require complete information and are achievable through learning, over repeated play. The satisfaction form is a game-theoretic formulation that models systems where players are interested not in maximizing their own utility, but rather in satisfying their own constraints [157].

Let us define the game as

$$\mathcal{G}' = \left(\mathcal{K}, \mathcal{A}^K, \{f_k\}_{k\in\mathcal{K}}\right), \tag{3.87}$$

where $\mathcal{K}$ and $\mathcal{A}^K$ follow the previous definitions and the correspondence $f_k : \mathcal{A}^{(K-1)} \to \mathcal{A}$, called *satisfaction* correspondence, is defined as

$$f_k(\mathbf{a}_{-k}) = \left(a_k \in \mathcal{A} : \sum_{\ell \in \mathcal{L}_k} \mathbf{1}_{\{\xi_\ell(a_k, a_{-k}, \geq \Gamma\}} = L_k \right). \tag{3.88}$$

Basically (3.86) is a correspondence that, given the action chosen by the other players, selects all the actions which satisfy the individual constraints. Here, a player can use any of its actions independently of all the other players. The dependence on the other players' actions plays a role only in determining whether a player is satisfied or not.

In this game formulation, the solution concept we adopt is the satisfaction equilibrium (SE) [157] defined as follows.

DEFINITION 65. *(Satisfaction equilibrium). A satisfaction equilibrium of game* $\mathcal{G}'$ *is an action profile* $\mathbf{a}' \in \mathcal{A}^K$ *such that* $\forall k \in \mathcal{K}$,

$$a'_k \in f_k\left(\mathbf{a}'_{-k}\right). \tag{3.89}$$

The SE is an action profile where all players are simultaneously satisfying their constraints. In other words, if there exists at least one SE, then $L^* = L$, since all players can be satisfied. However, an SE does not always exist for a given game. For instance, if not all the communications can simultaneously take place with the minimum required QoS in the network modeled by the game *G*, an SE simply does not exist. An extensive discussion on the existence and multiplicity of an SE in finite games is provided in [158].

Efficient satisfaction equilibrium (ESE)

Consider that player k assigns a cost to each of its actions a_k, which we denote by $c_k(a_k)$. For all $k \in \mathcal{K}$, the cost function $c_k : \mathcal{A}_k \to [0, 1]$ satisfies the following condition: $\forall (a_k, a'_k) \in \mathcal{A}_k^2$,

$$c_k(a_k) < c_k(a'_k), \tag{3.90}$$

if and only if a_k requires a lower effort than action a'_k when it is played by player k. In the QoS problem, the effort can be associated with the transmit power or the processing time required to implement a given transmit/receive configuration [159]. Thus, considering the effort or cost of individual actions, one SE is the one that requires the lowest individual effort.

DEFINITION 66. *(Efficient satisfaction equilibrium). An action profile* $\mathbf{a}^*$ *is an ESE for the game G, with cost functions* $\{c_k\}_{k\in\mathcal{K}}$*, if, for all* $k \in \mathcal{K}$*,*

$$\text{(i)} \quad a_k^* \in f_k(\mathbf{a}_{-k}^*) \text{ and} \tag{3.91}$$

$$\text{(ii)} \quad \forall a_k \in f_k(\mathbf{a}_{-k}^*),\ c_k(a_k) \geq c_k(a_k^*). \tag{3.92}$$

The effort associated with each player for each of its actions does not depend on the choices made by other players. Thus, an ESE $\mathbf{a}^* \in \mathcal{A}$, if it exists, is one SE at which player k is satisfied by using the action a_k^* which requires the minimum effort among all the actions in $f_k(\mathbf{a}_{-k})$. Nonetheless, the existence of an SE does not imply the existence of an ESE.

Modeling drop-ins and drop-outs

Consider a game played only by a subset $\mathcal{J} \subset \mathcal{K}$ of the players of the game G and denote it by

$$G(\mathcal{J}) = \left(\mathcal{J}, \{\mathcal{A}_k\}_{k\in\mathcal{J}}, \left\{f_k^{(\mathcal{J})}\right\}_{k\in\mathcal{J}}\right). \tag{3.93}$$

The function $f_k^{(\mathcal{J})} : \mathcal{A}_{\mathcal{J}} \to 2^{\mathcal{A}_k}$ determines the set of actions that satisfies the individual constraints of player k given the actions adopted by the subset of players $\mathcal{J}$. In the game in (3.93), players in $\mathcal{K} \setminus \mathcal{J}$ do not play any role in the decisions adopted by the players in $\mathcal{J}$. More precisely, the game in (3.93) is obtained when the players in the set $\mathcal{K} \setminus \mathcal{J}$ have decided to drop out of the original game G [160].

A player j drops out of the game G by playing the action corresponding to a standby state of the link which is denoted by $A_j^{(0)}$. In the game G, such an action $A_j^{(0)}$ satisfies the following condition for all $j \in \mathcal{J}$:

$$f_k^{(\mathcal{J})}(\mathbf{a}_{\mathcal{J}\setminus\{j\}}) = f_k\left(\mathbf{a}_{\mathcal{J}\setminus\{j\}}, \mathbf{A}^{(0)}_{\mathcal{K}\setminus\mathcal{J}}\right), \tag{3.94}$$

where the action profile $\mathbf{A}^{(0)}_{\mathcal{K}\setminus\mathcal{J}}$ represents an action profile in which all players $k \in \mathcal{K} \setminus \mathcal{J}$ use the action $A_k^{(0)}$.

The equality in (3.94) shows that when a set of players $\mathcal{K} \setminus \mathcal{J}$ choose to play their actions $A_k^{(0)}$ in the game G, they do not play any role in the choice of the actions of the players in $\mathcal{J}$.

The relevance of a game in (3.93), given a set $\mathcal{J} \subseteq \mathcal{K}$, stems from the fact that, if the game G does not have an SE, the set $\mathcal{J}$ can be chosen in order to allow the satisfaction of the largest population of players. That is, $\mathcal{J}$ can be constructed such that the subgame in (3.93) is the game with the largest population that possesses an SE. We refer to these action profiles as N-person satisfaction points (N-PSPs) of the game G.

DEFINITION 67. *N-person satisfaction point (N-PSP). Assume the game in satisfaction form G does not possess an SE. Then, an action profile* $(\mathbf{a}^*_{\mathcal{J}}, \mathbf{A}^{(0)}_{\mathcal{K}\setminus\mathcal{J}})$ *is said to be an N-PSP, if* $|\mathcal{J}| = N$ *and (3.93) is the subgame with the largest set of players that has an SE.*

When a game G possesses at least one SE, any SE is a K-PSP. That is, when the simultaneous satisfaction of all individual constraints is feasible, SE and K-PSP are identical notions.

---

[1] In economics, risk-neutral behavior is in between risk aversion and risk seeking. If offered either \$50 or a 50% chance of \$100, a risk-averse person will take the \$50, a risk-seeking person will take the 50% chance of \$100, and a risk-neutral person will have no preference between the two options.

[2] Since F is symmetric between the two buyers, this is an auction model with symmetric bidders.

[3] A simple exchange environment is one in which there are buyers and sellers, selling single units of the same good.

Part III

Resource management, cross-layer design, and security for D2D communications

4 Mode selection and resource allocation for D2D communications underlaying cellular networks

4.1 Introduction

Two major requirements for the LTE-A (Long Term Evolution-Advanced) standard for 4G (fourth-generation) cellular wireless networks are the need to improve spectrum efficiency and to enhance network throughput. D2D communications technology is a promising add-on component of LTE-A systems to satisfy those requirements. The concept of D2D communications is to allow direct communications among the user equipments (UEs) by reusing the cellular resources rather than using the uplink or downlink resources of the cellular networks (see Figure 4.1). D2D communications can achieve four types of gain [161], namely proximity gain, hop gain, reuse gain, and pairing gain. In D2D communications, the UEs can operate in one of three traditional modes as follows.

- *Reuse mode*: D2D UEs directly transmit data among themselves by reusing some radio resources used by cellular UEs to enhance the spectrum utilization.
- *Dedicated mode*: D2D UEs directly transmit data among themselves by using a dedicated portion of spectrum to avoid interference with cellular UEs.
- *Cellular mode*: Similarly to cellular UEs, D2D UEs relay their data through the base station.

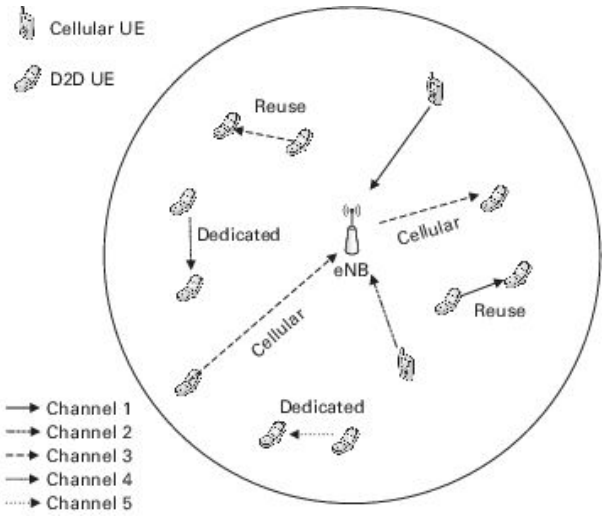

Figure 4.1. A single cell with multiple cellular links and D2D links using different D2D communication modes.

One key question here is how to select a transmission mode for each D2D link. In the cellular mode, more resources (e.g., the number of time slots) may be required for transmitting data to the receiver than in the reuse mode or dedicated mode; however, it is easier to manage interference with cellular users. The reuse mode can achieve a higher spectrum efficiency but D2D communications in this mode may interfere with cellular users and other D2D users using the cellular mode. By contrast, the dedicated mode can completely avoid interference, since some resources are reserved for the D2D communications; however, the spectrum utilization can be very poor in this mode. A simple method is to choose the mode by considering only the received signal strength over the D2D link or the distance between the terminals. However, the interference conditions and the differences between sharing cellular uplink and downlink also affect the overall network throughput.

In this chapter, an overview of LTE-A networks is given and the integration of D2D communications into LTE-A networks is discussed. The major research challenges and the current state-of-the-art D2D communications are then described. Then, we study the problem of mode selection and cooperative transmission for D2D communications via coalitional game theory where coalitions are formed for transmission-mode selection such that the cooperation among users in a coalition provides benefits to the D2D users (e.g., reduces transmission cost). The cooperation here implies that the D2D links within a coalition use orthogonal channels for transmission so that they do not experience any interference from the other D2D links in the same coalition. We define an appropriate *transmission cost* for each user in terms of transmit power and the price of channel occupancy. Since each user is rational, she may not want to cooperate with other users in a group or coalition if she is unable to achieve a lower transmission cost, even if the overall transmit power of the group is minimized. Thereby, the assumption that all users always

cooperate to use a single transmission mode to achieve the global optimality is relaxed. The stable solution for such a coalition-formation process can be considered as the solution for the mode-selection problem in D2D communications. The stable coalitions represent the system states in which no D2D link can change its communication mode and have a lower transmission cost without making others worse off. A discrete-time Markov-chain-based analysis and a distributed algorithm are presented to obtain the stable coalitions.

To this end, we consider the joint mode selection and resource-allocation problem for D2D communications considering both uplink and downlink transmissions of a cellular network. The objective is to minimize the transmission length, which is equivalent to minimizing the number of resource blocks (RBs) used for transmissions. Multiple D2D links can reuse the same RBs as long as the transmissions do not cause harmful interference with each other. We formulate a mixed-integer programming (MIP) for the optimization problem. Since the problem is NP-hard, we propose a column-generation-based algorithm to efficiently solve the problem with low complexity. In the column-generation method, the problem is decomposed into a restricted master problem and a pricing problem. An efficient heuristic algorithm was proposed to solve the pricing problem. To obtain the joint mode selection and resource-allocation solution, the restricted master problem and the pricing problem are iteratively solved.

4.2 LTE-A networks and D2D communications

4.2.1 An overview of LTE-A networks

To cope with the exponential growth of mobile broadband data traffic, the 3GPP has proposed the LTE-A standard to the International Telecommunication Union (ITU) as a candidate for the 4G cellular wireless systems. LTE-A is the evolution of the LTE standard which uses orthogonal frequency-division multiple access (OFDMA) for downlink and single-carrier FDMA (SC-FDMA) for uplink transmissions along with multiple-input and multiple-output (MIMO) technology and higher-order modulation [162]. There are two main requirements for LTE-A systems [163]. The first requirement is the backward compatibility with LTE systems. LTE-A systems should be deployed in the spectrum occupied by LTE systems without any impact on existing LTE terminals. It is necessary also to satisfy the capacity, data rates, and low-cost-deployment requirements of IMT-Advanced. The required peak data rates are up to 1 Gbps in the downlink and 500 Mbps in the uplink. More important than the peak-rate requirements is that the LTE-A systems should be able to provide high data rates over a larger portion of the cell.

To satisfy the above requirements, the authors of [164] described the specifications and features of LTE (in Releases 8 and 9) and LTE-A (in Release 10 and beyond) toward the commercial launch of these systems. In Release 10, LTE-A can deliver higher

efficiency and a smooth evolution in the deployment with several add-on features. Some examples of these add-on features are carrier aggregation (CA), enhanced downlink multiple-antenna transmission, uplink multiple-antenna transmission, relaying, and enhanced inter-cell interference coordination (eICIC) for non-CA-based heterogeneous networks (HetNets). However, further enhancements are required in Release 11 and beyond, some of which are as follows:

(i) extremely high network capacity with a significant decrease in cost per bit,

(ii) better spectrum efficiency and user-experienced throughput,

(iii) fairness in terms of user throughput in a cell, among cells, and even among users,

(iv) low capital expenditure (CAPEX) and operating expenditure (OPEX),

(v) energy efficiency and conservation,

(vi) scalability and flexibility to optimize systems for various environments and QoS requirements, and

(vii) low end-to-end latency.

Towards the above enhancement requirements, Release 11 provides several features both in the lower and in the upper layers of the protocol stack. Some examples of the lower-layer features are coordinated multiple-point transmission (CoMP) and reception, CA enhancements, eICIC enhancements, and advanced receiver techniques. Some examples of the upper-layer features are relaying for coverage extension, minimization of drive-test (MDT) enhancements, multimedia broadcast/multicast service (MBMS) enhancements, self-optimizing network (SON) enhancements, and machine-type communication (MTC) enhancements.

Considering the technology requirements for Release 11 and beyond, D2D communications underlaying an LTE-A network is a candidate feature to provide peer-to-peer services and thus enable MTC enhancements, and also achieve higher spectrum utilization and throughput experienced by users. Moreover, end-to-end latency in D2D communications can be reduced since the number of hops is reduced from two (due to the relaying via the base station) to one (due to direct communication).

4.2.2 D2D communications in LTE-A networks

D2D communications enable fast access to the radio spectrum with controlled interference levels. With underlay spectrum sharing, D2D communications can enhance the spectrum efficiency and network throughput, which are two important requirements for LTE-A networks. D2D communications engage four types of gains [161]. The first gain is *proximity gain*, where the short-range communication using a D2D link enables high bit rates, low delays, and low power consumption. The second gain is *hop gain*, where D2D transmission uses one hop rather than two hops (i.e., communicating via a BS, in which case both uplink and downlink resources are used). The third gain is *reuse gain*, where D2D and cellular links can simultaneously share the same radio resources. The last gain is *pairing gain*, which facilitates new types of wireless local-area services, and a UE can select either cellular or D2D communications mode. Furthermore, [165] suggested that the overall throughput in the network with D2D communications may increase by up to 65% compared with the case in which all the D2D traffic is transmitted through the cellular mode. Additionally, the D2D operation can be fully transparent to the users, and manual pairing or access point definition is not required as in WLAN and Bluetooth. The cellular network conceals the complexity of setting up the D2D connection from the users.

To enable D2D communications in the LTE-A networks, the authors of [165] and [166] proposed two mechanisms of D2D connectivity based on session initiation protocol (SIP) and Internet Protocol (IP). LTE systems with system architecture evolution (SAE) employ these protocols to operate fully in the packet-switched domain. In the SAE architecture, the mobility management entity (MME) works together with the packet data network (PDN) gateway to take care of the UE context, setting up the SAE bearers, IP tunnels, and IP connectivity between the UEs and the serving PDN gateway. A D2D session can be initiated either via the serving PDN by detecting the potential D2D traffic, or via the users or applications directly by selecting the SIP uniform resource indicator (URI) format with a local extension, such as .direct, .local, .peer, or .short, with the URI of the destination UE.

The two proposed mechanisms for D2D session setup as shown in Figure 4.2 are (i) detecting D2D traffic and (ii) dedicated SAE signaling.

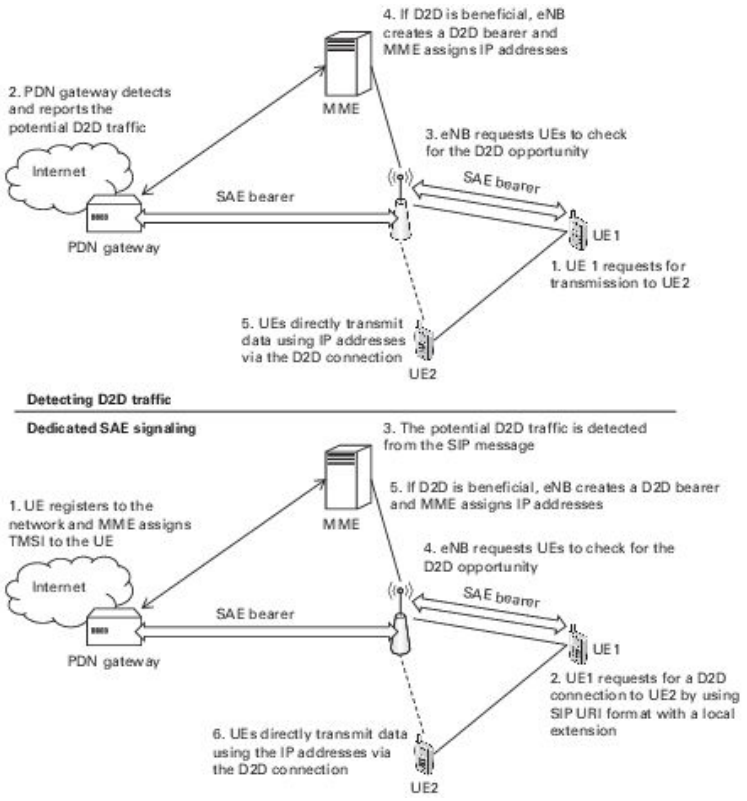

Figure 4.2. The network architecture and signaling of D2D communications.

The formal mechanism initiates a D2D session by allowing the serving PDN gateway to detect the potential D2D traffic. The gateway knows the eNB (evolved node B, is equivalent to the base transceiver station) which serves the UEs from the IP headers of the data packets and tunnel headers. The potential D2D traffic corresponds to any flow for which the source and destination IP addresses of the forward and reverse tunnels are assigned to the same eNB or the neighboring eNBs. Then the eNB(s) request the UE units to check whether both UE units are in the communication range and D2D communications provides higher throughput or not. If these criteria are met, the eNB(s) set up a D2D bearer for the direct communication between the two UE units. Moreover, the eNB(s) still maintain the SAE bearer between the UEs and the gateway for the cellular communication mode and control the radio resources for both cellular and D2D communications. By contrast, the UEs can transmit packets using the IP address of the peer UE via the D2D connection without the eNB or SAE gateway being involved in routing.

The latter mechanism employs dedicated SAE signaling for a session setup. The users or applications initiate the D2D session by selecting the SIP URI format with a local extension, such as .direct, .local, .peer, or .short, with the URI of the destination UE. Since this method provides a specific address format to separate a D2D SIP session request from a general SIP session request, it can avoid the overhead from detecting D2D traffic and

enhance the MME with a light SIP handler to facilitate session setup. To enhance the MME functionality in keeping track of the SIP addresses of the UE, the MME assigns a temporary mobile subscriber identity (TMSI) to the UE in the initial access. On receiving an NAS message type for a D2D session when the D2D UEs have been detected to be in the same or neighboring cells, the MME will request a setup of a D2D radio bearer from the serving eNB(s). Then the eNB(s) request the D2D UE to check for the possibility of D2D connection. If D2D communication is beneficial, a D2D bearer is set up and the eNB(s) confirm the successful D2D setup to the MME. With these operations, the D2D connection setup can be transparent to the users. Moreover, D2D communication is backward compatible with the existing LTE systems.

4.3 Research issues and challenges for D2D communications underlaying LTE-A networks

This section describes some challenges and research issues in D2D communications as an underlay in LTE-A networks. In the next section, we will review the current state-of-the-art approaches to deal with some of these challenges.

4.3.1 Mode selection

To achieve the maximum throughput, D2D communications should be able to choose to operate in multiple modes, i.e., reuse mode, dedicated mode, and cellular mode. In addition, D2D UEs can be in a silent mode. In the silent mode, when the available resources are not enough to support the D2D traffic and spectrum reuse is not possible due to the interference problem, the D2D devices cannot transmit data and have to stay silent.

As mentioned above, one of the main issues in D2D communications is how to select the optimal transmission mode for D2D links so that the overall network throughput is maximized and the QoS requirements of the communication links are satisfied.

4.3.2 Transmission scheduling

In LTE-A networks, the radio resources are divided into equal-sized physical resource blocks (RBs). A resource block occupies one slot in the time domain and 180 kHz in the frequency domain (i.e., 12 subcarriers with subcarrier spacing of 15 kHz) [167]. The amount of interference in each resource block is time- and space-dependent. Intelligent selection of the shared resource blocks would lead to better network throughput and spectrum utilization. Hence, efficient transmission scheduling is an important issue for D2D communications research.

4.3.3 *Power control and power efficiency*

Power control is a key mechanism to mitigate interference among users in an LTE-A network with D2D communications. Moreover, the transmit power should be allocated to satisfy the QoS requirements (e.g., SINR) of users in the network. With proper power allocation, the spectrum utilization can be improved by allowing more D2D pairs to share the same resource. Again, since mobile devices in the cellular network rely on their limited battery energy for their operations, minimization of power consumption is also an important issue in D2D communications. Consequently, power efficiency should consider the tradeoff between energy saving and achievable QoS.

4.3.4 *Distributed resource allocation*

Most of the existing work on D2D communications usually relies on centralized resource allocation where the eNB allocates the resources for both cellular and D2D users. However, due to their high complexity, centralized schemes may not be suitable when the network is large. Consequently, the resources should be allocated to the D2D links in a distributed way. Each D2D link has to sense the network environment and adaptively utilize the resources without causing any harmful interference to the cellular users. The distributed schemes can use either a fully distributed model or a message-passing model. In the former case, each D2D link will access the spectrum on the basis of local measurement without any communication with any other nodes. This model provides less signaling overhead and is highly distributed, but the solution may be far from the optimal solution. In the latter case, D2D nodes need to exchange local information with their neighbors to achieve near-optimal solutions. However, high rates of message exchange and low distributiveness are the main problems of this model. Therefore, the distributed resource-allocation schemes require efficient spectrum sensing and access schemes that take into account the tradeoff among the optimality, distributed implementation, and complexity.

4.3.5 *Coexistence with heterogeneous networks*

In the LTE-A networks, heterogeneous cellular architecture enables enhanced coverage and spectrum efficiency with flexible and low-cost deployment of macro, pico, and femto cells, and relays that can reuse the same wireless resources. For interference management, inter-cell interference coordination (ICIC) is used to coordinate among the interfering base stations for resource partitioning in terms of time, frequency, and spatial domains. In LTE-A networks, D2D communications will share the radio resources with these heterogeneous networks. For interference management, D2D nodes should be able to coordinate with other base stations. A simple way is to allow the coordination via the eNBs. Moreover, efficient resource allocation among D2D links, cellular communications, and heterogeneous networks is an important issue for the coexistence of D2D communications

with heterogeneous networks so that higher overall network throughput can be achieved with controlled interference.

4.3.6 Cooperative communications

Cooperative communications is a promising wireless technology that can improve the performance of D2D communications. D2D terminals can cooperate for transmitting data to efficiently utilize the radio resources, reduce the interference levels in the network, increase D2D coverage, and enhance the overall network throughput. The key question for cooperative communications is how to achieve the cooperation (e.g., by forming coalitions among users) so that the wireless resources are optimally utilized.

4.3.7 Network coding

Network coding is another promising technique to improve the overall throughput of the network and reduce the amount of routing information required in peer-to-peer networks to achieve near-optimal throughput. With network coding, the transmitting nodes can combine their data packets together before transmitting. This technique can assist cooperative communications among D2D nodes to enhance the possible information flow among the nodes. In another scenario, the D2D nodes may help the cellular users to relay cellular data to the destinations. During relaying, the D2D nodes can combine their own packets with the cellular packets and then transmit the data to both their destinations and the cellular destinations while reusing the cellular resources. A simple technique of network coding is linear coding, in which multiplication and addition over a finite field are used to combine multiple packets.

Despite the benefits of network coding, there are several difficulties of using network coding in D2D communications. Firstly, a large amount of time and radio resources may be required for a D2D node in decoding the received data. Secondly, when there are many packets to be combined, it can be difficult to guarantee the uniqueness of the coefficients. Thirdly, the topology of D2D communications is dynamic due to the addition and removal of D2D links, which may affect the network performance under network coding.

4.3.8 Interference cancellation and advanced receivers

Interference cancellation is an important technology to enhance the capacity of the cellular network without any change in the network infrastructure. Advanced D2D receivers can employ interference cancellation schemes to mitigate the interference. The interference can possibly be cancelled out at the receivers by modeling the structure of an interfering signal and then subtracting it out. However, there are some challenges for interference cancellation [168]. Firstly, this technology has some limitations in its functionality in terms of complex modulations, required link margin, and robustness to multiple senders.

Secondly, it is challenging to define the physical-layer schemes and parameters (e.g., modulation schemes) so that the maximum recovery can be achieved. Forward-error-correction (FEC) decoding and error-recovery techniques are important in interference cancellation to improve joint detection by correcting wrong symbol decoding and reducing ambiguity (i.e., reducing the possible symbol combinations).

4.3.9 Multiple-antenna technology and multiple-input and multiple-output (MIMO) schemes

D2D transceivers can use multiple antennas and MIMO schemes to increase the data throughput and link coverage without increased transmit power or bandwidth. The MIMO technique spreads the transmit power over the transmission antennas to achieve an array gain with higher rate and a diversity gain to mitigate the effect of fading. The major problem of using MIMO technology in D2D communications is the design of efficient precoders (i.e., how the multiple data streams should be independently emitted from the transmission antennas and properly weighted at the receivers to achieve the maximum link throughput). The precoder design should minimize the transmit power to minimize the interference caused to the neighbors while guaranteeing the QoS requirements (e.g., SINR). Recent research in this area has focused on advanced signal-processing techniques at the transceivers to reduce and cancel out the perceived interference. However, these proposed techniques require channel information and have high complexity, which may not be suitable for D2D communications.

4.3.10 Mobility management and handoff

Since the transmission range of D2D communication links is expected to be limited, the mobility management and handoff are important issues of D2D communications. The authors of [166] suggested that D2D communications should be designed for rather stationary links or nodes with limited mobility. Within a cell, the handoff can occur when either the D2D transceivers move or the interference is too high so that the D2D communication becomes impossible. Therefore, the D2D links can be handed over to the cellular links and vice versa. This is known as mode selection and vertical handoff, respectively. By contrast, horizontal handoff (i.e., moving from one cell to another cell) is also an open issue. An efficient horizontal handoff process is required in order to achieve seamless communications through the D2D links. The D2D links may be able to continue direct communications during moving from one cell to another cell or may need to switch to the cellular mode before handoff to another cell. Moreover, the inter-cell handoff can be either hard handoff or soft handoff. It also requires the study of the maximum D2D ranges that are feasible in different scenarios subject to the interference constraints for the cellular links.

4.3.11 Robust resource allocation

In wireless communications, the system information (e.g., channel gains, number of users, SINR measurement) is typically inaccurate, time-varying, or uncertain. Resource allocation without taking care of these uncertainties may lead to poor or even infeasible solutions to the realization. Robust optimization techniques can be used to tackle optimization problems with data uncertainty. The robust optimization seeks a solution that is near-optimal but remains feasible under the perturbation of parameters in the optimization problem without uncertainty (i.e., the nominal problem). The uncertainty sets can be modeled by ellipsoids, polyhedrons, and D-norm methods [169]. In D2D communications, the mode-selection and resource-allocation algorithms should take the inherently stochastic nature of link gains into account. Moreover, the number of cellular and D2D links can vary over time. The allocation results should be also robust against this uncertainty.

4.4 The state of the art of D2D communications underlaying LTE/LTE-A networks

4.4.1 Mode selection

Recently, the authors of [167, 170, 171] studied the mode-selection problem for spectrum sharing between D2D links and cellular users in the network. Simple mode-selection methods consider only the received signal strength over a D2D link or the distance between the terminals. However, the differences between sharing cellular uplink or downlink and the interference situation also affect the overall throughput of the network. Therefore, the authors of [170] proposed a mode-selection algorithm by considering the D2D and cellular link quality and the interference situation of each possible sharing mode. The mode-selection scheme selects the mode that provides the highest sum-rate while satisfying the SINR constraint of the cellular network in both single-cell and multiple-cell scenarios where each cell includes one D2D pair and a cellular user. However, the algorithm did not consider power control.

The work in [171] considered mode selection with power control in a single cell that includes one D2D link and one cellular user subject to spectral-efficiency restrictions and maximum-transmit-power or energy constraints. The authors first studied a greedy sum-rate maximization problem where cellular and D2D communications are competing services. Afterward, they studied the sum-rate maximization problem under rate constraints where cellular users have higher priority with a guaranteed minimum transmission rate. It is found that the optimization problem can be either solved in closed form or searched from a finite set except for the cellular mode with a maximum-power constraint. To generalize the system model, the authors of [167] investigated the resource-allocation problem for multiple cellular users and multiple D2D links. The RBs of cellular users in uplink and downlink are scheduled to D2D connections for which the network

throughput increases. The problem of maximizing the sum-rate of the primary cellular users and secondary D2D users was formulated as a mixed-integer nonlinear programing problem with SINR constraints for cellular and D2D communications. Then, a greedy heuristic algorithm was proposed to schedule the RBs in uplink and downlink. A D2D link is assigned with an RB used by a cellular user such that the interference channel gains from D2D communications to cellular communications are minimized. Note that the cellular user with a higher channel quality will share the resource with a D2D link which causes lower interference. However, the spectrum may not be efficiently utilized, since one RB can be shared with at most one D2D link.

4.4.2 Power control

Power control is a key research issue for D2D communications [172, 173]. A simple power-control method was proposed in [172], where the D2D transmit power is reduced to prevent there being too much interference with cellular communication. The authors of [174] then studied power optimization to maximize the sum-rate in the non-orthogonal sharing with the rate constraints to the cellular and D2D users in a single-cell scenario. The authors of [175] also proposed a dynamic power-control mechanism for a D2D link to reduce interference and improve cellular system performance. The transmit power of the D2D link is periodically adjusted by the eNB to exclude the cellular users and the eNB from their coverage areas. The eNB can calculate such power by using the channel gains between the D2D links and the cellular users. In [173], a power-efficient scheme was proposed to minimize the total downlink transmit power subject to users' QoS demands, and a heuristic scheme was used to jointly allocate subcarriers, adaptive modulation, and mode selection.

4.4.3 Distributed resource allocation

To improve the scalability of D2D communications, distributed resource-allocation methods were proposed in [176] and [161]. A distributed power-control algorithm was proposed in [176], where the SINR targets are iteratively determined in the mixed cellular and D2D environment with a cellular and a D2D link coexisting on the same uplink OFDM physical resource blocks (PRBs). The objective is to minimize the total power consumption under the constraints of sum-rate and SINR. The authors proposed a two-step algorithm with SINR- and power-setting steps. An augmented Lagrangian penalty-function (ALPF) method was used to obtain the optimal SINR target setting, aiming at setting the individual SINR targets such that the required sum power is minimized with respect to a sum-rate target. Then, an iterative transmit-power and power-loading algorithm was proposed to optimally allocate transmit power over multiple MIMO streams.

The authors of [161] proposed a distributed suboptimal algorithm for joint mode selection, scheduling, and power control among multiple cells where each eNB selects the proper mode and allocates PRBs to each mobile in a distributed way. The objective is to minimize the overall transmit power. The problem is formulated as a noncooperative game in which each eNB is a player and the payoff function is the total transmit power. The power vectors are iteratively computed from the interference perceived in each PRB while the allocation strategies of all the other players are kept fixed. The allocation strategies are the set of all possible mode selections and PRB allocations that each eNB can adopt. Each eNB plays the game until a Nash equilibrium is reached. Moreover, a load-control policy was proposed in order to improve stability by reducing the SINR target of the users who consume the most power and in turn interfere the most and cause higher instability.

4.4.4 Interference cancellation

Interference cancellation is a promising technique to manage the interference. The authors of [177] proposed a new interference-management scheme for advanced receivers to improve the reliability of D2D communications in the uplink without reducing the power of cellular UEs. Three receiving modes were studied to obtain the outage probabilities in closed forms. The first mode demodulates the desired signal and treats the interference as noise while the second mode demodulates interference first and cancels it out before demodulating the desired signal. In the third mode, retransmission of the interference from the base station is exploited to generate the desired interference as strong interference, and then the interference-cancellation process can be used to obtain the desired signal. The authors suggested mode-selection schemes based on the minimum of theoretical outage probabilities as follows: (i) the first mode for the low-interference regime, (ii) the second mode for the high-interference regime, and (iii) the third mode for the intermediate-interference regime.

4.4.5 MIMO-based D2D communications

Design and optimization of MIMO technology is also an interesting topic in D2D communications. In [178], MIMO schemes were proposed for cellular downlink transmission that avoid generating interference to an intra-cell D2D receiver underlaying the cellular network. The eNB can use any MIMO transmission scheme by designing transmitter weights for a projected cellular downlink channel and then the downlink precoding matrix can be calculated as the multiplication product of the projection matrix and the designed transmitter weights. Consequently, the D2D link quality can be improved in terms of SINR, and the overall link capacity can be increased.

4.5 Mode selection based on a coalitional game model

4.5.1 The system model and assumptions

We consider N cellular links and M D2D links sharing $\mathcal{L}$ subchannels in a cell (Figure 4.1). Each cellular link $i \in \mathcal{N} = \{1, \ldots, N\}$ is a connection between a cellular UE and the eNB (i.e., the base station) and has a rate requirement of R_i. Each D2D link $j \in \mathcal{M} = \{1, \ldots, M\}$ is a connection between the transmitter of a D2D UE and the receiver of a D2D UE, which are in the same cell and have a rate requirement of R_j. We assume that all the subchannels have the same bandwidth of B Hz. The cellular users use orthogonal subchannels to communicate with the eNB. Denoting either a cellular link or a D2D link by k, we define $g^l_{kk'}$ as the channel power gain between the transmitter of link k' and the receiver of link k on channel l. g^l_{Bk} and g^l_{kB} are defined as the channel power gains between the transmitter of link k and the eNB and the channel power gain between the eNB and the receiver of link k, respectively. Let p^l_k denote the transmit power used for transmitting data from the transmitter of link k to the receiver of link k on subchannel l. Also, let p^l_{kB} and p^l_{Bk} denote the transmit powers used for transmitting data from the transmitter of link k to the eNB and from the eNB to the receiver of link k on subchannel l, respectively. Next, let N_k and N_B denote the additive white-Gaussian-noise power at the receiver of link k and at the eNB, respectively, which is assumed to be constant over all the subchannels.

Each D2D link tries to choose the communication mode which gives the lowest transmission cost in terms of transmit power and cost of channel occupancy while satisfying the QoS requirements of the communication links. We use the concept of coalitional game theory to determine which communication mode should be used by each D2D link. We assume that the channel state information for all of the links involved is known by a coordinator at the base station. Then, the coordinator can distribute this information to all the links. In this coalitional game, the D2D links in the same coalition will not interfere with each other (e.g., by cooperatively using orthogonal subchannels) but they may interfere with links in different coalitions. In particular, the same subchannel can be used by multiple links in different coalitions at the same time.

4.5.2 The coalitional game model

In this section, we present a non-transferable-utility (NTU) coalitional game where M D2D links are *players*. The coalitions of players are denoted by $\mathcal{S}_c, \mathcal{S}_r, \mathcal{S}_d \subseteq \mathcal{M}$, where $\mathcal{S}_c$, $\mathcal{S}_r$, and $\mathcal{S}_d$ are coalitions of D2D links using the cellular mode, the reuse mode, and the dedicated mode, respectively. Since each link can use only one mode at a time, we have $\mathcal{S}_c \cap \mathcal{S}_r \cap \mathcal{S}_d = \emptyset$ and $\mathcal{S}_c \cup \mathcal{S}_r \cup \mathcal{S}_d = \mathcal{M}$.

Rates of links

Let $r_j(\mathcal{S}_c)$, $r_j(\mathcal{S}_r)$, and $r_j(\mathcal{S}_d)$ denote the rates of D2D link j when it is in the coalition using the cellular mode, the reuse mode, and the dedicated mode, respectively. We can find the rate of each D2D link when it is using each different communications mode as follows.

- Since in the cellular mode the eNB (i.e., the base station) needs to relay packets transmitted from the transmitter to the receiver of link j and the same subchannel is used for both uplink and downlink transmissions, the rate $r_j(\mathcal{S}_c)$ is half of the minimum value between the uplink rate from the transmitter of link j to the base station and the downlink rate from the base station to the receiver of link j. That is, $r_j(\mathcal{S}_c)$ is given by

$$r_j(\mathcal{S}_c) = \frac{1}{2} B \min \left\{ \log_2 \left(1 + \frac{g^l_{Bj} p^l_{jB}}{N_B + g^l_{Bj'} p^{l(\text{up})}_{j'}} \right), \log_2 \left(1 + \frac{g^l_{jB} p^l_{Bj}}{N_j + g^l_{jj'} p^{l(\text{down})}_{j'}} \right) \right\}, \quad (4.1)$$

  where $j \in \mathcal{S}_c$ and $j' \in \mathcal{S}_r$. Moreover, since a subchannel can be assigned to only one D2D link in each coalition, there may be interference from a D2D link using the reuse mode. Note that while the transmitter of D2D link j in the cellular mode is transmitting data to the base station with transmit power p^l_{jB}, $p^{l(\text{up})}_{j'}$ is the transmit power used for transmitting data from the transmitter to the receiver of link j' using the reuse mode. Similarly, while the receiver of D2D link j is receiving data relayed from the base station with transmit power p^l_{Bj}, $p^{l(\text{down})}_{j'}$ is the transmit power used for transmitting data from the transmitter to the receiver of link j' using the reuse mode. Then, the average transmit power of D2D link j can be calculated as $p^l_j = \frac{1}{2}\left(p^l_{jB} + p^l_{Bj}\right)$.

- In the reuse mode, D2D link j reuses the subchannel which is already being used by either a cellular link or a D2D link using the cellular mode. Then, the cellular or D2D link using the cellular mode may interfere with the transmission of link j using the reuse mode. If subchannel l is occupied by D2D link j' using the cellular mode, the rate of D2D link j is the average rate of the rate obtained by D2D link j' in its uplink transmission, i.e.,

$$B \log_2 \left(1 + \frac{g^l_{jj} p^{l(\text{up})}_j}{N_j + g^l_{jj'} p^l_{j'B}} \right),$$

  and the rate obtained by the D2D link j' in its downlink transmission, i.e.,

$$B\log_2\left(1+\frac{g_{jj}^{l}p_j^{l\,(\text{down})}}{N_j+g_{jB}^{l}p_{Bj'}^{l}}\right).$$

We assume that D2D link j needs to keep the rate requirement R_j constant by adjusting its $p_j^{l(\text{up})}$ and $p_j^{l(\text{down})}$, i.e.,

$$B\log_2\left(1+\frac{g_{jj}^{l}p_j^{l\,(\text{down})}}{N_j+g_{jB}^{l}p_{Bj'}^{l}}\right)=B\log_2\left(1+\frac{g_{jj}^{l}p_j^{l\,(\text{down})}}{N_j+g_{jB}^{l}p_{Bj'}^{l}}\right)=R_j.$$

Therefore, the required SINRs for both the cases are same. Moreover, the average transmit power of D2D link j can be calculated as $p_j^l=\frac{1}{2}(p_j^{l(\text{up})}+p_j^{l(\text{down})})$ when l is a subchannel shared with a D2D link using the cellular mode. The rate of D2D link j when it is in coalition $\mathcal{S}_\text{r}$ (i.e., using the reuse mode) is given by

$$r_j(\mathcal{S}_\text{r})=\begin{cases}\dfrac{1}{2}B\left(\log_2\left(1+\dfrac{g_{jj}^{l}p_j^{l(\text{up})}}{N_j+g_{jj'}^{l}p_{j'B}^{l}}\right)+\log_2\left(1+\dfrac{g_{jj}^{l}p_j^{l(\text{down})}}{N_j+g_{jB}^{l}p_{Bj'}^{l}}\right)\right),\\ \text{if subchannel } l \text{ is occupied by a D2D link using the cellular mode,}\\ B\log_2\left(1+\dfrac{g_{jj}^{l}p_j^{l}}{N_j+g_{ji}^{l}p_i^{l}}\right),\\ \text{if subchannel } l \text{ is occupied by a cellular link,}\end{cases}\tag{4.2}$$

where $j\in\mathcal{S}_\text{r}$, $j'\in\mathcal{S}_\text{c}$, and $i\in\mathcal{N}$.

- The rate of D2D link j when it is in coalition $\mathcal{S}_\text{d}$ (i.e., using the dedicated mode) is

$$r_j(\mathcal{S}_\text{d})=B\log_2\left(1+\frac{g_{jj}^{l}p_j^{l}}{N_j}\right),\quad \text{where } j\in\mathcal{S}_\text{d}.\tag{4.3}$$

Since in the dedicated mode D2D link j uses a reserved channel, there is no interference from any other transmitters.

Next, the rate of each cellular link i denoted by r_i can be obtained from

$$r_i=\begin{cases}B\log_2\left(1+\dfrac{g_{Bi}^{l}p_{iB}^{l}}{N_B+g_{Bj'}^{l}p_{j'}^{l}}\right), & \text{for uplink transmission,}\\ B\log_2\left(1+\dfrac{g_{iB}^{l}p_{Bi}^{l}}{N_i+g_{ij'}^{l}p_{j'}^{l}}\right), & \text{for downlink transmission,}\end{cases}$$

(4.4)

where $i \in \mathcal{N}$.

4.5.3 *Strategies of the D2D links*

In each coalition $\mathcal{S} \in \{\mathcal{S}_c, \mathcal{S}_r, \mathcal{S}_d\}$, the members of the coalition choose subchannels that minimize the sum of transmit powers while their rate requirements are satisfied as shown in (4.5), where $\mathcal{A}_{\mathcal{S}}$ is the set of available subchannels for each coalition $\mathcal{S} \in \{\mathcal{S}_c, \mathcal{S}_r, \mathcal{S}_d\}$, denoted by $\mathcal{A}_{\mathcal{S}_c}$, $\mathcal{A}_{\mathcal{S}_r}$, and $\mathcal{A}_{\mathcal{S}_d}$, respectively, and p_j^l is the transmit power of D2D link j on subchannel l,

$$\begin{aligned} \min \quad & \sum_{l \in \mathcal{A}_{\mathcal{S}}} \sum_{j \in \mathcal{S}} p_j^l \\ \text{s.t.} \quad & r_j \geq R_j, \quad \forall j \in \mathcal{S}. \end{aligned} \tag{4.5}$$

Let $\mathcal{A}_{\mathcal{N}}$ denote the set of subchannels occupied by the cellular links. Next, D2D links using the cellular mode choose subchannels from the set of available subchannels, i.e., $\mathcal{A}_{\mathcal{S}_c} \subseteq \mathcal{L} \setminus \mathcal{A}_{\mathcal{N}}$. Then, D2D links using the reuse mode will choose the subchannels already occupied by either cellular links or D2D links using the cellular mode, i.e., $\mathcal{A}_{\mathcal{S}_r} \subseteq \mathcal{A}_{\mathcal{N}} \cup \mathcal{A}_{\mathcal{S}_c}$, and the D2D links using the dedicated mode will choose unoccupied subchannels whose set is denoted by $\mathcal{A}_{\mathcal{S}_d} \subseteq \mathcal{L} \setminus (\mathcal{A}_{\mathcal{N}} \cup \mathcal{A}_{\mathcal{S}_c})$. Note that, when the subchannels are reused by D2D links, the other links which are using these subchannels (i.e., cellular links or D2D links using the cellular mode) need to adjust their minimum transmit powers such that their rate requirements are satisfied.

In coalition $\mathcal{S}$, a given subchannel l can be assigned to only one D2D link $j \in \mathcal{S}$. Then, $p_{j'}^l = 0$, for all other j' different from j (i.e., $j \neq j'$). R_j is the rate requirement at the receiver of D2D link j.

According to (4.1)–(4.4) and the given rate requirement R_j of each D2D link j, the corresponding SINR requirement of D2D link j denoted by γ_j can be found as follows:

$$\gamma_j = \begin{cases} 2^{(R_j/B)} - 1, & \text{if } j \in \mathcal{S}_r \text{ or } \mathcal{S}_d, \\ 2^{(2R_j/B)} - 1, & \text{if } j \in \mathcal{S}_c. \end{cases} \tag{4.6}$$

Additionally, given the rate requirement R_i of each cellular link i, the corresponding SINR requirement of cellular link i denoted by γ_i is given by

$$\gamma_i = 2^{(R_i/B)} - 1. \tag{4.7}$$

Hence, the rate requirement of each link k, which is either a cellular link or a D2D link, can be rewritten in terms of its SINR requirement as follows:

$$\mu_k \geq \gamma_k, \tag{4.8}$$

where μ_k is the achievable SINR.

Let $\mathcal{H}_l$ denote the set of all the links sharing the same subchannel l and $\vec{\mathbf{p}}$ denote a column vector whose element P_h is the transmit power of each link $h \in \mathcal{H}_l$. We can then find the transmit powers for all the links using the same subchannel that satisfy their SINR requirements as follows:

$$(\mathbf{I} - \mathbf{F})\vec{\mathbf{p}} = \vec{\mathbf{u}}, \tag{4.9}$$

where $\mathbf{I}$ is an identity matrix and $\vec{\mathbf{u}}$ is a column vector that can be written as

$$\vec{\mathbf{u}} = \begin{bmatrix} \cdots & \gamma_h N_h / g^l_{hh} & \cdots \end{bmatrix}^\top, \quad \forall h \in \mathcal{H}_l, \tag{4.10}$$

where $\top$ is the vector transpose. $\mathbf{F}$ is an $|\mathcal{H}_l| \times |\mathcal{H}_l|$ matrix ($|\mathcal{H}_l|$ is the number of links sharing subchannel l) whose (h, h')th element is

$$F_{h,h'} = \begin{cases} \gamma_k g^l_{hh'} / g^l_{hh}, & \text{if } h \neq h', \\ 0, & \text{if } h = h'. \end{cases} \tag{4.11}$$

Note that the transmit powers given by (4.9) can be obtained distributively by using the power-control algorithm proposed in [179]. Since we are considering the problem of transmit-power minimization, we do not impose any limit on the maximum transmit power.

The cost function

The transmission cost of D2D link j when it is a member of coalition $\mathcal{S} \in \{\mathcal{S}_\mathrm{c}, \mathcal{S}_\mathrm{r}, \mathcal{S}_\mathrm{d}\}$ is defined as a function of the transmit power and the cost associated with using the subchannel as follows:

$$u_j(\mathcal{S}, l) = \delta_j p_j^l(\mathcal{S}) + \alpha_j c_j^l(\mathcal{S}), \tag{4.12}$$

where $p_j^l(\mathcal{S})$ is the transmit power of link i on subchannel l (in mW), which can be obtained from the minimization problem in (4.5) and $c_j^l(\mathcal{S}) \geq 0$ is the price of using subchannel l when D2D link j is in coalition $\mathcal{S} \in \{\mathcal{S}_c, \mathcal{S}_r, \mathcal{S}_d\}$. Since the price of using a dedicated subchannel $c_j^l(\mathcal{S}_d)$ has to be higher than the price of using a shared channel $c_j^l(\mathcal{S}_c)$ and $c_j^l(\mathcal{S}_r)$, we assume $c_j^l(\mathcal{S}_c), c_j^l(\mathcal{S}_r) \leq c_j^l(\mathcal{S}_d)$. In (4.12), δ_j and α_j are the positive weight constants of the transmit power and the price of subchannel occupancy, respectively. Since we consider a non-transferable-utility (NTU) coalitional game, only the transmission cost of each D2D link j is considered in order to calculate its utility, which is individual and is non-transferable. Then, each D2D link aims at minimizing its transmission cost.

4.5.4 Coalition formation

Each D2D link or player j makes a decision to leave its current coalition and join another coalition if, in the new coalition, player j will incur a lower transmission cost and all the other players will not incur higher transmission costs than those incurred when they are in their current coalitions, i.e.,

$$\begin{aligned} u_j(\mathcal{S}' \cup \{j\}) &< u_j(\mathcal{S}), j \in \mathcal{S}, \\ u_{j'}(\mathcal{S}' \cup \{j\}) &\leq u_{j'}(\mathcal{S}'), \forall j' \in \mathcal{S}', \end{aligned} \tag{4.13}$$

where $\mathcal{S}, \mathcal{S}' \in \{\mathcal{S}_c, \mathcal{S}_r, \mathcal{S}_d\}$, $\mathcal{S} \neq \mathcal{S}'$, and $j \neq j'$.

The coalitional structure which has the properties of internal stability and external stability is considered as a stable solution of the proposed coalitional game [180].

- *Internal stability:* A coalition $\mathcal{S}$ possesses internal stability if no player can decrease its transmission cost by leaving its coalition and acting alone.
- *External stability:* A coalition $\mathcal{S}$ possesses external stability if leaving the coalition and then joining with another coalition $\mathcal{S}'$ does not decrease the transmission cost of the player leaving from coalition $\mathcal{S}$ and the transmission costs of all the players in $\mathcal{S}'$.

To find the solution of stable coalition formation and analyze stable coalitional structures, we can formulate a discrete-time Markov chain (DTMC). The state space of the DTMC can be expressed as the set of all the coalitional structures denoted by $\Upsilon = \{\mathcal{S}_c, \mathcal{S}_r, \mathcal{S}_d\}$. The transition from one state to another state depends on the decisions of the players to leave and join the coalitions. Given the probability that player j leaves its

coalition $\mathcal{S}$ and joins another coalition $\mathcal{S}'$, the transition probability from state Υ to Υ' can be found as

$$\rho_{\Upsilon,\Upsilon'} = \begin{cases} \frac{1}{2}(1/M)\prod_{x\in\mathcal{S}'\cup j}\varphi_x(\Upsilon'|\Upsilon), & \Upsilon \neq \Upsilon' \text{ and} \\ & \Upsilon' = ((\Upsilon\backslash\{\mathcal{S}\})\backslash\{\mathcal{S}'\}) \cup (\{\mathcal{S}' \cup \{j\}\} \cup \{\mathcal{S}\backslash\{j\}\}), \\ 1 - \sum_{\Upsilon'\in\Omega,\Upsilon'\neq\Upsilon}\rho_{\Upsilon,\Upsilon'}, & \Upsilon = \Upsilon', \\ 0, & \text{otherwise}, \end{cases} \tag{4.14}$$

where $1/M$ is the probability that D2D link or player j is selected to make her decision to leave and join, $\frac{1}{2}$ is the probability that player i selects one of the remaining two coalitions, i.e., the other two D2D communication modes, and $\varphi_x(\Upsilon'|\Upsilon)$ is the probability that each player in the new coalition $\mathcal{S}' \cup \{j\}$ will accept the change which makes the coalitional structure change from Υ to Υ', i.e.,

$$\varphi_x(\Upsilon'|\Upsilon) = \begin{cases} 1, & u_x(\mathcal{S}' \cup \{j\}) < u_x(\mathcal{S}), \\ 0, & \text{otherwise}, \end{cases} \tag{4.15}$$

where $\mathcal{S}, \mathcal{S}' \in \Upsilon$ and $\mathcal{S} \neq \mathcal{S}'$. The stable coalitions correspond to the absorbing states of the DTMC [180].

Given the transition matrix $\mathbf{Q}$ whose elements are $\rho_{\Upsilon,\Upsilon'}$, the stationary probability vector $\vec{\boldsymbol{\pi}}$ can be obtained by solving the following equation:

$$\vec{\boldsymbol{\pi}}^{\top}\mathbf{Q} = \vec{\boldsymbol{\pi}}^{\top}, \tag{4.16}$$

where $\vec{\boldsymbol{\pi}}^{\top}\vec{\mathbf{1}} = 1$, and $\vec{\mathbf{1}}$ is a vector of ones, $\vec{\pi} = [\pi_{\Upsilon_1} \cdots \pi_{\Upsilon_q} \cdots \pi_{\Upsilon_{3^M}}]^{\top}$, and π_{Υ_q} is the probability that the coalitional structure Υ_q will be formed.

The solution for the DTMC can be obtained in a centralized manner by the coordinator. We also propose a distributed algorithm (as shown in Algorithm 4) to find the solution based on the individual leave-and-join decision of each D2D link j.

Algorithm 4 Distributed coalition-formation algorithm based on individual leave-and-join decision of each D2D link

Initialize $\phi = 0$ and $\Upsilon(\phi)$.
loop
  At time ϕ, D2D link j is randomly selected to make a decision to leave $\mathcal{S}(\phi)$ and join any coalition $\mathcal{S}'(\phi)$.
  D2D link j randomly selects $\mathcal{S}'(\phi)$, one of two other modes (i.e., coalitions).
  D2D link j sends its request to the central coordinator to join $\mathcal{S}'(\phi)$ and the information required in order to solve the minimization problem is exchanged.
  All D2D links $j' \in \mathcal{S}'(\phi)$ compute and send their transmission costs $u_{j'}(\mathcal{S}'(\phi) \cup \{j\})$ to the central coordinator.
  D2D link j computes its transmission cost $u_j(\mathcal{S}'(\phi) \cup \{j\})$.
  if $u_j(\mathcal{S}'(\phi) \cup \{j\}) < u_j(\mathcal{S}(\phi))$ is true
    if $u_{j'}(\mathcal{S}'(\phi) \cup \{j\}) < u_{j'}(\mathcal{S}'(\phi)), \forall j' \in \mathcal{S}'(\phi)$, is true
      D2D link j joins $\mathcal{S}'(\phi)$
      $\Upsilon(\phi + 1) = ((\Upsilon(\phi) \setminus \{\mathcal{S}(\phi)\}) \setminus \{\mathcal{S}'(\phi)\}) \cup (\{\mathcal{S}'(\phi) \cup \{j\}\} \cup \{\mathcal{S}(\phi) \setminus \{j\}\})$
    else
      $\Upsilon(\phi + 1) = \Upsilon(\phi)$
    end
  else
    $\Upsilon(\phi + 1) = \Upsilon(\phi)$
  end
  $\phi = \phi + 1$
end loop when a stable coalitional structure Υ^* is reached (i.e., no D2D link prefers to move to another coalition).

4.5.5 *Numerical results*

We investigate the performance of the proposed mode-selection scheme by using MATLAB simulations. We simulate a single-cell system with D2D communications links in a rectangular area of 300 m × 300 m. The base station is located at the center of the area. There are four cellular links. The cellular links communicate with the base station in the uplink direction, where the locations of UEs are uniformly distributed within a range of 50 m from the base station. For D2D communications, there are eight D2D users (i.e., four D2D links) that are randomly located with the distance between a transmitter and a receiver of a link uniformly distributed within the range of 100 m. The path loss can be calculated from $\mathrm{PL}(k,k')\,(\mathrm{dB}) = \mathrm{PL}(d_0)\,(\mathrm{dB}) + 10n_{\mathrm{SF}}\log(d_{k,k'}/d_0)$, where $d_{k,k'}$ is the distance of transmitter of link k' to the receiver of link k. The noise powers at the base station and

all the D2D receivers are 10^{-10} W. We set the obstructed-path-loss exponent $n_{\mathrm{SF}} = 4$ and the measured line-of-sight (LOS) path loss at $d_0 = 1$m as $\mathrm{PL}(d_0) = 37.7$ dB. The required transmission rate for all the cellular and D2D links is set to 128 kbps. The number of subchannels is 10, where each subchannel has 180 kHz. The positive weight constants of the transmit power and the price of subchannel occupancy, i.e., δ_j and α_j, are set to 20 and 10, respectively. The price of using a dedicated subchannel is set to be $c_j^l(\mathcal{S}_\mathrm{d}) = 5$ and the price of using a shared channel is set to be $c_j^l(\mathcal{S}_\mathrm{c}) = c_j^l(\mathcal{S}_\mathrm{r})$ is 0 for all the D2D links and the subchannels.

Figure 4.3 shows how stable coalitional structures are obtained from the proposed distributed algorithm. As the algorithm runs, we observe different stable coalitional structures which are $\Upsilon^* = \{\mathcal{S}_\mathrm{c}, \mathcal{S}_\mathrm{r}, \mathcal{S}_\mathrm{d}\} = \{\{4\}, \{1,2\}, \{3\}\}$, $\{\{3\}, \{1,4\}, \{2\}\}$, and $\{\{4\}, \{1,3\}, \{2\}\}$ for each round, respectively. Using the DTMC analysis, the stationary probabilities for the stable states (i.e., stable coalitional structures) $\Upsilon^* = \{\{4\}, \{1,2\}, \{3\}\}$, $\{\{3\}, \{1,4\}, \{2\}\}$, and $\{\{4\}, \{1,3\}, \{2\}\}$ are obtained, with probabilities 0.109, 0.123, and 0.122, respectively. Figure 4.4 shows the subchannels occupied by the D2D links when they are using different D2D communications modes. The subchannels are assigned to the D2D links according to the minimization problem in (4.5).

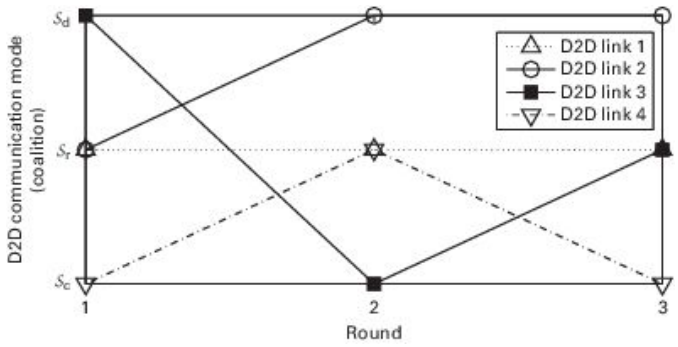

Figure 4.3. A stable coalitional structure obtained from the distributed algorithm which is composed of D2D links in coalition $\mathcal{S}_\mathrm{c}$ using the cellular mode, those in coalition $\mathcal{S}_\mathrm{r}$ using the reuse mode, and those in coalition $\mathcal{S}_\mathrm{d}$ using the dedicated mode.

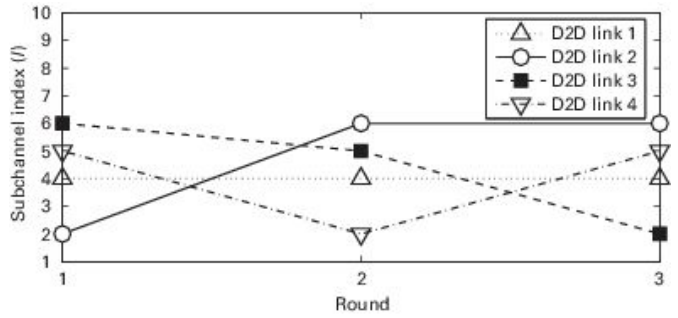

Figure 4.4. Subchannels occupied by D2D links when they are in different coalitions as shown in Figure 4.3.

Table 4.1 shows the average cost and transmit power of each D2D link, which are calculated by evaluating

$$E[u_j] = \sum_{q=1}^{D_M} \pi\Upsilon_q u_j(\mathcal{S}), \quad \text{for } j \in \mathcal{S} \text{ and } \mathcal{S} \in \Upsilon_q, \tag{4.17}$$

and

$$E[p_j] = \sum_{q=1}^{D_M} \pi\Upsilon_q p_j(\mathcal{S}), \quad \text{for } j \in \mathcal{S} \text{ and } \mathcal{S} \in \Upsilon_q, \tag{4.18}$$

where D_M is the number of coalitional structures and $\pi\Upsilon_q$ can be found from (4.16).

Table 4.1. Average transmission cost ($E[u_j]$) and transmit power ($E[p_j]$) of each D2D link

D2D link	Average cost	Average transmit power (mW)
1	6.84	9.6
2	17.53	162.0
3	10.77	18.1
4	9.39	106.7

4.6 Joint mode selection and resource allocation for D2D communications

D2D communications allow the user equipments (UEs) to directly transmit data among themselves by reusing the spectrum resources of the cellular network. If two UEs are within communication range of each other (i.e., can be called a D2D link), the link can select as transmission mode either the direct mode or the relay mode (i.e., via the cellular base station, BS, as in the traditional way). Moreover, the network needs to allocate the appropriate resource blocks (RBs) both in the time domain and in the frequency domain and the transmit power both for the cellular and for the D2D links in such a way as to avoid harmful interference. In this section, we consider the joint mode selection and resource allocation for D2D communications underlaying an LTE-A network. The objective is to minimize the transmission length (in terms of time slot), which is equivalent to minimizing the number of RBs used for transmissions in a frame subject to

the traffic demand of the links. We present an efficient algorithm that is based on a column-generation method to obtain the near-optimal solutions with low complexity. Numerical results show that the proposed algorithm provides an optimality gap of less than 10%.

4.6.1 The network model

We consider a cellular network where a set of cellular links $\mathcal{K}$, indexed by $k = 1, 2, \ldots, |\mathcal{K}|$, coexists with a set of D2D links $\mathcal{L}$, indexed by $l = 1, 2, \ldots, |\mathcal{L}|$. Each cellular link consists of one UE for either uplink or downlink transmission to or from the BS, while a D2D link consists of one transmitter and a corresponding receiver. Note that $\mathcal{K} = \mathcal{K}^{\text{up}} \cup \mathcal{K}^{\text{down}}$, where $\mathcal{K}^{\text{up}}$ and $\mathcal{K}^{\text{down}}$ denote, respectively, the set of cellular uplinks and the set of downlinks. The D2D links can communicate by either direct communication or relay communication through the BS. Each link requires a number of active time slots in a frame (i.e., traffic demand) u_i, where $i \in \mathcal{K} \cup \mathcal{L}$. We consider four transmission modes ($\mathcal{M}$), namely the *cellular mode* for cellular links ($m = 1$), *direct mode* for D2D links ($m = 2$), *relay mode* for D2D links in the *uplink* direction ($m = 3$), and *relay mode* for D2D links in the *downlink* direction ($m = 4$). The cellular and D2D links can share a set of RBs, where an RB contains one slot in the time domain and 180 kHz with 12 subcarriers in the frequency domain [167]. To avoid intra-cell interference at the BS, each RB can be assigned to either one cellular link or one D2D link in the relay mode. Consequently, one cellular link or one D2D link in the relay mode and a number of D2D links in the direct mode can be simultaneously scheduled in one RB. We consider a physical interference model where a receiver decodes its signal successfully if the SINR at the receiver is above a certain threshold (γ_i).

4.6.2 Feasible access patterns

A collection of feasible links is the subset of links that can simultaneously transmit data on an RB (i.e., on a subchannel in a time slot) to achieve spatial reuse of the radio spectrum. A feasible access pattern is a set of the collections of feasible links, on all RBs where a feasible access pattern consists of $|\mathcal{C}| \times T$ RBs. Therefore, a feasible access pattern consists of $|\mathcal{C}| \times T$ collections of feasible links, where $\mathcal{C}$ is the set of all subchannels and T is the number of time slots. Each access pattern requires two time slots for uplink and downlink transmissions (i.e., $T = 2$). Let us use $\mathcal{S}$ indexed by $s = 1, 2, \ldots, |\mathcal{S}|$ to denote the set of all access patterns.

Let $o_{i,s,m,t,f}$ be the binary variable, where $o_{i,s,m,t,f}$ is 1 if link i is in the access pattern $\mathcal{S}(s)$ using mode m to transmit in time slot t on subchannel f and is 0, otherwise. f is in the set of all subchannels $\mathcal{C}$ indexed by $f = 1, 2, \ldots, |\mathcal{C}|$ and t is in the set of $\{1, 2\}$, where 1 is for the uplink time slot and 2 is for the downlink time slot in a feasible access pattern. We denote by $\text{Tx}_{i,m}$ and $\text{Rx}_{i,m}$ the transmitter and receiver of link i in transmission

mode m. Let $g(\mathrm{Rx}_{i,m}, \mathrm{Tx}_{j,m})$ denote the link gain between $\mathrm{Tx}_{j,m}$ and $\mathrm{Rx}_{i,m}$. A collection of feasible links satisfies the following two key constraints.

- *The minimum SINR requirements*: the achievable SINR at the receiver $\mathrm{Rx}_{i,m}$ ($\mu_{i,s,m,t,f}$) has to be greater than the SINR threshold (γ_i) for all links in a feasible access pattern, where

$$\mu_{i,s,m,t,f} = \frac{g(\mathrm{Rx}_{i,m}, \mathrm{Tx}_{i,m}) o_{i,s,m,t,f} p_{i,s,m,t,f}}{\left\{ \sum_{\mathcal{S}(s), j \neq i} g(\mathrm{Rx}_{i,m}, \mathrm{Tx}_{j,m}) o_{j,s,m,t,f} p_{j,s,m,t,f} + n_{\mathrm{Rx}_{i,m}} \right\}}. \tag{4.19}$$

  Here $n_{\mathrm{Rx}_{i,m}}$ is the thermal noise of the receiver $\mathrm{Rx}_{i,m}$ and $p_{i,s,m,t,f}$ is the transmit power of link i in the access pattern $\mathcal{S}(s)$ using mode m in time slot t on subchannel f.
- *The maximum transmit power constraints*: the transmit power $p_{i,s,m,t,f}$ should be less than the maximum power $p_{i,m}^{\max}$.

4.6.3 Constraints of feasible access patterns

Let binary matrix **Q** represent the number of RBs that each link uses for transmissions in the feasible access patterns. The inner element of **Q** is

$$q_{i,s} = \sum\nolimits_{m \in \{1,2\}} \sum\nolimits_{t \in \{1,2\}} \sum\nolimits_{f \in \mathcal{C}} o_{i,s,m,t,f} + \frac{1}{2} \sum\nolimits_{m \in \{3,4\}} \sum\nolimits_{t \in \{1,2\}} \sum\nolimits_{f \in \mathcal{C}} o_{i,s,m,t,f}.$$

Since the access patterns require two time slots, we use a vector of constant $\vec{\mathbf{a}}$ to represent the number of time slots for each access pattern, where its element $a_s = 2, \mathcal{S}(s) \in \mathcal{S}$. The constraints of the feasible access patterns can be written as

$$\mu_{i,s,m,t,f} \geq \gamma_i o_{i,s,m,t,f}, \forall f \in \mathcal{C}, \forall t \in 1,2, \forall i \in \mathcal{S}(s), \forall s \in \mathcal{S}, \tag{4.20}$$

$$0 \leq p_{i,s,m,t,f} \leq p_{i,m}^{\max}, \forall f \in \mathcal{C}, \forall t \in \{1,2\}, \forall i \in \mathcal{S}(s), \forall s \in \mathcal{S}, \tag{4.21}$$

$$q_{i,s} = \sum_{m \in \{1,2\}} \sum_{t \in \{1,2\}} \sum_{f \in \mathcal{C}} o_{i,s,m,t,f} + \frac{1}{2} \sum_{m \in \{3,4\}} \sum_{t \in \{1,2\}} \sum_{f \in \mathcal{C}} o_{i,s,m,t,f}, \forall s \in \mathcal{S}, \tag{4.22}$$

$$\sum_{m\in\mathcal{M}}\sum_{f\in\mathcal{C}} o_{i,s,m,t,f} \le 1, \forall i \in \mathcal{K}\cup\mathcal{L}, \forall s \in \mathcal{S}, \forall t \in \{1,2\}, \tag{4.23}$$

$$\sum_{m=\{2,3,4\}}\sum_{t\in\{1,2\}}\sum_{f\in\mathcal{C}} o_{i,s,m,t,f} = 0, \forall i \in \mathcal{K}, \forall s \in \mathcal{S}, \tag{4.24}$$

$$\sum_{t\in\{1,2\}}\sum_{f\in\mathcal{C}} o_{i,s,1,t,f} = 0, \forall i \in \mathcal{L}, \forall s \in \mathcal{S}, \tag{4.25}$$

$$o_{i,s,3,1,f} = o_{i,s,4,2,f}, \forall i \in \mathcal{L}, \forall s \in \mathcal{S}, \forall f \in \mathcal{C}, \tag{4.26}$$

$$\sum_{f\in\mathcal{C}} o_{i,s,1,2,f} \le 0, \forall i \in \mathcal{K}^{\text{up}}, \forall s \in \mathcal{S}, \tag{4.27}$$

$$\sum_{f\in\mathcal{C}} o_{i,s,1,1,f} \le 0, \forall i \in \mathcal{K}^{\text{down}}, \forall s \in \mathcal{S}, \tag{4.28}$$

$$\sum_{f\in\mathcal{C}} o_{i,s,3,2,f} \le 0, \forall i \in \mathcal{L}, \forall s \in \mathcal{S}, \tag{4.29}$$

$$\sum_{f\in\mathcal{C}} o_{i,s,4,1,f} \le 0, \forall i \in \mathcal{L}, \forall s \in \mathcal{S}, \tag{4.30}$$

$$\sum_{i\in\mathcal{K}\cup\mathcal{L}}\sum_{m\in\{1,3,4\}} o_{i,s,m,t,f} \le 1, \forall s \in \mathcal{S}, \forall t \in \{1,2\}, \forall f \in \mathcal{C}, \tag{4.31}$$

$$o_{i,s,m,t,f} = \{0,1\}, \forall i \in \mathcal{K}\cup\mathcal{L}, \forall s \in \mathcal{S}, \forall m \in \mathcal{M}, \forall t \in \{1,2\}, \forall f \in \mathcal{C}. \tag{4.32}$$

The constraints in (4.20) and (4.21) are the constraints for the *collection of feasible links*. The constraints in (4.22) express the relationship between acquired bandwidth **Q** and scheduling variable **O**. The constraints in (4.23) ensure that one link can transmit at most in one mode on a channel at a time slot in a feasible access pattern. The constraints (4.24) ensure that cellular links cannot operate in the modes for D2D links (i.e., modes 2, 3, and 4) while constraints (4.25) ensure that D2D links cannot operate in the mode for cellular links (i.e., mode 1). The constraints in (4.26) guarantee that the numbers of uplink and downlink transmissions of a D2D link in the relay modes are equal in order to

complete the D2D transmission in a feasible access pattern. The constraints in (4.27)–(4.30) ensure that there is no downlink transmission in the first time slot of an access pattern and no uplink transmission in the second time slot of the access pattern. The constraints in (4.31) ensure that only one link can connect to the BS at a time on a channel in order to avoid intra-cell interference. Finally, the constraints in (4.32) guarantee that **O** is a matrix of binary variables.

4.6.4 Column generation for joint mode selection and resource allocation

Problem formulation

We consider the problem of transmission-length minimization of all of the links in the cellular network subject to the traffic demands of all the links and the constraints of the feasible access patterns. Let us denote by $\vec{\mathbf{y}}$ the decision variable vector, where its element y_s represents the number of times that the feasible access pattern $\mathcal{S}(s)$ is scheduled in a frame. With the traffic demands of all the links $\vec{\mathbf{u}}$, whose elements are denoted by u_i, and the constraints of the feasible access patterns, we can formulate an optimization problem as a mixed-integer program (MIP) as follows:

$$\min_{\vec{\mathbf{y}},\mathbf{Q}} \sum_{s\in\mathcal{S}} a_s y_s \tag{4.33}$$

$$\text{s.t.} \sum_{s\in\mathcal{S}} q_{i,s} y_s \geq u_i, \forall i \in \mathcal{K}\cup\mathcal{L} \tag{4.34}$$

$$y_s \geq 0 \text{ and } y_s \in \mathbb{Z}, \forall s \in \mathcal{S}. \tag{4.35}$$

The constraints in (4.34) guarantee the traffic demand of each link and the constraints in (4.35) ensure that y_s is an integer and greater than 0. Here, the matrices **O** and **Q** are the keys for this problem. However, it is difficult to find all feasible access patterns and the corresponding transmit power vectors with the constraints in (4.20)–(4.32). We have the following result on the complexity of our problem.

PROPOSITION 3. *The joint mode-selection and resource-allocation problem for D2D communications underlaying a cellular network is an NP-hard problem.*

Proof. It was shown in [161] that the problem of jointly optimizing mode selection, resource allocation, and power assignment (JOMSRAP) for uplink transmission in a cellular system is NP-hard. Since this problem is a special case of the problem under

consideration which considers both uplink and downlink cellular systems, the latter is also an NP-hard problem. □

This proposition implies that the joint mode selection and resource allocation cannot be solved by any algorithm without solving an NP-hard problem. For finding all feasible access patterns $\mathcal{S}$, the complete coefficient of matrix $\mathbf{O}$ is also difficult to specify. In addition, the size of $\mathcal{S}$ could grow exponentially with the number of links. Therefore, we propose an algorithm that is based on a column-generation method with low complexity. The details of this algorithm are provided in the next section.

An algorithm based on a column-generation method

The key idea of the column-generation method [181] is to generate only the potential variables that can improve the objective function. The problem is decomposed into a restricted master problem and a pricing problem. The restricted master problem is similar to the original problem except that it considers only the potential variables, not all variables. Therefore, the method generates a subset of all feasible access patterns ($\bar{\mathcal{S}}$) where $\bar{\mathcal{S}} \subseteq \mathcal{S}$ and the corresponding acquired bandwidth matrix $\bar{\mathbf{Q}}$ instead of $\mathbf{Q}$. The restricted master problem of the joint mode selection and resource allocation can be written as follows:

$$\min_{\vec{\mathbf{y}}} \sum_{s\in\mathcal{S}} \bar{a}_s y_s \tag{4.36}$$

$$\text{s.t.} \sum_{s\in\mathcal{S}} \bar{q}_{i,s} y_s \geq u_i, \forall i \in \mathcal{K} \cup \mathcal{L} \tag{4.37}$$

$$y_s \geq 0 \text{ and } y_s \in \mathbb{Z}, \forall s \in \mathcal{S}. \tag{4.38}$$

Note that the constraints in (4.20)–(4.32) will be considered in the pricing problem. The restricted master problem is solved to find the minimum transmission length for which the pricing problem is solved in order to find the new potential variables $\bar{\mathbf{q}}_s$ (i.e., a new column of variables) to be appended to the restricted master problem. The reduced price function of the pricing problem can be expressed as $\bar{a}_s - \boldsymbol{\zeta}'\bar{\mathbf{q}}_s$, where $\boldsymbol{\zeta}'$ is the row vector of the dual variables for constraints (4.37). The dual variables, also called shadow prices, express the marginal cost of strengthening the constraint. If ζ_i is high, this means that the change by one unit of the RB allocation of user i highly impacts the objective value. Therefore, the objective function of the pricing problem is to minimize the reduced price function subject to the constraints in (4.20)–(4.32), which can be expressed as follows:

$$\begin{aligned} \min_{\mathbf{O},\mathbf{P}} \quad & \bar{a}_s - \boldsymbol{\zeta}' \bar{\mathbf{q}}_s \\ \text{s.t.} \quad & \text{constraints in (4.20)–(4.32).} \end{aligned} \tag{4.39}$$

In this method, the restricted master problem is iteratively solved to determine the dual variables. These variables are passed to the pricing problem to generate a new column of acquired bandwidth from a new feasible access pattern. If the objective of the pricing problem is negative, new column variables will be appended to the matrix $\bar{\mathbf{Q}}$. The restricted master problem is repeatedly solved and new column variables are generated until no negative reduced price variable is identified. Then, the current solution to the restricted master problem is the optimal solution. The column-generation-based algorithm is shown in Algorithm 5.

Algorithm 5 Column-generation-based algorithm

1: Initialize matrix $\bar{\mathbf{Q}}$ by finding any feasible access patterns.
2: **repeat**
3: Add the new column variables in the matrix $\bar{\mathbf{Q}}$
4: Solve the dual problem in (4.36)–(4.38) to specify $\boldsymbol{\zeta}$
5: Solve the pricing problem in (4.39) to find $\bar{\mathbf{Q}}$, $\bar{\mathbf{O}}$, and $\bar{\mathbf{P}}$
6: **until** $a_s - \boldsymbol{\zeta}^{*\prime} \bar{\mathbf{q}}_s \geq 0$ or the number of iterations reaches a chosen limit
7: The optimization problem is solved to obtain the minimum transmission length with corresponding feasible access patterns and power assignment.

The heuristic algorithm for solving the pricing problem

Although the column generation can reduce the complexity by generating only the potential variables, the pricing problem for generating the new potential variables is still NP-hard. Note that the pricing problem is also an MIP, which is NP-hard. Consequently, the complexity of the column-generation method mainly relies on solving the pricing problem. Since the pricing problem is used to find the new feasible access patterns that provide the minimum reduced price, it suffices to obtain any feasible access pattern that provides a negative reduced price. We present a heuristic algorithm that is based on a greedy method to find the new feasible access patterns. Owing to the constraints for the feasible access patterns, the pricing problem can be seen as the joint admission and power-control problem. To minimize the reduced price in (4.39), $\boldsymbol{\zeta}' \bar{\mathbf{q}}_s$ needs to be maximized. Consequently, the key idea of the proposed heuristic algorithm is to maximize the number of active links that have high values of ζ_i while satisfying the constraints of the feasible access patterns. The links can be added to the collections of feasible links in descending order of their weights. We define the link weights by the value of $\boldsymbol{\zeta}$ and the interference measures.

Let us denote by **D** the relative channel gain matrix among all the links in $\mathcal{K}$ and $\mathcal{L}$, which is of order $(|\mathcal{K}| + |\mathcal{L}|) \times (|\mathcal{K}| + |\mathcal{L}|)$. Note that we consider the channel gains of D2D links when they use the direct transmission mode because D2D links are expected to use this mode (i.e., reuse the resource of the cellular network) in order to achieve efficient spectrum utilization. The elements of the matrix $\boldsymbol{D}$ are defined as follows:

$$d_{i,j} = \begin{cases} \gamma_i g^{(\mathrm{Rx}_i, \mathrm{Tx}_j)} / g^{(\mathrm{Rx}_i, \mathrm{Tx}_i)}, & \text{if } i \neq j, \\ 0, & \text{otherwise.} \end{cases} \tag{4.40}$$

The interference measures of the links can be obtained from

$$\omega_i = \max \left\{ \sum_j d_{i,j}, \sum_k d_{k,i} \right\}. \tag{4.41}$$

These interference measures express the maximum relative interference level either from the transmitter of link i to the receivers of other links or from the transmitters of other links to the receiver of link i. If the interference measure of link i is high, link i can cause high interference to other links or link i has low interference tolerance, and it is difficult to achieve its SINR requirement. Let ρ_i denote the weight of secondary link i, which can be obtained as follows:

$$\rho_i = \zeta_i + \frac{\omega_i}{\max(\boldsymbol{\omega})}, \tag{4.42}$$

where $\max(\boldsymbol{\omega})$ is the maximum value of the relative interference levels among all the links. This weight represents the value of $\boldsymbol{\zeta}_i$ and the relative interference level of link i. Therefore, the proposed heuristic algorithm first tries to find the feasible access patterns by including the links that have high values of $\boldsymbol{\zeta}$ and high relative interference levels. Since it is difficult to find spectrum-access opportunities for links with high relative interference levels, we should consider these links first in order to increase the chance of their being active in an access pattern. Consequently, the number of active links in an access pattern ($\boldsymbol{\zeta}' \bar{\mathbf{q}}_s$) can be maximized. The proposed heuristic algorithm is shown in Algorithm 6.

Algorithm 6 Heuristic algorithm to solve the pricing problem

Initialize: $o_{i,s,m,t,f} = 0, \quad \forall i \in \mathcal{K} \cup \mathcal{L}, \forall m \in \mathcal{M}, \forall f \in \mathcal{C}$.
Initialize the number of time slots used: $TS = 2$ and $t = 1$.
repeat
  Consider link i in the descending order of their weights
  repeat
    $Allocate = 0$ and $f = 1$
    if link $i \in \mathcal{K}$ **then**
      Run **Algorithm 7**
    else
      Run **Algorithm 8**
    end if
    $t = t + 1$
  until $t > TS$
  $t = 1$
until all links have been considered
Obtain $\mathbf{q}_s$ and a_s and return $\mathbf{O}$, $\mathbf{q}_s$, and a_s.

Initially, there is no link in the feasible access patterns. The links are considered one by one in descending order of their weights, which can be obtained from (4.42). Algorithm 7 is used for cellular links to jointly allocate RB and power, while Algorithm 8 is used for the D2D links. The process is repeated until all links have been considered for the resource allocation.

Algorithm 7 Resource-allocation algorithm for a cellular link

Consider subchannel f in ascending order of the interference levels of subchannels.
repeat
  if link $i \in \mathcal{K}^{\text{down}}$ **then**
    $t = t + 1$
  end if
  if there is a link using subchannel f for transmission with the BS **then**
    $f = f + 1$
  else
    $o_{i,s,1,t,f} = 1$ and calculate the new transmit power vector
    if the new transmit power vector $> \mathbf{P}^{\max}$ **then**
      $o_{i,s,1,t,f} = 0$ and $f = f + 1$
    else
      $Allocate = 1$
    end if
  end if
until $f > |\mathcal{C}|$ or $Allocate = 1$
if link $i \in \mathcal{K}^{\text{up}}$ **then**
  $t = t + 1$
end if
Return $\mathbf{O}$ and the transmit power vector.

Algorithm 8 Resource-allocation algorithm for a D2D link

Consider the subchannels f in the ascending order of the interference levels of subchannels
$m = 2$.
repeat
  repeat
    if $m = 3$ and there is a link using subchannel f for transmission with the BS **then**
      $f = f + 1$
    else
      $o_{i,s,m,t,f} = 1$ and calculate the new transmit power vector
      if the new transmit power vector $> \mathbf{P}^{\max}$ **then**
        $o_{i,s,m,t,f} = 0$ and $f = f + 1$
      else
        if $m = 2$ **then**
          $Allocate = 1$
        else
          $o_{i,s,4,2,f} = 1$
          if downlink transmission is not feasible **then**
            $o_{i,s,3,t,f} = o_{i,s,4,2,f} = 0$, and $f = f + 1$
          else
            $Allocate = 1$ and set $t = t + 1$
          end if
        end if
      end if
    end if
  until $f > |C|$ or $Allocate = 1$
  if $Allocate = 0$ and $t = 1$ **then**
    $m = m + 1$
  else
    $m = 4$
  end if
until $m > 3$ or $Allocate = 1$
Return $\mathbf{O}$ and the transmit power vector.

For the resource allocation in Algorithm 7, the cellular links can only be active in mode $m = 1$. Note that downlink transmissions can be performed only in the second time slot, whereas uplink transmissions can be performed only in the first time slot. Firstly, we keep updating the relative channel gains ($U_{i,j,t,f}$) on all of the subchannels f at every time slot t by using an equation similar to (4.40). Note that only the elements of links i and j which are active at time slot t on subchannels f are greater than 0. Otherwise, they are equal to 0. Then, the subchannels for link i are arranged in ascending order of $\alpha_{t,f}$, where $\alpha_{t,f} = \max\left\{\sum_j u_{i,j,t,f}, \sum_k u_{k,i,t,f}\right\}$. Cellular link i can be active at time t on subchannel f only if there is no link communicating with the BS at time t on subchannel f and the new transmit power after cellular link i has been included is not greater than the maximum power ($\mathbf{P}^{\max}$). The new transmit power can be obtained from $\vec{\mathbf{p}}_{t,f} = (\mathbf{I} - \mathbf{U}_{t,f})^{-1}\vec{\mathbf{v}}_{t,f}$ [182], where $\mathbf{I}$ is the identity matrix. $\vec{\mathbf{p}}_{t,f}$ is the transmit power vector at time t on subchannel f

and $\vec{\mathbf{v}}_{t,f}$ is the vector of the normalized noise power. The elements of $\vec{\mathbf{v}}_{t,f}$ are $v_{i,t,f} = \gamma_i n_{\mathrm{Rx}_i} / g(\mathrm{Rx}_i, \mathrm{Tx}_i)$, if link i is active at time t on subchannel f, and $v_{i,t,f} = 0$ otherwise. If link i fails to access the subchannel f at time t (i.e., the attempt results in an infeasible access pattern), another subchannel will be considered for link i to access. This process is repeated until all subchannels have been considered for access or link i has successfully been assigned to a subchannel.

In Algorithm 8, the process for D2D links is similar to that in Algorithm 7 except that the D2D link can operate in modes $m = 2, 3, 4$. For the direct mode ($m = 2$), D2D link i can reuse any subchannel as long as the new transmit power vector is less than or equal to $\mathbf{P}^{\max}$. However, if the D2D links cannot find a spectrum-access opportunity with the direct mode, they can use the relay modes ($m = 3, 4$). To find the feasible access at time t on subchannel f for the relay mode, the D2D links can use the same conditions as the cellular users, namely that there is no link communicating with the BS at time t on subchannel f and the new transmit power after including the D2D link i is not greater than $\mathbf{P}^{\max}$. The D2D link i first finds the access opportunity in the first time slot ($t = 1$) for uplink transmission ($m = 3$). If it can successfully access subchannel f for the uplink transmission, subchannel f will be also considered for downlink transmission ($m = 4$) of link i in the second time slot $t = 2$. This results in the completion of D2D transmission. Note that the second time slots are not allowed for transmission mode $m = 3$.

4.7 Numerical results

We investigate the performance of the proposed column-generation-based algorithm through simulations. We consider a cellular network setting in a rectangular area of $500\mathrm{m} \times 500\mathrm{m}$. A BS is located at the center of the area. A cellular user is randomly located within a range of 55 m from the BS. The D2D links are also randomly located in the area. The distance between each D2D link is randomly selected within a range of 76 m. We consider the following radio-propagation-loss model: $\mathrm{PL}(\mathrm{Rx}_i, Tx_j)\ (\mathrm{dB}) = \mathrm{PL}(d_0)\ (\mathrm{dB}) + 10 n_{\mathrm{SF}} \log(d_{i,j}/d_0)$. $\mathrm{PL}(d_0)$ is the measured line-of-sight (LOS) path loss at $d_0 = 1$ m, n_{SF} is the obstructed-path-loss exponent, and $d_{i,j}$ is the distance from transmitter Tx_j to receiver Rx_i. The link gain for link $(\mathrm{Rx}_i, \mathrm{Tx}_j)$ is given by $g(\mathrm{Rx}_i, \mathrm{Tx}_j) = 10^{-\mathrm{PL}(\mathrm{Rx}_i, \mathrm{Tx}_j)/10}$. We set $\mathrm{PL}(d_0) = 37.7$ dB and $n_{\mathrm{SF}} = 4$. The maximum transmit power of a transmitter is $p_i^{\max} = 100$ mW. The noise at the receivers is assumed to be $n_{\mathrm{Rx}_i} = 100$ dB. The target SINR for each of cellular link and D2D link is chosen as $\gamma_k = \gamma_i = 7$ dB. The simulation results were obtained by using MATLAB for 100 experiments.

First, we compare the performance of our proposed algorithm with the optimal solution. The optimal solution is obtained from the exhaustive search. We consider a

small-cellular-network scenario where there are two uplinks, two downlinks, and two D2D links sharing a subchannel. The transmission length (with 95% confidence interval) obtained from our proposed algorithm is compared with the optimal solution as shown in Figure 4.5. Our proposed algorithm can obtain a transmission length close to the optimal solution, although the bandwidth requirement of each link increases. The optimality gap is approximately 9.5%. However, the complexity of the exhaustive search can exponentially increase with the number of links in the network. By contrast, our proposed algorithm can provide complexity linear with the number of links. Consequently, our proposed algorithm can achieve near-optimal solutions with much lower complexity.

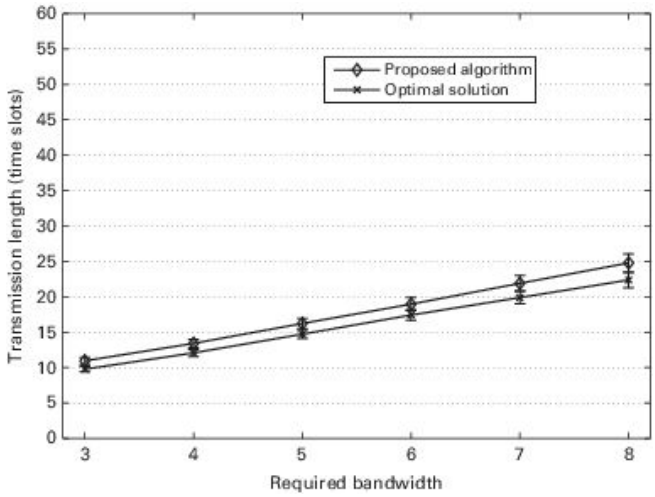

Figure 4.5. The transmission length of the proposed algorithm and the optimal solution.

Figure 4.6 shows the transmission length (i.e., duration with a 95% confidence interval) when the numbers of uplinks, downlinks, and D2D links in the network vary. When the number of a link type varies, the numbers of other link types are fixed at 10. We set the number of subchannels equal to five. The number of uplinks and downlinks mainly affects the transmission length because these links cannot reuse the same RBs to avoid intra-cell interference. The increasing number of downlinks can cause the greatest changes in the transmission length since the transmission in the downlink direction can easily interfere with other links. By contrast, the transmission length increases only very slightly when the number of D2D links increases. Since the spectrum reuse of D2D links can improve the spectrum utilization, the cellular network can accommodate more D2D links with only a slight increase in the transmission length.

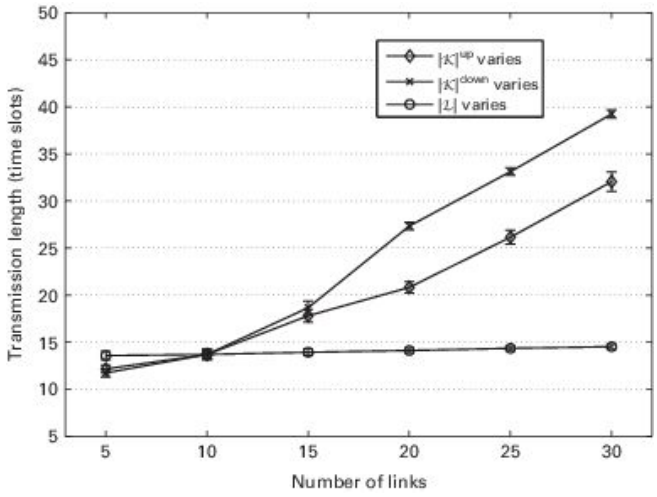

Figure 4.6. The transmission length of the proposed algorithm vs. the number of links.

4.8 Chapter summary

For D2D communications, we have presented a mode-selection framework that operates via a coalitional game. The D2D links are rational in order to form coalitions and to minimize the individual transmission costs. First, we have investigated the achievable rates of each D2D link when it uses different D2D communications modes (i.e., the cellular mode, the reuse mode, and the dedicated mode). D2D links using the same transmission mode are considered to be in the same coalition. The D2D links in the same coalition cooperatively select subchannels to minimize the total transmit power while their rate requirements are satisfied. Then, a coalitional game has been formulated to model the decision-making process of D2D links, that is, whether they will join a coalition on the basis of their incurred transmission costs. A Markov-chain-based analysis and a distributed algorithm have been proposed to find stable coalitional structures. The stable coalitional structures, i.e., three stable groups of D2D links using the different D2D communications modes, have been considered as the solution for the problem of mode selection.

To this end, we have presented a joint mode-selection and resource-allocation framework for D2D communications underlaying a cellular network. In particular, an optimization problem formulation has been presented to minimize the transmission length of LTE-A networks. We have also proposed a column-generation-based algorithm to solve the problem. We have further proposed an efficient heuristic algorithm for the pricing problem. The combination of the heuristic algorithm and the column-generation method provides a near-optimal solution with low complexity.

5 Interference coordination for D2D communications

D2D communication may cause undesirable interference to primary cellular users due to spectrum sharing. This chapter focuses on interference coordination for D2D communications underlaying cellular networks.

5.1 Interference analysis

D2D communication not only provides coverage at the customer's premises, but also radiates toward neighboring mobile users, introducing interference. Owing to this and given that D2D communication typically is performed within the coverage area of existing macro/micro cells, it can cause severe degradation of the cellular network's performance. Furthermore, the occurrence of new D2D networks could also disturb the normal functioning of already-existing D2D communications. Therefore, to reduce the appearance of dead zones within cellular networks and successfully enable a D2D LAN, interference avoidance, randomization, or cancellation techniques must be applied.

In the following, it is assumed that the D2D users are synchronized with the cellular networks as well as with other D2D users. Therefore, considering that the networks define two separate layers (the D2D and cellular layers), interference can be classified as follows.

- *Cross-layer interference:* This refers to situations in which the aggressor (e.g., a D2D user) and the victim (e.g., a cellular user) of

interference belong to different network layers.

- *Co-layer interference:* In this case the aggressor (e.g., a D2D user) and the victim (e.g., a neighboring D2D user) belong to the same network layer.

5.2 Interference avoidance

To overcome the adverse effects of interference, cancellation techniques have been proposed, but they are often disregarded due to errors in the cancellation process [183]. The use of multiple antenna beamforming at the mobile has also been suggested as a means of reducing interference by decreasing the number of interferers. By contrast, strategies based on interference avoidance also represent efficient alternatives (e.g., power and subchannel management).

Power-control algorithms and radio-resource management are tools that are often used in cellular systems to mitigate interference. If they are not applied, users located far from an eNB will be jammed by users in much closer positions. These techniques are also necessary in D2D communications for the same reasons plus the added problem of cross-layer interference.

5.3 Power control

In this section, power-control algorithms for D2D communications are presented. A simple power-control scheme is proposed in Section 5.3.1, and in Section 5.3.2 a joint beamforming and power control mechanism to avoid interference between cellular and D2D links as well as maximize system throughput is investigated.

5.3.1 Network-controlled power control

One of the major benefits of D2D communication is that the eNB can participate in the control process, and, in this section, a threshold-based

power-control scheme for D2D links is proposed in order to improve the performance of D2D underlay systems. Both interference management and power saving are considered in this scheme.

Figure 5.1 shows the radio-resource sharing of D2D and cellular links. It can be seen that the co-channel interference cannot be ignored. Uplink (UL) resource reuse has better performance in terms of D2D channel rate and operability than does downlink resource reuse. However, for efficiently sharing UL spectrum resource, it is necessary to mitigate the interference from the D2D transmitter to the eNB. Moreover, saving power as much as possible while satisfying a reliable level of performance for D2D users will promote the system efficiency.

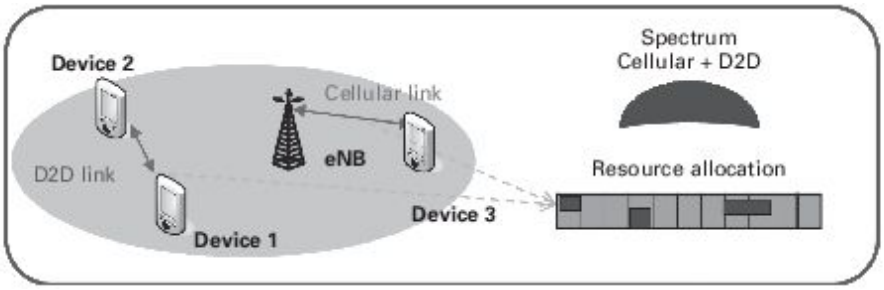

Figure 5.1. A scenario of resource reuse between D2D and cellular links.

Figure 5.2 shows the interference scenario of UL resource sharing. It can be seen that D2D transmitter UE1 causes interference to the eNB, while cellular user UE3 causes interference to D2D receiver UE2. The authors of [1, 3, 10] proposed some power-control schemes for D2D transmission. The authors of [1] employed the eNB to control the maximum transmit power of D2D transmitters, which achieves the purpose of limiting the co-channel interference. In [3], the D2D power is controlled by the eNB according to statistical results at the eNB. The authors of [10] proposed a greedy sum-rate-maximization optimization with the assumption that full channel-state information (CSI) is available. However, these schemes did not consider the practical communication constraints and detailed mechanism design. The patent [184] adjusted D2D transmit power according to HARQ feedback from the eNB to cellular UE, which is unreliable in judging the interference status by HARQ monitoring.

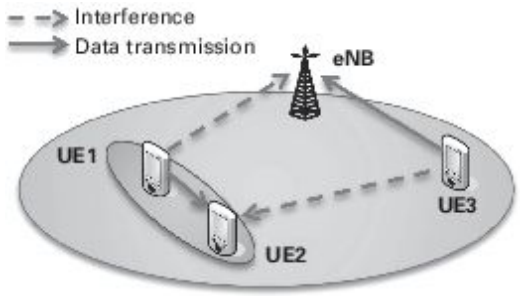

Figure 5.2. The interference scenario of D2D and cellular links under uplink resource sharing.

The patent [185] involves the following scheme: The eNB makes measurements of interference from a D2D transmitter to a cellular link, computes appropriate backoff or boost values, and sends a power-control command to a D2D transmitter. Although this scheme can control the interference relatively effectively, the quality of the D2D link is not accounted for in the system, which may cause performance loss. Further, it needs centralized scheduling since the eNB should control both D2D and cellular communications for interference measurement, which leads to large system overhead. Given the above, considering both cellular and D2D link performances, this section proposes a power-control method that can be utilized with distributed scheduling under uplink resource sharing.

The key ideas of this scheme are as follows.

(i) The eNB has no direct control on the D2D link but notifies an interference margin threshold to D2D transmitter.

(ii) The eNB feeds back the CSI of D2D transmitter UL channel (not needed for TDD system as the CSI can be obtained by channel symmetry).

(iii) D2D transmit power is calculated by a D2D transmitter itself with knowledge of the CSI and the interference margin threshold.

(iv) D2D transmitter can freely decide whether to transmit according to the allowed transmit power and D2D link status.

The key benefits of the above scheme are that the system satisfies D2D link quality while guaranteeing that a cellular link is not affected by destructive interference, which further improves system performance. Additionally, the scheme has better scalability as distributed characteristics. It could both restrict interference and guarantee the feasibility of D2D connection.

A simplified process of signaling interactions is shown in Figure 5.3, and Figure 5.4 lists the implementation process of the proposed D2D power control.

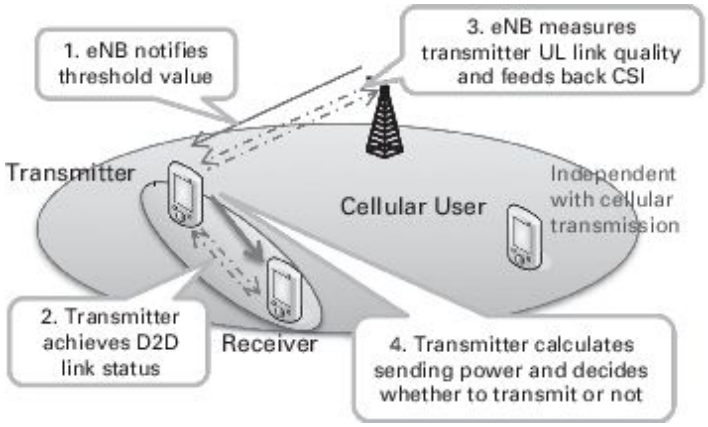

Figure 5.3. Signaling interaction of the threshold-based power-control scheme.

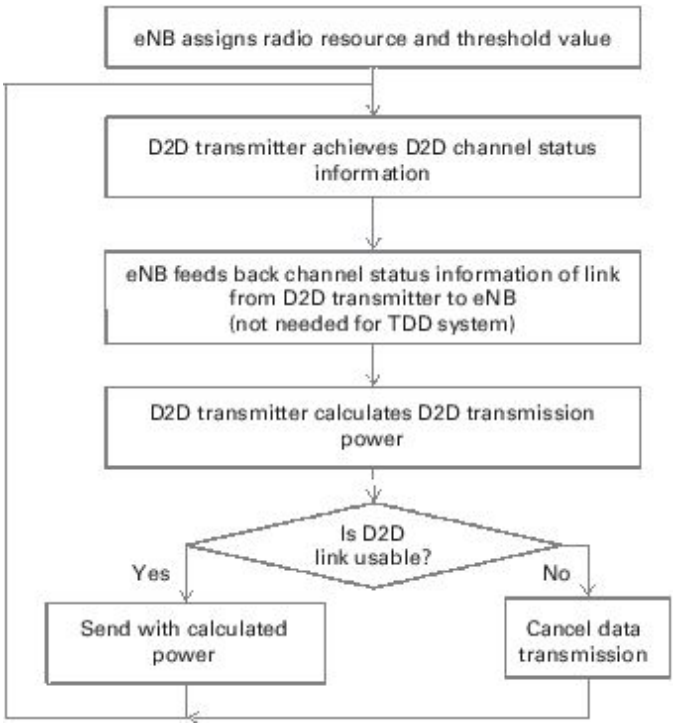

Figure 5.4. The implementation process of the threshold-based power-control scheme.

This subsection has proposed a distributed threshold-based power-control scheme that guarantees the feasibility of D2D connection, and at the same time limits cellular SINR degradation. The eNB has no direct control of the D2D link but notifies an interference margin threshold to the D2D transmitter, and the value can be tuned to meet corresponding SINR requirements. The transmit power is calculated by the D2D transmitter itself, which makes the operation flexible and convenient, improving the system efficiency.

5.3.2 Power control using MIMO

The same frequency–time resources could be shared by cellular and D2D links to enhance the system capacity, but co-channel interference exists. During downlink, D2D links receive more interference from the eNB. Interference management is necessary in order to optimize the system performance. On the one hand, it is hoped to achieve a reliable level of performance for both cellular and D2D users. On the other hand, to

maximize the system throughput is our objective. In this subsection, a joint beamforming and power-control method to reduce the interference and further improve the system performance is investigated.

In this scheme, a single-cell scenario is considered, and there is only one cellular user and one D2D pair in the model. It is assumed that the eNB is equipped with multiple antennas, while the UEs each have a single antenna. Figure 5.5 gives the system model, where the solid lines indicate the data transmissions and the dotted lines indicate the interference links. Moreover, the channel responses are assumed to be known by the eNB, and the SINR minimum thresholds of both cellular and D2D users are set by the eNB.

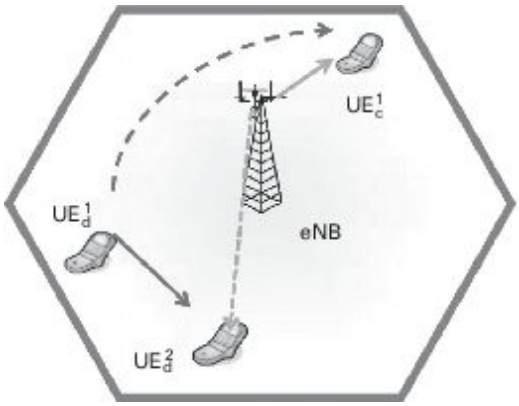

Figure 5.5. The system model of D2D communication underlaying cellular networks with downlink resource sharing.

Figure 5.6 gives an example of beamforming with two antennas equipped at the eNB. The channel-response matrix can be expressed as

$$\mathbf{H} = \begin{pmatrix} h_{11} & h_{12} \\ h_{21} & h_{22} \end{pmatrix}, \tag{5.1}$$

where h_{11} and h_{12} are the data-channel responses of the cellular link, and h_{21} and h_{22} are the interference-channel responses of the D2D link. The transmitted signal at the eNB is obtained by

$$\vec{\mathbf{x}} = \mathbf{WA}\vec{\mathbf{s}}. \tag{5.2}$$

Here, **W** is the beamforming matrix, **A** is the power-normalization matrix, and $\vec{\mathbf{s}}$ is the data vector. Thus, the received signal at cellular user $\mathrm{UE}_{\mathrm{c}}^{1}$ and D2D receiver $\mathrm{UE}_{\mathrm{d}}^{2}$ can be jointly written as

$$\vec{\mathbf{y}} = \mathbf{HWA}\vec{\mathbf{s}} + \vec{\mathbf{n}}. \tag{5.3}$$

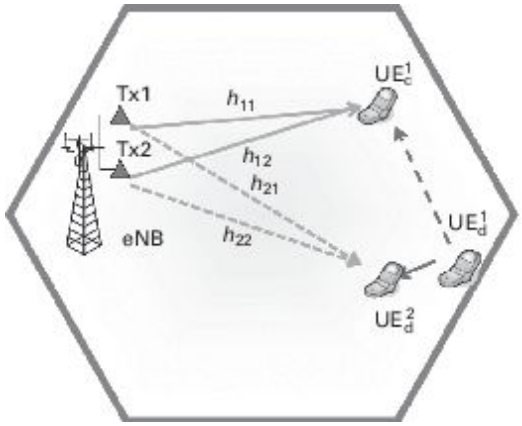

Figure 5.6. An example of beamforming with the eNB equipped with two antennas.

In this model, the eNB is a control center which performs both beamforming and power control simultaneously.

The key ideas of this scheme are as follows.

(i) The eNB performs beamforming to avoid D2D receiving excessive interference from the eNB.

(ii) The D2D receiver and the cellular user feed back downlink CSI to the eNB.

(iii) The eNB calculates the transmit power to maximize the system sum rate subject to the SINR thresholds of both cellular and D2D links.

The key benefit of the above scheme is that the system can better adapt to D2D link quality in downlink resource sharing. In general, the scheme can guarantee the performance of both cellular and D2D links, and can maximize system throughput as centralized characteristics.

A simplified representation of the process of signaling interactions is shown in Figure 5.7, and Figure 5.8 lists the implementation process of the proposed joint beamforming and power-control scheme.

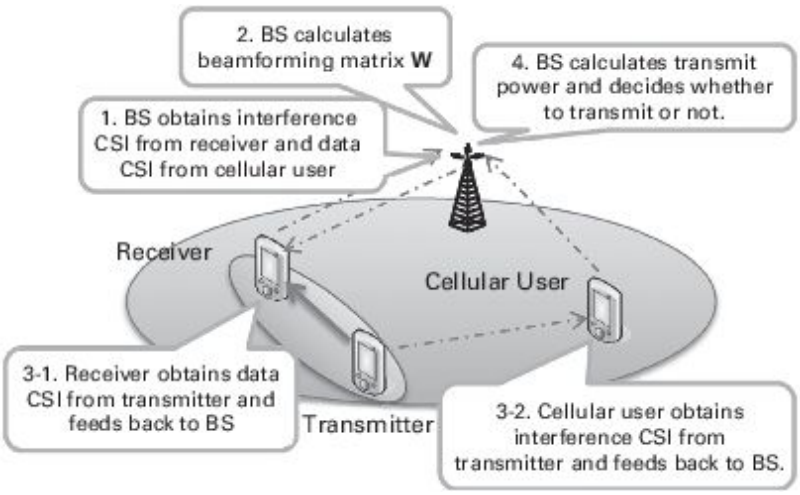

Figure 5.7. The signaling interaction of the joint beamforming and power-control scheme.

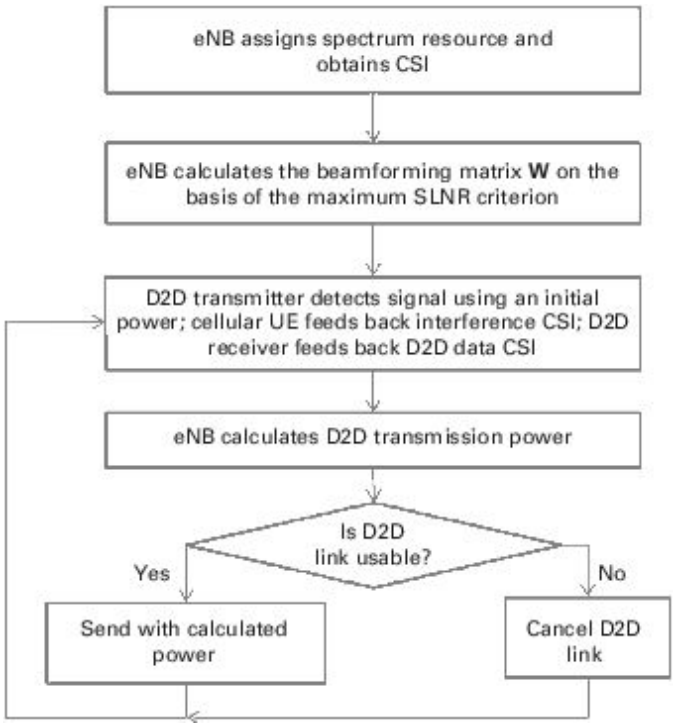

Figure 5.8. The implementation process of the joint beamforming and power-control scheme.

The eNB calculates the beamforming matrix according to the CSI that cellular and D2D users feed back to it. The received signal at the cellular user and D2D receiver can be written as follows:

$$y_{\mathrm{c}} = \mathbf{h}_{\mathrm{c}}^{\mathrm{H}}\mathbf{W}\sqrt{p_{\mathrm{B}}}s_{\mathrm{c}} + h_{dc}\sqrt{p_{\mathrm{d}}}s_{\mathrm{d}} + n, \tag{5.4}$$

$$y_{\mathrm{d}} = h_{\mathrm{dd}}\sqrt{p_{\mathrm{d}}}s_{\mathrm{d}} + \mathbf{h}_{\mathrm{d}}^{\mathrm{H}}\mathbf{W}\sqrt{p_{\mathrm{B}}}s_{\mathrm{c}} + n, \tag{5.5}$$

respectively. Here, $\mathbf{h}_{\mathrm{c}} = [\ h_{11}\quad h_{21}\ ]^{\top}$ is the signal-channel response of the cellular user, and $\mathbf{h}_{\mathrm{d}} = [\ h_{12}\quad h_{22}\ ]^{\top}$ is the interference-channel response of the D2D receiver. $\mathbf{W} = [\ w_1\quad w_2\ ]^{\top}$ is the beamforming matrix satisfying $\mathbf{W}^{\mathrm{H}}\mathbf{W} = 1$. s_{c} and s_{d} represent transmit signals from the eNB and D2D transmitter, respectively. p_{B} and p_{d} denote transmit power from the eNB and D2D transmitter, respectively. n is thermal noise with variance σ^2. Maximizing SINR is employed as the beamforming criterion. That is,

$$\max \quad \frac{\mathbf{W}^{\mathrm{H}}\mathbf{h}_{\mathrm{c}}\mathbf{h}_{\mathrm{c}}^{\mathrm{H}}\mathbf{W}}{\mathbf{W}^{\mathrm{H}}\mathbf{h}_{\mathrm{d}}\mathbf{h}_{\mathrm{d}}^{\mathrm{H}}\mathbf{W} + \sigma^2/p_{\mathrm{B}}}. \tag{5.6}$$

Thus, the beamforming matrix can be obtained by

$$\mathbf{W} = \frac{1}{\rho}\left(\mathbf{H}\mathbf{H}^{\mathrm{H}} + \frac{\sigma^2}{p_{\mathrm{B}}}\mathbf{I}\right)^{-1}\mathbf{h}_{\mathrm{c}}, \tag{5.7}$$

where $\mathbf{H} = (\ \mathbf{h}_{\mathrm{c}}\ \ \mathbf{h}_{\mathrm{d}}\ )$ is the channel response from the eNB to users, and $\rho = \left\|(\mathbf{H}\mathbf{H}^{\mathrm{H}} + (\sigma^2/p_{\mathrm{B}})\mathbf{I})^{-1}\mathbf{h}_{\mathrm{c}}\right\|$ is a normalization factor so that $\mathbf{W}^{\mathrm{H}}\mathbf{W} = 1$.

In this scheme, our objective is to maximize the system sum rate which is expressed as follows:

$$R = \log_2(1 + \gamma_{\mathrm{c}}) + \log_2(1 + \gamma_{\mathrm{d}}). \tag{5.8}$$

Additionally, the D2D transmit power p_{d} also must satisfy the SINR threshold of both cellular and D2D links, i.e.,

$$\gamma_{\mathrm{c}} = \frac{p_{\mathrm{B}}\left\|\mathbf{h}_{\mathrm{c}}^{\mathrm{H}}\mathbf{W}\right\|^2}{p_{\mathrm{d}}h_{\mathrm{dc}}^2 + \sigma^2} \geq \beta_{\mathrm{c}}, \tag{5.9}$$

$$\gamma_{\mathrm{d}} = \frac{p_{\mathrm{d}}h_{\mathrm{dd}}^2}{p_{\mathrm{B}}\left\|\mathbf{h}_{\mathrm{d}}^{\mathrm{H}}\mathbf{W}\right\|^2 + \sigma^2} \geq \beta_{\mathrm{d}}, \tag{5.10}$$

where β_{c} and β_{d} are the SINR minimum threshold of cellular user and D2D receiver, respectively. Thus, the objective function can be expressed as follows:

$$\max\ R = \log_2\left(1 + \frac{p_{\mathrm{B}}\left\|\mathbf{h}_{\mathrm{c}}^{\mathrm{H}}\mathbf{W}\right\|^2}{p_{\mathrm{d}}h_{\mathrm{dc}}^2 + \sigma^2}\right) + \log_2\left(1 + \frac{p_{\mathrm{d}}h_{\mathrm{dd}}^2}{p_{\mathrm{B}}\left\|\mathbf{h}_{\mathrm{d}}^{\mathrm{H}}\mathbf{W}\right\|^2 + \sigma^2}\right), \tag{5.11}$$

s.t.

$$\left(p_{\mathrm{B}}\left\|\mathbf{h}_{\mathrm{d}}^{\mathrm{H}}\mathbf{W}\right\|^2 + \sigma^2\right)\beta_{\mathrm{d}}h_{\mathrm{dd}}^{-2} \le p_{\mathrm{d}} \le \min\left(\left(p_{\mathrm{B}}\left\|\mathbf{h}_{\mathrm{c}}^{\mathrm{H}}\mathbf{W}\right\|^2\beta_{\mathrm{c}}^{-1} - \sigma^2\right)h_{\mathrm{dc}}^{-2}, p_{\max}\right), \tag{5.12}$$

where $p_{\max}$ is the maximum transmit power that UE can use.

Next, some simulation results and related analysis are given. The throughputs of cellular users, D2D users and the whole system are our main performance metrics. Some different interference-management schemes are compared with regard to the system performance, including the following.

(i) Proposed PC & BF: joint beamforming and power control.

(ii) No PC & BF: only beamforming is applied, and power is fixed.

(iii) PC & no BF: only power control is applied.

(vi) No PC & no BF: neither power control nor beamforming is applied.

The simulation parameters are listed in Table 5.1.

Table 5.1. Main simulation parameters

Parameter	Value
Cellular	Isolated cell, one-sector
System area	User devices are distributed in a hexagonal cell with radius 600 m

Noise spectral density	-174 dBm/Hz
System bandwidth	20 MHz
Subcarrier bandwidth	15 kHz
Subcarrier number of each user	64
Cluster radius (D2D user scattering)	50 m
Minimum SINR	5 dB (both cellular and D2D)
Number of cellular users (channels)	1
Number of D2D pairs	1/1:4
Device transmit-power upper bound	23 dBm
eNB total transmit power	46 dBm
Channel model	WINNER II

Figure 5.9 shows the system throughput distribution with different schemes. Obviously, the joint beamforming and power-control scheme improves the system performance. Figures 5.10 and 5.11 show the throughput distributions of D2D and cellular users. On the one hand, beamforming makes the performance of D2D communication better insofar as SINR criteria constrain the interference from the eNB to D2D receiver. On the other hand, power control makes the performance of cellular communication better insofar as it limits the interference from D2D users to cellular users.

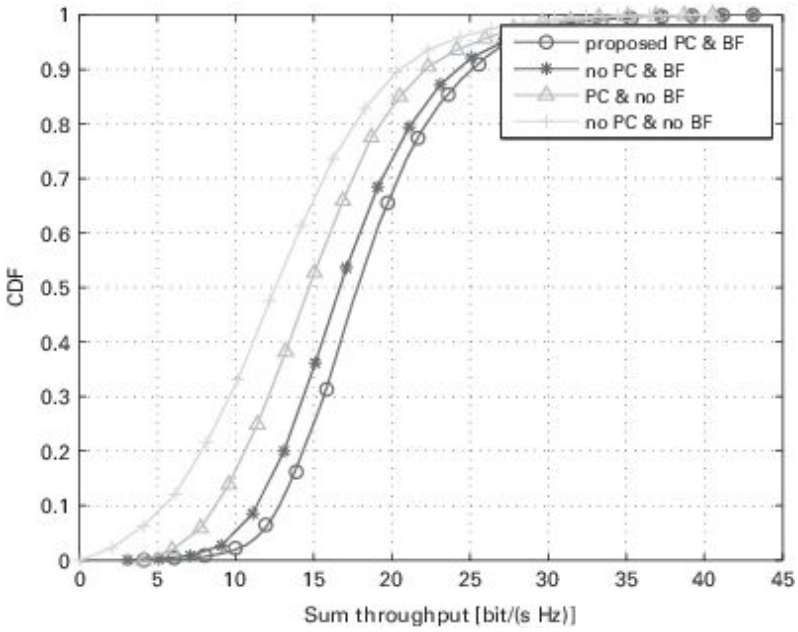

Figure 5.9. System throughput distribution with different interference-management schemes (CDF, cumulative distribution function).

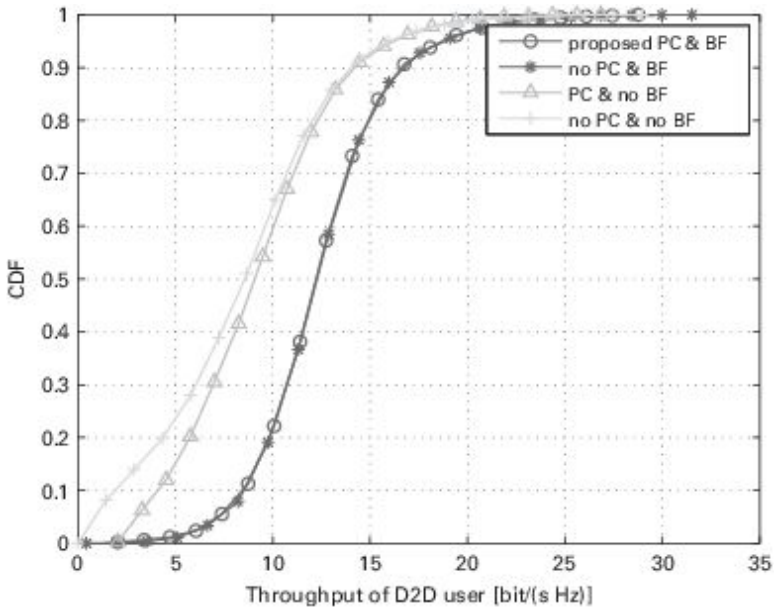

Figure 5.10. Throughput distribution of D2D communications with different interference-management schemes.

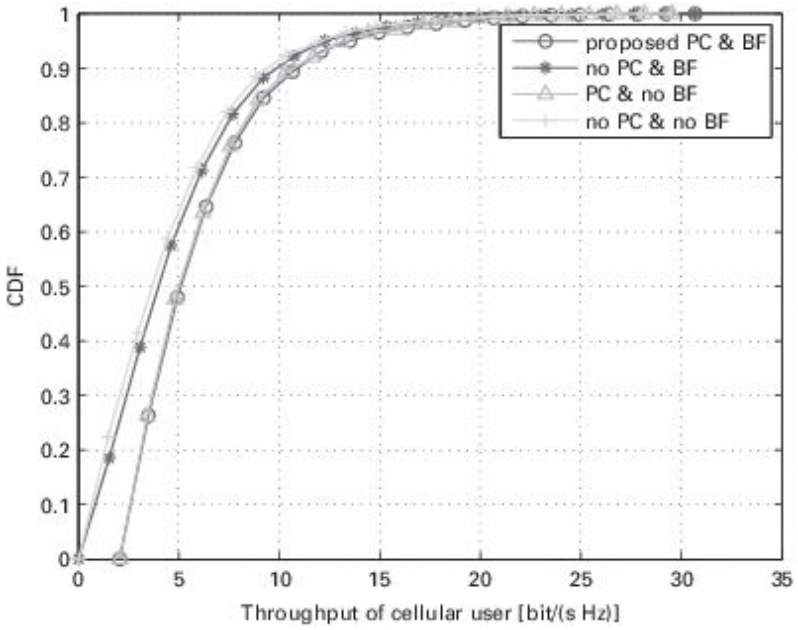

Figure 5.11. Throughput distribution of cellular communication with different interference-management schemes.

For multiple D2D pairs, the same objective function is considered as that of a single pair for simplicity. Figure 5.12 shows the result of the system throughput with different numbers of D2D pairs. It can be seen that the proposed scheme gives the optimal performance.

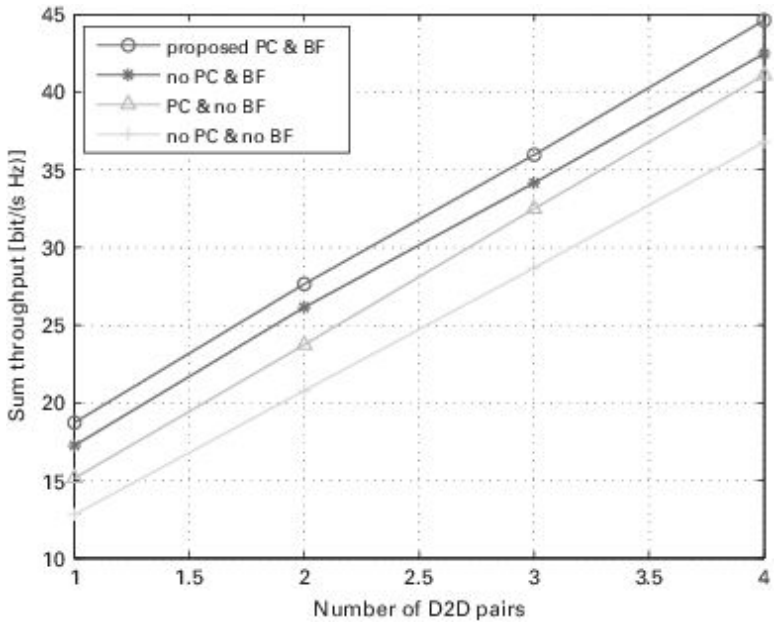

Figure 5.12. System throughput with different numbers of D2D pairs.

Figure 5.13 gives the system throughput with different cellular radii. When the radius is small, beamforming prevents interference from eNB to D2D effectively, which makes the performance gain obvious. When the radius increases, the received signal power of cellular user decreases. Thus, power control becomes more important as a means to prevent interference from D2D.

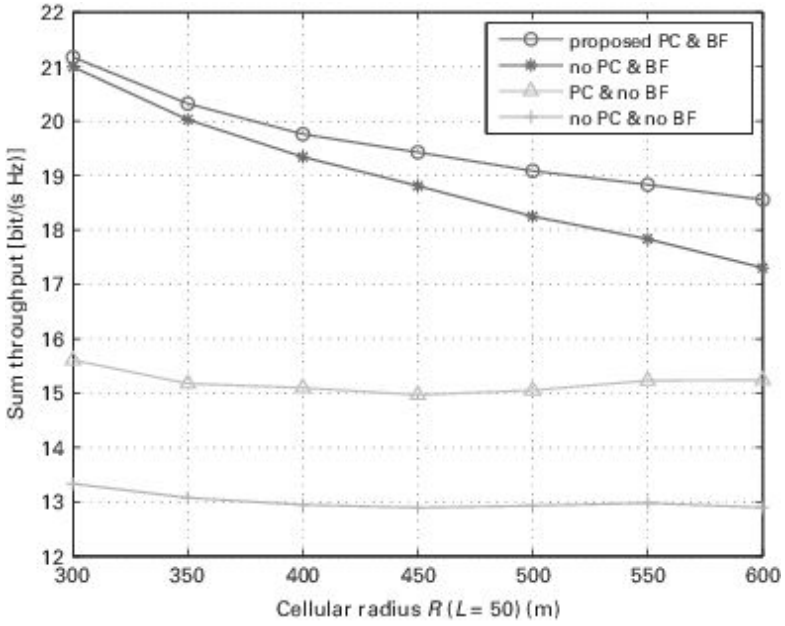

Figure 5.13. System throughput with different cellular radii.

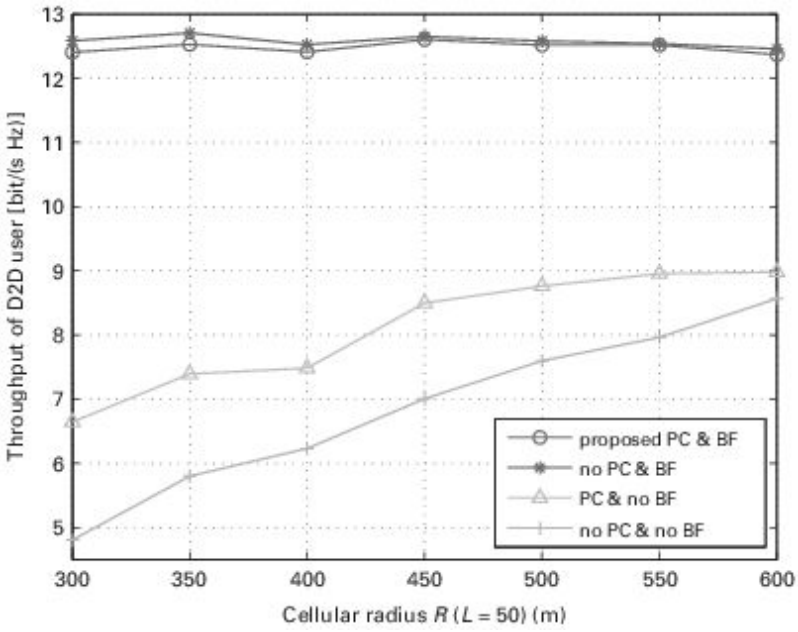

Figure 5.14. Throughput of D2D communications with different cellular radii.

Figure 5.14 shows the throughput of a D2D user with different cellular radii. The power control includes the mechanism which guarantees that the SINR of a D2D user will be above the threshold, and the objective function of power control is the system throughput. Focusing on the top two lines, it can be found that the gap between the proposed scheme and the other one is comparably obvious when the cellular radius is small. Because cellular communication is dominant when the radius is small, system throughput is improved due to reduced D2D power. Thus, fading of the D2D link becomes obvious.

This section has proposed a joint beamforming and power-control scheme that aims to maximize the system sum rate and guarantees the performance of both cellular and D2D connections. The eNB sets the SINR threshold for D2D and cellular links, and the value can be tuned to meet corresponding performance requirements. The eNB carries out beamforming to avoid subjecting D2D links to excessive interference. The D2D transmit power is calculated by the eNB to maximize the system sum rate. Additionally, the eNB determines the calculated D2D transmit power according to SINR thresholds of cellular and D2D links.

5.4 Chapter summary

Spectrum sharing leads to severe interference between D2D and cellular links, and also between different D2D links reusing the same subchannels. The undesirable interference leads to performance loss of the whole system. We have focused on interference coordination of D2D communications in this chapter. The interference is classified into two types: cross-layer interference from a D2D transmitter to a cellular receiver and co-layer interference from a D2D transmitter to a neighboring D2D receiver. The different approaches for interference avoidance include power control, spectrum-resource allocation, multiple-antenna beamforming, and other techniques. They aim to reduce co-channel interference. Finally, we have proposed a network-assisted power-control scheme that is based on an interference-margin threshold, and both interference reduction and power-saving are considered. We have further studied a joint beamforming and power control mechanism whose objective is to maximize the system sum rate, while, at the same time, achieving a reliable level of performance for both cellular and D2D users. The simulation results show that this joint beamforming and power-control scheme improves the overall system performance.

6 Subchannel allocation and time-domain scheduling for D2D communications

Since the co-channel interference between cellular and D2D links causes performance degradation, resource management is necessary for D2D communications underlaying cellular networks. This chapter introduces the subchannel allocation and time-domain scheduling schemes, which improve the system performance effectively.

6.1 Subchannel allocation

Note that, with regard to the underlay approach, to mitigate cross- and co-layer interference, there would be a central entity in charge of intelligently telling each cell which subchannels to use. This entity would need to collect information from the D2D users, and use it to find an optimal or at least a good solution within a short period of time. The presence of a large number of D2D users, and the allowance for the coexistence of multiple D2D users with cellular users, makes the optimization problem too complex. Additionally, latency issues arise when trying to facilitate the communication of femto cells with the central subchannel broker throughout the backhaul. A distributed approach to mitigate cross- and co-layer interference, whereby the D2D users can manage their own subchannels, is thus more suitable in this case (i.e., self-organization). In a noncooperative solution, i.e., a self-organized approach, each D2D user would plan its subchannels so as to maximize the throughput and QoS for its users. Furthermore, this would be done independently of the effects its allocation

might cause for co-channel D2D and cellular users, even if this implies greater interference. The access to the subchannels then becomes opportunistic, and it is possible that the method decays to greedy. By contrast, in a cooperative approach (the network-assisted approach), the D2D users can gather partial information about the subchannel usage situation and may perform its allocation taking into account the effect this would have on co-channel neighbors. In this way, the average cellular and D2D users' throughput and QoS, as well as their global performance, can be locally optimized.

6.1.1 Centralized (operator-managed) subchannel allocation

An innovative resource-allocation scheme is proposed to improve the performance of a mobile peer-to-peer, i.e., D2D communication, system as an underlay in downlink (DL) cellular networks. To optimize the system sum rate over the resource sharing of both D2D and cellular modes, a reverse iterative combinatorial auction is introduced as the allocation mechanism. In the auction, all the spectrum resources are considered as a set of resource units, which compete as bidders to obtain business while the packages of the D2D pairs are auctioned off as goods in each auction round. Firstly, the valuation of each resource unit is formulated, as a basis of the proposed auction. Then a detailed non-monotonic descending-price auction algorithm depending on the utility function that accounts for the channel gain from D2D and the costs for the system is explained. Further, it is proved that the proposed auction-based scheme is cheat-proof, and converges in a finite number of iteration rounds. Non-monotonicity in the price-update process is explained, and it is shown that this approach is of lower complexity then a traditional combinatorial allocation. The simulation results demonstrate that the algorithm efficiently leads to a good performance on the system sum rate.

A model of a single cell with multiple users is considered. As shown in Figure 6.1, UEs with data signals between each other are in the D2D communication mode while UEs that transmit data signals with the eNB keep operating in the traditional cellular mode. Each user is equipped with a single omnidirectional antenna. The locations of cellular users and D2D

pairs are randomly set and traverse the whole cell. Without loss of generality, the uniform distribution is employed to describe the user locations which are proposed for system simulation in [186]. Notice that, from stochastic geometry with Poisson distributions, the users are uniformly located as well if the number of users is known [187]. For simplicity and clarity, a co-channel interference scenario involving three UEs (UE_c, $UE_{d,1}$, and $UE_{d,2}$) is illustrated, and the interference and control signals among others are omitted. UE_c is a traditional cellular user that is distributed uniformly in the cell. $UE_{d,1}$ and $UE_{d,2}$ are close enough to satisfy the maximum-distance constraints of D2D communication, and at the same time they also have data-communication demands. One member of the D2D pair $UE_{d,1}$ is distributed uniformly in the cell, and the position of the other member $UE_{d,2}$ follows a uniform distribution inside a region at most L from $UE_{d,1}$.

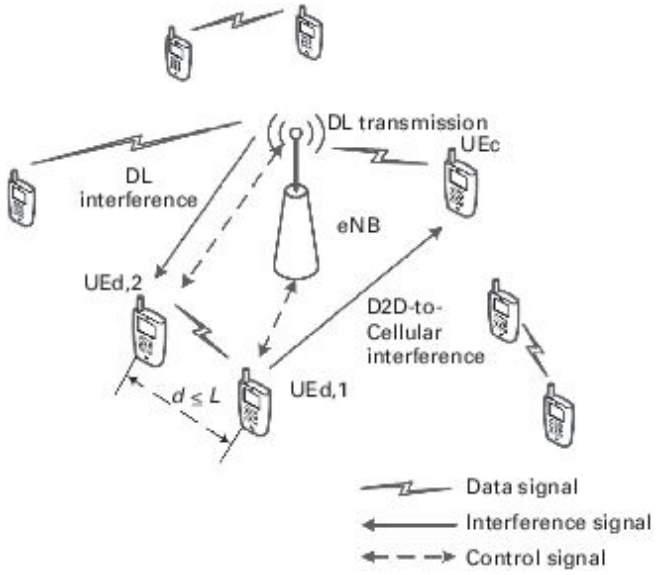

Figure 6.1. The system model of D2D communications underlaying cellular networks with downlink resource sharing.

The existing works [16, 17] confirm that, with a power-control or resource-scheduling mechanism, the inter-cell interference can be managed efficiently. Therefore, this work places an emphasis on the intra-cell interference, which is due to the resource sharing of D2D and cellular

communication. Generally speaking, the session setup of D2D communications requires the following steps [1].

(i) A request of communication is initiated by one UE pair.

(ii) The system detects traffic originating from and destined to the UE in the same subnet.

(iii) If the traffic fulfills a certain criterion (e.g., data rate), the system considers the traffic as potential D2D traffic.

(iv) The eNB checks whether the D2D mode offers higher throughput.

(v) If both UEs are D2D-capable and the D2D mode offers higher throughput, the eNB may set up a D2D bearer.

The cross-layer processes of resource control can be contained in the above steps, and are generally summarized as follows. The transmitters (both cellular and D2D users) send detecting signals. Then CSI would be obtained by corresponding receivers and be fed back to the control center (e.g., the eNB). The power control and spectrum allocation are conducted on the basis of certain principles. Finally, the eNB sends control signals to users according to allocation outcomes.

Even if the D2D connection setup is successful, the eNB still maintains the detection process in case a user should switch back to the cellular communication mode. Furthermore, the eNB maintains the radio-resource control both for cellular and for D2D communication. Given these communication features, this chapter mainly focuses on assigning cellular resources for D2D communication.

Here, a scenario of sharing DL resource of the cellular network as shown in Figure 6.1 is considered. $UE_{d,1}$ is the transmitter of the D2D pair sharing the same subchannel with the eNB, and, thus, $UE_{d,2}$ as the D2D receiver

receives interference from the eNB. Also, the cellular receiver UE_C is exposed to interference from $UE_{d,1}$. In addition, the D2D users feed back the CSI to the eNB, while the eNB transmits control signals to the D2D pair, in such a way that the system achieves D2D power control and resource allocation.

During the DL period of the cellular system, both cellular and D2D users receive interference because they share the same subchannels. Here, any cellular user's resource blocks (RBs) can be shared with multiple D2D pairs and each pair can use more than one user's RBs for transmission. Note that the numbers of cellular users and D2D pairs in the model are C and D, respectively. During the DL period, the eNB transmits signal x_i to the ith ($i = 1, 2, \ldots, C$) cellular user, and the jth ($d = 1, 2, \ldots, D$) D2D pair uses the same spectrum resources transmitting signal x_j. The received signals at UE i and D2D receiver j are written as

$$y_i = \sqrt{p_B} h_{Bi} x_i + \sum_j \beta_{ij} \sqrt{p_j} h_{ji} x_j + n_i, \tag{6.1}$$

$$y_j = \sqrt{p_j} h_{jj} x_j + \sqrt{p_B} h_{Bj} x_i + \sum_{j'} \beta_{jj'} \sqrt{p_{j'}} h_{j'j} x_{j'} + n_j, \tag{6.2}$$

where p_B, p_j, and $p_{j'}$ are the transmit powers of the eNB and D2D transmitters j and j', respectively. h_{ij} is the channel response of the i–j link that is from equipment i to j. n_i and n_j are the additive white Gaussian noise (AWGN) at the receivers with one-sided power spectral density (PSD) σ^2. β_{ij} represents the presence of interference satisfying $\beta_{ij} = 1$ when RBs of UE i are assigned to UE j, otherwise $\beta_{ij} = 0$. Since a cellular user can share resources with multiple D2D pairs, it also satisfies $0 \le \sum_j \beta_{ij} \le D$. Similarly, $\beta_{jj'}$ represents the presence of interference between D2D pairs j and j'.

The channel is modeled as the Rayleigh fading channel, thus the channel response follows the independent identical complex Gaussian distribution. The free-space-propagation path-loss model, $p = p_0 \cdot (d/d_0)^{-\alpha}$, is used, where

P_0 and P represent signal power measured at d_0 and d away from the transmitter, respectively. α is the path-loss exponent. Hence, the received power of each link can be expressed as follows:

$$p_{r,ij} = p_i \cdot h_{ij}^2 = p_i \cdot (d_{ij})^{-\alpha} \cdot h_0^2, \tag{6.3}$$

where $p_{r,ij}$ and d_{ij} are the received power and the distance of the i–j link, respectively. p_i represents the transmit power of equipment i and h_0 is the complex Gaussian channel coefficient that obeys the distribution $\mathcal{CN}(0, 1)$. The model is simplified by assuming that the received power at $d_0 = 1$ equals the transmit power.

For the purpose of maximizing the network capacity, the SINR should be considered as an important indicator. The SINR of user j is

$$\gamma_j = \frac{p_i h_{ij}^2}{P_{\text{int},j} + \sigma^2}, \tag{6.4}$$

where $p_{\text{int},j}$ denotes the interference signal power received by user j, and σ^2 accounts for the terminal noise at the receiver.

Determined by the Shannon capacity formula, the channel rate corresponding to the SINR of cellular and D2D users can be calculated. As cellular users suffer interference from D2D communication that is sharing the same spectrum resource, the interference power of cellular user i is

$$p_{\text{int},i} = \sum_j \beta_{ij} p_j h_{ji}^2. \tag{6.5}$$

While the interference of D2D receiver j is from both eNB and D2D users to which the same resources have been assigned, the interference power of user j can be expressed as

$$p_{\text{int},j} = p_{\text{B}} h_{\text{B}j}^2 + \sum_{j'} \beta_{jj'} p_{j'} h_{j'j}^2. \tag{6.6}$$

Using (6.4), (6.5), and (6.6), the channel rates of cellular user i and D2D receiver j can be obtained as

$$R_i = \log_2 \left(1 + \frac{p_{\text{B}} h_{\text{B}i}^2}{\sum_j \beta_{ij} p_j h_{ji}^2 + \sigma^2} \right), \tag{6.7}$$

$$R_j = \log_2 \left(1 + \frac{p_j h_{jj}^2}{p_{\text{B}} h_{\text{B}j}^2 + \sum_{j'} \beta_{jj'} P_{j'} h_{j'j}^2 + \sigma^2} \right), \tag{6.8}$$

respectively. Here, $j \neq j'$. So $\sum_{j'} \beta_{jj'} p_{j'} h_{j'j}^2$ represents the interference from the other D2D pairs that share spectrum resources with pair j.

The DL system sum rate can be defined as

$$\Re = \sum_{i=1}^{C} \left(R_i + \sum_{j=1}^{D} \beta_{ij} R_j \right). \tag{6.9}$$

Thus, the problem of designing β_{ij} for each D2D pair is considered as an optimization issue of maximizing $\Re$.

Since the D2D mode of communication shares the same spectrum resources with cellular communication at the same time slot, the co-channel interference should be limited as much as possible to optimize the system performance. The radio signals experience different degrees of fading, thus the amount of interference depends on the transmit power and spatial distances. Accordingly, this chapter focuses on assigning appropriate resource blocks (RBs) occupied by cellular users to D2D pairs to minimize

interference in order to achieve a higher system sum rate. Next, the relation between the allocation result and the rate of the shared channel is formulated, which can be defined as a value function whose target value is the channel rate.

Define $\mathcal{D}$ as a package of variables representing the index of D2D pairs that share the same resources, and the totality of pairs can form N such packages. Thus, if the members of the kth ($k = 1, 2, \ldots, N$) D2D user package share resources with cellular user i, the channel rates of UE i and D2D pair j ($j \in \mathcal{D}_k$) can be written as

$$R_i^k = \log_2 \left(1 + \frac{p_B h_{Bi}^2}{\sum_{j \in \mathcal{D}_k} p_j h_{ji}^2 + \sigma^2} \right), \tag{6.10}$$

$$R_j^k = \log_2 \left(1 + \frac{p_j h_{jj}^2}{p_B h_{Bj}^2 + \sum_{j' \in \mathcal{D}_k - \{j\}} p_{j'} h_{j'j}^2 + \sigma^2} \right), \tag{6.11}$$

respectively. The rate of the operating channel shared by UE i and D2D pairs $j \in \mathcal{D}_k$ is

$$R_{ik} = R_i^k + \sum_{j \in \mathcal{D}_k} R_j^k. \tag{6.12}$$

According to (6.10)–(6.12), when assigning resources of user i to the kth package of D2D pairs, the channel rate is given by

$$V_i(k) = \log_2\left(1 + \frac{p_{\mathrm{B}} h_{\mathrm{B}i}^2}{\sum_{j\in\mathcal{D}_k} p_j h_{ji}^2 + \sigma^2}\right) + \sum_{j\in\mathcal{D}_k} \log_2\left(1 + \frac{p_j h_{jj}^2}{p_{\mathrm{B}} h_{\mathrm{B}j}^2 + \sum_{j'\in\mathcal{D}_k - \{j\}} p_{j'} h_{j'j}^2 + \sigma^2}\right). \tag{6.13}$$

In the proposed mechanism, the spectrum resource unit occupied by cellular user i is considered as one of the bidders submitting bids to compete for the packages of D2D pairs to maximize the channel rate. It is obvious that there would be a gain of channel rate owing to D2D communication as long as the contribution to data signals from D2D pairs is larger than that to interference signals. Considering the constraint of a positive value, the performance gain is defined as

$$v_i(k) = \max\ (V_i(k) - V_i, 0)\,, \tag{6.14}$$

which is the private valuation of bidder i for the package of D2D pairs $\mathcal{D}_k$. Here, V_i denotes the channel rate of UE i without co-channel interference and is given by

$$V_i = \log_2\left(1 + \frac{p_{\mathrm{B}} h_{\mathrm{B}i}^2}{\sigma^2}\right). \tag{6.15}$$

Thus, we have the following definition.

DEFINITION 68. **A valuation model** $\mathcal{V} = \{v_i\,(k)\}$ *is a set of the private valuations of all bidders* $i \in \{1, 2, \ldots, C\}$ *for all packages* $\mathcal{D}_k \subseteq \{1, 2, \ldots, D\}$ $(k \in \{1, 2, \ldots, N\})$.

In the auction, the cellular resource denoted by i obtains a gain by getting a package of D2D communications. However, there exists some cost such as control-signal transmission and information feedback during the access process. The cost is defined as a pay price.

DEFINITION 69. *The price to be paid by the bidder i for the package* $\mathcal{D}_k$ *is called the* **pay price** *and denoted by* $\mathcal{P}_i(k)$. *The unit price of item j* ($\forall k$, $j \in \mathcal{D}_k$) *can be denoted by* $P_i(j)$.

Here, consider linear anonymous prices [188], which means that the prices are linear if the price of a package is equal to the sum of the prices of its items, and the prices are anonymous if the prices of the same package for different bidders are equal. Thus, the payment made by a bidder is

$$\mathcal{P}_i(k) = \sum_{j \in \mathcal{D}_k} P_i(j) = \sum_{j \in \mathcal{D}_k} P(j), \forall i = 1, 2, \ldots, C, \tag{6.16}$$

which is determined by the unit price $P(j)$ and the size of the bidding package $\mathcal{D}_k$.

DEFINITION 70. *The* **bidder utility**, *or* **bidder payoff**, $U_i(k)$ *expresses the satisfaction of bidder i which accrues from getting package* $\mathcal{D}_k$. *The bidder utility can be defined as follows:*

$$U_i(k) = v_i(k) - \mathcal{P}_i(k). \tag{6.17}$$

From (6.14), (6.16), (6.17), $V_i(k)$ in (6.13), and V_i in (6.15), the utility of bidder *i* can be considered as

$$U_i(k) = \log_2\left(1 + \frac{p_B h_{Bi}^2}{\sum_{j \in \mathcal{D}_k} p_j h_{ji}^2 + \sigma^2}\right) + \sum_{j \in \mathcal{D}_k} \log_2\left(1 + \frac{p_j h_{jj}^2}{p_B h_{Bj}^2 + \sum_{j' \in \mathcal{D}_k - \{j\}} p_{j'} h_{jj}^2 + \sigma^2}\right) - \log_2\left(1 + \frac{p_B h_{Bi}^2}{\sigma^2}\right) - \sum_{j \in \mathcal{D}_k} P(j). \tag{6.18}$$

To describe the allocation outcome intuitively, the definition below is helpful.

DEFINITION 71. *The result of the auction is a spectrum allocation denoted by* $\mathcal{X} = (X_1, X_2, \ldots, X_C)$*, which allocates a corresponding package to each bidder. The allocated packages may not intersect (*$\forall i, j,\ X_i \cap X_j = \emptyset$*).*

Consider a set of binary variables $\{x_i(k)\}$ to redefine the allocation as

$$x_i(k) = \begin{cases} 1, & \text{if } X_i = \mathcal{D}_k, \\ 0, & \text{otherwise.} \end{cases} \tag{6.19}$$

According to the literature, the two most popular bidding languages are exclusive-OR (XOR), which allows a bidder to submit multiple bids but at most one of the bids can win, and additive-OR (OR), which allows one to submit multiple bids and any non-intersecting combination of the bids can win. Here, consider the XOR bidding language. Thus, (6.19) satisfies $\sum_{k=1}^{N} x_i(k) \leq 1$ and $\sum_{k=1}^{N} x_i(k) = 0 \Rightarrow X_i = \emptyset$ for $\forall i = 1, 2, \ldots, C$. If one is given an allocation $\mathcal{X}$, the total bidder utility of all bidders can be denoted as $U_{\text{all}}(\mathcal{X}) = \sum_{i=1}^{C} \sum_{k=1}^{N} x_i(k) U_i(k)$. Furthermore, the auctioneer's revenue is denoted as $\mathcal{A}(\mathcal{X}) = \sum_{i=1}^{C} \sum_{k=1}^{N} x_i(k) \mathcal{P}_i(k)$, which is usually considered to be the auctioneer's gain.

As mentioned before, assume that the total spectrum resources are divided into C units, with each one already providing communication service to one cellular user. By the auction game, the spectrum units are assigned to N user packages $\{\mathcal{D}_1, \mathcal{D}_2, \ldots, \mathcal{D}_N\}$, with each package consisting of at least one D2D pair. In other words, the spectrum units compete to obtain D2D communication for improving the channel rate.

During an iterative combinatorial auction (ICA) game, the auctioneer announces an initial price for each item, and then the bidders submit to the auctioneer their bids at the current price. As long as the demand exceeds the supply, or on the contrary the supply exceeds the demand, the auctioneer

updates (raises or reduces) the corresponding price and the auction goes to the next round.

Obviously, it can be shown that the overall gain, which includes the total gain of the auctioneer and all bidders, does not depend on the pay price, but equals the sum of the allocated packages' valuations, i.e.,

$$\begin{aligned}\mathcal{A}(\mathcal{X}) + U_{\text{all}}(\mathcal{X}) &= \sum_{i=1}^{C}\sum_{k=1}^{N} x_i(k)\,\mathcal{P}_i(k) + \sum_{i=1}^{C}\sum_{k=1}^{N} x_i(k)\,U_i(k) \\ &= \sum_{i=1}^{C}\sum_{k=1}^{N} x_i(k)\,\mathcal{P}_i(k) + \sum_{i=1}^{C}\sum_{k=1}^{N} x_i(k)[(v_i(k) - \mathcal{P}_i(k))] \\ &= \sum_{i=1}^{C}\sum_{k=1}^{N} x_i(k)v_i(k).\end{aligned} \tag{6.20}$$

As was the original intention, we employ the ICA to obtain an efficient allocation of spectrum resources.

DEFINITION 72. *An* **efficient allocation** *denoted by* $\tilde{\mathcal{X}} = (\tilde{X}_1, \tilde{X}_2, \ldots, \tilde{X}_C) = \{\tilde{x}_i(k)\}$ *is an allocation that maximizes the overall gain.*

Given the private bidder valuations for all possible packages in (6.14), an efficient allocation can be obtained by solving the combinatorial allocation problem (CAP).

DEFINITION 73. *The* **combinatorial allocation problem (CAP)**, *also sometimes referred to as the* **winner-determination problem (WDP)**, *leads to an efficient allocation by maximizing the overall gain,*

$$\max_{\mathcal{D}_k = X_i \in \mathcal{X} \in \mathcal{Z}} \sum_{i=1}^{C} v_i(k),$$

where $\mathcal{X}$ *denotes the set of all possible allocations.*

An integer linear program using the binary decision variables $\{x_i(k)\}$ for the CAP is formulated as

$$\begin{aligned} &\max \sum_{i=1}^{C} \sum_{k=1}^{N} x_i(k) v_i(k), \\ &\text{s.t.} \sum_{k=1}^{N} x_i(k) \leq 1, \forall i \in \{1, 2, \ldots, C\}, \\ &\sum_{\mathcal{D}_k : j \in \mathcal{D}_k} \sum_{i=1}^{C} x_i(k) \leq 1, \forall j \in \{1, 2, \ldots, D\}. \end{aligned} \tag{6.21}$$

The objective function maximizes the overall gain, and the constraints guarantee that (1) at most one package can be allocated to each bidder; and (2) each item cannot be allocated more than once.

In fact, there might be multiple optimal solutions of the CAP with the same objective function. From the auctioneer's point of view, tie-breaking rules are needed to determine which of the optimal solutions is selected. In a real auction, the auctioneer does not know the private valuations of the bidders, and neither can he or she solve the NP-hard problem. To solve the CAP, the auctioneer selects the winners on the basis of the bids submitted in each round. Therefore, in the case of the XOR bidding language, the WDP formulation is similar to the CAP and the only difference is the objective function, i.e.,

$$\max \sum_{i=1}^{C} \sum_{k=1}^{N} x_i(k) \mathcal{P}_i^t(k), \tag{6.22}$$

where $\mathcal{P}_i^t(k)$ represents the pay price of bidder i for package $\mathcal{D}_k$ in round t.

In terms of Definition 5, the outcome of a CA is not always efficient. Here, the allocation efficiency is employed as a primary measure to benchmark auctions.

DEFINITION 74. *The* **Allocation efficiency** *in CAs can be expressed as the ratio of the overall gain of the final allocation to that of an efficient allocation [188],*

$$\mathcal{E}(\mathcal{X}) = \frac{\mathcal{A}(\mathcal{X}) + U_{\text{all}}(\mathcal{X})}{\mathcal{A}\left(\tilde{\mathcal{X}}\right) + U_{\text{all}}\left(\tilde{\mathcal{X}}\right)}, \tag{6.23}$$

which has $\mathcal{E}(\mathcal{X}) \in [0, 1]$.

Many ICA designs, especially for the centralized ICA design, are based on ask prices. The price-based ICA designs differ by the pricing scheme and price update rules. In the proposed algorithm, linear prices are used, since they are easy to understand for bidders and convenient to communicate in each auction round. Because of the interference from D2D links, cellular channels should guarantee the performance of the cellular system before allowing the D2D access. Hence, a descending-price criterion is considered in the algorithm. Prices are updated by a greedy mode such that, once a bidder has submitted a bid for items or packages, the corresponding prices are fixed. Otherwise, the prices are decreased.

At the beginning of the allocation, the eNB collects the location information of all of the D2D pairs. In addition, the round index $t = 0$, the initial ask price $P^0(j)$ for each item (D2D pair) j, and the fixed price reduction $\Delta > 0$ are set up. When the initial prices are announced to all the bidders (i.e., spectrum resources occupied by cellular UEs), each bidder submits bids, which consist of its desired packages and the corresponding pay prices. Jump bidding, where bidders are allowed to bid higher than the prices, is not allowed in our scheme, thus bidders always bid at the current prices. According to the CAP proposed in Definition 6 and the analysis of the WDP, the problem of maximizing the overall gain can be simplified as a

process of collecting the highest pay price. As a result, bidder i bids for package $\mathcal{D}_k$ as long as $U_i(k) \geq 0$. Combining (6.16) and (6.17), one has

$$v_i(k) \geq \mathcal{P}_i^t(k) = \sum_{j \in \mathcal{D}_k} P^t(j), \tag{6.24}$$

where the round index $t \geq 0$. In this case, let $b_i^t(k) = \{\mathcal{D}_k, \mathcal{P}_i^t(k)\}$ denote the bid submitted at the end of round t, and let $\mathcal{B}^t = \{b_i^t(k)\}$ denote all the bids. When (6.24) is not satisfied, bid $b_i^t(k) = \{\emptyset, 0\}$. If $\exists j \in \mathcal{D}_k$ satisfies $\forall b_i^t(k) \in \mathcal{B}^t, \mathcal{D}_k \notin b_i^t(k)$, this reveals that the supply exceeds the demand. Then, the eNB sets $t = t + 1$, $P^{t+1}(j) = P^t(j) - \Delta$, where j is the over-supplied item, and the auction moves on to the next round.

In a normal case, whenever the price of a package decreases below a bidder's valuation for that package, the bidder submits a bid for it. The eNB allocates the package to the bidder, and fixes the corresponding prices of items. At the same time, constrained by the XOR bidding language, the bidder is not allowed to participate in the following auction rounds. As the asking prices decrease discretely every round, there may exist a situation in which more than one bidder will bid for packages containing the same items simultaneously. The eNB detects the bids of all the bidders to assess whether it holds that (1) $b_{i_1}^t(k) = b_{i_2}^t(k) \neq \{\emptyset, 0\}$ $(i_1 \neq i_2, k \in \{1, 2, \ldots, N\})$; and (2) $b_{i_1}^t(k_1) = \{\mathcal{D}_{k_1}, \mathcal{P}_{i_1}^t(k_1)\}$ and $b_{i_2}^t(k_2) = \{\mathcal{D}_{k_2}, \mathcal{P}_{i_2}^t(k_2)\}$ $(k_1 \neq k_2, i_1, i_2 \in \{1, 2, \ldots, C\})$ satisfying $\mathcal{D}_{k_1} \cap \mathcal{D}_{k_2} \neq \emptyset$. If either of the above conditions is satisfied, the overall demand exceeds supply for at least one item. Then, the eNB sets a fine tuning $P^t(j) = P^t(j) + \delta$, where j is the temporarily over-demanded item, and δ can be set by $\delta = \Delta / n$, where n is an integer factor that affects the convergence rate. The allocation can be determined by multiple iterations.

The auction continues until all the D2D links have been auctioned off or every channel has won a package. Our algorithm is detailed in Table 6.1.

Table 6.1. The resource-allocation algorithm

Initial state:

The eNB collects the location information of all D2D pairs. The valuation of the ith resource unit for package k is $v_i(k), i = 1, 2, \ldots, C, k = 1, 2, \ldots, N$, which is given by (6.14). The round index $t = 0$, and the initial price $P^0(d)$, the fixed price reduction $\Delta > 0$ are set up.

Resource-allocation algorithm:

1. Bidder i submits bids $\{\mathcal{D}_k, \mathcal{P}_i(k)\}$ depending on its utility.

- bidder i bids for package $\mathcal{D}_k$ as long as $U_i(k) \geq 0$, which is represented by (6.24).
- If $U_i(k) < 0$, bidder i submits $\{\emptyset, 0\}$.

2. If $\exists j \in \mathcal{D}_k$ satisfies $\forall b_i^t(k) \in \mathcal{B}^t, \mathcal{D}_k \notin b_i^t(k)$, the eNB sets $t = t + 1$, $P^{t+1}(j) = P^t(j) - \Delta$, where j is the over-supplied item, and the auction moves on to the next round. Return to step 1.

3. The eNB detects the bids of all the bidders:

(1) there exists $b_{i_1}^t(k) = b_{i_2}^t(k) \neq \{\emptyset, 0\}$ $(i_1 \neq i_2, k \in \{1, 2, \ldots, N\})$;

(2) there exists $b_{i_1}^t(k_1) = \left\{\mathcal{D}_{k_1}, \mathcal{P}_{i_1}^t(k_1)\right\}$, $b_{i_2}^t(k_2) = \left\{\mathcal{D}_{k_2}, \mathcal{P}_{i_2}^t(k_2)\right\}$ ($k_1 \neq k_2, i_1, i_2 \in \{1, 2, \ldots, C\}$) satisfying $\mathcal{D}_{k_1} \cap \mathcal{D}_{k_2} \neq \emptyset$.

4. If neither of the conditions in step 3 is satisfied, go to step 5. Otherwise, the overall demand exceeds supply for at least one item. The eNB sets $P^t(j) = P^t(j) + \delta$, and δ can be set by $\delta = \Delta / i$, where i is an integer factor. Return to step 1.

5. The allocation can be determined by repeating the above steps. The auction continues until all D2D links have been auctioned off or every cellular channel has won a package.

Next, the important properties of the proposed auction-based resource-allocation mechanism are analyzed.

As the general definition, cheat-proof means that reporting the true demand in each auction round is a best response for each bidder.

PROPOSITION 4. *The resource-allocation algorithm based on the reverse ICA is cheat-proof.*

Proof. From (6.18), the utility of bidder $U_i(k)$ depends on the valuation of the package that it bids and unit prices of the items. In particular, it is the interference (between cellular and D2D communications) that mainly affects the utility. As the expression is extremely complex to obtain, consider the case that only one item constitutes the package without loss of generality. The utility of bidder i can be rewritten as

$$U_i(j) = \log_2\left(1 + \frac{p_B h_{Bj}^2}{p_j h_{ji}^2 + \sigma^2}\right) + \log_2\left(1 + \frac{p_j h_{jj}^2}{p_B h_{Bj}^2 + \sigma^2}\right) - \log_2\left(1 + \frac{p_B h_{Bi}^2}{\sigma^2}\right) - P^t(j), \tag{6.25}$$

and the differential expressions for the utility with respect to h_{ji} and h_{Bj} are

$$\frac{\partial U_i(j)}{\partial h_{ji}} = \frac{-2p_j h_{ji} p_B h_{Bi}^2}{(\ln 2)\left(p_j h_{ji}^2 + p_B h_{Bi}^2 + \sigma^2\right)\left(p_j h_{ji}^2 + \sigma^2\right)} < 0, \tag{6.26}$$

$$\frac{\partial U_i(j)}{\partial h_{Bj}} = \frac{-2p_B h_{Bj} p_j h_{jj}^2}{(\ln 2)\left(p_B h_{Bj}^2 + p_j h_{jj}^2 + \sigma^2\right)\left(p_B h_{Bj}^2 + \sigma^2\right)} < 0, \tag{6.27}$$

respectively. Accordingly, the utility $U_i(j)$ is a monotonically decreasing function with respect to both h_{ji} and h_{Bj}. Thus, the optimal strategy is to bid the D2D link that has a lower channel gain with the cellular transmitter and receiver.

In a descending-price auction, items are always too expensive to afford at the beginning. With the number of iterations t increasing, the prices of items drop off. Given a package $\mathcal{D}_k$ in round t, bidder i has the right to submit bid $\{\mathcal{D}_k, \mathcal{P}_i^t(k)\}$ or $\{\emptyset, 0\}$. Given that all the other bidders submit their true demands according to (6.24), consider the strategy of bidder i in two cases: (1) if i bids $\{\emptyset, 0\}$ when its true valuation for $\mathcal{D}_k$ satisfies $U_i(k) \geq 0$, it will quit this round and lose the package which maximizes its channel rate; (2) if i bids $\{\mathcal{D}_k, \mathcal{P}_i^t(k)\}$ when its true valuation for $\mathcal{D}_k$ satisfies $U_i(k) < 0$ and finally wins the package, it will obviously get a negative surplus that is unwanted.

From the above analysis, it can be concluded that the optimal strategy for cellular channel i is to submit its true demand in each round, or it will get a loss in its utility as a result of any deceiving. That is, the proposed resource-allocation algorithm is cheat-proof. □

PROPOSITION 5. *The resource-allocation algorithm based on the reverse ICA has the convergence property that the number of the iterations is finite.*

Proof. According to Theorem 1, all the bidders submit their true demands in each auction round, to obtain the utility from winning. From (6.18), it can be derived that

$$U_i^{t+1} - U_i^t = \Delta > 0, \tag{6.28}$$

where U_i^t denotes the utility of bidder i in round t. According to the algorithm, bidder i will get zero utility with no bid if $U_i^t < 0$, and have an opportunity to win a positive utility with bid $\{\mathcal{D}_k, \mathcal{P}_i^t(k)\}$ if $U_i^t \geq 0$. Therefore, at the beginning, bidder i plays a waiting game, and, once $U_i^t(k) \geq 0$, it will bid for $\mathcal{D}_k$. As long as it is the only one that submits a bid, it will get the package. With a sufficiently large t and $\Delta > 0$, it can be finally got that $x_i(k) = 1$. Similarly, if more than one bidder bids for the same item, the algorithm performs an allocation by ascending price process with the step size $\delta < \Delta$. Subject to

$$\sum_{\mathcal{D}_k : j \in \mathcal{D}_k} \sum_{i=1}^{C} x_i(k) \leq 1$$

in (6.21), the package cannot be allocated again. Thus, for a finite number of packages N, the number of iterations is finite. That is, the proposed scheme would reach convergence. □

Additionally, the value of the price step Δ has a direct impact on the speed of convergence of the proposed scheme. The scheme converges fast when Δ is large, whereas it converges slowly when Δ is small. The fine tuning δ also has the same nature, but has less impact on convergence.

In an ICA game, the price updates in several ways, i.e., through monotonically increasing, monotonically decreasing, and non-monotonic modes. Here, we focus on the price non-monotonicity in the proposed reverse ICA algorithm.

PROPOSITION 6. *In the proposed descending-price auction, the raising of item prices in a round may be necessary in order to reflect the competitive situation. Moreover, it brings about an improvement in efficiency.*

Proof. From the algorithm proposed in Table 6.1, there exists a situation in which more than one bidder submits bids for the same package or different packages with intersection when the prices are reduced to some particular values. However, auctions do not allow one item to be obtained by multiple bidders, as the second constraint in (6.21) shows. In this situation, raising the corresponding prices by a fine tuning $\delta = \Delta/n$ makes bidders reinspect their utility functions. Once a bidder finds its utility less than zero, it quits the competition. By a finite number of iterations, the winner converges to one bidder. Since the ascending-price process maximizes the auctioneer's revenue as shown in (6.22), the allocation has higher efficiency than that of a random allocation in that situation. □

As mentioned before, a traditional CAP in fact is an NP-hard problem, the normal solution of which is the centralized exhaustive search. Assume that the number of items to be allocated is m, and the number of bidders is n. For an exhaustive optimal algorithm, an item can be allocated with n possible results. Thus, all the m items are allocated with n^m possible results. The complexity of the algorithm is $\mathcal{O}(n^m)$. In the proposed reverse ICA scheme, bidders reveal their entire utility function. In particular, they calculate valuations for all possible packages, the number of which is $\mathcal{C}_m^1 + \mathcal{C}_m^2 + \cdots + \mathcal{C}_m^m = 2^m - 1$. If the total number of iterations is t, the complexity of the auction-based scheme is $\mathcal{O}(n\,(2^m - 1) + t)$. From the proposed algorithm, one has $P^t\,(j) = P^0\,(j) - \Delta \cdot t \geq 0$.[1] Consequently, the worst case is $t = P^0\,(j)/\Delta$. It is obvious that, for sufficiently large values of m and n, with general values of $P^0(j)$ and Δ, much lower complexity is obtained by using the proposed reverse ICA scheme. That is, $\mathcal{O}(n^m) > \mathcal{O}(n\,(2^m - 1) + P^0\,(j)/\Delta)$. On constraining the number of D2D pairs sharing the same channel to one, the complexity would be further reduced to $\mathcal{O}(n \cdot m + P^0\,(j)/\Delta)$. The performance of this reduced scheme is shown in the simulation.

In the D2D underlay system, the eNB is still the control center of resource allocation, and the global CSI should indeed be available at the eNB for the proposed scheme. In addition to the CSI detection, feedback, and the control signaling transmission, the reverse ICA scheme does not entail additional signaling overhead compared with existing resource-scheduling schemes such as maximum carrier to interference (max C/I) and proportional fair (PF), which also need the global CSI to optimize the system performance. The difference is that the reverse ICA scheme requires more complicated CSI due to the interference between the D2D and cellular networks.

At the beginning of the allocation, the transmitters need to send some packets containing detection signals. Then, the CSI obtained at each terminal (D2D or cellular receiver) would be fed back to the eNB. After that, the iteration process would be conducted at the eNB, and no signaling needs to be exchanged among the network nodes until the forwarding of the control signal.

Methods such as CSI feedback compression, and signal flooding would help reduce the overhead. In addition, future work on D2D communications could consider some mechanism that would limit the number of D2D pairs sharing the same channel by, e.g., imposing a distance constraint, which would obviously help reduce the overhead. However, for this chapter, the target is to obtain the most nearly optimal solution possible, so the simplification is not considered.

The main simulation parameters are listed in Table 6.2. As shown in Figure 6.1, simulations are performed in a single cell. Both the path-loss model and shadow fading are considered for cellular and D2D links. The wireless propagation is modeled according to WINNER II channel models [18], and the D2D channel is based on an office/indoor scenario while the cellular channel is based on the urban microcell scenario.

Table 6.2. Main simulation parameters

Parameter	Value
Cellular layout	Isolated cell, one-sector
System area	The radius of the cell is 500 m
Noise spectral density	-174 dBm/Hz
Subchannel bandwidth	15 kHz
Noise figure	9 dB at device
Antenna gains	eNB: 14 dBi; device: 0 dBi
Maximum distance of D2D	5 m
Transmit power	eNB: 46 dBm; device: 23 dBm

The system sum rate with different numbers of D2D pairs and different numbers of resource units using the proposed auction algorithm is illustrated in Figures 6.2 to 6.4. The sum rate can be obtained from (6.9).

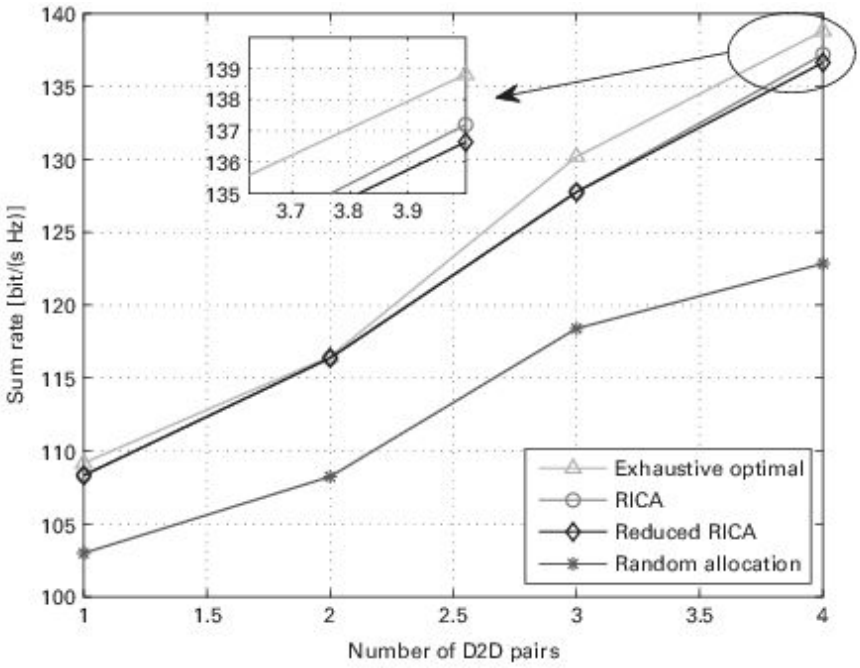

Figure 6.2. System sum rates for different allocation algorithms in the case of eight resource units.

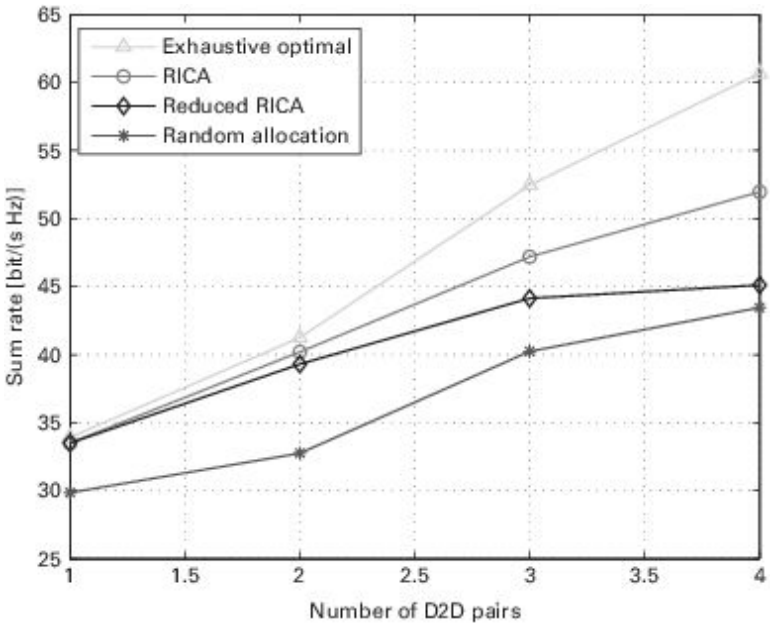

Figure 6.3. System sum rates for different allocation algorithms in the case of two resource units.

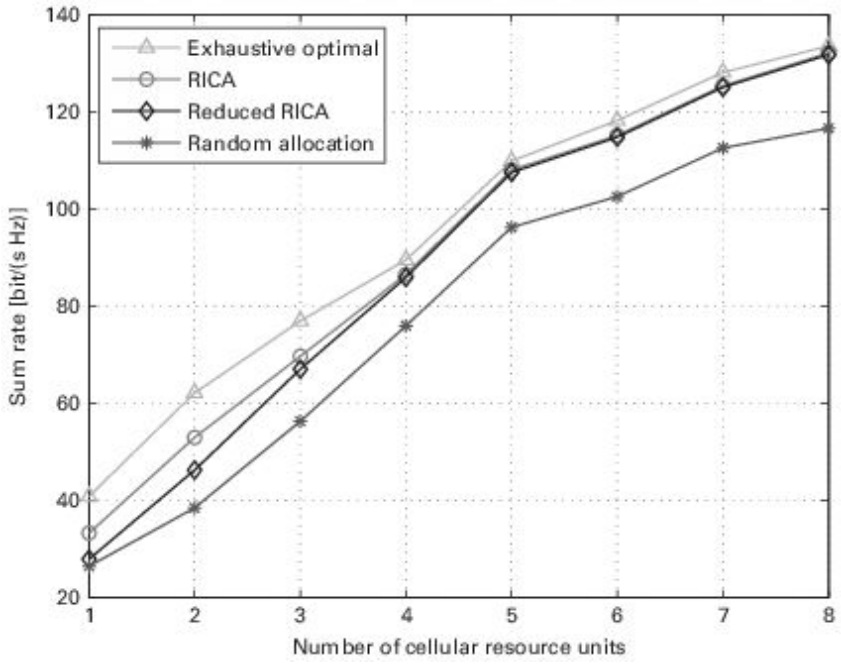

Figure 6.4. System sum rates for different allocation algorithms in the case of four D2D pairs.

From Figures 6.2 and 6.4, it can be seen that the system sum rate goes up with both the number of D2D pairs and the number of resource units increasing. On the one hand, when the amount of resource is fixed, more D2D users contribute to a higher system sum rate. On the other side, as the amount of resource increases, the probability of resources with less interference to D2D links being assigned to them enhances, which can lead to an increased sum rate. This phenomenon is similar to the effect of multi-user diversity. Definitely, cellular users also contribute to the performance.

From another perspective, Figures 6.2 to 6.4 show the system sum rate for different allocation algorithms. The curve labeled as exhaustive optimal is simulated by the exhaustive search method, which guarantees an upper bound of the system sum rate. The curve labeled reduced RICA is the result of a reduced reverse ICA scheme, in which the number of D2D pairs sharing the same cellular resources is constrained to one. The curve labeled RICA represents the performance of the proposed reverse ICA algorithm, and the last one is the simulation result obtained using a random allocation of spectrum resources. Firstly, the proposed auction algorithm is much superior

to the random allocation. Secondly, the optimal allocation results in the highest system sum rate, but the superiority compared with RICA is relatively small, especially when the number of cellular resource units increases, as Figure 6.4 shows. Moreover, the performance of reduced RICA approximates to that of the RICA scheme in the case of eight resource units, but obviously differs in the case of two resource units as shown in Figure 6.3. The reason for this result is that the constraint of the reduced RICA limits D2D pairs' access to the network when the number of resource units is less than that of D2D pairs. As a result, a large capacity loss ensues.

Define the system efficiency as $\eta = \Re/\Re_{\text{opt}}$, where $\Re_{\text{opt}}$ represents the exhaustive optimal sum rate. Figure 6.5 shows the system efficiency with different numbers of D2D pairs and different numbers of resource units. The simulation result indicates that the proposed algorithm provides high (the lowest value of η is around 0.7) system efficiency. Moreover, the efficiency is stable over different parameters of users and resources.

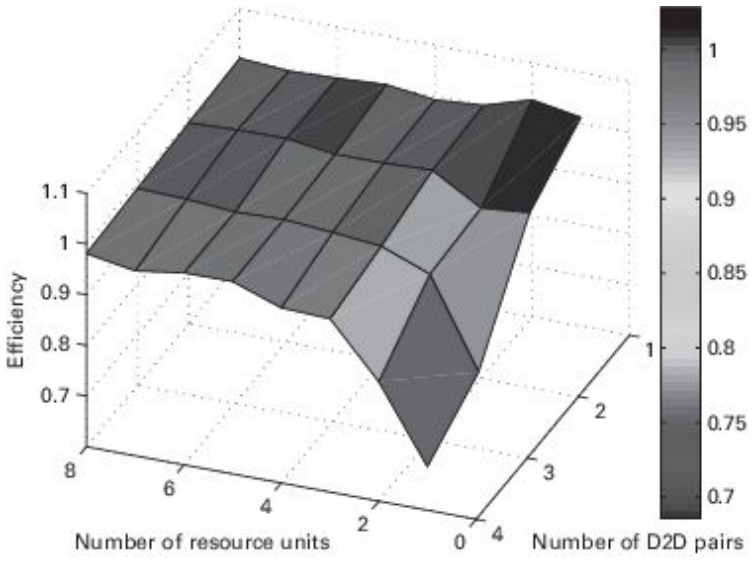

Figure 6.5. System efficiency: η with different numbers of D2D pairs and different numbers of resource units.

Regarding the point of the efficiency value being about 0.7, the number of resource units and the number of D2D pairs are both small. The linear price rule prevents bidders from bidding for the maximal-valuation

packages; instead, they are constrained to bid for the packages having maximal average unit valuation. For this reason, the efficiency decreases slightly.

Regarding other points, the efficiency is stable above 0.9, which reflects a small performance gap between the proposed algorithm and the exhaustive-search scheme. In fact, the descending-price rule determines that the bidder who has the highest bid on current items would win the corresponding package, which maximizes the current overall gain. However, the gap cannot be avoided because the algorithm essentially follows a local, or an approximately global, optimum principle.

Figure 6.6 shows an example of the price non-monotonicity in the reverse ICA scheme. The four curves represent unit prices of four D2D pairs. As the enlarged detail shows, the unit price of D2D pair 2 ascends during the auction. Since the step size δ is much less than the descending step Δ, the phenomenon of an ascending price is hard to observe. When the items have been allocated, their prices are fixed to the selling value. From the figure, it can be found that D2D pair 2 is the last one to be allocated.

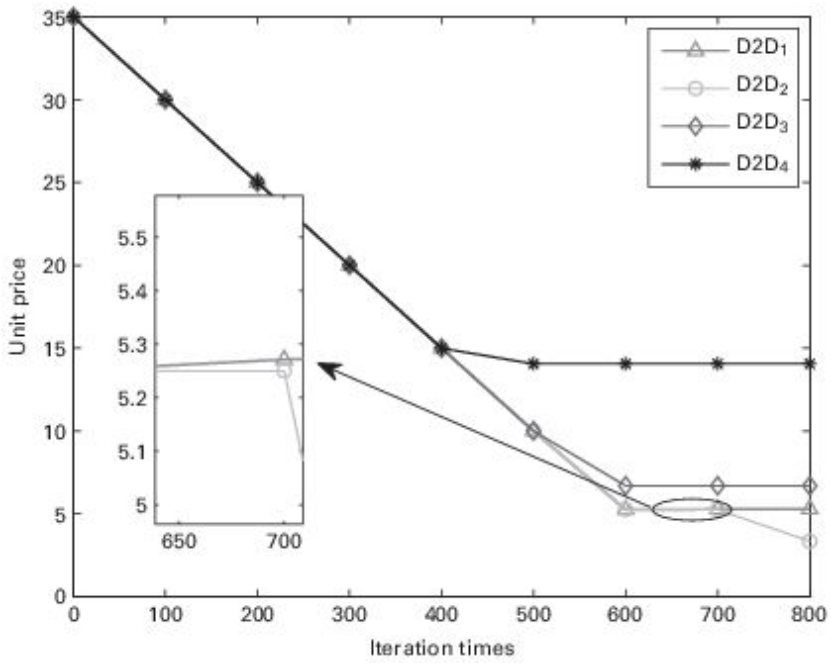

Figure 6.6. Price monotonicity: an example of price non-monotonicity in the reverse ICA scheme.

In this section, we have investigated how to reduce the effects of interference between D2D and cellular users, in order to improve the system sum rate for a D2D underlay network. The reverse ICA has been proposed as the mechanism to allocate the spectrum resources for D2D communications with multiple user pairs. We have formulated the valuation of each D2D pair for each resource unit, and then explained a detailed auction algorithm depending on the utility function. A non-monotonic descending-price iteration process has been modeled and analyzed to be cheat-proof, to converge in a finite number of rounds, and to be of low complexity. The simulation results show that the system sum rate increases as both the number of D2D pairs and the number of resource units increase. The proposed auction algorithm is much superior to random allocation, and provides high system efficiency, which is stable over different parameters of users and resources.

6.2 Time-domain scheduling

D2D communications as an underlay to cellular networks brings significant benefits to system throughput and energy efficiency. However, since D2D UEs can cause interference to cellular UEs, the scheduling and allocation of channel resources and power to D2D communication need elaborate coordination. Thus, both system throughput and fairness are taken into account in this section. Joint time-domain scheduling and spectrum allocation schemes are studied.

6.2.1 Stackelberg game-based scheduling in the time domain

In this subsection, we develop a Stackelberg game framework in which a cellular UE and a D2D UE are grouped to form a leader–follower pair. The cellular user is the leader, and the D2D UE is the follower who buys channel resources from the leader. We analyze the equilibrium of the game, and propose an algorithm for joint scheduling and resource allocation.

We still consider a single-cell scenario with multiple UEs and one eNB located at the center of the cell. Both the UEs and the eNB are equipped with

a single omni-directional antenna. The system includes two types of UEs, namely D2D UEs and cellular UEs. The D2D UEs are in pairs, each consisting of one transmitter and one receiver. Consider a dense D2D environment, where the numbers of cellular UEs and D2D UEs are K and D $(D > K)$, respectively. The sets of cellular UEs and D2D pairs are denoted by $\mathcal{K}$ and $\mathcal{D}$, respectively. There are K orthogonal channels, which is occupied by the corresponding cellular UEs. The channels allocated to the cellular UEs are fixed, and D2D communications share the channels with cellular UEs. One channel is allowed to be used only by one cellular UE and one D2D UE. In LTE, scheduling takes place every transmission time interval (TTI) [183], which consists of two time slots. Channels are allocated among D2D UEs according to their priority. During each TTI, K D2D pairs are selected to share the K channels with the cellular UEs while other D2D UEs wait for transmission.

A scenario of uplink resource sharing is illustrated in Figure 6.7, which includes one cellular UE (UE_1) and two D2D pairs (UE_2 and UE_3, UE_4 and UE_5). UE_2 and UE_4 are transmitters while UE_3 and UE_5 are receivers. The two D2D UEs in a pair are close enough to satisfy the maximum-distance constraint of D2D communications, to guarantee the quality of D2D services. D2D pair 1 is selected to share the channel resource with UE_1 while D2D pair 2 cannot transmit. During the uplink period of the cellular network, UE_1 transmits data to the eNB, while the eNB suffers interference from UE_2. Also, D2D pair 1 is in communication while UE_3 is exposed to interference from UE_1.

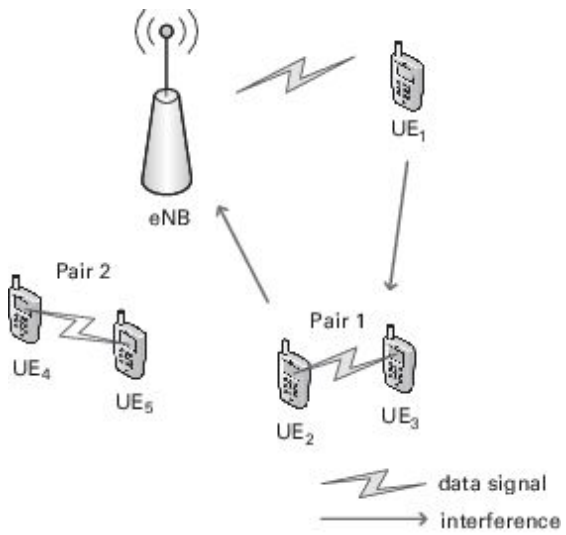

Figure 6.7. The system model of D2D underlay communications with uplink resource sharing. UE_1 is a cellular user while the pairs UE_2 and UE_3, UE_4 and UE_5 are D2D UEs.

During the downlink period, the cellular UE receives data from the eNB and interference from the D2D transmitter sharing the same channel. The D2D receivers suffer interference from the eNB. The transmit power of the eNB is too large, causing serious interference to the D2D UEs, and hence it is hard to guarantee the quality of D2D services. Therefore, we focus on the uplink frame of the network.

Define a set of binary variables $\{x_{ik}\}$ $(i \in \mathcal{D}, k \in \mathcal{K})$ to denote the current D2D pair in communication. $x_{ik} = 1$ if the ith D2D pair is selected to use channel k; $x_{ik} = 0$ otherwise. From the analysis above, during the uplink period, the kth cellular UE transmits s_k to the eNB, and the ith D2D transmitter transmits s_i. The signals received at the eNB and D2D receiver i are written as follows:

$$y_k^c = \sqrt{p_k g_{ke}} s_k + \sum_{i=1}^{D} x_{ik} \sqrt{p_i g_{ie}} s_i + n_k, \tag{6.29}$$

$$y_i^{\mathrm{d}} = \sqrt{p_i g_{ii}} s_i + \sum_{k=1}^{K} x_{ik} \sqrt{p_k g_{ki}} s_k + n_i, \tag{6.30}$$

where p_k and p_i are the transmit powers of the kth cellular UE and the ith D2D transmitter, respectively. g_{ki} denotes the channel gain between the kth cellular UE and the ith D2D receiver. g_{ii} denotes the channel gain between the ith D2D transmitter and the ith D2D receiver, which are in a pair. g_{ke} is the channel gain between cellular UE k and the eNB, and g_{ie} is the channel gain between D2D transmitter i and the eNB. n_k and n_i denote the additive white Gaussian noise (AWGN). Without loss of generality, we assume all UEs observe the same noise power σ^2.

The received SINR at the ith D2D receiver can be expressed as follows:

$$\gamma_i^{\mathrm{d}} = \frac{p_i g_{ii}}{\sum_k x_{ik} p_k g_{ki} + \sigma^2}. \tag{6.31}$$

The SINR at the eNB corresponding to cellular UE k is

$$\gamma_k^{\mathrm{c}} = \frac{p_k g_{ke}}{\sum_i x_{ik} p_i g_{ie} + \sigma^2}. \tag{6.32}$$

The channel rate of UEs is given by

$$r = \log_2(1 + \gamma). \tag{6.33}$$

Since D2D communication takes place underlaying the primary cellular network, we focus on the power control and scheduling of the D2D UEs, while the transmit power and channel of the cellular UE are assumed to be fixed. D2D communication can utilize the proximity between UEs to improve the throughput performance of the system. In the meantime, the interference from the D2D network to the cellular network should be limited.

Thus, the transmit power of the D2D UEs should be properly controlled. Another goal is to guarantee fairness among D2D UEs when scheduling.

The interactions among the selfish cellular and D2D UEs sharing a channel can be modeled as a noncooperative game. When the players choose their strategies independently without any coordination, it usually leads to an inefficient outcome. If we simplify the D2D scenario as a noncooperative game, D2D UEs will choose to use the maximum transmit power to maximize their own payoffs regardless of other players, while cellular UEs will choose not to share the channel resources with D2D UEs. This is an inefficient outcome, as the interference is too strong or D2D cannot get access to the network.

Therefore, the Stackelberg game is employed to coordinate the scheduling, in which the cellular UEs are the leaders and the D2D UEs are the followers. Focus on the behavior of a one-leader–one-follower pair. The leader owns the channel resource and it can charge the D2D UE some fees for using the channels. The fees are fictitious money to coordinate the system. Thus, the cellular UE has an incentive to share the channel with the D2D UE if it is profitable, and the leader has the right to decide the price. For the D2D UE, under the charging price, it can choose the optimal power to maximize its payoff. In this way, an equilibrium can be reached.

Next, analyze the behavior of a one-leader–one-follower pair, which includes cellular UE k as the leader and D2D pair i as the follower. The utility of the leader can be defined as its own throughput performance plus the gain it earns from the follower. The fee should be decided according to the leader's own consideration. Thus, we set the fee proportional to the interference that the leader observes. The utility function of the leader can be expressed as follows:

$$u_k(\alpha_k, p_i) = \log_2\left(1 + \frac{p_k g_{ke}}{p_i g_{ie} + \sigma^2}\right) + \alpha_k \beta p_i g_{ie}, \tag{6.34}$$

where α_k is the charging price ($\alpha_k > 0$). β is a scaling factor to denote the ratio of the leader's gain and the follower's payment ($\beta > 0$). β is a key parameter to influence the outcome of the game, which will be discussed later. The optimization problem for the leader is to set a charging price that maximizes its utility, i.e.,

$$\max u_k(\alpha_k, p_i), \quad \text{s.t.} \alpha_k > 0. \tag{6.35}$$

For the follower, the utility is its throughput performance minus the cost that it pays for using the channel, which can be expressed as follows:

$$u_i(\alpha_k, p_i) = \log_2\left(1 + \frac{p_i g_{ii}}{p_k g_{ki} + \sigma^2}\right) - \alpha_k p_i g_{ie}. \tag{6.36}$$

The optimization problem for the follower is to set the appropriate transmit power to maximize its utility, i.e.,

$$\max \ u_i(\alpha_k, p_i), \quad \text{s.t.} \ p_{\min} \le p_i \le p_{\max}. \tag{6.37}$$

In the Stackelberg game, the leader moves first and the follower moves subsequently. That is, the leader sets the price first, and the follower selects its best transmit power on the basis of the price. The leader knows ex ante that the follower observes its action. The game can be solved by backward induction.

Given α_k decided by the leader, when p_i approaches 0, the utility approaches 0 as well. As p_i increases, u_i also increases. If p_i grows too large, u_i will begin to decrease since the logarithmic function grows slower than the cost. The follower wants to maximize its utility by choosing the appropriate transmit power. The best response is derived by solving

$$\frac{\partial u_i}{\partial p_i} = \frac{1}{\ln 2} \frac{g_{ii}}{p_i g_{ii} + p_k g_{ki} + \sigma^2} - \alpha_k g_{ie} = 0. \tag{6.38}$$

The solution is

$$\hat{p}_i = \frac{1}{\alpha_k g_{ie} \ln 2} - \frac{p_k g_{ki} + \sigma^2}{g_{ii}}. \tag{6.39}$$

The second-order derivative is

$$\frac{\partial^2 u_i}{\partial p_i^2} = -\frac{1}{\ln 2} \left(\frac{g_{ii}}{p_i g_{ii} + p_k g_{ki} + \sigma^2} \right)^2 < 0. \tag{6.40}$$

Thus, the solution in (6.39) is a maximum point.

From (6.39), it can be seen that the power is monotonically decreasing with α_k, which means that, when the price is higher, the amount of power bought is smaller. Note that $p_{\min} \leq p_i \leq p_{\max}$, thus, the best response is sought in $\{p_{\min}, p_{\max}, \hat{p}_i\}$.

The leader knows ex ante that the follower will react to his price by searching in $\{p_{\min}, p_{\max}, \hat{p}_i\}$. If the leader sets the price too low, the follower will buy only $p_{\max}$, and the leader will earn more if he raises the price. Besides, the price is restricted to be set too high, to prevent the occurrence of an inefficient outcome. Thus, the leader will set the price such that $p_{\min} \leq \hat{p}_i \leq p_{\max}$. On solving the inequalities, one has

$$\alpha_{k\min} = \frac{g_{ii}}{(g_{ii} p_{\max} + p_k g_{ki} + \sigma^2) g_{ie} \ln 2}, \tag{6.41}$$

$$\alpha_{k\max} = \frac{g_{ii}}{(g_{ii} p_{\min} + p_k g_{ki} + \sigma^2) g_{ie} \ln 2}, \tag{6.42}$$

and $\alpha_{k\min} \leq \alpha \leq \alpha_{k\max}$.

On substituting the follower's strategy (6.39) into the leader's utility function, one has

$$u_k(\alpha_k) = \frac{\beta}{\ln 2} - \alpha_k \beta g_{ie} \frac{p_k g_{ki} + \sigma^2}{g_{ii}} + \log_2 \left[1 + p_k g_{ke} \left(\frac{1}{\alpha_k \ln 2} - g_{ie} \frac{p_k g_{ki} + \sigma^2}{g_{ii}} + \sigma^2 \right)^{-1} \right]. \tag{6.43}$$

There is a tradeoff between the gain from the leader itself and the gain from the follower. When the leader raises the price, it will gain less from the follower according to (6.43), but the follower will buy less power, which will lead to an increase in the leader's rate. Therefore, there is an optimal price for the leader to ask for.

On letting $A = p_k g_{ke}, B = 1/\ln 2$, and $C = -g_{ie}(p_k g_{ki} + \sigma^2)/g_{ii} + \sigma^2$, one has

$$u_k(\alpha_k) = \log_2 \left(1 + \frac{A\alpha_k}{C\alpha_k + B} \right) + (C - \sigma^2)\beta\alpha_k + B\beta. \tag{6.44}$$

To obtain the optimal price, by taking the first-order derivative, it is obtained that

$$\frac{du_k}{d\alpha_k} = \frac{AB^2}{(C\alpha_k + B)[(A + C)\alpha_k + B]} + (C - \sigma^2)\beta. \tag{6.45}$$

Consider the following cases.

(1) $C = 0$. The first-order condition is

$$\frac{du_k}{d\alpha_k} = \frac{AB}{A\alpha_k + B} - \sigma^2\beta = 0. \tag{6.46}$$

The solution is

$$\hat{\alpha}_k = \frac{B}{\sigma^2\beta} - \frac{B}{A}. \tag{6.47}$$

The second-order derivative is

$$\frac{d^2u_k}{d\alpha_k^2} = -B\left(\frac{A}{A\alpha_k + B}\right)^2 < 0. \tag{6.48}$$

Note that $\alpha_{k\min} = B/(p_{\max} g_{ie} + \sigma^2 - C)$ and $\alpha_{k\max} = B/(p_{\min} g_{ie} + \sigma^2 - C)$. Thus, the optimal α_k is sought in $\{\hat{\alpha}_k, \alpha_{k\min}, \alpha_{k\max}\}$.

(2) $A + C = 0$. The optimal price α_k can be solved similarly. The solution is sought in $\{B/A - B/[(A+\sigma^2)\beta], \alpha_{k\min}, \alpha_{k\max}\}$. If $C \neq 0$ and $A + C \neq 0$, denote $f(\alpha_k) = (C\alpha_k + B)[(A+C)\alpha_k + B]$, which is a quadratic function of α_k. It can be noticed that roots for the $f(\alpha_k)$ are $\alpha_{k1} = -B/C$ and $\alpha_{k2} = -B/(A+C)$. From $\alpha_k \leq \alpha_{k\max}$, there is $(C - \sigma^2)\alpha_k + B \geq 0$. Thus, $C\alpha_k + B > 0$ and $(A+C)\alpha_k + B > 0$. The following three cases are discussed in terms of the sign of C and $A + C$.

(3) $C > 0$. One has $\alpha_k \geq \alpha_{k\min} > 0 > \alpha_{k2} > \alpha_{k1}$. $f(\alpha_k)$ is monotonically increasing with α_k and $f(\alpha_k) > 0$ for $\alpha_k > \alpha_{k\min}$. Thus, the first-order derivative of the utility $u_k'(\alpha_k)$ is monotonically decreasing with α_k and it follows that

$$\lim_{\alpha_k \to \infty} u_k'(\alpha_k) = (C - \sigma^2)\beta < 0.$$

If $u_k'(\alpha_{k\min}) \leq 0$, it satisfies the condition $u_k'(\alpha_k) \leq 0, \alpha_k \in [\alpha_{k\min}, \alpha_{k\max}]$. Thus, the optimal price is $\alpha_{k\min}$. Otherwise, if $u_k'(\alpha_{k\min}) > 0$, there exists a unique point such that $u_k'(\alpha_k) = 0$. Solving for $u_k'(\alpha_k) = 0$ gives

$$\alpha_k = \frac{-B(A+2C) \pm \sqrt{\Delta}}{2C(A+C)}, \tag{6.49}$$

where $\Delta = AB^2[A + 4C(A+C)/[(\sigma^2 - C)_\beta]]$. The maximum point must be the larger root or on the boundary of the feasible region of α.

(4) $C < 0$ and $A + C > 0$. One has $\alpha_{k2} < 0 < \alpha_{k\min} \le \alpha_k < \alpha_{k1}$ and $f(\alpha_k) > 0$. If $\min u_k'(\alpha_k) \le 0, \alpha_k \in [\alpha_{k\min}, \alpha_{k\max}]$, with α_k increasing, $u_0'(\alpha_k)$ is increasing, decreasing, and increasing sequentially. Thus, the maximum point is either on the maximum boundary of the feasible region or is the smaller root of $u_k'(\alpha_k) = 0$, i.e.,

$$\alpha_k = \frac{-B(A+2C) + \sqrt{\Delta}}{2C(A+C)}. \tag{6.50}$$

Otherwise, $u_k(\alpha_k)$ is increasing with α_k, and the maximum point is $\alpha_{k\max}$.

(5) $A+C < 0$. One has $0 < \alpha_k < \alpha_{k1} < \alpha_{k2}$ and $f(\alpha_k) > 0$, and $u_k'(\alpha_k)$ is monotonically increasing with α_k. Thus, there does not exist a maximum point within the feasible region. By similar analysis, the optimal price α_k is derived to be that on the boundary of the feasible region.

From the discussion above, the optimal α_k can be uniquely decided. The strategies of the leader and the follower establish a Stackelberg equilibrium defined below.

DEFINITION 75. *A pair of strategies (α_k, p_i) is a Stackelberg equilibrium if no unilateral deviation in strategy by the leader or the follower is profitable, i.e.,*

$$u_i(\alpha_k, p_i) \ge u_i(\alpha_k, p_i'), \tag{6.51}$$

$$u_k(\alpha_k, p_i(\alpha_k)) \geq u_k(\alpha_k', p_i(\alpha_k')). \tag{6.52}$$

The equilibrium is a stable outcome of the Stackelberg game where the leader and the follower compete through self-optimization and reach a point from which no player wishes to deviate. The analysis of the leader and the follower above shows the existence and uniqueness of the Stackelberg equilibrium.

6.2.2 *Joint frequency–time-domain scheduling*

The scheduling process is conducted at each TTI. The D2D UEs form a priority queue for each channel. During each TTI, the eNB selects K D2D UEs with the highest priority for each channel sequentially, and other D2D UEs have to wait.

In our Stackelberg game framework, the priority is based on the utilities of the followers, which quantify the satisfaction of the followers. In the design of a scheduling scheme, fairness is considered as an important goal. The scheme should take the outcome in the previous TTIs into account. This can be achieved by adjusting the prices for using the channel. The follower has to pay an additional fee for using the channel at TTI t if it has been selected in previous TTIs, which will lead to a decrease in the priority. The additional fee is decided by the cumulative utility of follower. The priority for follower i at TTI t can be defined as

$$P_{ik}(t) = u_i(\alpha_k^*(t), p_i^*(t)) - c_i(t), \tag{6.53}$$

where $\alpha_k^*(t)$ and $p_i^*(t)$ are the optimal strategy pair under the Stackelberg equilibrium at TTI t. $c_i(t)$ is the additional cost, and can be defined as follows:

$$c_i(t) = \sum_{\tau=0}^{t-1} \sum_{k=1}^{K} \delta x_{ik}(\tau) u_i(\alpha_k^*(\tau), p_i^*(\tau)), \tag{6.54}$$

where $\delta > 0$ is the fairness coefficient. For a larger δ, the cumulative utility has a larger influence on the priority. If $\delta = 0$, the scheduling scheme does not take fairness into account.

From the above discussion, during each TTI, every cellular UE and D2D UE will form a leader–follower pair and play the Stackelberg game. The optimal price and power can be decided for each pair. The priority for each pair can be calculated, and they form a priority queue. Then, the eNB schedules the D2D pairs sequentially according to their order in the queue. If there is a tie, such that one channel has been allocated to another D2D pair, or the D2D pair has been scheduled to another channel, the pair is skipped. When each channel has been allocated to one D2D pair, the eNB records the outcome and the scheduling finishes. The algorithm is summarized in Algorithm 9.

Algorithm 9 Joint scheduling and resource-allocation algorithm

1: Given CSI, TTI t, the scaling factor β, the fairness coefficient δ, and the additional cost $c_i(t), \forall i$.

2: Initialize $x_{ik} = 0, \forall i, k$.

3: Search for the optimal $\alpha_{ik}^*, \forall i, k$ in

$$\left\{ \frac{B}{p_{\max} g_{ie} + \sigma^2 - C}, \frac{B}{p_{\min} g_{ie} + \sigma^2 - C} \right\}$$

and

$$\left\{ \frac{B}{\sigma^2 \beta} - \frac{B}{A}, \frac{B}{A} - \frac{B}{(A + \sigma^2)\beta}, \frac{-B(A + 2C) + \sqrt{\Delta}}{2C(A + C)} \right\}.$$

4: Calculate the optimal power

$$p_{ik}^* = \frac{1}{\alpha_{ik}^* g_{ie} \ln 2} - \frac{p_k g_{ki} + \sigma^2}{g_{ii}}, \forall i, k.$$

5: Calculate priorities

$$P_{ik} = \log_2 \left(1 + \frac{p_{ik}^* g_{ii}}{p_k g_{ki} + \sigma^2} \right) - \alpha_{ik}^* g_{ie} p_{ik}^* - c_i(t), \forall i, k.$$

6: Sort P_{ik} in descending order to form a priority queue.

7: **while** $\sum_i x_{ik} = 0, \exists k$ **do**

8: Select the head of the queue. The pair is (i^*, k^*).

9: **if** $\sum_i x_{ik^*} = 0$ **and** $\sum_k x_{i^*k} = 0$ **then**

10: Schedule the pair (i^*, k^*).

11: Set $x_{i^*k^*} = 1$ and $c_{i^*}(t + 1) = c_{i^*}(t) + \delta u_{i^*k^*}$.

12: **end if**

13: Delete the head of the queue.

14: **end while**

The algorithm has a low complexity, since the optimal strategy for each leader–follower pair is sought in a set with a constant number of elements.

To form the priority queue with length $K \times D$, the complexity is $O(KD)$.

To evaluate the performance of the proposed algorithm, several simulations are performed. Consider a single-circular-cell environment. The cellular UEs and D2D pairs are uniformly distributed in the cell. The two D2D UEs in a D2D pair are close enough to satisfy the maximum-distance constraint of D2D communication. The received signal power is $p_i = p_j d_{ij}^{-2} |h_{ij}|^2$, where p_i and p_j are the received power and transmit power, respectively. d_{ij} is the distance between the transmitter and the receiver. h_{ij} represents the complex Gaussian channel coefficient that satisfies $h_{ij} \sim \mathcal{CN}(0, 1)$. The scheduling takes place every TTI. The simulation parameters are summarized in Table 6.3.

Table 6.3. Simulation parameters and values

Parameter	Values
Cell layout	One isolated, circular
Cell radius	500 m
Number of cellular UEs	5
Number of D2D pairs	10
Maximum D2D communication distance	50 m
Cellular UE transmit power	23 dBm
D2D UE transmit power	0–23 dBm
Thermal noise power density	-174 dBm/Hz
Bandwidth	180 kHz
Transmission time interval	1 ms

In Figure 6.8, the effect of the fairness coefficient δ is studied. The cumulative distribution function (CDF) of the UE rate is plotted. δ has little effect on the performance of the cellular UEs. For a small δ, D2D UE rate is distributed in a large range, and has a tendency to converge with a larger δ. Thus, scheduling with a larger δ achieves better fairness. If one sets δ too large, the scheduling algorithm behaves like the round-robin scheduling, in

which the previous utility is the deciding factor and the utility of the current TTI has little influence. If D2D scheduling is not considered, there will be only C D2D pairs that can get access to the network, with the result that a proportion $1 - C/D$ of D2D UEs cannot achieve any data transmission.

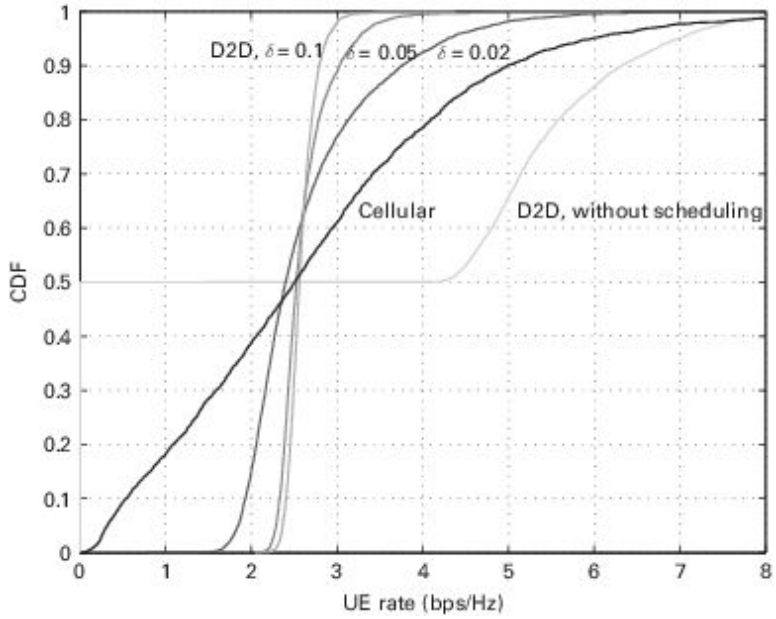

Figure 6.8. The UE rate distribution under different δ.

In Figures 6.9 and 6.10, the CDFs of the UE transmit power and UE rate under different values of the scaling factor β are plotted. β is the ratio of the leader's gain and the follower's payment. For a larger β, the payment for the follower is relatively lower, and thus the follower will choose a larger transmit power. This is illustrated in Figure 6.9. With a larger transmit power of D2D UEs, the rate of D2D UEs is larger. In the meantime, D2D UEs cause more interference to cellular UEs, causing a decrease in the rate of cellular UEs. This effect is illustrated in Figure 6.10. It can also be observed that D2D UEs use a much smaller transmit power than that of the cellular UEs.

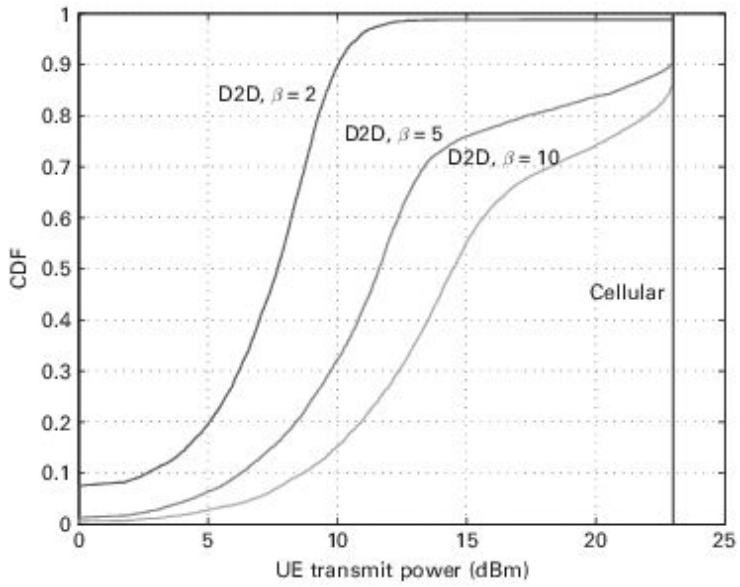

Figure 6.9. The UE power distribution under different β.

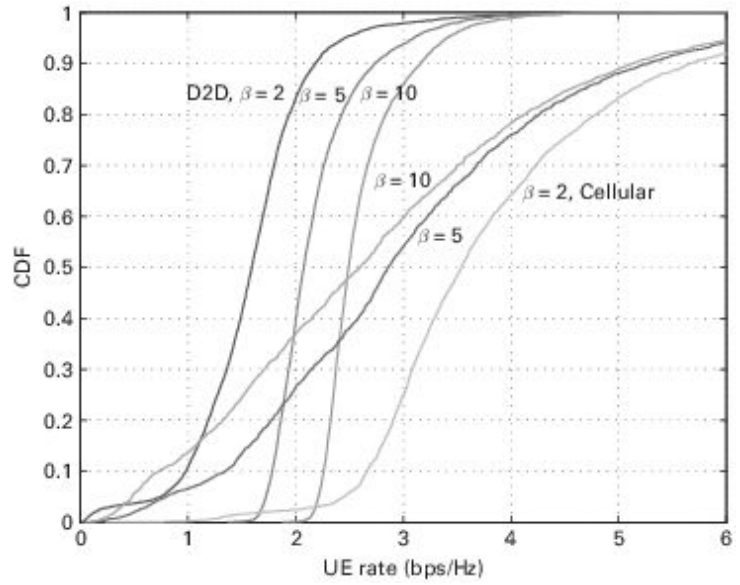

Figure 6.10. The UE rate distribution under different β.

In Figures 6.11 and 6.12, the average rate of UEs and the system sum rate with different numbers of cellular UEs are plotted. Figure 6.11 shows that, when the number of cellular UEs increases, the rate performance of D2D UEs is improved. This is due to the fact that D2D UEs have more

resources to use. It is observed that, when $C = 10$, the rate performance of D2D UEs is much better than that of cellular UEs. The effects of the scaling factor β and fairness coefficient δ are shown clearly in the two figures. It can be seen that the interference is properly managed and the cellular UEs achieve a reasonable rate performance. Besides, since there are C resources and D D2D UEs, the average transmission time of D2D UEs is D/C that of cellular UEs. In Figure 6.11, it is observed that D2D UEs achieve a rate similar to or higher than that of cellular UEs. The D2D communication obviously has higher efficiency.

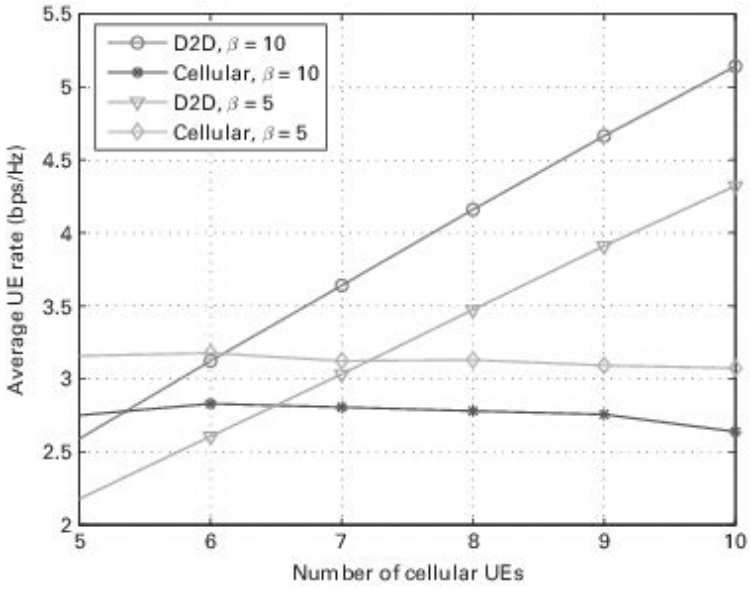

Figure 6.11. Cellular and D2D average UE rates with different numbers of cellular UEs.

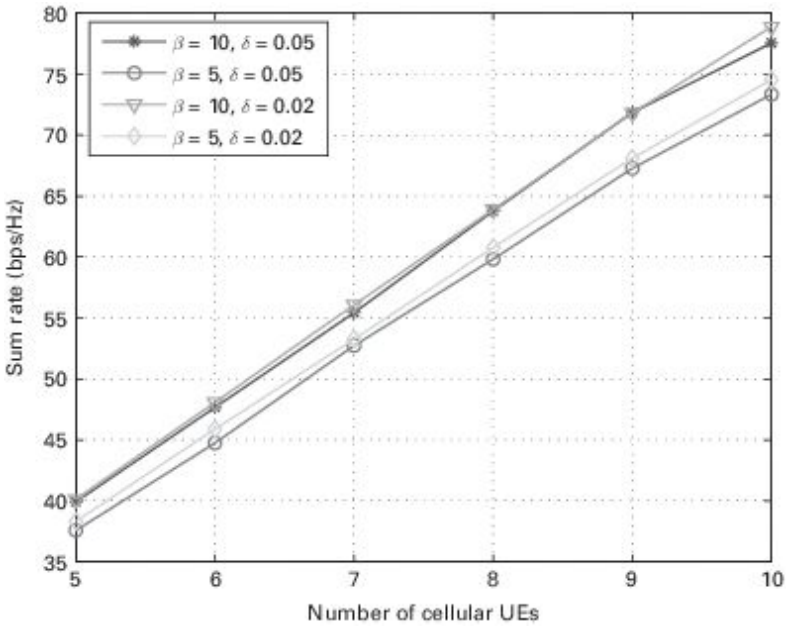

Figure 6.12. The system sum rate with different numbers of cellular UEs.

In this section, we have developed a Stackelberg game framework for joint power control, channel allocation, and scheduling of D2D communication. The optimal strategy for the game has been analyzed, and an algorithm to allocate resources and schedule D2D UEs has been proposed. Throughput, interference management and the fairness of the system have been considered. Simulation results show that the proposed algorithm can achieve good throughput performance both for the cellular and for the D2D UEs. The D2D UEs can be fairly served. The scaling factor β and fairness coefficient δ have important effects on the performance of the algorithm. It is also shown that D2D communication can improve the throughput of the system.

6.3 Capacity offloading through D2D local area networks

For D2D direct communication, the main function is to offload data from the eNBs by proper resource allocations. In this section, we study a capacity-offloading model based on cooperative game theory.

In a cooperative game, players are able to make enforceable contracts. The players cooperate to maximize a common objective of their coalition. In this case, the players can coordinate strategies and agree on how the total payoff is to be divided among the players. The Nash bargaining solution and coalitional games are two major types of cooperative game. Owing to the space limit, this section explains solely the coalition-formation game, which is a coalitional game involving a set of players who are looking for cooperative groups (i.e., coalitions). A coalition, which represents an agreement among the players in order to act as a single entity, can be formed by players in order to gain a higher payoff (i.e., utility), and the worth of this coalition is called the coalitional value. Two common forms of coalitional game are the strategic form and the partition form. In the former case, the value of a coalition depends on the members of that coalition only. In the latter case, the value of a coalition strongly depends on how the other players outside the coalition are structured. Coalitional game models can be developed with either transferable utility (TU) or non-transferable utility (NTU). In a TU coalitional game, utility serves like money and can be allocated to different players. In an NTU coalitional game, different players have different interpretations of utilities, and the utilities cannot be distributed among players arbitrarily.

For strategic-form coalitional games, a typical algorithm is the merge-and-split algorithm. The only two operations are given as follows.

- *Merge:* A set of coalitions is merged to a single coalition whenever the merged form is preferred.
- *Split:* A coalition is split whenever a split form is preferred.

For comparing collections of coalitions, there are two categories of preference relations that can be defined. For TU games, coalition-value orders are often defined, e.g., the utilitarian order, which states that a new form of collection is preferred if and only if the total social welfare is strictly increased. For NTU games, individual-value orders are often defined, e.g., the Pareto order, which states that a new form of collection is preferred if and only if the individual payoff of each player is not decreased and the individual payoff for at least one player is strictly increased. It is to be noted

that individual-value orders are suitable irrespective of whether the payoff is transferable or non-transferable. It has been proved that the merge-and-split algorithm will always converge to a stable partition, in which no group of players has an interest in performing a merge or a split operation. Driven by commercial interests, popular content distribution, as one of the key services in many hotspots such as stadium networks or concert networks, has recently received considerable attention. Next, one of the most representative scenarios, namely *group communication*, is considered. A simple but basic scenario for distributing a popular file to D2D LANs through traditional cellular networks is presented, and the use of a coalition game for efficient content dissemination is introduced, as shown in Figure 6.13. In this scenario, N UEs want exactly the same file from the Internet, while only K "*seeds*" have already downloaded it. Instead of using more RBs to download the file directly from the eNB, the remaining $N - K$ "*normal*" UEs can ask the seeds to send the file using D2D communications. The performance of this approach is determined by which subchannels are selected and with which D2D links they share their spectrum [189].

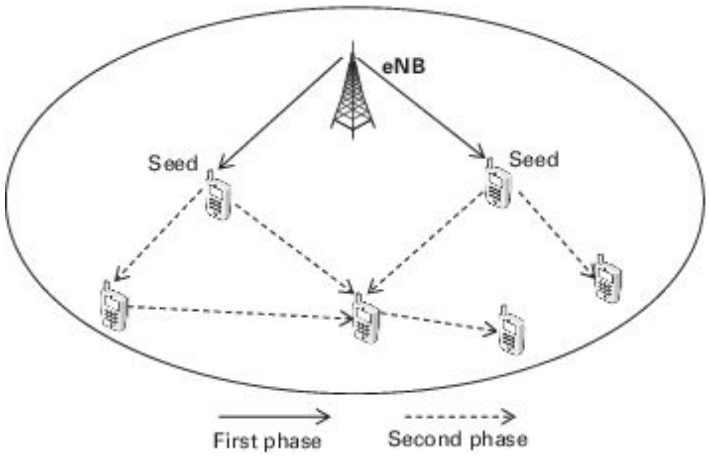

Figure 6.13. Popular content downloading in hotspot areas, such as concert and stadium networks.

A coalition-formation game can be used in this scenario, which consists of the following components.

- *Players: N* D2D UEs and *M* cellular UEs.
- *Coalition:* Each coalition contains one and only one cellular UE. The remaining members are the D2D UEs using the same subchannel.

- *Coalition value:* In a specific coalition, the seeds and the normal UEs form D2D links between themselves. The coalition value is the sum rate of all D2D links and the cellular link.

Since each coalition uses a different subchannel, the links in different coalitions do not interfere with each other, and thus the coalition-formation game has a strategic form. The algorithm for this game can be based on "*switch*" operations, by which one means that a player may leave the current coalition and join a new coalition if the total value of both coalitions is strictly increased. The switch operation can be simply seen as a combination of a split and a merge using the utilitarian order. Since the total value of the entire system is strictly increased by each switch operation, we expect a stable partition in which no switch operation is preferred. Note that the formerly stable partition might not be stable, since the D2D transmissions transform the normal UEs into seeds, and thus further switch operations may be preferred until all the UEs have turned into seeds.

Figure 6.14 shows the cumulative service curves both for the proposed coalition-game-theoretic approach and for the noncooperative approach. It can be seen that the proposed approach performs much better than the noncooperative approach. In the noncooperative approach, each user makes individual decisions, which may lead to severe data collisions. However, in the proposed approach, the users cooperate with each other to maximize the utility function, which is highly dependent on the network throughput of the current slot. Consequently, the proposed approach achieves a better performance in terms of the service rate.

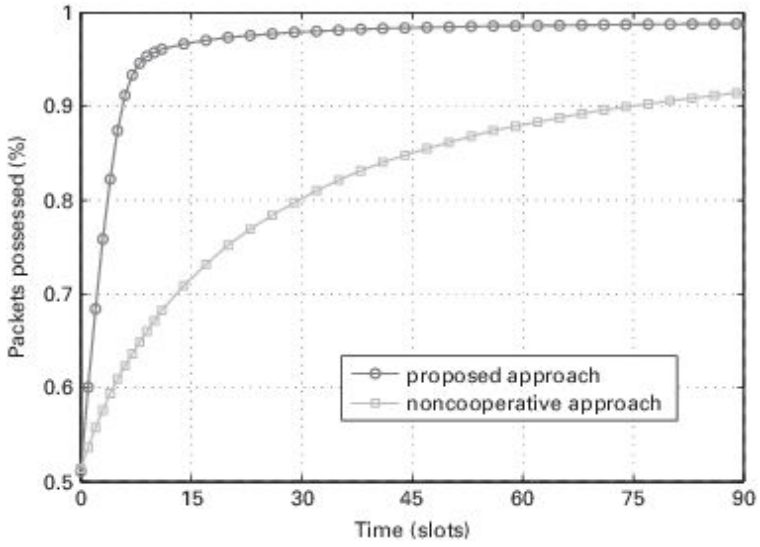

Figure 6.14. The total percentages of packets possessed obtained by use of the proposed coalition-game-theoretic approach and the noncooperative approach.

6.4 Chapter summary

In this chapter, we have analyzed the spectrum-sharing mode of D2D communications, namely the underlay mode (non-orthogonal channel sharing) and the overlay mode (orthogonal channel sharing). We have introduced a centralized subchannel allocation scheme for a D2D underlaying network, which efficiently reduces the co-channel interference, thus improving the whole system performance. The reverse iterative combinatorial auction has been proposed as the mechanism by which to allocate the spectrum resources for D2D communications with multiple user pairs. Simulation results show that the proposed auction algorithm is much superior to the random allocation, and provides high system efficiency.

Moreover, we have considered the problem of time-domain scheduling in D2D communications. We have developed a Stackelberg game framework in which a cellular user (leader) and a D2D user (follower) are grouped to form a leader–follower pair. On the basis of this game, we have proposed an algorithm for joint power control, time-domain scheduling, and spectrum resource allocation of D2D communications. Throughput, interference management, and the fairness of the system have been considered.

Simulation results show that the proposed algorithm can achieve a good throughput performance both for cellular and for D2D users.

D2D communications can offload data from cellular networks. For D2D direct communications, the main function is to offload data from the eNBs by appropriate resource allocations. We have introduced a capacity-offloading scheme that uses cooperative game theory (i.e., a coalition-formation game). Simulation results show that the proposed approach performs much better than the noncooperative approach.

---

[1] The fine tuning has only a small impact on the result and can be omitted here.

7 Cross-layer design for device-to-device communication

Traditional communication systems were built using a layered structure to provide well-defined but limited interfaces among protocols in adjacent layers. The modular design of the layered structure, where the details of each protocol are hidden, promotes the interoperatability of the communication protocols. Although the protocol details (e.g., states and internal functions) are encapsulated in each layer, this structure prevents the protocols sharing, accessing, and controlling the operations of other protocols, which might be required for efficient data transmission. Therefore, the concept of cross-layer design has been introduced to allow tighter integration of different protocols. It is not necessary for these protocols to be in adjacent layers. The benefits of cross-layer design are that it allows one to improve both the flexibility of protocol implementations and network performance. Cross-layer design and optimization have been adopted in various wireless systems. A few surveys on cross-layer design exist in the literature, e.g., [190, 191, 192, 193].

The cross-layer design has been adopted for optimizing D2D communication. In this chapter, we give an overview of the cross-layer design by introducing its definition and different approaches. Then, we present one of the most commonly used cross-layer design models, i.e., the coordination model, which incorporates different functionalities. These functionalities are security, QoS, mobility, and wireless link adaptation. We next present the cross-layer implementation and challenges.

We introduce cross-layer optimization, which is part of the cross-layer design. We provide examples of the cross-layer optimization problems,

including opportunistic scheduling, OFDM resource allocation, and congestion control. We then review the cross-layer design framework proposed for D2D communications. They are information correlation routing, routing in sensor networks, and traffic scheduling for a video application. Finally, we outline some research directions of the cross-layer design and D2D communications.

7.1 An overview of cross-layer design

In this section, we first introduce the basic concepts including the definition of, and approaches to, cross-layer design. Then, we discuss the coordination model, which incorporates other functionalities (i.e., security, QoS, mobility, and wireless link adaptation) into the protocols.

7.1.1 Definitions and approaches

The design of communications systems is usually based on a layered architecture, defined as the seven-layer open systems interconnection (OSI) model. In this architecture, network operations are divided into layers with different groups of functions. Different layers are organized in a hierarchical structure with interfaces defined for interactions between adjacent layers only. Additionally, each layer cannot interact with nonadjacent layers, and the interaction must be based on the predefined interfaces only. Communication protocols can be developed on the basis of this layer structure. Specifically, the protocol in a higher layer can utilize the services provided through the interfaces of a lower layer, and vice versa. The protocol in one layer does not need to be concerned about the mechanisms and implementation details of protocols in other layers. Consequently, the protocol-implementation complexity is reduced, since the protocols interact through well-defined interfaces. The reliability improves since a problem and bug in one protocol will be confined by the interfaces and will not propagate to other protocols. More importantly, interoperatability is enhanced because one protocol can work, can be modified, or can be replaced by another protocol with minimal impact.

By contrast, instead of following the layer-based protocol structure, cross-layer design allows protocols in one layer to access services and interfaces of the protocols in nonadjacent layers. For example, a routing protocol in the network layer may access channel-quality information in the physical layer. In addition, the protocol is permitted to access data and functions inside a protocol in another layer. For example, a transport protocol (e.g., TCP) may obtain a cause of packet loss, namely whether it is due to congestion or transmission error, from the MAC and physical layers, respectively [194]. Therefore, the authors of [195] state the definition of cross-layer design as follows: "Protocol design by the violation of a reference layered communication architecture is cross-layer design with respect to the particular layered architecture." The ultimate goal of the cross-layer design, which violates the classical rule of layer-based protocol structure, is to improve network performance using the following approaches [195].

- *Solutions to the unique problems created by wireless links:* Owing to its large size, high complexity, and highly sophisticated mobile and wireless applications and networks, there are several problems that could not be addressed efficiently using standard approaches in the traditional layer-based protocol structure. As mentioned, when the TCP protocol is used for data transfer over a wireless link, the protocol might not be able to distinguish between packet loss due to network congestion, transmission collision, or physical transmission error without accessing information associated with the protocols in other layers.
- *Opportunistic communication over wireless links:* Different types of diversity (e.g., spatial diversity, user diversity, and time diversity) can be utilized to improve the transmissions of multiple users in wireless networks. The information about diversity is usually located in one layer (e.g., in the physical layer), and hence, with the cross-layer design approach, this information can be shared across different layers. For example, a routing algorithm can utilize interference information to optimize its packet-forwarding strategy.
- *New modalities of communications:* New data-transmission schemes can be implemented on the basis of cross-layer design. For example, a

routing protocol can be optimized by taking advantage of network coding techniques, which require information in the MAC layer.

Figure 7.1 shows typical approaches in cross-layer design.

- *Upward information flow:* This refers to the case when a protocol in a higher layer accesses information of a protocol in a lower layer. For example, the transport-layer protocol can observe whether packet loss happens due to wireless transmission error or for some other reasons.
- *Downward information flow:* This refers to the case when a protocol in a lower layer accesses information of a protocol in a higher layer. For example, a routing protocol can access application content in a packet to optimize a packet-forwarding strategy.
- *Back-and-forth information flow:* In this approach, protocols in nonadjacent layers access information of each other. For example, in a wireless mesh network, a routing protocol can be optimized jointly with channel allocation and power control [196].

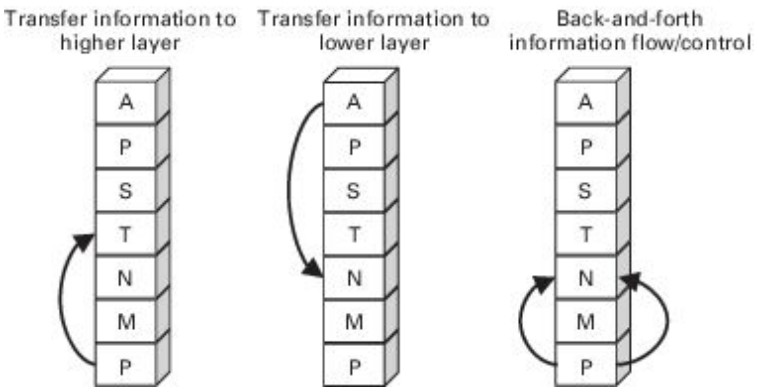

Figure 7.1. Typical approaches in cross-layer design.

However, other approaches also exist. For example, protocols in adjacent layers can be merged to have tighter integration of functions. To implement cross-layer design efficiently, three approaches have been suggested [195] (Figure 7.2).

- *Direct communications between layers:* This is the simplest form of implementing cross-layer design. Protocols in different layers are

allowed to interact with each other. New sets of interfaces can be defined and are available for different layers. For example, a physical-layer protocol can provide two sets of interfaces, i.e., one for a MAC-layer protocol and another for a routing protocol. While this approach provides more flexibility for the protocol design and operation, the protocol maintenance could be complicated and inefficient due to an untidy structure of interfaces.

- *Shared database across layers:* Instead of allowing protocols to communicate directly, there could be a central and shared database that acts as a broker to interface among protocols in different layers. The services of a protocol are available to protocols in other layers through this database. This approach improves the protocol-maintenance process compared with the aforementioned direct-communication mechanism. Additionally, the special logic and functions can be implemented at the shared database to enhance the performance of the whole system.
- *New abstraction:* Instead of relying on a hierarchical structure of protocols and layers, protocols are considered as modules that can interact with each other as a graph. This approach, which is based on a modular design, provides the highest flexibility, but at the cost of lower interoperability. Additionally, the protocol maintenance will be more complicated.

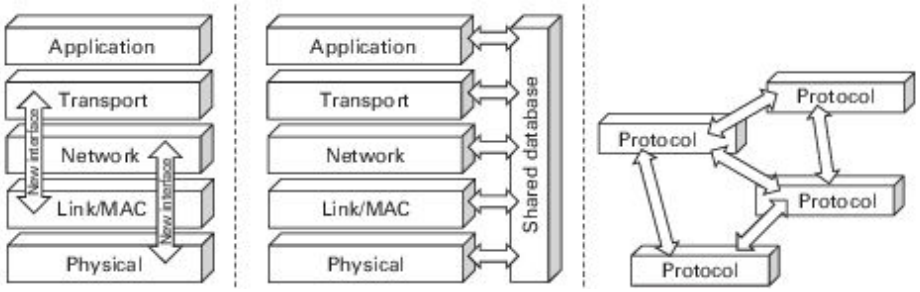

Figure 7.2. Implementation approaches for cross-layer design.

7.1.2 The cross-layer coordination model

The authors of [197] introduced a cross-layer coordination model, which incorporates necessary functions not specified in the typical seven-layer OSI

protocol stacks. These functions are presented as coordination planes, connected vertically to the hierarchy, as shown in Figure 7.3.

- *Security:* The security plane provides different functions to the protocols across different layers. These functions could be encryption, digital-signature, authentication, and authorization mechanisms, and key management. For example, the secure socket layer (SSL) and secure shell (SSH) can provide encryption functions at the transport and application layers, while IPSec provides them at the network layer. Similarly, for wireless networks, IEEE 802.11x provides various security functions at the MAC layer. These protocols can operate independently, which might be redundant. Therefore, having a coordination plane could help to integrate different security functions in the different layers.
- *Quality-of-service (QoS):* QoS can be supported in protocols at different layers. For example, the end-to-end delay is related to the transport and network layers, while the single-hop delay is related to the MAC and physical layers. In the transport layer, there is the real-time protocol (RTP), which interacts with the application layer. In the network layer, there is the IP QoS-for-routing protocol. For wireless transmission, IEEE 802.11e supports QoS functions (e.g., service differentiation) in the MAC layer.
- *Mobility:* Mobility is supported by a handoff mechanism for the mobile users in order to provide seamless connectivity. In the network layer, there is the mobile IP, which supports the relocation of mobile nodes and addressing. In the MAC and physical layers, a handoff algorithm can be implemented on the basis of the signal strength. Handoff could be vertical or horizontal. Vertical handoff happens when a user changes a connection from one type of network (cell) to a different type of network (e.g., from a cellular network to WLAN). By contrast, horizontal handoff happens when the user changes the connection in the same network or same type of the cells. Additionally, the handoff could be soft or hard. Hard handoff happens if the user has the connection on a single channel only. In soft handoff, by contrast, the user can hold the connection on two or more channels of two or more cells, to ensure smooth transition of the movement.
- *Wireless link adaptation:* Since the wireless channels are time-varying, to achieve the best performance, data transmission can be made

adaptively to an environment and the channel-quality information can be used by protocols at different layers to optimize their operations. The channel-quality information may include the signal-to-interference-plus-noise ratio (SINR), bit error rate (BER), channel fading, and delay. For example, the TCP protocol in the transport layer can be notified about the cause of packet loss from the physical and MAC layers in order to adapt the congestion window accordingly. The automatic repeat request (ARQ) in the data-link layer can adapt the data-retransmission strategy on the basis of the BER.

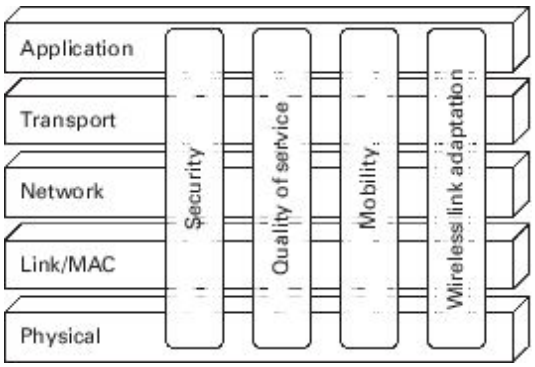

Figure 7.3. The cross-layer coordination model.

To implement the cross-layer design and coordination model, supporting components and entities must be provided in order to optimize network performance. The authors of [192] categorized different types of entities related to the cross-layer design. Firstly, the entities can be classified according to whether they are internal or external to mobile devices and base stations. If the entities are internal, they can be classified into intralayer or interlayer. By contrast, if the entities are external, they can be classified into centralized or decentralized.

- *Internal interlayer entities:* These entities are located in the same device. Two important entities are the interlayer cross-layer manager and optimizer. The manager is responsible for coordination and information exchange among protocols in a different layer, while the optimizer implements protocol optimization to determine optimal operation parameters of the protocol. The manager receives notifications of events happening at a protocol layer and sends them to

an appropriate protocol. The manager may keep track of the protocol state and information about each protocol. The optimizer uses the notification together with the protocol state and information to optimize the best action to be performed by the protocol given an objective function and a set of constraints. For example, in handoff management, the manager can be notified about the change of cell and channel quality by the MAC and physical-layer protocols, respectively. Then, the optimizer retrieves the state and other information to determine the best handoff decision (e.g., the channel to move to) to maximize the data-transmission rate given the interference constraint.

- *Internal intralayer entities:* These entities are parts of a protocol, providing direct interfaces to protocols in other layers. Examples of these entities are the intralayer cross-layer optimizer and scheduler. The optimizer is again designed to implement protocol optimization to determine the best actions of the protocols. The optimizer interacts to collect and access the state and information of other protocols and use them to provide the optimal policy/strategy. The scheduler performs slightly different functions that are divided into traffic scheduling and resource allocation. The schedulers are typically implemented in the MAC and physical layers. The scheduler determines the number of packets to be transmitted and is integrated with a queue/buffer-management mechanism. The resource allocation will determine the suitable channel and its parameters (e.g., transmit power) for packet transmission.
- *External centralized entities:* The cross-layer entities can be deployed outside the devices. The external centralized cross-layer optimizer could be located at a base station to optimize the data transmission by mobile devices. The centralized optimizer is able to collect the state and information about the network (e.g., the channel quality of other devices), and uses that information to optimize the protocol operations globally. As an example, information on users' contexts in the application layer can be gathered by the base station. The base station uses that context information to match and optimize content delivery. The channel to be used and mode of data transmission (e.g., D2D communications) can be chosen according to the context and channel quality in the application and physical layers, respectively. Usually, the

external centralized entities are suitable for a single-hop network with a single controller.

- *External decentralized entities:* By contrast, the external cross-layer entities could be decentralized. The optimizer can be located at different locations (e.g., base station, gateway, and devices) to optimize protocols. The external decentralized optimizer is suitable for multihop networks without the centralized controller. For example, a decentralized routing protocol can have the optimizer collect and learn about the interference at different hops in the network. The optimizer then uses that interference information to choose the best route for data transfer. The routing protocol, with help from the optimizer, can also optimize the transmit power to avoid severe interference to other nodes in the network.

7.1.3 Cross-layer implementation

To implement cross-layer design, it is important to collect and analyze communication and protocol requirements. The requirements can be classified into two types.

- *Application requirements:* These requirements relate to the functionality of the end-application. For example, real-time interactive applications (e.g., multimedia) require QoS support. Delay-tolerant networks (DTNs) have to take the mobility of devices into account to determine the best packet-forwarding strategy. Vehicular networks could support safety and transportation efficiency applications, which require integration of functions in different layers.
- *Performance requirements:* These requirements define a set of performance criteria that need to be fulfilled. For example, such performance criteria include throughput, delay, and loss. While the performance can be defined as layer-specific requirements (e.g., the collision probability in the MAC layer or the number of hops in a routing protocol), some types of performance should be defined as the system requirements (e.g., the total latency which could be incurred due to application processing, route selection, channel contention, and transmission delays).

After a set of requirements and their attributes have been specified, the objective and constraint of the cross-layer design will be defined. For example, the protocols could be optimized to maximize throughput, while the constraint could be the need to maintain delay and interference to other users below the maximum bounds. After the objective and constraints have been defined, the list of layers and their protocols to be modified or developed will be identified. These protocols depend on the requirements. For example, if the objective is to maximize the throughput in a single-hop network (e.g., a cellular network), then the physical and MAC layers should be involved. However, if the constraint is the end-to-end delay in a multihop network, then the network and transport layers might need to be considered. Additionally, if requirements are related to an application (e.g., video), the application layer may need to be revisited.

In addition to the requirements, the implementation cost and design complexity must also be taken into account. In many cases, when the cross-layer design involves many layers, giving more opportunities to improve performance, the implementation cost and complexity could increase. Therefore, the tradeoff and the algorithms to be used in the implementation must be evaluated and chosen carefully. The strategy to implement the cross-layer design can be chosen (e.g., upward, downward, or back-and-forth information flow). It could be based on the coordination model.

The levels of changes and integration of existing protocols must be analyzed and specified. Although opening and modifying much detail of the protocol could improve the performance and reduce complexity, the extensibility will be adversely affected since there could be too much cohesion among layers. By contrast, defining clear interfaces will involve a simple data structure and exchange, which make the protocol extensible and interoperatable with other protocols and other entities in the system. Therefore, the tradeoff among performance, implementation cost, and complexity, as well as extensibility, has to be investigated and optimized.

7.1.4 Cross-layer design considerations and challenges

Although cross-layer design brings many benefits, especially the ability to improve the transmission performance, there are some considerations and challenges relating to applying the cross-layer design concept in general [193].

- *Coexistence and signaling:* When implementing the cross-layer design in a device or network, a few more components and entities have to be deployed, and must coexist in the system. It is important to implement the integration of different protocols in an efficient and seamless manner to achieve a design goal. Furthermore, the signaling for information exchange among them has to be carefully designed. Firstly, the design and implementation must ensure there is no conflict in the protocols' functionality. Secondly, the cross-layer entities must have proper control of and access to functions of the protocols. Thirdly, there must be some prevention mechanism to avoid having a problem in one protocol propagate to other protocols.
- *Overhead:* Adding components and entities to existing protocols and systems could create more computational and communication overhead. The cross-layer design must be implemented in such a way as to avoid and minimize such overhead.
- *Lack of universal framework:* The cross-layer design can be implemented arbitrarily without any clear and well-defined structure. As a result, the strict interface and control will be loosened, which could lead to poorer function and information encapsulation. One of the solutions is to introduce a universal framework to implement the cross-layer design. However, having such a universal framework requires the protocol developers and manufacturers to agree on and follow the guideline, which is a complicated task. Additionally, it is important to employ some verification methods to ensure that all the protocols and cross-layer entities can work efficiently.
- *Unintended consequence:* The authors of [198] highlight that the cross-layer design may result in an unexpected deterioration in performance. This could be the tradeoff in designs in a different protocol layer. An example of a rate-adaptive MAC protocol and minimum-hop routing is given. In the rate-adaptive MAC protocol, the data-transmission rate can be adjusted on the basis of channel quality. If the channel quality is good (e.g., nearby nodes), the transmission rate can be increased. By

contrast, the transmission rate will be decreased if the channel quality is poor (e.g., faraway nodes). This rate adaptation is to guarantee minimum loss probability. In the minimum-hop routing, a source node will choose the route with the minimum number of relay nodes involved (e.g., to minimize energy consumption and radio-resource usage) for packet forwarding. The downstream relay node is chosen only from a set of nodes that are within transmission range of the upstream transmitting node. When the cross-layer rate-adaptive MAC protocol is used with the minimum-hop routing, an unexpected deterioration in performance is observed. That is, the routing protocol will choose the most distant relay node to minimize the number of hops. However, the rate-adaptive MAC protocol will use a very low transmission rate. This arises from the fact that the channel quality of the long-distance transmission is usually favorable due to signal attenuation. As a result, the end-to-end throughput is adversely affected. Therefore, when the cross-layer design is implemented, all of the protocols must be optimized holistically.

7.2 Cross-layer optimization

The intrinsic part of the cross-layer design approach is a type of optimization that is generally referred to as cross-layer optimization. The purpose of the optimization is to find a set of optimal protocol parameters such that an objective is achieved, given a set of resource and/or performance constraints. Various cross-layer optimization formulations and techniques have been developed and applied to solve the optimal cross-layer design. The authors of [199] provide a comprehensive tutorial on applying optimization techniques (e.g., convex optimization) to cross-layer design of wireless networks.

7.2.1 Opportunistic scheduling

The authors of [200] present the cross-layer optimization for the opportunistic scheduling in a centralized cellular network. The system is assumed to be time-slotted, and one user is scheduled to transmit a packet in any particular time slot. Since the channel quality can be time-varying, the

users will be opportunistically allocated the time slot for their transmission. In other words, the scheduling algorithm determines which user can transmit its packet in a time slot on the basis of the performance or utility that all the users can receive if they are scheduled for transmission. In wireless networks, the utility is commonly used to quantify a user's satisfaction from data transfer. Let U_i denote the utility that user i can receive from the transmission in a certain time slot. The utility is an increasing function of the channel quality (e.g., the transmission rate). The scheduling policy π is a mapping from the vector of utilities $\vec{\mathbf{u}}$ to the particular user that will transmit its packet in that time slot. The vector of utilities of all the users is defined as $\vec{\mathbf{u}} = [\ U_1(x_1) \ \cdots \ U_N(x_N)\ ]^\top$, where N is the total number of users and x_i is a function of the channel quality.

The simple scheduling policy can be defined as follows:

$$\pi^* = \arg\max_i U_i(x_i). \tag{7.1}$$

In other words, the user whose transmission yields the largest utility will be scheduled to transmit. With this scheduling policy, the system throughput will be maximized, since the scheduling algorithm favors those users whose channel quality is good in the long run. For example, if there are users 1 and 2, the channel quality of each of these users could be good or bad. If the probabilities of good channel quality of users 1 and 2 are 0.8 and 0.1, respectively, the probabilities that users 1 and 2 will be scheduled to transmit their packets are 0.85 and 0.15, respectively. This is based on the assumption that, if both users have good or bad channel quality, they will be randomly scheduled for transmission with equal probability. The probabilities that the users will be scheduled for transmission can be calculated as follows. The probability that both users have good channel quality is $0.8 \times 0.1 = 0.08$ and each user has an equal chance to transmit with probability 0.04. The probability that user 1 has good channel quality while user 2 has bad channel quality is $0.8 \times 0.9 = 0.72$. User 1 will always be scheduled for transmission in this case. The probability that user 1 has bad channel quality while user 2 has good channel quality is $0.2 \times 0.1 = 0.02$. User 2 will always be scheduled for transmission in this case. Finally, the probability that users 1 and 2 have bad channel quality

is $0.2 \times 0.9 = 0.18$, and each user has an equal chance to transmit with probability 0.09. Clearly, the fairness of this scheduling policy is poor, since user 2 will have much less opportunity to transmit its packet. Therefore, the optimization problem can be extended to include a constraint on the minimum transmission requirement as follows:

$$\begin{aligned} \max_{\pi} \quad & \sum_{i=1}^{N} \mathbb{E}[U_i(x_i)], \\ \text{s.t.} \quad & P(\pi(\vec{\mathbf{u}}) = i) \geq r_i, \quad i = 1, \ldots, N, \end{aligned} \tag{7.2}$$

where $P(\pi(\vec{\mathbf{u}}) = i)$ is the probability that the policy schedules user i to transmit its packet and r_i is the minimum fraction of time slots scheduled for the transmission by user i. In this optimization problem, the fairness in terms of time share is incorporated. Alternatively, the fairness can be defined as the ratio of the system utility. The corresponding optimization problem is defined as follows:

$$\begin{aligned} \max_{\pi} \quad & \sum_{i=1}^{N} \mathbb{E}\left[U_{\pi(\vec{\mathbf{u}})}\right] = \sum_{i=1}^{N} \mathbb{E}\left[U_i \mathbf{1}_{\pi(\vec{\mathbf{u}})=i}\right], \\ \text{s.t.} \quad & \mathbb{E}\left[U_i \mathbf{1}_{\pi(\vec{\mathbf{u}})=i}\right] \geq w_i \mathbb{E}\left[U_{\pi(\vec{\mathbf{u}})}\right], \quad i = 1, \ldots, N, \end{aligned} \tag{7.3}$$

where $\mathbf{1}_{\pi(\vec{\mathbf{u}})=i}$ gives the value of one, if the condition $\pi(\vec{\mathbf{u}}) = i$ is true (i.e., the policy schedules user i for transmission), and zero otherwise. w_i is the ratio of the system utility that user i should receive. In this case, we have $w_i \geq 0$ for all i and $\sum_{i=1}^{N} w_i \leq 1$. The optimization problem defined in (7.3) is that of how to achieve the maximum system utility given that all users must achieve the minimum ratio of the system utility.

Alternatively, the proportional fairness criterion [201] can be applied to the objective function to determine an optimal scheduling policy. In this case, the optimization problem becomes

$$\max_{\pi} \sum_{i=1}^{N} \log(\mathbb{E}(x_i)). \tag{7.4}$$

The interpretation of the proportional fairness is that, if the mean throughput of one user increases by y%, then the mean throughput of all other users will decrease by more than y% [199].

The authors of [200] discuss the solution methods and properties of the optimal scheduling policies for the above cross-layer optimization problems for opportunistic scheduling.

7.2.2 OFDMA wireless networks

The authors of [202] and [203] present the theoretical and implementation framework to provide the cross-layer optimization for OFDM wireless networks jointly at the physical and MAC layers. In addition, the tradeoff between fairness and efficiency is analyzed. Specifically, the cross-layer optimization is divided into the dynamic subcarrier-allocation and adaptive power-allocation problems.

Theoretical framework

Under the theoretical framework, the network is assumed to have an infinite number of orthogonal subcarriers, and hence the bandwidth of each subcarrier is infinitesimal. Let $\mathcal{B}$ denote the set of total bandwidths, and let $\mathcal{D}_i$ denote the set of bandwidths allocated to user i. All the bandwidth should be allocated to one or other user, i.e., $\bigcup_{i=1}^{N} \mathcal{D}_i = \mathcal{B}$. Additionally, the bandwidth of each user must not overlap with that of another, i.e., $\mathcal{D}_i \cap \mathcal{D}_j = \emptyset$ for $i \neq j$. Given this assumption, the transmission throughput of user i can be expressed as follows:

$$r_i = \int_{\mathcal{D}_i} \log_2(1 + \beta p(f)\rho_i(f))df, \tag{7.5}$$

where $\beta = -1.5/\ln(5\text{BER})$, $p(f)$ is the transmit power density at frequency f, and $\rho_i(f)$ is the ratio between the channel gain and noise.

While the transmission throughput r_i is based on the performance in the physical layer, the user's satisfaction in the MAC and higher layers can be quantified by the utility function. For the best-effort traffic, the following utility function can be used:

$$U(r) = 0.16 + 0.8\ln(r - 0.3), \tag{7.6}$$

where r is the transmission rate in bits per second. The function and its parameters can be obtained from subjective surveys as performed in [204]. Then, the cross-layer optimization problem can be formulated as follows:

$$\max \ \frac{1}{N}\sum_{i=1}^{N} U_i(r_i), \tag{7.7}$$

$$\text{s.t.} \ \bigcup_{i=1}^{N} \mathcal{D}_i \subseteq \mathcal{B}, \tag{7.8}$$

$$\mathcal{D}_i \cap \mathcal{D}_j = \emptyset, \quad i \neq j, i, j = 1, \ldots, N. \tag{7.9}$$

For the dynamic subcarrier allocation, the subcarrier should be allocated on the basis of the transmission-rate ratio among users. For the two-user case (i.e., users 1 and 2), any frequency f will be allocated to user 1 if $c_2(f)/c_1(f) < \alpha$, where $c_i(f) = \log_2(1 + \beta\rho_i(f))$ and α is the constant which determines the subcarrier allocation preference of the users. Here $c_i(f)$ is the achievable transmission efficiency (i.e., the data rate per Hz) of user i on subcarrier f. Then, the frequency f will be allocated to user 2 if $c_2(f)/c_1(f) > \alpha$. Figure 7.4 shows an example of subcarrier allocation.

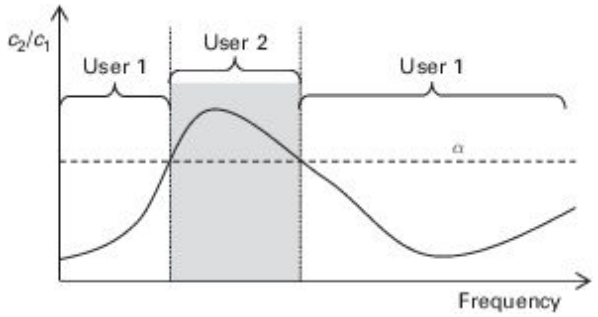

Figure 7.4. Dynamic subcarrier allocation on the basis of the transmission ratio $c_2(f)/c_1(f) < \alpha$.

It is found that the optimal α^* is obtained from

$$\alpha^* = \frac{U_1'(r_1^*)}{U_2'(r_2^*)}, \tag{7.10}$$

where $U_i'(r) = dU_i(r)/dr$. Clearly, the value of α can be used to make a tradeoff between efficiency and fairness. While the optimal performance (i.e., the highest efficiency) can be obtained at α^*, the fairness among users can be improved by deviating from α^* toward giving more subcarrier to the users with inferior performance.

Then, the adaptive power allocation is performed given the fixed subcarrier allocation. The optimization problem is expressed as follows:

$$\max_{p(f)} \frac{1}{N} \sum_{i=1}^{N} U_i \left(\int_{\mathcal{D}_i} \log_2(1 + \beta p(f) \rho_i(f)) df \right), \tag{7.11}$$

$$\text{s.t.} \quad \frac{1}{|\mathcal{B}|} \int_{\mathcal{B}} p(f) df \leq 1, \tag{7.12}$$

$$p(f) \geq 0, \tag{7.13}$$

where $|\mathcal{B}|$ is the size of the total amount of subcarrier. Using the water-filling procedure, the optimal power allocation is obtained from

$$p^*(f) = \left[\frac{U_i'(r_i^*)}{\lambda} - \frac{1}{\beta\rho_i(f)}\right]^+, \tag{7.14}$$

for $\lambda > 0$ and $f \in \mathcal{D}_i$, where λ is a constant used to normalize the optimal power density. $[x]^+ = x$ if $x \geq 0$ and $[x]^+ = 0$ otherwise. It is important to note that the water-filling algorithm which is applied to obtain $p^*(f)$ is different from the traditional water-filling method, since the objective is to maximize the average utility rather than the system capacity. As a result, the water levels of $U_i'(r_i^*)/\lambda$ will be different for different users. Additionally, the constraint is on the total transmit power, not on the individual transmit power.

Then, the joint dynamic subcarrier allocation and adaptive power allocation for the cross-layer optimization can be formulated. The authors of [202] established the necessary conditions for the globally optimal solution as follows. Firstly, given that the subcarrier allocation is fixed, any change of power allocation will not increase the total utility. Secondly, given that the power allocation is fixed, any change of subcarrier allocation will not increase the total utility. The optimal solution is defined as follows:

$$\mathcal{D}_i^* = \left\{f \in \mathcal{B}; \rho_i(f) = \max_{i'} \rho_{i'}(f)\right\}, \tag{7.15}$$

$$p^*(f) = \left[\frac{U_i'(r_i^*)}{\lambda} - \frac{1}{\beta \max_{i'} \rho_{i'}(f)}\right]^+ \tag{7.16}$$

$$1 = \frac{1}{|\mathcal{B}|}\int_{\mathcal{B}} p^*(f)df. \tag{7.17}$$

It has been proved that, if the utility function $U_i(r)$ is concave, then the locally optimal solution is also the globally optimal solution.

Implementation framework

However, the above optimization is not implementable. This is due to the fact that the problem considers an infinite set of subcarriers and the size of each subcarrier is assumed to be infinitesimal. In an actual OFDM system, the set of available subcarriers is finite and there is a certain size of the subcarrier. Therefore, the authors of [203] extended the theoretical framework and introduced the implementation framework of the cross-layer dynamic subcarrier-allocation and adaptive power-allocation problem.

The dynamic subcarrier allocation is formulated as the nonlinear binary-integer programming problem as follows:

$$\max_{x_{i,k}} \sum_{i=1}^{N} U_i \left(\Delta f \sum_{k=1}^{K} c_i^{\vec{\mathbf{p}}}[k] x_{i,k} \right), \tag{7.18}$$

$$\text{s.t.} \sum_{i=1}^{N} x_{i,k} = 1, \quad k \in \{1, \ldots, K\}, \tag{7.19}$$

$$x_{i,k} \in \{0, 1\}, \quad i \in \{1, \ldots, N\}, k \in \{1, \ldots, K\}. \tag{7.20}$$

- Δf is the bandwidth of one of the subcarriers, all of which are assumed to be of identical size.
- K is the total number of subcarriers.
- $c_i^{\vec{\mathbf{p}}}[k]$ is the achievable transmission efficiency of user i on subcarrier k, given the fixed power-allocation vector $\vec{\mathbf{p}}$.
- $x_{i,k}$ is a binary variable indicating whether the subcarrier k is allocated to user i or not.

Let $\vec{\mathbf{x}}$ denote a vector of $x_{i,k}$. The optimal solution of $\vec{\mathbf{x}}^*$ will satisfy the condition

$$\nabla_{\vec{\mathbf{x}}} U(\vec{\mathbf{x}}^*)^\top (\vec{\mathbf{x}}^* - \vec{\mathbf{x}}) \geq 0 \tag{7.21}$$

for all $\vec{\mathbf{x}}$, where

$$U(\vec{\mathbf{x}}^*) = \sum_{i=1}^{N} U_i \left(\Delta f \sum_{k=1}^{K} c_i^{\vec{\mathbf{p}}}[k] x_{i,k} \right), \tag{7.22}$$

and the gradient of $U(\vec{\mathbf{x}})$ is given by

$$\nabla_{\vec{\mathbf{x}}} U(\vec{\mathbf{x}}) = \begin{bmatrix} U_1'(r_1) c_1^{\vec{\mathbf{p}}}[1] \Delta f \\ \vdots \\ U_1'(r_1) c_1^{\vec{\mathbf{p}}}[K] \Delta f \\ \vdots \\ U_N'(r_N) c_N^{\vec{\mathbf{p}}}[1] \Delta f \\ \vdots \\ U_N'(r_N) c_N^{\vec{\mathbf{p}}}[K] \Delta f \end{bmatrix}. \tag{7.23}$$

In other words, we have

$$U_i'(r_i^*) c_i^{\vec{\mathbf{p}}}[k] \geq U_{i'}'(r_{i'}^*) c_{i'}^{\vec{\mathbf{p}}}[k], \tag{7.24}$$

for all $i' \neq i$ and

$$r_i^* = \sum_{k=1}^{K} c_i^{\vec{\mathbf{p}}}[k] \Delta f x_{i,k}^*. \tag{7.25}$$

To obtain the optimal solution of the subcarrier allocation $\vec{\mathbf{x}}^*$, the sorting-search algorithm is applied. Consider a two-user, three-subcarrier case. We can compute the ratio between the transmission efficiencies of the two users. Suppose they are $c_2^{\vec{\mathbf{p}}}[1]/c_1^{\vec{\mathbf{p}}}[1] \leq c_2^{\vec{\mathbf{p}}}[2]/c_1^{\vec{\mathbf{p}}}[2] \leq c_2^{\vec{\mathbf{p}}}[3]/c_1^{\vec{\mathbf{p}}}[3]$. Then, there are four possibilities of allocation, where $\mathcal{D}_1 = \emptyset$, $\mathcal{D}_1 = \{1\}$, $\mathcal{D}_1 = \{1, 2\}$, $\mathcal{D}_1 = \{1, 2, 3\}$, and $\mathcal{D}_2 = \{1, 2, 3\} \setminus \mathcal{D}_1$. The algorithm has the threshold α that, if $c_2^{\vec{\mathbf{p}}}[k]/c_1^{\vec{\mathbf{p}}}[k] > \alpha$, then subcarrier k will be allocated to user 2, while the rest of the subcarriers will be allocated to user 1. It can be shown that the optimal value of the threshold α should be close to $U_1'(r_1)/U_2'(r_2)$. The same concept is applied for any number of users and subcarriers, where the binary search is identified as the efficient algorithm to obtain the threshold.

For the adaptive power allocation, if the subcarrier allocation is fixed, the optimization problem becomes

$$\max_{\vec{\mathbf{p}}} \sum_{i=1}^{N} U_i(r_i), \tag{7.26}$$

$$\text{s.t.} \sum_{k=1}^{K} p[k] \leq \overline{P}, \tag{7.27}$$

$$p[k] \geq 0. \tag{7.28}$$

Similarly to the theoretical framework, the optimal solution of the power allocation is given by

$$p^*[k] = \left[\frac{U_i'(r_i^*)}{\lambda} - \frac{1}{\beta\rho_i[k]}\right]^+, \tag{7.29}$$

for $\lambda > 0$. To obtain the optimal solution, the sequential-linear-approximation water-filling algorithm is proposed. This algorithm is for continuous-rate adaptation, i.e., the transmission efficiency is based on a

logarithmic function. However, in an actual system, discrete rates are used. Therefore, to obtain the optimal solution, greedy power allocation based on maximizing the total utility is introduced. In this greedy algorithm, the allocation of bits and power is iterative. In each iteration, the bits and power are allocated such that they maximize the (marginal) utility gained.

Finally, we present the joint dynamic subcarrier allocation and adaptive power allocation. The algorithm to obtain the optimal solution is given in Algorithm 10, where t is an iteration index. ϕ is the updating step size.

Algorithm 10 Joint dynamic subcarrier-allocation and adaptive power-allocation algorithm for continuous-rate adaptation

repeat
  for $k = 1, \ldots, K$ **do**
    Obtain the new subcarrier allocation from $\hat{i}(k) \leftarrow \arg\max_{i \in \{1,\ldots,N\}} \gamma_i[t] c_i^{\vec{\mathbf{p}}}[k]$, where $\hat{i}(k)$ is the user to which subcarrier k is allocated
    Update the set of allocated subcarriers, i.e., $\mathcal{D}_{\hat{i}} \leftarrow \mathcal{D}_{\hat{i}} \cup \{k\}$
  end for
  for $k = 1, \ldots, K$ **do**
    Obtain the new power allocation from $p[k] \leftarrow [\gamma_{\hat{i}(k)}[k]/\lambda - 1/(\beta \rho_{\hat{i}(k)}[k])]^+$
  end for
  for $i = 1, \ldots, N$ **do**
    Obtain the data rate from $r_i[t+1] \leftarrow \sum_{k \in \mathcal{D}_i} \log_2(1 + \beta p[k] \rho_i[k]) \Delta f$
  end for
  for $i = 1, \ldots, N$ **do**
    Update $\gamma_i[t+1] \leftarrow (1 - \phi)\gamma_i[t] + \phi U_i'(r_i[t+1])$
  end for
until $\sum_{i=1}^{N} U_i'(r_i[t]) |r_i[t+1] - r_i[t]| \leq \epsilon$

7.2.3 *Cross-layer congestion control and scheduling*

The transport-layer protocol (e.g., TCP) controls the traffic-transmission rate of source nodes to avoid congestion in a network. In wireless networks, congestion control of the transport layer may lead to poor performance, since the protocol cannot identify whether packet loss is due to congestion or wireless transmission error. If the packet loss arises from wireless error, reducing the transmission rate would reduce the end-to-end throughput unnecessarily. Additionally, wireless networks generally have limited bandwidth. The traffic-sending rate must be carefully controlled in order to avoid not only congestion, but also collision due to many nodes transmitting many packets in the same network. The cross-layer optimization can be formulated and solved to determine the appropriate rate region (i.e., transmission-rate allocation to each node) to achieve optimal end-to-end performance given that traffic scheduling is implemented to support multiple access.

The authors of [205] studied congestion control in a wireless multihop network similar to a D2D communications context with traffic scheduling. Specifically, the cross-layer design involves transmission-rate control in the transport layer and scheduling in the physical layer. In the system model under consideration, a multihop network is modeled as a graph with N nodes. A link is denoted by (i,j) for a pair of nodes i and j that can communicate with each other. A set of links is denoted by $\mathcal{L}$. The data rate of the link denoted by $r_{i,j}$ depends on the transmit power $p_{i,j}$. Note that, in this case, $p_{i,j}$ is the transmit power used by node i to transmit the data to node j. The transmit power $p_{i,j}$ may differ from $p_{i,j'}$, where $j \neq j'$ in order to achieve a different transmission rate to node j'. Multiple access employing CDMA can be adopted. The vectors of transmit power and rate are denoted by $\vec{\mathbf{p}}$ and $\vec{\mathbf{r}}$, respectively. Taking interference into account, we can express the rate vector as a function of transmit power of all nodes, i.e., $\vec{\mathbf{r}} = c(\vec{\mathbf{p}})$. $c(\cdot)$ is a rate-power function, which is usually nonconvex. The total transmit power of any node i is bounded by the maximum transmit power, i.e., $\sum_j p_{i,j} \leq p_{i,\max}$.

In the network, the source and destination nodes are denoted by s and d, respectively. x_s is the end-to-end rate over multiple hops between source node s and the destination node d. The satisfaction of a user on the rate is

quantified by a utility function, denoted by $U_s(x_s)$. This function is assumed to be strictly concave, non-decreasing and continuously differentiable. The scheduling is implemented to allocate transmit power (i.e., the transmit power vector $\vec{\mathbf{p}}$), which can be translated into the rate vector $\vec{\mathbf{r}}$. The scheduling also selects data to transmit on each path. The cross-layer optimization problem is formulated to address not only the scheduling, but also the congestion control. Specifically, the congestion control determines the end-to-end rates of all users which maximize the sum of the utilities of all users, i.e., $\sum_s U_s(x_s)$, given that the system is stable (i.e., the queue length of each node is finite). The scheduling determines the transmission rate (single hop) of each node to meet end-to-end rates obtained from the congestion control.

Figure 7.5 shows an example network with seven nodes and two sources. Source nodes 1 and 2 transmit their data to destination nodes 6 and 7, respectively. Here the congestion control is done to determine the end-to-end rates x_{s1} and x_{s2} of source nodes 1 and 2. The scheduling is done to determine the one-hop rates $r_{1,3}$, $r_{2,3}$, $r_{1,5}$, $r_{3,4}$, $r_{3,5}$, $r_{5,4}$, $r_{5,7}$, $r_{4,6}$, and $r_{4,7}$ by adjusting the transmit power.

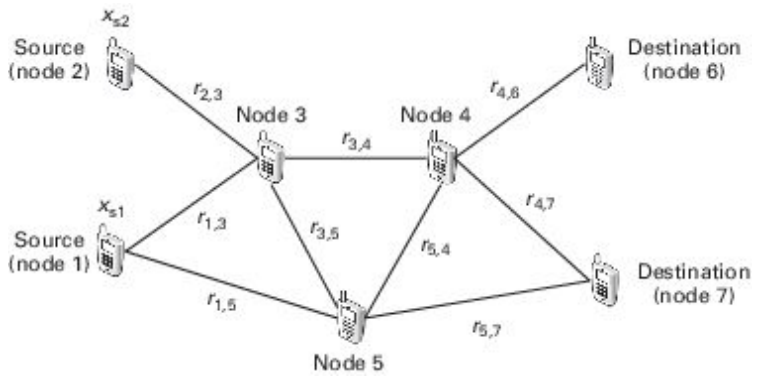

Figure 7.5. An example scenario of congestion control and scheduling.

The joint cross-layer optimization for the congestion control can be expressed as follows:

$$\max_{x_s} \sum_{s \in \mathcal{S}} U_s(x_s), \tag{7.30}$$

$$\text{s.t. } x_s \leq x_{s,\max}, \tag{7.31}$$

$$\vec{\mathbf{x}} \in \Lambda, \tag{7.32}$$

where Λ is the capacity region of the system, $\mathcal{S}$ is a set of source nodes in the network, and $x_{s,\max}$ is the maximum rate of source s. The capacity region Λ can be obtained by evaluating the feasible rate allocation of each destination node d. Let $\vec{\mathbf{r}}^d$ denote the rate vector of destination node d whose element is $r_{i,j}^d$. $r_{i,j}^d$ denotes the transmission rate from node i to node j for the traffic heading to destination d. The condition of the transmission rate which must be met to determine the capacity region is defined as follows:

$$\underbrace{\sum_{j} r_{i,j}^d}_{\text{Outgoing rates}} \geq \underbrace{\sum_{j'} r_{j',i}^d}_{\text{Incoming rates}} + \underbrace{x_{si}}_{\text{Self-generated rate}}, \tag{7.33}$$

for any node i that is not a destination. This constraint is applied to all destinations. x_{si} is the transmission rate generated at node i as a source (i.e., the traffic-generation rate of node i). Figure 7.6 shows a schematic diagram of the flow balance.

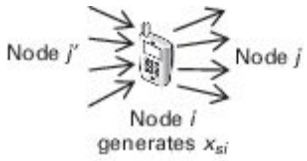

Figure 7.6. Flow balance.

However, due to the nonconvexity of the transmission rate (e.g., because of interference), it becomes much more complex to solve the problem and

obtain an optimal solution. Therefore, it is proposed that the rate-power function must be in the closed and bounded convex hull, i.e., $\mathcal{R} = \{c(\vec{\mathbf{p}})\}$ [199]. Under this assumption, the cross-layer optimization problem has a dual without any duality gap. Letting μ_i^d denote a Lagrange multiplier for each constraint defined in (7.33), the solution can be obtained as follows.

The data rates of source nodes are obtained from

$$x_s^* = \arg\max_{x_s} \left(U_s(x_s) - x_s \mu_s^d \right), \tag{7.34}$$

where destination d is associated with source s. This is basically the solution of the congestion-control problem. Then, the scheduling solution is obtained from

$$\vec{\mathbf{r}}^* = \arg\max_{\vec{\mathbf{r}} \in \mathcal{R}} r_{i,j} \max_d (\mu_i^d - \mu_j^d). \tag{7.35}$$

The suitable rate and the corresponding power for each link (i.e., $r_{i,j}$ and $p_{i,j}$ which are the elements of vectors $\vec{\mathbf{r}}$ and $\vec{\mathbf{p}}$, respectively) will be chosen. Then, the element of a rate vector for the destination $\vec{\mathbf{r}}^d$ is obtained as follows:

$$r_{i,j}^d = \begin{cases} r_{i,j}, & d = \arg\max_d (\mu_i^d - \mu_j^d), \\ 0, & \text{otherwise.} \end{cases} \tag{7.36}$$

Finally, the Lagrange multiplier is updated as follows:

$$\mu_i^d = \left[\mu_i^d - \phi \left(\sum_j r_{i,j}^d - \sum_{j'} r_{j',i}^d - x_{si} \right) \right]^+, \tag{7.37}$$

where ϕ is the updating step size. The update is proved to converge, where $\phi \to 0$.

7.3 Cross-layer design for vehicular ad-hoc networks

Vehicular ad-hoc networks (VANETs) are considered to be a type of D2D communication whereby devices (i.e., vehicular nodes) are allowed to communicate and exchange various data used for intelligent transportation systems (ITSs). More details about ITSs and VANETs, especially from the D2D communication perspective, are given in Chapter 9. In this section, we give an overview of cross-layer design for VANETs. In addition, the authors of [206] provide a comprehensive survey on this topic.

VANETs have specific characteristics different from those of typical mobile ad-hoc networks (MONETs). These differences are typically vehicle mobility, constant topology changes, and strict QoS requirements for safety applications. The authors of [206] categorize the cross-layer design for VANETs in terms of interactions among layers as follows.

7.3.1 Physical and MAC layers

The channel quality of the physical layer is significantly affected by a vehicle's mobility (e.g., shadowing and fading). Therefore, a few solutions focus on an integration of channel adaptation and contention in the physical and MAC layers, respectively.

- *Transmission-rate adaptation:* A modulation mode can be adjusted adaptively on the basis of packet-loss or signal-to-noise ratio (SNR) level-change events [207]. The loss-triggered scheme is transmitter-based. If the transmitter does not receive an acknowledgement for its transmitted packet, the transmitter will reduce modulation mode in order to achieve better reliability (i.e., lower BER). By contrast, the SNR-triggered scheme is a receiver-based method, in which the receiver evaluates the channel quality of a request-to-send (RTS) message. Then, the receiver chooses the best modulation mode, and informs the transmitter through a clear-to-send (CTS) message. While the transmission rate is adjusted in the physical layer, the RTS and CTS

messages are used in the MAC layer, and this constitutes the cross-layer design concept.

- *Handoff management and channel selection:* VANETs can be based on hybrid topology, combining multihop transmission with a vehicle-to-infrastructure (V2I) communications capability. In such a setting, a vehicular node has to choose whether it should communicate with a roadside unit (i.e., a base station) directly or access relay nodes to forward data to the roadside unit [208]. Since the communications over multihop networks and to the roadside unit may use different connections (e.g., IEEE 802.11 or 802.16, respectively), the vehicular node must choose the transmission channel on the basis of a suitable connectivity. [208] introduced a vehicular fast handover scheme that is able to use channel and location information to switch between direct and relay transmissions. For example, a vehicular node can choose relay nodes that travel in the same direction with good channel quality to forward data to the roadside unit.
- *Transmission-range adaptation:* By adjusting the transmit power, the transmission range of a vehicular node can be controlled. The long transmission range may help one to reach a destination node sooner. However, it will create more interference and contention in a network. Figure 7.7 illustrates such a situation. Clearly, with a long transmission range, the interference area is much larger than that with a short transmission range. However, the short transmission range requires relay transmission, which incurs more delay. Therefore, one solution to achieve an optimal end-to-end performance is to adapt the transmission range to suit the vehicle density. The transmission range can be increased when the vehicle density is low. The vehicle density can be extracted from the MAC-layer protocol (e.g., the contention rate). Using this MAC-layer information, the transmission range can be adjusted in the physical layer.

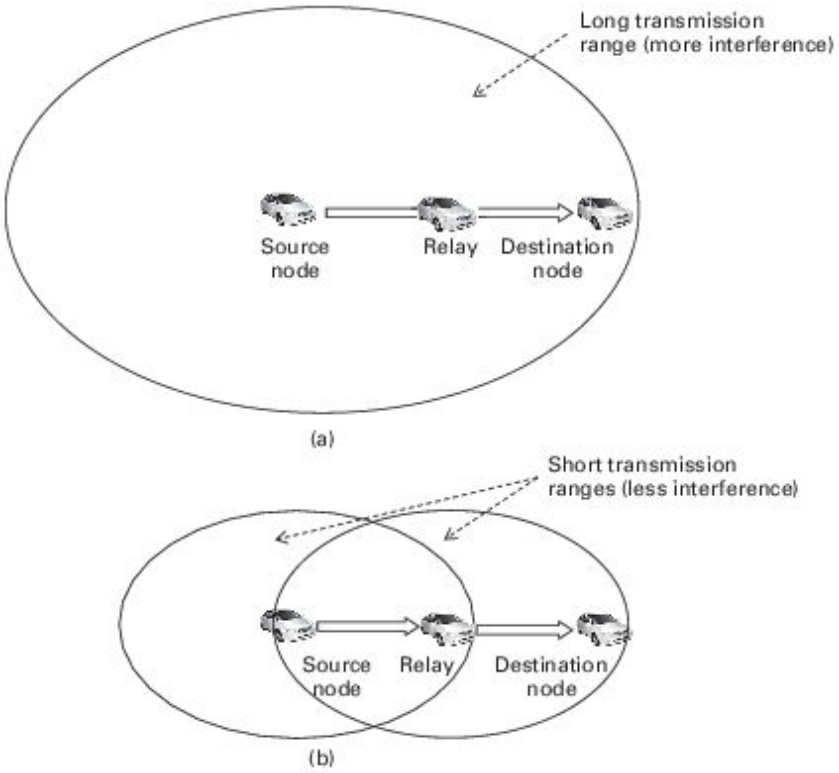

Figure 7.7. Transmission range adaptation for (a) one long transmission range and (b) two short transmission ranges.

7.3.2 Physical and network layers

In VANETs, routing has to be updated frequently to maintain up-to-date information about a network topology. However, updating routing information is an overhead, which could interrupt data transmission. Therefore, the routing information update must be performed appropriately to minimize the overhead while maintaining accurate routing information of the network. The authors of [209] introduced the link-residual-time (LRT) metric. This LRT is computed from the received power strength measured in the physical layer. By using the LRT to evaluate the change of signal strength, one can estimate the remaining time of a connection. The protocols in higher layers can use this information to adapt the routing, scheduling, and handoff accordingly. Along the same lines, the authors of [210] introduced signal-strength-assessment-based route selection for the optimized-link-state-routing (OLSR) protocol. In this protocol, relay nodes

are chosen according to the strongest signal strength to perform routing and topology-information broadcasting.

7.3.3 Network and MAC layers

Routing protocols can utilize geographical information, which is available in the MAC layer, to optimize packet transfer.

- *Contention-aware route selection:* Routing protocols can utilize the contention information (e.g., a collision probability) from the MAC layer to optimize route selection in order to achieve optimal end-to-end performance. For example, the protocol should avoid a route with heavy contention, even though that route may be the shortest path. The highly congested route could result in a high collision probability and a long delay due to the need for many retransmissions. Figure 7.8 illustrates such a scenario.
- *Link prediction:* Mobility information (e.g., current position, speed, and direction from a global positioning system [GPS]) can be used to predict the new location, and hence the links available for routing. The authors of [211] introduced the movement-prediction-based-routing (MOPR) protocol. The protocol utilizes vehicle movement information from the MAC layer, including position, speed, and direction, together with topology information to predict the availability of relay nodes. By using geographical and network information jointly, the MOPR protocol can determine a stable route, providing a reliable and more efficient routing mechanism.
- *Cluster-based routing:* Instead of allowing any vehicular nodes to route their packets directly, the concept of clustering is adopted, leading to hierarchical VANETs. Specifically, a network is divided into clusters (i.e., groups). Each cluster has a cluster head and cluster members. The cluster member first transmits its data to the cluster head. Then, the cluster head relays that packet to the cluster heads of other clusters, until the packet reaches the cluster of a destination. The cluster head stops forwarding the packet and just transmits to the destination. This cluster-based routing in the network layer can avoid collision in the MAC layer. The authors of [212] presented a segment-based routing framework. A road is divided into segments. Each segment corresponds

to a cluster of vehicles. The transmission could be divided into intracluster and intercluster components. The scheduling can be employed at the cluster head to control the intracluster and intercluster transmission in order to avoid collisions.

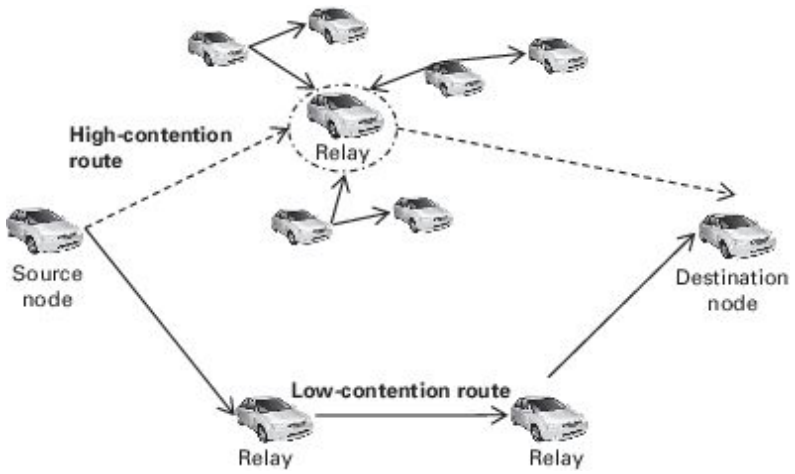

Figure 7.8. Routing to avoid highly congested route.

7.3.4 Transport, network, and MAC layers

TCP is the most commonly used transport protocol. The aim of cross-layer design using TCP in VANETs is to differentiate among incidents of packet loss due to congestion (i.e., buffer overflow), MAC collision, and wireless transmission error.

- *Vehicular transport protocol (VTP):* VTP integrates the transport-layer protocol with position-based routing, by allowing nodes in the network to feed back a type of packet loss to a source node [213]. The protocol has two states, i.e., connected and disrupted. As long as the acknowledgement message is received, the protocol will be in the connected state. However, if the acknowledgement message cannot be received, the protocol will compute the expected connection duration using distance and past-transmission records (e.g., whether a relay node receives an acknowledge message or not) between the source and the receiver. The state changes to disrupted if the duration is less than a predefined threshold. The state and data rate are estimated at the source

node using per-packet feedback from other relay nodes. Then the protocol uses the computed data rate to estimate control packet transmission in order to avoid congestion.

- *Joint optimal control (JOC):* The authors of [214] presented a cross-layer design with the objective of maximizing the path utility by controlling the flow rate at the transport layer. The joint-optimal-control (JOC) algorithm was developed for link-capacity estimation, routing, and network flow control at the MAC, network, and transport layers, respectively. The relay nodes in the network will report the link-persistence probability to a source node. The source node uses this information to compute suitable flow rates in all possible paths. Then, the best path is selected for data transfer.
- *Distributed rate control for VANETs (DRCV):* The authors of [215] proposed a transmission-rate-control algorithm for road-safety applications. The objective is to improve the reliability of safety messages while achieving a small delay. Each node monitors channel activities locally to estimate the number of neighbors, channel idle time, and number of beacons per unit of time. From the monitored data, the DRCV estimates the traffic load and determines the transmission rate of periodic messages used in non-safety applications in the transport layer. If an emergency message has to be transmitted urgently, the periodic message-transmission rate will be reduced to give more priority to the emergency message.
- *Power allocation:* The authors of [216, 217] investigated a transmit-power-control problem with TCP. It was found that, when the vehicle traffic density decreases, the number of hops required in order to reach a destination node increases, and hence the throughput decreases (due to there being fewer choices of relay nodes). However, under a heavy traffic density, interference and congestion can easily happen. In addition, the vehicular nodes near a roadside unit can have higher transmission rate and the nodes do not need to use high power to avoid there being a high collision probability. According to these observations, the transmit power of vehicular nodes should be adjusted depending on the traffic density and road scenario.

Cross-layer design can be applied also to vehicle-to-infrastructure (V2I) communications. The authors of [218] introduced the Cabernet, which is a

protocol for V2I communications that is intended to reduce the connection time. The Cabernet transport protocol (CTP) is introduced by using a probing mechanism to monitor whether the packet loss arises from channel error or congestion, so that the transmission rate in the transport layer can be controlled properly. The CTP also incorporates a dynamic addressing mechanism. By using a proxy, the CTP can maintain a connection session even though the IP address changes (e.g., due to handoff).

7.4 Cross-layer design in D2D communication

In this section, the cross-layer designs, particularly those applied to D2D communication, are reviewed. Firstly, we present the routing scheme based on information correlation in the D2D networks. Secondly, we present the cross-layer routing scheme for D2D sensor networks. Then, the cross-layer video-transmission scheme is presented.

7.4.1 Information correlation routing

The authors of [219] introduced the novel idea of analyzing information in content and using that information to optimize the content distribution in multihop D2D communications. This is a similar idea to context-aware communication. For example, the information associated with a location of a user can be transmitted if the user's GPS data is available. Additionally, a service provider can recommend some service (e.g., file downloading) to the users, depending on their interests and preferences. Furthermore, the context information can be used to optimize the performance of data transfer. For example, video packets should be forwarded to users before web packets. However, in traditional D2D communications, this context information is not incorporated for allocating radio resources for peer-to-peer and possibly multihop communication. The authors of [219] bridged this gap by proposing a new routing algorithm among D2D users considering their information requirements.

To achieve good performance of content forwarding and relaying, the concept of information correlation between content and user's context is

introduced in [219]. This correlation quantitatively measures the similarity between information stored in the content and the requirement stored in the context of a user. In other words, the correlation provides the worth of information in the content. With this information, a base station can allocate radio resources to different devices appropriately. For example, the base station may detect that there are some devices holding the content needed by many other nearby devices. Therefore, instead of letting those devices connect to and download the content through the base station, the base station can allow those devices to form a group of D2D links so that they can download the content directly. Figure 7.9 shows such a scenario. In addition, the base station can allocate more radio resources to the devices which hold the demanded content in order to improve the performance. Furthermore the channel quality in the physical layer can be incorporated into this radio-resource allocation. For example, the base station may assign only a few source devices with favorable channel quality to supply the content to other devices, thereby reducing interference and congestion in the group of D2D links.

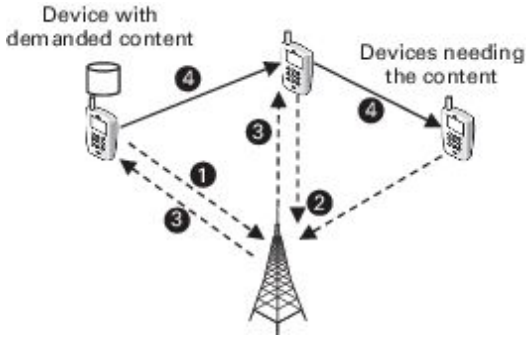

Figure 7.9. A typical scenario considered in [219]. (1) The device with content informs the base station. (2) Other devices inform the base station of their demand for the content. (3) The base station organizes the group of D2D links and assigns radio resources accordingly. (4) The content is transferred using the allocated radio resources from the base station.

The authors of [219] considered specifically the routing problem in a group of D2D links. The cross-layer routing algorithm based on an application layer is motivated as follows. Figure 7.10 shows the group of D2D devices D1, … , D5. Device D1 has the content needed by devices D3 and D5. Devices D3 and D5 inform the base station of their demand. Since the base station knows the channel quality and connectivity in the group, the

base station instructs device D1 to choose the route through device D4 instead of that through D2.

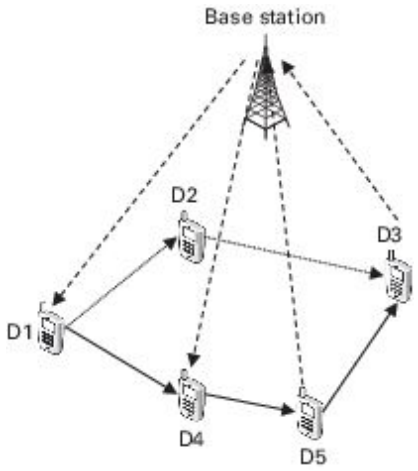

Figure 7.10. An example scenario of an application-layer-based cross-layer routing algorithm.

The information correlation is the parameter which determines the correlation between a given content and the context information (demand) of a user. If the correlation is high, there is a higher chance that the content will be needed by that user, and the user will be more willing to obtain and forward that content. Let C_j denote a particular content needed by user j, and let S_i denote the content chosen by the base station to transfer to user i. Specifically, C_j and S_i denote demand and supply, respectively. Here C_j could be interpreted as context information indicating the demand of user j. The conditional probability of context information C_j given the content S_i is denoted by $P(C_j|S_i)$. The mutual information can be considered as the effectiveness of the content. In general, we have $P(C_j|S_i) \leq 1$. The entropy metric and mutual information are defined as follows: $H(C_j|S_i)$ and $I(C_j;S_i)$, respectively; and $I(C_j;S_i) \leq H(C_j)$. If the value of $I(C_j;S_i)/H(C_j)$ is large, the content S_i can reduce much uncertainty of the context of user j (i.e., the content S_i is useful for user j). If the context C_j is identical to content S_i, then we have $P(C_j|S_i) = 1$, $H(C_j|S_i) = 0$, and $I(C_j;S_i) = H(C_j)$, where the content S_i completely removes the uncertainty of the context of user j. Here, the information correlation is defined according to the mutual information as follows:

$$\sigma_{j,i} = \frac{I(C_j; S_i)}{H(C_j)}. \tag{7.38}$$

In other words, the information correlation is the ratio of the demanded information of user j which is satisfied by content S_i.

Let us consider a particular application of scientific-article transfer. One user may want to download a particular scientific article. However, this user has only the abstract of that article. This abstract is considered as the context C_j of user j. If the user i has the full article denoted by S_i, the following scenarios can happen.

- *The mutual information is small* if the article is in a different research area from that of the abstract which user j has (e.g., S_i is an article on medical science but C_j is the abstract of an article on electrical engineering).
- *The mutual information is large* if the article is in the same area as that of the abstract which user j has (e.g., S_i is an article related to wireless communication and C_j is the abstract of an article about D2D communication).
- *The mutual information is the largest (i.e., $I(C_j; S_i) = H(C_j)$)* if the abstract that user j has is from the same article as that which user i has.

The users will send an indication message that contains the information about the context of the content that the user needs and the content that the user already has. The base station collects the indication messages from all of the users in the network and constructs a context table, which contains the context information. Another table is built by the base station to store the mapping from demand to the content-supplier users and the candidate route. The information correlation, which is computed again by the base station, is used to link these two tables together. When the base station receives a request for content, it uses the computed information correlation to determine the best content-supplier user from

$$i^* = \arg\max_i \sigma_{j,i}. \tag{7.39}$$

Given the best content supplier, the best route will be determined in such a way as to maximize the total mutual information of all users in the networks.

The base station can allocate radio resources to different users according to their priority. The link with higher information correlation will be accorded higher priority. The priority $\rho_{j,i}$ can be simply determined by the information correlation, i.e., $\rho_{j,i} = \sigma_{j,i}$. However, some users with low information correlation may suffer from low priority. Therefore, the modified priority assignment is defined as follows:

$$\rho_{j,i} = \sigma_{j,i}(1 + \beta d_j), \tag{7.40}$$

where d_j is the delay of user j from the last time the user has been served and β is the weight of the delay.

Two major performance metrics are considered to evaluate the application-layer-based cross-layer routing algorithm. The system effectiveness is defined as follows:

$$\eta = \sum_{m=1}^{M} \frac{\sum_{k=1}^{K} V_m \sigma_{m,k} \delta_{m,k}}{\sum_{k=1}^{K} B_m \delta_{m,k}}, \tag{7.41}$$

where M and K are the total number of contents and number of users in the system, respectively. V_m is the size and B_m is the bandwidth used to transfer the content m. $\delta_{m,k}$ is the indication, where $\delta_{m,k} = 1$ if the content m is transferred through user k, and $\delta_{m,k} = 0$ otherwise. Basically, the system effectiveness indicates the amount of content transferred per unit of bandwidth. The satisfaction of user k is another important metric, and it is defined as follows:

$$u_k = \frac{\sum_{m=1}^{M} \sigma_{m,k} \delta_{m,k}}{\sum_{m=1}^{M} \delta_{m,k}}. \tag{7.42}$$

Here u_k is the ratio between the amount of needed content received and the total amount of content demanded. The average user satisfaction is obtained from $\bar{u} = (1/K)\sum_{k=1}^{K} u_k$.

The system-level simulation is conducted for an LTE system to evaluate the performance of the proposed cross-layer routing algorithm for D2D users. The results show that the proposed cross-layer routing algorithm can achieve much higher effective throughput (i.e., the throughput which is used to transfer the content needed by users) than that of round-robin scheduling. Therefore, the limited radio resource is more effectively used for useful information transfer. The simulation results also show that, if the value of β used to weight the delay in allocating the priority of content transfer increases, the system throughput will be decreased. However, users with poor channel quality will have more opportunity to receive demanded content.

7.4.2 Cross-layer routing in wireless sensor networks

The authors of [220] introduced a cross-layer routing algorithm for wireless sensor networks for machine-to-machine (M2M) communications to support hazard-monitoring applications. The cross-layer routing algorithm is integrated with power control and link scheduling to guarantee a high probability of interference-aware and delay-sensitive data delivery.

The M2M network considered in [220] is composed of sensors randomly deployed in a target area. The sensor can adjust its transmission range by controlling its transmit power. Specifically, the sensor chooses the transmit power from a set of $\{p_0, p_1, \ldots, p_{\max}\}$. Each transmit-power level corresponds to the transmission range whose set is defined as $\{r_0, r_1, \ldots, r_{\max}\}$. The data generated at the sensor must be delivered to the destination (i.e., a sink) within a delay deadline denoted by $T_{\max}$. The transmissions of the sensors are based on time slots, where the synchronization is assumed to be available and perfect for all the sensors. Figure 7.11 shows a frame structure adopted in the cross-layer routing

algorithm. A frame is divided into three phases, i.e., the control, schedule, and ACK phases.

- *Control phase:* The main purposes of this phase are to provide synchronization for the sensors in the network and to exchange assigned slots for data transmission among sensors. This slot exchange is used to avoid interference among sensors one or two hops away. Additionally, the possible interference area (PIA), which is the estimate of an interference area (i.e., minimum separation at which two transmissions can be performed simultaneously without collision), is also exchanged in this phase. The information exchanges by the sensors are performed through the contention-based protocol, where the collision is assumed to be negligible.
- *Schedule phase:* Given information exchanged in the control phase (e.g., the PIA), the sensor performs local interference-aware link slot allocation. Specifically, the sensor selects available slots according to its transmission demand and allocates the slots to transmit data on different links (i.e., link scheduling).
- *ACK phase:* The sensor observes the interference during its transmission (e.g., from the feedback from its destination). The sensor acknowledges the allocated slot. There are two cases. If there is no interference, the sensor can reuse this slot again in the future. Otherwise, the sensor will mark this slot as an interference slot, and try to choose other available slots in the next frame.

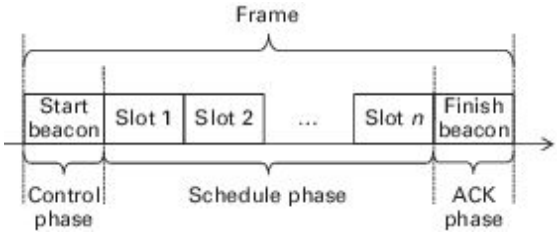

Figure 7.11. A frame structure of the cross-layer routing algorithm in wireless sensor networks.

Using these three phases, the sensor keeps track of the frame-length and slot-allocation information. In addition, the sensor maintains the PIA through message exchange in the control phase.

The frame is divided into two types for the transmissions of high priority and normal data. By differentiating the different types of data, the proposed routing protocol can then optimize the power control (by choosing a transmit power level) and link scheduling to meet the delay deadline of the data. The major steps in the protocol are as follows.

(i) The sensor searches for the route with minimum end-to-end power allocation.

(ii) All links of the route must be interference-free, which can be achieved through the slot allocation.

(iii) The end-to-end delay of the route must be less than or equal to the threshold $T_{\max}$.

(iv) The high-priority data can utilize the slot in two transmission frames to meet the delay requirement. Otherwise, another frame will be used for transmitting normal data.

The protocol is formally divided into two parts, i.e., routing with admission control and dynamic link scheduling. For the routing with admission control, the sensor will choose the next hop for data forwarding such that the data becomes closest to the destination, given that the delay deadline has been estimated to be satisfied. The sensor can gradually increase the transmit power to find the best next hop. The sensor performs admission control in routing to ensure that the delay of that data will meet its deadline, given available slots. Otherwise, the sensor will not accept and forward the data. In other words, if the sensor accepts and forwards the data whose delay cannot be met, this sensor will waste its energy and radio resources as the data becomes useless. For the dynamic link scheduling, if the high-priority data cannot reach the destination before the deadline, the sensor will try to obtain more transmission opportunity for this data. In particular, the sensor will expand and double its frame size. The sensor will piggyback the request for frame expansion with the neighbor exchange message and broadcast this message during the control phase. If the

neighbors agree to expand the frame size, they will update the frame size for synchronization purposes and send an acknowledgement message back to the requesting sensor in the ACK phase. Having two frames for transmitting high-priority data will ensure that the data will have a higher chance of reaching the destination earlier, since there is no interruption from interference and transmission collision.

The performance evaluation is performed by simulations, by comparison with the real-time and robust routing (RTRR) [221] and real-time power-aware routing (RPAR) [222] protocols. A constant-bit-rate (CBR) sensor is considered. The simulation results clearly show that the proposed cross-layer routing protocol can increase the probability of data delivery within the delay deadline, compared with the RTRR and RPAR protocols. This is due to cross-layer adaptation of the power control, admission control, routing, and link scheduling, which can be optimized jointly.

7.4.3 Cross-layer distributed scheduling for peer-to-peer video streaming

The authors of [223] introduced a cross-layer distributed scheduling algorithm for video streaming services on peer-to-peer networks. The proposed cross-layer framework focuses on the video-distortion estimation at the application layer, packet scheduling at the P2P overlay layer, packetization and fragmentation at the MAC layer, and adaptive modulation and coding (AMC) at the physical layer. This distributed framework is designed such that different devices can interact with each other independently to achieve the performance goal.

Figure 7.12 shows the structure of the cross-layer design framework for peer-to-peer video streaming services. The main component of the cross-layer design is the controller which collects protocol information (e.g., link information including SNR and queue length) to optimize the network performance by controlling the protocol parameters. These parameters are the video quantization step size and prediction mode at the application layer, the packet size at the MAC layer, and the modulation and coding parameter at the physical layer. With the proposed structure, the framework has the

flexibility to adjust a few protocol parameters given the feedback information. For example, the quantization step size and prediction mode can be adjusted on the basis of the tradeoff that increasing the size of encoded video will improve the video quality. If the packet size is large, the delay will be lower because a lot of data can be transmitted at once, but, due to the bit error rate, the error could be higher. Additionally, if the SNR is low, the device may reduce the modulation mode and coding rate to achieve a lower transmission error in order to achieve reliable transmission. All these parameters should be optimized jointly to achieve the optimal application performance and user satisfaction.

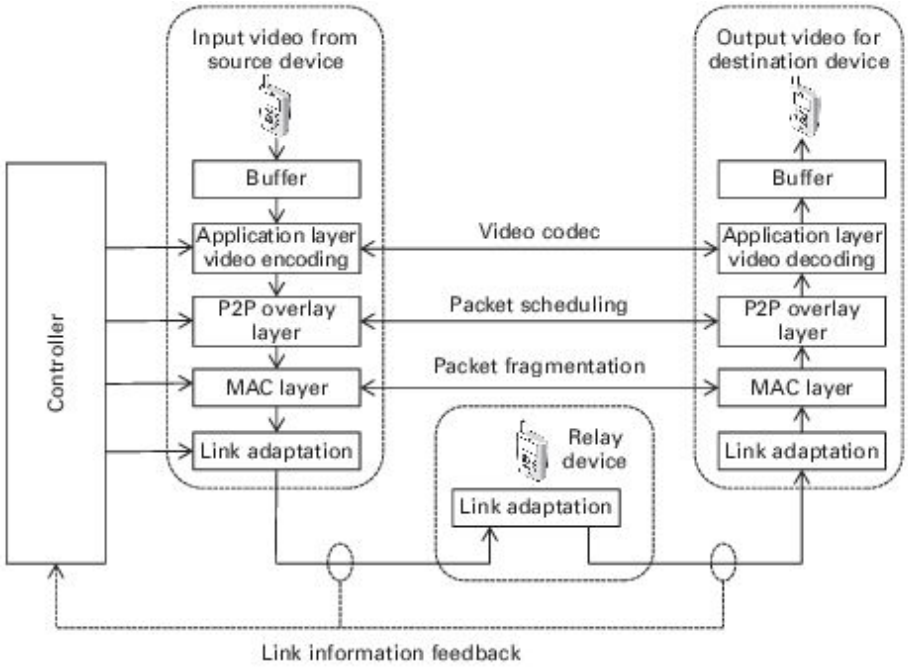

Figure 7.12. The cross-layer design framework for peer-to-peer video streaming.

The proposed scheduling algorithm works when a device detects a lost packet. Then, the device will send requests to its partner (i.e., the devices in the same overlay network). The partners will perform cross-layer optimization of the scheduling algorithm to determine the optimal set of protocol parameters (i.e., the quantization step size, prediction mode, packet size, modulation mode, and coding rate) for retransmitting the lost packet. Next, the partners reply with the estimated distortion of the video. After the device has received the responses, it will choose the partners with the

smallest expected video distortion to obtain the missing packet. The selected partners will use the optimized protocol parameters to transmit the missing packet. The video distortion is defined as follows:

$$\mathbb{E}[D] = \sum_{f=1}^{F} \sum_{i=1}^{I} \sum_{j=1}^{J} \mathbb{E}[D_{j,i,f}], \tag{7.43}$$

where F is the total number of video frames, I is the total number of packets for one video frame, and J is the total number of pixels in one packet. Let $d_{j,i,f}$ denote the original value of pixel j of packet i of frame f at the source, and let $\tilde{d}_{j,i,f}$ denote the reconstructed pixel at the destination. The distortion can be computed from

$$\mathbb{E}[D_{j,i,f}] = \left(d_{j,i,f} - \tilde{d}_{j,i,f}\right)^2, \tag{7.44}$$

which follows the concept of mean-squared error (MSE). In this case, the optimization problem can be formulated as follows:

$$\begin{aligned} \min_{q_{f,i}, p_{f,i}, l_{f,i}, a_{f,i}, c_{f,i}} & \sum_{f=1}^{F} \sum_{i=1}^{I} \sum_{j=1}^{J} \mathbb{E}[D_{j,i,f}] \\ \text{s.t.} \quad & t_{f,i} \leq T_{f,i}, \end{aligned} \tag{7.55}$$

where $q_{f,i}$ is the quantization step size, $p_{f,i}$ is the prediction mode, $l_{f,i}$ is the packet size, and $a_{f,i}$ and $c_{f,i}$ are the modulation mode and coding rate, respectively. These decision variables are for packet i of video frame f. $T_{f,i}$ is the video-playback deadline for packet i of frame f. $t_{f,i}$ is the delay of transferring missing packet i of frame f, and is expressed as follows:

$$t_{f,i} = \sum_{z=1}^{Z} \sum_{h=1}^{H} \left(\frac{l_{f,i,z}(\vec{\epsilon}, \vec{\mathbf{q}}, \vec{\mathbf{p}})}{R_h(a_h, c_h) b_h} + T_h + Q_h \right), \tag{7.46}$$

where Z and H are the number of MAC packets and number of hops from the selected partner employed to transfer the missing packet, respectively. $l_{f,i,z}$ is the number of bits in packet i of the video frame f. This $l_{f,i,z}$ depends on the vectors of the packet-loss rate $\vec{\epsilon}$, quantization step size $\vec{\mathbf{q}}$, and prediction mode $\vec{\mathbf{p}}$ of the partners. $R_h(a_h, c_h)$ is the transmission rate given the modulation mode a_h and coding rate c_h, and b_h is the bandwidth at hop h. T_h and Q_h are the propagation delay and queueing delay at hop h, respectively. While the propagation delay is fixed, the queueing delay is obtained from

$$Q_h = \frac{R_h(a_h, c_h)b_h}{R_{h+1}(a_{h+1}, c_{h+1})b_{h+1}(R_{h+1}(a_{h+1}, c_{h+1})b_{h+1} - R_h(a_h, c_h)b_h)}, \tag{7.47}$$

which follows the delay model of the M/M/1 queue. Figure 7.13 shows a schematic diagram of this queueing delay.

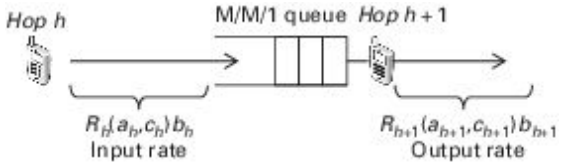

Figure 7.13. A schematic diagram of queueing delay.

To obtain the solution, the optimization problem defined in (7.45) is cast as the directed acyclic graph (DAG) and the dynamic programming algorithm is applied. First, the minimum total video-distortion function of packet i is defined as $G_i(v_{i-x}, v_{i-x+1}, \ldots, v_i)$, where $v_{i'}$ is the composite variable of protocol parameters for packet i', i.e., $v_{i'} = (q_{f,i'}, p_{f,i'}, l_{f,i'}, a_{f,i'}, c_{f,i'})$. Here the video-decoder concealment strategy is used (i.e., the quality of the current video frame depends on the quality of the previous frames back for x packets). Therefore, the minimum total distortion of the entire video clip defined in (7.45) can be reformulated as follows:

$$\min_{v_{S-x},\ldots,v_S} G_S(v_{S-x}, v_{S-x+1}, \ldots, v_S), \tag{7.48}$$

where $S = F \times I$ is the total number of packets of the video sequence. It is observed that the selection of variable v_i is independent of the selection of the previous variables $v_{i-x-1}, v_{i-x-2}, \ldots, v_1$. Therefore, this relation can be represented by the directed acyclic graph, which can be solved using the dynamic programming algorithm.

The performance evaluation of the proposed cross-layer scheduling algorithm is based on simulation on NS2. A comparison with the gossip-based protocol [224] is provided. Firstly, the packet playback deadline is varied. It is shown that the packet scheduling failure rate (i.e., the ratio of the packet loss that cannot be replaced within the deadline to the total packet loss) of the proposed cross-layer scheduling algorithm decreases as the deadline increases. Additionally, the proposed cross-layer scheduling algorithm achieves a much lower failure rate than that of the traditional protocol. Similarly, the peak signal-to-noise ratio (PSNR) of the proposed algorithm is higher.

7.5 Chapter summary

Cross-layer design has been introduced as an alternative to the layer-based protocol structure. Allowing parameters and functions to be shared across protocols in different layers can improve the performance of data communication. In this chapter, we have presented an overview of the cross-layer design. We have given the definition and presented different approaches to achieve efficient and effective cross-layer design. Then, we have introduced the cross-layer coordination model, which incorporates the security, quality of service, mobility, and wireless link adaptation functions in the protocols. Next, we have discussed the implementation and some challenges in adopting the cross-layer design concept to develop new protocols.

As part of the cross-layer design, cross-layer optimization plays an important role in achieving an optimal data-communication and networking performance. We have given examples of the cross-layer optimization for the opportunistic scheduling, OFDM resource allocation, and congestion

control. We have briefly reviewed some related works in the cross-layer design and optimization for device-to-device (D2D) communications including vehicular ad-hoc networks (VANETs), routing in sensor networks, and traffic scheduling for peer-to-peer video services.

Some research directions for cross-layer design and optimization in D2D communications are as follows.

- *Energy efficiency:* While most of the existing cross-layer design frameworks focus on data communication and network performance, energy efficiency is also a crucial issue. The protocols in different layers used in D2D communications must be optimized to reduce energy consumption. While energy-efficient algorithms can be implemented in different layers, their holistic integration could provide superior performance. For example, in wireless sensor networks, routing protocols can determine the route with the largest energy supply and harvesting and the least amount of collision, which incurs energy wastage. The cross-layer coordination model can be modified to include energy efficiency as one of its planes.
- *Coordination through a base station:* In D2D communications, a base station can control the spectrum access and data transmission of D2D devices. Different levels of control can be applied (e.g., devices can be loosely controlled by allowing D2D devices to use a certain channel or tightly controlled by adjusting all parameters of all transmissions). The cross-layer design can be implemented both at D2D devices and at a base station. However, the information and control signaling must be invented to maximize transmission performance and reduce overhead.
- *Application specific cross-layer design:* D2D communications can be applied to broad applications. The cross-layer design must be customized to account for application-specific requirements. In mobile social networks, for example, the cross-layer design involves not only the system parameters from different layers, but also social metrics extracted from users' application and mobility. Cross-layer optimization can utilize such information to achieve optimal network performance and user satisfaction.

8 Security for D2D communications

D2D communications can be prone to potential security threats. For example, D2D mobiles need to know who else is located nearby so as to pair up. If the location information is spoofed, the interference caused by wrongly paired D2D users can significantly lower the system performance. Additionally, D2D communications between neighboring D2D nodes provide alternative security approaches (physical-layer security) by using channel statistics. In this chapter, we will study the following two security problems in detail.

- Location security: D2D networks need to pair D2D users on the basis of location information so as to use locally available spectrum. This creates a critical loophole for global-positioning-system (GPS)-spoofing attack, where the adversary attacks the GPS signals received by D2D devices, so that D2D devices obtain false available spectrum information with false location information. This security loophole can potentially result in large-scale malfunctioning of mobile D2D networks.
- Data transmission security: Security in D2D communications is traditionally implemented using cryptography, as in other wireless communication systems. Alternatively, physical-layer security provides additional security provided by the channel statistics, which fits well the D2D communications scenarios. We will consider physical-layer security in D2D communications as an underlay to cellular networks with an eavesdropper. Benefiting from the underlaid spectrum reuse, D2D users can contribute to the system's secrecy capacity, while D2D users may interfere with cellular users and decrease their secrecy capacity.

8.1 Location security

8.1.1 Problem overview

Dynamic-spectrum-access (DSA) technology has received much attention in industry and academic environments due to its promise of better utilization of spectrum resources compared with the current static spectrum-allocation method. Traditionally, spectrum allocation is static, where FCC assigns communities licenses to use specific frequencies, such as AM, FM, short-wave and citizens' bands, and VHF and UHF television channels, as well as hundreds of less familiar bands that serve cellular and cordless telephones, GPS trackers, air-traffic-control radars, security alarms, radio-controlled toys, and the like. While some of these assigned spectrum bands have been overloaded due to the growth of their users, other spectrum bands are scarcely used. The uneven utilization of spectrum resources promotes the development of DSA, so as to take advantage of the spectrum white space opportunistically. This innovative method of dynamic spectrum management can greatly enhance the utilization of spectrum resources and has been called out in the federal government's National Broadband Plan [225] recently as one of the major technologies to provide broadband services to millions of US residences.

DSA techniques can be used for resource allocation for D2D communications. One of the most important requirements on DSA operation for D2D is that D2Ds must not interfere with regular mobile users. To achieve this, D2D users need to know the location information of the nearby nodes. The geolocation information is stored in the database, from which the resource allocation such as D2D pairing is determined. However, the above database-based approaches have a critical security loophole that can potentially result in large-scale malfunction of mobile D2D networks. This loophole is caused by the fact that, in a geolocation database approach, a D2D user usually calculates its own location using GPS and then uses this location to query the database for resource allocation. Unfortunately, GPS is a very insecure system. As a narrow-band technology that relies on weak satellite signals with a poor authentication mechanism, the GPS signal can be easily jammed, delayed, or emulated in a large area with a small amount

of emit power. The availability and relatively low price of software-defined radio has made building GPS-spoofing devices a fairly easy task [226, 227]. Multiple incidents of GPS-spoofing attacks have also been reported recently [228, 229]. The vulnerability of GPS systems means that an adversary can easily launch a GPS-spoofing attack to cause incorrect location computation at D2D mobiles. Such incorrect location computations lead to incorrect spectrum-query results, which then causes D2D users to impose dangerous interference on other mobile users. For example, the FCC is moving to push the 3.5-GHz radar band for use in DSA technology [230]. Many military facilities are using this band currently. In normal DSA networks, mobiles in the vicinity of these military facilities are informed by a geolocation database that the radar band is not available in their current location. However, a terrorist can potentially launch a GPS-spoofing attack on mobiles in that neighborhood to make them believe that they are in a different location where the radar band is not in use. These mobile devices then start to operate on the radar band, creating a harmful jamming attack on the neighboring military facilities. As DSA D2D technology moves to a more mature stage and becomes more densely deployed in the near future, the danger of such GPS-spoofing attacks will also grow proportionally.

8.1.2 Literature

Wireless localization has been a long-standing research topic, and the recent location-based services (LBSs) have greatly promoted the rapid development of localization techniques. In terms of the mechanisms used for position estimation, the existing localization schemes can be grouped roughly into four categories: range-based, fingerprinting-based, connectivity-based, and hybrid positioning.

In range-based localization systems, the distance information can be obtained from received-signal-strength (RSS) and time-of-arrival (TOA) measurements. For RSS-based schemes, the distance from the transmitter to the receiver is estimated using radio-signal propagation and attenuation models [231, 232, 233]. Similarly, TOA-based schemes use the signal-propagation delay to calculate the distance [234, 235, 236]. With these estimated distances, the localization result is obtained geometrically by

trilateration. Besides trilateration, another range-based mechanism of positioning is triangulation, where the wireless signal's angle of arrival (AOA) is measured by receivers equipped with antenna arrays [237, 238]. Positioning using triangulation is based on the principle that, in a triangle graph, if the positions of the vertices are already known, then, given the angles from a point inside this triangle to the vertices, the position of the interior point can be determined.

Fingerprinting-based schemes follow a common two-phase framework for location estimation, although they may use different kinds of signal measurements. Before the positioning system can operate, an off-line phase is necessary in order to collect sensing data that carries location-dependent features and create the fingerprint database. During the on-line phase, the location of the wireless radio is estimated using classification algorithms based on the fingerprint database. RSS of wireless LAN signals is the most widely used measurement for fingerprinting-based schemes [239, 240, 241, 242, 243, 244]. In addition, in [245] FM broadcast radio signals are used for indoor fingerprinting because they are less susceptible to human presence, multipath effects, and fading. The authors of [246] constructed a fingerprint by combining the optical, acoustic, and motion attributes captured by sensors on a mobile phone.

As the name suggests, connectivity-based algorithms use merely the connectivity information to estimate the position of wireless radios. In [247], a node calculates the centroid of its proximate reference points to localize itself using a simple connectivity metric. An approximate point-in-triangle test (APIT) positioning scheme is presented in [248]. Location algorithms using multidimensional scaling are introduced in [249, 250].

Recently, smartphone localization has attracted tremendous interest, and the variety of sensors in smartphones enable new hybrid positioning schemes that take advantage of multimodal sensing to achieve better location accuracy and independence from infrastructure. Constandache *et al.* developed a war-driving free-human localization system that uses the accelerometer and compass readings from smartphones to capture users' movement traces [251, 252]. The authors of [253] proposed a technique

called EV-Loc, which integrates electronic and visual signals to improve the accuracy of wireless localization. Acoustic ranging estimates among peer phones are utilized to assist Wi-Fi-based localization for improved accuracy in [254]. Other localization schemes based on multimodal sensing can be found in [255, 256, 257].

Owing to the open nature of wireless networks, wireless localization is vulnerable to malicious attacks. In [258], it is experimentally shown that, by attenuating or amplifying the RSS readings at the anchors, the localization system may conclude in false location estimation. Bauer *et al.* showed that attackers with directional antennas [259] have the ability to bias the location estimation to a direction of their choice in addition to introducing significant localization errors. The requirements for successful GPS-spoofing attacks are analyzed in [260].

A few robust localization schemes have been proposed as countermeasures against malicious attacks. Some of the solutions proposed require additional infrastructure support, such as using directional antennas [261, 262] and fixed locators [263, 264, 265]. Some solutions rely on the analysis of the abnormality in the timing and signal characteristics [258, 266, 267, 268, 269, 270, 271, 272, 273], which may be compromised by the attacker if the attacker is aware of the type of analysis algorithm in use. Bao and Liang proposed an algorithm that uses the threshold idea and vote with sensor nodes to improve the safety performance of node positioning in wireless sensor networks [274]. The Secure Walking GPS scheme [275] is based on tracing human mobility through motion sensors, which cannot be used if the mobility of nodes is not caused by walking human.

8.2 Data-transmission security

In order to provide the secure communications, the concept of *physical-layer security* was recently proposed to describe the physical characteristics of wireless channels [276]. To quantify the security of the transmission, the concept of *secrecy capacity*, defined as the maximum rate of trustworthy information sent from the transmitter to the receiver under the threat of

eavesdroppers, is widely used [277]. In [278], the average secrecy capacity in a non-interference network is calculated. The authors of [279] studied the influence of interference on the secrecy capacity in a cognitive-radio network. Hence, the issue of how the D2D communications can affect the physical-layer security is worthy of study. However, to the best of our knowledge, there have been only a few works investigating this problem.

In this section, we explore the secrecy capacity of cellular networks with D2D underlaying communications, and propose to improve the secrecy capacity in the cellular network with the help of D2D communication as an underlay. Specifically, we consider a single-cell OFDMA network, with a number of cellular users (CUs) and D2D users, and one eavesdropper who can listen to all the users. We assume that each CU can share its channel with only one D2D user pair, since the signals transmitted by D2D pairs may lead to a collision and thus impair the CU's channel performance. Besides, we assume that each D2D pair can access only one channel.

First, we introduce the concept of secrecy capacity into the D2D underlaying cellular networks, and provide the expression for the corresponding secrecy capacity. When a D2D pair accesses the spectrum of a CU, it generates interference with the corresponding CU and decreases its secrecy capacity. However, when it comes to the system's secrecy capacity, D2D underlay communications may be beneficial and can improve the system's secrecy capacity. This shows that the system's secrecy capacity can be greatly improved by the use of D2D underlay communications.

Second, we consider the radio-resource-allocation problem by using a graph model, and formulate it as the matching problem in a weighted bipartite graph. In the constructed weighted bipartite graph, the vertices in the graph denote the CUs and the D2D pairs, and the edge weight represents the increase of secrecy capacity when CUs share their channels with D2D pairs. Maximizing the secrecy capacity in the cellular network equals maximizing the sum weight of the constructed graph, which yields the maximal weight matching of the above bipartite graph. With the help of the *Kuhn–Munkres* (KM) algorithm, the problem can be solved in polynomial time with maximum sum secrecy capacity for both cellular and D2D users.

Besides, we also provide several other means of channel allocation, such as the random and greedy algorithms, to compare with our proposed method.

In the following, first the system model will be described and then the radio-resource-allocation problem will be given as an optimization problem. Then, we will model the radio-resource-allocation problem as a matching problem in the weight bipartite graph and introduce the KM algorithm to obtain the optimal solution in polynomial time. Finally, simulation results will be presented.

8.2.1 The system model and problem formulation

The system model

We consider an uplink scenario in a cellular network with N CUs in N orthogonal channels respectively, M D2D user pairs accessing the cellular channel with the underlay mode, and a malicious eavesdropper that can overhear the information in all channels, as shown in Figure 8.1. We denote the set of cellular users, the set of D2D user pairs, and the eavesdropper by $\mathcal{U} = \{u_1, u_2, \ldots, u_N\}$, $\mathcal{D} = \{d_i = (d_{\mathrm{T}}^i, d_{\mathrm{R}}^i) | d_1, d_2, \ldots, d_M\}$, and $\mathbb{E}$, respectively, where d_{T}^i and d_{R}^i denote the transmitter and receiver of D2D user pair d_j, respectively. The transmit powers of CU and D2D transmitters are denoted by P_{c} and P_{d}, respectively. We assume that each CU can share its channel with at most one D2D user pair and each D2D pair can access at most one cellular channel. Additionally, all users are assumed to have perfect knowledge of the channel information.[1]

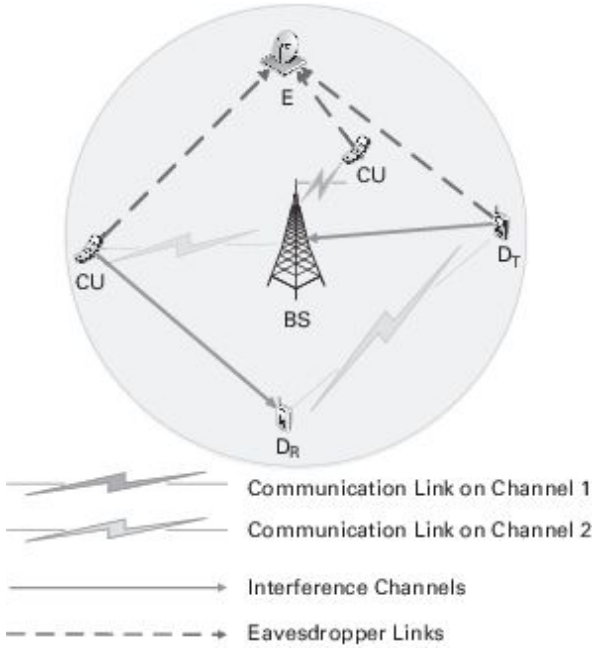

Figure 8.1. The system model.

When CU U_i shares its channel with D2D user pair d_j, the signals received at the base station, at the eavesdropper, and at the D2D receiver d_{R}^{j} are written as, respectively,

$$y_{\mathrm{b}}^{i,j} = \sqrt{P_{\mathrm{c}}} h_{\mathrm{c}}^{i} x_{\mathrm{c}}^{i} + \sqrt{P_{\mathrm{d}}} h_{\mathrm{d,b}}^{j} x_{\mathrm{d}}^{j} + n_{\mathrm{b}}, \tag{8.1}$$

$$y_{\mathrm{d}}^{i,j} = \sqrt{P_{\mathrm{c}}} h_{\mathrm{c,d}}^{i,j} x_{\mathrm{c}}^{i} + \sqrt{P_{\mathrm{d}}} h_{\mathrm{d}}^{j} x_{\mathrm{d}}^{j} + n_{\mathrm{d}}^{j}, \tag{8.2}$$

$$y_{\mathrm{e}}^{i,j} = \vec{\mathbf{h}}_{i,j} \vec{\mathbf{x}}_{i,j} + n_{\mathrm{e}}, \tag{8.3}$$

where $\vec{\mathbf{h}}_{i,j} = \left[\sqrt{P_{\mathrm{c}}} h_{\mathrm{c,e}}^{i} \quad \sqrt{P_{\mathrm{d}}} h_{\mathrm{d,e}}^{j} \right]^{\top}$, $\vec{\mathbf{x}}_{i,j} = \left[x_{\mathrm{c}}^{i} \quad x_{\mathrm{d}}^{j} \right]^{\top}$, and $h_{\mathrm{d,e}}^{j}$, h_{d}^{j}, and $h_{\mathrm{d,b}}^{j}$ denote the direct channel gain from D2D transmitter d_{T}^{j} to eavesdropper $\mathbf{E}$, D2D receiver d_{R}^{j} and the base station, respectively. $h_{\mathrm{c,e}}^{i}$, h_{c}^{i}, and $h_{\mathrm{c,d}}^{i,j}$ denote the direct channel gain from CU U_i to eavesdropper $\mathbf{E}$, the base station, and D2D receiver d_{R}^{j}, respectively. n_{b}, n_{e}, and n_{d}^{j} are the Gaussian noise terms with zero mean and σ^2 variance.

For CU u_i and D2D pair d_j that share the same channel, their total capacity is given by

$$C(u_i, d_j) = \log_2\left(1 + \frac{|h_{\mathrm{c}}^i|^2 P_{\mathrm{c}}}{\sigma^2 + \gamma |h_{\mathrm{d,b}}^j|^2 P_{\mathrm{d}}}\right) + \log_2\left(1 + \frac{|h_{\mathrm{d}}^j|^2 P_{\mathrm{d}}}{\sigma^2 + \gamma |h_{\mathrm{c,d}}^{i,j}|^2 P_{\mathrm{c}}}\right), \tag{8.4}$$

where γ $(0 \leqslant \gamma \leqslant 1)$ is a scaling factor associated with the decoding method. When γ is zero, this means that CU and D2D receivers can decode their own messages completely and experience no interference.

Since the eavesdropper overhears both CU u_i and D2D pair d_j, the channel capacity of the wire-tap channel is given by

$$C_{\mathrm{e}}(u_i, d_j) = \log\left(1 + \frac{\vec{\mathbf{h}}_{i,j}\vec{\mathbf{h}}_{i,j}^{\top}}{\sigma^2}\right). \tag{8.5}$$

Hence, the total secrecy capacity of CU u_i and D2D pair d_j is given by [277]

$$C_{\mathrm{s}}(u_i, d_j) = \left[C(u_i, d_j) - C_{\mathrm{e}}(u_i, d_j)\right]^+, \tag{8.6}$$

where $[\cdot]^+ \triangleq \max(\cdot, 0)$.

For CU u_i, without sharing its channel with other D2D user pairs, its secrecy capacity is given by

$$C_{\mathrm{s}}(u_i) = \left[\log\left(1 + \frac{|h_{\mathrm{c}}^i|^2 P_{\mathrm{c}}}{\sigma^2}\right) - \log\left(1 + \frac{|h_{\mathrm{c,e}}^i|^2 P_{\mathrm{c}}}{\sigma^2}\right)\right]^+. \tag{8.7}$$

Problem formulation

We define an $N \times M$ matrix $\mathbf{A} = [\alpha_{i,j}]$, $1 \leqslant i \leqslant N$, $1 \leqslant j \leqslant M$, where $\alpha_{i,j} = 0$ or 1, to denote whether a CU shares its channel with a D2D user pair or not. If CU u_i shares its channel with D2D user pair d_j, $\alpha_{i,j}$ is 1; otherwise $\alpha_{i,j}$ is zero.

The resource-allocation problem is given by

$$\max_{\mathbf{A}} \sum_{i=1}^{N} C_{\mathrm{s}}^{i} \tag{8.8}$$

$$\text{s.t.} \begin{cases} \sum_{j=1}^{M} \alpha_{i,j} \leqslant 1, \ 1 \leqslant i \leqslant N, \\ \sum_{i=1}^{N} \alpha_{i,j} \leqslant 1, \ 1 \leqslant j \leqslant M, \end{cases} \tag{8.9}$$

where C_{s}^{i}, which denotes the actual secrecy capacity corresponding to CU u_i's channel, is given by

$$C_{\mathrm{s}}^{i} \triangleq \begin{cases} C_{\mathrm{s}}(u_i), & \nexists \ \alpha_{i,j} = 1, \ 1 \leqslant j \leqslant M, \\ C_{\mathrm{s}}(u_i, d_j), & \exists \ \alpha_{i,j} = 1, \ 1 \leqslant j \leqslant M. \end{cases} \tag{8.10}$$

The first constraint, $\sum_{j=1}^{M} \alpha_{i,j} \leqslant 1$, is due to the fact that each CU can share its channel with at most one D2D pair. The second constraint, $\sum_{i=1}^{N} \alpha_{i,j} \leqslant 1$, is due to the fact that each D2D pair can access at most one channel.

8.2.2 Graph-based resource allocation

In this subsection, we formulate the above radio-resource-allocation problem as a matching problem in a weighted bipartite graph. Then, the KM algorithm is introduced to obtain the optimal solution in polynomial time.

Graph construction

The first step is to model the scenario as a bipartite graph $G = (\mathcal{V}, \mathcal{E})$, where $\mathcal{V}$ denotes the set of vertices and is partitioned into two disjoint sets, set U and set D, and $\mathcal{E} \subseteq U \times D$ denotes the set of edges in the graph. Vertex v_U^i in subset U denotes CU u_i, and vertex v_D^j in subset D denotes D2D user pair d_j. For each CU u_i and D2D user pair d_j, we obtain an edge $e_{i,j} = (v_U^i, v_D^j)$ and define its weight $W_{i,j}$ as

$$W_{i,j} = C_s(u_i, d_j) - C_s(u_i), \tag{8.11}$$

which represents the increase of total secrecy capacity when CU u_i shares its channel with D2D user pair d_j. An illustrative example is given in Figure 8.2. Notice that $W_{i,j} \leqslant 0$, which means that CU u_i cannot gain any benefits if it shares its channel with D2D user pair d_j. In this case, we let $W_{i,j} = 0$.

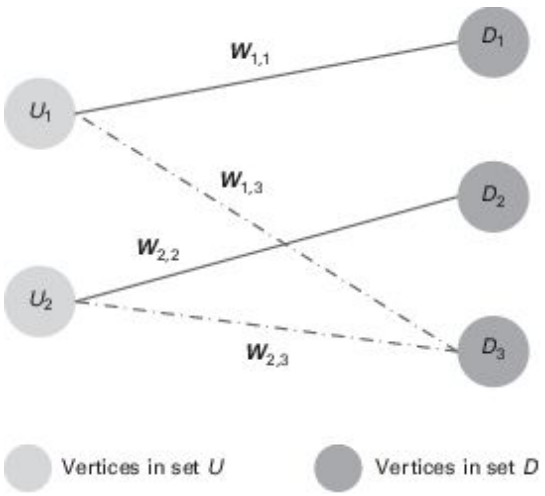

Figure 8.2. An illustrative example of the graph.

DEFINITION 76. *A matching of an undirected graph $G = (\mathcal{V}, \mathcal{E})$ is defined as a nonempty edge set $\mathcal{M}$ that satisfies the following.*

- *Edge set $\mathcal{M}$ is a subset of edge set $\mathcal{E}$, $\mathcal{M} \subseteq \mathcal{E}$.*

- *For all vertex $v \in \mathcal{V}$, at most one edge $e \in \mathcal{M}$ connects to vertex v.*

We define the mapping $f : \mathbf{A} \longrightarrow \mathcal{A}$, where $\mathcal{A}$ is the defined edge set that is solely depended on matrix $\boldsymbol{A}$,

$$\begin{cases} \text{if } \alpha_{i,j} = 1,\ (v_U^i, v_D^j) \in \mathcal{A}, \\ \text{if } \alpha_{i,j} = 0,\ (u_U^i, v_D^j) \notin \mathcal{A}. \end{cases} \tag{8.12}$$

LEMMA 1. *Edge set $\mathcal{A}$ is a matching of graph $G = (\mathcal{V}, \mathcal{E})$ as long as $\mathcal{A} \neq \varnothing$.*

Proof. For every vertex $v \in \mathcal{V}$, function $d(v)$ is defined to denote the degree of vertex v. In a new graph $G' = (\mathcal{V}, \mathcal{A})$, for all vertices $v_U^i \in U(1 \leqslant i \leqslant N)$, the function $d(v_U^i)$ satisfies the relationship

$$d(v_U^i) = \sum_{j=1}^{M} \alpha_{i,j} \leqslant 1, \tag{8.13}$$

which implies that, for an arbitrary vertex v in subset U, at most one edge in $\mathcal{A}$ connects to it. Similarly, for an arbitrary vertex $v_D^j \in D$, the function $d(v_D^j)$ satisfies the relationship

$$d(v_D^j) = \sum_{i=1}^{N} \alpha_{i,j} \leqslant 1, \tag{8.14}$$

which indicates that at most one edge in $\mathcal{A}$ connects to vertex v_D^j. Since set $\mathcal{V} = U \cup D$ and edge set $\mathcal{A}$ is a subset of edge set $\mathcal{E}$, edge set $\mathcal{A}$ is a matching of graph $G = (\mathcal{V}, \mathcal{E})$ as long as edge set $\mathcal{A}$ is nonempty. □

Notice that the system's secrecy capacity $\sum_{i=1}^{N} C_s^i$ in the cellular network can be divided into two parts $\sum^{\text{alone}} + \sum^{\text{coop}}$, which are written as follows:

$$\sum^{\text{alone}} = \sum_{i=1}^{N} C_s(u_i), \tag{8.15}$$

$$\sum^{\text{coop}} = \sum_{i=1}^{N} C_s^i - \sum^{\text{alone}}, \tag{8.16}$$

where the first term $\sum^{\text{alone}}$ denotes the sum secrecy capacity when no CU shares its channel with other D2D pairs, while the second term $\sum^{\text{coop}}$ denotes the increase in secrecy capacity brought about when some CUs share their channels with D2D pairs. Since the item $\sum^{\text{alone}}$ is constant, the total secrecy capacity is maximized as long as the item $\sum^{\text{coop}}$ is maximized. Notice that the item $\sum^{\text{coop}}$ can also be written as

$$\sum^{\text{coop}} = \sum_{i=1}^{N} \sum_{j=1}^{M} I_{\{(v_U^i, v_D^j) \in \mathcal{A}\}} W_{i,j}, \tag{8.17}$$

where the function $I_{\{(v_U^i, v_D^j) \in \mathcal{A}\}}$ is defined as

$$I_{\{(v_U^i, v_D^j) \in \mathcal{A}\}} \triangleq \begin{cases} 1, & (v_U^i, v_D^j) \in \mathcal{A}, \\ 0, & (u_U^i, v_D^j) \notin \mathcal{A}. \end{cases} \tag{8.18}$$

Hence, maximizing the item $\sum^{\text{coop}}$ is the same as finding the maximum weighted bipartite matching $\mathcal{A}$ of graph G.

A graph-based resource-sharing algorithm

Using the constructed graph, we propose to apply the KM algorithm to obtain the maximum weighted bipartite matching $\mathcal{A}$ of graph G.

DEFINITION 77. *The edge set* $\mathcal{M}$ *is a match of the graph* $G = (\mathcal{V}, \mathcal{E})$. *Vertices* $u, v \in \mathcal{V}$ *are covered by matching* $\mathcal{M}$ *if edge* $e = (u, v) \in \mathcal{M}$.

DEFINITION 78. *In a weighted bipartite graph* $G = (\mathcal{V}, \mathcal{E})$, *we define a function-vertex labeling* $l : \mathcal{V} \longrightarrow R$. *A vertex labeling* l *is feasible labeling if the relationship* $l(v_U^i) + l(v_D^j) \geqslant W_{i,j}, \forall\, v_U^i \in U,\ v_D^j \in D$ *holds.*

DEFINITION 79. *A weighted bipartite graph* $G = (\mathcal{V}, \mathcal{E}_l)$ *is an equality graph if the relationship* $l(v_U^i) + l(v_D^j) = W_{i,j}$ *holds for every* $(v_U^i, v_D^j) \in \mathcal{E}_l, v_U^i \in U, v_D^j \in D$.

DEFINITION 80. *Edge set* $\mathcal{M}$ *is a match of graph* $G = (\mathcal{V}, \mathcal{E})$. *Path* $(v_1, v_2, \ldots, v_k)$ *is called an augmenting path if it satisfies the following:*

(i) *its starting vertex and ending vertex are uncovered by match* $\mathcal{M}$; *and*

(ii) *its edges are alternately in and out of the match* $\mathcal{M}$.

Without loss of generality, we suppose that $N \leqslant M$. In order to obtain the maximal weight matching $\mathcal{M}$, the first step is to define a feasible vertex labeling for the vertex in set $\mathcal{V}$,

$$\begin{aligned} l(v_U^i) &= \max\ W_{i,j},\ v_U^i \in U, \\ l(v_D^j) &= 0,\ v_D^j \in D. \end{aligned} \tag{8.19}$$

Using the above vertex labeling, we construct the set $\mathcal{E}_l = \{(v_U^i, v_D^j) : l(v_U^i) + l(v_D^j) = W_{i,j}\}$ and create an initial matching $\mathcal{M}$ in an equality graph $G^e = (\mathcal{V}, \mathcal{E}_l)$.

LEMMA 2. *Matching* $\mathcal{M}$ *of graph* $G = (\mathcal{V}, \mathcal{E}_l)$ *maximizes the sum weight if matching* $\mathcal{M}$ *covers all vertices in set* $\mathcal{V}$.

Proof. Take an arbitrary matching $\mathcal{M}'$. Since the defined vertex labeling is feasible, the following relationship holds for all edges $e_{i,j} = (v_U^i, v_D^j)$:

$$\sum_{e_{i,j} \in \mathcal{M}'} W_{i,j} \leqslant \sum_{e_{i,j} \in \mathcal{M}'} (l(v_U^i) + l(v_D^j)) \leqslant \sum_{v \in \mathcal{V}} l(v). \tag{8.20}$$

Since matching $\mathcal{M}$ belongs to the set $\mathcal{E}_l$ and covers all vertices in $\mathcal{V}$, we obtain the relationship

$$\begin{aligned} \sum_{e_{i,j} \in \mathcal{M}} W_{i,j} &= \sum_{e_{i,j} \in \mathcal{M}} [l(v_U^i) + l(v_D^j)] \\ &= \sum_{v \in \mathcal{V}} l(v) \geqslant \sum_{e_{i,j} \in \mathcal{M}'} W_{i,j}. \end{aligned} \tag{8.21}$$

Since the selection of matching $\mathcal{M}'$ is arbitrary, we have proved that matching $\mathcal{M}$ of graph $G = (\mathcal{V}, \mathcal{E}_l)$ maximizes the sum weight if matching $\mathcal{M}$ covers all vertices in set $\mathcal{V}$. □

Hence, if the initial matching $\mathcal{M}$ covers all vertices in $\mathcal{V}$, the sum weight is maximized and the algorithm can stop. Otherwise, methods that can cover more vertices in $\mathcal{V}$ need to be employed.

LEMMA 3. *For set $\mathcal{S} \subseteq U$, its neighbor set $N_l(\mathcal{S})$ is defined as $N_l(\mathcal{S}) = \{v_D^j \in D | v_U^i \in \mathcal{S}, (v_U^i, v_D^j) \in \mathcal{E}_l\}$. If set $N_l(\mathcal{S}) \neq D$, more vertices in $\mathcal{V} = U \cup D$ can be covered by $\mathcal{E}_l$ through adjusting the vertex labeling.*

Proof. Set number $\beta_{\min}$ as

$$\beta_{\min} = \min_{v_U^i \in \mathcal{S}, v_D^j \notin N_l(\mathcal{S})} \{l(v_U^i) + l(v_D^j) - W_{i,j}\}. \tag{8.22}$$

Then the labeling of a vertex in $\mathcal{S}$ and $N_l(\mathcal{S})$ is adjusted according to the following rule:

$$\begin{cases} l'(v_U^i) = l(v_U^i) - \beta_{\min}, & v_U^i \in \mathcal{S}, \\ l'(v_D^j) = l(v_D^j) + \beta_{\min}, & v_D^j \in N_l(\mathcal{S}). \end{cases} \tag{8.23}$$

It is easy to verify that the new vertex labeling l' is still feasible after the adjustment. Besides, more vertices may be covered by $\mathcal{E}_l$ since

(i) if edge $(v_U^i, v_D^j) \in \mathcal{E}_l$ initially, edge (v_U^i, v_D^j) is still in edge set $\mathcal{E}_l$ after the adjustment; and

(ii) if edge $(v_U^i, v_D^j) \notin \mathcal{E}_l, v_U^i \in \mathcal{S}, v_D^j \notin N_l(\mathcal{S})$ initially, it may be added to set $\mathcal{E}_l$ after the adjustment since $l'(v_U^i) + l'(v_D^j)$ declines.

Hence, matching $\mathcal{E}_l$ may cover more vertices in graph G and the sum weight $\sum_{e_{i,j} \in \mathcal{E}_l} w_{i,j} = \sum_{e_{i,j} \in \mathcal{E}_l} [l(v_U^i) + l(v_D^j)]$ increases. □

According to the above lemma, the second step begins with the iteration of an uncovered vertex $u_i \in U$. We define set $\mathcal{S}$ as $\{u_i\}$ and set the initial state of set $\mathcal{T}$ as $\varnothing$. If $N_l(\mathcal{S}) \neq \mathcal{T}$, we skip the third step and take the fourth step directly. Otherwise, we continue with the third step to cover more vertices.

The third step is mainly used to adjust the vertex labeling using the rule (8.23) in this step. After the adjustment, some new edges may be added to the set $N_l(\mathcal{S})$, and that leads to $N_l(\mathcal{S}) \neq \mathcal{T}$. Then the next step is to be taken.

The fourth step begins as long as $N_l(\mathcal{S}) \neq \mathcal{T}$. If $N_l(\mathcal{S}) \neq \mathcal{T}$, we can find a vertex $d_j \in N_l(\mathcal{S}) - \mathcal{T}$. If vertex d_j is matched by another vertex z, replace set $\mathcal{S}$ and set $\mathcal{T}$ by $\mathcal{S} \cup \{z\}$ and $\mathcal{T} \cup \{d_j\}$, respectively. Since more vertices are added to set $\mathcal{S}$ and set $\mathcal{T}$, take the third step again to adjust the vertex labeling to add more edges to $\mathcal{E}_l$. If vertex d_j is unmatched, it is proved that

we can find an augmenting path $\mathcal{P} = (u_i, \ldots, d_j)$. Then, replace the matching $\mathcal{M}$ by $\mathcal{M}' = \mathcal{M} \cup \mathcal{P} - \mathcal{M} \cap \mathcal{P}$. In this way, vertex d_j is covered by the new matching $\mathcal{M}'$, leading to an increase of the sum weight. After that, restart the second step and match more uncovered vertices in $\mathcal{V}$.

Complexity analysis

If we use the enumeration method to find the maximal sum weight, the computational complexity of the algorithm $\mathcal{C}_{\text{enum}}$ can be written as follows:

$$\mathcal{C}_{\text{enum}} = \mathcal{O}((\max\{M, N\})!). \tag{8.24}$$

In the proposed algorithm, the computational complexity reduces to polynomial time. Since the computational complexity of finding an augmenting path is $\mathcal{O}(N)$, the computational complexity of changing the top index of vertices in the augmenting path is $\mathcal{O}(M)$, and the computational complexity of adjusting the feasible vertex labeling is $\mathcal{O}(M)$, the total computational complexity of the algorithm $\mathcal{C}_{\text{prop}}$ is

$$\mathcal{C}_{\text{prop}} = \mathcal{O}(NM^2). \tag{8.25}$$

Therefore, Algorithm 11 can solve the problem in polynomial time.

Algorithm 11 Distributed merge-and-split coalition formation algorithm

Stage I: Initial state

Calculate the weight $W_{i,j}$ between each two CUs and each D2D user pair. Construct the bipartite graph $G = (\mathcal{V}, \mathcal{E})$ using the above information and initialize the feasible vertex labeling as $l(v_U^i) = \max W_{i,j}, v_U^i \in U,\ l(v_D^j) = 0, v_D^j \in D$.

Stage II: Sharing scheme

$*$ **initialize** Construct the first matching $\mathcal{M}$ in equality graph $G = (\mathcal{V}, \mathcal{E}_l)$.

$*$ **repeat**

(i) Find an uncovered vertex $u_i \in U$. Set the initial states of set $\mathcal{S}$ and set $\mathcal{T}$ as $\mathcal{S} = \{u_i\}$ and $\mathcal{T} = \varnothing$, respectively. Set $N_l(\mathcal{S})$ is defined as $N_l(\mathcal{S}) = \{v_D^j \in D | v_U^i \in \mathcal{S}, (v_U^i, v_D^j) \in \mathcal{E}_l\}$.

(ii) If $N_l(\mathcal{S}) = \mathcal{T}$, adjust the vertex labeling in the following way:

$$\beta_{\min} = \min_{v_U^i \in \mathcal{S}, v_D^j \notin N_l(\mathcal{S})} \{l(v_U^i) + l(v_D^j) - W_{i,j}\}$$

$$\text{s.t.} \begin{cases} l'(v_U^i) = l(v_U^i) - \beta_{\min},\ v_U^i \in \mathcal{S}, \\ l'(v_D^j) = l(v_D^j) + \beta_{\min},\ v_D^j \in N_l(\mathcal{S}). \end{cases}$$

(iii) If $N_l(\mathcal{S}) \neq \mathcal{T}$, find a vertex $d_j \in N_l(\mathcal{S}) - \mathcal{T}$.

(a) If vertex d_j is unmatched, find an augmenting path $\mathcal{P} = (u_i, \ldots, d_j)$. Replace the matching $\mathcal{M}$ by the new matching $\mathcal{M}' = \mathcal{M} \cup \mathcal{P} - \mathcal{M} \cap \mathcal{P}$. Then go to step (i).

(b) If vertex d_j is matched to another vertex z, replace set $\mathcal{S}$ by $\mathcal{S} \cup \{z\}$ and set $\mathcal{T}$ by $\mathcal{T} \cup \{d_j\}$. Then go to step (ii) to adjust the vertex labeling.

$*$ **until** Each of the vertices in set U is covered by matching $\mathcal{M}$.

Stage III: Secure transmission

After all of the CUs have chosen their cooperation D2D user pair partner, they share the channel and transmit their own information in a cellular mode.

8.2.3 *Simulation results*

We model the cellular network as a 1000 m × 1000 m square region. The distance between the base station and the eavesdropper is set as 50 m. Cellular users and D2D pairs are uniformly scattered in the square region. The maximal distance between the D2D transmitter and its corresponding receiver is set as 20 m. We consider only the path loss without small scaling fading. The transmit power of CUs and D2D transmitter is set as 10 dBm. The noise power is –70 dBm and the propagation loss factor is set as 3. The scaling factor γ which is associated with the decoding method is set as 1, which means that one user cannot decode the other user's signals and treat them the same as interference. All these parameters are listed in Table 8.1.

Table 8.1. Simulation parameters

Parameter	**Value**
Length of square side	1000 m
Distance between base station and eavesdropper	50 m
Maximum D2D pair separation	20 m
Transmit power of cellular user P_C	10 dBm
Transmit power of D2D pair P_D	10 dBm
Noise power	-70 dBm
Propagation loss factor	3
Decoding factor γ	1

In Figure 8.3, we study the relationship between the system's secrecy capacity and the number of CUs. In this scenario, the number of D2D pairs is fixed as 30. When no D2D pair is allowed to access the spectrum, the system's secrecy capacity linearly increases with increasing number of CUs. This is because the increasing number of CUs means that there are more channels and hence leads to an increase in the system's secrecy capacity. The system's secrecy capacity also increases when D2D underlay communications are introduced into the network. In the random scheme, the D2D pairs access the channel randomly. In the greedy scheme, the D2D pairs join the cellular network sequentially and make their decisions on the

basis of the current state. In the proposed scheme, the D2D pairs join the spectrum on the basis of the result of the proposed algorithm. The curves show that the system's secrecy capacity achieves the highest gains when our proposed algorithm is adopted. This fact verifies the efficiency of the proposed algorithm. Besides, we find that the trend of increase in the system's secrecy capacity becomes slow once the number of CUs exceeds the number of D2D pairs. This is because some CUs cannot receive any help from D2D pairs to improve the system's secrecy capacity when the number of CUs exceeds that of D2D pairs. Hence, it leads to a slower increase of the secrecy capacity.

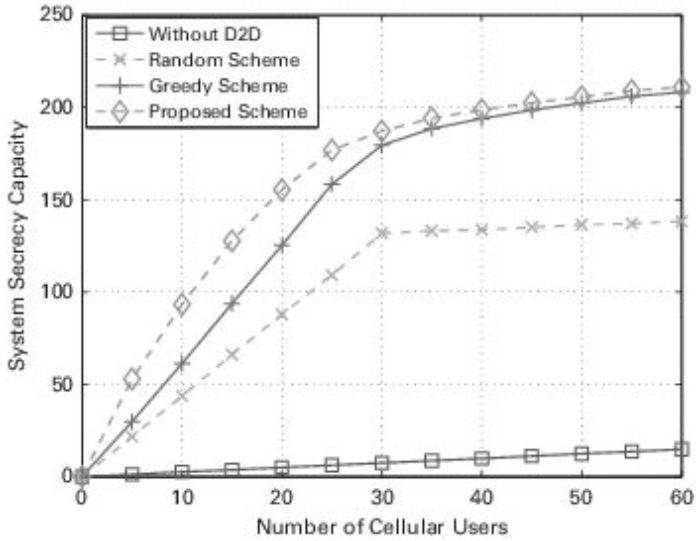

Figure 8.3. The system's secrecy capacity, with N cellular users (for $M = 30$ D2D pairs).

In Figure 8.4, we study the relationship between the system's secrecy capacity and the number of D2D pairs in the network. In this scenario, the number of CUs in the cellular network is fixed as 30. The curve in Figure 8.4 shows that the system's secrecy capacity increases with increasing number of D2D pairs. Define a function $f(n, m)$ to denote the average sum weight when there are n D2D user pairs and m CUs in the network such that

$$f(n,m) = \lim_{N\to\infty} \frac{1}{N} \sum_{i=1}^{N} |\mathcal{M}(\vec{X}, \vec{Y})|, \tag{8.26}$$

where $\mathcal{M}(\vec{X}, \vec{Y})$ denotes the matching of the weighted bipartite graph that can maximize the system's secrecy capacity, $\vec{X} = (\vec{x}_1, \vec{x}_2, \ldots, \vec{x}_n)$ denotes the positions of D2D user pairs in the network, and $\vec{Y} = (\vec{y}_1, \vec{y}_2, \ldots, \vec{y}_m)$ denotes the positions of CUs in the network. This fact can be interpreted by invoking the following two properties.

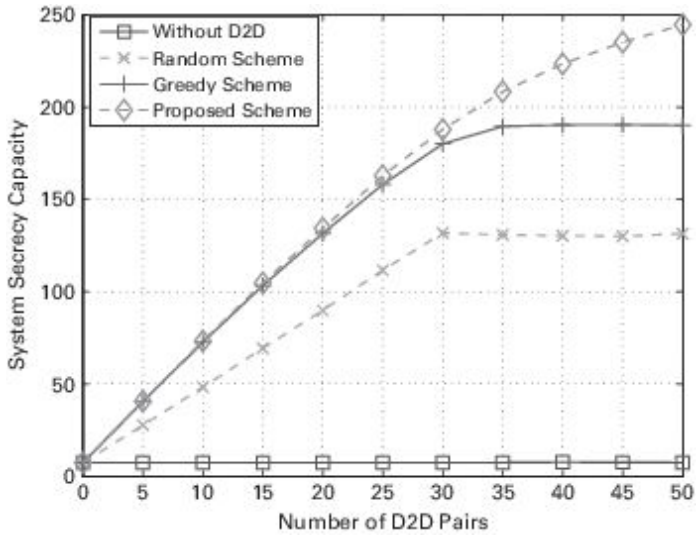

Figure 8.4. The system's secrecy capacity, with *M* D2D pairs (for $N = 30$ cellular users).

Hence, we have proved that the system's secrecy capacity can be improved when there are more potential D2D pairs in the cellular network. Besides, we notice that our proposed algorithm can reach a higher value of system secrecy capacity than that reached by the other two schemes. This result also verifies the correctness and efficiency of the proposed algorithm.

In Figure 8.5, we study the cumulative distribution function (CDF) of the system's secrecy capacity. The curves in Figure 8.5 show that the average system secrecy capacity is improved when more CUs or D2D pairs join the cellular network. This result can be interpreted in the following ways. As the number of CUs increases, there are more channels in the cellular network. Since the secrecy capacity of each channel is non-negative, the increasing number of channels means an increase of system secrecy capacity. Differently from what happens for CUs, increasing the number of D2D pairs provides a greater variety of potential matchings and can improve the

average system secrecy capacity. Besides, the curves show that increasing the number of D2D pairs has a more efficient effect on increasing the system's secrecy capacity. This fact verifies that we can increase the system's secrecy capacity efficiently by introducing D2D underlay communication into the cellular network.

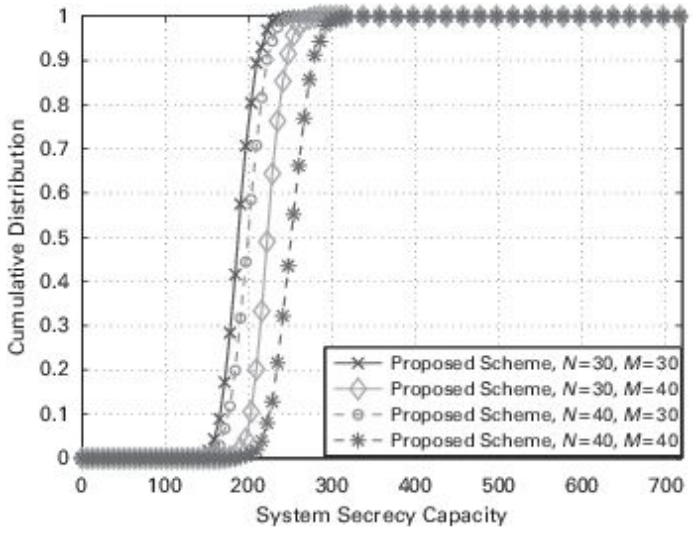

Figure 8.5. The cumulative distribution, with *M* D2D pairs, with $N = 30$ cellular users.

8.3 Chapter summary

We have studied the potential security problems in two phases of D2D communication: neighbor discovery and data transmission. For neighbor discovery, we have investigated the location security by providing an overview of the problem and a literature survey. For the data transmission, to enhance the security, we have used physical-layer security as an alternative to ensure secure transmission. By formulating the radio-resource allocation as a matching problem in a weighted bipartite graph, we introduced the *Kuhn–Munkres* (KM) algorithm to obtain the optimal solution, which can be solved in polynomial time. Simulation results indicate that the system's secrecy capacity increases with the number of CUs and D2D pairs in the cellular network. In particular increasing the number of D2D pairs can improve the system's secrecy capacity more efficiently than can increasing the number of CUs. The proposed graph-based algorithm can provide better

performance than can be obtained with the random and greedy spectrum-sharing ones.

Many other directions can be studied further. For example, for a D2D LAN, denial-of-service (DoS) attacks have to be prevented. User identity is also important for security in D2D networks, so there is a need for a novel method to generate and verify user identity.

---

[1] This is a common assumption made when one wants to study the secrecy capacity.

Part IV

Applications of D2D communications

9 Vehicular ad-hoc networks

9.1 Introduction

Vehicular networks play an important role in data communications and networking to support intelligent-transportation-system (ITS) applications. The many ITS applications related to vehicles, road traffic, drivers, passengers, and pedestrians have diverse quality-of-service (QoS) requirements, which need to be offered by the vehicular networks [280]. Vehicular networks can be based on vehicle-to-infrastructure (V2I) communications, in which the data transmission happens between a network infrastructure (e.g., a base station or a roadside unit) and vehicular nodes, i.e., on-board units (OBUs) in vehicles. Therefore, V2I communication relies on a centralized network that can be supported efficiently by cellular networks or broadband wireless access. However, V2I communication has limitations in some ITS applications. The transmission latency in V2I communication can be considerable due to relaying through the roadside unit. By contrast, vehicular networks can be based on vehicle-to-vehicle (V2V) communication, in which the data can be transmitted from one vehicular node to another node directly, reducing latency significantly. Therefore, V2V communication is suitable for many real-time ITS applications (e.g., vehicle collision avoidance). V2V communication is inherently D2D communication in which the vehicular node can establish local direct transmission without the help of any network infrastructure (i.e., roadside units). D2D communication in vehicular networks has some unique features, making it different from other typical D2D communication scenarios.

- *High-speed mobility:* In vehicular networks, the network nodes are basically vehicles. Therefore, the mobility of vehicular nodes has a unique feature. Firstly, the nodes generally move relatively fast (e.g., 100 km/h on a highway or 30 km/h in an urban area). Secondly, the nodes move along a road structure (e.g., there is straight-line motion on a highway, but drivers are able to turn at an intersection). As a result, the topology of vehicular networks can change quickly. This makes wireless data transmission and routing challenging due to there being only an intermittent connection.
- *Energy constraint:* A wireless transceiver (i.e., an OBU) of a vehicular node has an abundant energy supply from a gas combustion engine or from a large battery array, in gasoline-powered cars and electric cars, respectively. This is different from most mobile devices and sensors, which operate solely by means of a small-sized battery.
- *High computational power:* Similarly to the case of the energy supply, the OBU can be based on a small-scale or full-scale computer, providing sufficient computational power and memory space for running different algorithms, including packet routing and radio-resource management.
- *Absolute positioning capability:* Most vehicles nowadays are equipped with positioning devices, e.g., a global positioning system (GPS). Therefore, the absolute geographical location of a vehicular node can be available with a certain accuracy. This information can be used in data transmission and routing effectively. The availability of the location information also introduces a new type of data transmission, i.e., geocast. In geocast, data is transmitted to vehicular nodes in a particular geographical area.

Owing to these differences, many of the D2D communication issues in vehicular networks have to be addressed differently.

In this chapter, we focus on D2D communication for vehicular ad-hoc networks (VANETs), which use V2V communications. Starting with a review of the applications, network architecture, and protocol issues for vehicular networks, we review several D2D communication issues in vehicular networks. Three specific issues are considered, namely intracluster relay transmission, BitTorrent-based information transfer, and dynamic

channel access in vehicular networks. Additionally, some research directions are outlined.

9.2 Vehicular networks

This section first presents the typical applications of an intelligent transportation system (ITS). These applications define the requirements for the vehicular networks.

9.2.1 ITS applications

ITS applications can be classified into three major types, as follows.

- *Road safety:* The main aim of road-safety applications is to reduce the number of road accidents, damage to vehicles, and loss of life among drivers, passengers, and pedestrians due to vehicle collisions. Therefore, vehicular networks are required to transfer information and assistance to drivers in order to help them to avoid collisions. In this application, information about the position and speed of vehicles and environments can be exchanged among vehicles and infrastructure, giving necessary assistance and warnings (e.g., in the case of speeding vehicles and a nearby pedestrian). Some road-safety applications are intersection collision warning, lane-change assistance, and warnings regarding overtaking vehicles, head-on collisions, and rear-end collisions.
- *Traffic management:* The objective of road-traffic-management applications is to increase the transportation efficiency. The vehicle traffic flow, traffic coordination, and traffic assistance will be improved by providing drivers with complete information about road, map, and traffic conditions. Two major approaches of road-traffic-management applications are speed management and cooperative navigation. In speed management, the driver will be assisted to use the optimal speed in order to avoid stopping needlessly. In cooperative navigation, the driver will be provided with navigation information, leading to better routing.

- *Infotainment:* The infotainment applications aim to provide a better journey experience for drivers and passengers. Accessing the Internet is one of the infotainment applications, since many multimedia applications can run over it. Additionally, interest notification, local electronic commerce, and media downloading are typical infotainment applications.

Different ITS applications post different requirements on the vehicular networks. The authors of [281] provide comprehensive detail of different requirements that are necessary in order to support ITS applications. The requirements related to wireless transmission are as follows [281].

- *Radio communication capability:* This is related to the single-hop radio-transmission range, radio-frequency channels, available bandwidth, and bit rate. The reliability of radio and signal propagation is also included in this type of requirement.
- *Network communication capability:* This is related to unicast, broadcast, multicast, and geocast data transfer, data aggregation, congestion control, data scheduling, medium-access control, IP addressing, mobility management, and quality of service (QoS).
- *Vehicle communication security capability:* This is related to the privacy, anonymity, integrity and confidentiality of data. Immunity to security attacks, authenticity of received data, and system reliability are also included in this type of requirement.

In addition to the above requirements, the system performance requirements are also important. For example, most road-safety applications require the maximum latency for data transmission to be less than 100 ms. Additionally, some applications require periodic message broadcasting (e.g., intersection collision warnings), while some applications require event- and state-dependent broadcast or unicast transmission. The transmission range should be between 300 and 20 000 meters, depending on the application.

9.2.2 Vehicular network architecture and IEEE 802.11p

Vehicular network architecture can be divided into two major types, i.e., vehicle-to-infrastructure (V2I)[1] and vehicle-to-vehicle (V2V) communication architecture. The latter can also be referred to as a VANET, in which vehicular nodes form clusters and perform their data transmission without help from infrastructure. The data transfer in VANETs could be single-hop or multihop, depending on the application and scenario. The vehicular network could be a hybrid of V2I and V2V. In this case, vehicular nodes can communicate directly with each other to transfer data. However, in some cases, the data can be transferred with an infrastructure. Again, in this hybrid architecture, the data transfer to the infrastructure can be multihop, where some vehicular nodes act as relays. Figure 9.1 shows a typical architecture of vehicular networks.

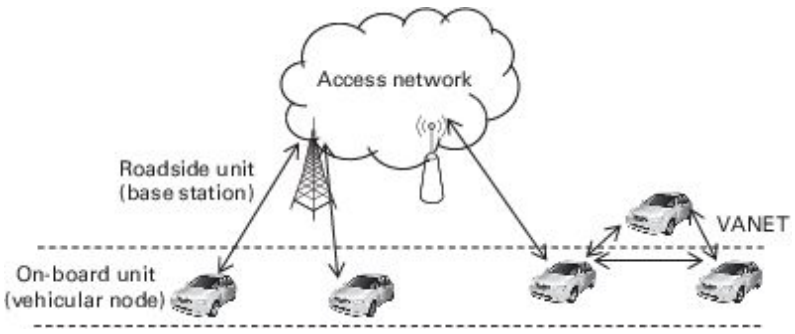

Figure 9.1. The typical architecture of a vehicular network.

Wireless communication in vehicular networks can use different parts of the frequency spectrum. In the USA, the major frequency spectrum allocated for dedicated short-range communications (DSRC) is 5.85–5.925 GHz with a bandwidth of 75 MHz. Additionally, there is the spectrum at 902–928 MHz for general ITS services (e.g., automated toll collection). However, in other regions, the frequency allocation could be different. For example, in Japan the spectrum 5.77–5.85 GHz is used for ITS applications, while in the EU the spectrum 5.875–5.905 GHz is allocated. The ITU Radiocommunication Sector (ITU-R) has allocated the spectrum in the 5.725–5.875 GHz band for ITS applications. To access the frequency spectrum 5.85–5.925 GHz, IEEE Task Group p has developed IEEE 802.11p as an extension of IEEE 802.11 for a vehicular environment, i.e., wireless access in vehicular environments

(WAVE). The protocol aims to support various ITS applications. Then, IEEE working group 1690 has introduced more detail of the protocol suit.

- *IEEE 802.11p* provides the details in the physical and MAC layers. IEEE 802.11p defines the physical-layer management entity (PLME) and the MAC-layer management entity (MLME) for physical-layer and MAC-layer management, respectively.
- *IEEE 802.2* defines the specification of the logical link control (LLC).
- *IEEE 1609.1* describes services and interfaces for an application to let an OBU interact with other components.
- *IEEE 1609.2* defines the security concept for WAVE and also secure message formats and their processing for message exchange.
- *IEEE 1609.3* provides routing and addressing services. These services are required at a network layer. The WAVE short-message protocol (WSMP) is defined as part of this service to support routing and group addressing for traffic-safety and traffic-efficiency applications.
- *IEEE 1609.4* specifies a multichannel operation.

Figure 9.2 shows the protocol structure of IEEE 802.11p. In the EU, IEEE 802.11p has been adopted as a basis for the ITS-G5 standard. This standard supports the GeoNetworking protocol for V2V and V2I communications.

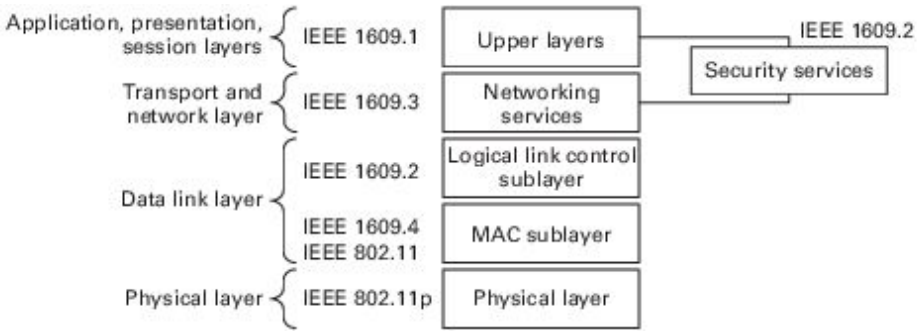

Figure 9.2. The protocol structure of IEEE 802.11p.

The physical layer of IEEE 802.11p is similar to that of IEEE 802.11a, which operates in the 5.9-GHz spectrum band. The transmission is based on orthogonal frequency-division multiplexing (OFDM). There are 64 subcarriers, where 52 inner subcarriers are used. Of the 52 subcarriers, 48 of

them are used for data transmission, while 4 of them are used to transmit a fixed pattern for mitigating frequency and phase offsets at the receiver side. These four subcarriers are called pilot subcarriers. For data transmission, the modulation could be BPSK, QPSK, 16QAM, or 64QAM, where the symbol duration is 3 μs and the guard interval time is 1.6 μs. Each channel of IEEE 802.11p has a bandwidth of 10 MHz. There is enough guard interval to avoid inter-symbol interference (ISI) being caused by the multipath channel during the transmission. As a result, IEEE 802.11p is suitable for the high-speed mobility of vehicular networks.

A channel in IEEE 802.11p can be either a control channel (CCH) or a service channel (SCH). The control channel is reserved for safety applications, while the service channel can be used for safety and non-safety (e.g., infotainment) applications. IEEE 802.11p adopts the IEEE 802.11a protocol for a vehicular environment. Two types of messages are adopted in IEEE 802.11p, i.e., a central access message (CAM) and a decentralized environmental notification message (DENM). The CAM is sent periodically and contains information about the vehicle's mobility, including its speed, position, and direction. By contrast, the DENM is sent on an event-driven basis and contains application-specific information (e.g., an emergency warning). Both CAMs and DENMs received from other nodes are used to update the local dynamic map (LDM) database.

IEEE 802.11p has a physical-layer convergence protocol (PLCP) defining a frame format. In this case, the protocol converts the data to be sent in a PLCP service data unit (PSDU) into a PLCP protocol data unit (PPDU), where the preamble and header are added.

- The preamble is composed of 12 training symbols. Ten symbols are short, and are used for establishing automatic gain control (AGC), diversity selection, and the coarse frequency-offset estimate of the carrier signal. The purpose of AGC is to set the signal gain to a level that is suitable for the received signal power. This control is required in order to ensure that the signal arriving at the receiver always has the same power level. The other two long training symbols are used for channel and fine frequency-offset estimation, which will take up to 16 ms to train a receiver after the receiver detects a signal on a channel.

- The header has a SIGNAL field of a PPDU frame. A transmitter always transmits the header with BPSK modulation at 6 Mbps. The header is composed of information about the data rate and type of modulation used. This is in a RATE field. The LENGTH field contains the length in octets of the PSDU. The parity field contains a parity bit calculated from the first 17 bits. The tail field contains all-zero bits.

The header is followed by a DATA field, which is composed of a service field, PSDU, tail field and pad bits field. For the service field, its first seven bits are zeros and used to synchronize the descrambler of the receiver. Its next nine bits are reserved for future use and currently are set as zeros. The PSDU is appended with the tail field and pad bits field. They contain the number of bits that makes a DATA field a multiple of the number of coded bits in an OFDM symbol. The number of coded bits could be 48, 96, 192, and 288.

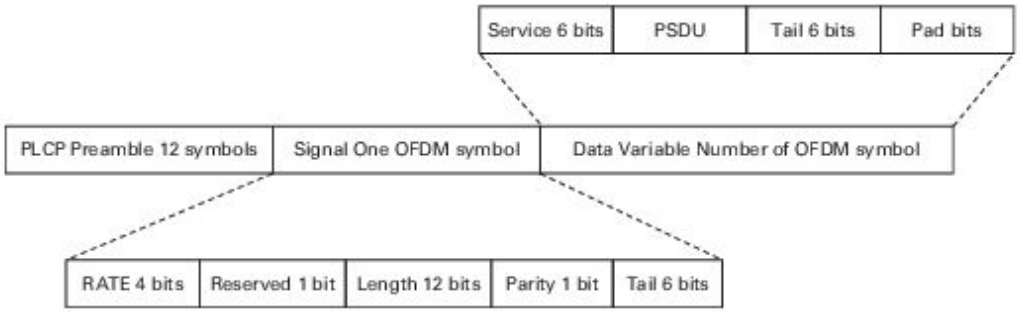

Figure 9.3. The IEEE 802.11p frame format.

The MAC layer of IEEE 802.11p is the same as that of IEEE 802.11a, where enhanced distributed channel access (EDCA) is adopted. EDCA is able to support quality of service (QoS) in IEEE 802.11 networks. The data service supports MAC service-data-unit (MSDU) exchange through the physical-layer protocol for the components in the logical link control (LLC) MAC sublayer. The exchange of MSDU is done asynchronously on a connectionless basis. The MSDU transmission can also be broadcast and multicast. Although the MSDU exchange is based on a best-effort fashion, there is a traffic identifier (TID) that can be used to support QoS services for each MSDU. IEEE 802.11p supports three architectures as in 802.11a, i.e.,

the point coordination function (PCF), hybrid coordination function (HCF), and distributed coordination function (DCF). The DCF is based on CSMA/CA, while the PCF is based on a polling mechanism. The HCF is provided to support QoS services by combining the DCF and PCF together with some special enhancement features. The HCF is composed of the HCF contention-based channel access (i.e., EDCA) and the HCF controlled channel access (HCCA) for contention-based and contention-free accesses, respectively. In HCCA, similarly to what happens with the PCF, there is a QoS-aware centralized controller, i.e., a hybrid coordinator (HC), to manage the network transmission and to support QoS services.

EDCA is a contention-based form of channel access that supports traffic differentiation and prioritization. There are four access categories (ACs) in the EDCA mechanism, each of which has a separate queue for traffic differentiation. Figure 9.4 shows the mechanism for traffic differentiation and prioritization of EDCA. Each queue of an access category works as an independent DCF station with an enhanced distributed channel access function (EDCAF). These access categories contend for transmission opportunity (TXOP) using their own EDCA parameters. As in IEEE 802.11 DCF, interframe space (IFS) is used to reduce collision by including short interframe spacing (SIFS), PCF IFS (PIFS), and DCF IFS (DIFS). In EDCA, the new IFS (i.e., AIFS) is used for transmission prioritization. The duration of AIFS depends on the access category, where the access category with the smallest duration of AIFS has the highest priority for transmission. Additionally, the different smallest and largest sizes of contention windows (i.e., CW_{min} and CW_{max}) are assigned to different access categories. Again, with smaller contention window size, the access category has higher priority to access the channel due to there being a relatively shorter waiting time. The default values of CW_{min} and CW_{max} in the IEEE 802.11p standard are 15 and 1023, respectively.

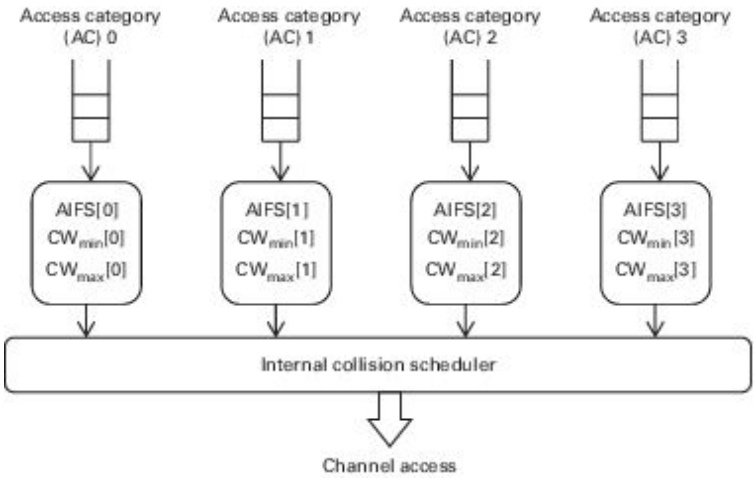

Figure 9.4. The traffic differentiation and prioritization of IEEE 802.11p EDCA.

The channel access of EDCA works as follows (Figure 9.5). If the queue of access category *i* has a packet waiting, it first checks whether the channel is idle or not. If the channel is idle, then it waits for AIFS[*i*]. Next, the backoff timer for the EDCAF will be checked. If the backoff timer is not zero, it will decrease by one. If the timer is zero, the DECAF will try to initiate a data-transmission sequence. Notably, it is possible that two or more queues of different access categories in the same station initiate the data-transmission sequences at the same time. In this case, the internal collision scheduler will resolve this virtual (internal) collision by allowing the access category with the highest priority to gain a transmission opportunity and initiate the transmission sequence. The other, lower-priority, access categories will apply the backoff mechanism again. If there is more than one station transmitting data on a channel, an external collision occurs. Similarly to what happens with a virtual internal collision, the backoff mechanism will be re-executed. Since there is no prioritization among collided stations, they have the same priority to initiate the transmission sequences again, depending on their access category. Note that the difference between virtual (internal) collision and external collision is that the retry bit in the MAC header will not be set for the lower-priority access categories in the case of a virtual internal collision.

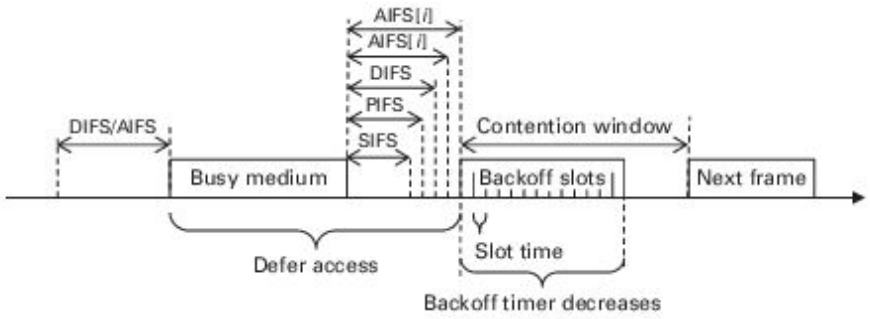

Figure 9.5. The backoff mechanism of IEEE 802.11p.

There have been studies related to performance analysis and improvement of IEEE 802.11p. For example, the authors of [282] proposed an analytical model of IEEE 802.11p for a network with devices operated on a single channel. The Markov-chain model was developed for the backoff mechanism, which is able to analyze the throughput metric and collision effects. Additionally, quite a few authors have performed experiments on 802.11p protocols [283, 284, 285, 286, 287, 288, 289]. The authors of [290] proposed a vehicular IP-in-WAVE (VIP-WAVE) framework to support an IP transport-layer protocol on the IEEE 802.11p protocol. The framework provides an IP configuration for extended and non-extended IP services, and also a mobility-management scheme supported by proxy mobile IPv6 over WAVE.

9.2.3 VANETs

VANETs are basically mobile ad-hoc networks (MONETs) whose nodes are vehicles (i.e., vehicular nodes). VANETs can support various V2V-based ITS applications such as cooperative collision warning (e.g., avoiding rear-end collision) and traffic-light optimal control, and video conferencing among passengers. In VANETs, there is no communication coordinator, and hence the protocols to support VANETs must be based on decentralized communication. Figure 9.6 shows the components of typical vehicular networks. In this case, the VANETs can be integrated with V2I communications, and the information connector provides a convergence function among networks.

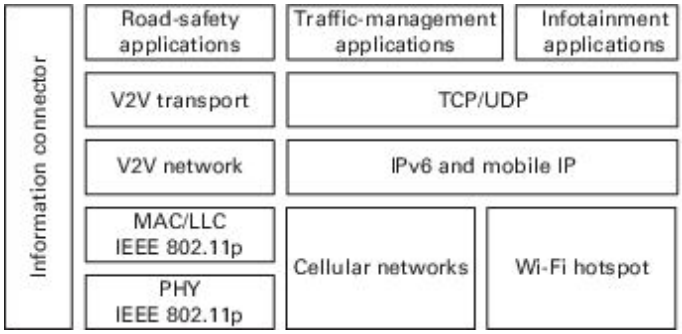

Figure 9.6. The vehicle-to-vehicle (V2V) communication protocol.

In VANETs, data communication can be divided into three different domains.

- *Intra-vehicle domain:* The data communication can be among nodes (e.g., sensors, actuators, processors, an OBU) inside a vehicle. These nodes are installed and used for different applications (e.g., engine monitoring and collision-detection sensors). The data communication in the intra-vehicle domain can be based on short-range wireless transmission (e.g., ultra-wideband) or wired communication. In the vehicle, there are application units, which provide the capability to run particular applications (e.g., collision warning). The application unit collects and processes data from sensors. This data can be transmitted to the actuator for performing certain actions. Alternatively, if the data has to be transmitted to external entities (e.g., other vehicles), the data will be first transferred to the OBU. Then, the OBU will forward that data to the destination through inter-vehicle ad-hoc communication.
- *Inter-vehicle ad-hoc domain:* This is referred to as data communication between vehicles, i.e., between OBUs. The communication can be a single hop or multihop. The transmission can be unicast, where one vehicular node transmits data to a particular vehicular node (e.g., an overtaking-warning message). The transmission can be multicast, where one vehicular node transmits data to a group of vehicular nodes (e.g., cooperative navigation). The transmission can be broadcast, where one vehicular node transmits data to all vehicular nodes (e.g., a collision-warning message).

- *Infrastructure domain:* VANETs can communicate with a roadside unit to extend the data transfer and facilitate ITS applications (e.g., traffic-light control). Internet access is a typical type of data transfer in the infrastructure domain. In this domain, a vehicular node can transmit data to the roadside unit using different available wireless technologies including cellular networks or Wi-Fi hotspots. While a cellular connection supports high-speed vehicles, Wi-Fi offers a higher data-transfer rate for relatively slow moving vehicles and parked vehicles.

Routing and data transmission is the major function of vehicular networks. In VANETs, the routing and data transmission has different challenges from those in other wireless systems.

- *Shadowing effect:* In VANETs, the communication between two vehicular nodes could be affected by obstacles (e.g., other cars and trucks, or buildings along roads). The signal transmitted from the vehicular node could be severely attenuated. Additionally, the signal quality can fluctuate abruptly due to the high speed of vehicles.
- *Limited radio resource:* Although a dedicated spectrum is allocated to VANETs (e.g., IEEE 802.11p), its size is small compared with demand. In an urban environment, hundreds of cars may communicate with each other in a hotspot area, hence making the 75 MHz bandwidth of 5.9 GHz for WAVE easily congested. The contention to access available spectrum will result in performance degradation, including a high collision rate and long latency.
- *Random connectivity:* Owing to the high speed and unpredictable mobility of vehicles, the topology of VANETs can change quickly. Such topology changes can disconnect some part of the network. Data routing needs to be updated promptly to ensure continuity of data transfer.
- *Strict QoS requirements:* Many ITS applications have strict requirements in terms of latency and loss (e.g., collision-warning messages must be transmitted within 100 ms). Additionally, there could be multiple applications running on the same vehicular nodes or accessing the same spectrum. Traffic and service differentiation is needed in order to meet diverse QoS requirements of vehicular nodes.

- *Security and privacy:* Security and privacy of data transfer in VANETs have to be customized to ITS applications. Additionally, geographical information of vehicular nodes could be used in the security framework for VANETs in order to meet the application requirements.

Next, we discuss one of the most important issues in VANETs, i.e., routing. Routing protocols in VANETs can be classified into five major types, i.e., ad-hoc, position-based, cluster-based, broadcast, and geocast routing [291]. In the following, we discuss their details.

Ad-hoc routing

VANETs share many similar characteristics with MONETs (e.g., they have no fixed infrastructure support and there is self-organization). Therefore, some ad-hoc routing protocols in MONETs can be used in VANETs. Some examples of such protocols designed for general-purpose MONETs are ad-hoc on-demand distance vector (AODV) [292] and dynamic source routing (DSR) [293]. The AODV and DSR protocols are forms of on-demand-based routing. The route will be determined only when there is data to be transmitted from a source to a destination. The difference is that, in AODV, routing relies on the routing table in intermediate nodes, whereas in DSR, routing is based on the information collected at the source node. Some authors have studied the use of general-purpose ad-hoc routing protocols in VANETs [294, 295]. However, they confirm that the general-purpose routing protocols for MANETs cannot perform well in VANETs. This is mostly due to the slow route convergence, which is not suitable for the fast-changing topology in VANETs. The situation becomes worse with a long route connection (i.e., more than a few hops), where the connection remains usable for only a short period of time (e.g., a few second). Consequently, it is impossible to use typical transport protocols (e.g., TCP) running on these routing protocols. Some improvements could be beneficial for the general-purpose routing protocols. For example, the authors of [296] introduced prediction-based routing protocols, in which the information about routing (e.g., a routing table) is predicted. As a result, the protocol can adapt to the fast-changing topology slightly better than can the traditional protocols which rely on the recent past information.

Position-based routing

In VANETs, the vehicular nodes' movement is directional and constrained by road structures. Therefore, routing protocols in VANETs can utilize information about the roads and streets to optimize the performance. This information includes the geographical location and mobility obtained from the street map, traffic model, and navigation system available in vehicles. One of the general position-based routing protocols is greedy perimeter stateless routing (GPSR) [297]. In the GPSR protocol, a node makes a decision of data forwarding on the basis of information about immediate neighbors in a network. The forwarding decision is based on selecting the region to reach the destination as much as possible (i.e., greedy). If the forwarding is not possible, the routing protocol will recover by considering the nodes in the nearby perimeter of the region. Since the routing maintains only the state of local topology, the protocol is highly scalable. The authors of [298] showed that GPSR performs better than the DSR protocol in a highway environment. This is because, if the location information is available, GPSR can utilize such information to forward data efficiently. However, GPSR might not perform well in an urban environment due to there being a complex road structure and many obstacles so that a greedy approach does not provide an optimal route. The authors of [299] introduced three improvements of the greedy-based protocol. The first improvement is to avoid using a location server to maintain the location information of all nodes in the network. Instead, they proposed that one should use a destination-discovery message, which can collect location information from message passing in an on-demand basis. The second improvement is to avoid flooding the route-request (RREQ) message for route finding. Instead, a unicast message is used. The third improvement avoids the path-break problem by allowing the routing protocol to opportunistically find the next hop for data forwarding from neighbor nodes only.

Cluster-based routing

In cluster-based routing, nodes must create a virtual structure by grouping nearby neighbors together as a cluster. The cluster has a cluster head to facilitate data forwarding, control-channel access (i.e., MAC protocols), and security. Structuring a network into multiple clusters improves the scalability

of routing protocols substantially since the nodes do not need to maintain global information of the whole network. By contrast, the nodes keep track of local information about their own cluster. Nodes in the same cluster can communicate with each other directly. For nodes in different clusters, the nodes will first send data to the cluster head. Then, the cluster head will forward the data to another cluster head. This is repeated until the cluster of the destination has been reached. One of the cluster-based routing protocols developed for VANETs is presented in [300]. Specifically, the protocol uses information about the location and direction of motion of vehicular nodes to optimize data forwarding among clusters in VANETs. The cluster head is responsible for receiving data from a cluster member. The cluster head decides on the data forwarding to other cluster heads according to its location, the location of the destination, and the direction of motion of the cluster.

Broadcast routing

Broadcast transmission and routing are typical in VANETs, which support many applications. The simplest form of broadcast routing is through flooding. In flooding, all nodes forward the newly received data. As a result, if the network is not disconnected, all the nodes in the network will be guaranteed to receive the data. In general, flooding is not only simple to implement, but also efficient as a means to achieve good performance in a small-sized network. However, in a large-scale network, flooding becomes a suboptimal choice and its performance drops quickly. The reason is that flooding simply forwards the data, and hence the number of data transmitted increases exponentially as the number of nodes increases, consuming a large amount of bandwidth and creating substantial contention and congestion in the network. Therefore, a protocol that performs selective data forwarding and reduces the flooding overhead is preferred (e.g., [301, 302, 303]). For example, the BROADCOMM protocol proposed in [301] considers an emergency broadcast enhancement for vehicles on a highway. The protocol divides the highway into multiple segments (i.e., clusters or cells). Some nodes located near to the center of a cluster are assigned to be cluster reflectors, which perform as cluster heads. These reflectors receive emergency messages from other nodes in the same cluster or from other clusters and forward to other nodes in the same cluster. Additionally,

reflectors can act as relays that receive emergency messages from and forward to neighboring clusters. This cluster-based broadcast transmission improves the performance and reduces overhead significantly compared with flooding.

The authors of [304] provide a comprehensive review of different information-dissemination or broadcast protocols for VANETs. The broadcast transmission can be classified into single-hop and multihop broadcast. Single-hop broadcast can be divided into two major types depending on the type of broadcast interval.

- *Fixed broadcast interval:* When a vehicular node has data to transmit, it will broadcast the data repeatedly. In fixed-broadcast-interval protocols, the data broadcast is performed periodically. The authors of [305] proposed TrafficInfo, which is one example of such a protocol. TrafficInfo has an algorithm to choose the most relevant data to be broadcast so that bandwidth is utilized efficiently.
- *Adaptive broadcast interval:* Instead of having a fixed broadcast interval, the broadcast interval can be optimized adaptively. In this case, the protocol has to consider the following tradeoff. If the broadcast interval is short, the latency is smaller, but it could increase the communication overhead, resulting in higher congestion of the network. One example of this protocol is proposed in [306], i.e., the collision-ratio control protocol (CRCP). In CRCP, a vehicular node periodically broadcasts traffic and mobility information. However, the broadcast interval is adjusted according to the number of collided packets. The CRCP aims to maintain the collision ratio at a target level. In this case, when the packet-collision ratio increases above the threshold, the interval will be doubled. Otherwise, the interval will be decreased by one second.

In multihop broadcast protocols, a vehicular node can receive data from other nodes and rebroadcast it. There are three major approaches for multihop broadcast protocols.

- *Delay-based:* When the vehicular node receives data, it can decide on the broadcast of that data on the basis of delay information. A delay-

based multihop broadcast protocol called efficient directional broadcast (EDB) is proposed in [307]. In this protocol, after a vehicular node has received data transmitted by another node, the data will be rebroadcast. To avoid exhaustive data rebroadcasting, the vehicular node receiving data will calculate a waiting time, which corresponds to the normalized transmission range minus the distance from the upstream node. The node with the largest waiting time (i.e., the one farthest from the transmitter) will be given priority to rebroadcast. The rationale behind this mechanism is that the rebroadcast should be performed by the node which waits longest. The node waiting longest is equivalent to the node which is farthest from the source. By choosing the farthest node, one can reduce the unnecessary rebroadcasting by nearby nodes.

- *Probabilistic:* In this scheme, the vehicular node receiving data from other nodes will rebroadcast the data with some assigned probability. As a result, the number of rebroadcasts reduces. However, the major challenge of this probabilistic multihop broadcast is how to obtain an optimal rebroadcast probability. In the simplest form, the rebroadcast probability can be fixed and determined by other nodes considering the network structure. By contrast, the rebroadcast probability can be adjusted adaptively on the basis of the current mobility properties of the node. One example of a probabilistic broadcast protocol is weighted p-persistence [308]. In this protocol, when a node receives data from other nodes, the node computes a rebroadcast probability that is based on the distance to the transmitter. Specifically, the node has a higher rebroadcast probability if it is farther from the transmitter.
- *Network coding-based:* The network coding aims to improve the transmission throughput by allowing a relay to forward coded data among multiple nodes. Consider Figure 9.7 as an example. Node A wants to transmit data to node B, and node B wants to transmit data to node A via a relay. Traditionally, node A must transmit the data, and the relay forwards this data to node B. Then, node B transmits the data and the relay forwards this data to node A. In total, it requires four time slots for such data transmission. However, with network coding, node A transmits data to the relay, and node B transmits data to the relay. Then, the relay combines data from nodes A and B together (e.g., using an XOR operation), and then broadcasts the coded data to nodes A and B in the same time slot. Since nodes A and B have their own transmitted

data, they can decode correctly the data from nodes B and A, respectively. With this approach, it requires only three time slots for completing data transmission between nodes A and B. One of the network coding-based broadcast protocols, i.e., CODEB, is introduced in [309].

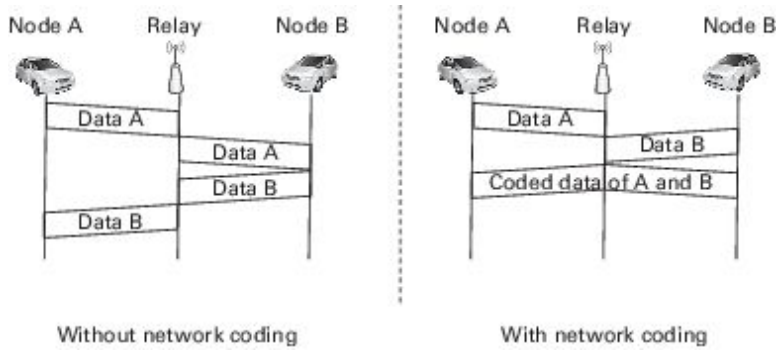

Figure 9.7. An example scenario of a network coding broadcast.

Geocast routing

Geocast routing is similar to position-based routing. The slight difference is that geocast routing aims to transmit data to the nodes in a particular geographical area. Therefore, geocast routing is similar to multicast routing rather than to unicast routing as was the case for position-based routing. Therefore, geocast routing can be implemented by extending the multicast routing to consider the locations of target nodes. There are many applications of geocast routing in VANETs. For example, when an accident happens, warning messages must be sent to incoming vehicles (i.e., those vehicles in the area which are moving in the direction towards the accident site). The concept of a zone of relevance (ZOR) [310] is typically used in geocast routing. The geocast-routing protocols aim to deliver data to the nodes in a ZOR, while nodes outside ZOR should not receive the data in order to reduce unnecessary congestion.

9.3 D2D communications in vehicular networks

In this section, we review works related to D2D communications in vehicular networks. The first work introduces the retransmission algorithm with optimal resource utilization. The second work proposes BitTorrent content distribution for VANETs. The third work presents the optimal channel access in cognitive-radio-based VANETs.

9.3.1 An intracluster device-to-device retransmission algorithm

The authors of [311] introduced an intracluster D2D retransmission algorithm. The algorithm is optimized to achieve optimal resource usage. Figure 9.8 shows the system model considered in [311]. There are nodes (e.g., vehicles) organized into clusters. The cluster formation is done by the base station (e.g., a roadside unit), which one supposes to have complete information about the channel quality to all nodes and among nodes in the same cluster. If a node wants to join an existing cluster, this node will send a request message to the base station. The base station decides which cluster this node can join. After receiving acknowledgement from the base station to join the cluster, this new coming node will evaluate the channel quality to all other nodes in the same cluster. This channel quality will be used to establish D2D transmission (i.e., relay) later. The base station transmits multicast data to each cluster. Specifically, nodes in the same cluster expect data from the base station. In this case, there could be some nodes in the cluster that cannot receive the transmitted data correctly. Nodes in the same cluster will establish D2D communication by relaying the multicast data among nodes. As a result, the base station does not need to retransmit data in, which would consume a considerable amount of radio resources. The local D2D relay transmission among the nodes reuses the same licensed spectrum as that of the base station, improving spectrum utilization. The D2D retransmission is done by retransmitters, which are the node in the same cluster (e.g., cluster A and cluster B in Figure 9.9, respectively). Figure 9.8 shows the components of the algorithm. Firstly, the number of retransmitters will be determined. Then, given the number of retransmitters, the cluster will be partitioned accordingly. Finally, in each subcluster, there could be multiple nodes that receive data successfully from the base station. Therefore, one of them will be chosen as the retransmitter.

Figure 9.8. Components of intracluster D2D retransmission.

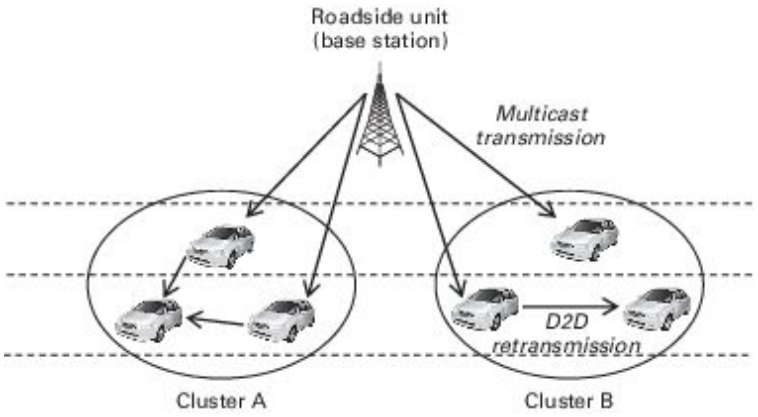

Figure 9.9. Intracluster relay transmission.

After the base station has transmitted data to a cluster, the nodes can receive or cannot receive the data successfully (the two types of nodes are called successful and unsuccessful nodes), whose sets are denoted as $\mathcal{D}_s$ and $\mathcal{D}_u$, respectively. Let $e_{i,j}$ denote the spectrum efficiency of the D2D link between nodes i and j. This spectrum efficiency depends on the channel quality between these nodes. Then, given a bandwidth of $B_{i,j}$ between these nodes assigned by the base station, the maximum transmission rate is $r_{i,j} = e_{i,j} \times B_{i,j}$. Figure 9.10 shows an example of a cluster. In this case, the sets of nodes are $\mathcal{D}_s = \{1, 2\}$ and $\mathcal{D}_u = \{3, 4\}$. The spectrum efficiency can be presented as follows:

	Node 1	Node 2
Node 3	$e_{3,1}$	$e_{3,2}$
Node 4	$e_{4,1}$	$e_{4,2}$

$$\text{where } \mathbf{E} = \begin{bmatrix} e_{3,1} & e_{3,2} \\ e_{4,1} & e_{4,2} \end{bmatrix}. \tag{9.1}$$

$\mathbf{E}$ is the matrix of spectrum efficiency between nodes that can and cannot receive data from the base station successfully.

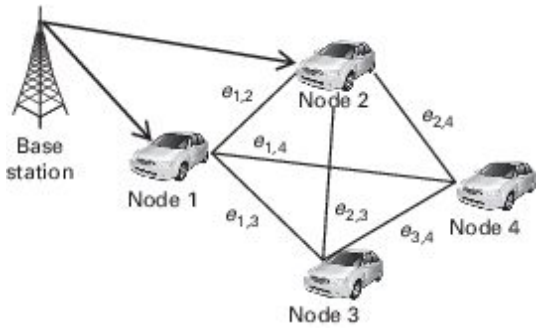

Figure 9.10. Sets of nodes that can and cannot receive data successfully from a base station.

Cost of retransmission and retransmitter selection

The cost of retransmission in the same cluster can be calculated. In this case, the cost depends on how many successful nodes will be selected to be retransmitters. The cost of retransmission is given by

$$C_1(\mathbf{E}) = \min_{j \in \mathcal{D}_s} \left(\frac{L}{\min\limits_{i \in \mathcal{D}_u} e_{i,j}} \right), \tag{9.2}$$

where L is the size of the data. The term $\min_{i \in \mathcal{D}_u} e_{i,j}$ is to identify the unsuccessful node with the worst spectrum efficiency given any retransmitter (i.e., a successful node). In other words, other unsuccessful nodes in the network will have better spectrum efficiency given the same retransmitter. Then, the term $\min_{j \in \mathcal{D}_s}$ is to find the retransmitter which yields the lowest cost (i.e., maximum resource utilization). For example, consider the following spectrum efficiency matrix:

$$\mathbf{E} = \begin{bmatrix} e_{3,1} = 1 & e_{3,2} = 2 \\ e_{4,1} = 3 & e_{4,2} = 4 \end{bmatrix}. \tag{9.3}$$

If $L = 1$, then it will cost 1/1 and 1/2 if nodes 1 and 2 are selected to be the retransmitter, respectively, where the highest cost comes from the unsuccessful node 3. Therefore, the maximum resource utilization is achieved when node 2 is chosen as the retransmitter, which yields a cost of 1/2.

Then, we can consider two retransmitters. The cost is given by

$$C_2(\mathbf{E}) = \min_{j,k\in\mathcal{D}_s, j\neq k, \mathcal{S}_j\cup\mathcal{S}_k=\mathcal{D}_u} \left(\frac{L}{\min\limits_{i\in\mathcal{S}_j} e_{i,j}} + \frac{L}{\min\limits_{i\in\mathcal{S}_k} e_{i,k}} \right). \tag{9.4}$$

In this case, the base station will allocate resource blocks (RBs in an LTE system) to the retransmitters to avoid interference. Therefore, the retransmissions can be performed simultaneously. The cost of two retransmitters for retransmission is similar to that of the single-retransmitter case. However, in this case, there are two subsets (i.e., subclusters) for the unsuccessful nodes, i.e., $\mathcal{S}_j$ and $\mathcal{S}_k$, which are associated with the retransmitters j and k, respectively. Again, the cost is the sum of the data size divided by the minimum spectrum efficiency (i.e., the worst case) of the unsuccessful nodes from these subclusters. Note, however, that a solution of the retransmission cost depends on the subclusters $\mathcal{S}_j$ and $\mathcal{S}_k$. Later, the partitioning algorithm used to achieve the optimal subcluster will be discussed.

Then, in general, the cost of retransmission with K retransmitters is given by

$$C_K(\mathbf{E}) = \min_{\substack{j_k\in\mathcal{D}_s, k=1,\ldots,K, j_1\neq\cdots\neq j_K, \\ \mathcal{S}_{j_1}\cup\cdots\cup\mathcal{S}_{j_K}=\mathcal{D}_u}} \left(\sum_{k=1}^{K} \frac{L}{\min\limits_{i\in\mathcal{S}_{j_k}} e_{i,j_k}} \right). \tag{9.5}$$

The number of retransmitters is bounded by the number of nodes receiving data from the base station successfully. However, the number of retransmitters can be less than the bound. When there are more retransmitters, the multiple retransmissions can be performed in parallel. One retransmitter has to handle fewer unsuccessful nodes, which increases the chance of having a higher transmission rate. By contrast, the cluster needs more resource blocks to perform such parallel retransmissions (i.e., the summation term from $k = 1$ to $k = K$). Therefore, it is suggested in [311] that the number of retransmitters should be also chosen optimally to minimize the cost.

Cluster partitioning

Observing the cost functions defined in (9.4) when there is more than one retransmitter in a cluster (i.e., 2 and K, respectively), we have to partition the cluster into multiple subclusters depending on the number of retransmitters. Then, each subcluster is served by a particular retransmitter. The authors of [311] introduced a cluster-partitioning algorithm to achieve the minimum cost. Since the cost is the data size divided by the spectrum efficiency, we can calculate the normalized resource cost denoted by $r = 1/e_{i,j}$. Then, the normalized resource cost vector is created by sorting the normalized resource costs into ascending order. Since two retransmitters are considered, two vectors are created as follows:

$$\vec{\mathbf{r}}_j = \begin{bmatrix} r_{1,j} & \cdots & r_{|\mathcal{D}_u|,j} \end{bmatrix}^\top, \tag{9.6}$$

$$\vec{\mathbf{r}}_k = \begin{bmatrix} r_{1,k} & \cdots & r_{|\mathcal{D}_u|,k} \end{bmatrix}^\top, \tag{9.7}$$

where $r_{1,j} \leq \cdots \leq r_{|\mathcal{D}_u|,j}$ and $r_{1,k} \leq \cdots \leq r_{|\mathcal{D}_u|,k}$. The main idea of the algorithm is that, when we consider the normalized resource costs $r_{1,j}$ and $r_{1,k}$, there will be at least one unsuccessful node in each subcluster. If there are still some unsuccessful nodes not in these subclusters, we can consider the costs $r_{2,j}$ and $r_{2,k}$, since there will be two unsuccessful nodes in each subcluster. This increment is repeated until all of the unsuccessful nodes are

in these subclusters. Therefore, the subsets of the subclusters are defined as follows:

$$\mathcal{S}_j = \left\{ i \middle| \frac{1}{e_{i,j}} \leq r_j, i \in \mathcal{S}_{\mathrm{u}} \right\}, \tag{9.8}$$

$$\mathcal{S}_k = \left\{ i \middle| \frac{1}{e_{i,k}} \leq r_k, i \in \mathcal{S}_{\mathrm{u}} \right\}, \tag{9.9}$$

where r_j and r_k are the smallest normalized resource costs associated with the retransmitters j and k, respectively. The detailed algorithm is described in [311].

Finally, the number of retransmitters K can be chosen optimally to minimize the cost as follows:

$$K^* = \arg \min_{K \in \{1,\ldots,|\mathcal{D}_{\mathrm{s}}|\}} C_K, \tag{9.10}$$

where C_K is the cost obtained from (9.5) given the cluster partitioning defined in (9.8) and (9.9).

Performance analysis

Given the retransmission algorithm, the cumulative distribution function (CDF) of the cost can be derived from the fact that the spectrum efficiency is independently random. Let $F(e)$ denote the CDF of the spectrum efficiency $e_{i,j}$. The conditional CDF of the cost c given that a single retransmitter is j is obtained from

$$
\begin{aligned}
F_1(c|j) &= P\left(\frac{L}{\min_{i\in\mathcal{D}_u}(e_{i,j})} < c\right) \\
&= \prod_{i\in\mathcal{D}_u} P(e_{i,j} > L/c) \\
&= (1 - F(L/c))^{|\mathcal{D}_u|}.
\end{aligned}
\tag{9.11}
$$

Then, the CDF of the resource cost can be obtained from

$$
\begin{aligned}
F_1(c) &= P(C_1 < c) \\
&= 1 - P\left(\min_{j\in\mathcal{D}_s}\left(\frac{L}{\min\limits_{i\in\mathcal{D}_u} e_{i,j}}\right) > c\right) \\
&= 1 - \prod_{j\in\mathcal{D}_s}(1 - F_1(c|j)) \\
&= 1 - \left(1 - (1 - F(L/c))^{|\mathcal{D}_u|}\right)^{|\mathcal{D}_s|}.
\end{aligned}
\tag{9.12}
$$

For the case with K retransmitters, the conditional CDF of the cost for the retransmitter j_k is expressed as follows:

$$
\begin{aligned}
F_K\left(c_k|j_k, \mathcal{S}_{j_k}\right) &= P\left(\frac{L}{\min\limits_{i\in\mathcal{S}_{j_k}} e_{i,j_k}} < c_k\right) \\
&= \prod_{i\in\mathcal{S}_{j_k}} P\left(e_{i,j_k} > \frac{L}{c_k}\right) \\
&= \prod_{i\in\mathcal{S}_{j_k}} \left(1 - F\left(\frac{L}{c_k}\right)\right).
\end{aligned}
\tag{9.13}
$$

Then, the CDF of resource costs for K retransmitters can be obtained from

$$\begin{aligned} F_K(c) &= P\left(C_K(\mathbf{E}) < c\right) \\ &= 1 - P\left(\min_{\substack{j_k \in \mathcal{D}_s, k=1,\ldots,K, j_1 \neq \cdots \neq j_K, \\ \mathcal{S}_{j_1} \cup \cdots \cup \mathcal{S}_{j_K} = \mathcal{D}_u}} \left(\sum_{k=1}^{K} \frac{L}{\min\limits_{i \in \mathcal{S}_{j_k}} e_{i,j_k}} \right) > c \right) \\ &= 1 - \prod_{\substack{j_k \in \mathcal{D}_s, k=1,\ldots,K, j_1 \neq \cdots \neq j_K, \\ \mathcal{S}_{j_1} \cup \cdots \cup \mathcal{S}_{j_K} = \mathcal{D}_u}} \left(1 - F_K\left(c \middle| j_1, \mathcal{S}_{j_1}, \ldots, j_K, \mathcal{S}_{j_K}\right)\right), \end{aligned} \tag{9.14}$$

where

$$F_K\left(c \middle| j_1, \mathcal{S}_{j_1}, \ldots, j_K, \mathcal{S}_{j_K}\right) = \int_{c_1 + \cdots + c_K < c} \cdots \int \prod_{k=1}^{K} dF_K\left(c_k \middle| j_k, \mathcal{S}_{j_k}\right). \tag{9.15}$$

In addition to the performance analysis, the simulation is carried out to evaluate the performance of the proposed retransmission algorithm. The evaluation focuses on the ratio between successful and unsuccessful nodes in a cluster. As expected, when the ratio is larger, there could be more retransmitters to relay data to unsuccessful nodes. As a result, the resource cost decreases.

9.3.2 BitTorrent-based wireless access in vehicular networks

One of the challenges in WAVE is due to the rapid change of the communication environment. Additionally, the duration of a connection between vehicular nodes could be very short (e.g., when vehicles are moving in opposite directions). However, there are many applications that require sizable amounts of data to be transferred within a certain period of time. To address this challenge, the authors of [312] introduced BitTorrent-based data transfer among vehicles based on the IEEE 802.11p protocol. Here

BitTorrent is used to distribute the data among vehicular nodes in a D2D fashion. For example, the road-traffic information can be transferred through BitTorrent when vehicles pass each other. To achieve a fair share of radio resources and data transfer, a bargaining framework considering different fairness criteria is established.

BitTorrent [313] is a peer-to-peer (P2P) file-sharing communication protocol. BitTorrent can support distributing large-sized data. BitTorrent can offload data transfer from data sources by allowing multiple nodes in a network to collaboratively distribute the data, reducing the cost and improving performance and redundancy. In WAVE, a roadside unit can be a data source distributing large amounts of data to vehicles. Different vehicles may receive different parts of the data. A receiver can receive these parts of the data and combine them to obtain the original data. The fairness of data transfer and resource allocation can be optimized using the concept of a bargaining game. Specifically, invoking BitTorrent and sequential bargaining, the authors of [312] proposed formulations of the vehicle-to-roadside (V2R) problem and vehicle-to-vehicle (V2V) problem. The V2R problem is that of deciding how to distribute different parts of data to the vehicles according to the traffic pattern and the average transmission time between OBUs and roadside units. The V2V problem is that of how to optimize the communication between the vehicles according to the channel variations, so that the maximal mutual benefit (i.e., the exchange of data) can be achieved.

The WAVE system model

For the channel model, the authors of [312] used the two-ray ground-reflection model [314] for large-scale fading and Rayleigh fading as a small-scale fading. The receiver signal-to-noise ratio (SNR) can be expressed as follows:

$$\Gamma = \frac{P_t G_t G_r h_t^2 h_r^2}{\sigma^2 d^4}, \tag{9.16}$$

where P_t is the transmit power, G_t is the transmitter antenna gain, G_r is the receiver antenna gain, h_t is the transmitter antenna height, h_r is the receiver antenna height, d is the distance from the transmitter to the receiver, and σ^2 is the thermal noise level.

For WAVE, the channel quality varies rapidly and one must ensure that the minimum link quality is maintained. This can be achieved with appropriate modulation and channel coding to maintain the bit error rate (BER) below some target BER threshold, which is assumed to be 10^{-5} in the system. Table 9.1 shows the required SNRs and the adopted modulation with coding rates to achieve different supported transmission rates under different BER requirements [315]. Given the target BER, there is a one-to-one mapping between the selected transmission rate and the chosen modulation scheme with coding rate when the required SNR is satisfied.

Table 9.1. The required SNR and transmission rate using adaptive modulation and coding rates [315]

Mode	Rate *R*	Modulation	Convolutional coding rate	SNR (dB) for BER $\leq 10^{-5}$
1	1	QPSK	1/2	4.09
2	1.33	QPSK	2/3	5.86
3	1.5	QPSK	3/4	6.84
4	1.75	QPSK	7/8	8.44
5	2	16QAM	1/2	10.04
6	2.66	16QAM	2/3	12.13
7	3	16QAM	3/4	13.29
8	3.5	16QAM	7/8	15.01
9	4	64QAM	2/3	17.70
10	4.5	64QAM	3/4	18.99
11	5.25	64QAM	7/8	21.06

Suppose the data source has a total of L packets to distribute. All of the packets have the same size. All vehicles want to receive all of the packets. However, different packets may have different priorities, which are pre-assigned. Specifically, for the kth and lth packets ($k, l \in \{1, 2, \ldots, L\}$) of OBU i, we have the weights $w_i(k) \geq w_i(l)$, if $k < l$. Suppose the channels are stable within a time period t_0 (i.e., quasi-static). Specifically, the channel quality remains the same within a transmission slot. The number of packets that can be transmitted within t_0 is defined as follows:

$$n \leq Rt_0/M. \tag{9.17}$$

V2V and V2R communications

The authors of [312] first formulated the V2V and V2R communications problems for an OBU and a roadside unit, respectively. Then, the bargaining algorithms for the V2V problem were discussed.

9.3.3 Problem formulation

Figure 9.11 shows the WAVE scenario under consideration. When the vehicles with OBUs pass by the roadside units which are located in places such as toll booths and gas stations, data can be transferred from the roadside unit to the OBU. However, since the communication duration for the OBUs and roadside units is usually limited, each vehicle can receive only a few packets from the total of L packets from the roadside unit. To overcome this problem, the roadside units randomly distribute the packets to the OBUs, and then let OBUs exchange information on the road.

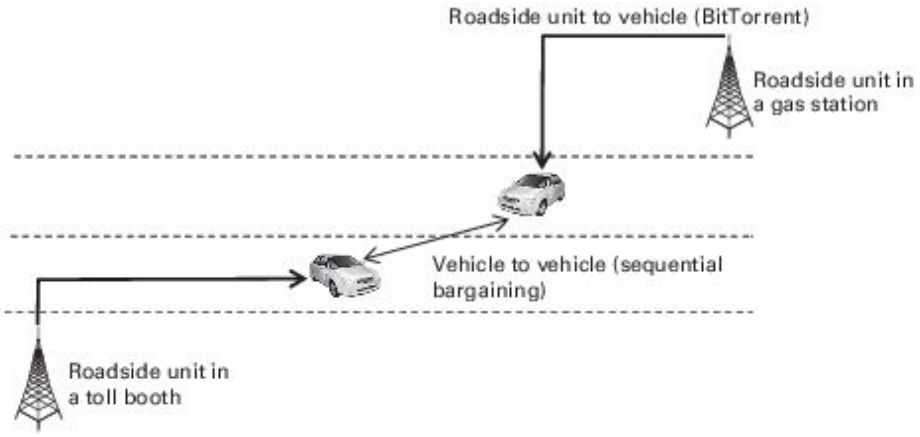

Figure 9.11. Vehicle-to-vehicle and vehicle-to-roadside communications.

For each individual vehicle, the *i*th vehicle's utility is defined as the sum of weights for the set $\mathcal{I}_i$ of packets that it currently has, i.e.,

$$U_i = \sum_{k \in \mathcal{I}_i} w_i(k). \tag{9.18}$$

This utility function corresponds to the user's satisfaction gained from an application-specific data packet. For example, the utility of a road-traffic data packet is higher than that of a data packet of an entertainment video.

For vehicle *i* and vehicle *j*, if each has some packets that the other does not have, they will exchange. In other words, the conditions for exchange are $\mathcal{I}_i \not\subset \mathcal{I}_j$ and $\mathcal{I}_j \not\subset \mathcal{I}_i$. For bargaining between two vehicles, the problem formulation is stated as follows:

$$\begin{aligned} &\max \ F(U_i, U_j), \\ &\text{s.t.} \sum_{k \notin \mathcal{I}_i, k \in \mathcal{I}_j} 1 + \sum_{l \notin \mathcal{I}_j, l \in \mathcal{I}_i} 1 \le n_{i,j}, \end{aligned} \tag{9.19}$$

where $n_{i,j}$ is the maximal number of packets that can be exchanged within the time period of t_0. $F(\cdot)$ is a function that represents the social welfare.

This social welfare indicates how the bargaining can benefit both users. The different definitions of $F(\cdot)$ which represent different criteria of fairness will be discussed later.

For roadside units, the objective is to maximize the overall utility by changing the probability distribution function (PDF) for distributing the L different packets. The optimization problem is expressed as follows:

$$\max_{\Pr(l)} \sum_{i=1}^{K} U_i$$
$$\text{s.t.} \sum_{l=1}^{L} \Pr(l) = 1, \tag{9.20}$$

where $\Pr(l)$ is the probability of packet l being sent to the OBU. The PDF is affected by the traffic pattern. For example, during a low-traffic period, it is very unlikely that a particular vehicle will meet other vehicles. In this case, it is better to send the higher priority packet first. By contrast, during a traffic jam, a more uniform distribution might be preferred, since there are plenty of opportunities for an OBU to exchange all information with other OBUs.

Bargaining between on-board units

The authors of [312] considered three fairness criteria for OBU bargaining. Then, the algorithms for data exchange and those for bargaining solutions are introduced. First, the authors of [312] studied the Nash bargaining solution (NBS) [71] for a two-player game. The definition of the NBS is given as follows. Define $\mathcal{U}$ as the feasible region, $\vec{\mathbf{u}}$ as the utility vector after users' bargaining, and $\vec{\mathbf{u}}^0$ as the utility vector before the negotiation. $\phi(\mathcal{U}, \vec{\mathbf{u}}^0)$ is the NBS which maximizes the product of utility from both players as follows:

$$\phi(\mathcal{U}, \vec{\mathbf{u}}^0) = \arg \max_{\vec{\mathbf{u}} \geq \vec{\mathbf{u}}^0, \vec{\mathbf{u}} \in \mathcal{U}} \prod_{i=1}^{2} \left(U_i - U_i^0 \right). \tag{9.21}$$

Two other bargaining solutions are considered as alternatives to the NBS, i.e., the Kalai–Smorodinsky solution (KSS) [71] and the egalitarian solution (ES). To define these solutions, the concept of restricted monotonicity can be defined and described as follows. If $\mathcal{V} \subset \mathcal{U}$ and $H(\mathcal{U}, \vec{\mathbf{u}}^0) = H(\mathcal{V}, \vec{\mathbf{u}}^0)$ then $\phi(\mathcal{U}, \vec{\mathbf{u}}^0) \geq \phi(\mathcal{V}, \vec{\mathbf{u}}^0)$, where $H(\mathcal{U}, \vec{\mathbf{u}}^0)$, called the *utopia point*, is defined as

$$H(\mathcal{U}, \vec{\mathbf{u}}^0) = \left[\max_{\vec{\mathbf{u}} > \vec{\mathbf{u}}^0} U_1(\vec{\mathbf{u}}) \quad \max_{\vec{\mathbf{u}} > \vec{\mathbf{u}}^0} U_2(\vec{\mathbf{u}}) \right]. \tag{9.22}$$

Then, the KSS is defined as follows. Let Λ be a set of points on the line containing $\vec{\mathbf{u}}^0$ and $H(\mathcal{U}, \vec{\mathbf{u}}^0)$. $\phi(\mathcal{U}, \vec{\mathbf{u}}^0)$ is the KSS, which can be expressed as follows:

$$\phi(\mathcal{U}, \vec{\mathbf{u}}^0) = \max \left\{ \vec{\mathbf{u}} > \vec{\mathbf{u}}^0 \left| \frac{1}{\theta_1}(U_1 - U_1^0) = \frac{1}{\theta_2}(U_2 - U_2^0) \right. \right\}, \tag{9.23}$$

where $\theta_i = H_i(\mathcal{U}, \vec{\mathbf{u}}^0) - U_i^0$. The solution is in Λ.

The ES is defined as follows. $\phi(\mathcal{U}, \vec{\mathbf{u}}^0)$ is the ES, which can be expressed as follows:

$$\phi(\mathcal{U}, \vec{\mathbf{u}}^0) = \max \left\{ \vec{\mathbf{u}} > \vec{\mathbf{u}}^0 | U_1 - U_1^0 = U_2 - U_2^0 \right\}. \tag{9.24}$$

The KSS assigns as the bargaining solution the point in the boundary of a feasible set that intersects the line connecting the disagreement point and the utopia point. The ES assigns as the bargaining solution the point in the feasible set where all players achieve maximal equal increase in utility relative to the disagreement point.

Algorithm 12 shows the detail for data exchanged between OBUs. First, the OBU tries to find the neighboring OBUs within its communication range. Among all the reachable OBUs, the one that has the best channel quality (e.g., estimated using a pilot signal) is paired. The expected transmission rate $r_{i,j}$ between on-board units i and j is computed for a certain transmission duration t_0. After the OBUs have been paired, the negotiation between OBUs is performed to exchange information about the available data packets and their weights. The authors of [312] assumed that OBU i initiates the negotiation by sending a message containing information about its available packets to OBU j. After receiving this information, OBU j checks whether it has data packets of OBU i or not. Then, OBU j replies with a message containing information about the needed packets from OBU i and their weights. Additionally, the information about the data packets available at OBU j is piggybacked with this message sent back to OBU i. From this information, OBU i has complete information about data and their weights from OBU j. Therefore, this OBU i applies Algorithm 13 to compute a solution of the bargaining game. Note that, in Algorithm 13, Kalai–Smorodinsky and egalitarian solutions are approximated since the strategy space of OBUs is discrete (i.e., the number of packets transmitted is an integer).

Algorithm 12 Data-exchange algorithm

1: **repeat**
2: Neighbor discovery: Evaluate and determine vehicles with the best channel and most mutual benefited packets
3: Negotiation: OBUs exchange information regarding available data packets and their weights.
4: Bargaining: The solution of the bargaining game is obtained from Algorithm 13.
5: Data transmission: An OBU transmits packets to another OBU.
6: Adaptation: Monitor the channels and adjust the modulation and coding rate.
7: **until** Both OBUs have all the same packets or the connection is lost.

Algorithm 13 Bargaining algorithm

1: INPUT: Weight of available packet k from OBUs $i \in \{1,2\}$ (i.e., $w_i(k) \in \mathcal{I}_i$), transmission rate between OBUs i and j (i.e., $n_{i,j}$), where $i \neq j$.
2: Sort packets according to their weights, i.e., $w_i(1) > \cdots > w_i(k) > \cdots > w_i(\langle \mathcal{I}_i \rangle)$, where $\langle \mathcal{I}_i \rangle$ gives the number of elements in a set $\mathcal{I}_i$.
3: Define a set of numbers of packets transmitted by OBUs i and j as $\{(n_i, n_j) : n_i = \{0, \ldots, n_{i,j}\}, n_j = n_{ij} - n_i\}$. $U_i(n)$ can be obtained from (9.18), i.e., $U_i(n) = \sum_{k=1}^{n} w_i(k)$.
4: **if** Nash bargaining solution **then**
5: Obtain solution in terms of $(n_i^*, n_j^*) = \arg\max_{(n_i,n_j)} (U_i(n_i) - U_i^0) \times (U_j(n_j) - U_j^0)$.
6: **else if** Kalai–Smorodinsky solution **then**
7: Define the normalized utility $\hat{U}_i(n_i) = (1/\theta_i)(U_i(n_i) - U_i^0)$, where $\theta_i = \max_{n_i \{0,\ldots,n_{i,j}\}} U_i(n_i) - U_i^0$.
8: $(n_i^*, n_j^*) = \arg\min_{(n_i,n_j)} \left| \hat{U}_i(n_i) - \hat{U}_j(n_j) \right|$.
9: **else if** egalitarian solution **then**
10: The solution is obtained from $(n_i^*, n_j^*) = \arg\min_{(n_i,n_j)} \left| \left(U_i(n_i) - U_i^0\right) - \left(U_j(n_j) - U_j^0\right) \right|$.
11: **end if**
12: $\phi(\mathcal{U}, \mathrm{U}^0) = (U_i(n_i^*), U_j(n_j^*))$
13: OUTPUT: The indexes of the packets to be transmitted by OBUs i and j, i.e., (n_i^*, n_j^*), respectively.

9.3.4 *Data transfer from roadside units*

To solve the problem in (9.20), the probability distribution $\Pr(l)$ needs to be optimized. To reduce the search space, it is assumed that the weight of the packet is ordered (i.e., $w_i(k) > w_i(l)$ for $k < l$) and the probabilities corresponding to the different packets have the following relation:

$$\Pr(l+1) = \beta \Pr(l), \; l = 1, \ldots, L-1, \tag{9.25}$$

where $0 < \beta \leq 1$. As a result, we have

$$\Pr(l) = \begin{cases} 1/L, & \beta = 1, \\ \beta^{l-1}/[(1-\beta^L)/(1-\beta)], & 0 < \beta < 1, \end{cases} \tag{9.26}$$

and the problem in (9.20) can be expressed as follows:

$$\max_{\beta} \sum_{i=1}^{K} U_i. \tag{9.27}$$

When β is equal to 1, the uniform distribution is obtained, which models the situation in which the OBUs have enough opportunities to exchange information with other OBUs. When the road traffic is light, the value of β should be small. Since there will be few vehicles on the road, only the high-priority packets should be transmitted in order to maximize the utility. The solution in (9.27) is suboptimal to the problem in (9.20). However, only one parameter is needed, and the solution can be much easier to obtain.

Figure 9.12 shows the different solutions of the bargaining game (i.e., Nash bargaining, Kalai–Smorodinsky, and egalitarian solutions) for V2V communications. Additionally, Figure 9.12 shows the Pareto optimality. At the Pareto optimality, one vehicle cannot increase its utility without decreasing the utility of another vehicle. In other words, the Pareto optimality indicates that an efficient sharing of the utility between vehicles has been achieved. It is observed that Nash bargaining, Kalai–Smorodinsky, and egalitarian solutions can be located differently. However, all of them are on the line of Pareto optimality.

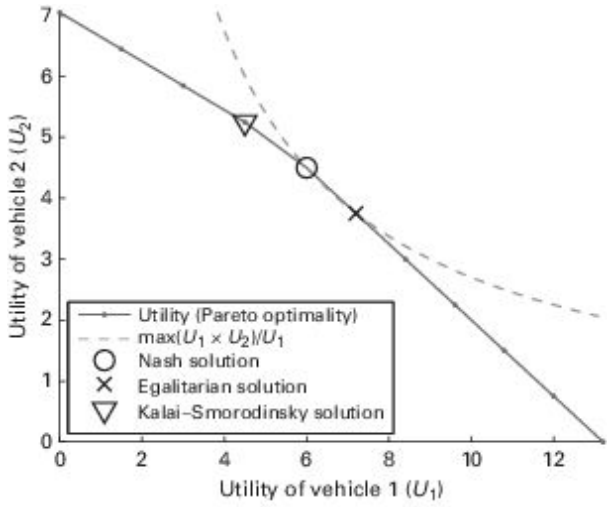

Figure 9.12. Nash bargaining, Kalai–Smorodinsky, and egalitarian solutions, and Pareto optimality.

9.3.5 Optimal channel access in vehicular networks

The authors of [311, 312] considered data dissemination by D2D communication. However, it is also important to investigate the channel access in such an environment. The problem of channel access becomes more challenging with the introduction of cognitive-radio capability. In particular, the vehicular nodes can opportunistically access licensed channels. The authors of [316] present an optimal channel-access scheme to provide quality of service (QoS) for data transmission in cognitive vehicular networks. In the networks, the vehicular nodes can opportunistically access the radio channels (referred to as shared-use channels) which are allocated to licensed users (i.e., primary users). Additionally, the vehicular nodes are able to reserve a channel for dedicated access (referred to as an exclusive-use channel) for data transmission. A channel-access management framework is developed for cluster-based communication among vehicular nodes. This framework has three components: opportunistic access to shared-use channels, reservation of an exclusive-use channel, and cluster-size control. A hierarchical optimization model based on a constrained Markov decision process (CMDP) is then developed for this framework in order to obtain the optimal policy. The objective of the optimization model is to maximize the utility of the vehicular nodes in a cluster and to minimize the cost of reserving an exclusive-use channel while the QoS requirements of data

transmission (for vehicle-to-vehicle and vehicle-to-roadside communications) are met, while satisfying the constraint on the probability of collision with licensed users. This hierarchical optimization model consists of two CMDP formulations – one for opportunistic channel access, and the other for joint exclusive-use channel reservation and cluster-size control. An algorithm is presented to solve this hierarchical optimization model.

The network model

The authors of [316] consider a cognitive vehicular network which uses clustering-based communication (Figure 9.13). A vehicular cluster is composed of a cluster head and cluster members. Data from a cluster member, i.e., the OBU of a vehicle, is first transmitted to the cluster head and then forwarded to the destination, which could be a neighboring cluster head. To achieve the required QoS level, the cluster head has to control the cluster size by limiting the number of cluster members. The intercluster and intracluster communication rely on two types of channels, i.e., shared-use channels and an exclusive-use channel [317].

- The shared-use channels are allocated to the licensed users. However, the vehicular nodes are allowed to access these channels opportunistically as unlicensed users. Owing to the imperfect nature of channel sensing, transmissions of vehicular nodes may collide with those of licensed users. The probability of collision with licensed users has to be maintained below a target level.
- The exclusive-use channel can be reserved for data transmission by the vehicular nodes in a dedicated mode. However, reserving the exclusive-use channel will incur some cost to the vehicular nodes.

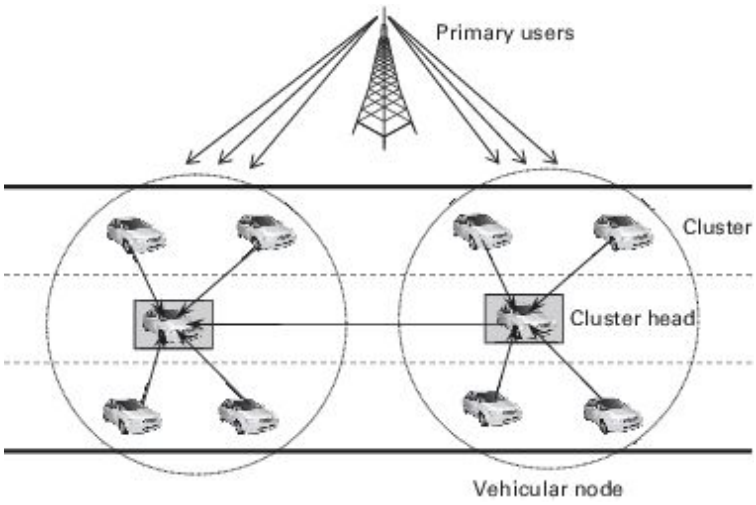

Figure 9.13. Cluster-based communication in a cognitive vehicular network.

A MAC protocol similar to that in [318] is adopted. Each time slot in a transmission frame is divided into a sensing period, a reporting period, a handshaking period, and a data-transmission period (Figure 9.14). Independent or cooperative sensing can be adopted to observe the status of the shared-use channels. The sensing results are sent to the cluster head using the exclusive-use channel. The cluster head obtains the sensing results (i.e., states) of all shared-use channels. The state could be *idle* or *occupied* by licensed users. Afterward, the decision on channel access (i.e., which among the shared-use channels is to be accessed) is made. Next, this decision as well as the information regarding the exclusive-use channel (i.e., the amount of bandwidth reserved) are sent to the cluster member (which is scheduled for data transmission during that time slot) in the handshaking period. Then, the cluster member transmits data using the shared-use channel and/or the exclusive-use channel. This data-transmission period is divided into two parts, i.e., transmission from a cluster member to a cluster head, and transmission from a cluster head to a destination. Since each of the vehicular nodes has two interfaces, transmission on the shared-use channel and on the exclusive-use channel can be performed simultaneously. The transmission on the exclusive-use channel is based on the reserved bandwidth. In one time slot, a maximum of B units of bandwidth can be reserved by the cluster.

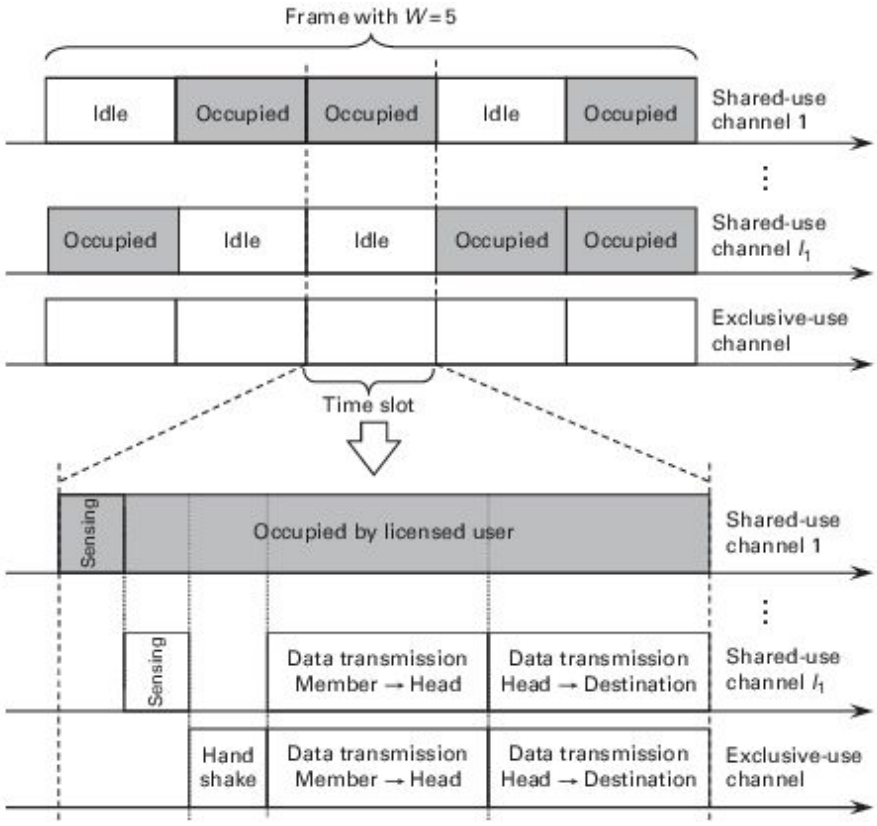

Figure 9.14. The frame structure and time slots of shared-use channels and an exclusive-use channel.

Traffic scheduling among the vehicular nodes in the cluster is weighted round-robin (WRR). With WRR scheduling, let n denote the total number of nodes in a cluster, including the cluster head. The weight of node m is denoted by $w_m \in \{1, 2, \ldots\}$. Each transmission frame has a length of $W = \sum_{m=1}^{n} w_m$ time slots. The same frame structure applies to the shared-use channels and the exclusive-use channel. In a frame, w_m time slots are allocated to vehicular node m in the cluster. In these allocated time slots, the nodes can transmit data packets using the exclusive-use channel, and a shared-use channel if it is free from licensed users.

The authors of [316] introduced a channel-access management framework for the cognitive vehicular network. The objective of this framework is to maximize the utility of a vehicular cluster. The utility is a function of the transmission rates of the vehicular nodes in the cluster and

the cost of reserving bandwidth for dedicated channel access. The constraints are the maximum packet-loss probability and the maximum packet delay for the vehicular nodes, and the maximum probability of collision with the licensed users. The framework is designed to have three components, as follows.

- *Queue-aware opportunistic channel access:* The opportunistic channel-access component determines which among the shared-use channels to access. This decision is made every time slot.
- *Exclusive-use channel reservation:* This is called the *bandwidth-reservation* component in short. The bandwidth-reservation component determines the amount of bandwidth to be reserved by the vehicular cluster in the exclusive-use channel.
- *Cluster-size control:* The cluster-size-control component determines whether to accept or refuse the request of a vehicular node requesting to join the cluster. The cluster head makes the decisions regarding channel reservation and cluster-size control when there is a new vehicular node requesting to join or leave the cluster, or when the cluster changes its location due to mobility of the vehicles.

Figure 9.15 shows the structure of the proposed channel-access management framework. The decision on opportunistic channel access is made at the first level, which corresponds to the short-term decision made every time slot. The decision on joint bandwidth reservation and cluster-size control is made at the second level, which corresponds to the long-term decision. Owing to the different time scales of the decisions, a hierarchical optimization model that is based on two CMDP formulations is developed.

- *CMDP for opportunistic channel access:* The formulation for opportunistic channel access is based on the state of the shared-use channels, the number of packets in the queue of a vehicular node, the service index of WRR scheduling, and the phase of packet arrival. The action is to access a shared-use channel.
- *CMDP for joint bandwidth reservation and cluster-size control:* The formulation for joint bandwidth reservation and cluster-size control is based on the location of a cluster and the cluster size. The action is to

reserve bandwidth in the exclusive-use channel and to accept or to refuse the request of a vehicular node requesting to join the cluster.

These two CMDP formulations interact through the QoS performance measures (e.g., packet-loss probability), the location, the cluster size, and the available bandwidth in the exclusive-use channel.

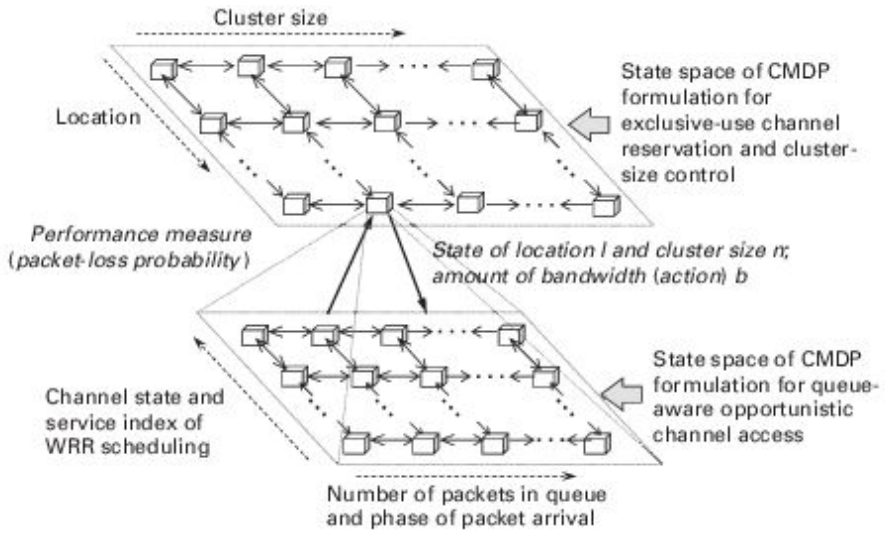

Figure 9.15. The structure of the channel-access management framework.

Mobility and packet-arrival processes

The residence time of a vehicular cluster at any location (i.e., the duration during which all the vehicular nodes in the cluster remain in the same cell) is assumed to be exponentially distributed. It is assumed that the movement of a vehicular cluster depends only on the current location. Therefore, the mobility of a cluster is modeled by the transition-rate matrix $\mathbf{M}$, which can be expressed as follows:

$$\mathbf{M} = \begin{bmatrix} M(1,1) & \cdots & M(1,l_m) \\ \vdots & \ddots & \vdots \\ M(l_m,1) & \cdots & M(l_m,l_m) \end{bmatrix}, \tag{9.28}$$

where $l_m = |\mathbb{L}|$ is the total number of locations in a service area, and $|\mathbb{L}|$ is the cardinality of set $\mathbb{L}$. The element $M(l, l')$ denotes the rate (i.e., speed) at which a cluster changes its location from L_l to $L_{l'}$. This transition-rate matrix can capture the different speeds of a cluster in different locations in a service area.

Let $\vec{\boldsymbol{\Omega}} = [\ \omega(L_1) \ \cdots \ \omega(L_l) \ \cdots \ \omega(L_{l_m})\ ]^\top$ denote the steady-state probability vector whose element $\omega(l)$ represents the probability of the cluster being at location L_l. This vector can be obtained by solving $\vec{\boldsymbol{\Omega}}^\top \mathbf{M} = \vec{\mathbf{0}}$ and $\vec{\boldsymbol{\Omega}}^\top \vec{\mathbf{1}} = 1$, where $\vec{\mathbf{0}}$ and $\vec{\mathbf{1}}$ are the vectors of zeros and ones, respectively.

For each vehicular node, the authors of [316] adopt a batch Markovian process with H phases for the packet-arrival process. The transition probability matrix for the packet-arrival process is given by $\mathbf{A}_a$ (as in (9.29)) for $a \in \{0, 1, \ldots, a_m\}$ arriving packets, where a_m is the maximum batch size, i.e.,

$$\mathbf{A}_a = \begin{bmatrix} A_a(1,1) & \cdots & A_a(1,H) \\ \vdots & \ddots & \vdots \\ A_a(H,1) & \cdots & A_a(H,H) \end{bmatrix}. \tag{9.29}$$

In (9.29), $A_a(h, h')$ denotes the probability that a packets arrive in the queue and the phase changes from h to h'. The matrix $\mathbf{A}$ is defined as $\mathbf{A} = \mathbf{A}_0 + \mathbf{A}_1 + \cdots + \mathbf{A}_{a_m}$. Let $\vec{\boldsymbol{\alpha}} = [\ \alpha(1) \ \cdots \ \alpha(h) \ \cdots \ \alpha(H)\ ]^\top$ denote the stationary probability vector of packet arrival. The element $\alpha(h)$ of this vector is the steady-state probability that the phase of packet arrival is h. This vector can be obtained by solving $\vec{\boldsymbol{\alpha}}^\top \mathbf{A} = \vec{\boldsymbol{\alpha}}^\top$ and $\vec{\boldsymbol{\alpha}}^\top \vec{\mathbf{1}} = 1$. The average packet-arrival rate can be obtained by weighting the probability of all phases with steady-state probability $\alpha(h)$ as follows:

$$\overline{\lambda} = \sum_{a=1}^{a_m} a \left(\vec{\boldsymbol{\alpha}}^\top \mathbf{A}_a \right) \vec{\mathbf{1}}. \tag{9.30}$$

Channel-state and packet transmission models

The activity of licensed users in a shared-use channel is modeled by a two-state Markov chain, i.e., an ON–OFF model. The ON and OFF states correspond, respectively, to the case when the channel is *occupied* and *idle*, respectively. For shared-use channel i, the channel state is modeled by the following transition probability matrix:

$$\hat{\mathbf{C}}_i = \begin{bmatrix} \tilde{C}_i(0,0) & \tilde{C}_i(0,1) \\ \tilde{C}_i(1,0) & \tilde{C}_i(1,1) \end{bmatrix} \begin{matrix} \leftarrow \text{idle} \\ \leftarrow \text{occupied} \end{matrix} \tag{9.31}$$

where 0 and 1 indicate the actual *idle* and *occupied* states, respectively. The probability P_i^{id} of shared-use channel i being idle can be obtained from

$$P_i^{\text{id}} = \frac{1 - \tilde{C}_i(1,1)}{\tilde{C}_i(0,1) - \tilde{C}_i(1,1) + 1}.$$

Adaptive modulation is used to enhance the transmission rate on both exclusive-use and shared-use channels with slowly varying flat fading. The average SNR at the receivers corresponding to the links between a cluster member and the cluster head, and to the link between the cluster head and the destination, are denoted by $\overline{\gamma}_i^{(\text{s1})}$ and $\overline{\gamma}_i^{(\text{s2})}$ for shared-use channel i, and by $\overline{\gamma}^{(\text{e1})}$ and $\overline{\gamma}^{(\text{e2})}$ for the exclusive-use channel, respectively.

With the maximum of F transmission modes, the SNR at the receiver γ can be partitioned into $F+1$ non-overlapping intervals by thresholds Γ_f ($f \in \{0, 1, \ldots, F\}$), where $\Gamma_0 = 0 < \Gamma_1 < \cdots < \Gamma_F = \infty$. The channel is said to be in mode f if $\Gamma_f \le \gamma < \Gamma_{f+1}$. In mode f, it is assumed that c_f packets can be transmitted in one time slot on the shared-use channel, and $c_f b$ packets can be transmitted on the exclusive-use channel where b for $b \in \{0, 1, \ldots, B\}$ is the amount of bandwidth reserved by the cluster and B is the maximum bandwidth. Given the Nakagami-m fading channel and average SNR $\overline{\gamma}$, the probability of the transmission in mode f can be obtained from [319]

$$\Pr(f) = \frac{\Gamma(m, m\Gamma_f/\overline{\gamma}) - \Gamma(m, m\Gamma_{f+1}/\overline{\gamma})}{\Gamma(m)}, \tag{9.32}$$

where $\Gamma(\cdot,\cdot)$ is the complementary incomplete gamma function, and $\Gamma(\cdot)$ is the gamma function. Note that the average SNR is denoted by $\overline{\gamma} \in \{\overline{\gamma}_i^{(s1)}, \overline{\gamma}_i^{(s2)}, \overline{\gamma}^{(e1)}, \overline{\gamma}^{(e2)}\}$.

With an infinite-persistent automatic-repeat-request (ARQ) error control, the probability that c packets can be successfully transmitted on shared-use channel i from a cluster member to the cluster head can be obtained from

$$\hat{D}_i^{(s1)}(c) = \sum_{c'=c_f}^{c_F} \Pr(f) \binom{c'}{c} (1 - \overline{\mathrm{PER}}_f)^c (\overline{\mathrm{PER}}_f)^{c'-c} (1 - \vartheta), \tag{9.33}$$

for $c_f \geq c$, where $\overline{\mathrm{PER}}_f$ is the average packet error rate in transmission mode f and ϑ is the collision probability. Collisions can occur when multiple clusters exist in the same cell. The collision probability can be obtained from

$$\vartheta = 1 - \prod_{j=1}^{J} \chi_j, \tag{9.34}$$

where J is the number of clusters in the same cell and χ_j is the probability of there being no transmission by cluster j. For transmission from the cluster head to the destination, this probability $\hat{D}_i^{(s2)}(c)$ can be obtained in the same way. However, $\Pr(f)$ could be different from that used to compute $\hat{D}_i^{(s1)}(c)$ in (9.33) due to the different average SNR. Similarly, for transmission on the exclusive-use channel given b units of bandwidth, this probability is obtained from

$$\hat{D}_b^{(e1)}(c) = \sum_{c'=c_f b}^{c_F b} \Pr(f) \binom{c'}{c} (1 - \overline{\mathrm{PER}}_f)^c (\overline{\mathrm{PER}}_f)^{c'-c}, \tag{9.35}$$

for $c_f b \geq c$. The probability $\hat{D}_b^{(e2)}(c)$ can be obtained in a similar way.

The probability that c packets will be transmitted from the cluster member to a destination (i.e., from cluster member to cluster head and then from cluster head to destination) using shared-use channel i can be obtained from

$$D_i^{(s)}(c) = \sum_{\{c',c''|\min(c',c'')=c\}} \hat{D}_i^{(s1)}(c')\hat{D}_i^{(s2)}(c''), \tag{9.36}$$

for $c = \{0, 1, \ldots, c_F\}$, where $\hat{D}_i^{(s1)}(c')$ and $\hat{D}_i^{(s2)}(c'')$ denote the probabilities that c' and c'' packets will be successfully transmitted from a cluster member to the cluster head and from the cluster head to the destination, respectively. These probabilities can be obtained from (9.33). Similarly, given b units of bandwidth, the probability that c packets will be transmitted from a cluster member to the destination using the exclusive-use channel can be obtained from

$$D_b^{(e)}(c) = \sum_{\{c',c''|\min(c',c'')=c\}} \hat{D}_b^{(e1)}(c')\hat{D}_b^{(e2)}(c''). \tag{9.37}$$

That is, this probability is determined from the minimum transmission rates from cluster member to cluster head and from cluster head to destination.

CMDP formulation for queue-aware opportunistic channel access

The decision on opportunistic channel access is to determine which shared-use channel to access. The decision will minimize the packet-loss probability and keep the probability of collision with the licensed users below the target threshold. A CMDP model is formulated for a tagged vehicular node and solved for each location (e.g., L_l) in the service area. The policy is for a certain cluster size n given the amount of bandwidth b reserved in the exclusive-use channel.

The composite state of the CMDP formulation for channel access of the tagged node in a cluster is defined as follows:

$$\Delta = \{(\mathcal{X}, \mathcal{Y}, \mathcal{C}, \mathcal{A}); \mathcal{X} \in \{0, 1, \ldots, X\}, \mathcal{Y} \in \{0, 1, \ldots, W\}, \mathcal{C} \in \mathbb{C}, \mathcal{A} \in \{1, \ldots, H\}\}, \tag{9.38}$$

where $\mathcal{X}$ is the number of packets in the queue of the tagged cluster member, X is the maximum queue size, $\mathcal{Y}$ is the service index assigned by the WRR scheduler, and $W = \sum_{m=1}^{n} w_m$. $\mathcal{C}$ is the composite state of the shared-use channels, and $\mathcal{A}$ is the phase of packet arrival. The set $\mathbb{C}$ is defined as $\mathbb{C} = \{(\mathcal{C}_1, \ldots, \mathcal{C}_{I_l}); \mathcal{C}_i \in \{0, 1\}\}$, where $\mathcal{C}_i$ is the sensed state of shared-use channel i. The action space is defined as $\mathbb{U}(s) \in \{0, 1, \ldots, I_l\}$, where $s \in \Delta$. Action $u \in \mathbb{U}(s)$ corresponds to use of the shared-use channel for packet transmission, where $u = 0$ indicates that none of the shared-use channels will be accessed.

The authors of [316] assume that the state of the tagged vehicular node (i.e., the number of packets in the queue, the state of the shared-use channel, and the phase of packet arrival) is observed at the beginning of each time slot. Then, the cluster head makes a decision on channel access accordingly. The decision could be to access the exclusive-use channel only, or to access both a shared-use channel and the exclusive-use channel. At the end of a time slot, an acknowledgement message is used to inform the cluster member whether the packets have successfully been transmitted or not.

The transition probability matrix $\mathbf{P}(u)$ for the states defined in space Δ can be derived on the basis of the action $u \in \mathbb{U}(s)$. The authors of [316] provide detailed derivations of this transition matrix. The CMDP formulation for opportunistic channel access can be expressed as follows:

$$\begin{aligned} \min_{\pi} \quad & \mathcal{J}_{\mathrm{L}}(\pi) \\ \text{s.t.} \quad & \mathcal{J}_{\mathrm{C},i}(\pi) \leq C_{i,\max}, \quad \forall i \\ & \mathcal{J}_{\mathrm{D}}(\pi) \leq D_{\max}. \end{aligned} \tag{9.39}$$

$\mathscr{J}_{\mathrm{L}}$ is the packet-loss probability (due to buffer overflow). $\mathscr{J}_{\mathrm{C}}$ is the collision probability. $\mathscr{J}_{\mathrm{D}}$ is the average packet delay (from the transmission queue). These performance metrics can be defined as follows:

$$\mathscr{J}_{\mathrm{L}} = \lim_{t\to\infty} \sup \frac{1}{t} \sum_{t'=1}^{t} E(\mathscr{L}(\mathcal{S}_{t'}, \mathcal{U}_{t'})), \tag{9.40}$$

$$\mathscr{J}_{\mathrm{C},i} = \lim_{t\to\infty} \sup \frac{1}{t} \sum_{t'=1}^{t} E(\mathscr{C}_i(\mathcal{S}_{t'}, \mathcal{U}_{t'})), \tag{9.41}$$

$$\mathscr{J}_{\mathrm{D}} = \lim_{t\to\infty} \sup \frac{1}{t} \sum_{t'=1}^{t} E(\mathscr{D}(\mathcal{S}_{t'}, \mathcal{U}_{t'})), \tag{9.42}$$

where $\mathcal{S}_{t'} \in \Delta$ and $\mathcal{U}_{t'} \in \mathbb{U}(\mathcal{S}_{t'})$ are the state and action variables, respectively, for the tagged node at time t', and $E(\cdot)$ denotes the expectation. $\mathscr{L}(s, u)$, $\mathscr{C}_i(s, u)$, and $\mathscr{D}(s, u)$ for $s \in \Delta$ and $u \in \mathbb{U}(s)$ denote the immediate packet-loss probability, immediate collision probability corresponding to shared-use channel i, and immediate delay functions, respectively. They are defined as functions of composite state s and action u. Note that the composite state s is defined as $s = (s_{\mathrm{x}}, s_{\mathrm{w}}, s_{\mathrm{c}}, s_{\mathrm{a}})$. The elements of this composite state s are the realization of the state variables defined in (9.38), i.e., the number of packets in the transmission queue $\mathcal{S}_{\mathrm{x}}$, the service index $\mathcal{S}_{\mathrm{w}}$ of WRR scheduling, the channel state $\mathcal{S}_{\mathrm{c}}$, and the phase of packet arrival $\mathcal{S}_{\mathrm{a}}$. In this case, $\mathcal{S}_{\mathrm{c}}$ is also a composite state which is defined as $s_{\mathrm{c}} = (\ldots, s_{\mathrm{c},i}, \ldots)$, where $s_{\mathrm{c},i}$ is the state for the shared-use channel i ($i \in \{1, \ldots, I_l\}$).

The objective function and constraints given in (9.39) are defined as functions of policy π. A policy π is a mapping of state s to action u, i.e., $u = \pi(s)$ for $u \in \mathbb{U}(s)$ and $s \in \Delta$. The authors of [316] consider a randomized policy in which action u to be taken at state s is chosen randomly according to the probability distribution denoted by $\nu(\pi(s))$ for

which $\sum_{\pi(s)\in\mathbb{U}(s)} \nu(\pi(s)) = 1$. The solution of the CMDP formulation is referred to as the optimal policy π^* which minimizes the packet-loss probability while maintaining the collision probability below the threshold $C_{i,\max}$ and the average packet delay below the threshold $D_{\max}$. The standard method is adopted to transform the CMDP formulation into an equivalent linear-programming (LP) problem to obtain the optimal policy π^* [320].

CMDP formulation for exclusive-use channel reservation and cluster-size control

The decision regarding the exclusive-use channel reservation is that one must determine the amount of bandwidth to be reserved for the vehicular cluster in the exclusive-use channel. The decision regarding the cluster-size control is that one must determine whether the request of a vehicular node requesting to join the cluster can be accepted or not. These decisions are made in such a way as to maximize the utility of the vehicular cluster while the target QoS performance can be achieved at all locations. Note that, to guarantee the QoS performance at a particular location (e.g., to minimize the packet-loss probability and to bound the average packet delay), the CMDP formulation for opportunistic channel access is used. To guarantee the QoS performance at all locations in a service area, bandwidth reservation from the exclusive-use channel should be implemented, and also the cluster size needs to be controlled. This CMDP formulation is based on the QoS performance measure (i.e., packet-loss probability) of the tagged vehicular node at a certain location, for a particular cluster size and amount of bandwidth reserved. Additionally, the optimal policy π^* for opportunistic channel access is applied.

The composite state of the CMDP formulation for joint bandwidth reservation and cluster-size control is defined as follows:

$$\Psi = \{(\mathcal{L},\mathcal{N}); \mathcal{L} \in \mathbb{L}, \mathcal{N} \in \{1,\ldots,N\}\}, \tag{9.43}$$

where $\mathcal{L}$ is the location of the cluster, and $\mathbb{L}$ is the set of locations in a service area. $\mathcal{N}$ is the cluster size, and N is the maximum cluster size. It is assumed that there is at least one node in the cluster.

The action of this CMDP formulation is a composite action of joint bandwidth reservation and cluster-size control. The action space is defined as follows:

$$\mathbb{V} = \{(b, g); b \in \{0, 1, \ldots, B\}, g \in \{0, 1\}, \tag{9.44}$$

where b is the amount of bandwidth to be reserved for transmission using the exclusive-use channel, and B is the maximum amount of bandwidth that can be reserved. The values of $g = 0$ and $g = 1$ correspond, respectively, to the decisions of refusing and accepting the request of a vehicular node requesting to join the cluster. The system state (i.e., the location and cluster size) is observed when a vehicular node requests to join or leave the cluster, and/or when the location of the cluster changes. Then, the cluster head makes the decision to reserve bandwidth in the exclusive-use channel and either to accept or to refuse the request of the vehicular node according to the optimal policy.

The authors of [316] assume that the interarrival time of requests from vehicular nodes to join or leave the tagged cluster is exponentially distributed. Let $1/\sigma$ denote the mean interarrival time of requests from vehicular nodes to join the cluster, and let $1/\beta$ denote the mean duration for which a vehicular node will be in the cluster. The transition-rate matrix $\mathbf{Q}(v)$ for the states defined in state space Ψ can be derived on the basis of action $v \in \mathbb{V}$. The authors of [316] provide detailed derivations of this transition matrix.

The CMDP formulation for joint bandwidth reservation and cluster size control can be expressed as follows:

$$\begin{aligned} \max_{\delta} \quad & \mathcal{K}_{\mathrm{U}}(\delta), \\ \text{s.t.} \quad & \mathcal{K}_{\mathrm{L}}(\delta) \leq L_{\max} \\ & \mathcal{K}_{\mathrm{D}}(\delta) \leq D_{\max}. \end{aligned} \tag{9.45}$$

$\mathscr{K}_{\mathrm{U}}$ is the utility of a cluster. $\mathscr{K}_{\mathrm{L}}$ is the packet-loss probability. $\mathscr{K}_{\mathrm{D}}$ is the average packet delay. They are measured across a service area as follows:

$$\mathscr{K}_{\mathrm{U}} = \lim_{t\to\infty} \sup \frac{1}{t} \sum_{t'=1}^{t} E(\mathscr{U}(\mathcal{R}_{t'}, \mathcal{V}_{t'})), \tag{9.46}$$

$$\mathscr{K}_{\mathrm{L}} = \lim_{t\to\infty} \sup \frac{1}{t} \sum_{t'=1}^{t} E(\mathscr{J}_{\mathrm{L}}(\mathcal{R}_{t'}, \mathcal{V}_{t'}, \pi^*)), \tag{9.47}$$

$$\mathscr{K}_{\mathrm{D}} = \lim_{t\to\infty} \sup \frac{1}{t} \sum_{t'=1}^{t} E(\mathscr{J}_{\mathrm{D}}(\mathcal{R}_{t'}, \mathcal{V}_{t'}, \pi^*)). \tag{9.48}$$

$\mathcal{R}_{t'} \in \Psi$ and $\mathcal{V}_{t'} \in \mathbb{V}$ denote, respectively, the state and action variables of the cluster at time t' for joint bandwidth reservation and cluster-size control. $\mathscr{U}(r, v)$, $\mathscr{J}_{\mathrm{L}}(r, v, \pi^*)$, $\mathscr{J}_{\mathrm{D}}(r, v, \pi^*)$ for $r \in \Psi$ and $v = (b, g) \in \mathbb{V}$ are the immediate utility, packet-loss probability, and delay, respectively, in a particular location. These are functions of composite state r and action v. Note that the composite state r is defined as $r = (l, n)$. l and n are the realizations of the state variables defined in (9.38), i.e., the location and cluster size, respectively. These performance metrics are defined, given that the optimal policy π^* for opportunistic channel access is used.

The objective and constraints given in (9.45) are defined as functions of policy δ. The policy to map the state $r \in \Psi$ to action $v \in \mathbb{V}$ is expressed as $v = \delta(r)$. A randomized policy in which the probability distribution is denoted by $\mu(\delta(r))$ is considered. In this case, $\mu(v = (b, g))$ is the probability of the cluster reserving b units of bandwidth in the exclusive-use channel and either accepting or refusing the request of a vehicular node requesting to join the cluster. The optimal policy is denoted by δ^*, which maximizes the utility of cluster $\mathscr{K}_{\mathrm{U}}(\delta)$ while maintaining the packet-loss probability $\mathscr{K}_{\mathrm{L}}(\delta)$ and delay $\mathscr{K}_{\mathrm{D}}(\delta)$ at a steady state below the thresholds

$L_{\max}$ and $D_{\max}$, respectively. Again, to obtain the optimal policy δ^*, the CMDP formulation is transformed into an equivalent LP problem.

An algorithm for computing the optimal policy for the hierarchical MDP model

Given the two CMDP formulations, i.e., one for joint bandwidth reservation and cluster-size control, and the other for opportunistic channel access, the joint optimal policy can be obtained by the cluster head using Algorithm 14.

Algorithm 14 Joint optimal policy

1: **for** State $r = (l, n) \in \Psi$ **do**
2: **for** Action $g = \{0, 1\}$ and $b = \{0, 1, \ldots, B\}$ **do**
3: Obtain optimal policy π^* for channel access by solving the linear-programming problem given location l, cluster size n, and bandwidth of exclusive-use channel b.
4: Obtain the packet-loss probability $\mathcal{J}_{\mathrm{L}}(r, v, \pi^*)$ and delay $\mathcal{J}_{\mathrm{D}}(r, v, \pi^*)$ given the optimal policy π^*.
5: **end for**
6: **end for**
7: Obtain the optimal policy δ^* for joint bandwidth reservation and cluster-size control by solving the linear-programming problem.
8: The cluster head makes a decision according to π^* on a time-slot basis, and according to δ^* when the cluster location changes, or a vehicular node requests to join or leave the cluster.

In Algorithm 14, the packet-loss probability and delay for the opportunistic channel access are obtained for a given state $r(l, n)$. Then, the policy for the joint bandwidth reservation and cluster-size control is obtained afterward.

The authors of [316] provide a comprehensive performance evaluation of the proposed optimization for optimal channel access in vehicular networks.

Figures 9.16(a) and (b) show examples of the impact of the channel quality on the packet-loss probability and average packet delay of a vehicular node (i.e., a cluster member), respectively, given an optimal policy of opportunistic channel access. When the cluster can opportunistically access the shared-use channels in addition to the transmission in the exclusive-use channel, the packet-loss probability and average packet delay significantly decreases. The same result is expected when the average SNR of the exclusive-use channel improves. As the adaptive modulation and coding is applied, the number of packets successfully transmitted in a time slot increases. Therefore, the probability that the data queue of the node will be full is lower.

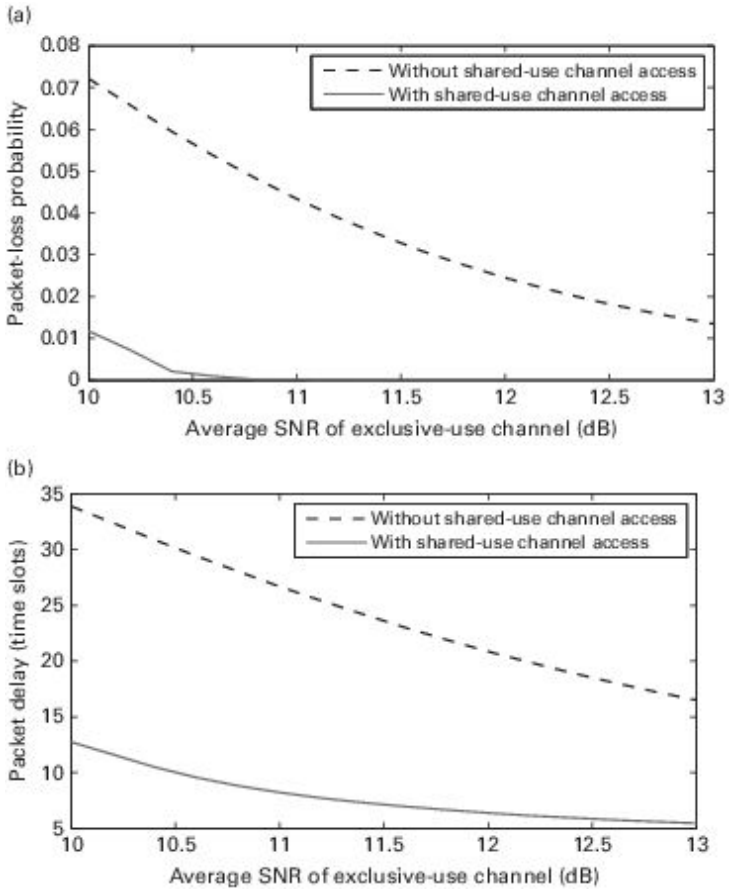

Figure 9.16. (a) The packet-loss probability and (b) average delay for a vehicular node with and without opportunistic access to shared-use channels.

Figure 9.17(a) shows the amount of average bandwidth reserved for the exclusive-use channel. Clearly, to meet the QoS requirements in terms of the packet-loss probability and average packet delay, more bandwidth has to be reserved as the packet-arrival rate increases. Conversely, due to channel sharing, the cluster size reduces so that each node has more chance to transmit packets (due to the use of weighted round-robin scheduling).

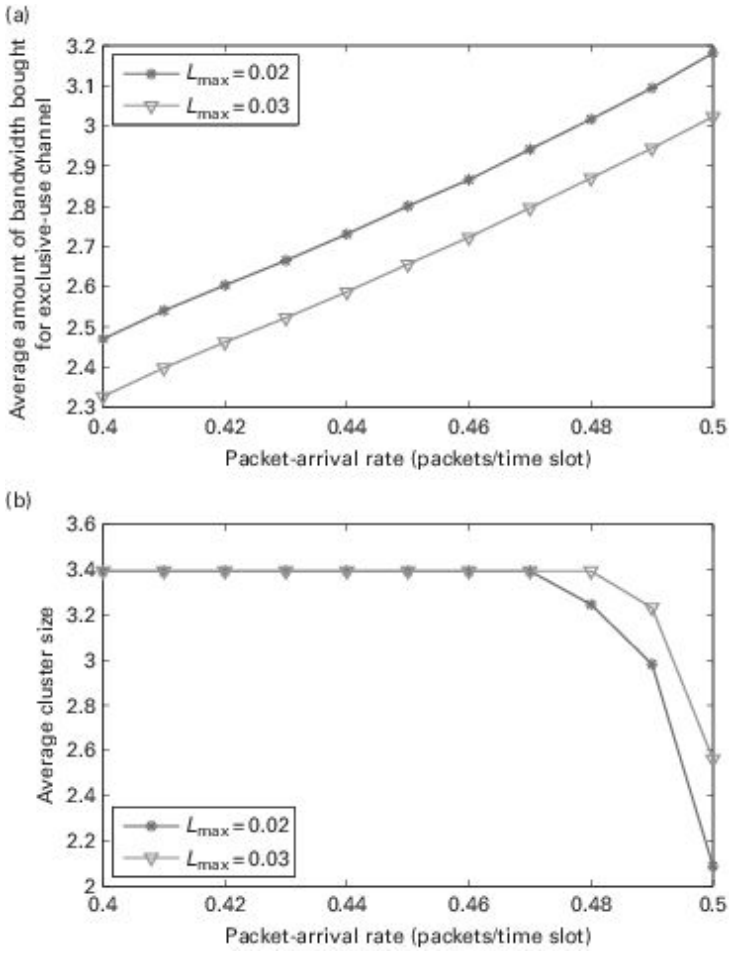

Figure 9.17. (a) The average amount of bandwidth reserved under different packet-arrival rates and (b) the average cluster size.

9.4 Chapter summary

We have introduced one important application of D2D communications in vehicular networks. D2D communications can support direct data transfer

among vehicular nodes in VANETs. D2D communications in VANETs can support many intelligent-transportation-system applications including safety, transportation efficiency, and infotainment applications. We first provided an overview of vehicle-to-infrastructure and vehicle-to-vehicle communication. The latter, which can use D2D communications techniques, allows data transfer among vehicular nodes directly. Afterward, we discussed the applications, protocols (i.e., IEEE 802.11p), and routing in vehicular networks. Then we discussed three specific issues in D2D communications in a vehicular environment, i.e., D2D retransmission, data distribution using BitTorrent, and channel access.

Some research directions for D2D communications and vehicular networks are as follows.

- *Network and mode selection:* In vehicular networks, the communications can be vehicle-to-vehicle. However, in many cases, the vehicular nodes can communicate with a roadside unit, improving the radio-resource efficiency and performance of applications. For example, a collision-warning message can be broadcast directly from vehicle to vehicle. However, the reachability of the message can be improved if the warning message is relayed by a nearby base station. Therefore, the important issue is how data will be transmitted (vehicle-to-vehicle and/or vehicle-to-infrastructure), which is referred to as mode selection. Additionally, if the infrastructure is used, the network (e.g., base stations) to be used for data transfer has to be optimally chosen.
- *Heterogeneous environment:* Vehicular networks can be integrated with sensor networks or human-centric networks (e.g., mobile social networks). Such integration can broaden the vehicular applications (e.g., vehicle-to-pedestrian communication). Therefore, D2D communication has to be integrated and adapted to different environments with diverse topology, channel quality, and mobility. The integration becomes more challenging when the QoS must be supported in an end-to-end fashion.
- *Adoption of advanced transmission technologies:* Different wireless transmission technologies can be adopted to improve D2D communication in vehicular networks. Some examples are adaptive

beamforming, multiple-input multiple-output (MIMO) antenna systems, and cooperative diversity. With these advanced transmission technologies, protocol layers of vehicular networks must be modified to optimally utilize the capability. For example, beamforming and MIMO can be used to enhance the transmission performance due to the rich spatial diversity in a vehicular environment.

---

[1] This is sometimes referred to as vehicle-to-roadside (V2R) communication architecture.

10 Mobile social networks

10.1 Introduction

Traditional D2D communications take place among any mobile units to transfer "data." However, current and emerging mobile applications pose the new challenges of "information" transfer. Typically, information is related to social relations of people. Therefore, social information and social networks have been integrated with wireless and mobile communication to serve the new demand of users for information transfer. When the social information is used or the social network is operated on wireless systems, we can refer to it as a mobile social network [321, 322]. The mobile social network can be integrated or used in D2D communications with the following approaches.

- *D2D communications to support mobile social network:* In this approach, typical social-network applications and mobile social networks will utilize D2D communications to transfer data and information. Instead of using a fixed wireless infrastructure (e.g., a base station of a cellular network) to transfer social-network information, the information can be conveyed through D2D networks. The typical advantages of D2D communications are inherited in this case for the mobile social network, including reducing radio-resource usage, alleviating network overload, and improving the data- and information-dissemination and -delivery performance.
- *Social-based D2D communications:* In this approach, D2D communications supporting other applications can utilize social information of users to improve the efficiency and effectiveness of data and information transfer. For example, packet routing of D2D LAN can be enhanced by taking social ties among devices and users into account

to determine an optimal route. Such an optimal route may not only minimize a network cost, but also maximize the social impact, improving the satisfaction of D2D communications and networking.

In this chapter, we focus on the mobile social network and its role in D2D communications. Firstly, Section 10.2 presents an overview of mobile social networks. Their architecture, applications, issues, and approaches are reviewed. Section 10.4 presents some seminal works in the field of social-aware data routing and dissemination. Section 10.5 introduces a detailed formulation for cooperative content delivery in mobile social networks. Finally, Section 10.6 gives a summary of the chapter.

10.2 An overview of mobile social networks

Social networks are the form of human relations which can be represented by a graph. Study of the "small-world" phenomenon [323] clearly shows that people usually belong to different communities and come into contact with others with similar interests. Recently, social networks have become important applications for people to share and exchange data and information. Social networks are adopted in such applications due to the fact that every entity (e.g., people, devices, or systems) has relationships in one form or another. In social science, relationships can be analyzed using a social-network analysis. The analysis can extract many interesting and useful attributes of the network (e.g., centrality metrics). In computer science, social-network applications gain tremendous popularity where the social information can be used to improve the effectiveness of information exchange and sharing. In wireless communications and mobile networking, the concept of a mobile social network, in which the mobility of users together with their social relationship can be used to optimize data dissemination and delivery, has been introduced. The authors of [321] provide a comprehensive survey of the applications, architecture, and protocol-design issues for mobile social networks. This section presents an overview of a mobile social network, which is closely related to the issue of D2D communications.

10.2.1 Types and components of mobile social networks

A mobile social network is a combination of two concepts, i.e., a social network and mobile networking. In general, the mobile social network is a mobile system involving social relationships of the users. In other words, the mobile social network is a user-centric mobile system in which the users not only transmit data, but also provide context information to optimize the operations of the network. Two major types of mobile social networks are as follows.

- *Web-based mobile social networks:* This is a typical form of providing social network websites (e.g., Facebook) over a mobile network. In this case, social network data will be transferred between servers and mobile users over a wireless connection. The web-based mobile social network is based on a centralized data-access topology and structure. The context information of mobile users (e.g., locations) can be used by the social-network website to optimize the data transferred.
- *Decentralized mobile social networks:* In this type, mobile users form a group to transfer data among each other according, for example, to a social relation or shared interest. The mobile users may not need to have permanent connections to a centralized server as in a web-based mobile social network. Instead, the mobile users can transfer data directly among themselves through multihop networking or carry-and-forward data transfer (e.g., similarly to a delay-tolerant network [DTN] [324, 325]). While the former could be an ad-hoc network or mesh networks for users with and without mobility, respectively, the latter uses opportunistic contact due to mobility of users to receive, store, and forward data. In this case, the data transfer can be performed using short-range wireless technologies (e.g., Wi-Fi), reducing radio-resource demand and energy consumption compared with long-range transmission (e.g., cellular networks). Figure 10.1 shows an example scenario of the decentralized mobile social network. First, the content provider (e.g., a content server) transfers the data to the wireless infrastructure (e.g., a Wi-Fi access point). Then, when one of the mobile users moves into the coverage area of this access point, the data is transferred. The mobile user “1” can move, and, when it meets with another mobile user “2” who is interested in that data, the data can be directly transferred. As a result, the mobile user “2” does not need to have a direct connection with the Wi-Fi access point or a cellular base

station. The decentralized mobile social network is directly related to D2D communications, where the data transfer can be performed locally among users or devices by means of their mobility.

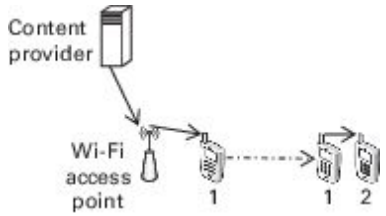

Figure 10.1. A decentralized mobile social network.

The typical components of mobile social networks are as follows.

- *Content provider:* The content provider's role is to supply data to users in mobile social networks (e.g., news feeders). The content provider can be a fixed dedicated server (e.g., a web server) connected to the Internet. The content provider can also be a gateway providing data collection from the Internet and transfer to the mobile users.
- *Mobile users/devices:* The mobile users or devices are the clients receiving data through different connections. In one way, the users can receive data from the content provider through a network infrastructure. In another way, the users can receive data from other users through local contact and direct data transmission. In this case, mobile users are not only the data consumers, but also data forwarders.
- *Network infrastructure:* The network infrastructure, both wired and wireless, provides a connection for data transfer between the content provider and mobile users. The network infrastructure could be a cellular network or a wireless local area network (WLAN).
- *Ad-hoc and opportunistic networks:* Instead of relying on the network infrastructure, data could be transferred using a multihop network (e.g., a mobile ad-hoc network). The data could be transmitted and routed through multiple nodes to the destination. Alternatively, the opportunistic network [326] can be used for data transfer in mobile social networks. As the mobile users move and meet each other, the data can be transferred. The use of an opportunistic network can reduce the cost of the cellular and wireless broadband connection. In addition,

due to the high transmission rate of a local connection, the opportunistic network can support the transfer of amounts of large data (e.g., a few GB), which cannot be efficiently and economically done through cellular networks. However, the shortcoming of the opportunistic network arises from its nature, i.e., mobility-driven, and the long delay of data transfer. Therefore, the opportunistic network is not suitable for delay-sensitive data transfer and dissemination.

10.2.2 Social-network analysis

Since mobile social networks rely on social relation and attributes for data delivery, the social-network analysis [327, 328] from social science becomes a useful tool to obtain such information. Furthermore, D2D communications can adopt social-network analysis to identify some important properties. These properties can be used to enhance the performance of data transfer and utilization of radio resources. Social-network analysis is an approach employed to analyze social relationships by using network and graph theory. A network composed of nodes and ties is constructed from the analysis. Each node represents an entity, while the ties represent relationships between entities. Each tie could be directed or undirected. A directed tie links between source and target (i.e., destination) entities. By contrast, an undirected tie links between entities in such a way that the direction of the relationship is not specified. Graphically, the directed and undirected ties are the lines with and without arrows, respectively. The ties may have different weights. The simplest form of the weight is "0" for no tie and "1" indicating the presence of the tie. The strength of a relationship can be represented by the weight. For example, the stronger the relationship, the larger the tie weight. Figure 10.2 shows examples of networks with directed and undirected ties and with weights of ties. In constructing a network, the ties among entities can represent a single type or multiple types of relation. The former and latter are referred to as simple and multiplex networks, respectively. In addition to representing a network using a graph, the social network can also be shown as a matrix. The rows and columns of a matrix represent the entities while the entries of the matrix represent relations or ties. An example of a matrix is expressed as follows:

	A	B	C	D
A	0	2	0	1
B	2	0	3	1
C	0	3	0	2
D	1	1	2	0

(10.1)

A network with directed ties can be represented in a similar way.

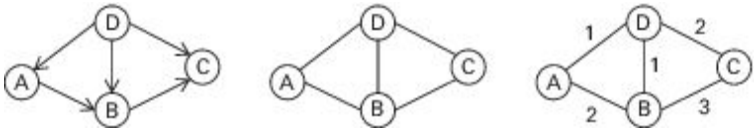

Figure 10.2. Networks with directed and undirected ties.

Some basic metrics of the network are as follows.

- *Size:* The network size could be determined by the number of nodes or the number of ties. The network size indicates the structure of the entities and their relationships. For a bigger network there are many entities with many relationships of interest. For example, in D2D communications, if the network size is large, there could be more devices sharing the same interest in data (e.g., video) to be transferred.
- *Density:* The network density is calculated from the number of actual ties divided by the number of all possible ties. Let n denote the number of nodes in a network. The numbers of all possible ties are $n(n-1)$ and $n(n-1)/2$ for networks with directed and undirected ties, respectively. The network density could indicate the network connectivity. Networks with high density tend to have more connectivity, which is useful for data dissemination. In D2D communications, if the network is highly dense, there will be more opportunity for transferring data. However, highly dense networks are susceptible to congestion.
- *Degree:* In an undirected network, the degree of a node indicates the number of ties that the node has. In a directed network, the tie can be an incoming link (in-degree) and an outgoing link (out-degree). Therefore, a node could be a source of ties by measuring the out-degree (i.e., the

number of outgoing links) and a target or a sink of ties by measuring the in-degree (i.e., the number of incoming links). In this case, the out-degree indicates how important the node is in terms of its influence on other nodes. By contrast, the in-degree indicates how much the node will be influenced by other nodes.

In addition to the above node-based metrics, some important metrics related to a network are as follows.

- *Distance between nodes:* The distance is measured by counting the minimum number of hops from one node to another node. The distance can indicate how easily one node will be reached by another node.
- *Path:* A path is a sequence of nodes and ties from a source to a target. For example, for the undirected network in Figure 10.2, there are the following paths from node A to node C: A → D → C and A → B → C with a length of 2, and A → D → B → C and A → B → D → C with a length of 3. A path and its length have many applications in data delivery (e.g., they are used to find the shortest path).
- *Eccentricity:* The eccentricity is the largest distance from one node to another node in a network.
- *Diameter of a network:* The diameter of a network is the maximum eccentricity for all the nodes in the network. In particular, it is the largest distance in the network, indicating the maximum number of hops that will be required in order to reach any node in the network. In other words, it is the minimum path length that can connect any pair of nodes in the network.
- *Radius:* The radius of a network is the minimum eccentricity for all nodes in the network. It is the smallest number of hops to cover the largest distance between any pair of nodes in the network. The diameter of the network is less than or equal to twice the radius.
- *Reachability:* The reachability of a pair of nodes in the network determines whether there is a path between the nodes or not. One node is reachable by another node if there exists a set of paths that connect them regardless of the number of hops.

The centrality is a commonly used social-network metric. The centrality of a node measures its structural importance or how much the node is considered to be a center of a network. For example, the centrality measures how much a node influences every other node in the same network. In this case, the importance of the node can be determined by invoking the concepts of degree, closeness, and betweenness. Again, the degree quantifies the importance of the node in terms of the number of its ties (i.e., a node with ties is more important). The closeness quantifies the importance in terms of the ability to reach other nodes in the network with a shorter distance. The betweenness quantifies the importance in terms of the location of the node between other nodes in the network.

Figure 10.3 shows an example network with degree centrality measure, which is the number of ties of each node. In this example, nodes C and E have the highest degree centrality since they have more ties with other nodes. While the degree centrality is a meaningful measure of the importance of the node, it relies only on a direct connection. However, it could also be useful to measure an indirect connection over multiple ties (e.g., data can be forwarded by intermediate nodes). This is the concept of closeness centrality, which measures the distance from each node to all other nodes. Basically, the closeness centrality is the sum of distances to all other nodes in the network. The closeness centrality of node i can be expressed as follows:

$$\frac{N-1}{\sum_{j=1}^{N} d(i,j)}, \tag{10.2}$$

where N is the total number of nodes and $d(i,j)$ is the shortest distance from node i to node j. Figure 10.4 shows an example network with closeness centrality measures. In this example, the closeness centrality of node A is obtained from $(7-1)/(1+1+2+3+4+4) = 6/15 = 0.4$, where $N = 5$ and the distances from node A to nodes B, C, D, E, F, and G are 1, 1, 2, 3, 4, and 4, respectively. The closeness centrality measures of other nodes can be calculated in the same way.

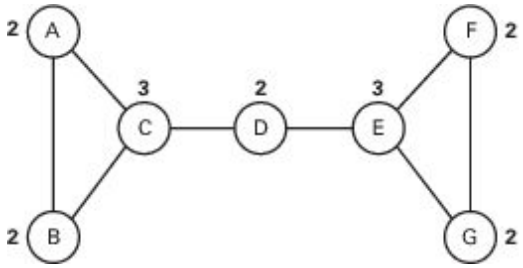

Figure 10.3. The degree centrality measure.

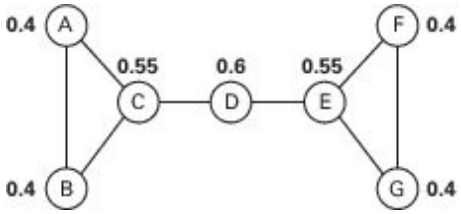

Figure 10.4. The closeness centrality measure.

The betweenness centrality measures how much a node is between other nodes. If the betweenness centrality of one node is high, this node will be important as an intermediate entity to the connections of all other nodes in the network. The betweenness centrality is calculated as the total number of occurrences for which the node is on the shortest paths between other nodes. Figure 10.5 shows an example network with betweenness centrality measures. In this example, the betweenness centrality of nodes A, B, F, and G is zero since these nodes are never on the shortest path of other pairs of nodes. Nodes C and E have the betweenness centrality of 8. Consider node C. Node C is in the shortest paths of the following pairs of nodes: A–D, A–E, A–F, A–G, B–D, B–E, B–F, and B–G. The betweenness centrality of node D is 9 since node D is in the shortest paths of the following pairs of nodes: A–E, A–F, A–G, B–E, B–F, B–G, C–E, C–F, and C–G. The normalized betweenness centrality can be obtained by dividing the number of occurrences for which the node is on the shortest paths between other pairs of nodes by the total number of shortest paths between other pairs of nodes in the network.

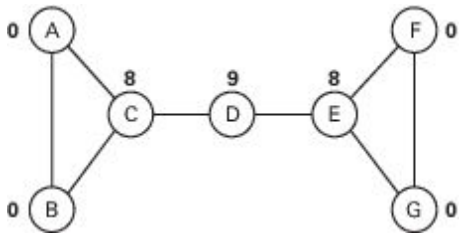

Figure 10.5. The betweenness centrality measure.

In addition to the above metrics, some other metrics such as the similarity and clustering coefficient are also useful in social-network analysis. The similarity metric measures how much two nodes have similar ties. In particular, if two nodes have similar ties to the other nodes, then the similarity metric is high for these two nodes. Considering the network shown in Figure 10.2, we can say that the similarity of nodes B and D is higher than that of nodes A and B. In this case, nodes B and D have an identical set of ties to other neighbors (i.e., ties to nodes A, D, and C), while node A has a different set of ties (i.e., node A has ties with nodes B and D).

The clustering coefficient measures how much nodes in a network tend to cluster together. In other words, the nodes have many ties with each other (i.e., there is a high density of ties among nodes). The clustering coefficient of a node can be defined as the number of pairs of other nodes (neighbors) connected by ties divided by the number of pairs of neighbors [323]. Consider node A in the network as shown in Figure 10.6. Node A has five neighbors (B, C, D, E, and F). Among these neighbors, three of them have ties with each other (i.e., B–C, C–D, and E–F). Since there are five neighbors, the total number of possible pairs of neighbors is

$$\binom{5}{2},$$

where “2” is for a pair of nodes. Therefore, the clustering coefficient is

$$\frac{3}{\binom{5}{2}} = \frac{3}{\frac{5!}{3!2!}} = \frac{3}{10} = 0.3.$$

To utilize social-network analysis in mobile social networks, the "contact graph" has to be built on the basis of the contact or encounter event [324]. A tie between nodes in the contact graph determines whether two nodes have encountered each other before or not. This past information can be used to predict that the nodes could encounter each other again in the future. The contact graph can be constructed for a certain period of time. The aggregated contact graph is a result of merging contact graphs of different times together. It has been shown that the aggregated contact graph and social graph (i.e., the graph capturing the actual social relation) could be statistically similar, depending on how the aggregated contact graph is created (e.g., one factor is the length of the time period) [329]. If an effective algorithm is applied, the aggregated contact graph can represent the social graph and can be used to analyze different social metrics as given above.

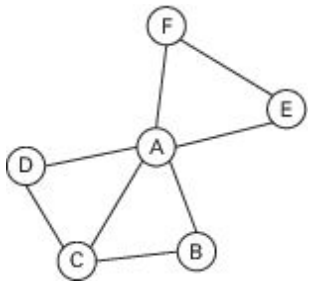

Figure 10.6. An example network for calculating the clustering coefficient.

10.3 Community detection

Since the mobile social network is composed of mobile users, it is important to group the mobile users together on the basis of some criterion. The community-detection mechanism [330, 331] is to determine clusters or groups of mobile users on the basis of social behavior, interests, and relationships. Using the clusters obtained from the community detection, the data forwarding can be optimized to achieve the objective of the mobile

social network. For example, mobile users belonging to the same organization can be grouped into the same cluster. As a result, if there is any data related to that organization to be disseminated, the data could be transferred and forwarded efficiently by the members of the same cluster. Community detection is similar to graph partitioning in graph theory. Graph partitioning aims to divide a network into subnetworks with some predefined size. However, community detection will use not only the edges among nodes as in graph partitioning, but also the social relationship and mobility to determine the clusters.

The community-detection mechanism can be divided into two major types, i.e., self-reported and detected network. In self-reported community detection, the mobile users will declare their social relationships among each other, so that the algorithm can use and determine suitable clusters. In this case, community detection can utilize available social information (e.g., from social-network services), where the users have to permit the information to be used. Alternatively, users can provide the social information needed by the community-detection algorithm only on an on-demand basis, without allowing the algorithm to access social information arbitrarily. By contrast, without social information having been provided, community detection can analyze various parameters (e.g., the mobility pattern) to determine the detected network. One of the commonly used approaches is based on the encounter traces and patterns of mobile users. Such parameters include the intercontact time, location, mobility pattern, contact frequency and duration.

The self-reported and detected-network community-detection mechanisms have their own advantages and disadvantages. Self-reported network detection incurs a lower data delivery cost since the mobile nodes will already know the social relation and attribute [332]. As a result, a mobile node does not need to spend time and resources to collate this information when building the routing table. The authors of [333] confirmed this fact by showing that a routing algorithm that utilizes available social information and profiles of mobile users can perform much better than when a dynamic algorithm to collect such information and build the social community is required.

10.3.1 Dynamic community detection

Different social metrics (e.g., modularity [334] and betweenness [335]) can be used in community-detection algorithms. However, the authors of [336] took a different approach by considering the "force" to determine communities. Specifically, they present an adaptive algorithm, called quick community adaptation (QCA), to detect the community structure of dynamic online social networks. Although the algorithm was developed for any social-network services (e.g., ENRON email and Facebook networks), its application to social-aware routing in mobile ad-hoc networks (MONETs) is also demonstrated. The dynamic algorithm has an advantage over the static community-detection algorithms (e.g., [334, 337]) in that the dynamic algorithm can adapt to the environment and parameter changes. In this case, under a dynamic environment, the static algorithms suffer from long convergence, especially for large-scale networks. A static algorithm can become trapped in a local optimum, and cannot confine the change to a local part of the network. These shortcomings are solved in the proposed QCA algorithm.

The main idea of the QCA algorithm is that, when the network evolves, the change is treated as a simple operation. The algorithm divides such operations into four types as follows.

- *Add new node:* A new node can be introduced into a network. There could be new ties associated with the new node.
- *Add new tie:* A new tie between nodes can be introduced.
- *Remove existing node:* An existing node can be removed from a network. The ties associated with the removed node will also be eliminated.
- *Remove existing tie:* An existing tie between nodes could be removed.

Figure 10.7 shows an example network with three existing communities (i.e., the first community is composed of nodes A, B, C, D, E, and F; the second community is composed of nodes G, H, I, and J; and the third community has only node K). When node A is removed, the ties with nodes B, C, D, E, and F will also be removed automatically. In this case, the first community

will be broken into two communities (i.e., one with nodes B, C, and D and another with nodes E and F). Alternatively, when the tie between nodes D and F is added, the strength of the first community will be improved (i.e., there will be more ties within the same community). By contrast, when the ties between nodes E and G and between nodes B and H are added, the first and second communities have more inter-community ties, making there be less strength within these communities.

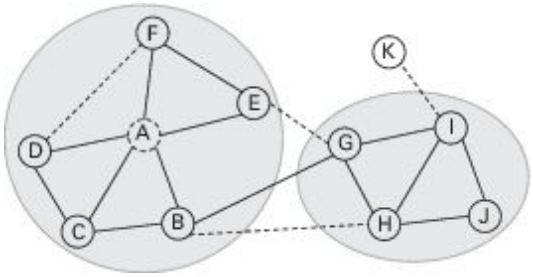

Figure 10.7. An example of adding or removing nodes.

Given the above intuition, the QCA algorithm is developed for four different operations, given that there are communities in a network.

Adding a new node: There are the following cases when a new node is added into the network.

- A new node has no ties. In this case, a new community will be defined for the new node, while the rest of the communities remain the same.
- A new node has a tie. In this case, the new node will join any community. The QCA adopts the physical approach [338]. In particular, similarly to gravity, the force will attract the new node to stay within or to join the community. The force is determined by the number of nodes and ties in each community. The node will join one community that has the highest force (e.g., a greater number of ties with the nodes in that community). It has been shown that using the concept of force to determine a community for a new node can improve the local gained modularity of the network.

Adding a new tie: A new tie linking a pair of nodes is introduced. There are again two cases.

- The new tie is within a community. In this case, a new tie is created between a pair of nodes in the same existing community (i.e., an intra-community link). Therefore, the new tie will strengthen the inner structure of the community, and the existing communities remain unchanged.
- The new tie is between communities. The new tie is created between two nodes in different communities. In this case, the new tie could change the community of the nodes. The criterion is defined on the basis of the number of ties and nodes in the communities to determine whether the node should change its community or not. An example shown in Figure 10.7 illustrates this case, where the tie between nodes I and K is created. In this case, node K could join the community of node I.

Removing an existing node: When the existing node is removed, the ties associated with this node will also be removed. The following consequences can happen.

- There is no change of the existing community.
- The community is divided into smaller communities. In this case, the new small community may be a standalone community, or it may join with another community.

To handle this case, the clique percolation method [339] is used. In this case, a 3-clique is applied to one of the removed node's neighbors. The clique is percolated until no node in the existing community is found. Then, the remaining communities (e.g., those resulting from dividing an existing community) will decide with which of other communities it would be best to merge.

Removing an existing tie: The following consequences can happen when one of the ties is removed.

- If one of the nodes associated with the removed tie has only one tie, then that node will become a singleton community.
- If the tie is between nodes in different communities, then removing the tie will strengthen the structure of existing communities. Therefore, there is no change to the existing communities.
- If the tie is intra-community (i.e., the tie links nodes in the same community), there are two possible outcomes. If the density of an existing community is high, there will be no change to the community. However, removing the intra-community tie can divide the existing community into smaller communities. The condition based on the maximum quasi-cliques within the existing community is used to determine whether the community should be divided or not.

The authors of [340] experimented with the QCA algorithm for identifying and updating the network community structure in social-aware routing algorithms. Specifically, the QCA algorithm is compared with the following algorithms.

- *WAIT:* In this algorithm, the source node waits and keeps sending or forwarding a packet until the packet has reached the destination node.
- *MCP:* A node keeps forwarding data until the packet has reached the maximum number of hops. Once this limit has been reached, the packet will be discarded.
- *LABEL:* A node forwards or sends a packet to all members in the destination community [341].
- *MIEN:* The social-aware routing algorithm from [342] is adopted.

The simulation evaluates the delivery ratio (i.e., the number of successfully delivered packets divided by the total number of packets), average delivery time (i.e., the time duration from when the packet is generated until it is received successfully by the destination), and average number of packets duplicated for each packet sent. The simulation results show that the QCA algorithm achieves better performance in terms of all metrics. This is due to the fact that the QCA can adapt to the structural change of the MONETs, which cannot be done efficiently by other algorithms.

10.3.2 Mobility-based distributed community detection

While the QCA algorithm proposed in [336] can be applied to any network, algorithms that take the mobility of nodes into account are also important. The authors of [343] propose a mobility-based distributed community-detection algorithm for delay-tolerant networks (i.e., opportunistic networks). Contacts between mobile nodes are used in the algorithm to detect communities. Specifically, the concepts of familiarity and regularity are introduced. The familiarity depends on the duration of contact between nodes (i.e., the longer the contact, the higher the familiarity). The regularity depends on the number of contacts (i.e., the higher the frequency of contact, the higher the familiarity). Using familiarity and regularity measures, the authors of [343] divide the relationship among mobile nodes into four categories (Figure 10.8).

- *Community:* Nodes in the same community must have high frequency and long duration of contacts. For example, employees in an organization will meet each other on a regular basis with long duration (e.g., in a business meeting).
- *Familiar stranger:* The nodes are defined to be familiar strangers if they meet each other frequently, but with a short contact duration. For example, customers of a book store could meet each other frequently in the store, but they do not know each other and hence the contact duration is short.
- *Stranger:* The nodes are strangers if they have infrequent and short contact.
- *Friend:* The nodes are friends of each other if their contact duration is long, but they meet infrequently. For example, friends usually meet a couple of times a week, but they spend an appreciable amount of time together.

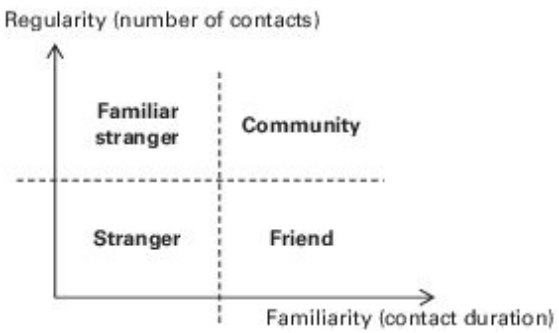

Figure 10.8. Relationship categories.

The first simple algorithm is based on a local community concept, which is defined on a familiar set. As an example, two nodes are classified to be in the familiar set if their contact duration is longer than a threshold value. Graphically, these two nodes will have a tie between them. The local community then is defined to contain all the nodes in its familiar set and their neighbors are selected by applying the proposed algorithm. The algorithm works as follows.

(i) The mobile node initializes by defining itself to be a local community.

(ii) If the node meets another node, they exchange mobility information regarding the network. The information includes a list of the nodes encountered and their contact durations, and the familiar set and local community of each node.

(iii) The node decides to include the contacting node in its familiar set or not (i.e., by checking the contact duration). Alternatively, the node could decide to include the contacting node in its local community.

The decision to add the contacting node to the community depends on the following different criteria.

- *SIMPLE:* The contacting node is added to the local community subject to the condition that the normalized size of a familiar set of the contacting node and the local community must be greater than a merging threshold.
- *k-CLIQUE:* The contacting node is added to the local community subject to the condition that the size of a familiar set of the contacting node and the local community must be greater than the number of members of the local community minus one.
- *MODULARITY:* The contacting node is added if the difference of local modularity between before and after adding the contacting node is above a certain threshold. The local modularity is defined on the basis

of the boundary set of the local community. Figure 10.9 shows an example of a local community, its boundary set, and the adjacent set.

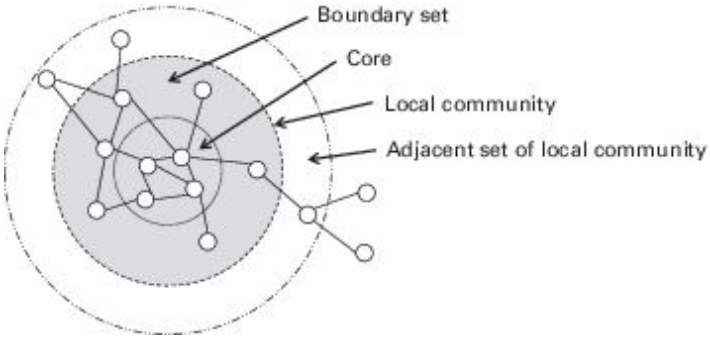

Figure 10.9. An example of a local community.

The performance evaluation of the proposed algorithms is based on the traces from the Cambridge Haggle Project [344], MIT Reality Mining Project [345], and UCSD wireless experiment [346]. In the Haggle Project, the mobility trace is based on two groups of students at the University of Cambridge. The Reality Mining Project distributes smart phones to students and staff at MIT for 9 months. The smartphone keeps the mobility log through Bluetooth and cellular interfaces. In the UCSD wireless experiment, personal digital assistants (PDAs) are used to keep the visibility of Wi-Fi access points, which is capable of detecting device-to-device transmission opportunity.

To verify the ability to detect communities, similarity measures that are based on the fraction of vertices correctly identified [330] and normalized mutual information [331] measures are used. The results show that *k*-CLIQUE and MODULARITY perform better than SIMPLE, which is as expected due to the consideration of network-wide parameters rather than just the contact duration used in SIMPLE.

10.3.3 Influence-based community detection

While the above community-detection methods are general and can be applied to any application, in some cases the community detection can be

designed with a specific purpose. In this case, dissemination of data and information is the most important application, and the community detection can be developed by considering the influence of nodes in a network to support data delivery. Influence can be defined in different ways, e.g., "word-of-mouth," which reflects the ability of some people to recommend a product to their friends or other people [347]. The classical approach is the influence-maximization problem [348], which aims to find a set of nodes (e.g., k nodes) in a network that maximize the spread of data dissemination. The influence-maximization problem can be formulated as an optimization problem, but it has been shown to be NP-hard, meaning that it is difficult to solve [349]. Some heuristic algorithms based on a greedy method are also considered (e.g., cost-effective lazy forward (CELF) in [350], MixedGreedy in [351], and community-based greedy algorithm (CGA) in [352]).

In mobile social networks and D2D communications, this problem is important since it can reduce the radio-resource usage and improve the speed of data transfer. The authors of [352] discuss the idea of finding a set of the most influential nodes in mobile social networks and propose the community-based greedy algorithm (CGA). The mobile social network considered in [352] is composed of mobile phones as nodes. A tie corresponds to communication between nodes. Therefore, the network can be represented as a directed weighted graph. A node has two states, i.e., active and inactive. An active node can influence (i.e., transfer data to) other inactive, neighboring nodes. Furthermore, an active node can be influenced by other active nodes. The influence can be quantified by the "diffusion speed," which depends on the weight of the graph. Let $w_{i,j}$ be the weight of a directed tie from node i to node j. Then, the diffusion speed is defined as follows:

$$\lambda_{i,j} = 2\overline{\lambda}\frac{w_{i,j}}{w_{\max} + w_{\min}}, \tag{10.3}$$

where $\overline{\lambda}$ is the average diffusion speed of the network. $w_{\max}$ and $w_{\min}$ are the maximum and minimum weights in the network, respectively. The degree of influence is measured as the number of nodes influenced by a set of active nodes divided by the total number of nodes in the network.

The main idea of the CGA is that the network is divided into communities. Then, the k most influential nodes within the communities are chosen. The community is defined on the basis of the frequency of contacts. Nodes in the same community will frequently encounter each other, while nodes in different communities will encounter each other much less often. The algorithm proceeds to choose from which community to obtain the k most influential nodes. A simple algorithm based on dynamic programming is proposed to choose communities. First, the increase of influence when the community is selected is computed. On the basis of the increase of influence associated with each community, a certain number of communities will then be selected. Then, k nodes are chosen from this set of communities. To choose the most influential nodes, the MixedGreedy algorithm [351] is adopted.

Community detection is an integral part of the CGA. The authors of [352] propose two steps, i.e., community partition and combination.

- *Community Partition:* First, each node is assigned a unique community label. Then, each node computes a set of its influenced neighbors according to a diffusion speed calculation. Then, the community label of each node is propagated to other nodes in the network. This propagation is performed within a limited number of iterations by deciding that a node should be a member of the community which contains the maximum number of its influenced neighbors.
- *Community Combination:* While the community-partition step is used to determine communities for nodes in a network, the community-combination step is used to decide whether any communities can be merged. The idea is to compute the community-combination entropy between communities. If this entropy is above the threshold, then the communities will be merged. Here the combination entropy is defined as the maximum ratio between the degree of influence of the node outside the community divided by the degree of influence of the node inside the community.

The performance evaluation is performed for the CGA using the detailed call-record data obtained from the largest mobile communication service

provider in China. The data set contains more than 700 000 nodes. The experimental results show that the CGA not only achieved a faster speed, but also detected more stable communities.

After the community detection has been done, nodes in mobile social networks can utilize the community information to facilitate data routing and dissemination for D2D communications. In the following section, we discuss some seminal work on social-aware data-routing and -dissemination schemes.

10.4 Social-aware data routing and dissemination

Data and information distribution is the most important issue in mobile social networks and also D2D communications. An important component of any means of data and information distribution is the need to find the best forwarding node to improve the delivery performance (i.e., provide a high success ratio and small delay). This is also referred to as a routing problem. However, in mobile social networks, this issue becomes more challenging due to the mobility, opportunistic contact among nodes, limited radio resources, and diverse network components. To overcome these limitations, social information of nodes in a network can be used in data routing and dissemination. The social information can be the detected community and other social metrics. The typical approach to data routing and dissemination in mobile social networks is optimization. Note that, since the mobile social network is composed of opportunistic networks, the routing protocols developed for opportunistic networks can be adopted [324].

In delay-tolerant networks (DTNs), routing protocols are based on "store" and "forward" mechanisms. That is, nodes receive and store data in their memory. When the nodes move and meet each other, the data can be transferred to other nodes as the next hop. Three types of routing protocols exist [324].

- *Message-ferry-based protocols:* In the message-ferry-based protocols, there are some dedicated nodes that perform data routing to perform data delivery. The mobility of these nodes can be controlled and

optimized to achieve the optimal performance. However, having the dedicated nodes could introduce an extra cost into the network.

- *Opportunity-based protocols:* In these protocols, data is transferred upon random contacts of nodes. Since the nodes may encounter each other randomly, there is no certain performance guarantee of data delivery. Therefore, multiple copies of data will be generated to increase the chance of successful delivery.
- *Prediction-based protocols:* Some mobility and other nodes' parameters could be estimated and used to determine a suitable data-forwarding policy. For example, data should be forwarded to a node that has recently met a destination.

Different routing metrics (e.g., delivery probability, available network resource, and mobility pattern) could be defined for the routing protocols for DTNs. However, it is likely that mobile nodes in DTN could have social relationships (e.g., among humans). Therefore, routing protocols that take social metrics into account have been developed.

10.4.1 A routing protocol based on betweenness and similarity

The authors of [353] presented one of the first routing protocols, called SimBet, using social-network analysis for DTNs. The main idea is to identify bridge nodes on the basis of their centrality measures (i.e., egocentric betweenness and similarity). The bridge nodes have the capability to deliver and exchange data among disconnected nodes. Firstly, the centrality measures are calculated on the basis of a contact graph. The ties in the contact graph are presented in the adjacency matrix denoted by $\mathbf{A}$ whose element $A_{i,j}$ is defined as follows:

$$A_{i,j} = \begin{cases} 1, & \text{if nodes } i \text{ and } j \text{ have contact,} \\ 0, & \text{otherwise.} \end{cases} \tag{10.4}$$

The size of the adjacency matrix $\mathbf{A}$ is $N \times N$, where N is the number of nodes in a network. It is assumed that the contact is bidirectional, i.e.,

$A_{i,j} = A_{j,i}$. In this case, the egocentric betweenness of a node i is calculated from

$$B_i = \mathbf{A}^2[1 - A]_{i,j}. \tag{10.5}$$

If there is a new node in the network, the new node will send a list of nodes that it has encountered to other nodes. All the nodes in the network update their betweenness metrics accordingly.

The similarity metric is calculated from

$$S_{i,j} = |N(i) \cap N(j)|, \tag{10.6}$$

where $N(i)$ is a set of neighbors of node i. The use of similarity is based on the fact that, if two nodes share similar groups of neighbors, the chance that two nodes will be contacted by the same neighbor is higher. Consider the example network shown in Figure 10.10. In this case, the similarity metrics of node A with nodes B, C, D, and E are 2, 2, 3, and 3, respectively.

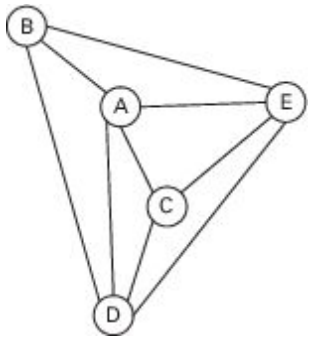

Figure 10.10. An example network for calculating similarity.

Now, to select the best carrier to forward data, the utility function of node i to destination d is defined from betweenness and similarity metrics as follows:

$$U_i(d) = w_1 \frac{S_{i,d}}{S_{i,d} + S_{j,d}} + w_2 \frac{B_i}{B_i + B_j}, \tag{10.7}$$

where w_1 and w_2 are the weights for similarity and betweenness, respectively.

Given the utility, the SimBet routing algorithm works as follows.

(i) When node *i* meets node *j*, node *i* sends a "hello" message to inform node *j* that they are neighbors of each other.

(ii) If node *j* is a destination of the data kept by node *i*, then node *i* simply sends the data to node *j*. Otherwise, node *j* replies to node *i* by sending it a list of nodes that it has encountered.

(iii) Node *i* uses this list to update betweenness and similarity metrics, and so does node *j*.

(iv) Nodes *i* and *j* exchange lists of the destination nodes which they have the data for as well as the betweenness and similarity metrics to those destination nodes.

(v) For each destination node, nodes *i* and *j* calculate the utility. If node *i* has a utility to the destination node higher than that of node *j*, the destination node is added to the list of node *i*. Node *j* forwards the data to node *i* and removes this data from its buffer.

A simulation was conducted to evaluate the performance of the SimBet routing protocol, where the mobility trace from the MIT Reality Mining Project [345] is used. The protocol is compared with the epidemic protocol. The simulation results show that the SimBet protocol can achieve approximately the same number of messages successfully delivered but with a much lower number of forwards (i.e., less resources used for data forwarding). However, using the SimBet protocol incurs a longer end-to-end

delay and a greater number of hops because the protocol limits the neighbors to which one can forward the data.

10.4.2 A routing protocol based on community and degree centrality

Instead of using a similarity metric as in the SimBet protocol, the authors of [354] proposed the BUBBLE protocol, which uses the community and degree-centrality measures to optimize data forwarding in DTN. The protocol was designed with the intuition that people generally form communities in their society depending on interests and relationships (e.g., communities involving co-workers or family members). Furthermore, inside the community, people have different roles and ability to make contact with others. Therefore, in the BUBBLE algorithm, the mobile nodes will be first clustered into communities. Then, from the community, some important nodes will be selected for data forwarding.

Before data will be forwarded, the following information must be prepared. Firstly, a node must belong to one of the communities only. Secondly, a node must be ranked in terms of popularity (i.e., degree centrality). The degree centrality is basically the number of direct neighbors which have direct contact with the node. By defining based on the degree centrality, popularity reflects the ability to forward data of a particular node. There are two ranks, i.e., local in a community and global among communities. Then, when the node has data to transfer to a destination, the node will refer to the global rank and forward (i.e., "bubble") the data to the more popular node. Until the data has reached a node in the same community as the destination, the node receiving the data will refer to the local rank and forward the data to a node with greater popularity. The bubble process terminates when the data reaches the destination or the maximum delay is reached. The advantage of this process is that a node does not need to know and maintain information about a global network. Merely local information can be used to decide on data forwarding.

Consider Figure 10.11 as an example. Node A wants to transfer data to node J. There is one predefined community composed of nodes F, H, I, and

J. The size of circle determines the popularity of nodes (i.e., the bigger the circle, the higher the popularity). In this example, node A forwards the data to nodes B and C, since they have higher popularity. However, node B will not forward the data to node D since node D has lower popularity. Node C will forward the data to node E. Then, node E will forward the data to node F, since node F is in the same community as node J (i.e., the destination), even though the popularity of node F is lower than that of node E. Next, node F forwards the data to nodes I and, subsequently, J.

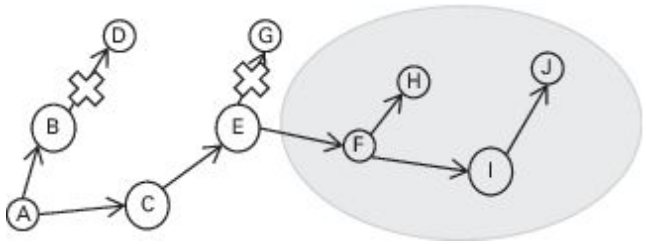

Figure 10.11. An example BUBBLE protocol.

The BUBBLE protocol adopts the *k*-clique algorithm [355] or weighted-network analysis [356] depending on whether the network under consideration is unweighted or weighted, respectively. For the weighted-network analysis, the modularity is used to determine the strength of a community. The modularity is defined as follows:

$$M = \sum_{i,j} \left(\frac{W_{i,j}}{2m} - \frac{k_i k_j}{(2m)^2} \right) \delta(c_i, c_j), \tag{10.8}$$

where $W_{i,j}$ is the weight of the edge between nodes i and j. $m = \frac{1}{2}\sum_{i,j} W_{i,j}$ and k_i is the degree of node i (i.e., $k_i = \sum_j W_{i,j}$). C_i is the community of node i, and

$$\delta(c_i, c_j) = \begin{cases} 1, & i = j, \\ 0, & \text{otherwise.} \end{cases} \tag{10.9}$$

In the performance evaluation, the mobility traces from various sources are used (e.g., the Cambridge Haggle Project and MIT Reality Mining

Project). The BUBBLE protocol has been compared with the PROPHET protocol [357] which relies only on the encounter history and mobility to calculate the probability that a node can deliver data to a destination. The simulation results show that the BUBBLE protocol achieves a similar successful-delivery ratio (i.e., ratio between the number of successfully delivered messages and the total number of messages delivered) to that of the PROPHET protocol. However, using the BUBBLE protocol incurs much fewer copies of the same data begin delivered, leading to less resources being used.

10.4.3 Friendship-based routing

The authors of [358] introduced the use of friendship among mobile nodes (i.e., users) to facilitate data routing in DTN. Unlike community-based routing (e.g., the BUBBLE protocol), this friendship-based routing protocol relies on the interrelationship between nodes. The interrelationship depends on the opportunistic contact in DTN.

The authors of [358] highlight that using any contact statistic (e.g., encounter frequency, total or average contact period, and average separation period) individually might not well represent the interrelationship between two nodes. Figure 10.12 shows six encounter scenarios between two nodes *i* and *j*, where a grey box is an encounter event. The following are observed from these scenarios.

- In cases (a) and (b) of Figure 10.12, the encounter frequencies are the same (i.e., four per unit time). However, the contact period in case (b) is longer than that in case (a). As a result, case (b) is more suitable for transferring data.
- In cases (b) and (c) of Figure 10.12, the encounter durations are the same, while the encounter frequency of case (c) is twice that of case (b). If the amount of data is not too large, case (c) will be more suitable for data transfer since node *i* does not need to wait too long to encounter node *j*.
- In cases (c) and (d) of Figure 10.12, the encounter duration and frequency are the same. However, the uniformity of encounter events of case (c) is higher than that of case (d). As a result, case (c) is preferable

due to the even distribution and greater predictability of an encounter event.

- In Figure 10.12, using an average separation duration cannot distinguish among cases (b), (e), and (f) if $t_1 = t_2 = t_3$. Apparently, cases (b) and (e) might be preferable. However, it is indistinguishable whether case (b) or case (e) is more suitable for data transfer.

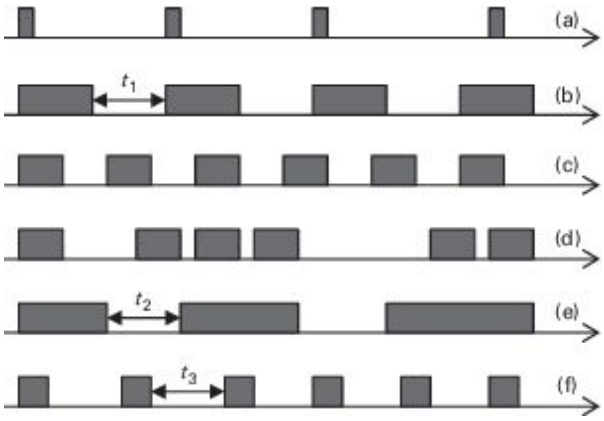

Figure 10.12. Different inter-encounter patterns.

Given the above observations, the authors of [358] suggested that the link quality (e.g., the strength of friendship) should be long in duration, and high and even in frequency. With this consideration, case (c) of Figure 10.12 will be the most suitable for data transfer. Formally, the authors of [358] introduced a new social metric, called the "social pressure metric" (SPM), which measures the social pressure in terms of friendship (i.e., the tendency to meet and share data). The link quality is defined on the basis of the SPM as follows:

$$w_{i,j} = \frac{1}{\text{SPM}_{i,j}} = \frac{T}{\int_{t=0}^{T} f(t)dt}, \tag{10.10}$$

where T is the time period of interest, and $f(t)$ is a function of the remaining time to the first encounter between nodes i and j after time t, which is

initialized to be zero. Clearly, the link quality $w_{i,j}$ increases as the friendship between nodes i and j becomes closer (i.e., stronger tie strength).

However, data might need to be transferred over multiple nodes to a destination. In this case, the authors of [358] additionally introduced the concept of community with friendship. The community is established by comparing the link quality with a threshold τ. A node is included in a community if it has a link quality higher than the threshold. The community is defined beyond the direct encounter between two nodes. In this case, nodes having friends in common can be classified as close indirect friends. As a result, a new metric, called the conditional SPM (CSPM), between two nodes is defined. Consider nodes i, j, and k, where nodes i and k need not be close direct friends of each other. However, nodes i and k could be the close friends of node j. The CSPM denoted by $\text{CSPM}_{j,k|i}$ is the average time taken for node j to transfer data received from node i to node k. The community of friends of node i is defined as follows:

$$F_i = \{j | w_{i,j} > \tau, i \neq j\} \cup \{k | w_{i,j,k} > \tau, w_{i,j} > \tau, i \neq j \neq k\}, \tag{10.11}$$

where the indirect link weight is given by

$$w_{i,j,k} = \frac{1}{\text{SPM}_{i,j} + \text{CSPM}_{j,k|i}}. \tag{10.12}$$

Unlike the SPM, which can be computed from local encounter information of a node, the CSPM requires periodic exchange of encounter information among multiple nodes. The SPM and CSPM can be computed at the steady state (e.g., for periods of many days). However, they could suffer from transient behavior of mobile nodes. Therefore, the authors of [358] proposed to compute the SPM and CSPM for different periods of a day (e.g., morning, afternoon, and evening), which will help these metrics to quantify the actual friendship more accurately.

If node *i* has data to transfer to node *d*, the data forwarding (i.e., routing) works as follows. If node *i* meets node *j*, then the data is forwarded from node *i* to node *j* only if node *j* is in the same friendship community as node *d* and node *j* has stronger friendship to node *d* than does node *i*. This forwarding rule ensures that node *j* will receive the data from node *i* only if it is classified to be in the same community as the destination. Otherwise, node *i* will keep its data and wait for other nodes to encounter.

The performance evaluation of the friendship-based routing was done using the mobility trace from the MIT Reality Mining Project. A comparison with epidemic, PROPHET [357], and SimBet [353] protocols was provided. The simulation results show that the friendship-based routing achieves a higher data-delivery rate than that of PROPHET and SimBet but still lower than that of the epidemic protocol. This is due to the fact that friendship-based routing can better classify the interrelationship between nodes. In terms of the cost (i.e., number of forwards), friendship-based routing is similar to SimBet and much less costly than epidemic and PROPHET. It is highlighted that the friendship-based routing achieves the highest ratio between delivery rate and cost.

However, most of the works related to social-aware routing do not take the location information of mobile nodes into account. The location information can be helpful in determining the social community and optimizing the data routing and dissemination, as we will discuss in the following.

10.4.4 Geocommunity-based routing

The authors of [359] argue that the social ties and community among nodes are highly correlated with a location. For example, students in the same class will have a very high probability of meeting each other regularly with long duration in the same classroom. Therefore, when computing a centrality metric and detecting a community, the geographical information must be taken into account. The authors of [359] introduced a new location-based social metric and community-detection mechanism, i.e., geocentrality and geocommunity. They also considered the scheduling of data distribution to

destinations by an entity called a "supernode." The supernode aims to distribute data to other nodes in the networks by moving among different locations. Figure 10.13 shows an example scenario.

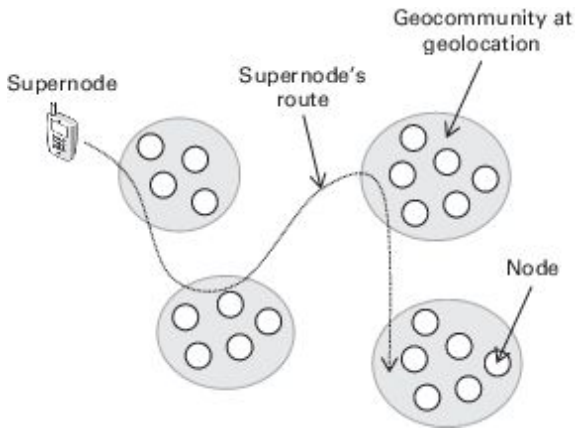

Figure 10.13. Geolocations, geocommunities, and supernode routing.

Firstly, the geocommunity concept is introduced as a cluster of mobile nodes that are tightly linked to each other. The link could be direct or indirect (e.g., through other nodes). The community can be associated with geolocation. In this case, the "contact user set" of a geolocation l is defined for time period $[t_1, t_2]$. This is the set of user i whose sojourn time $T_{i,l}$ at geolocation l is larger than a threshold τ. Then, a set of geolocation l with regular user mobility is defined as the "contact geolocation set." In this case, a node can belong to different geocommunities, but it will be in just one geocommunity at any time. The authors of [359] also introduced the geocentrality metric. This metric measures the probability that a particular mobile node in a network will be in a geocommunity (i.e., at the corresponding geolocation). The geocentrality of a geocommunity k is defined as follows:

$$C_k(t_k) = 1 - \frac{1}{N}\sum_{i=1}^{N}(1 - \phi_{i,k})^{t_k}, \tag{10.13}$$

where N is the number of nodes in the network, and $\phi_{i,k}$ is the steady-state probability per unit time that node i will be in geocommunity k. The

geocentrality $C_k(t_k)$ is basically the average probability that any node in the network will be in geocommunity k within time duration t_k.

After the geocommunity at a geolocation and its geocentrality have been computed, the route of the supernode to perform data distribution can be optimized. The authors of [359] considered the case that the supernode will visit different geolocations and try to distribute data to the nodes or members of the geocommunities (Figure 10.13). However, since the nodes may be in any geocommunity randomly due to their mobility, the supernode has to decide how long to stay in each geocommunity and in which order to meet a data-distribution requirement. This scheduling can be formulated as an optimization problem to choose the waiting time t_k and order for the supernode to be in geocommunity k. The static and greedy adaptive route algorithms are proposed.

In the static route algorithm, there could be two formulations for the supernode, i.e., to minimize the total duration of a route or to maximize the data-distribution ratio. The algorithm is divided into two steps, i.e., to choose the geocommunities and to construct a route through them. In the first step, the geocommunities are chosen using the traveling-salesman problem. Then, the waiting time in each geocommunity is optimized using the following optimization formulation:

$$\min \quad \sum_{k=1}^{K} t_k, \tag{10.14}$$

$$\text{s.t.} \quad \sum_{k=1}^{K} C_k(t_k) \geq p \tag{10.15}$$

$$t_k \geq 0, \quad k = 1, \ldots, K, \tag{10.16}$$

where K is the total number of geocommunities and p is the total data-distribution ratio. In this case, the term $\sum_{k=1}^{K} t_k$ is the total duration of the

route of the supernode, which is to be minimized. The constraint is to ensure that the data-distribution ratio is above the requirement. This optimization problem can be transformed into a convex optimization problem (i.e., by taking a logarithmic function of the constraint). Therefore, a standard solver can be applied to obtain an optimal solution efficiently.

By contrast, the supernode can optimize to achieve the maximum data-distribution ratio. The optimization problem is formulated for this case as follows:

$$\max \quad p = \sum_{k=1}^{K} C_k(t_k) \tag{10.17}$$

$$\text{s.t.} \quad \sum_{k=1}^{K} t_k + T_t(t_0, t_1, \ldots, t_K) \leq T \tag{10.18}$$

$$t_k \geq 0, \quad k = 1, \ldots, K, \tag{10.19}$$

where T_t is the total traveling time that the supernode spends to visit geocommunities. The objective here is to maximize the geocentrality, which is equivalent to the data-distribution ratio. The constraint is to ensure that the total route duration is maintained below the maximum time T. This optimization can be reformulated as a knapsack problem by considering the geocentrality-to-traveling-time ratio defined for each geocommunity. This ratio can be referred to as the efficiency of a community. The knapsack algorithm is applied where the traveling time from one community to another community is chosen and put in the knapsack.

Unlike the static route algorithm, which assumes that all geocentralities are fixed, the greedy adaptive route algorithm is developed to allow dynamic updating of geocommunity. Using the optimization formulations to minimize the total duration of a route or to maximize the data-distribution ratio, in the adaptive route algorithm, the supernode visits a geocommunity and then

gradually updates its decision to wait for data distribution and moves to the next geocommunity. Therefore, the supernode can adjust its decision dynamically without assuming a-priori information.

In all of the social-aware data routing and dissemination, the radio-resource usage is not taken into account. However, in reality, data transfer requires radio resources for wireless transmission among mobile nodes. In the next section, we will discuss how the radio-resource (i.e., bandwidth) allocation affects the content distribution, where the content can be transferred through the network infrastructure (i.e., a base station) and opportunistic contacts among mobile nodes.

10.5 Cooperative content delivery in mobile social networks

In this section, we introduce cooperative data delivery in mobile social networks. The authors of [360] considered a mobile social network, whose content delivery uses not only a broadband connection from an access point, but also a local connection when mobile nodes move and encounter one another. The benefit of such a content-delivery scheme is that it reduces the radio-resource usage of the access point. As a result, the cost for content providers can be lowered by exploiting the social relations and physical mobility of the mobile users. The authors of [360] considered the issue of wireless-connection sharing of the content providers in such a mobile social network. Furthermore, the rationality and self-interested behavior of a network operator allocating radio resources in terms of the bandwidth are taken into account. Specifically, multiple content providers can buy a wireless connection from a network operator so as to deliver content to the mobile nodes of subscribers. The content providers can cooperate by forming coalitions to efficiently share the wireless connection and forward content. Despite achieving a lower cost due to connection sharing, the performance of content distribution may be degraded (e.g., due to a greater delay). For the network operator, the amount of bandwidth allocated to a wireless connection used by content providers can be controlled so that its revenue is maximized. The scenario under consideration is shown in Figure 10.14.

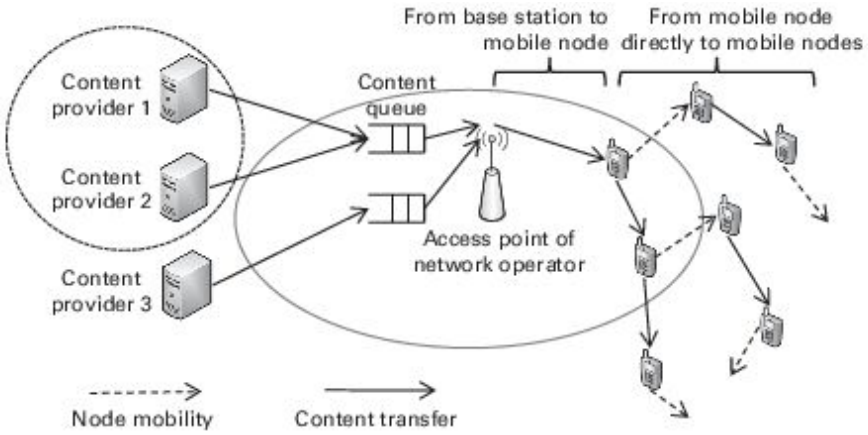

Figure 10.14. The system model of cooperative data delivery in mobile social networks.

To address the above issues, the authors of [360] introduced the concept of a *controlled coalitional game*. This game jointly addresses the cooperative content forwarding and bandwidth sharing of multiple content providers, and the bandwidth allocation of a network operator. This game consists of a coalition-formation subgame among the content providers and an optimization formulation for the network operator. In this game, the network operator can effectively "adjust" its own action to control the coalition formation of the content providers. This game is similar to the Stackelberg framework (i.e., a hierarchical optimization model); the proposed controlled coalitional game can be used to obtain a solution for the scenarios where these two formulations are interrelated and depend on each other. The structure of this game is shown in Figure 10.15. In the following, the detail of different analytical models proposed in [360] will be presented.

- An analytical model for cooperative content forwarding among heterogeneous groups of mobile nodes that are subscribers to different content providers is introduced. Since the mobile nodes that are subscribers to different content providers may have a varied mobility behavior, a multi-dimensional absorbing Markov chain [361] is used to obtain important performance metrics of the content delivery, including the delay for content forwarding and the probability of receiving the content within the deadline for all subscribed mobile nodes.
- A general coalition-formation game among content providers with a composite strategy of cooperative content forwarding and bandwidth

sharing is developed. Along with the composite strategy of coalition formation (e.g., coalitions of content forwarding and bandwidth sharing can be formed jointly or independently), a two-dimensional Markov chain [361] is used to analyze the dynamics of coalition formation and to obtain the stable coalitional state of the content providers.

- Given the dynamics of coalition formation of the content providers, the optimization model used by the network operator to allocate bandwidth to the wireless connection is presented. This constrained Markov decision process (CMDP) optimization model is used to maximize the revenue of the network operator. The constraint on the QoS requirement of the network operator's nodes is imposed. The optimal policy can be obtained from this optimization model. The policy provides a mapping from a coalitional state to the amount of bandwidth allocated.

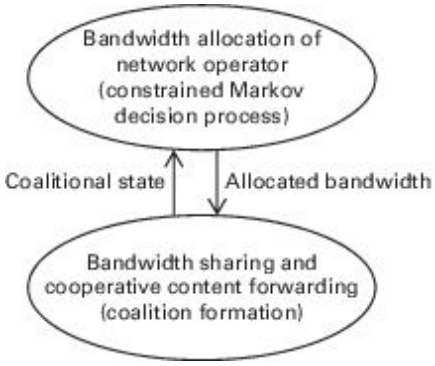

Figure 10.15. The optimization structure of the cooperative data-delivery scheme.

10.5.1 Mobile social networks with content providers and a network operator

The mobile social network under cooperative content delivery is composed of the following components.

- *Content providers:* In the mobile social network, there are I content providers or "providers." We denote by $\mathcal{I} = \{1, \ldots, I\}$ the set of all providers. These providers create a content for their subscribed mobile nodes (e.g., news, business data, and mobile applications). To transfer content, each content provider uses a wireless connection of an access

point. The access point belongs to a network operator. The objective of the content providers is to minimize the cost of content distribution, which is a function of the content-distribution delay, the bandwidth usage, and the content-forwarding overhead.

- *Network Operator:* A network operator provides a wireless data-transfer service (i.e., a wireless connection) to the content providers. There is a queue at the access point of the network operator to buffer the content received from the providers. The content in the queue is transferred to the mobile nodes by the access point (e.g., using broadband wireless access) in a first-in, first-out fashion. The network operator can control the amount of bandwidth b (i.e., the number of channels) allocated by the access point for transferring content to the mobile nodes in the coverage area. The price charged for each wireless connection is denoted by $b\theta$, where θ is a price constant. Note that the available bandwidth at the access point is shared by mobile nodes subscribed to the content provider and "normal nodes," i.e., nodes that are not part of the mobile social network. The objective of the network operator is to maximize the revenue from selling wireless connections to content providers. At the same time, the QoS performance of the normal nodes is maintained at a given threshold.
- *Mobile nodes:* For any content provider $i \in \mathcal{I}$, there are N_i subscribed mobile nodes. However, only U_i subscribed mobile nodes will receive the new content via the access point (i.e., $U_i < N_i$). The rest of the mobile nodes can obtain the content via direct transfer from other nodes. In particular, the content can be transferred directly between the subscribed mobile nodes when they move and encounter each other.

It can be assumed that the transmission rate of direct content transfer between mobile nodes (i.e., from the opportunistic contact) is much larger than that between an access point and mobile node. This is due to the fact that the wireless connection between mobile nodes is from the local network, while that between the access point and mobile node is based on the broadband wireless access network, which is expensive and speed-limited (e.g., Wi-Fi and 3G cellular networks, respectively).

To model the decision-making process between the content providers and a network operator, where they have different objectives (i.e., to

minimize their cost and to maximize its revenue given the QoS constraints, respectively), we formulate a hierarchical optimization model, referred to as the *controlled coalitional game*. The controlled coalitional game is similar to the Stackelberg game. In this model, the *leader* is the network operator and the *followers* are the content providers. The leader can announce its strategy before the followers make their strategy choices (Figure 10.15). As a leader, the network operator can optimize its reward (i.e., revenue) by controlling its action (i.e., amount of allocated bandwidth) given the state of the followers. The followers can observe the action of the leader and adapt their strategies (i.e., coalition formation) so as to minimize the cost. The coalition formation of followers is divided into two parts, i.e., cooperative content forwarding and bandwidth sharing. For cooperative content forwarding, a coalition $\mathcal{F}$ is formed among the content providers in which their subscribed mobile nodes will forward the content between themselves. For bandwidth sharing, a coalition $\mathcal{B}$ is formed between the providers to share the allocated bandwidth (i.e., a wireless connection) of the network operator's access point. In general, the coalition of bandwidth sharing $\mathcal{B} \subseteq \mathcal{I}$ can be different from that of content forwarding $\mathcal{F} \subseteq \mathcal{I}$.

The controlled coalitional game is decomposed into two interrelated problems to obtain the optimal action and strategies of leaders and followers. The first problem is an optimization based on a constrained Markov decision process (CMDP) for the network operator. The second problem is a coalitional game for the content providers. With this structure, the optimal action of the network operator is obtained, given the coalitional structure of the content providers. Furthermore, the coalitional state transition of the content providers is controlled by the action of the network operator.

10.5.2 The Markov chain model of content forwarding among mobile nodes

To analyze the performance of content-delivery services offered by content providers, the analytical model based on an absorbing continuous-time Markov chain is presented. The model is for content forwarding among the mobile nodes.

State space

We consider the content-forwarding process of the mobile nodes subscribed to content provider i. This content provider belongs to (i.e., is a member of) coalition $\mathcal{F} \subseteq \mathcal{I}$ (i.e., $i \in \mathcal{F}$). The number of members of coalition $\mathcal{F}$ is $|\mathcal{F}|$, where $|\cdot|$ denotes the cardinality of a set (i.e., coalition). In other words, $\mathcal{F}$ is a set of content providers that cooperate by allowing the mobile nodes of their subscribers to forward each other's content.

We introduce an absorbing continuous-time Markov chain to analyze the performance of the content-forwarding process of the cooperative content providers. The content is forwarded from the access point to mobile nodes. One important performance metric is the delay, which is measured from when the access point finishes transferring its content to the mobile nodes to when all mobile nodes of provider i receive the content (or when the deadline is reached). Therefore, we define the state of the content-forwarding process as the number of mobile nodes that have already received the content from provider i. The states can be further divided into the *transient state* and the *absorbing state*. The transient state is the state in which not all mobile nodes of provider i have received the content, and the absorbing state is the state in which all of the mobile nodes of provider i have received the content.

The state space of the transient state can be defined as follows:

$$\Delta_{i,\mathcal{F}} = \mathbb{M}_i \times \prod_{j \in \mathcal{F}, j \neq i} \mathbb{N}_j, \tag{10.20}$$

where both $\times$ and $\prod$ are Cartesian products. Set $\mathbb{M}_i$ is defined as $\mathbb{M}_i = \{1, \ldots, N_i - 1\}$. Set $\mathbb{N}_j$ is defined as $\mathbb{N}_j = \{0, \ldots, N_j\}$. The absorbing state can be defined as follows:

$$\delta_{i,\mathcal{F}} = \{N_i\}, \tag{10.21}$$

where N_i is the total number of mobile nodes subscribed to content provider i.

The transition matrix

Mobile nodes first receive content from an access point. Then, the mobile nodes transfer/forward this content directly to other nodes as they move and encounter one another. We assume that the time interval between two encounter events is random and follows an exponential distribution. The mean time taken for the mobile nodes of provider i to encounter those of provider j is denoted by $1/\Lambda_{i,j}$ [362]. Therefore, $\Lambda_{i,j}$ is the mean encounter rate. We assume $\Lambda_{i,j} = \Lambda_{j,i}$ for $i, j \in \mathcal{F}$. Given the spaces for the transient and absorbing states (i.e., $\Delta_{i,\mathcal{F}}$ and $\delta_{i,\mathcal{F}}$), the transition matrix of the content-forwarding process can be defined as follows:

$$\mathbf{Q}_{i,\mathcal{F}} = \left[\begin{array}{c|c} \mathbf{S}_{i,\mathcal{F}} & \vec{\mathbf{s}}_0 \\ \hline \mathbf{0} & 0 \end{array}\right], \tag{10.22}$$

where $\mathbf{S}_{i,\mathcal{F}}$ is the transition matrix of the transient states in $\Delta_{i,\mathcal{F}}$. $\mathbf{0}$ is a matrix of zeros with an appropriate size. Both $\mathbf{0}$ and 0 at the bottom of matrix $\mathbf{Q}_{i,\mathcal{F}}$ correspond to the absorbing state $\delta_{i,\mathcal{F}}$. $\vec{\mathbf{s}}_0$ is the vector whose elements are the transition rates from the transient state to the absorbing state.

The matrix $\mathbf{S}_{i,\mathcal{F}}$ can be expressed as follows:

$$\mathbf{S}_{i,\mathcal{F}} = \begin{bmatrix} \mathbf{N}_{0,0}^{(j)} & \mathbf{N}_{0,1}^{(j)} & & & \\ & \mathbf{N}_{1,1}^{(j)} & \mathbf{N}_{1,2}^{(j)} & & \\ & & \ddots & \ddots & \\ & & & \mathbf{N}_{N_j-1,N_j-1}^{(j)} & \mathbf{N}_{N_j-1,N_j}^{(j)} \\ & & & & \mathbf{N}_{N_j,N_j}^{(j)} \end{bmatrix}, \tag{10.23}$$

where each row of the matrix $\mathbf{S}_{i,\mathcal{F}}$ corresponds to the number of mobile nodes of content provider j for $j \neq i$, $j \in \mathcal{F}$ that have received the content from provider i. In other words, $\mathbf{N}^{(j)}_{n_j,n'_j}$ is the transition matrix for the number of mobile nodes changing from n_j to n'_j. Matrix $\mathbf{N}^{(j)}_{n_j,n_j+1}$ accounts for the transition from state n_j to n_j+1 for mobile nodes of provider j. Matrix $\mathbf{N}^{(j)}_{n_j,n_j+1}$ is composed of the diagonal element $\eta^{(j)}_{(\ldots,n_k,\ldots)}$ corresponding to the number of mobile nodes n_k of the other providers $k \in \mathcal{F}$ and $k \neq j$. The diagonal element $\eta^{(j)}_{(\ldots,n_k,\ldots)}$ can be obtained from

$$\eta^{(j)}_{(\ldots,n_k,\ldots)} = (N_j - n_j)\left(\sum_{k\in\mathcal{F}} n_k \Lambda_{j,k}\right), \tag{10.24}$$

where $\Lambda_{i,k}$ is the mean encounter rate between mobile nodes of providers i and k.

Matrix $\mathbf{N}^{(j)}_{n_j,n_j}$ represents the transition of the number of mobile nodes of provider $k \in \mathcal{F}$ for $k \neq j$ that have received the content from provider i. The structure of matrix $\mathbf{N}^{(j)}_{n_j,n_j}$ is similar to that of $\mathbf{S}_{i,\mathcal{F}}$ in (10.23) and can be expressed as follows:

$$\mathbf{N}^{(j)}_{n_j,n_j} = \begin{bmatrix} \mathbf{N}^{(k)}_{0,0} & \mathbf{N}^{(k)}_{0,1} & & & & \\ & \mathbf{N}^{(k)}_{1,1} & \mathbf{N}^{(k)}_{1,2} & & & \\ & & \ddots & \ddots & & \\ & & & \mathbf{N}^{(k)}_{N_k-1,N_k-1} & \mathbf{N}^{(k)}_{N_k-1,N_k} & \\ & & & & \mathbf{N}^{(k)}_{N_k,N_k} \end{bmatrix}. \tag{10.25}$$

Again, matrix $\mathbf{N}^{(k)}_{n_k,n_k+1}$ represents the transition from state n_k to n_k+1 for the mobile nodes of provider k. The diagonal element $\eta^{(k)}_{(\ldots,n_l,\ldots)}$ is for the number of mobile nodes n_l of the providers $l \in \mathcal{F}$ and $l \neq k$ that have received the content from provider i. The diagonal element $\eta^{(k)}_{(\ldots,n_l,\ldots)}$ can be obtained similarly to that in (10.24). The element $\mathbf{N}^{(k)}_{n_k,n_k}$ in $\mathbf{N}^{(j)}_{n_j,n_j}$ can be obtained similarly to that in (10.25). The same steps are repeated for the rest of the

providers in $\mathcal{F}$ until one reaches the innermost matrix $\mathbf{N}^{(i)}_{n_i,n_i}$. The matrix $\mathbf{N}^{(i)}_{n_i,n_i}$ accounts for the change in the number of mobile nodes of provider *i* having the content.

The diagonal element of matrix $\mathbf{S}_{i,\mathcal{F}}$ corresponds to the number of mobile nodes of all providers $m \in \mathcal{F}$. It can be obtained from

$$\eta_{(\ldots,n_m,\ldots)} = -\sum_{m\in\mathcal{F}} \left(\eta^{(m)}_{(\ldots,n_{m'},\ldots)} + \zeta_{(\ldots,n_{m'},\ldots)}\right), \tag{10.26}$$

for $m' \in \mathcal{F}$, where $\zeta_{(\ldots,n_{m'},\ldots)}$ is the element of vector $\vec{\mathbf{s}}_0$ defined as follows:

$$\zeta_{(\ldots,n_{m'},\ldots)} = \begin{cases} (N_i - 1)\sum_{m\in\mathcal{F}} n_m \Lambda_{i,m}, & \text{if } n_i = N_i - 1, \\ 0, & \text{otherwise.} \end{cases} \tag{10.27}$$

$\zeta_{(\ldots,n_{m'},\ldots)}$ is the rate at which the last mobile nodes of provider *i* will receive the content from the mobile nodes of providers $m \in \mathcal{F}$.

10.5.3 Performance measures

From the absorbing continuous-time Markov chain with the transition matrix defined in (10.22), the performance measures for the content-forwarding process can be obtained for any provider *i*. Let $\vec{\xi}$ denote the initial probability vector of the content-forwarding process, with each element denoted by $\xi_{(\ldots,n_i,\ldots)}$. Since U_i mobile nodes of content provider *i* will receive the content from the network operator's access point, $\xi_{(\ldots,n_i,\ldots)}$ can be obtained from

$$\xi_{(\ldots,n_i,\ldots)} = \begin{cases} 1, & \text{if } n_i = U_i, \\ 0, & \text{otherwise.} \end{cases} \tag{10.28}$$

In other words, the transient state starts at U_i.

The average content-forwarding delay experienced by all mobile nodes of provider i is the average time taken to reach the absorbing state [361] and can be obtained from

$$D_i^{\mathrm{fd}}(\mathcal{F}) = -\vec{\xi}^{\top}\mathbf{S}_{i,\mathcal{F}}^{-1}\vec{\mathbf{1}}, \tag{10.29}$$

where $\vec{\mathbf{1}}$ is a column vector of ones with an appropriate size.

We can calculate the probability that the content will be received by all mobile nodes before a deadline. Firstly, we assume that, at an initial time 0, the access point finishes transferring the content of provider i to U_i mobile nodes. If the content of provider i has the deadline denoted by $\Gamma > 0$, the probability that all mobile nodes of provider i will receive the content is the probability that the absorbing state will be reached at time Γ [361] and can be obtained from

$$P_i^{\mathrm{all}}(\mathcal{F}, \Gamma) = 1 - \vec{\xi}^{\top} \exp\left(\Gamma \mathbf{S}_{i,\mathcal{F}}\right)\vec{\mathbf{1}}. \tag{10.30}$$

Similarly, we can calculate the average number of mobile nodes receiving the content of provider i by the deadline Γ. It is obtained from the transient-state probability. The transient-state probability vector $\vec{\mathbf{q}}(\Gamma)$ is

$$\vec{\mathbf{q}}(\Gamma) = \vec{\xi}^{\top} \exp\left(\mathbf{Q}_{i,\mathcal{F}}\Gamma\right), \tag{10.31}$$

where the element $q_{(\ldots,n_j,\ldots)}$ of vector $\vec{\mathbf{q}}(\Gamma) = [\ \cdots\ \ q_{(\ldots,n_j,\ldots)}(\Gamma)\ \ \cdots\ ]^{\top}$ corresponds to the probability that n_j mobile nodes of provider $j \in \mathcal{F}$ have received the content of provider i. The average number of mobile nodes of provider i that have received the content from provider i at time Γ is given by

$$\overline{n}_i(\Gamma) = \sum_{n_i=1}^{N_i} n_i \left(\sum_{j\in\mathcal{F};j\neq i} \sum_{n_j=1}^{N_j} q_{(\ldots,n_j,\ldots)}(\Gamma) \right). \tag{10.32}$$

The performance measures can be used by content provider *i* to optimize its coalition-formation strategy.

10.5.4 Controlled coalitional-game formulation

The controlled coalitional game is to jointly address the coalition-formation process between the content providers and the bandwidth-allocation problem of the network operator. Firstly, the cost of the content provider is defined. Then, the coalitional-game formulation of content providers is presented. The optimization problem of the network operator is introduced.

The cost function of the content provider

A content provider aims to deliver its content, in a timely manner, to the mobile nodes of its subscribers while at the same time minimizing the cost. This cost is composed of the following components.

- The price paid to the network operator to allow the content provider to transfer content from the access point to the mobile nodes.
- The content-forwarding overhead (e.g., energy consumption) among the mobile nodes.

The cost of content provider *i* that is a member of coalition $\mathcal{F}$ for content forwarding and a member of coalition $\mathcal{B}$ for bandwidth sharing (i.e., $i \in \mathcal{F}$ and $i \in \mathcal{B}$) is expressed as follows:

$$C_i(\mathcal{F}, \mathcal{B}, b) = \omega_{\text{td}} D_i^{\text{td}}(\mathcal{B}, b) + \omega_{\text{bu}} C_i^{\text{bu}} + \omega_{\text{fd}} D_i^{\text{fd}}(\mathcal{F}) + \omega_{\text{cf}} C_i^{\text{cf}}. \tag{10.33}$$

ω_{td}, ω_{bu}, ω_{fd}, and ω_{cf} are the cost weights of the content-transmission delay, bandwidth, content-forwarding delay, and content-forwarding overhead, respectively. The objective of content provider *i* is to minimize this cost $C_i(\mathcal{F}, \mathcal{B}, b)$.

- $D_i^{\text{td}}(\mathcal{B}, b)$ is the content-transmission delay from the access point to U_i mobile nodes. This content-transmission delay depends on the coalition $\mathcal{B}$ and the amount of bandwidth b.
- $C_i^{\text{bu}}(b)$ is the bandwidth cost charged by the network operator. This cost depends on the amount of bandwidth b only.
- $D_i^{\text{fd}}(\mathcal{F})$ is the average content-forwarding delay experienced by all mobile nodes of provider i. It is obtained from (10.29).
- C_i^{cf} is the overhead of content forwarding. In this case, if the mobile nodes forward too much content, the battery power of mobile nodes can be depleted very quickly or the nodes cannot use the local network for other applications. This overhead negatively affects the satisfaction of mobile users. Therefore, the content provider can provide an incentive and compensate for this dissatisfaction experienced by the owners of the mobile nodes by giving payments to mobile nodes participating in cooperative content forwarding. This payment can be a discount on the service fee of mobile nodes charged by the content provider.

The time taken for content distribution can be divided into two parts.

- The content-transmission delay is the time used to transfer the content from the access point to the mobile nodes.
- The content-forwarding delay is the time used to forward content among the mobile nodes, and can be obtained using (10.29).

Given the coalition of bandwidth sharing $\mathcal{B}$, any content received from content provider $i \in \mathcal{B}$ is buffered in a queue at the access point. We assume that content generation follows a Poisson process with an average rate of α_i. Using an M/D/1 queueing model, the content transmission delay from the access point to U_i mobile nodes is expressed as follows:

$$D_i^{\text{td}}(\mathcal{B}, b) = \frac{LU_i}{b\kappa/|\mathcal{B}|}\left(1 + \frac{\rho_{\mathcal{B}}}{2(1-\rho_{\mathcal{B}})}\right). \tag{10.34}$$

- L is the content size.
- b is the amount of bandwidth measured in terms of the number of channels allocated by the network operator.

- κ is the data rate per channel.
- $\rho_{\mathcal{B}}$ is the traffic intensity defined as $\rho_{\mathcal{B}} = LU_i\alpha_i/(b\kappa/|\mathcal{B}|)$.

The cost of bandwidth due to the price paid to the network operator for provider *i* is obtained from

$$C_i^{\text{bu}} = \theta b/|\mathcal{B}|. \tag{10.35}$$

The cost of the content-forwarding overhead is considered to be a function of the amount of content generated from all providers belonging to the same coalition and the number of subscribed mobile nodes, i.e.,

$$C_i^{\text{cf}} = N_i \sum_{m\in\mathcal{F}} \alpha_m. \tag{10.36}$$

Coalitional-game formulation for the content providers

Consider the content providers' coalitional game. Given the amount of bandwidth *b* allocated by the network operator (i.e., leader), a content providers' coalitional game is defined by the players (i.e., content providers) which are the followers. Hence, the set of players in this coalitional game is $\mathcal{I}$. The strategy of any player is to form the coalitions $\mathcal{F}$ and $\mathcal{B}$, respectively, for cooperative content forwarding and bandwidth sharing. The negative payoff of any player $i \in \mathcal{I}$ is the cost $C_i(\mathcal{F}, \mathcal{B}, b)$ as defined in (10.33). The players have self-interested behavior and aim at minimizing their individual costs. This is the *non-transferable-utility (NTU)* coalitional game, since the value (i.e., cost) of any coalition of content providers is a function of delay components that cannot be transferred (divided) arbitrarily among the members of a given coalition.

In the coalitional game, each content provider has two coalitions to form, i.e., for cooperative content forwarding (i.e., $\mathcal{F}$) and bandwidth sharing (i.e., $\mathcal{B}$). As a result, the strategies of any content provider can be defined as follows.

- *Split from a cooperative content-forwarding coalition:* Consider a coalition $\mathcal{F}$ formed between content providers for the purpose of cooperative content forwarding. The content providers in this coalition $\mathcal{F}$ can decide to split into multiple new coalitions $\mathcal{F}^{\dagger}$, if the following conditions are satisfied:

$$C_i(\mathcal{F}^{\dagger}, \mathcal{B}, b) \leq C_i(\mathcal{F}, \mathcal{B}, b), \quad \forall i \in \mathcal{F}, \tag{10.37}$$

  where $\mathcal{F} = \bigcup \mathcal{F}^{\dagger}$. The content providers split into multiple coalitions $\mathcal{F}^{\dagger}$ used for cooperative content forwarding if the costs of all content providers $i \in \mathcal{F}^{\dagger}$ are lower than or equal to those of the ones in the original coalition $\mathcal{F}$.
- *Split from a bandwidth-sharing coalition:* Consider a coalition $\mathcal{B}$ formed between a group of content providers and used for bandwidth sharing. The content providers in this coalition $\mathcal{B}$ can split from this coalition into multiple new coalitions $\mathcal{B}^{\dagger}$, if the following conditions are satisfied:

$$C_i(\mathcal{F}, \mathcal{B}^{\dagger}, b) \leq C_i(\mathcal{F}, \mathcal{B}, b), \quad \forall i \in \mathcal{B}, \tag{10.38}$$

  where $\mathcal{B} = \bigcup \mathcal{B}^{\dagger}$. The content providers can split a bandwidth-sharing coalition into multiple new coalitions if, on doing so, the cost of the content providers in the new coalition $\mathcal{B}^{\dagger}$ is lower than that of the original coalition $\mathcal{B}$.
- *Merge into a cooperative content-forwarding coalition:* The content providers from multiple coalitions $\mathcal{F}$ can collectively merge into a single new coalition $\mathcal{F}^{\ddagger}$, if the following conditions are satisfied:

$$C_i(\mathcal{F}^{\ddagger}, \mathcal{B}, b) \leq C_i(\mathcal{F}, \mathcal{B}, b), \quad \forall i \in \mathcal{F}^{\ddagger}, \tag{10.39}$$

  where $\mathcal{F}^{\ddagger} = \bigcup \mathcal{F}$. The content providers will merge and act as a single coalition if all content providers (in all coalitions) achieve a lower cost.
- *Merge into a bandwidth-sharing coalition:* The content providers from multiple coalitions $\mathcal{B}$ can collectively form (i.e., merge into) a single new coalition $\mathcal{B}^{\ddagger}$, if the following conditions are satisfied:

$$C_i(\mathcal{F}, \mathcal{B}^{\ddagger}, b) \leq C_i(\mathcal{F}, \mathcal{B}, b), \quad \forall i \in \mathcal{B}^{\ddagger}, \tag{10.40}$$

where $\mathcal{B}^{\ddagger} = \bigcup \mathcal{B}$. The content providers can merge and act as a single coalition if all content providers in the new coalition achieve a lower cost.

The stable coalitional state

We can analyze the coalition-formation process using a Markov chain. First, the state space is defined on the basis of the following coalition structures. The set of coalitions of all content providers in the bandwidth sharing is defined as a coalitional structure $S = \{\mathcal{B}_1, \ldots, \mathcal{B}_x, \ldots, \mathcal{B}_X\}$, where $\mathcal{B}_x \cap \mathcal{B}_{x'} = \emptyset$, for $x \neq x'$, and $\bigcup_{x=1}^{X} \mathcal{B}_x = \mathcal{I}$, and X is the total number of coalitions in the structure S, i.e., $X = |S|$. Similarly, the set of coalitions of all content providers in the cooperative content forwarding is defined as a coalitional structure $R = \{\mathcal{F}_1, \ldots, \mathcal{F}_y, \ldots, \mathcal{F}_Y\}$, where $\mathcal{F}_y \cap \mathcal{F}_{y'} = \emptyset$, for $y \neq y'$, and $\bigcup_{y=1}^{Y} \mathcal{F}_y = \mathcal{I}$, and Y is the total number of coalitions in structure R, i.e., $Y = |R|$.

The state space of the Markov chain for the coalition-formation process is composed of coalitional structures for bandwidth sharing and cooperative content forwarding. The state space is defined as follows:

$$\Omega = \{(S_k, R_l) | k, l = \{1, \ldots, B_I\}\}, \tag{10.41}$$

where B_I is the Bell number given a total of I content providers. A change in the coalitional state occurs when the content providers choose strategies (i.e., split or merge).

Given the amount of bandwidth b from the network operator, the transition probability matrix of a coalitional state is denoted by $\mathbf{P}(b)$ and can be expressed as follows:

$$\mathbf{P}(b) = \begin{bmatrix} \hat{\mathbf{P}}_{1,1}(b) & \cdots & \hat{\mathbf{P}}_{1,k'}(b) & \cdots & \hat{\mathbf{P}}_{1,B_I}(b) \\ \vdots & \ddots & \vdots & \ddots & \vdots \\ \hat{\mathbf{P}}_{k,1}(b) & \cdots & \hat{\mathbf{P}}_{k,k'}(b) & \cdots & \hat{\mathbf{P}}_{k,B_I}(b) \\ \vdots & \ddots & \vdots & \ddots & \vdots \\ \hat{\mathbf{P}}_{B_I,1}(b) & \cdots & \hat{\mathbf{P}}_{B_I,k'}(b) & \cdots & \hat{\mathbf{P}}_{B_I,B_I}(b) \end{bmatrix}, \tag{10.42}$$

where element $\hat{\mathbf{P}}_{k,k'}$ is the transition probability matrix of the content providers that want to change their bandwidth-sharing coalition structure from S_k to $S_{k'}$. The block element $\hat{\mathbf{P}}_{k,k'}(b)$ is obtained from

$$\hat{\mathbf{P}}_{k,k'}(b) = \begin{bmatrix} P^{k,k'}_{1,1}(b) & \cdots & P^{k,k'}_{1,l'}(b) & \cdots & P^{k,k'}_{1,B_I}(b) \\ \vdots & \ddots & \vdots & \ddots & \vdots \\ P^{k,k'}_{l,1}(b) & \cdots & P^{k,k'}_{l,l'}(b) & \cdots & P^{k,k'}_{l,B_I}(b) \\ \vdots & \ddots & \vdots & \ddots & \vdots \\ P^{k,k'}_{B_I,1}(b) & \cdots & P^{k,k'}_{B_I,l'}(b) & \cdots & P^{k,k'}_{B_I,B_I}(b) \end{bmatrix}, \tag{10.43}$$

where $P^{k,k'}_{l,l'}(b)$ is the probability that the coalitional state changes from (S_k, R_l) to $(S_{k'}, R_{l'})$. $P^{k,k'}_{l,l'}(b)$ is at row $(k-1)B_I + l$ and column $(k'-1)B_I + l'$ of matrix $\mathbf{P}(b)$.

To derive the transition probability further, we define the following notion.

- $\mathbb{C}_{k,k'} \subseteq \mathcal{I}$ denotes the set of content providers that are candidates to perform split and merge strategies that result in a change in the *bandwidth-sharing* coalition from S_k to $S_{k'}$.
- $\mathbb{D}_{l,l'} \subseteq \mathcal{I}$ denotes the set of candidate content providers that result in a change in the *cooperative content-forwarding* coalition from R_l to $R_{l'}$.
- $F((S_{k'}, R_{l'})|(S_k, R_l))$ is a feasibility condition. The feasibility condition is defined as follows. If the coalitional state $(S_{k'}, R_{l'})$ is reachable from

(S_k, R_l) given the strategies of all content providers in $\mathbb{C}_{k,k'}$ and $\mathbb{D}_{l,l'}$, then the condition $F((S_{k'}, R_{l'})|(S_k, R_l))$ is true, and it is false otherwise.

The transition probability $P_{l,l'}^{k,k'}(b)$ can be obtained from

$$P_{l,l'}^{k,k'}(b) = \begin{cases} \prod_{i \in \mathbb{C}_{k,k'}; i \in \mathbb{D}_{l,l'}} \gamma \tau_i((S_{k'}, R_{l'})|(S_k, R_l)), & \text{if } F((S_{k'}, R_{l'})|(S_k, R_l)), \\ 0, & \text{otherwise,} \end{cases} \tag{10.44}$$

where γ is the probability that the content providers perform a merge or split strategy. $\tau_i((S_{k'}, R_{l'})|(S_k, R_l))$ is the best-reply rule. That is, $\tau_i((S_{k'}, R_{l'})|(S_k, R_l))$ is the probability that the content provider i changes strategies and the coalitional state changes from (S_k, R_l) to $(S_{k'}, R_{l'})$. This best-reply rule can be formally defined as follows:

$$\tau_i((S_{k'}, R_{l'})|(S_k, R_l)) = \begin{cases} \hat{\tau}, & \text{if } C_i(\mathcal{B} \in S_{k'}, \mathcal{F} \in R_{l'}, b) \leq C_i(\mathcal{B} \in S_k, \mathcal{F} \in R_l, b), \\ \epsilon, & \text{otherwise,} \end{cases} \tag{10.45}$$

for $i \in \mathcal{B} \in S_{k'}$, $i \in \mathcal{B} \in S_k$, $i \in \mathcal{F} \in R_{l'}$, and $i \in \mathcal{F} \in R_l$, where $0 < \hat{\tau} \leq 1$ is a constant, and ϵ is a small probability (e.g., $\epsilon = 10^{-2}$) that a content provider chooses an irrational strategy. The irrational strategy results in higher cost, which could happen if the content provider does not have complete information about the outcome of the strategy and coalition formation.

Given the amount of bandwidth b allocated by the network operator, we can obtain the stationary probability of the Markov chain defined by the state space in (10.41) and the transition probability in (10.44). The vector of the stationary probabilities is denoted by $\vec{\mathbf{p}}_b = [p_b(S_1, R_1), \ldots, p_b(S_k, R_l), \ldots, p_b(S_{B_I}, R_{B_I})]^\top$. This vector is obtained by solving $\vec{\mathbf{p}}_b^\top \mathbf{P}(b) = \vec{\mathbf{p}}_b^\top$ and $\vec{\mathbf{p}}_b^\top \vec{\mathbf{1}} = 1$. If the probability of an irrational decision made by content providers approaches zero (i.e., $\epsilon \to 0^+$), there could be absorbing states. Once the Markov chain has transited to the absorbing states, the chain will remain in these states forever.

Therefore, this corresponds to the stable coalitional structure, in which, after the content providers have reached this structure, they will remain in that structure forever. In other words, the absorbing state is named the *stable coalitional state*. Within this stable coalitional state, no player has an incentive to change its decision given the prevailing coalitional state.

Optimization formulation for bandwidth allocation by the network operator

With the decisions of content providers to split or merge coalitions, the network operator can optimize its bandwidth allocation action to maximize revenue. In other words, given the underlying coalitional game among the content providers, the optimization formulation for the network operator in the controlled coalitional game is a constrained Markov decision process (MDP) with the 4-tuple $(\Omega, \Xi, P_{l,l'}^{k,k'}(b), V(S_k, R_l, b))$.

- Ω is a finite set of coalitional states as defined in (10.41).
- Ξ is a finite set of action b.
- $P_{l,l'}^{k,k'}(b)$ is the transition probability defined in (10.44).
- $V(S_k, R_l, b)$ is the immediate reward (i.e., revenue) received for coalitional structures S_k and R_l with action b.

An action, i.e., amount of allocated bandwidth, b for the network operator represents the amount of bandwidth allocated to each wireless connection. The wireless connection is used by the content providers. Therefore, the action space is denoted by $\Xi = \{1, 2, \ldots, b_{\max}\}$, where $b_{\max}$ is the maximum amount of bandwidth allocated. The action takes a value from a discrete finite set (i.e., $b \in \Xi$), which is the number of channels (e.g., a subcarrier or time slot in an OFDM or TDMA system, respectively).

The immediate reward or immediate revenue of the network operator is defined as follows:

$$V(S_k, R_l, b) = b\theta|S_k|, \tag{10.46}$$

where $|S_k|$ is the number of coalitions for bandwidth sharing of content providers. Each coalition is allocated a bandwidth b, and θ is a price constant charged per connection.

For the CMDP in the controlled coalitional-game framework, the network operator aims to optimize its bandwidth-allocation policy. The policy is a mapping from a coalitional structure or state $(S_k, R_l) \in \Omega$ to the action $b \in \Xi$. The optimal policy aims to maximize the long-term revenue of the network operator. However, since the available bandwidth of the access point is used not only by the content providers, but also by normal nodes (i.e., non-content-distribution service users), the performance of the normal nodes has to be taken into account. In this case, if all the bandwidth (i.e., all channels) of the access point denoted by $B_{\max}$ is reserved for the mobile nodes of the content providers and occupied by the normal ongoing nodes, any new normal nodes will be unable to connect to the access point. Dissatisfaction occurs for these blocked users. As a result, the network operator must ensure that the connection-blocking probability of the new normal nodes is maintained at a certain threshold P_{bl}. Therefore, the CMDP-based optimization problem of the network operator can be formulated as follows:

$$\max_{\pi} \quad J_V = \lim_{T\to\infty} \inf \frac{1}{T} \sum_{t=1}^{T} E_\pi \left(V(S_k(t), R_l(t), b(t))\right), \tag{10.47}$$

$$\text{subject to} \quad J_K = \lim_{T\to\infty} \sup \frac{1}{T} \sum_{t=1}^{T} E_\pi \left(K(S_k(t), R_l(t), b(t))\right) \leq P_{\text{bl}}, \tag{10.48}$$

where

- J_V is the long-term average revenue,
- J_K is the connection-blocking probability of the network operator,
- $S_k(t)$ is the coalition used for bandwidth sharing at time t,
- $R_l(t)$ is the cooperative content forwarding at time t,

- $b(t)$ is the bandwidth allocated,
- $E_\pi(\cdot)$ denotes the expectation over policy π,
- π is a policy defined as $\pi = \{\psi(S_k, R_l, b)|k, l = \{1, \ldots, B_I\}, \forall b \in \Xi\}$
- $\psi(S_k, R_l, b)$ is the probability of taking action b in coalitional state (S_k, R_l), and
- $K(S_k, R_l, b)$ is the immediate connection-blocking probability obtained by using the Erlang-B (or loss) formula.

The immediate connection-blocking probability is obtained from

$$K(S_k, R_l, b) = \frac{(\lambda\mu)^{B_{\max} - b|S_k|}/(B_{\max} - b|S_k|)!}{\sum_{x=0}^{B_{\max} - b|S_k|} (\lambda\mu)^x/x!}, \tag{10.49}$$

where

- $B_{\max} - b|S_k|$ is the number of channels available for normal nodes,
- λ is the arrival rate of new normal nodes, and
- μ is the connection holding time of normal nodes.

We formulate and solve a linear-programming (LP) model to obtain the optimal policy of CMDP defined in (10.47) and (10.48). The solution of the LP model is the stationary probability of the coalitional state and action denoted by $\phi(S_k, R_l, b)$. The LP model with decision variable $\phi(S_k, R_l, b)$ for $(S_k, R_l) \in \Omega$ and $b \in \Xi$ is defined as follows:

$$\max_{\phi(S_k, R_l, b)} \quad \sum_{(S_k, R_l) \in \Omega} \left(\sum_{b \in \Xi} \phi(S_k, R_l, b) V(S_k, R_l, b) \right), \tag{10.50}$$

$$\text{subject to} \quad \sum_{(S_k, R_l) \in \Omega} \left(\sum_{b \in \Xi} \phi(S_k, R_l, b) K(S_k, R_l, b) \right) \leq P_{\text{bl}}, \tag{10.51}$$

$$\sum_{b\in\Xi}\phi(S_{k'},R_{l'},b)=\sum_{(S_k,R_l)\in\Omega}\left(\sum_{b\in\Xi}P_{l,l'}^{k,k'}(b)\phi(S_k,R_l,b)\right),$$
$$\text{for } (S_{k'},R_{l'})\in\Omega, \tag{10.52}$$

$$\sum_{(S_k,R_l)\in\Omega}\left(\sum_{b\in\Xi}\phi(S_k,R_l,b)\right)=1,\quad \phi(S_k,R_l,b)\geq 0. \tag{10.53}$$

The optimal solution $\phi^*(S_k,R_l,b)$ of the LP model defined in (10.50)–(10.53) is used to obtain the optimal randomized policy of the network operator as follows:

$$\psi^*(S_k,R_l,b)=\frac{\phi^*(S_k,R_l,b)}{\sum_{b'\in\Xi}\phi^*(S_k,R_l,b')}, \tag{10.54}$$

for $\sum_{b'\in\Xi}\phi^*(S_k,R_l,b')>0$, where $\psi^*(S_k,R_l,b)$ is the probability that the network operator allocates bandwidth b when the coalitional state of content providers is (S_k,R_l). The optimal policy is then defined as $\pi^*=\{\psi^*(S_k,R_l,b)|k,l=\{1,\ldots,B_I\},\forall b\in\Xi\}$.

Given the optimal policy of the network operator, different performance measures can be obtained.

- The average revenue of the network operator is

$$\overline{V}=\sum_{(S_k,R_l)\in\Omega}\left(\sum_{b\in\Xi}\phi^*(S_k,R_l,b)b\theta|S_k|\right). \tag{10.55}$$

- The average cost of content provider $i\in\mathcal{I}$ is obtained from

$$\overline{C}_i=\sum_{(S_k,R_l)\in\Omega}\left(\sum_{b\in\Xi}\phi^*(S_k,R_l,b)C_i(\mathcal{F},\mathcal{B},b)\right),$$

(10.56)

where $C_i(\mathcal{F}, \mathcal{B}, b)$ is the cost of content provider i defined in (10.33).

10.5.5 *Performance evaluation*

We first describe the parameter setting and then present some numerical results. The following parameter setting is used.

- There are three content providers in the mobile social network under evaluation.
- The number of mobile nodes subscribed to provider i is $N_i = 7$.
- The mean inter-encounter time among mobile nodes subscribed to the same and to the different providers is $1/\Lambda_{i,j} = 1$ hour.
- The average size of an item of content is $L = 12.5$ MB.
- The average content generation rate is $\alpha_i = 1$ item of content per hour.
- For the access point of the network operator, the transmission rate per channel is $\kappa = 28$ kbps.
- The network operator can allocate at most $b_{\max} = 9$ channels to each wireless connection for the content provider.
- The average connection arrival rate of normal nodes is $\lambda = 12$ connections/hour.
- The average connection holding time is $\mu = 20$ minutes.
- The threshold of the connection-blocking probability is $P_{\text{bl}} = 0.05$.
- The content is transferred from an access point to one mobile node (i.e., $U_i = 1$).
- The price constant is $\theta = 0.3$.
- For a provider, the cost weights of content-transmission delay, bandwidth usage, content-forwarding delay, and content-forwarding overhead are $\omega_{\text{td}} = 1$, $\omega_{\text{bu}} = 1$, $\omega_{\text{fd}} = 1$, and $\omega_{\text{cf}} = 0.1$, respectively.
- The parameters of the controlled coalitional game are $\gamma = 0.5$, $\hat{\tau} = 0.99$, and $\epsilon = 0.01$.

The coalitional structures (i.e., states) are denoted as follows: $S_1, R_1 = \{\{1\}, \{2\}, \{3\}\}$, $S_2, R_2 = \{\{1, 2\}, \{3\}\}$, $S_3, R_3 = \{\{1, 3\}, \{2\}\}$, $S_4, R_4 = \{\{1\}, \{2, 3\}\}$, and $S_5, R_5 = \{\{1, 2, 3\}\}$.

We consider two coalition formation schemes.

- In scheme 1, the providers form the same coalition for sharing bandwidth and cooperatively performing content forwarding (i.e., $\mathcal{F} = \mathcal{B}$).
- In scheme 2, the content providers can form any coalitions for bandwidth sharing and cooperative content forwarding.

With three channels allocated to each connection for content providers, Figure 10.16(a) shows the cost of content provider 1 due to content-forwarding delay and overhead of mobile nodes under different numbers of subscribed nodes N_1 (i.e., $\omega_{\text{fd}} D_1^{\text{fd}} + \omega_{\text{cf}} C_1^{\text{cf}}$). Noncooperatively, without forming any coalition with other providers (i.e., $\{1\}$), the cost first decreases as the number of mobile nodes increases. Since a greater number of mobile nodes can help each other to forward the content, the content-forwarding delay decreases (Figure 10.17). However, at a certain number of mobile nodes, the cost increases due to the higher content-forwarding overhead resulting from the increased number of mobile nodes. A similar effect is observed for different coalitions. As shown in Figure 10.16(b) for coalitions $\{1, 2\}$, when the bandwidth is less than five channels, the cost first decreases and then increases. It is also observed that, at different network sizes, the lowest cost of content-forwarding delay and overhead can be achieved under different coalitional structures. For example, when the number of nodes reaches $N_1 = 6$ or 7, the lowest cost is achieved when providers 1 and 2 merge into a single coalition (i.e., $\{1, 2\}$). If the number of nodes is large (e.g., $N_1 > 10$), provider 1 will not form any coalition. This is due to the fact that the cost increment from the overhead incurred by carrying and forwarding the content of the other providers is higher than the cost decrement arising from the smaller delay.

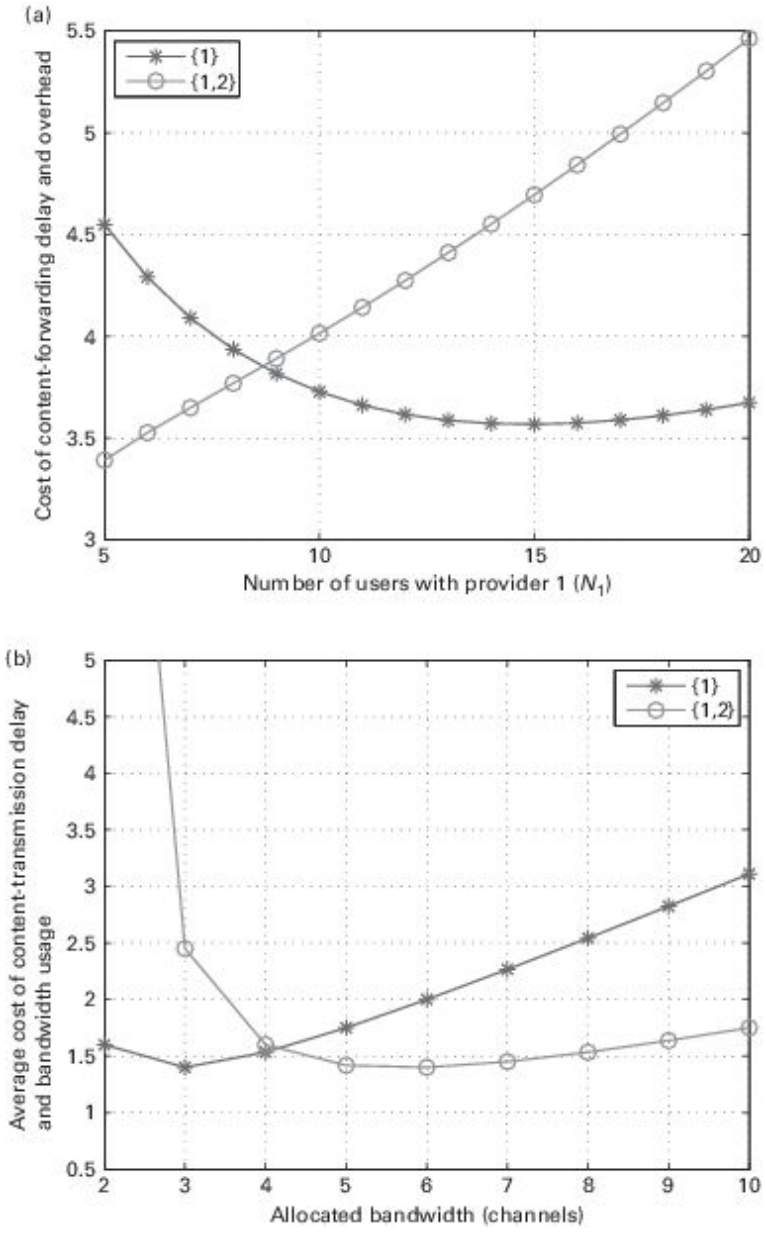

Figure 10.16. (a) The cost incurred by content provider 1 due to content-forwarding delay and overhead and (b) the cost incurred by content provider 1 due to content transmission delay and bandwidth usage under coalitions with provider 2.

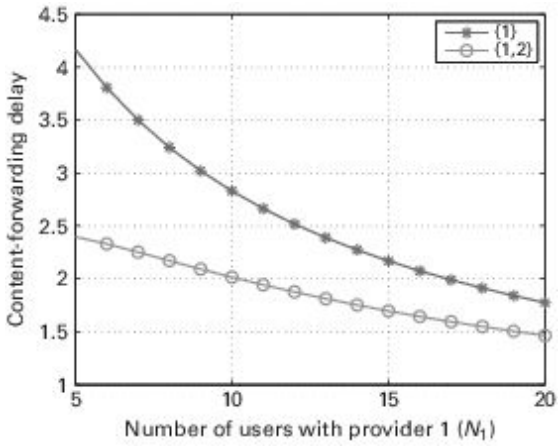

Figure 10.17. The average content-forwarding delay.

Figure 10.16(b) shows some similar results regarding the cost of provider 1 due to the content-transmission delay and the bandwidth usage (i.e., $\omega_{\text{td}} D_1^{\text{td}}(\mathcal{B}, b) + \omega_{\text{bu}} C_1^{\text{bu}}$). Under different coalitions of content providers, the lowest cost can be achieved. In this case, when the allocated bandwidth per connection increases, the cost decreases due to the smaller content-transmission delay. However, when the allocated bandwidth is large, the cost of bandwidth usage increases, and the total cost increases.

Figure 10.18(a) shows the average cost incurred by the providers under different bandwidth allocations. First, we note that, since we consider homogeneous providers, their average costs are the same. Using coalition formation in schemes 1 and 2, the cost of providers fluctuates as the allocated bandwidth increases due to the coalition-formation dynamics. One important observation from Figure 10.18(a) is that the costs of all providers are not the lowest compared with those of the case with no coalition (i.e., $\{\{1\}, \{2\}, \{3\}\}$) or a grand coalition (i.e., $\{\{1, 2, 3\}\}$) since the coalitions are formed rationally. Therefore, some providers might not achieve the lowest cost if the rest have already done so. For example, providers 1 and 2 have an incentive to form a coalition to achieve the lowest costs, but provider 3 does not. Figure 10.18(a) also shows the average costs from the "no-coalition" and "grand-coalition" cases. They can be used as benchmarks for average costs for providers.

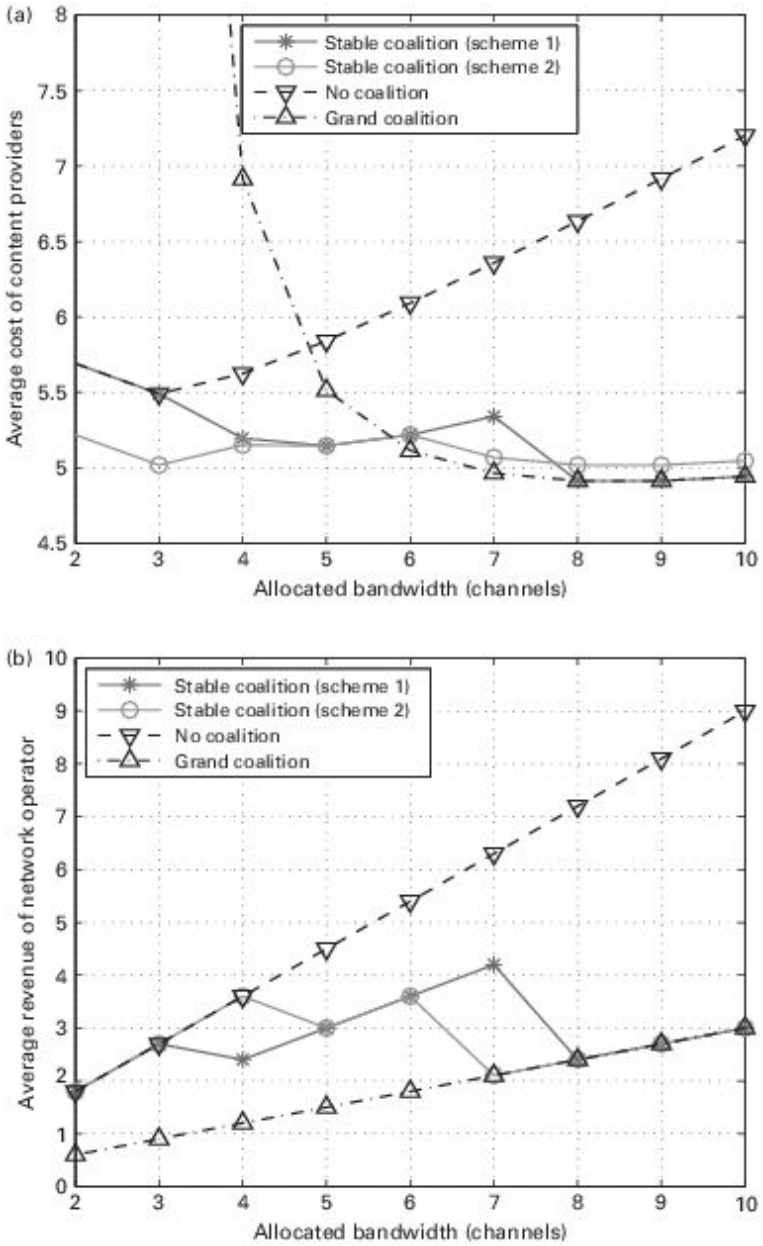

Figure 10.18. (a) The average cost incurred by content providers and (b) the average revenue of the network operator under different bandwidth allocations.

Figure 10.18(b) shows the average revenue for the network operator given the coalition-formation process of the providers. The average network operator's revenue fluctuates due to the coalition-formation decisions of the providers. Note that, in this case, the "no-coalition" and "grand-coalition" cases can be used, respectively, to indicate the upper and lower bounds on

the average revenue of the network operator. This is due to the fact that the "no-coalition" and "grand-coalition" cases will result in the largest and smallest amount of bandwidth usage, respectively.

Next, we consider the case in which the network operator can optimize the bandwidth allocation Using the CMDP model. The optimal policy of bandwidth allocation is shown in Figures 10.19(a) and (b) for connection-blocking probability thresholds of $P_{\text{bl}} = 0.05$ and $P_{\text{bl}} = 0.10$, respectively. For coalitional states S_1, S_2, S_3, and S_4, the network operator will allocate a large bandwidth to reduce the possibility of coalition formation between the content providers. The bandwidth allocation, given these states S_1, S_2, S_3, and S_4, must also ensure that the connection-blocking probability is maintained below or at the threshold. However, for the grand-coalition state S_5, the network operator will allocate the bandwidth such that the content providers will break their coalitions so that its revenue is maximized. The allocation for state S_5 is not constrained by the connection-blocking probability threshold since only one connection will be used by all content providers.

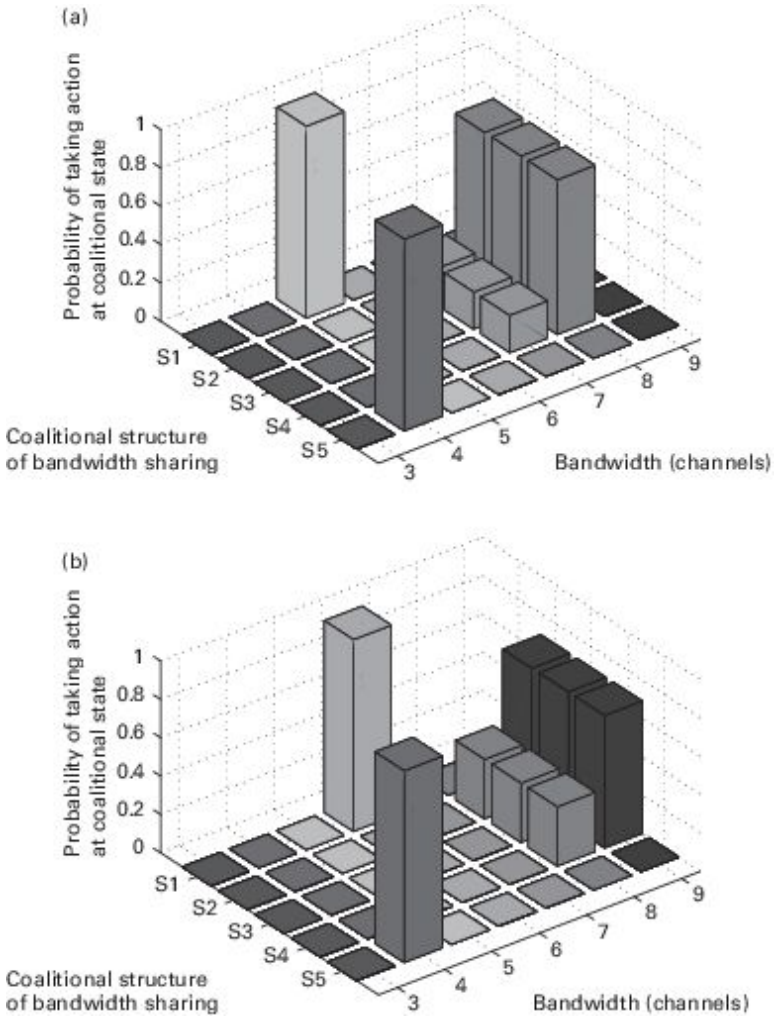

Figure 10.19. The optimal policy used by the network operator for bandwidth allocation under different coalitional states for content providers with connection-blocking probability thresholds of (a) $P_{\text{bl}} = 0.05$ and (b) $P_{\text{bl}} = 0.10$.

10.6 Chapter summary

Data transfer in mobile social networks can be done through direct local transmission to reduce the demand for radio and energy resources, while improving the data-transfer performance. Mobile social networks can utilize social attributes of mobile nodes to optimize data transfer. In this chapter, we first provided an overview of mobile social networks and some preliminary detail of social-network analysis. Then, we reviewed some important work on mobile social networks, including community detection and social-aware

data routing. Finally, we presented a cooperative content-delivery scheme developed for mobile social networks. Game theory is used as a tool to analyze and obtain the solution among entities in the mobile social network (i.e., content providers and a network operator).

Some research directions for mobile social networks and D2D communications are as follows.

- *Radio-resource management:* In D2D communications, the use of radio resources has to be optimized to achieve an objective (e.g., minimize resource usage) and meet constraints (e.g., QoS requirements). The radio-resource-management framework can be developed for mobile social networks with D2D communications. In this case, the social metrics can be used contributively for radio-resource allocation to support data transmission and transfer.
- *Context-aware communications:* D2D communications can be used in particular applications (e.g., sensor networks), where the mobile social networks have to be customized to use not only social metrics but also the context of applications to optimize data routing and dissemination. In this case, prioritization of different data for different applications under different contexts needs to be implemented to ensure that the satisfaction of the users is maximized and the goal of applications is achieved.
- *Noncooperative behavior:* D2D communications can be composed of noncooperative entities. For example, nodes with a social relationship may be willing to transfer data among themselves only when they gain some benefits exceeding particular thresholds. In this case, game theory can be applied to analyze the equilibrium solution for data transfer in D2D communications-based mobile social networks. The equilibrium solution can be compared with the optimal solution which is derived when the nodes are cooperative.

11 Machine-to-machine (M2M) communications

11.1 Introduction

Wireless connectivity is rapidly expanding beyond traditional mobile devices used by humans. In the near future, many wireless devices (e.g., sensors and actuators) will be connected in the framework of the Internet-of-Things (IoT) [363]. In cellular networks, hundreds or thousands of devices can exist in one cell. Therefore, the concept of machine-to-machine (M2M) communications has been introduced to handle the transmission of a number of devices in the network. M2M communication, also known as machine-type communications (MTC), refers to mobile nodes communicating over a network without (or with minimal) human intervention.[1] M2M communication enables ubiquitous connectivity among autonomous devices and/or Internet connectivity of MTC devices (i.e., communications between an MTC device and an M2M server or between two MTC devices). M2M communication is different from human-to-human (H2H) communication, which mainly involves voice calls, messaging, and web browsing. The goal of M2M communications is to increase the level of system automation by allowing the devices and systems to exchange and share data. Therefore, the protocol and data format are the major issues in M2M communications owing to the need to ensure seamless data and control flows.

D2D communication can be considered as a type of M2M communication when the D2D user equipments UEs are in close proximity and have small amounts of data to transmit among themselves (e.g., in application scenarios relating to the control of appliances in the home). In this chapter, we provide an overview of M2M communications in Section 11.2. Specifically, we focus on MTC in Long Term Evolution (LTE) and LTE-Advanced (LTE-A). Section 11.3 presents the mechanisms to support MTC, i.e., a random-access (RA) procedure

and random-access-channel (RACH)-overload control mechanisms. Section 11.4 introduces a performance-modeling technique based on queueing theory to analyze the performance of the RA mechanism for M2M communications. Finally, Section 11.5 gives a summary of the chapter and lists some important research directions.

11.2 Machine-to-machine (M2M) communications

M2M communication, which is undergoing the process of standardization by the Third Generation Partnership Project (3GPP), can support a wide range of applications (e.g., secured access and surveillance, metering and smart grid, and Internet-of-Things). In contrast to traditional human-to-human (H2H) services (e.g., voice), M2M communication has different requirements due to its specific features. M2M communications will accommodate various types of transmission, including scheduled services that are periodic and frequent but delay-tolerant and emergency services that are infrequent but have tight delay bounds. More importantly, the transmission in M2M communications is mostly for small amounts of data, but massive numbers of messages and sources. Additionally, M2M communications may need to support time-controlled access (i.e., transmission allowed only during an access-granted period) [364]. According to the 3GPP proposal, higher-layer connections among MTC devices are provided by attaching MTC devices to an existing cellular infrastructure (e.g., LTE-A).

For M2M communication, there are huge numbers of devices with small amounts of data needing to be transmitted. Therefore, the devices perform an initial and periodic RA for delivering resource requests to the network. In LTE-A networks, M2M and H2H devices can perform RA using the physical random access channel (PRACH). Here, the random access channel (RACH) is a transport layer channel in LTE-A that directly maps with the physical-layer PRACH.[2]

11.2.1 Machine-type communications in LTE-A networks

The overall LTE-A network consists of two parts: the core network (CN) and the radio-access network (RAN) [365]. The CN is responsible for overall control of mobile devices and establishment of IP packet flow. The RAN is based on a base station, which provides necessary user and control-plane protocols for communicating with mobile devices. In LTE-A, the base station is called an enhanced node-B (eNodeB or eNB) and each mobile device is called a user

equipment (UE). A UE can be either an H2H device or an MTC device. The eNBs are interconnected through an interface known as the "X2" interface. Besides that, the RAN (i.e., eNB) is connected to the CN by means of the "S1" interface. An overview of the LTE-A network architecture, with X2 and S1 interfaces, can be found in [366]. A higher-level architecture of LTE-A networks with M2M communications is shown in Figure 11.1, where MTC devices are connected to the eNB either directly or via the MTC Gateway (MTCG). The MTC Gateway is responsible for managing power consumptions of the network and providing suitable path for communicating between MTC devices. MTC devices can also communicate with each other locally, which can be considered as D2D communications. This peer-to-peer transmission can reduce power consumption since the MTC devices do not need to constantly scan for local access points. The eNB-to-MTC Gateway wireless link should follow the 3GPP LTE-A specification. However, MTC Gateway-to-M2M and M2M-to-M2M links can be based on either LTE-A or other wireless protocols such as 3G and WiMAX [367]. To reduce the signaling overhead, the minimum scheduling unit for downlink and uplink is referred to as a resource block (RB).

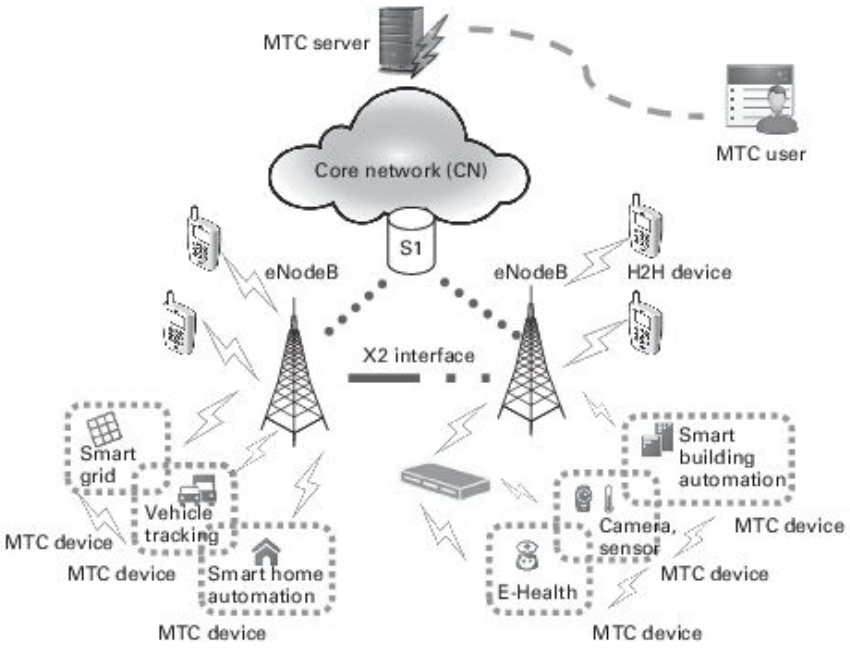

Figure 11.1. The architecture of machine-type communications in LTE-A networks.

When a UE has packets to transmit, it performs an RA during an allowable time slot, termed an access grant time interval (AGTI) or RA opportunity (i.e., RA-slots). The time–frequency resource (i.e., RB) on which RA is performed is

known as the physical random access channel (PRACH). RA allows the MTC device to request a connection initialization. An overview of the LTE-A RA procedure is provided next.

11.2.2 An overview of the random-access procedure

Random Access (RA) is a process [365, 368, 369] initiated by a UE when the device is turned on, but loses or has not acquired the uplink timing synchronization, or performs handover from one eNB to another. In LTE-A, RA can be used for initial access to establish a radio link, a resource request when no uplink radio resource is allocated, a scheduling request if no dedicated scheduling request has been configured (i.e., no dedicated physical uplink control channel (PUCCH) is available), and re-establishing a radio link after failure.

In LTE-A, RA is classified into two types: *contention-based* and *contention-free*. A UE normally initiates RA in a contention-based manner by randomly choosing a code sequence known as a preamble. More than one device can possibly choose the same preamble, which necessitates further contention-resolution processes. In contention-free RA, an eNB has explicit control over devices to initiate RA by using dedicated preambles. Hence, it is faster than the contention-based approach and mainly used in handover when time is crucial. These two types of RA procedure are described in the following.

(i) *Contention-based RA*. Figure 11.2(a) illustrates contention-based RA, which consists of the following four steps.

   (a) *Preamble transmission:* Each cell is assigned 64 preamble sequences, some of which are reserved for contention-free RA. According to [370], 54 preambles are available for contention-based RA and the remaining 10 are reserved for other purposes. The UE (which can be an M2M or H2H device) selects one of the available contention-based preamble sequences and transmits it using PRACH. Contention-based preambles are subdivided into two groups and, by choosing an appropriate subgroup, the UE signals the eNB about the amount of uplink radio resources that it wants to transmit in step (c). The eNB can control the number of preamble sequences in each subgroup according to the channel load. If two or more devices simultaneously transmit different preamble sequences, no collision will occur.

However, collision occurs when devices are trying to transmit the same preamble on PRACH. The eNB broadcasts the information about time–frequency resources (i.e., PRACH resources, referred to as RA-slots) in which RA preamble transmission is allowed. Each of the RA-slots, as illustrated in Figure 11.3, has a bandwidth corresponding to six RBs (1.08 MHz) in the frequency domain. The basic duration for an RA-slot is 1 ms in the time domain, but it can be extended according to the preamble format configuration. Random-access preambles consist of a cyclic prefix (CP), a preamble sequence, and a guard period (GP). The CP is used to reduce frequency-domain processing at the eNB and mitigate maximum-delay spreads over a cell. Since the devices are not uplink time synchronized, the GP is used to avoid interference with subsequent subframes.

(b) *Random-access response (RAR):* After receiving an RA preamble, the eNB transmits a random-access response (RAR) on the physical downlink shared channel (PDSCH). When the eNB detects multiple requests from different eNBs, the individual RAR for multiple eNBs can be combined into a single transmission. Hence, the RAR is scheduled on the PDSCH, which is the main data-bearing download channel. Even if multiple UEs select the same preamble, the eNB cannot detect collisions due to the structure of a preamble sequence. As a result, each of the UEs receives the RAR. Each RAR contains an ID indicating the time–frequency slot in which the preamble was detected, an uplink scheduling grants for transmitting the next-step message, uplink-timing information to synchronize subsequent uplink transmissions, and assignment of a temporary identifier, i.e., a cell radio network temporary identifier (C-RNTI) for further communication between the UE and the eNB. The UE expects to receive a RAR within a timing window, and, if the UE does not receive the response within the configured time window, the access attempt is considered to have failed and the UE will retransmit the preamble. The eNB may include a *backoff indicator* in the RAR message to inform the UE to back off for a period of time before retrying the RA procedure. After receiving the RAR, the UE synchronizes its uplink transmission timing and continues to the next step.

(c) *Scheduled transmission (terminal identification):* A packet transmitted in this step contains an actual RA message (i.e., a radio-resource request, a scheduling request, or a tracking area update). It also includes temporary C-RNTI and either C-RNTI (if the device has assigned C-RNTI) or a unique identity, i.e., international mobile subscriber identity (IMSI). The UE transmits this message using the physical uplink shared channel (PUSCH). Inclusion of C-RNTI or a unique identity helps to resolve collision in the last step. If preamble collision occurs in step (a), the colliding devices will receive the same temporary C-RNTI in the RAR. Consequently, the colliding UEs may possibly not be decoded by the eNB (even if one UE is decoded, the other UEs may be unaware of collision), and a further contention-resolution procedure will be required in the next step.

(d) *Contention resolution:* The last step of an RA procedure is contention resolution using PDSCH. In this case, the eNB echoes the terminal identity received in step (c). This step works as an early indication of collision before actual data transmission and guides the UE to re-initiate the RA procedure. If the eNB can decode any of the step (c) messages, it replies with the identifier (i.e., C-RNTI or IMSI). Only the UE, which can detect its own ID, acknowledges the message using a hybrid automatic repeat request (HARQ). The rest of the colliding devices should discard the message and try to initiate another RA procedure after random backoff.

(ii) *Contention-free RA*. A contention-free RA procedure, shown in Figure 11.2(b), is simplified with three steps by allocating dedicated preamble signatures to a UE. The procedure starts with the RA preamble assignment by the eNB. After the transmission of an assigned RA preamble by the UE, the eNB responds with the RAR. This is the last step of the contention-free RA since there is no need to resolve further collision.

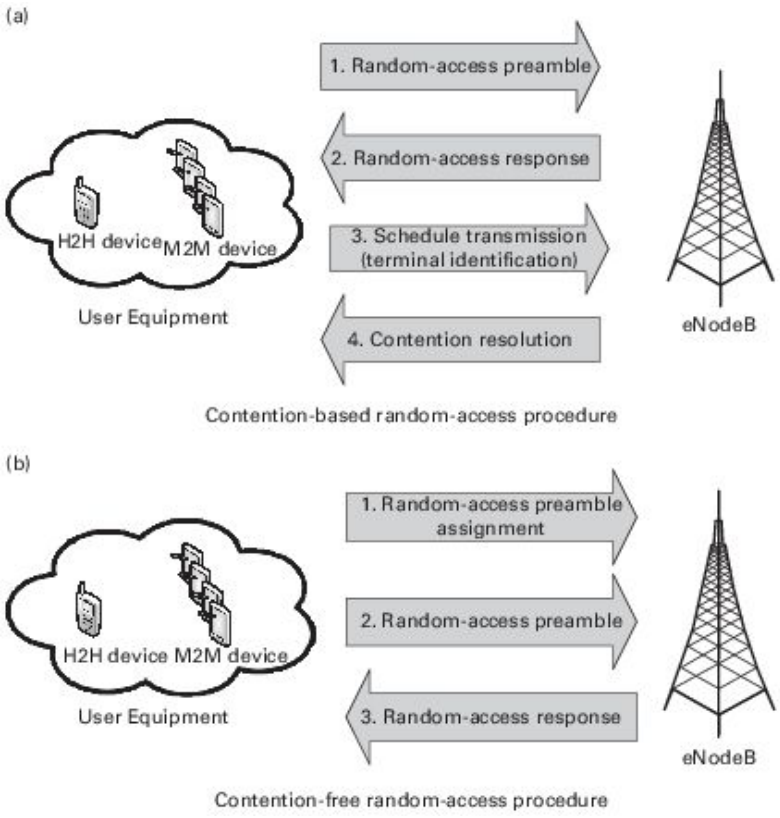

Figure 11.2. LTE-A RA procedures between user equipment and eNodeB.

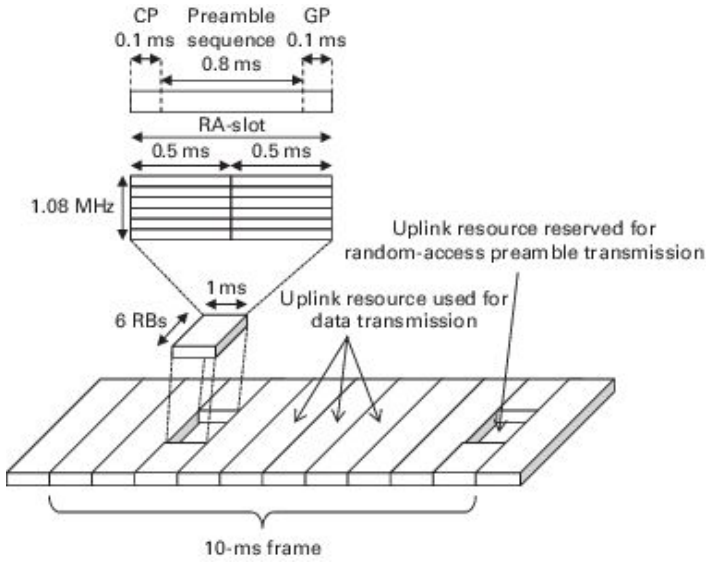

Figure 11.3. Preamble transmission and PRACH time–frequency resources.

One subframe (1 ms) of an LTE-A frequency-division duplexing (FDD) mode contains two RA opportunities to send preambles. Before a UE transmits a preamble to the eNB, the UE must know the required parameters (i.e., the RAR window size, maximum number of allowable retransmissions, power of transmission in terms of retransmission times, and set of available PRACH resources for transmitting preambles). These parameters are broadcast by the eNB [369]. In the following, we concentrate on contention-based RA since devices mainly perform RA in a contention-based manner. Although most of the recent literature addresses RA overload with respect to contention-based RA, contention-free RA can also be a potential candidate to control congestion centrally (i.e., through the CN) since the eNB has full control to deliver the preambles. As mentioned earlier, if the UE fails to receive a RAR within the specified timing window or does not receive its own ID in step (d), the RA is considered unsuccessful and the devices need to re-initiate the procedure after random backoff. In the backoff procedure, the UE randomly selects an integer between zero and the maximum backoff counter as an initial counter value. This counter is decreased in every time slot and, when the counter value becomes zero, the UE selects a random real number between zero and one. If this real number is less than the given persistence probability, the UE transmits the preamble. Otherwise, the preamble will not be transmitted and the UE performs the backoff procedure again. This process can be repeated until the retransmission is successful or until the maximum number of allowable retransmissions is reached. However, when many devices are trying to perform RA on the same channel in a short interval, network congestion cannot be avoided, and one requires further overload control mechanisms.

11.3 RACH overload control mechanisms

Rapid growth in number of MTC devices and their frequent access within a short time causes the radio network to overload. When many MTC devices try to access the network simultaneously, this leads to low RA success rate and network congestion in PRACH. This may cause unexpected delays, packet loss, waste of radio resources, extra battery consumption, and even service interruption. Both H2H and MTC devices (or M2M devices) can communicate over the same channel. As a result, the devices may suffer continuous collisions on the PRACH. The amounts of data transmitted by MTC devices are small in most cases. However, since the number of MTC devices is larger (i.e., more than 30 000 per cell compared with 50 active H2H devices per cell [370]) and their frequency of making data connection is much higher than that of H2H devices, this can

significantly degrade the QoS performance of the H2H devices. The channel can be further overloaded when the MTC devices repeat their access attempts after collision. This may cause starvation of some devices even after a couple of RA attempts. To support MTC in LTE-A, the 3GPP has proposed the following solutions [370] for controlling PRACH overload.

(i) *The access-class-barring (ACB) scheme:* In a legacy access-class-barring (ACB) mechanism, initially the eNB broadcasts an access probability and ACB time. When a device initiates RA, the device draws a random number and compares it with the access probability. If this number is less than the access probability, the device is allowed to proceed the RA process. Otherwise, the device delays for the ACB duration. In the recent releases of LTE-A (release 10 and onwards), the existing ACB mechanism is extended to allow one or more new access classes for MTC devices and an individual access barring factor can be assigned for each of the classes. The 3GPP also proposes an *extended-access-barring (EAB)* scheme in which, when the EAB is activated, the devices that belong to a certain access class (i.e., delay-tolerant devices) are not allowed to perform RA. Using the ACB mechanism, the eNB can control PRACH overload by lowering the value of the access probability. Although this reduces the number of RA attempts, it may cause longer RA delays for some devices.

(ii) *RACH resource-separation scheme:* When H2H and MTC devices share the same resource, the contention for RA may overload the channel and degrade the QoS performance of H2H devices. Therefore, this resource-separation scheme allocates orthogonal PRACH resources (i.e., preamble) to H2H and MTC devices. For overall system efficiency and resource utilization, the resource allocation to MTC devices should be adjusted dynamically according to a traffic condition.

(iii) *MTC-specific backoff scheme:* A backoff scheme is used to delay the RA attempts of H2H and MTC devices separately. In this scheme, the backoff time for H2H devices is set to a small value, while the backoff time for MTC devices is set to a large one. Though it improves performance in low channel overload, it cannot solve congestion problems in high-overload situations when a huge number of MTC devices will be performing RA at the same time.

(iv) *Slotted access scheme:* In this scheme, each MTC device is allowed to perform RA only in its dedicated access slot. The MTC device can calculate the allowable access slots through its ID (i.e., IMSI) and RA-cycle. The RA-cycle is the integer multiple of a radio frame that is broadcast by the eNB. If the total number of unique access slots is smaller than the number of MTC devices in a particular cell, multiple MTC devices share the same access slot and collision occurs. Increasing the RA-cycle can reduce collisions but create unacceptable delay to an RA request.

(v) *Pull-based scheme:* In the pull-based scheme, an MTC server requests the eNB to page MTC devices. Upon receiving a paging message from the eNB, the MTC device will start the RA procedure. In this centralized scheme, the eNBs can control the number of devices to be paged according to the PRACH load and resource availability. However, one requires extra control channel resources to page massive MTC devices.

Simulation results in [371] show that a better contention resolution, including the conditions of lower access probability and large backoff value and longer waiting time, is attained, but with a longer delay. In practice, the tradeoff between success probability and delay is unavoidable since the RACH resource is very limited compared with the huge number of MTC devices. Owing to the increasing number of MTC devices and their frequent massive access, the 3GPP proposals in the current specification cannot completely overcome channel overload in all practical scenarios. Two approaches have been introduced in the recent literature to control RACH overload in line with the 3GPP proposals. As mentioned earlier in Section 11.2.1, the three types of transmission modes available in MTC are

- direct communication between eNB-to-MTC devices,
- multihop transmission using MTC Gateway, and
- peer-to-peer communication between MTC devices (i.e., a D2D mode).

However, most of the schemes proposed in the literature consider only the direct communication mode. In the following, we give an overview of these overload control approaches.

11.3.1 Grouping of MTC devices

To support a large number of MTC devices and their frequent access in RACH, a group-based communication scheme is an efficient way to reduce traffic overhead. According to 3GPP-defined features [364] in M2M communications, MTC devices can form groups for radio-resource allocation and the system shall be optimized to handle MTC groups. There should also be a mechanism to associate MTC devices with one or more MTC groups. A group-based scheme is proposed in [372] to control massive access of MTC devices by forming clusters based on QoS requirements. The QoS requirements are characterized by the packet (i.e., preamble) arrival rate and maximum tolerable jitter. The higher packet-arrival rate indicates higher priority. The eNB allocates an AGTI for each cluster depending on the arrival rate. Each device in clusters is allowed to transfer packets only during the corresponding AGTI. If the AGTI for a different cluster is allocated in the same subframe, the cluster with lower priority (i.e., lower arrival rate) is delayed until the following subframe. An upper bound of the jitter (the total amount of time the packet has to wait) for a new cluster is calculated by summing up the arrival ratios (i.e., the arrival rate of existing clusters divided by the arrival rate of a new cluster) and adding this value to the AGTI. When the MTC device needs to perform an RA procedure, it sends the QoS requirements to the eNB. If there is already a cluster with the same QoS requirements and there are enough RBs in that AGTI to support the new device, the eNB allows the device to join the existing cluster. Otherwise, the device cannot be served. However, if there is no cluster with the QoS parameters for the requesting device, the upper bound of the jitter is calculated. If this bound is less than the maximum tolerable jitter for the device and for all other clusters, the eNB creates a new cluster. Although the computational complexity is less in this scheme, this scheme cannot handle the RAN overload completely because it fails to consider the number of MTC devices in each group. When the number of devices in each cluster grows larger, the access attempts of devices overload the channel and network congestion happens.

Devices can be grouped according to an application type or geographical location. Then, a group head or coordinator that will communicate with the eNB on behalf of group members is selected. Since the peer-to-peer communication between MTC devices is supported by the LTE-A, a group head can receive requests from group members and relay the request to the eNB. A group-based scheme considering energy efficiency is proposed in [373], where a coordinator (i.e., a group head) guarantees low energy consumption by limiting the access among MTC devices and the eNB (Figure 11.4). The achievable data rate between links (eNB-to-coordinator and M2M-to-coordinator) can be calculated using the channel gain and the link bandwidth. Using this data rate, the energy consumed by

each MTC device in a group is calculated and the total energy consumed by the group is determined. The objective of this scheme is to minimize the overall system energy consumption. The formation of groups is done by application of the *K-means algorithm*. In this algorithm, *K* randomly chosen devices are considered as the initial members of *K* groups and the rest of the devices join the groups according to their channel gains. The group coordinator can be selected in several ways, e.g., choosing the device with the maximum arithmetic/geometric mean of the channel gain. In summary, however, this scheme considers only the channel gain for grouping and the issues regarding preamble allocation to groups are not considered.

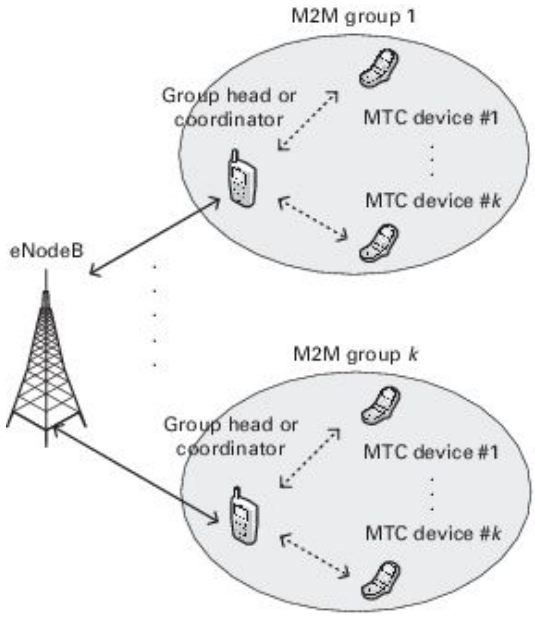

Figure 11.4. A group-based MTC overload control scheme using group heads.

11.3.2 An access-class-barring-based scheme

In [374], Lien *et al.* propose a cooperative ACB-based scheme whereby the eNBs select the ACB parameter jointly. As discussed in Section 11.2.1, the eNBs can communicate directly by means of an X2 interface. Using this cooperation, the eNBs can jointly decide the ACB parameter according to the level of network congestion. In this centralized scheme, an MTC device within the overlapping coverage area of several eNBs can access the unattached eNB. For example, as shown in Figure 11.5, if the MTC device is attached to eNB1, and within the overlapping area of eNB1 and eNB2, it can possibly access eNB2.

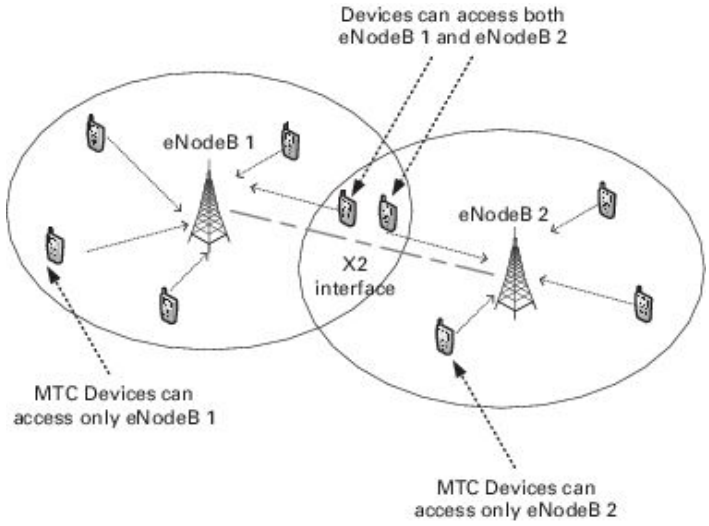

Figure 11.5. Machine-type communications (MTC) devices belonging to overlapping coverage areas of multiple eNBs.

The objective of this approach is to take a joint decision probability that minimizes the number of access attempts even under the highest level of congestion (i.e., when the number of accesses is maximum). An optimization problem is formulated to balance the number of devices attached to each eNB. Since the number of MTC devices which can access any particular eNB is random, the eNBs must be aware of the eNB selection strategy employed by the MTC devices. The authors of [374] consider all the MTC devices with equal priority, so the devices can choose the same strategy. After providing the strategy of each MTC device, the eNBs can obtain the number of devices attached to each of the specific eNBs. When this number is known, the decision probability can be obtained iteratively. Simulation results show that cooperative ACB is computationally inexpensive and can achieve around 30% improvement in the average and worst-case delay performance without significant degradation of throughput. However, this scheme requires overall system information (i.e., the number of devices attached to the eNBs, number of devices that can access the eNBs, and number of eNBs that a particular MTC device can access). Unfortunately, this information might not be available all the time in practice. Besides, the issues related to preamble allocation by the eNBs are not considered in this approach.

The approach discussed above does not consider priorities among devices. A prioritized random-access (PRA) scheme is proposed in [375], where RACH opportunities (i.e., RA-slots) are pre-allocated to different MTC classes. Using a

class-dependent backoff procedure, the occurrence of a large number of simultaneous access attempts can be avoided. In this case, the devices are classified into five priority classes, i.e., H2H, low priority, high priority, scheduled, and emergency, but this can be extended to more classes. Available RACH opportunities are virtually allocated to different priority classes. The eNB coordinates this virtual resource allocation and stores it in the system information block (SIB). As expected, H2H devices should be unaffected by MTC devices. As a result, the H2H devices can use all the available RA-slots. Multiple classes (i.e., emergency and scheduled) can share the same virtual slot, and collisions can be resolved using an individual backoff procedure. When a device fails to receive a RAR within a RAR window, the device detects a collision and backs off for its class-specific backoff period. Emergency situations can be handled by triggering an emergency flag in SIB. That is, when this flag is asserted, multiple classes, which share common virtual slots and try to access a channel for the first time, should delay their access attempts for a predefined time period. Although pre-allocation of slots to different classes can reduce the chance of collision, it cannot completely avoid collisions since the number of MTC devices can be too large and they can frequently access the channel within a short time. Therefore, a dynamic access-barring (DAB) mechanism has been proposed. In this mechanism the expected number of successfully decoded RA preambles is a function of the total number of RA attempts at that RA-slot and used as a loading factor. The eNB continuously monitors this loading factor and changes a loading state from *low*, via *medium*, to *high*. The loading state transits from low to medium if the average loading factor of two successive preamble transmissions is greater than or equal to some predefined threshold, and further transits to the high state if this average loading factor is less than or equal to another predefined threshold. DAB is disabled if it remains in the high state for a predefined number of slots, or the average loading factor is zero, or it remains in the medium and high states for more than a predefined amount of time. Simulation results show that, in typical MTC use-case scenarios (e.g., smart meters or hospital e-care), the PRA scheme provides a higher RA success probability and a lower access delay than those of the 3GPP-proposed EAB.

11.3.3 Separation of random-access preambles

As specified by the 3GPP, separation of RA resources can reduce the number of RA attempts in RACH. In [376], two RA preamble-separation approaches are compared on the basis of a throughput metric. In the first approach (method 1), the set of available RA preambles is completely split into two subsets, i.e., one solely for H2H devices and another for MTC devices. In the second approach (method

2), the preambles are again split into two subsets. However, in method 2, one set of preambles is dedicated solely to H2H devices and another set is shared by both H2H and MTC devices. After passing the ACB procedure, the devices can transmit preambles using the RA procedure. RACH throughputs are calculated assuming that the arrival of RA attempts is a Poisson process. Simulation results show that there is an RA load boundary below which the throughput of method 2 is slightly better than that of method 1. However, if the RA load is above that boundary, the throughput drops significantly. To this end, the selection of eNBs and the backoff procedure are not considered in any of these preamble-separation methods.

11.3.4 Dynamic allocation of random-access resources

In a dynamic resource-allocation approach, eNBs can dynamically allocate PRACH resources on the basis of the PRACH overload and the overall network load. As discussed in Section 11.2.2, when many devices are trying to transmit the same RA preamble in the same subframe as that being used for the RACH (i.e., in the same RA-slot), the transmissions collide, and the devices need to retransmit the preambles. Increasing the number of subframes for the RACH can reduce delay. However, when a subframe is used for the RACH, part of that subframe cannot be used for data transmission. As a result, there exists a tradeoff between selecting the RACH subframe and the data-transmission subframe. To meet the QoS requirement and reduce delay, the eNB in a cell should use a certain number of subframes for the RACH. Choi *et al.* address this issue in [377] and model a tradeoff between RACH and data transmission for contention-based RA. When the arrival rate of the RA preambles is known, the success and collision probabilities of the RA procedure can be calculated from the Poisson process. Using the collision probability, the expected RA delay can be found. A higher collision probability (i.e., fewer subframes allocated for the RACH) results in a longer delay. However, allocating more subframes to the RACH reduces the data-transmission opportunity. By measuring the delay bound and resource availability for data transmission, each cell can adjust the number of subframes for the RACH. An optimization problem is formulated to minimize the number of subframes allocated to the RACH, where the expected RA delay is less than a given delay bound. Each cell solves this optimization problem to determine the number of subframes allocated to the RACH. The collision probability is a function of the preamble-arrival rate. In practice, the arrival rate may vary over time and needs to be estimated correctly in order to calculate the collision probability as well as to solve the optimization problem. The authors propose an estimation framework using two baseline models, i.e., a *profile-based scheme* and a *moving-average*

scheme. The profile-based scheme keeps a weekly profile of RA preambles by averaging the arrival rate of RA requests at a specific time and day. The moving-average scheme reflects the current trend by giving more weight to recent observations. The proposed framework is the weighted sum of these two baseline models, where the weighting factor has a value between 0 and 1. Simulation results show that the proposed scheme uses fewer subframes for the RACH while satisfying a delay bound that can reduce that channel overload and improve the data-transmission opportunity. However, this scheme needs information about the RA preamble-arrival rate. Besides, the backoff procedure after collision is not considered in this approach.

Using the 3GPP-proposed slotted-access scheme, Anthony *et al.* [378] propose a self-optimizing algorithm whereby eNBs can automatically increase or decrease the number of RA-slots for preamble transmission depending on the channel load. As mentioned earlier, when a device fails to receive a response from the eNB in the last step of the RA procedure, the device performs a simple access-barring check. First, a random number between 0 and 1 is drawn, and this number is compared with the access probability (AP). If the number is less than the AP, the device proceeds to transfer preambles. Otherwise, the same procedure is repeated in the next RA-cycle. Two new access classes have been added to this scheme for high- and low-priority MTC devices. A lower AP results in a longer delay. When an MTC device receives an RAR in step (b) of the RA procedure, the MTC device includes an overload indicator in the next step. The overload indicator counts how many times that MTC device performs RA attempts. A higher overload indicator means that the level of congestion is increasing. According to the value of the overload indicator, the eNB dynamically increases or decreases the number of RA-slots for preamble transmission using an iterative algorithm. The number of RA-slots required can be calculated using the RA collision probability and the total number of RA resources. The collision probability and total number of RA resources are calculated by the eNB at the end of each RA-cycle. The collision probability is estimated by summing the overload indicators of all MTC devices and dividing this by the total number of RA attempts in one RA-cycle. The total number of RA resources can be found by taking the product of the number of RA-slots per second, the number of RA-frequency bands, and the number of preamble sequences. When the collision probability and total number of RA resources are known, the number of RA-slots required can be calculated accordingly. Using this value, the amount of RA resources available for the next cycle can be found. Finally, the eNB broadcasts this amount of available RA resources for the next RA-cycle. The responsiveness (i.e., how often the resources are adjusted in congestion) of this scheme is determined by the period of the RA-cycle. The short

RA-cycle period can react to congestion quickly. However, this will create a high signaling overhead.

11.3.5 A qualitative comparison of random-access overload control approaches

A qualitative comparison among different RA overload control schemes is provided in Table 11.1. The *efficiency* of a scheme depends on whether the scheme

- explicitly considers co-existence of H2H devices,
- considers preamble allocation to devices (and/or groups),
- considers mode selection (i.e., direct or via MTC Gateway),
- provides an eNB or MTC Gateway selection mechanism,
- takes a backoff procedure into account,
- is responsive (i.e., reacts quickly to changes of QoS parameters or of the traffic pattern),
- is scalable (i.e., can accommodate a large number of MTC devices) or not, and
- how much system information is required (a greater information requirement creates a higher signaling overhead).

If any scheme can satisfy more than five of these attributes, we consider the efficiency of that scheme to be *high*. The efficiency of a scheme is considered to be *Moderate* if it attains three to five of the above attributes. For example, the efficiency of the prioritized ACB scheme (proposed in [375]) is considered to be *moderate* since it explicitly considers the coexistence of MTC devices with H2H devices, and takes a backoff procedure into account, although it is not scalable but responsive and does not require much system information. In fact, mode selection and the selection of eNB or MTC Gateway are not addressed in any of these schemes. Since the schemes are unable to satisfy more than five of the attributes, we do not rank the efficiency of any of these schemes *high* in our comparison.

Table 11.1. A qualitative comparison of different random-access overload control schemes

Schemes	Explicit H2H co-existence schemes	Consideration of preamble allocation	Mode	Scalability	Computational complexity	Efficiency

Grouping of MTC devices						
Without group head (in [372])	No	No	Direct	No	Inexpensive	Low
Using group head (in [373])	No	No	Direct, peer-to-peer	Yes	Expensive	Moderate
Access-class barring						
Non-prioritized (in [374])	No	No	Direct	Yes	Moderate	Moderate
Prioritized (in [375])	Yes	No	Direct	No	Inexpensive	Moderate
Separation of preambles (in [376])	Yes	Yes	Direct	No	Inexpensive	Moderate
Dynamic allocation of resources						
Based on arrival rate (in [377])	No	No	Direct	Yes	Moderate	Moderate
Based on slotted access (in [378])	Yes	No	Direct	Yes	Moderate	Moderate

The *computational complexity* increases with increasing complexity of group formation, prediction of arrival rate, calculation of backoff period, amount of information exchange between eNB and device (and device to device), computational time of the algorithm, and the frequency with which it needs to be executed. For example, the complexity of the group-based scheme (proposed in [373]) is considered *expensive* because the formation of groups is based on the *K*-means algorithm. Besides, this group-based scheme needs to monitor the channel gain and update the group members frequently.

11.4 Performance modeling of the random-access channel (RACH)

In this section, we introduce a tractable queueing analytical model for MTC UEs with RA to initiate connections for transmitting data to an eNB. The queueing model enables us to analyze the data-transmission performances of heterogeneous MTC UEs with energy-saving capability.

11.4.1 The network model

We consider a cellular network with a macro eNB (Figure 11.6). In the macrocell, there are two types of UE, i.e., machine-type communications (MTC) and human-to-human (H2H). The H2H and MTC UEs require preambles to initiate a connection to the macrocell eNB for data transmission. The H2H and MTC UEs can contend to obtain RBs through the RA mechanism.

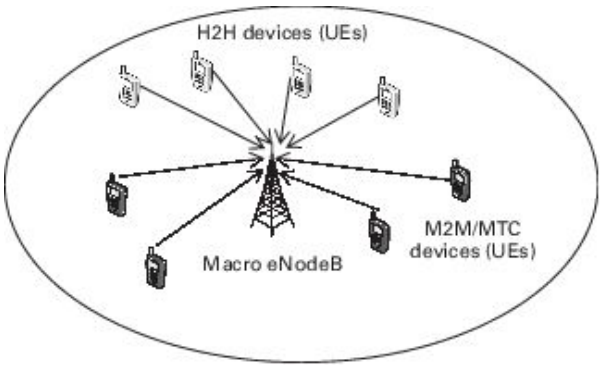

Figure 11.6. The network model for the performance modeling of the random-access channel (RACH).

In the following, we state the protocol adopted in the queueing analytical model. It is similar to that of LTE-A systems, which supports contention-based and contention-free RA [379]. A frame is divided into subframes, each of which has a length of 1 ms. We assume that the contention-free RA is used for H2H UEs, which allows the eNB to assign a preamble, and, hence, an RB to the target H2H UE in a timely manner. By contrast, the MTC UEs with lower priority will use the contention-based RA to obtain a preamble for initiating a connection to a target eNB for data transmission. When an MTC UE wants to transmit its packets to an eNB, the MTC UE randomly chooses one preamble from the set broadcast by the target eNB. More than one MTC UE may choose the same preamble, and hence, a collision will occur. The contention-based RA procedure is composed of four steps (Figure 11.2), i.e., preamble transmission, RAR, scheduled transmission (terminal identification), and contention resolution. The eNB broadcasts necessary parameters for the RA to MTC UEs, including the RAR window size and the

maximum number of allowable retransmissions. Here, let U denote the maximum backoff counter and L denote the maximum retransmissions. If the transmission failure occurs for L times, the packets in the buffer of the MTC UEs will be dropped to reduce the congestion and allow other MTC UEs to transmit their packets.

11.4.2 MTC user equipment and its packet transmission

We consider the MTC UE with a finite buffer (i.e., a queue) to store packets. The MTC UE can operate in two modes, i.e., active and inactive modes. In the active mode, the MTC UE turns on its transmitter and performs the contention-based RA. In the inactive mode, the MTC UE turns off its transmitter. However, the MTC UE can still receive and store the generated packets in its buffer. Initially, the MTC UE is in the inactive mode. When the number of packets in the buffer is greater than or equal to the wakeup threshold, the MTC UE will switch to the active mode. Conversely, when the number of packets in the buffer is zero, the MTC UE switches to the inactive mode again.

In the active mode, after the successful RA, the RB is allocated to the MTC UE for packet transmission in the uplink direction. Typically, the packet in M2M communications has a small size (e.g., sensor data and location update with a size of a few bytes). Therefore, we assume that all the packets in the buffer can be transmitted during one successful preamble contention (i.e., the buffer of the MTC UE is cleared immediately in a subframe). Once the queue size of the MTC UE has become zero, the MTC UE disconnects the connection to the eNB and switches back to the inactive mode waiting for new incoming packets.

11.4.3 Coexistence of MTC and H2H user equipments

Since H2H and MTC UEs coexist in the same cell, the eNB allocates the preambles to H2H and MTC UEs. The H2H UEs have higher priority and we assume that the eNB will always allocate the preambles to H2H UEs when they need to transmit packets. When the preambles are not used by the H2H UEs, the MTC UEs opportunistically contend for the preambles. We assume that the demand for a particular preamble by H2H UEs is modeled as a two-state Markov chain, from which the probability of a preamble being free (i.e., H2H UEs do not use the preamble) can be derived. The two states correspond to when the preamble is needed and not needed by H2H UEs, respectively. Let ψ_m and χ_m denote the

probabilities that H2H UEs remain in the states that need and do not need preamble m, respectively. The state-transition matrix is expressed as follows:

$$\boldsymbol{\psi}_m = \begin{bmatrix} \psi_m & 1-\psi_m \\ 1-\chi_m & \chi_m \end{bmatrix}. \tag{11.1}$$

Therefore, the probability that the preamble m is free and can be used by an MTC UE can be obtained from

$$P_m^{\text{free}} = \frac{1-\psi_m}{2-\psi_m-\chi_m}. \tag{11.2}$$

11.4.4 A queueing model

Without keeping track of the global state of the network, an *approximate* queueing model is adopted by taking advantage of the independence of the MTC UEs' states. The MTC UEs share the same pool of preambles allocated by the eNB. Figure 11.7 shows the system of queues of I MTC UEs contending for the preambles of the same eNB. The system of queues is composed of multiple individual queueing models – one for each MTC UE. However, solving each individual queueing model for MTC UE i requires not only the probability of availability of the preambles (after they have been allocated to H2H UEs), but also the collision probability p_{cl}^{i} of accessing the preambles allocated to MTC UEs. The collision probability for MTC UE i depends on the transmission probabilities $p_{\text{tr}}^{i'}$ of all other MTC UEs i' connected to the same eNB (i.e., sharing the same pool of preambles). The transmission probability of MTC UE i' depends on its own queue state, backoff, and retransmission counters, and the MTC UE's mode (i.e., either inactive or active mode). The transmission probability can be obtained by solving the individual queueing model (i.e., the expression in (11.22) in Section 11.4.6), which again requires the collision probability to compute. With this cyclic relationship, the steady-state transmission and collision probabilities will be obtained by using the iterative algorithm.

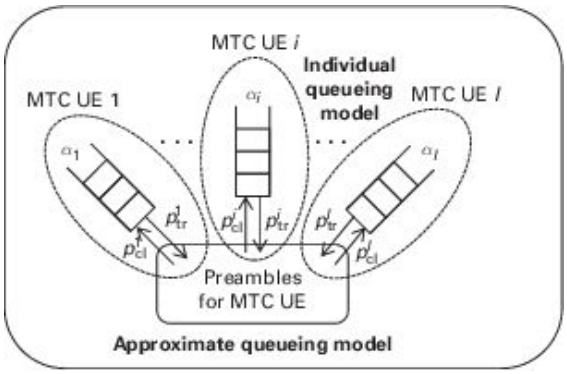

Figure 11.7. The queueing model of MTC UEs.

11.4.5 The state space and transition matrix for queueing at each MTC UE

For simplicity of presentation, we omit the index of MTC UE (i.e., *i*), for the individual queueing model. We consider a tagged MTC UE with a queue with a finite buffer size of Q packets. The contention-based RA and uniform backoff mechanisms are used by MTC UEs. The state of the tagged MTC UE is observed at the end of a subframe. Therefore, the discrete-time Markov chain (DTMC) is applied for modeling. The state space of the individual queueing model for the tagged MTC UE for contention-based RA can be defined as follows:

$$\Omega = \Big\{(\mathscr{Q}, \mathscr{B}, \mathscr{L}, \mathscr{K}), \mathscr{Q} \in \{0, \ldots, Q\}, \mathscr{B} \in \{0, \ldots, U\}, \mathscr{L} \in \{0, \ldots, L\}, \mathscr{K} \in \{\text{inact}, \text{act}\}\Big\}, \tag{11.3}$$

where $\mathscr{Q}$, $\mathscr{B}$, $\mathscr{L}$, and $\mathscr{K}$ are the random variables. $\mathscr{Q}$ represents the number of packets in the queue of the MTC UE, $\mathscr{B}$ represents the backoff counter, and $\mathscr{L}$ represents the retransmission counter. U is the maximum backoff counter and L is the maximum retransmission value. $\mathscr{K}$ represents the mode of the MTC UE, where $\mathscr{K} = \text{inact}$ and $\mathscr{K} = \text{act}$ are for inactive and active modes, respectively. The transition-probability matrix of the MTC UE can be defined as follows:

$$\mathbf{P} = \begin{bmatrix} \mathbf{P}_{\text{act}}\mathbf{M}_{\text{act,act}} & \mathbf{P}_{\text{act}}\mathbf{M}_{\text{act,inact}} \\ \mathbf{P}_{\text{inact}}\mathbf{M}_{\text{inact,act}} & \mathbf{P}_{\text{inact}}\mathbf{M}_{\text{inact,inact}} \end{bmatrix}, \tag{11.4}$$

where $\mathbf{P}_{\text{act}}$ and $\mathbf{P}_{\text{inact}}$ are the transition matrices of the queue state, backoff counters, and retransmission counter when the MTC UE is in active and inactive modes, respectively. $\mathbf{M}_{k,k'}$ is the transition matrix when the MTC UE switches from mode k to k', where $k, k' \in \{\text{inact}, \text{act}\}$.

The derivations of the matrices $\mathbf{P}_{\text{act}}$, $\mathbf{P}_{\text{inact}}$, and $\mathbf{M}_{k,k'}$ are presented below.

$\mathbf{P}_{\text{act}}$: The transition matrix of the MTC UE in an active mode

The transition matrix of the MTC UE in the active mode can be expressed as follows:

$$\mathbf{P}_{\text{act}} = \begin{bmatrix} \alpha' & \vec{\boldsymbol{\alpha}}^{\top} & & & \\ \vec{\boldsymbol{\beta}} & \mathbf{p}_{1,1} & \mathbf{p}_{1,2} & & \\ \mathbf{p}_{2,0} & \mathbf{p}_{2,1} & \mathbf{p}_{2,2} & \mathbf{p}_{2,3} & \\ \vdots & \vdots & & \ddots & \ddots \\ \mathbf{p}_{Q,0} & \mathbf{p}_{Q,1} & \cdots & \cdots & \mathbf{p}_{Q,Q} \end{bmatrix}. \tag{11.5}$$

Each row of the matrix $\mathbf{P}_{\text{act}}$ represents the number of packets q in the queue of the tagged MTC UE, i.e., $q = 0, 1, \ldots, Q$. For example, the probability α' and vector $\vec{\boldsymbol{\alpha}}^{\top}$ correspond to the state of there being zero packets in the queue (i.e., $q = 0$). Likewise, the vector $\vec{\boldsymbol{\beta}}$ and matrices $\mathbf{p}_{1,1}$ and $\mathbf{p}_{1,2}$ correspond to the state of one packet in the queue (i.e., $q = 1$), and so on. The probability matrices $\mathbf{p}_{q,0}$, $\mathbf{p}_{q,1}$, $\mathbf{p}_{q,q}$, and $\mathbf{p}_{q,q+1}$ are for the cases in which the number of packets in the queue of the MTC UE becomes zero, decreases to 1, remains the same, and increases by one, respectively. The case corresponding to $\mathbf{p}_{q,0}$ is based on the assumption that MTC data is typically small in size. Once the connection between the MTC UE and eNB has been established (i.e., a preamble is transmitted successfully), all the packets in the queue of the MTC UE will be transmitted to eNB in a single frame.

Note that the elements of $\mathbf{P}_{\text{act}}$ not shown in (11.5) are zeros. Additionally, to ease presentation of the notation, the matrix $\mathbf{p}_{q,q'}$ is derived for the case of MTC

UE in active mode without superscript act or subscript act when there is no ambiguity.

When the number of packets in the queue of the tagged MTC UE is zero, $\alpha' = 1 - \alpha$ is the probability of there being no packet generated, and hence the number of packets in the queue remains zero, where α is the packet-generation probability for the MTC UE. The vector $\vec{\boldsymbol{\alpha}}$ captures the case when there is a new generated packet at the MTC UE. In this case, the backoff counter will be randomly selected to be any number between 0 and U with equal probability. Additionally, the retransmission counter is reset to zero. Therefore, the vector $\vec{\boldsymbol{\alpha}}$ is defined as follows:

$$\vec{\boldsymbol{\alpha}}^{\top} = \left[\begin{array}{cccccc} \alpha/(U+1) & \cdots & \alpha/(U+1) & 0 & \cdots & 0 \end{array} \right]. \tag{11.6}$$

The first $U+1$ elements of $\vec{\boldsymbol{\alpha}}$ correspond to the retransmission counter of zero. The next $U+1$ elements correspond to the retransmission counter of one, and so on. Therefore, the zero elements of vector $\vec{\boldsymbol{\alpha}}$ correspond to the cases in which the retransmission counter is non-zero.

When the number of packets in the queue of the tagged MTC UE is positive, the transitions of backoff and retransmission counters must be taken into account. Let $\mathbf{L}_0$ and $\mathbf{L}_1$ denote the transition matrices when the transitions of backoff and retransmission counters result in there being no packet departure and packet departure, respectively. The matrix $\mathbf{L}_0$ (i.e., the case with no packet departure) can be defined as follows:

$$\mathbf{L}_0 = \begin{bmatrix} \mathbf{B}_{0,0} & \mathbf{B}_{0,1} & & & \\ & \mathbf{B}_{1,1} & \mathbf{B}_{1,2} & & \\ & & \ddots & \ddots & \\ & & & & \mathbf{B}_{L,L} \end{bmatrix}, \tag{11.7}$$

where $\mathbf{B}_{l,l'}$ represents the transition matrix of the backoff counter when the current and next retransmission counters are l and l', respectively. Each element of matrix $\mathbf{B}_{l,l'}$ corresponds to the backoff counter, and can be expressed as follows:

$$\mathbf{B}_{l,l} = \begin{bmatrix} 0 & 0 & \cdots & 0 \\ 1 & 0 & & \\ & \ddots & \ddots & \\ & & 1 & 0 \end{bmatrix}, \quad \mathbf{B}_{l,l+1} = \begin{bmatrix} p_{\mathrm{fl}} & \cdots & p_{\mathrm{fl}} \\ 0 & \cdots & 0 \\ \vdots & & \vdots \\ 0 & \cdots & 0 \end{bmatrix}. \tag{11.8}$$

For $\mathbf{B}_{l,l}$, when the backoff counter is zero (i.e., the first row), the MTC UE will perform preamble transmission. If the transmission fails (e.g., due to collision with the transmissions of other MTC UEs or channel error), the retransmission counter will be increased, which corresponds to $\mathbf{B}_{l,l+1}$. The probability that the transmission fails and the new backoff counter will be chosen is denoted by

$$p_{\mathrm{fl}} = \frac{1 - p_{\mathrm{sc}}(1 - p_{\mathrm{cl}})}{U + 1}, \tag{11.9}$$

where p_{sc} and p_{cl} are the probability of successful preamble transmission (i.e., no channel error) and the collision probability observed by the tagged MTC UE, respectively. We can obtain this probability from the performance analysis of preamble detection (e.g., as in [380]). Note, however, that the collision probability depends on the access strategy (i.e., transmission probability) of other MTC UEs connected to the same eNB. This probability will be obtained from the iterative algorithm to be presented later.

If the preamble transmission is successful, the RB will be allocated from the eNB to the MTC UE and the connection between the MTC UE and eNB will be established. Under the assumption that MTC data is typically small, once the connection has been established, all the packets in the queue will be transmitted. In this case, the probability matrix corresponding to the packet transmission is denoted by $\mathbf{L}_1$, i.e.,

$$\mathbf{L}_1 = \begin{bmatrix} \mathbf{C}_0 & \mathbf{0} & \cdots & \mathbf{0} \\ \vdots & \vdots & \ddots & \vdots \\ \mathbf{C}_L & \mathbf{0} & \cdots & \mathbf{0} \end{bmatrix}, \tag{11.10}$$

where $\mathbf{C}_l$ is the transition matrix when the retransmission counter is l and the packet departs from the queue, and $\mathbf{0}$ is a matrix of zeros with an appropriate size.

If the preamble transmission is successful, the retransmission counter will be reset to zero, and hence $\mathbf{C}_l$ is the leftmost element of matrix $\mathbf{L}_1$ (i.e., when the next state is $l = 0$). For $l < L$, the packet departs from the queue only when the preamble is successfully transmitted. However, for $l = L$, where the retransmission counter reaches its maximum value, the packet will be dropped if its current preamble transmission fails. The probability matrices corresponding to the above cases are defined as follows:

$$\mathbf{C}_l = \begin{bmatrix} p_{\text{sc}}(1-p_{\text{cl}})/(U+1) & \cdots & p_{\text{sc}}(1-p_{\text{cl}})/(U+1) \\ 0 & \cdots & 0 \\ \vdots & \ddots & \vdots \\ 0 & \cdots & 0 \end{bmatrix} \text{ for } l < L,$$

$$\mathbf{C}_L = \begin{bmatrix} 1/(U+1) & \cdots & 1/(U+1) \\ 0 & \cdots & 0 \\ \vdots & \ddots & \vdots \\ 0 & \cdots & 0 \end{bmatrix}. \tag{11.11}$$

The matrix $\mathbf{C}_l$ where $l < L$ corresponds to the case in which the preamble transmission is successfully transmitted. The matrix $\mathbf{C}_L$ corresponds to the transition regardless of whether the preamble is successfully transmitted or not (since the maximum retransmission value is reached).

Then, the elements of matrix $\mathbf{P}_{\text{act}}$ defined in (11.5) can be obtained as follows.

- $\mathbf{p}_{q,q+1} = \mathbf{L}_0\alpha$: The number of packets in the queue increases by one if there is a new packet generated with probability α and the preamble transmission is not successful.
- $\mathbf{p}_{q,q} = \mathbf{L}_0(1-\alpha)$: The number of packets in the queue remains the same if the preamble transmission is not successful and no new packet is generated. Except for $q = Q$, the element becomes $\mathbf{p}_{Q,Q} = \mathbf{L}_0$. That is, regardless of whether there is a new packet generated or not, if the preamble transmission is not successful, the queue remains full (i.e., the incoming packet will be blocked).
- $\mathbf{p}_{q,1} = \mathbf{L}_1\alpha$: The number of packets in the queue decreases to one if the preamble transmission is successful and there is a new packet generated.

- $\mathbf{p}_{q,0} = \mathbf{L}_1(1-\alpha)$: The number of packets decreases to zero if the preamble transmission is successful and no new packet is generated.

Finally, the vector $\vec{\boldsymbol{\beta}}$, which corresponds to the case in which there is no packet waiting in the queue in the next state (i.e., backoff and retransmission counters are not used), can be obtained from $\vec{\boldsymbol{\beta}} = (\mathbf{L}_1(1-\alpha))\vec{\mathbf{1}}$, where $\vec{\mathbf{1}}$ is a vector of ones with an appropriate size.

$\mathbf{P}_{\text{inact}}$: The transition matrix of the MTC UE in an inactive mode

The transition matrix of the MTC UE in the inactive mode can be expressed as follows:

$$\mathbf{P}_{\text{inact}} = \begin{bmatrix} \alpha' & \vec{\boldsymbol{\alpha}}^{\top} & & & \\ & \mathbf{p}_{1,1} & \mathbf{p}_{1,2} & & \\ & & \mathbf{p}_{2,2} & \mathbf{p}_{2,3} & \\ & & & \ddots & \ddots \\ & & & & \mathbf{p}_{Q,Q} \end{bmatrix}. \tag{11.12}$$

The structure of matrix $\mathbf{P}_{\text{inact}}$ is similar to that of $\mathbf{P}_{\text{act}}$ defined in (11.5). However, when the MTC UE is in the inactive mode, there is no preamble transmission attempt. Consequently, there is no packet departure (i.e., there is no element $\mathbf{p}_{q,q'}$, where $q' < q$).

The matrix $\mathbf{L}_0$ which corresponds to the case of no packet departure can be defined as follows:

$$\mathbf{L}_0 = \begin{bmatrix} \mathbf{B}_{0,0} & & & \\ & \mathbf{B}_{1,1} & & \\ & & \ddots & \\ & & & \mathbf{B}_{L,L} \end{bmatrix},$$

$$\text{where } \mathbf{B}_{l,l} = \begin{bmatrix} 1/(U+1) & 1/(U+1) & \cdots & 1/(U+1) \\ & 1 & & \\ & & \ddots & \\ & & & 1 \end{bmatrix}. \tag{11.13}$$

Specifically, the backoff and retransmission counters are always the same when the MTC UE is inactive. Since there is no packet departure when the MTC UE is in the inactive mode, we obtain the matrix $\mathbf{L}_1 = \mathbf{0}$. The first row of the matrix $\mathbf{B}_{l,l}$ corresponds to the case when the backoff counter is zero but the MTC UE is in the inactive mode. In this case, a new value of the backoff counter will be randomly generated.

Then, the elements of matrix $\mathbf{P}_{\text{inact}}$ defined in (11.12) can be obtained as follows: $\mathbf{p}_{q,q+1} = \mathbf{L}_0\alpha$ and $\mathbf{p}_{q,q} = \mathbf{L}_0(1-\alpha)$. Specifically, the number of packets in the queue of the MTC UE increases and remains the same when there is packet arrival and when there is no packet arrival with the probabilities α and $1-\alpha$, respectively.

$\mathbf{M}_{k,k'}$: The transition matrix for the mode of the MTC UE

The matrices $\mathbf{M}_{\text{act,act}}$ and $\mathbf{M}_{\text{act,inact}}$ represent the state transition of the MTC UE from the active mode to the active mode and to the inactive mode, respectively. Similarly, the matrices $\mathbf{M}_{\text{inact,inact}}$ and $\mathbf{M}_{\text{inact,act}}$ represent the state transitions of the MTC UE from the inactive mode to the inactive mode and to the active mode, respectively. The transition matrices which result in the mode change to the active mode can be expressed as follows:

$$\mathbf{M}_{\text{act,inact}} = \begin{bmatrix} 1 & 0 & \cdots & 0 \\ 0 & 0 & & \\ \vdots & & \ddots & \vdots \\ 0 & & \cdots & 0 \end{bmatrix}, \quad \mathbf{M}_{\text{inact,act}} = \begin{bmatrix} 0 & & & & \\ & \ddots & & & \\ & & 0 & & \\ & & & 1 & \\ & & & & \ddots \\ & & & & & 1 \end{bmatrix}, \tag{11.14}$$

where $\mathbf{M}_{\text{act,act}} = \mathbf{I} - \mathbf{M}_{\text{act,inact}}$ and $\mathbf{M}_{\text{inact,inact}} = \mathbf{I} - \mathbf{M}_{\text{inact,act}}$. $\mathbf{I}$ is an identity matrix with an appropriate size.

In the case of $\mathbf{M}_{\text{act,inact}}$, the MTC UE switches from the active mode to the inactive mode only when the queue is empty (i.e., only the top-left corner is one). In the case of $\mathbf{M}_{\text{inact,act}}$, the diagonal elements corresponding to the queue size $0, \ldots, Q_{\text{wake}} - 1$ are zeros. Q_{wake} is the wakeup threshold (i.e., MTC UE switches from an inactive mode to an active mode if the number of packets in its queue is equal to this threshold). Otherwise, the diagonal elements corresponding to the queue size $Q_{\text{wake}}, \ldots, Q$ are ones.

11.4.6 Queueing performance measures at an MTC user equipment

With the transition probability matrix $\mathbf{P}$ defined in (11.4), the stationary probability whose vector is denoted by $\vec{\boldsymbol{\pi}}$ of the states of the tagged MTC UE can be obtained by solving $\vec{\boldsymbol{\pi}}^{\top} = \vec{\boldsymbol{\pi}}^{\top}\mathbf{P}$ and $\vec{\boldsymbol{\pi}}^{\top}\vec{\mathbf{1}} = 1$, where $\vec{\mathbf{1}}$ is a vector of ones with an appropriate size. The elements of the vector $\vec{\boldsymbol{\pi}}$ are denoted by $\pi_{q,b,l,k}$, each of which refers to the stationary probability when the number of packets in the queue of the MTC UE is q, the backoff and retransmission counters are b and l, respectively, and the mode of the MTC UE is k. From the stationary probabilities, various performance measures of the MTC UE can be obtained.

The average number of packets in the queue of the MTC UE can be obtained from

$$\overline{q} = \sum_{q=1}^{Q} q \left(\sum_{b=0}^{U} \sum_{l=0}^{L} \sum_{k \in \{\text{act,inact}\}} \pi_{q,b,l,k} \right). \tag{11.15}$$

The packet-dropping probability is the probability that the packet is dropped due to reaching the retransmission limit (i.e., L). First, the packet-dropping rate (i.e., the average number of dropped packets per subframe) is obtained as follows:

$$\overline{D} = \left(\sum_{q=1}^{Q} \pi_{q,0,L,k} \right) (1 - p_{\text{sc}}(1 - p_{\text{cl}})), \tag{11.16}$$

for $k = \text{act}$. Then, the packet-dropping probability is obtained from $p_{\text{dr}} = \overline{D}/\alpha$.

The packet-blocking probability is the probability that the newly generated packet cannot be buffered when the queue of the MTC UE is full. First, the packet-blocking rate (i.e., the average number of blocked packets per subframe) is obtained as follows:

$$\overline{B} = \underbrace{\left[\pi_{Q,0,0,\text{act}} \quad \cdots \quad \pi_{Q,b,l,k} \quad \cdots \quad \pi_{Q,U,L,\text{act}} \right] \left(\mathbf{L}_0 \alpha \vec{\mathbf{1}} \right)}_{\text{active mode}} + \underbrace{\alpha \sum_{q=1}^{Q} \sum_{b=0}^{U} \sum_{l=0}^{L} \pi_{q,b,l,\text{inact}}}_{\text{inactive mode}}, \tag{11.17}$$

where the first and second terms are for the cases when the MTC UE is in the active and inactive modes, respectively. Then, the packet-blocking probability can be obtained from $p_{\text{bl}} = \overline{B}/\alpha$.

The average packet delay is measured from the time when the packet is generated to when the MTC UE successfully transmits a preamble. As a result, the MTC UE can establish a connection and transmit packets to the eNB in the next subframe. The average packet delay can be obtained using Little's law from

$$\overline{W} = \frac{\overline{q}}{\alpha - \overline{B}} + W_{\text{RAR}}, \tag{11.18}$$

where $\alpha - \overline{B}$ is the effective packet-arrival rate at the queue (i.e., the blocked packet is ignored), and W_{RAR} is the size of a RAR window.

The queue throughput of the MTC UE can be obtained from $\tau = \alpha - \overline{D} - \overline{B}$. The normalized throughput is calculated from

$$\overline{\tau} = \tau/\alpha. \tag{11.19}$$

The duty cycle is the proportion of time that the MTC UE is in the active mode. The duty cycle can be obtained from

$$T = \sum_{q=1}^{Q} \sum_{b=0}^{U} \sum_{l=0}^{L} \pi_{q,b,l,\text{act}}. \tag{11.20}$$

The net transmission probability of the MTC UE (i.e., probability that the MTC UE transmits using any preamble) is obtained from

$$p_{\text{ntr}} = \left(\sum_{q=1}^{Q} \sum_{l=1}^{L} \pi_{q,0,l,\text{act}} \right). \tag{11.21}$$

Since the eNB can allocate M preambles to all MTC UEs, the transmission probability of the MTC UE on one of the preambles is obtained from

$$p_{\text{tr}} = \frac{p_{\text{ntr}}}{M}. \tag{11.22}$$

In (11.22), it is assumed that the MTC UE chooses to transmit on any allocated preamble uniformly.

11.4.7 An iterative algorithm

The performance measures are for a particular MTC UE given the transmission probabilities of other MTC UEs (notice from p_{cl} in (11.9)). To obtain the steady-state performance measures, the steady-state transmission probabilities of all the MTC UEs contending for preambles from the same eNB are required. The steady-state performance measures can be obtained iteratively using Algorithm 15. The iterative algorithm calculates the collision probability of a particular MTC UE

(i.e., $p_{\text{cl}}^{i}[t]$ for MTC UE i) given the transmission probabilities of other MTC UEs (i.e., $p_{\text{tr}}^{i'}[t]$ for MTC UEs i'). However, since the number of available preambles is random due to the demand by H2H UEs, first we obtain the probability that n preambles are available as follows:

$$\rho(n) = \sum_{\sum y_m = n} \prod (P_m^{\text{free}})^{y_m} (1 - P_m^{\text{free}})^{1-y_m}, \tag{11.23}$$

where P_m^{free} is the probability that the preamble m is free and can be obtained from (11.2). y_m is an auxiliary indicator function that takes a value of one if the preamble m is free and a value of zero if it is used by an H2H UE. The collision probability (i.e., the probability of unsuccessful preamble access) is then obtained from

$$p_{\text{cl}}^{i}[t] = 1 - \sum_{n=1}^{M} \rho(n) \left(\prod_{i'=1; i' \neq i}^{\tilde{I}} (1 - p_{\text{tr}}^{i'}[t]) \right), \tag{11.24}$$

where $\tilde{I}$ is the total number of MTC UEs contending for preambles from the same eNB. Observe that $p_{\text{cl}}^{i}[t]$ of an MTC UE i is obtained from $p_{\text{tr}}^{i'}[t]$ of other UEs i' and also the probability of a preamble being free. Then, the collision probability $p_{\text{cl}}^{i}[t]$ is used to solve the individual queueing model (line 5 in Algorithm 15). Then, the transmission probability is obtained (line 6 in Algorithm 15). These steps are repeated for all MTC UEs contending for preambles from the same eNB. The iterative algorithm stops when the transmission probability converges, i.e., the change is less than the tolerable threshold ε (line 9 in Algorithm 15).

Algorithm 15 Iterative algorithm to obtain the steady-state performance measures for the MTC UEs.

1: Initialize transmission probabilities of all MTC UEs $p_{\text{tr}}^{i}[t]$ for $i = 1, \ldots, \tilde{I}$, where $t = 0$.
2: **repeat**
3: **for** $i = 1, \ldots, \tilde{I}$ **do**
4: Calculate the collision probability $p_{\text{cl}}^{i}[t]$ observed by MTC UE i from (11.24)
5: Solve the individual queueing model given $p_{\text{cl}}^{i}[t]$
6: Obtain the transmission probability of MTC UE i from (11.22)
7: **end for**
8: $t = t + 1$
9: **until** $\max_i \left| p_{\text{tr}}^{i}[t] - p_{\text{tr}}^{i}[t-1] \right| < \epsilon$

11.4.8 Numerical results

We consider the coexistence of MTC UEs and H2H UEs transmitting data to the eNB. The H2H UEs access a preamble with probability 0.5, where the total number of preambles is $M = 2$. The queue size for an MTC UE is assumed to be five packets. The packet-generation probability of the MTC UE is $\alpha = 0.001$. The maximum backoff and retransmission counters are $U = 15$ and $L = 5$, respectively. The threshold for the iterative algorithm to terminate is $\epsilon = 10^{-10}$. To validate the correctness of the proposed analysis, the simulation to emulate the contention-based RA mechanism is implemented. The simulation follows the backoff algorithm as used in the UMTS-LTE standard.

The simulation of the RA procedure is done on a time-slot (i.e., frame) basis, where the different events (e.g., packet arrival, backoff, and transmission) happen and are observed at the end of a transmission frame. Firstly, the availability of RBs, which is associated with whether H2H UEs are active or not is determined. Secondly, each MTC UE checks whether a packet is generated or not. The generated packet will be blocked if the queue of the MTC UE is full. Then, if the queue of the M2M EU is not empty, the M2M EU will initiate a backoff algorithm. The backoff counter decreases for every frame and, if the counter is zero, the MTC UEs will transmit an RA preamble. If the preamble is successfully transmitted, the eNB will reply with a RAR and the MTC UE will transmit the packet. If the collision occurs, the MTC UE will implement the backoff

mechanism and try to retransmit the RA preamble again. The MTC UE observes its state and switches between active and inactive modes. The performance metrics (e.g., average queue size, number of blocked packets, delay, and throughput) are measured in each frame.

The convergence of the queueing model

First, we consider the queueing performance of the MTC UEs. Figure 11.8 shows the convergence of the performance measure in terms of the numbers of packets in the queue of four selected MTC UEs which is obtained from the approximate queueing model. This performance measure is obtained when there are 100 MTC UEs with packets to transmit to an eNB. The packet-arrival probability of each MTC UE is between 0.001 and 0.0015 packets per subframe. From Figure 11.8, we can observe that the queueing performance of an MTC UE converges to the steady state within a few iterations, which shows that the proposed approximate queueing model can be used efficiently.

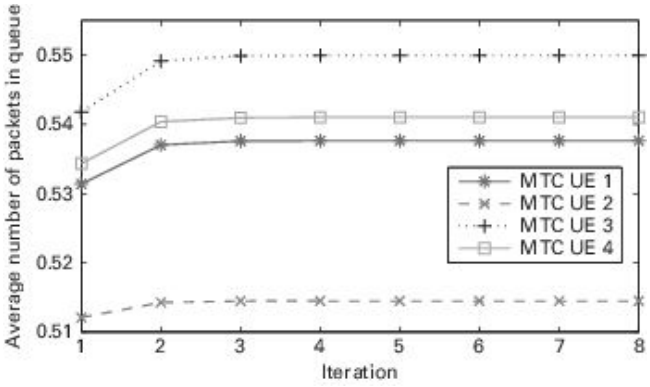

Figure 11.8. The convergence of the MTC UE's performance (i.e., the average number of packets in the queue).

The impact of the probability of a preamble being free

Figure 11.9 shows the normalized throughput of the MTC UE when the probability of a preamble being free is varied. In this case, we assume that all preambles have the same parameters of ψ_m and χ_m and all the MTC UEs have the same packet-arrival probability (i.e., $\alpha = 0.001$) for ease of presentation. There are 500 MTC UEs. When the probability of a preamble being free increases, the normalized throughput increases, since the MTC UEs have a higher chance of being able to use preambles to establish connections and transmit packets to the

eNB. Additionally, when the number of preambles available increases, the normalized throughput increases significantly. The eNB can use this performance metric to allocate the preambles so that the performance of the MTC UEs can be guaranteed.

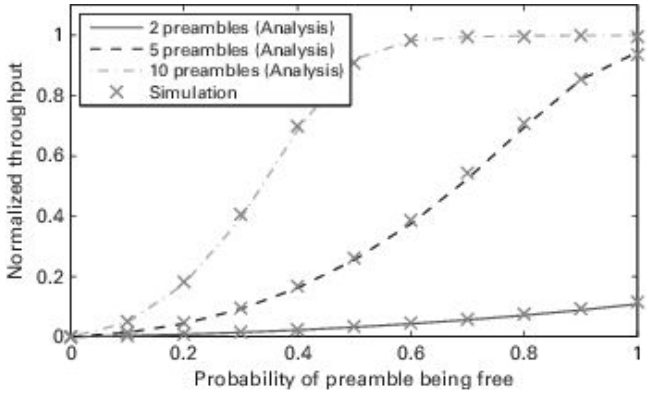

Figure 11.9. The normalized throughput of the MTC UE when the probability of a preamble being free is varied.

The impact of heterogeneous MTC UEs

Next, we consider the case of heterogeneous MTC UEs whose packet-arrival rate is different. The packet-arrival probabilities of 100 MTC UEs are random between 0.001 and 0.0015. The average packet delays of these 100 MTC UEs are shown in Figure 11.10. Since the number of MTC UEs is small, the average packet delay is large if the packet-arrival rate is large, which is to be expected. Nevertheless, the simulation results follow the numerical results obtained from the analysis closely.

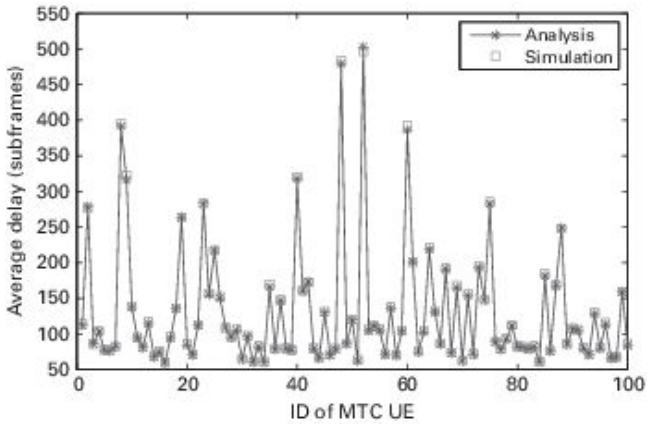

Figure 11.10. Packet delay under a heterogeneous packet-arrival rate.

The impact of active and inactive modes

When the queue of an MTC UE is empty, the MTC UE will switch to the inactive mode to reduce energy. The MTC UE will switch back to the active mode if the number of packets in its queue is equal to the wakeup threshold Q_{wake}. We study the impact of this threshold. Figure 11.11 shows the normalized throughput when the number of MTC UEs is varied between 100 and 1000. When the number of MTC UEs increases, the normalized throughput decreases due to congestion in the network (i.e., to contend for preambles from an eNB). However, interestingly, when the wakeup threshold (i.e., the threshold to switch from an inactive to an active mode) increases to two, the throughput increases. This result is counter-intuitive since, when the wakeup threshold is large, the MTC UEs tend to be more likely to be in an inactive mode (i.e., they have a smaller duty cycle as shown in Figure 11.12(a)) and their performance should be negatively affected. However, in fact, the performance in terms of normalized throughput is improved (Figure 11.11). The reason is that when most of the MTC UEs are active, they aggressively contend for the limited number of available preambles, resulting in high collision and packet-dropping probabilities. However, when some MTC UEs spend more time in the inactive mode, the congestion is alleviated. As a result, the probability of successful preamble transmission increases and the throughput of MTC UEs increases.

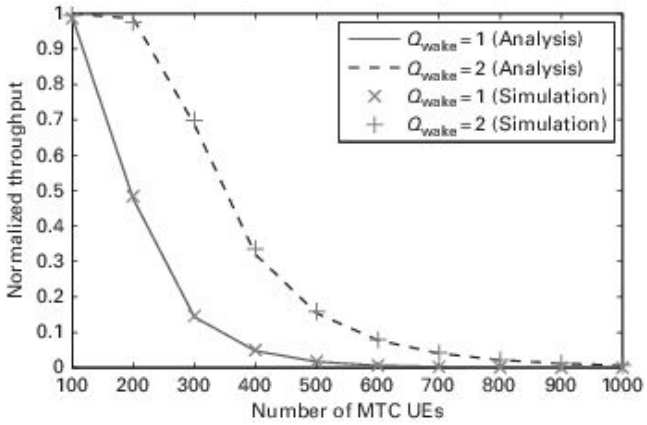

Figure 11.11. The normalized throughput under different numbers of MTC UEs.

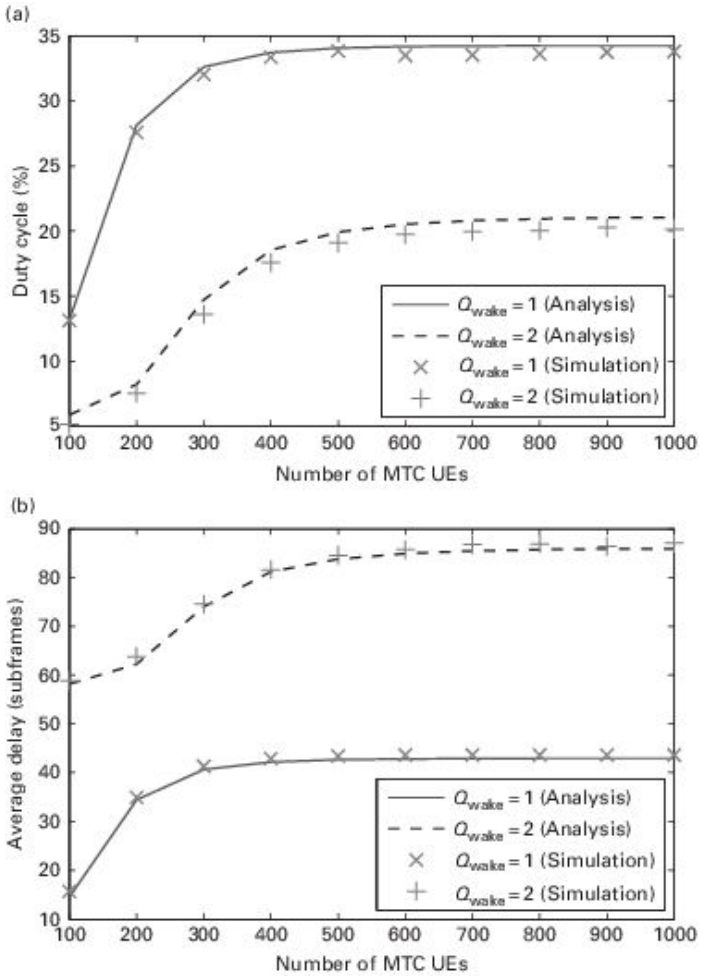

Figure 11.12. (a) The duty cycle and (b) the average packet delay under different numbers of MTC UEs.

However, one important side effect when the wakeup threshold increases is the larger delay, as shown in Figure 11.12(b). Therefore, it is important to optimize the wakeup threshold such that the performances (i.e., throughput and delay) as well as the energy consumption are traded off.

11.5 Chapter summary

Machine-to-machine communications will be an important part of the Internet-of-Things (IoT) for connecting machine-type communications devices. The major challenge here is to provide connectivity for a very large number of devices and avoid network congestion. Therefore, it is necessary to control radio-network traffic by using an efficient random-access procedure. In this chapter, we have

provided a comprehensive survey of various approaches to control network congestion. A comparison of existing schemes has been presented. By applying an effective RA procedure, it will be possible to improve overall network stability and guarantee quality of service (QoS) performance.

Efficient overload control for supporting a large number of devices in MTC is an ongoing area of research. In addition, coexistence with H2H devices without compromising their QoS requirements and distinguishing MTC devices from H2H devices makes the problems more challenging in MTC. In this chapter, we have identified a couple of research directions related to practical overload problems.

- *Mode selection and QoS provisioning:* As expected, MTC devices should not collide with H2H devices, and should at the same time satisfy their own QoS requirements. As noted above, the MTC devices can communicate either directly with the eNB or via the MTC Gateway. The choice of selection of the eNB or MTC Gateway may depend on the signal strength or link condition (channel gain). However, in some practical cases, the choice of the optimal mode might need to be analytically evaluated. For example, although the signal strength is strong in direct mode, selecting an MTC Gateway may provide a better success probability or a lower delay. In our viewpoint, *queueing theory* can be applied to evaluate an optimal choice of the mode selection and QoS provisioning (i.e., measuring throughput) in the context of MTC.
- *Selection of eNB and MTC Gateway:* Besides mode selection, when the MTC devices are in the coverage region of multiple eNBs (MTC Gateways), the selection of eNB (MTC Gateway) might be crucial. To guarantee QoS and balance the network load, it is necessary to adopt an efficient eNB (MTC Gateway) selection mechanism. Unfortunately, most of the approaches proposed in the literature so far do not consider eNB- or MTC Gateway-selection mechanisms while addressing RA overload control. However, in our perspective, *reinforcement learning* approach (i.e., *Q*-learning) whereby MTC devices select an eNB or MTC Gateway on the basis of their perceived QoS parameters can be helpful.
- *Efficient group management:* Group management and addressing (i.e., selection of a group coordinator) of MTC devices are vital. When both the number of groups and the number of members in the groups grow larger, it will be a challenging issue to allocate RA slots and reduce signaling overhead. In addition, an efficient algorithm for preamble allocation is necessary. *Game theory* can be a useful tool to optimize preamble allocation competitively. In addition, the formation and reformation of groups should be

done adaptively on the basis of traffic change. Additionally, there must be provision for peer-to-peer communication between group members even if peer-to-peer communication has to coexist with other communication standards.

- *Opportunistic random access (cognitive M2M):* Owing to the increasing number of MTC devices, there may not be enough resources to accommodate all MTC devices. It would be beneficial to control network congestion if the MTC devices were able to access the channel opportunistically. Enabling cognitive-radio capability in M2M RA might be a propitious area of research.

---

[1] "M2M" and "MTC" can be used interchangeably, depending on the context.

[2] "PRACH" and "RACH" are used interchangeably.

Part V

Standardization of D2D communications

12 Network-controlled D2D over LTE/LTE-A

This chapter mainly introduces the motivation and requirement for using D2D communications over Long Term Evolution (LTE)/LTE-Advanced (LTE-A). The agreed working scenarios and working assumptions are discussed and also the methods for link- and system-level performance evaluation are provided.

12.1 D2D communications in LTE-A networks

Now that more and more new multimedia-rich services are becoming available to mobile users, there is an ever-increasing demand for higher-data-rate wireless access. As a consequence, new wireless technologies such as LTE have been introduced. These technologies are capable of providing high-speed, large-capacity, and mobile services with guaranteed quality of service (QoS) [183]. With the technological evolution of cellular networks, new techniques, such as small cells, which are able to improve network capacity by reducing cell size and effectively controlling interference, have been developed. However, most attempts still rely on the centralized network topology which requires mobile devices to communicate with an evolved Node B (eNB). Such a centralized network topology can easily suffer from congestion with a large number of communicating devices. Additionally, the eNB might not have complete information about transmission parameters among devices, which is required in order to achieve optimal network performance. Consequently, the concept of D2D communications has been introduced to allow local peer-to-peer transmission among mobile devices by bypassing the eNB and AP [1].

Many technical groups such as the 3GPP and the IEEE are currently addressing the standardization of D2D communications in the licensed band. A major breakthrough was achieved in due course when the 3GPP agreed on starting a study item for D2D technology. The objective of this study item is to investigate the operator-controlled communications between user equipments (UEs) that are in proximity, under continuous network control, and in 3GPP network coverage. Specifically, besides cellular operation, where the UEs can be served by the network via the eNB in the LTE system, some UEs may communicate with each other directly over direct links for proximity services [381].

In addition to commercial use cases of D2D, direct communication can have a crucial role in public-safety use cases. For example, firefighters can communicate with each other directly even under no network coverage where a network is unavailable after a tsunami or a wild fire. In December 2012, the 3GPP RAN plenary approved the start of a study item (SI) on LTE device-to-device (D2D) proximity-based services (ProSe). In 3GPP LTE release 12, it was also agreed to focus on broadcast D2D communications for the public-safety use case and discovery for both general and public-safety use cases. In the public-safety use case, inside-, partial-, and outside-network-coverage scenarios should be supported. Hence the 3GPP technology has the opportunity to become the platform of choice to enable D2D communications, for which two important services of ProSe have been defined.

- The first one is proximity discovery, with which users can discover each other when they are in close mutual proximity.
- The second is direct communication, with which users can communicate with each other when they are in close mutual proximity.

12.2 Requirements and working assumptions

In a 3GPP technical report [381], the requirement contents cover operational, charging, and security requirements.

12.2.1 Operational requirements

The operator network shall be able to continuously control the use of evolved universal terrestrial radio access (E-UTRA) resources for ProSe discovery and ProSe communications between UEs, as long as at least one of these UEs is under E-UTRA coverage and using the operator spectrum. ProSe communications and ProSe discovery shall not adversely affect other E-UTRA services. ProSe services are available to ProSe-enabled UEs that are registered to a PLMN, and are under coverage of the E-UTRA of said PLMN, potentially served by different eNBs. In this case E-UTRA resources involved in ProSe services will be under real-time 3GPP network control. The network should be able to collect discovery information regarding which ProSe-enabled UEs have been discovered to be in the proximity of a given UE. Restrictions from contracts and regulation on data collection apply. ProSe services are not available to ProSe-enabled UEs outside the E-UTRA coverage except in the following case: ProSe-enabled public-safety UEs can use ProSe services when operating on public-safety spectrum even when not under E-UTRA coverage. In this case, at least a one-time pre-authorization to use ProSe services is needed. Re-authorization and specific configurations, including spectrum configurations, of public safety UEs shall be subject to public-safety operator policy. When operating ProSe, the evolved packet system (EPS) shall be able to support regional or national regulatory requirements. The ProSe system shall

- allow a UE to selectively discover other UEs of interest;
- ensure that 3GPP UE/subscriber identifiers are not disclosed to unauthorized parties when ProSe discovery and communications are used;
- allow both granting and revocation of discovery permissions; and
- enable applications to individually request the setting of discovery parameters, such as discovery range class.

Subject to operator policies, multi-operator core network (MOCN) networks shall support establishing ProSe communications between two UEs camping on the same radio-access network but served by different MOCN PLMNs.

12.2.2 Charging requirements

When a ProSe-enabled UE uses ProSe communications or ProSe-assisted WLAN direct communications, both the home public land mobile network (HPLMN) and visited public land mobile network (VPLMN) operators shall be able to collect accounting data for this communication, including its

- activation/deactivation;
- initiation/termination;
- duration and amount of data transferred;
- QoS, if via E-UTRAN (e.g., levels of availability, resources allocated);
- inter-operator communication; and
- inter-operator signaling.

12.2.3 Security requirements

The system shall ensure the confidentiality and the integrity of user data and network signaling over the ProSe communications path and ProSe-assisted WLAN direct communication to a level comparable to that provided by the existing 3GPP system. The level of security provided by the existing EPS shall not be adversely affected when ProSe discovery and communications are enabled. The system shall ensure the authenticity of the ProSe discovery information used by an application that is authorized by the operator and the user. At the same time, the system shall be able to restrict ProSe discovery information to the ProSe-enabled UEs and applications that have been authorized. The permission to be discoverable is given by the user and shall be executed by the system, subject to operator control, on a per-application basis. An operator shall be able to configure a UE with the permission to be discoverable or not by one or more UEs, without prior registration to the network, for example, to provide the means for an enterprise or public-safety organization to set permissions for its users. Existing 3GPP security mechanisms shall be reused whenever possible and appropriate. ProSe services shall respect local regulatory frameworks on the use of licensed spectrum. ProSe discovery and communications shall support regional or national regulatory requirements (e.g., regarding lawful interception). The

system shall ensure that the user's identity and privacy are protected when ProSe is used.

12.3 Key working scenarios

From the year 1995 until now, as shown in Figure 12.1, wireless cellular technologies have evolved from the second generation to the fourth generation of mobile communication systems due to new services' requirements. For each generation, new communication techniques have been explored, which include frequency, code, and space to improve the network capacity. Ever since D2D communications was introduced [1], it has attracted a great deal of attention from both academia and industrial communities investigating another communication domain: that of mobile devices.

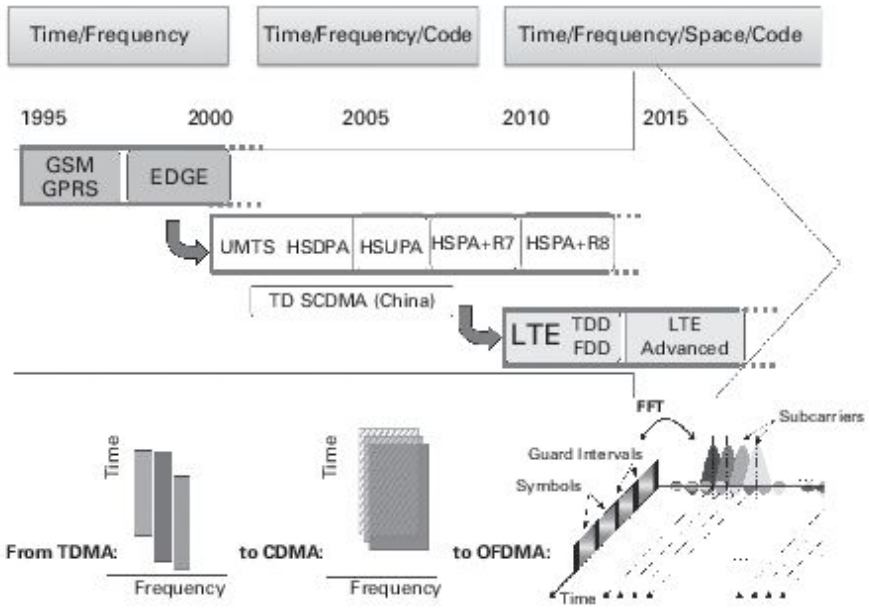

Figure 12.1. Cellular technology's evolution by exploring new communication dimension.

The technology-evolution roadmap of D2D-enabled communication is from simple device-to-device short-range communications that are network-unaware (Figure 12.2) such as the use of Bluetooth among mobiles, to cellular-aware short-range communications, and finally to cellular-controlled

D2D communications in the licensed spectrum in a fully coordinated manner. For scenario A, the cellular networks and the D2D networks work separately using different radio-access technologies (RATs), and operate in different spectrum ranges, e.g., UMTS and Wi-Fi. Scenario B grants mobile devices partial control functions via the eNB and core networks (CNs), which allows mobiles to intelligently switch between licensed and unlicensed bands. In a third scenario, devices can form a cooperative network in the licensed band to realize maximal flexibility and performance.

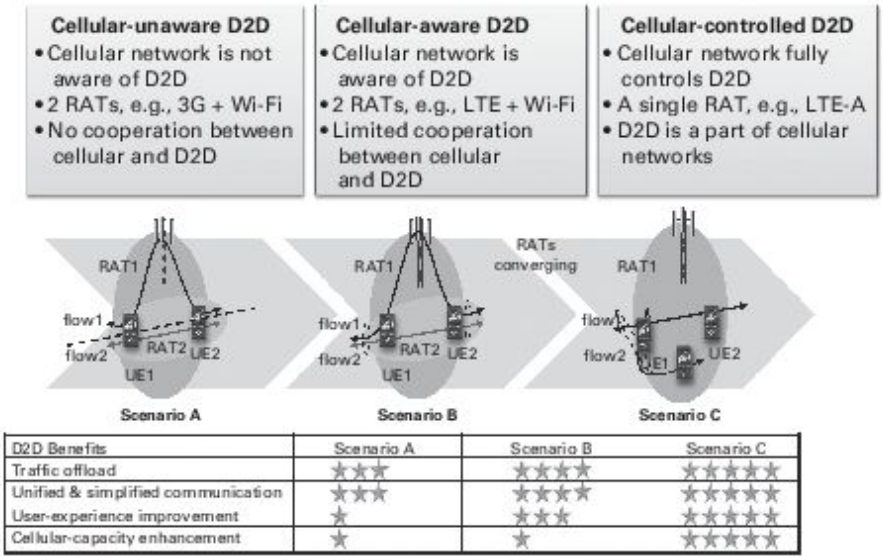

D2D Benefits	Scenario A	Scenario B	Scenario C
Traffic offload	★★★	★★★★	★★★★★
Unified & simplified communication	★★★	★★★★	★★★★★
User-experience improvement	★	★★★	★★★★★
Cellular-capacity enhancement	★	★	★★★★★

Figure 12.2. A wireless device-to-device communications evolution roadmap.

Besides, the LTE platform would have an advantage over others, such as Wi-Fi and Bluetooth, that operate device-to-device protocols using license-exempt spectrum, and the 3GPP is working on enhancing the LTE Evolved Packet Core (EPC) platform to support these capabilities. Proximity-based applications and services represent a recent and enormous social–technological trend.

- These applications and these services are based on the awareness that two devices or two users are close to each other.
- Awareness of proximity carries value, and generates demand for an exchange of traffic between them.

Direct D2D communication is also essential for public-safety services in case of a lack of network infrastructure in disaster situations. The 3GPP provides two general scenarios for D2D communications and network, i.e., public safety and commercial use. Specifically, Table 12.1 summarizes the corresponding application scenarios, when the UE is within or outside the eNB coverage.

Table 12.1. Key applications

Application	Within network coverage	Outside network coverage
Discovery	Non-public-safety and public-safety requirements	Public safety only
Direct communication	At least public-safety requirements	Public safety only

12.4 LTE-A architecture enhancements to support proximity-based services (ProSe)

The overall solution for ProSe incorporates/covers the UE, radio-access network, and CN. In the core, a new network element is added to provide the proximity services. This element is called the "proximity server," and for direct communication the system architecture is the same as that used for LTE-A. For the access part, the proximity discovery is the same, while for the direct communication, it is different. D2D uses a cellular link for the control part, which is the same as for the control plan. For the data plan, D2D uses new direct mobile communication, as shown in Figure 12.3.

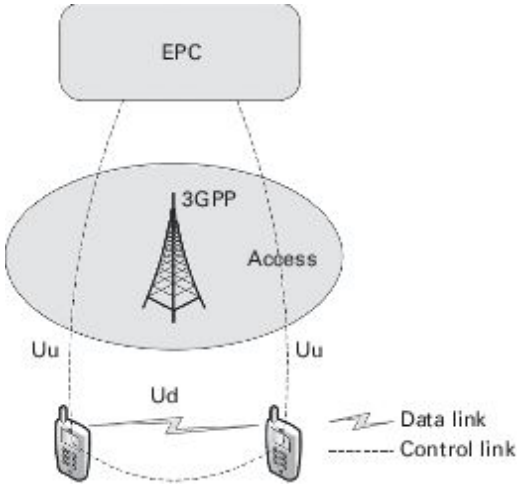

Figure 12.3. The access architecture for D2D communications.

Figure 12.4 shows the D2D control plan, which reuses the LTE-A control protocol stack, and Figure 12.5 introduces the new interface named Ud for the data plan, which reuses the LTE-A data protocol stack.

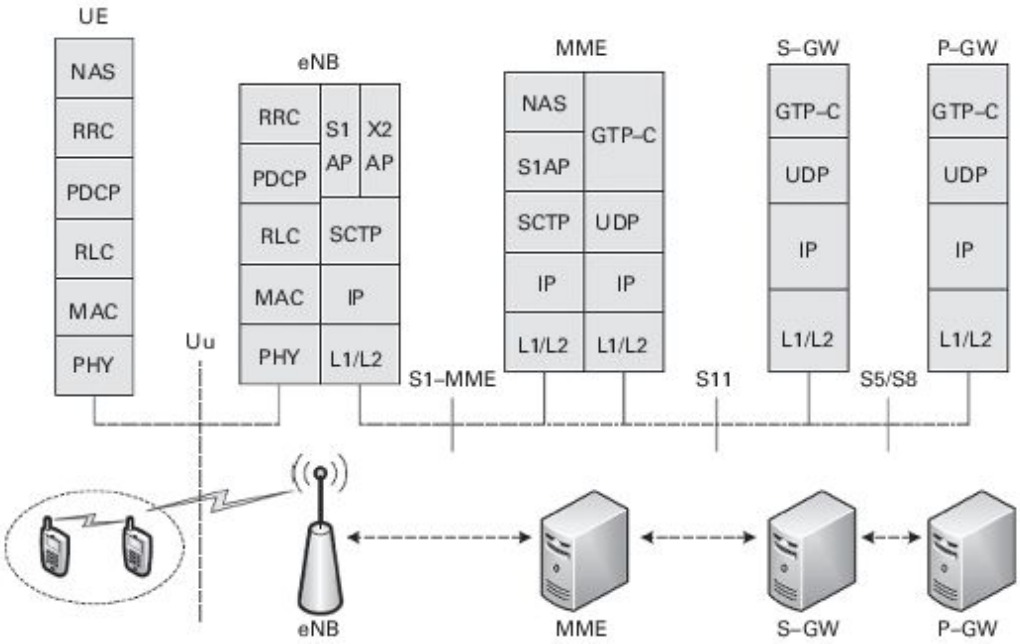

Figure 12.4. LTE-A control-protocol stack for D2D communications.

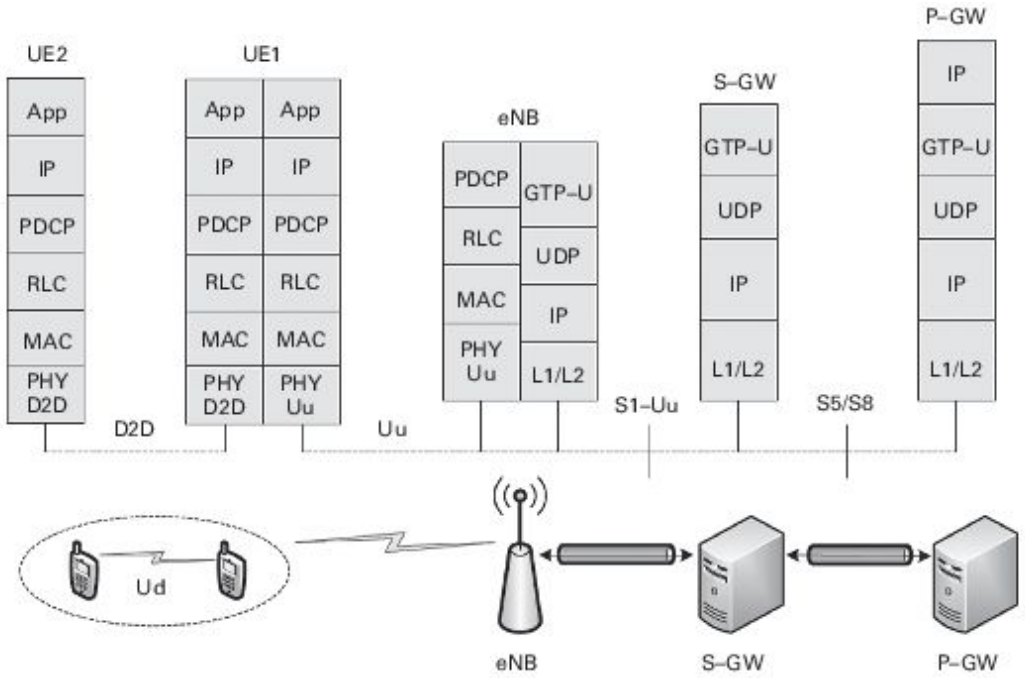

Figure 12.5. LTE-A data-protocol stack for D2D communications.

To enable D2D communications in the LTE-A networks, the authors of [1, 5] proposed two mechanisms of D2D connectivity based on the session initiation protocol (SIP) and the Internet Protocol (IP). LTE-A works fully in the packet-switched domain. Therefore, D2D connectivity that is based on Internet connectivity is a plausible proposal. This IP-based method provides two types of benefits for D2D connectivity. Firstly, the operator has control over D2D connectivity. Secondly, operators need only update some software functionalities in their infrastructure to fit the D2D network. An LTE-A architecture with D2D communications functionality is presented in Figure 12.6.

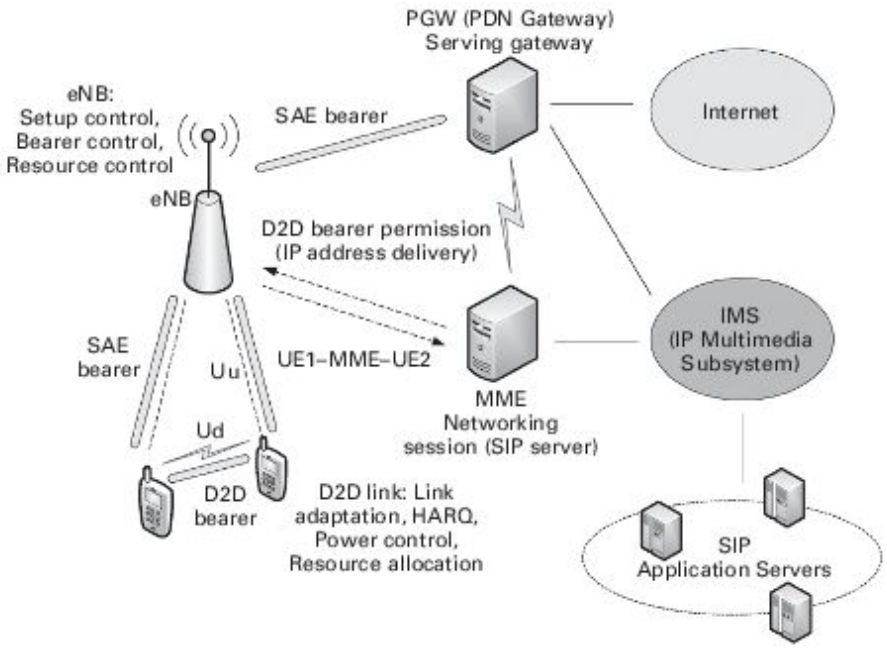

Figure 12.6. The D2D functional block in LTE-A SAE.

The mobility management entity (MME) is responsible for providing IP connectivity using serving packet data network (PDN) gateways. This IP connectivity is then used to acquire IP addresses to the UE. Therefore, MME works as the connector between the IP address SAE identification and subscription information. The above-mentioned points justify that a D2D session-initiation request should be delivered to the MME. Hence, the MME is responsible for initiating the D2D radio bearer setup using the Ud interface and delivery of an IP address for D2D terminating devices. These IP addresses for D2D communications are created using the local subnet scope, which is identical to a local breakout solution. This IP base connectivity helps D2D communications to offer seamless operations to the higher-layer protocol stack, such as TCP/IP and UDP/IP, which eventually simplifies mobility processes between D2D and cellular networking [5].

Once the D2D bearer has been established between peer devices, the eNB must control the radio resources which are used by D2D communications. It is also very important for D2D users to remain connected with the Internet for a voice/video call. In LTE-A, this is achieved because the SAE bearer is preserved and connectivity to the gateway is

maintained. In order to do this, the UE remains in EPS mobility management (EMM) (i.e., the NAS connected state) and the radio-resource control (RRC) connected state using Uu interface for outbound and inbound calls, respectively, which will assist the UE to rapidly move from D2D communications to cellular communication for outbound or inbound voice/video calls. Note that the handover from the D2D network to the cellular network takes place when cellular connection attains a higher throughput and lower energy consumption than that of D2D.

Generally, the session setup of D2D communications requires the following steps [1].

(i) A request to communicate is initiated by one UE pair.

(ii) The system detects traffic originating from and destined to the UE in the same subnet.

(iii) If the traffic fulfills a certain criterion (e.g., data rate), the system considers the traffic as the potential D2D traffic.

(iv) The eNB checks whether D2D communication offers a higher throughput.

(v) If both UEs are D2D-capable and D2D communication offers a higher throughput, the eNB may set up a D2D bearer.

The cross-layer processes of resource control can be contained in the above steps, and can be generally summarized as follows. The transmitters (both cellular and D2D users) send detecting signals. Then CSI would be obtained by corresponding receivers and be fed back to the control center (e.g., the eNB). The power control and spectrum allocation are conducted on the basis of certain principles. Finally, the eNB sends control signals to users according to allocation results.

Even if the D2D connection setup is successful, the eNB still maintains the detection process to evaluate whether a user should switch back to the cellular communication mode. Furthermore, the eNB maintains the radio resource control for both cellular and D2D communications.

12.5 Performance evaluation

This section briefly introduces the key methods and system parameters to evaluate the performance of D2D communications by simulations. Typically, network simulations are divided into two parts: link-level and system-level simulation. Although a single simulator approach would be preferred, the complexity of such a simulator is far too high with the required simulation resolutions and simulation times. Additionally, the time granularities of the two domains are dramatically different: at link level bit transmissions take place with durations on the order of milliseconds, while at the system level traffic and mobility models require time intervals of some tens of seconds to minutes. Therefore, it is necessary to separate link-level and system-level simulations. Link-level simulation is done by assuming that there are single-cell and multiple users, i.e., cellular UEs and D2D UEs. The output of the link-level simulator is in the form of look-up tables, which reflect the function of SNR versus block error rate (BLER) performance curves. These look-up tables then feed to the system-level simulation platform. Specifically, depending on the specific D2D communications configuration, the BER or BLER performance of physical and logic channels such as the physical uplink shared channel (PUSCH), physical downlink shared channel (PDSCH), physical uplink control channel (PUCCH), and physical downlink control channel (PDCCH) will need to be produced. The system-level simulator then computes the number of successfully transmitted packets given the traffic and channel profiles employed. Specifically, the outputs are the parameters that usually characterize packet transmissions: throughput, BLER, packet delay, etc. The traffic-generation block contains non-real traffic with a full queue.

System-level simulation is an effective method to evaluate the system performance and analyze the radio-resource-management (RRM)

algorithms. The core feature of system-level simulation lies in the fact that more attention has been paid to the higher level of a system, while the specific signal-processing procedure has been simplified. In a system-level scenario, many UEs are distributed in a certain manner (usually uniformly, or in a hotspot drop for D2D communications [381]) throughout the entire network, and each will establish communication links with its own serving eNB according to a specific access algorithm. Each eNB allocates the resource available to its UEs using particular scheduling algorithms and each UE would calculate its received SINR and make a decision regarding whether the received transport block can be decoded successfully. If the received SINR is greater than the target threshold, it is more probable that the transport block will be decoded without error, otherwise the failure probability becomes higher.

In the system-level simulator, the RRM block comprises a call-admission control algorithm to regulate the operation of the network, a link-adaptation algorithm to select the appropriate parameters as a function of the current radio conditions, and a scheduler that decides how to allocate the appropriate resources according to the service type, the amount of data, the current load in the cell, etc. The packet-scheduler module includes three well-known packet-scheduling algorithms, i.e., round robin, proportional fair, and maximum carrier-to-interference ratio, to evaluate the network performance under the different types of packet scheduler. The interference block determines the average interference power received by the central base station, i.e., the inter-cell interference. Finally, the computations of the system-level metrics block return the network results, such as the service throughput (average spectral efficiency), BLER, and packet delay. The propagation block models path loss and shadow fading. Channel models for indoor environments and for outdoor urban and rural environments are available. The scheduler mechanism will generate the arrival process of the users, according to a Poisson arrival process. HARQ is employed for non-real-time services.

The features of system-level simulation prominently include the wraparound technique, the channel interface, and the SINR mapping method.

- Wraparound technique: In system-level simulations, cellular-network modeling is limited to a certain finite number of cells with strict boundaries. If a certain UE is located in the boundary cells, the interference received from surrounding cells may be much less than that when the UE is positioned in a central cell, because no interference is received from the area outside the boundaries. Besides, when mobility is taken into consideration, a UE may leave the network and lose its link to the network due to the limited boundaries. To avoid these problems, a wraparound technique can be implemented in the system-level simulator. The wraparound technique considered here is essentially a geometry-mapping method to create an infinitely large network.
- Channel interface: In an LTE system-level simulator, an extended spatial channel model (SCME) is used to model the fading for cellular UEs. Regarding D2D UEs, the channel model can reuse the D2D outdoor-to-outdoor channel model with a uniform distribution, or a hotspot drop (two thirds of the UEs are within a 40-m radius) [381].
- SINR mapping: A key issue for accurate system-level simulation is the need to be able to go from an instantaneous channel state to a corresponding block error probability (BLEP). Instead of directly finding the BLEP, an effective SIR mapping (ESM) that maps the instantaneous channel state can be used. The effective SNR is then used to find an estimate of the BLEP from basic AWGN link-level performance.

Besides, overhead calculation should be considered. To make the transmission reliable, some resources are reserved as reference signals or for controlling. The existence of the overheads necessitates a tradeoff between efficiency and reliability. For example, the reference signals are commonly used for channel measurement, and it is well known that the more resources are reserved as reference signals, the more accurate the measurement results and the more reliable the communication which can be expected. However, if more resources are used for channel measurement, then less resources can be used for data transmission, which leads to a loss of efficiency. Note that, for D2D communications, additional signaling overhead will be used for synchronization, channel estimation, etc.

Finally, the 3GPP RAN1 agreed on VoIP as the baseline traffic model in designing D2D communications, with the parameters summarized in Table 12.2.

Table 12.2. Simulation parameters and values

Parameter	Values
Codec	Source rate 12.2 kbps
Encoder frame length	20 ms
Voice activity factor	0.75
Talk spurt	Exponential distribution: mean 2.5 s
Voice payload per speech frame during active talk	Baseline: with header compression 41 bytes (328 bits)
	Optional: without header compression 70 bytes (560 bits)
Outage definition	0.02 (may be revisited)

12.6 Application in proximity services

The LTE platform would have the advantage over others, such as Wi-Fi and Bluetooth, that operate device-to-device protocols, because they use license-exempt spectrum. Proximity-based applications and services represent a recent and enormous social–technological trend. These applications and services are based on the awareness that two devices or two users are close to each other. Awareness of proximity carries value, and generates demand for an exchange of traffic between them.

Proximity is determined ("a UE is in the proximity of another UE") when given proximity criteria are fulfilled. There are two important proximity services (ProSes). One is proximity discovery, with which users

can discover each other when they are in mutual proximity. The other is direct communication, with which users can communicate with each other when they are in mutual proximity. The proximity criteria for discovery and communication can be different. There is no causal relationship between proximity discovery and direct communication. Proximity discovery can be provided as a standalone service to users and does not always trigger direct communication. Users may initiate direct communication without proximity discovery. However, users can implement direct communication easily when they know the proximity information. This chapter introduces the use case of ProSe from the 3GPP draft [381].

12.6.1 Proximity discovery over E-UTRA

ProSe discovery is a process to identify that a UE is in the proximity of another, using evolved universal terrestrial radio access (E-UTRA). The proximity range is a rough indication of distance for use in ProSe discovery, for example, on the basis of geographical distance and radio conditions. ProSe discovery shall support a minimum of three range classes, for example short, medium, and maximum range. The operator shall be able to authorize per subscription the maximum range class ProSe discovery is allowed to use.

The **restricted ProSe discovery use case** is a general use case, which describes a basic scenario for ProSe discovery that can be used for any application. A social networking application is used as an example to illustrate this use case. Friends on social networks find others in close proximity, and then transfer data between them. In practice, an operator offers a service that makes use of the ProSe feature. In particular, a ProSe-enabled UE of a given user is able to discover and be discoverable by the ProSe-enabled UEs of his/her friends, and a social-networking application is enabled to use this ProSe feature.

Here, we explain an example that will be continued in the following sections. Assume that A, B, and C are persons using a given networking application. A and B are friends, and B and C are friends, but A and C are not friends. There might be hundreds of other ProSe-enabled UEs in the vicinity of A using the same or other applications. Additionally, A, B, and C

use ProSe-enabled UEs, being subscribers to the same cellular operator, currently residing on their home public land mobile network (HPLMN). They have given friends permission to discover them. The social-networking application used by A, B, and C is enabled by the operator to benefit from ProSe. A decides to look for a friend via his application, and so do B and C. Thus (e.g., following interaction with his application), as A's UE comes into the proximity of B's and C's UEs, the user experience is such that, without any further user interaction with the device,

- A's UE detects (for example using direct radio signals or via the operator's network) that B's UE is in its proximity;
- B's UE detects that A's UE is in its proximity;
- A's social-networking application learns that B is in or out of her proximity;
- B's social-networking application learns that A and C are in or out of his proximity;
- A's UE does not detect that C's UE is in its proximity;
- C's UE does not detect that A's UE is in its proximity;
- A's social-networking application does not detect that C is in or out of her proximity;
- C's social-networking application does not detect that A is in or out of his proximity.

When the social-network application of A detects that B is in her proximity, A may decide to transfer data to B via the social-networking application. ProSe discovery is achievable without any location information.

Another use case is the **open ProSe discovery use case**. This describes a case in which UEs discover other UEs without permission by the discoverable UEs.

Person A uses a given application. A, Store S and Restaurants X, Y, and Z use ProSe-enabled UEs. A and the owners of the store and restaurant UEs are subscribers to an operator service that allows them to use ProSe. There might be hundreds of other stores/restaurants with ProSe-enabled UEs in the vicinity of A, and the operator has enabled the application to access this

ProSe feature. As A walks into the neighborhood where Store S is located, A is notified of the proximity of Store S. A then decides to look for a restaurant, and thus (e.g., following interaction with his application), A is notified of the proximity of Restaurant X. A is not notified of the proximity of other establishments, which are not determined to be of interest according to the application he is using. After he starts walking towards Restaurant Y, A is notified of the proximity of Restaurant Y, and also of Restaurant Z.

The **discovery use case with subscribers from different PLMNs** describes discovery between UEs camped on different PLMNs. This case has the same assumptions as in the restricted ProSe discovery use case except that A is a subscriber to operator A and camps on operator A's network, while B is a subscriber to operator B and camps on operator B's network. As B moves towards A, A is notified that B is in his proximity and B is notified that A is in his proximity.

The **discovery use case with roaming subscribers** describes discovery between UEs in different PLMNs under roaming conditions. This case has the same assumptions as in the restricted ProSe discovery use case except that A is a subscriber to operator A and camps on operator A's network (i.e., his HPLMN), while B is a subscriber to operator C in a different country and roams in operator B's network, which is located in the same country as operator A's network. As B moves towards A, A is notified that B is in his proximity and B is notified that A is in his proximity.

Another use case is the **network ProSe discovery use case**, in which the 3GPP network provides ProSe discovery for ProSe-enabled UEs. A and C use ProSe-enabled UEs, subscribe to the same mobile network operator (MNO), and reside on the HPLMN. The MNO network supports ProSe discovery and communications. A uses an application on his UE to connect with C, causing his UE to request ProSe discovery from the MNO network. The MNO network verifies that A's UE has permission to discover C's UE and is in proximity of C's UE. Then, the network informs A's and C's UEs that they are in proximity.

An operator A can use ProSe to **enhance location and presence services**. For example, user A's UE receives real-time parking-space information that helps him to find his parking space easily. One can provide more information than is given by a GPS-based application by means of ProSe.

12.6.2 Proximity communications over E-UTRA

ProSe communications amount to communication between two UEs in proximity by means of an E-UTRA communication path established between the UEs. The communication path could, for example, be established directly between the UEs or routed via local eNB(s).

ProSe communication has two data-path scenarios. If UEs are in mutual proximity, they may be able to use a "direct mode" or a "locally routed" path. For example, in the 3GPP LTE spectrum, the operator can move the data path (user plane) off the access network and CN onto direct links between the UEs. Another example is when the data path is locally routed via the eNB(s).

For ProSe-enabled UEs, the 3GPP proposes a requirement of **service continuity** between infrastructure and E-UTRA ProSe communications paths. In this case, UEs communicate initially via an infrastructure path, then via a ProSe communications path, and finally return to an infrastructure path. An operator offers a service making use of the ProSe feature, in which the operator is able to establish a new traffic session using E-UTRA ProSe communications and is also able to switch user traffic from an infrastructure communication path to an E-UTRA ProSe communications path.

Assume that A and B use ProSe-enabled UEs that have been subscribed to the same cellular operator. A and B are subscribers to an operator service that allows them to use ProSe. Now, they have performed ProSe discovery and initiation of ProSe communications. They are engaged in a data session that is being routed over the MNO's CN infrastructure. As B moves within the proximity of A, one or more flows of the data session will switch to an

E-UTRA ProSe communications path. At some later time, the data session is switched back to the infrastructure path. The switching of the data path is not perceived by the users, and any un-switched data flows are not negatively impacted by the switching of other data flows.

The **ProSe-assisted WLAN direct-communications use case** describes how WLAN direct communication can be used between ProSe-enabled UEs. A and B are subscribers to a mobile data service from an MNO. They both carry UEs that have WLAN capabilities and are enabled for ProSe discovery and communications. The 3GPP network has the capability to provide WLAN configuration information to ProSe-enabled UEs. A has clicked the ProSe-enabled UE to send a video to B. The 3GPP EPC determines the proximity of A's and B's UEs and provides them with WLAN configuration information to assist them to establish WLAN direct connection. Then, A's and B's UEs use the configuration information to verify the feasibility of the WLAN direct connection and establish ProSe-enabled WLAN direct communication. The ProSe-enabled application on A's UE streams a video to the ProSe-enabled application on B's UE using the established WLAN connection.

Being the same as ProSe communications, ProSe-assisted WLAN communications need service management and continuity. The 3GPP system is capable of switching an infrastructure communication path to a WLAN ProSe communications path and back again. A and B are engaged in a data session that is being routed over the MNO's CN infrastructure. When A and B move within WLAN communication range, the 3GPP system switches their data session to the WLAN ProSe communications path. Later, when A and/or B move out of WLAN communication range, the 3GPP system switches their data session back to the MNO's infrastructure path.

With **Concurrent E-UTRA infrastructure and WLAN proximity communications** E-UTRA infrastructure communication and WLAN ProSe communications between ProSe-enabled UEs can be used concurrently. A, B, and C are subscribers to a mobile data service from an MNO. They all carry UEs that have WLAN capabilities. The UEs are within mutual proximity of each other and enabled for ProSe discovery and

communications. B and C are within the WLAN range and have entered a preference to use WLAN ProSe communications. A chats with B once A's and B's UEs have established an E-UTRA infrastructure communication. C's UE looks for B's UE, triggering C's UE to discover B's UE using ProSe discovery. C's UE then streams the video to B's UE after establishing WLAN ProSe communications, while A continues to chat with B using their existing E-UTRA infrastructure communication.

Networking data offloading can be achieved via WLAN ProSe communications. B and C are engaged in a data session that is being routed over the MNO's CN, which is currently congested. Owing to the congestion, the 3GPP EPC checks whether any data sessions can be offloaded and finds that B's and C's data session can be offloaded to a WLAN direct connection. The 3GPP EPC sends them a request to connect directly via WLAN. B's and C's UEs determine whether they are willing to connect directly via WLAN. After B's and C's UEs have responded to the 3GPP EPC positively, the 3GPP EPC moves their data session from the infrastructure path to their WLAN direct path to reduce the system congestion. Later, when the MNO's network congestion has subsided, the 3GPP EPC shall be able to request to switch B's and C's data session back to the MNO's infrastructure path.

12.6.3 Public-safety services

This section explains the use cases and requirements of public-safety services, which are specific needs in addition to the general cases and requirements in the preceding sections.

ProSe discovery within network coverage describes the scenario where a given UE discovers one or more other UEs while in E-UTRAN coverage, with ProSe discovery always enabled. Assume that A, B, and C all use ProSe-enabled public-safety UEs, and are within E-UTRA coverage. They also have configured ProSe discovery on their UEs such that they can discover other UEs and be discovered by others. At first, A is not in the proximity of B and C, who are both within proximity of each other. When A moves into the proximity of B and C, A's UE discovers B's and C's UEs

upon entering proximity, and also B's UE and C's UE discover A's UE upon entering proximity.

ProSe discovery out of network coverage describes the scenario where a given UE discovers one or more other UEs while out of E-UTRAN coverage, with ProSe discovery always enabled. In the above scenario, assume that A is in E-UTRA coverage while B and C are out of E-UTRA coverage. Thus, A is not in the proximity of B and C. When A moves into the proximity of B and C, again they will discover each other.

A UE is able to discover other UEs, but is not discoverable by other UEs, which can be named "**can discover but not discoverable**." A, B, and C use ProSe-enabled public-safety UEs, and some or all of them are out of E-UTRA coverage. A and B have configured ProSe discovery on their UEs such that they can discover other UEs and be discovered by other UEs. C has enabled ProSe discovery on his UE that is configured such that it can discover other UEs but cannot be discovered by other UEs. Thus, when A, B, and C are all within proximity of each other, A's and B's UEs discover each other. C's UE discovers A's and B's UEs, while they do not discover C's UE.

Basic ProSe one-to-one direct user traffic initiation in public-safety spectrum supports the initiation by a given public-safety UE of a one-to-one direct user traffic session with another UE. A and B are subscribers to a public-safety service that allows them to use ProSe. They may, or may not, be in E-UTRA coverage. The two public-safety UEs discover each other via ProSe discovery. If A wants to communicate with B, A's and B's public-safety UEs are able to initiate a direct connection and exchange user traffic over the air using the public-safety spectrum.

In the case of a **UE with multiple one-to-one direct user traffic sessions in public-safety spectrum** a given UE can concurrently maintain one-to-one user traffic sessions with several other UEs. Here, besides A and B, C is also a subscriber to a public-safety service that allows him to use ProSe. The three UEs discover each other via ProSe discovery. Now, A wants to communicate with B and C concurrently. While A's UE and B's UE

exchange user traffic via a direct connection, A's UE and C's UE are able to initiate an additional ProSe direct connection and exchange user traffic over the air using the public-safety spectrum.

A **ProSe group** describes the scenario where a user wants to communicate the same information concurrently to two or more other users using ProSe group communications. The UEs of all users in the scenario belong to a common communications group. A's, B's, and C's UEs are configured to belong to communications group X, and C has disabled ProSe discovery on his UE. All the users are subscribers to a public-safety service that allows them to use ProSe. A's UE has discovered B's UE via ProSe discovery, but has not discovered C's UE. The users' UEs may, or may not, be in E-UTRA coverage. A's UE transmits data using ProSe group communications to B's and C's UEs concurrently. It is to be noted that a public safety UE in or out of E-UTRAN coverage shall be capable of transmitting data to a group of public-safety UEs using ProSe group communications with a single transmission, assuming that they are within transmission range, authenticated, and authorized. Authentication shall allow for security enablement of large groups, regardless of whether group members have discovered each other in or out of E-UTRAN coverage.

ProSe broadcast describes the scenario where a given UE initiates a ProSe broadcast communication transmission to all UEs within transmission range. In a firefighting scenario, firefighters A, B, C, and D and an incident commander use ProSe-enabled public-safety UEs, being subscribers to a public-safety service that allows them to use ProSe. Firefighter A's and firefighter B's UEs are configured to belong to communication group X, and C's and D's UEs are configured to belong to group Y, which is separate from firefighters A and B. The incident commander's UE is configured to belong to communication group X and communication group Y. The firefighters may, or may not, be in E-UTRA coverage. After arriving at the scene of a fire, firefighters A's and B's UEs discover each other and communicate among themselves in communications group X using ProSe group communications. Later, firefighters C and D also arrive on the fire scene and communicate with each other in communications group Y using ProSe group communications. At some point, the incident commander wants to provide the same information concurrently to all of the firefighters at the scene of the

incident who are within transmission range. The incident commander's UE transmits a ProSe broadcast communications message to all of the firefighters' UEs. A single transmission is received by all of the firefighters' UEs rather than individual transmissions being sent to each of the firefighters.

The **ProSe relay** use case describes the scenario where a given UE acts as a communication relay for one or more UEs. Assume that A, B, and C use ProSe-enabled public safety UEs. B's UE has a relay capability allowing it to receive and retransmit ProSe communications. The three users' UEs have been configured to belong to communication group X. A's UE is within transmission range of B's UE, and B's UE is within transmission range of C's UE, but C's UE is not within transmission range of A's UE. When A wants to communicate with B and C in communication group X via ProSe group communications, B enables his UE to act as a relay for ProSe group communications. After A's UE has transmitted a message to B's UE, B's UE relays (receives and then retransmits) the communication from A's UE to C's UE, all using ProSe group communications. B continues to act as a ProSe group communications relay until C is back within transmission range of A and B.

ProSe hybrid and range extension describes the scenario where a given UE communicates using the network infrastructure and using ProSe communications concurrently. This use case also includes the scenario where a given UE acts as a communication relay for one or more other UEs so that the latter UE(s) can get communication towards the network. Assume that A's UE has a relay capability allowing it to receive and retransmit UE- and network-originated communications. A, B, and C are subscribers to a public-safety service that allows them to use ProSe, and their UEs have been configured to belong to communication group X. A and B are within E-UTRA coverage and not in ProSe group communications range of each other, while C is out of E-UTRAN coverage but within ProSe group communications transmission range of A. A communicates information to B and C in group X. When A transmits, A's and C's UEs exchange data using ProSe group communications, while A's and B's UEs exchange data using group communication via the network. C wants to communicate with B, who can be reached via the network, in communications group X via ProSe group

communications. A enables his UE to act as a relay for ProSe communications and network communication. Thus, A's UE relays (receives and then retransmits) the communication between B's UE and C's UE. A is able to continue to act as the relay until B is back within transmission range of A and C.

ProSe range describes the scenario where a given UE is within a building and uses ProSe communications to exchange user traffic to/from UEs outside a building. A, B, and C are subscribers to a public-safety service that allows them to use ProSe. C has disabled ProSe discovery on his UE. A is inside a building, and B and C are outside the same building. A is not within E-UTRAN coverage, while B and C are within E-UTRAN coverage. A's UE discovers B's UE via ProSe discovery, but A's UE does not discover C's UE via ProSe discovery. A's UE can still exchange data using ProSe communications to/from B's and C's UEs. An authorized public-safety UE in or out of E-UTRAN coverage supports the capability to exchange data via ProSe from within a building to public-safety UEs outside the building.

Public-safety implicit discovery gives a scenario in which public-safety officials need to communicate without an explicit ProSe discovery event. Public-safety officials arrive at a disaster site with their ProSe-enabled UEs. ProSe discovery has been disabled on each UE by agreement among the officials. The officials' UEs may, or may not, be in E-UTRAN coverage. If the public-safety officials assess the situation and decide that they need to use ProSe communications, they activate ProSe communications on their UEs and communicate with each other as they proceed about their duties on the site. As the officials move about the site, the communications will be received when the UEs are within communication range. Since ProSe discovery is not performed, there is no explicit prior indication whether communication with a particular official will succeed at any given time. Authorized ProSe-enabled public-safety UEs in or out of E-UTRAN coverage shall be able to communicate with other authorized ProSe-enabled public-safety UEs irrespective of whether or not ProSe discovery is used.

In ProSe safety services, **coexistence of ProSe communications and E-UTRA communications** is allowed just as in the general use case. ProSe

discovery and communications have been established between two UEs when no E-UTRAN coverage is available. The two UEs, while still performing ProSe communications, then move back into E-UTRA coverage with minimal impact on communication via the network. Assume that A and B are at a disaster site with ProSe-enabled UEs, and they are underground where there is no E-UTRA coverage. A's UE and B's UE are in the proximity of each other. C and D are at a disaster site with ProSe-enabled UEs and are in E-UTRA coverage. C and D are in communication via the E-UTRA network. A's UE discovers B's UE using ProSe discovery, and establishes ProSe communications with B. When A and B emerge from the building, they are once again in E-UTRA coverage and are in the proximity of C and D. The ProSe-enabled public-safety UEs using ProSe communications should have no impact on other UEs communicating via E-UTRAN, and vice versa.

12.7 Chapter summary

As the demand for high-data-rate wireless communication grows rapidly, new wireless technologies such as LTE/LTE-A have been introduced. D2D communication, as a new potential type of communication, is being developed to work over LTE/LTE-A. This chapter has mainly introduced the motivation, requirements, and application scenarios for using D2D communications over LTE/LTE-A. In accord with a 3GPP technical report, the requirements cover operational, charging, and security requirements. We have summarized the requirements and introduced the key working scenarios. To support ProSe in D2D, necessary enhancements of LTE-A architecture have been studied. The session setup of D2D communications has been discussed, and the performance evaluation is provided. We have briefly introduced key methods and system parameters to evaluate the performance of D2D communications by computer simulation. Furthermore, we have given some applications of proximity services in D2D communications. Proximity is determined when given proximity criteria are fulfilled. There are two important proximity services: proximity discovery and proximity communication. Additionally, the use cases and requirements of public-safety services, which are specific needs in addition to the general cases and requirements, have been explained.

References

[1] K. Doppler, M. Rinne, C. Wijting, C. Ribeiro, and K. Hugl, "Device-to-device communication as an underlay to LTE-advanced networks," *IEEE Commun. Mag.*, vol. 47, no. 12, pp. 42–49, Dec. 2009.

[2] S. Basagni, M. Conti, S. Giordano, and I. Stojmenovic, *Mobile Ad Hoc Networking*. Wiley-IEEE Press, 2004.

[3] C.-H. Yu, O. Tirkkonen, K. Doppler, and C. Ribeiro, "On the performance of device-to-device underlay communication with simple power control," in *Proc. IEEE Vehicular Technology Conference 2009 – Spring*, Barcelona, Apr. 2009.

[4] T. Koskela, S. Hakola, T. Chen, and J. Lehtomaki, "Clustering concept using device-to-device communication in cellular system," in *Proc. IEEE Wireless Communications and Networking Conference*, Sydney, Apr. 2010.

[5] K. Doppler, M. Rinne, P. Janis, C. Ribeiro, and K. Hugl, "Device-to-device communications; functional prospects for LTE-advanced networks," in *Proc. IEEE International Conference on Communications Workshops*, Dresden, Jun. 2009.

[6] K. Doppler, C.-H. Yu, C. Ribeiro, and P. Janis, "Mode selection for device-to-device communication underlaying an LTE-advanced network," in *Proc. IEEE Wireless Communications and Networking Conference*, Sydney, Apr. 2010.

[7] H. Min, W. Seo, J. Lee, S. Park, and D. Hong, "Reliability improvement using receive mode selection in the device-to-device uplink period underlaying cellular networks," *IEEE Trans. Wireless Commun.*, vol. 10, no. 2, pp. 413–418, Feb. 2011.

[8] S. Hakola, C. Tao, J. Lehtomaki, and T. Koskela, "Device-to-device (D2D) communication in cellular network – performance analysis of optimum and practical communication mode selection," in *Proc. IEEE Wireless Communications and Networking Conference*, Sydney, Apr. 2010.

[9] C.-H. Yu, K. Doppler, C. Ribeiro, and O. Tirkkonen, "Performance impact of fading interference to device-to-device communication underlaying cellular networks," in *IEEE 20th International Symposium on Personal, Indoor and Mobile Radio Communications*, Tokyo, Sept. 2009, pp. 858–862.

[10] C.-H. Yu, O. Tirkkonen, K. Doppler, and C. Ribeiro, "Power optimization of device-to-device communication underlaying cellular communication," in *Proc. International Conference on Communications*, Dresden, Jun. 2009.

[11] H. Xing and S. Hakola, "The investigation of power control schemes for a device-to-device communication integrated into OFDMA cellular system," *in Proc. IEEE 21st International Symposium on Personal Indoor and Mobile Radio Communications (PIMRC)*, Istanbul, Sept. 2010, pp. 1775–1780.

[12] P. Janis, V. Koivunen, C. Ribeiro, K. Doppler, and K. Hugl, "Interference-avoiding MIMO schemes for device-to-device radio underlaying cellular networks," in *Proc. IEEE 20th International Symposium on Personal, Indoor and Mobile Radio Communications*, Tokyo, Sept. 2009, pp. 2385–2389.

[13] T. Peng, Q. Lu, H. Wang, S. Xu, and W. Wang, "Interference avoidance mechanisms in the hybrid cellular and device-to-device systems," in *Proc. IEEE 20th International Symposium on Personal, Indoor and Mobile Radio Communications*, Tokyo, Sept. 2009, pp. 617–621.

[14] P. Janis, V. Koivunen, C. Ribeiro *et al.*, "Interference-aware resource allocation for device-to-device radio underlaying cellular networks," in *Proc. IEEE Vehicular Technology Conference 2009 – Spring*, Barcelona, Apr. 2009.

[15] M. Zulhasnine, C. Huang, and A. Srinivasan, "Efficient resource allocation for device-to-device communication underlaying LTE network," in *Proc. IEEE 6th International Conference on Wireless and Mobile Computing, Networking and Communications*, Niagara Falls, Oct. 2010, pp. 368–375.

[16] S. Xu, H. Wang, T. Chen, Q. Huang, and T. Peng, "Effective interference cancellation scheme for device-to-device communication underlaying cellular networks," in *Proc. IEEE Vehicular Technology Conference 2010 – Fall*, Ottawa, Sept. 2010.

[17] C.-H. Yu, K. Doppler, C. Ribeiro, and O. Tirkkonen, "Resource sharing optimization for D2D communication underlaying cellular networks," *IEEE Trans. Wireless Commun.*, vol. 10, no. 8, pp. 2752–2763, Aug. 2011.

[18] WINNER II D1.1.2, "WINNER II channel models," https://www.istwinner.org/deliverables.html, Sept. 2007.

[19] 3GPP, Technical Report TS 36.213 V8.2.0, "E-UTRA physical layer procedures."

[20] S. Boyd and L. Vandenberghe, Eds., *Convex Optimization*. Cambridge University Press, 2004, http://www.stanford.edu/~boyd/cvxbook.html.

[21] M. K. Wood and G. B. Dantzig, "Programming of interdependent activities. I. general discussion," *Econometrica*, vol. 17, pp. 193–199, 1949.

[22] G. B. Dantzig, "Programming of interdependent activities. II. Mathematical model," *Econometrica*, vol. 17, pp. 200–211, 1949.

[23] L. G. Khachian, "A polynomial algorithm in linear programming," *Dokl. Akad. Nauk SSSR*, English translation in *Soviet Math. Dokl.*, vol. 244, pp. 1093–1096, 1979.

[24] N. Karmarkar, "A new polynomial-time algorithm for linear programming," *Combinatorica*, vol. 4, pp. 373–395, 1984.

[25] E. Wallace, "Altruism helps swarming robots fly better," Genevalunch News, May 2011. http://genevalunch.com/2011/05/04/altruism-helps-swarming-robots-fly-better-study-shows/.

[26] M. Waibel, D. Floreano, and L. Keller, "A quantitative test of Hamilton's rule for the evolution of altruism," *PLOS Biol.*, vol. 9, no. 5, p. e1000615, May 2011.

[27] T. S. Marco Dorigo, *Ant Colony Optimization*. MIT Press, 2004.

[28] P. Rabanal, I. Rodrguez, and F. Rubio, *Ant Colony Optimization and Swarm Intelligence*. Springer, 2008, ch. Finding minimum spanning/distances trees by using river formation dynamics, pp. 60–71.

[29] D. Karaboga, "Artificial bee colony algorithm," *Scholarpedia*, vol. 5, no. 3, p. 6915, 2010.

[30] U. Aickelin and D. Dasgupta, *Search Methodologies: Introductory Tutorials in Optimization and Decision Support Techniques*. Springer, 2006, ch. Artificial immune systems.

[31] E. Rashedi, H. Nezamabadi-pour, and S. Saryazdi, "GSA: A gravitational search algorithm," *Science Direct*, vol. 179, no. 13, pp. 2232–2248, Jun. 2009.

[32] H. Nobahari, M. Nikusokhan, and P. Siarry, "Non-dominated sorting gravitational search algorithm," in *International Conference on Swarm Intelligence, ICSI*, Cergy, Jun. 2011.

[33] K. N. Krishnanand and D. Ghose, *Swarm Intelligence*. Springer, 2009, ch. Glowworm swarm optimization for simultaneous capture of multiple local optima of multimodal functions, pp. 87–124.

[34] K. Krishnanand and D. Ghose, "Glowworm swarm based optimization algorithm for multimodal functions with collective robotics applications," *Multiagent and Grid Systems*, vol. 2, no. 3, pp. 209–222, 2006.

[35] H. Shah-Hosseini, "The intelligent water drops algorithm: A nature-inspired swarm-based optimization algorithm," *Int. J. Bio-Inspired Computation*, vol. 1, no. 1/2, pp. 71–79, 2009.

[36] K. E. Parsopoulos and M. N. Vrahatis, "Recent approaches to global optimization problems through particle swarm optimization," *Natural Computing*, vol. 1, no. 2–3, pp. 235–306, 2002.

[37] M. Clerc, *Particle Swarm Optimization*. Wiley, 2006.

[38] M. M. al Rifaie, M. J. Bishop, and T. Blackwell, "An investigation into the merger of stochastic diffusion search and particle swarm optimisation," in *Proc. 13th Conference on Genetic and Evolutionary Computation, (GECCO)*, Dublin, Jun. 2011, pp. 37–44.

[39] P. Rabanal, I. Rodríguez, and F. Rubio, *Unconventional Computation*. Springer, 2007, ch. Using river formation dynamics to design heuristic algorithms, pp. 163–177.

[40] P. Rabanal, I. Rodríguez, and F. Rubio, *Nature-Inspired Algorithms for Optimisation*. Springer, 2009, ch. Applying river formation dynamics to solve NP-complete problems, pp. 333–368.

[41] P. Rabanal, I. Rodríguez, and F. Rubio, "Testing restorable systems: Formal definition and heuristic solution based on river formation dynamics," *Formal Aspects of Computing*, vol. 25, no. 5, pp. 743–768, 2013.

[42] A. Czirk and T. Vicsek, "Collective behavior of interacting self-propelled particles," *Physica A: Statist. Mech. Appl.*, vol. 281, no. 1–4, pp. 17–29, 2000.

[43] E. Bertin, M. Droz, and G. Grégoire, "Hydrodynamic equations for self-propelled particles: Microscopic derivation and stability analysis," *Physics A: Math. Theor.*, vol. 42, p. 445001, 2009.

[44] Y.-X. Li, R. Lukeman, and L. Edelstein-Keshet, "Minimal mechanisms for school formation in self-propelled particles," *Physica D: Nonlinear Phenomena*, vol. 237, no. 5, pp. 699–720, 2008.

[45] S. J. Nasuto, M. J. Bishop, and S. Lauria, "Time complexity analysis of the stochastic diffusion search," in *Proc. Neural Computation*, Vienna, Sept. 1998, pp. 260–266.

[46] D. Myatt, J. Bishop, and S. Nasuto, "Minimum stable convergence criteria for stochastic diffusion search," *Electron. Lett.*, vol. 40, no. 2, pp. 112–113, 2004.

[47] M. M. al Rifaie, J. M. Bishop, and T. Blackwell, "Information sharing impact of stochastic diffusion search on differential evolution algorithm," *Memetic Computing*, vol. 4, no. 4, pp. 327–338, 2012.

[48] M. al Rifaie and A. Aber, "Identifying metastasis in bone scans with stochastic diffusion search," in *Information Technology in Medicine and Education (ITME)*, Hokodate, Hokkaido, Aug. 2012, pp. 519–523.

[49] M. al Rifaie, A. Aber, and A. Oudah, "Utilising stochastic diffusion search to identify metastasis in bone scans and microcalcifications on mammographs," in *Bioinformatics and Biomedicine Workshops (BIBMW)*, Philadelphia, PA, Oct. 2012, pp. 280–287.

[50] C. Li and S. Yang, "Fast multi-swarm optimization for dynamic optimization problems," in *Fourth International Conference on Natural Computation, ICNC*, Jinan, Oct. 2008, pp. 624–628.

[51] J. McCaffrey, "Test run - multi-swarm optimization," *MSDN Mag.*, Sept. 2013.

[52] M. W. Cooper and K. Farhangian, "Multicriteria optimization for nonlinear integer-variable problems," *Large Scale Systems*, vol. 9, pp. 73–78, 1985.

[53] S. Martello and P. Toth, *Knapsack Problems: Algorithms and Computer Implementations*. John Wiley & Sons, 1990.

[54] M. L. Fisher, "The Lagrangian method for solving integer programming problems," *Management Sci.*, vol. 27, pp. 1–18, 1981.

[55] M. Guignard and S. Kim, "Lagrangian decomposition: A model yielding stronger Lagrangian bounds," *Math. Programming*, vol. 39, pp. 215–228, 1987.

[56] J. F. Benders, "Partitioning procedures for solving mixed-variables programming problems," *Numerische Math.*, vol. 4, pp. 238–252, 1962.

[57] H. Weyl, "Elementare Theorie der konvexen Polyeder," *Commentarii Math. Helv.*, 1935, vol. 7, pp. 290–306 [English translation "The elementary theory of convex polyhedra," in H. W. Kuhn and A. W. Tucker, *Contributions to the Theory of Games*, "Elementare Theorie der konvexen Polyeder," vol. 1, p. 3, 1950].

[58] R. E. Gomory, "Outline of an algorithm for integer solution to linear programs," *Bull. Am. Math. Soc.*, vol. 64, no. 5, pp. 275–278, 1958.

[59] D. P. Bertsekas, *Dynamic Programming and Optimal Control*. Athena Scientific, 1995.

[60] R. V. Slyke and R. J. Wets, "L-shaped linear program with application to optimal control and stochastic linear programming," *SIAM J. Appl. Math.*, vol. 17, pp. 638–663, 1969.

[61] W. P. Ziemer, *Weakly Differentiable Functions: Sobolev Spaces and Functions of Bounded Variation*. Springer, 1989.

[62] S. Kullback, "The Kullback–Leibler distance," *Am. Statistician*, vol. 41, no. 4, pp. 340–341, 1987.

[63] S. Kullback, *Information Theory and Statistics*. Dover, 1997.

[64] D. Hosmer and S. Lemeshow, *Applied Logistic Regression*. Wiley-Interscience, 2000.

[65] J. Duchi, S. Shalev-Shwartz, Y. Singer, and T. Chandra, "Efficient projections onto the ℓ_1-ball for learning in high dimensions," in *Proc. 25th International Conference on Machine Learning*. ACM, pp. 272–279.

[66] A. Quattoni, X. Carreras, M. Collins, and T. Darrell, "An efficient projection for $\ell_{1,\infty}$ regularization," in *Proc. 26th Annual International Conference on Machine Learning, ICML '09*. ACM, pp. 857–864.

[67] J. Liu and J. Ye, "Efficient Euclidean projections in linear time," in *Proc. 26th Annual International Conference on Machine Learning, ICML '09*. ACM, pp. 657–664.

[68] E. van den Berg and M. Friedlander, "Probing the Pareto frontier for basis pursuit solutions," *SIAM J. Scient. Computing*, vol. 31, no. 2, pp. 890–912, 2008.

[69] E. van den Berg, M. Schmidt, M. Friedlander, and K. Murphy, "Group sparsity via linear-time projection," *Optimization Online*, 2008.

[70] Z. Han, H. Li, and W. Yin, *Compressive Sensing for Wireless Networks*. Cambridge University Press, 2012.

[71] D. Fudenberg and J. Tirole, *Game Theory*. MIT Press, 1991.

[72] G. Owen, *Game Theory*, 3rd edn. Academic Press, 2001.

[73] V. Krishna, *Auction Theory*. Academic Press, 2002.

[74] http://www.gametheory.net

[75] C. U. Saraydar, N. B. Mandayam, and D. J. Goodman, "Efficient power control via pricing in wireless data networks," *Bull. Am. Math. Soc.*, vol. 50, no. 2, pp. 291–303, Feb. 2002.

[76] H. Yaiche, R. R. Mazumdar, and C. Rosenberg, "A game theoretic framework for bandwidth allocation and pricing in broadband networks," *IEEE/ACM Trans. Networking*, vol. 8, no. 5, pp. 667–678, Oct. 2000.

[77] Z. Han, Z. Ji, and K. J. R. Liu, "Power minimization for multi-cell OFDM networks using distributed non-cooperative game approach," in *IEEE Global Telecommunications Conference*, Dallas, TX, Nov.–Dec. 2004, pp. 3742–3747.

[78] Z. Han, Z. Li, and K. J. R. Liu, "A referee-based distributed scheme of resource competition game in multi-cell multi-user OFDMA networks," *IEEE J. Selected Areas Commun., Special Issue on Non-cooperative Behavior in Networking*, vol. 25, no. 6, pp. 1079–1090, Aug. 2007.

[79] V. Srinivasan, P. Nuggehalli, C. F. Chiasserini, and R. R. Rao, "Cooperation in wireless ad hoc networks," in *Proc. IEEE Conference on Computer Communications (INFOCOM 2003)*, San Francisco, CA, Mar. 2003.

[80] E. Altman, A. A. Kherani, P. Michiardi, and R. Molva, "Non-cooperative forwarding in ad-hoc networks," INRIA, Technical Report, May 2005.

[81] R. H. Porter, "Optimal cartel trigger price strategies," *J. Economic Theory*, vol. 29, pp. 313–318, Apr. 1983.

[82] N. Vieille, "Stochastic games: Recent results," in *Handbook of Game Theory*. Elsevier Science, pp. 1833–1850, 2002.

[83] L. Shapley, "Stochastic games," *Proc. Nat. Acad. Sci. USA*, vol. 39, pp. 1095–1100, 1953.

[84] A. Neyman, *Stochastic Games and Applications*. Springer, 2003.

[85] J. Filar and K. Vrieze, *Competitive Markov Decision Processes*. Springer, 1996.

[86] E. Altman, *Advances in Dynamic Games*. Birkhäuser, 2005, vol. 7, ch. Applications of dynamic games in queues, pp. 309–342.

[87] E. Altman, T. Jimenez, R. N. Queija, and U. Yechiali, "Optimal routing among ./m/1 queues with partial information," INRIA, Technical Report, 2004.

[88] W. van den Broek, J. Engwerda, and J. Schumachar, "Robust equilibria in indefinite linear-quadratic differential games," *J. Optimization Theory Appl.*, vol. 119, no. 3, pp. 565–595, 2003.

[89] T. Basar and G. J. Olsder, *Dynamic Noncooperative Game Theory*, 2nd edn. Academic Press, 1995.

[90] T. Basar and P. Bernhard, *H8-Optimal Control and Related Minimax Design Problems: A Dynamic Game Approach*. Birkhäuser, 1995.

[91] M. G. Crandall and P.-L. Lions, "Viscosity solutions of Hamilton–Jacobi equations," *Trans. Am. Math. Soc.*, vol. 277, no. 1, pp. 1–42, 1983.

[92] A. D. Polyanin and F. Z. Valentin, *Handbook of Nonlinear Partial Differential Equations*. Chapman and Hall/CRC, 2003.

[93] W. Fleming and P. Souganidis, "On the existence of value functions of two-player, zero-sum stochastic differential games," *Indiana Univ. Math. J.*, vol. 38, no. 2, pp. 293–314, 1989.

[94] D. Grosu, A. T. Chronopoulos, and M. Leung, "Load balancing in distributed systems: An approach using cooperative games," in *Proc. IPDPS*, Fort Lauderdale, FL, Apr. 2002, pp. 52–61.

[95] W. Rhee and J. M. Cioffi, "Increase in capacity of multiuser OFDM system using dynamic subchannel allocation," in *Proc. IEEE Vehicular Technology Conf. (VTC 2000 Spring)*, Tokyo, May 2000, pp. 1085–1089.

[96] Z. Han, Z. Ji, and K. J. R. Liu, "Fair multiuser channel allocation for OFDMA networks using Nash bargaining and coalitions," *IEEE Trans. Commun.*, vol. 53, no. 8, pp. 1366–

1376, Aug. 2005.

[97] C. Peng, H. Zheng, and B. Y. Zhao, "Utilization and fairness in spectrum assignment for opportunistic spectrum access," *Mobile Networks Appl.*, vol. 11, no. 4, pp. 555–576, Aug. 2006.

[98] J. E. Suris, L. DaSilva, Z. Han, and A. MacKenzie, "Cooperative game theory approach for distributed spectrum sharing," in *IEEE International Conference on Communications, ICC*, Glasgow, Jun. 2007, pp. 5282–5287.

[99] K. Lee and V. Leung, "Fair allocation of subcarrier and power in an OFDMA wireless mesh network," *IEEE J. Selected Areas Commun.*, vol. 24, no. 11, pp. 2051–2060, Nov. 2006.

[100] H. Park and M. van der Schaar, "Bargaining strategies for networked multimedia resource management," *IEEE Trans. Signal Process.*, vol. 55, no. 7, pp. 3496–3511, Jul. 2007.

[101] K. Apt and A. Witzel, "A generic approach to coalition formation," in *Proc. International Workshop on Computational Social Choice (COMSOC)*, Amsterdam, Dec. 2006.

[102] K. Apt and A. Witzel, "A generic approach to coalition formation," arXiv:0709.0435[cs.GT], Sept. 2007.

[103] K. Apt and T. Radzik, "Stable partitions in coalitional game," arXiv:cs/0605132[cs.GT], May 2006.

[104] D. T. Mortensen, *The Matching Process as a Non-Cooperative/Bargaining Game*. John McCall, 1982.

[105] A. E. Roth and E. Peranson, "The redesign of the matching market for American physicians: Some engineering aspects of economic design," *Am. Economic Rev.*, vol. 89, no. 4, pp. 748–780, Sept. 1999.

[106] D. M. Gusfield and R. W. Irving, *The Stable Marriage Problem: Structure and Algorithms*. MIT Press, 1989.

[107] Wikipedia, "Stable marriage problem," 2013. http://en.wikipedia.org/wiki/Stable_marriage_problem.

[108] D. Gale and L. S. Shapley, "College admissions and the stability of marriage," *Am. Math. Monthly*, vol. 69, no. 1, pp. 9–15, Jan. 1962.

[109] S. Bayat, R. H. Y. Louie, Z. Han, Y. Li, and B. Vucetic, "Distributed stable matching algorithm for physical layer security with multiple source-destination pairs and jammer nodes," in *Proc. IEEE Wireless Communications and Networking Conference (WCNC)*, Paris, Apr. 2012.

[110] S. Bayat, R. H. Y. Louie, Z. Han, B. Vucetic, and Y. Li, "Physical-layer security in distributed wireless networks using matching theory," *IEEE Trans. Information Forensics*

Security, vol. 8, no. 5, pp. 717–732, May 2013.

[111] *Annual Averages of Employed Multiple Job Holders by Industry*. US Bureau of Labor Statistics, 2002.

[112] J. Green and J. J. Laffont, "On coalition incentive compatibility," *Rev. Economic Studies*, vol. 46, no. 2, pp. 243–254, Apr. 1979.

[113] T. Groves, "Incentives in teams," *Econometrica*, vol. 45, pp. 617–631, 1973.

[114] A. Gibbard, "Manipulation of voting schemes: A general result," *Econometrica*, vol. 41, no. 4, pp. 587–601, 1973.

[115] M. A. Satterthwaite, "Strategy-proofness and arrow's conditions: Existence and correspondence theorems for voting procedures and social welfare functions," *J. Economic Theory*, vol. 10, pp. 187–217, Apr. 1975.

[116] L. Hurwicz, *Decision and Organization: On Informationally Decentralized Systems*, 2nd edn. University of Minnesota Press, 1972.

[117] R. B. Myerson and M. A. Satterthwaite, "Efficient mechanisms for bilateral trading," *J. Economic Theory*, vol. 29, pp. 265–281, 1983.

[118] K. J. Arrow, *Economics and Human Welfare: The Property Rights Doctrine and Demand Revelation under Incomplete Information*. Academic Press, 1979.

[119] C. d'Aspremont and L. Gerard-Varet, "Incentives and incomplete information," *J. Public Economics*, vol. 29, no. 45, pp. 11–25, 1979.

[120] V. Krishna, *Auction Theory*, 2nd edn. Academic Press: San Diego, CA, 2010.

[121] R. Wilson, "Auctions of shares," *Q. J. Economics*, vol. 93, pp. 675–698, 1979.

[122] L. Ausubel and P. Cramton, "Demand reduction and inefficiency in multi-unit auctions," University of Maryland, Technical Report, 1998, http://www.cramton.umd.edu/papers1995-1999/98wp-demand-reduction.pdf.

[123] C. Maxwell, "Auctioning divisible commodities: A study of price determination," Harvard University, Technical Report, 1983.

[124] K. Back and J. F. Zender, "Auctions of divisible goods: On the rationale for the treasury experiment," *Rev. Financial Studies*, vol. 6, pp. 733–764, 1993.

[125] J. J. D. Wang and J. F. Zender, "Auctioning divisible goods," *Economic Theory*, no. 19, pp. 673–705, 2002.

[126] A. Hortacsu, "Mechanism choice and strategic bidding in divisible good auctions: An empirical analysis of the Turkish treasury auction market," Stanford University, Technical Report, 2000, http://home.uchicago.edu/~hortacsu/ttreas.pdf.

[127] K. J. Sunnevag, "Auction design for the allocation of emission permits," Technical Report, University of California at Santa Barbara, 2001.

[128] G. Federico and D. Rahman, "Bidding in an electricity pay-as-bid auction," *J. Regulatory Economics*, vol. 24, no. 2, pp. 175–211, 2003.

[129] R. Johari and J. N. Tsitsiklis, "Efficiency loss in a network resource allocation game," *Math. Operations Res.*, vol. 29, no. 3, pp. 407–435, Aug. 2004.

[130] S. Yang and B. Hajek, "Revenue and stability of a mechanism for efficient allocation of a divisible good," Technical Report, Department of Electrical and Computer Engineering, University of Illinois at Urbana–Champaign.

[131] R. Maheswaran and T. Başar, "Nash equilibrium and decentralized negotiation in auctioning divisible resources," *Group Decision and Negotiation*, vol. 12, no. 5, pp. 361–395, 2003.

[132] R. T. Maheswaran and T. Başar, "Coalition formation in proportionally fair divisible auctions," in *AAMAS '03 Proc. Second International Conference on Autonomous Agents and Multi-Agent Systems*, 2003, pp. 25–32.

[133] R. T. Maheswaran and T. Başar, "Decentralized network resource allocation as a repeated noncooperative market game," in *Proc. 40th IEEE Conference on Decision and Control (CDC 2001)*, Orlando, FL, Dec. 2001, pp. 4565–4570.

[134] P. Milgrom, *Putting Auction Theory to Work*. Cambridge University Press, 2004.

[135] D. Friedman, D. P. Friedman, and J. Rust, *The Double Auction Market: Institutions, Theories, and Evidence*. Westview Press, 1993.

[136] "Contract theory." http://en.wikipedia.org/wiki/Contract_theory.

[137] L. Gao, X. Wang, Y. Xu, and Q. Zhang, "Spectrum trading in cognitive radio networks: A contract-theoretic modeling approach," *IEEE J. Selected Areas Commun.*, vol. 29, no. 4, pp. 843–855, Apr. 2011.

[138] L. Gao, J. Huang, Y. Chen, and B. Shou, "Contrauction: An integrated contract and auction design for dynamic spectrum sharing," in *46th Annual Conference on Information Sciences and Systems (CISS)*, Princeton, NJ, Mar. 2012.

[139] L. Gao, J. Huang, Y. Chen, and B. Shou, "An integrated contract and auction design for secondary spectrum trading," *IEEE J. Selected Areas Commun.*, vol. 31, no. 3, pp. 581–592, Mar. 2013.

[140] P. Bolton and M. Dewatripont, *Contract Theory*. MIT Press, 2004.

[141] D. M. Kreps and R. Wilson, "Sequential equilibria," *Econometrica*, vol. 50, no. 4, pp. 863–894, 1982.

[142] D. Monderer and L. S. Shapley, "Potential games," *Games and Economic Behavior*, vol. 14, no. 1, pp. 124–143, 1996.

[143] A. MacKenzie and L. DaSilva, *Game Theory for Wireless Engineers*. Morgan & Claypool Publishers, 2006.

[144] G. Scutari, S. Barbarossa, and D. P. Palomar, "Potential games: A framework for vector power control problems with coupled constraints," in *IEEE International Conference on Acoustics, Speech and Signal Processing, ICASSP*, vol. 4, Toulouse, May 2006, p. IV.

[145] J. Neel, J. Reed, and R. Gilles, "Game models for cognitive radio analysis," in *SDR Forum Technical Conference*, vol. 4, Phoenix, AZ, Nov. 2004.

[146] J. Neel, J. Reed, and R. Gilles, "Convergence of cognitive radio networks," in *Wireless Communications and Networking Conference*, vol. 4, Atlanta, GA, Mar. 2004, pp. 2250–2255.

[147] J. Neel, J. Reed, and R. Gilles, "The role of game theory in the analysis of software radio networks," in *SDR Forum Technical Conference*, San Diego, CA, Nov. 2002.

[148] A. Fattahi and F. Paganini, "New economic perspectives for resource allocation in wireless networks," in *American Control Conference*, Portland, OR, Jun. 2005.

[149] E. Altman and Z. Altman, "S-modular games and power control in wireless networks," *IEEE Trans. Automatic Control*, vol. 48, pp. 839–842, May 2003.

[150] G. Scutari, S. Barbarossa, and D. P. Palomar, "Potential games: A framework for vector power control problems with coupled constraints," in *ICASSP*, May 2006, pp. 241–244.

[151] R. Menon, A. MacKenzie, R. Buehrer, and J. Reed, "Game theory and interference avoidance in decentralized networks," in *SDR Forum Technical Conference*, Phoenix, AZ, Nov. 2004.

[152] J. Hicks, A. MacKenzie, J. Neel, and J. Reed, "A game theory perspective on interference avoidance," in *Globecom*, vol. 1, Dallas, TX, Nov.–Dec. 2004, pp. 257–261.

[153] J. Hicks and A. B. MacKenzie, "A convergence result for potential games," in *11th International Symposium on Dynamic Games and Applications*, Tucson, AZ, Dec. 2004.

[154] R. J. Aumann, "Subjectivity and correlation in randomized strategy," *J. Math. Economics*, vol. 1, no. 1, pp. 67–96, 1974.

[155] R. J. Aumann, "Correlated equilibrium as an expression of Bayesian rationality," *Econometrica*, vol. 55, no. 1, pp. 1–18, Jan. 1987.

[156] S. Hart and A. Mas-Colell, "A simple adaptive procedure leading to correlated equilibrium," *Econometrica*, vol. 68, no. 5, pp. 1127–1150, Sept. 2000.

[157] S. M. Perlaza, H. Tembine, S. Lasaulce, and M. Debbah, "Satisfaction equilibrium: A general framework for qos provisioning in self-configuring networks," in *GLOBECOM*, Miami, FL, Dec. 2010, pp. 1–5.

[158] S. M. Perlaza, H. Tembine, S. Lasaulce, and M. Debbah, "Quality of service provisioning in decentralized networks: A satisfaction equilibrium approach," *IEEE J. Selected Topics Signal Process.*, vol. 6, no. 2, pp. 104–116, Feb. 2012.

[159] L. Rose, S. M. Perlaza, C. L. Martret, and M. Debbah, "Achieving Pareto optimal equilibria in energy efficient clustered ad hoc networks," in *Proc. IEEE International Conference on Communications (ICC)*, Budapest, Jun. 2013, pp. 1491–1495.

[160] S. Perlaza, H. Poor, and Z. Han, "Learning efficient satisfaction equilibria via trial and error," in *Proc. Asilomar Conference on Signals, Systems and Computers (ASILOMAR)*, Pacific Grove, CA, Nov. 2012, pp. 676–680.

[161] M. Belleschi, G. Fodor, and A. Abrardo, "Performance analysis of a distributed resource allocation scheme for D2D communications," in *Proc. IEEE Workshop on Machine-to-Machine Communications*, Dec. 2011, pp. 358–362.

[162] N. S. Networks, "The advanced LTE toolbox for more efficient delivery of better user experience," Nokia Siemens Networks, Technical Report, 2011.

[163] S. Parkvall, A. Furuskar, Y. Jading *et al.*, "LTE-advanced – evolving LTE towards IMT-advanced," in *Proc. VTC2008 – Fall*, Sept. 2008, pp. 1–5.

[164] S. Abeta, "Toward LTE commercial launch and future plan for LTE enhancements (LTE-advanced)," in *Proc. IEEE International Conference on Communication Systems (ICCS)*, Nov. 2010, pp. 146–150.

[165] K. Doppler, M. Rinne, C. Wijting, C. Ribeiro, and K. Hugl, "Device-to-device communication as an underlay to LTE-advanced networks," *IEEE Commun. Mag.*, vol. 47, no. 12, pp. 42–49, Dec. 2009.

[166] K. Doppler, M. Rinne, C. Wijting, C. Ribeiro, and K. Hugl, "Device-to-device communications: Functional prospects for LTE-advanced networks," in *Proc. IEEE International Communications (ICC) Workshops*, Jun. 2009, pp. 1–6.

[167] M. Zulhasnine, C. Huang, and A. Srinivasan, "Efficient resource allocation for device-to-device communication underlaying LTE network," in *Proc. IEEE 6th International Conference on Wireless and Mobile Computing*, Oct. 2010, pp. 368–375.

[168] D. Halperin, J. Ammer, T. Anderson, and D. Wetherall, "Interference cancellation: Better receivers for a new wireless MAC," in *Proc. Hot Topics in Networks (HotNets – VI)*, Nov. 2007.

[169] K. Yang, Y. Wu, J. Huang, X. Wang, and S. Verdu, "Distributed robust optimization for communication networks," in *Proc. IEEE 6th International Conference on Wireless and Mobile Computing*, Apr. 2008.

[170] K. Doppler, C. H. Yu, C. B. Ribeiro, and P. Janis, "Mode selection for device-to-device communication underlaying an LTE-advanced network," in *Proc. IEEE Wireless Communications and Networking Conference (WCNC)*, Sydney, Apr. 2010.

[171] C. Yu, K. Doppler, C. Ribeiro, and O. Tirkkonen, "Resource sharing optimization for device-to-device communication underlaying cellular networks," *IEEE Trans. Wireless Commun.*, vol. 10, no. 8, pp. 2752–2763, Aug. 2011.

[172] C. Yu, O. Tirkkonen, K. Doppler, and C. Ribeiro, "On the performance of device-to-device underlay communication with simple power control," in *Proc. IEEE 69th Vehicular Technology Conference (VTC – Spring)*, Apr. 2009.

[173] X. Xiao, X. Tao, and J. Lu, "A QoS-aware power optimization scheme in OFDMA systems with integrated device-to-device (D2D) communications," in *Proc. IEEE Vehicular Technology Conference Fall*, Sept. 2011.

[174] C. Yu, K. Doppler, C. Ribeiro, and O. Tirkkonen, "Power optimization of device-to-device communication underlaying cellular communication," in *Proc. IEEE International Conference on Communications*, Jun. 2009.

[175] J. Gu, S. J. Bae, B. G. Choi, and M. Y. Chung, "Dynamic power control mechanism for interference coordination of device-to-device communication in cellular networks," in *Proc. IEEE 70th Vehicular Technology Conference Fall*, Jun. 2009.

[176] G. Fodor and N. Reider, "A distributed power control scheme for cellular network assisted D2D communications," in *Proc. IEEE Global Telecommunications Conference*, Dec. 2011.

[177] H. Min, W. Seo, J. Lee, S. Park, and D. Hong, "Reliability improvement using receive mode selection in the device-to-device uplink period underlaying cellular networks," *IEEE Trans. Wireless Commun.*, vol. 10, no. 2, pp. 413–418, Feb. 2011.

[178] P. Janis, V. Koivunen, C. Ribeiro, K. Doppler, and K. Hugl, "Interference-avoiding MIMO schemes for device-to-device radio underlaying cellular networks," in *Proc. IEEE 20th International Symposium on Personal, Indoor and Mobile Radio Communications*, Sept. 2009.

[179] S. A. Grandhi and J. Zander, "Constrained power control," *IEEE Trans. Wireless Commun.*, vol. 1, no. 4, pp. 257–270, 1995.

[180] T. Arnold and U. Schwalbe, "Dynamic coalition formation and the core," *J. Economic Behavior Organization*, vol. 49, no. 3, pp. 363–380, Nov. 2002.

[181] P. Gilmore and R. Gomory, "A linear programming approach to the cutting stock problem part II," *Operations Res.*, vol. 11, no. 6, pp. 94–120, Dec. 1963.

[182] L. Le and E. Hossain, "QoS-aware spectrum sharing in cognitive wireless networks," in *Proc. IEEE GLOBECOM*, Washington, DC, 2007, pp. 3563–3567.

[183] L. Song and J. Shen, *Evolved Cellular Network Planning and Optimization for UMTS and LTE*. CRC Press, 2010.

[184] "Apparatus and method for transmitter power control for device-to-device communications in a communication system," patent US 2012/0028672 A1.

[185] "Method, apparatus and computer program for power control to mitigate interference," patent US 2009/0325625 A1.

[186] ITU-R M.2135-1, "Guidelines for evaluation of radio interface technologies for IMT-advanced," http://www.itu.int/pub/R-REP-M.2135-1-2009, Dec. 2009.

[187] M. Haenggi, J. G. Andrews, F. Baccelli, O. Dousse, and M. Franceschetti, "Stochastic geometry and random graphs for the analysis and design of wireless networks," *IEEE J. Selected Areas Commun.*, vol. 27, no. 7, pp. 1029–1046, Sept. 2009.

[188] A. Pikovsky, "Pricing and bidding strategies in iterative combinatorial auctions," Ph.D. Dissertation, 2008.

[189] T. Wang, L. Song, Z. Han, and B. Jiao, "Dynamic popular content distribution in vehicular networks using coalition formation games," *IEEE J. Selected Areas Commun.*, vol. 31, no. 9, pp. 538–547, Sept. 2013.

[190] T. Ma, M. Hempel, D. Peng, and H. Sharif, "A survey of energy-efficient compression and communication techniques for multimedia in resource constrained systems," *IEEE Commun. Surveys Tutorials*, vol. 15, no. 3, pp. 963–972, Jul.–Sept. 2013.

[191] S. Mantzouratos, G. Gardikis, H. Koumaras, and A. Kourtis, "Survey of cross-layer proposals for video streaming over mobile ad hoc networks (MANETS)," in *Proc. IEEE International Conference on Telecommunications and Multimedia (TEMU)*, Jul.–Aug. 2012, pp. 101–106.

[192] F. Foukalas, V. Gazis, and N. Alonistioti, "Cross-layer design proposals for wireless mobile networks: A survey and taxonomy," *IEEE Commun. Surveys Tutorials*, vol. 10, no. 1, pp. 70–85, Jan.–Mar. 2008.

[193] B. Fu, Y. Xiao, H. Deng, and H. Zeng, "A survey of cross-layer designs in wireless networks," *IEEE Commun. Surveys Tutorials*, vol. 16, no. 1, pp. 110–126, Jan.–Mar. 2014.

[194] S. Shakkottai, T. S. Rappaport, and P. C. Karlsson, "Cross-layer design for wireless networks," *IEEE Commun. Mag.*, vol. 41, no. 10, pp. 74–80, Oct. 2003.

[195] V. Srivastava and M. Motani, "Cross-layer design: A survey and the road ahead," *IEEE Commun. Mag.*, vol. 43, no. 12, pp. 112–119, Dec. 2005.

[196] K. Karakayali, J. H. Kang, M. Kodialam, and K. Balachandran, "Cross-layer optimization for OFDMA-based wireless mesh backhaul networks," in *Proc. IEEE Wireless Communications and Networking Conference (WCNC)*, Mar. 2007, pp. 276–281.

[197] G. Carneiro, J. Ruela, and M. Ricardo, "Cross-layer design in 4G wireless terminals," *IEEE Commun. Mag.*, vol. 11, no. 2, pp. 7–13, Apr. 2004.

[198] V. Kawadia and P. R. Kumar, "A cautionary perspective on cross-layer design," *IEEE Wireless Commun.*, vol. 12, no. 1, pp. 3–11, Feb. 2005.

[199] X. Lin, N. B. Shroff, and R. Srikant, "A tutorial on cross-layer optimization in wireless networks," *IEEE J. Selected Areas Commun.*, vol. 24, no. 8, pp. 1452–1463, Aug. 2006.

[200] X. Liu, E. K. P. Chong, and N. B. Shroff, "A framework for opportunistic scheduling in wireless networks," *Computer Networks*, vol. 41, no. 4, pp. 451–474, Mar. 2003.

[201] F. Kelly, "Charging and rate control for elastic traffic," *European Trans. Telecommun.*, vol. 8, no. 1, pp. 33–37, Feb. 1997.

[202] G. Song and Y. Li, "Cross-layer optimization for OFDM wireless networks – part I: Theoretical framework," *IEEE Trans. Wireless Commun.*, vol. 4, no. 2, pp. 614–624, Mar. 2005.

[203] G. Song and Y. Li, "Cross-layer optimization for OFDM wireless networks – part II: Algorithm development," *IEEE Trans. Wireless Commun.*, vol. 4, no. 2, pp. 625–634, Mar. 2005.

[204] Z. Jiang, Y. Ge, and Y. G. Li, "Max-utility wireless resource management for best effort traffic," *IEEE Trans. Wireless Commun.*, vol. 4, no. 1, pp. 100–111, Jan. 2005.

[205] X. Lin and N. B. Shroff, "The impact of imperfect scheduling on cross-layer congestion control in wireless networks," *IEEE/ACM Trans. Networking*, vol. 14, no. 2, pp. 302–315, Apr. 2006.

[206] B. Jarupan and E. Ekici, "A survey of cross-layer design for VANETS," *Ad Hoc Networks*, vol. 9, no. 5, pp. 966–983, Jul. 2011.

[207] J. Camp and E. Knightly, "Modulation rate adaptation in urban and vehicular environments: Cross-layer implementation and experimental evaluation," in *Proc. ACM International Conference on Mobile Computing and Networking (MobiCom)*, Sept. 2008, pp. 315–326.

[208] K.-L. Chiu, R.-H. Hwang, and Y.-S. Chen, "Cross-layer design vehicle-aided handover scheme in VANETS," *Wireless Commun. Mobile Computing*, vol. 11, no. 7, pp. 916–928, Jul. 2011.

[209] N. Sofra, A. Gkelias, and K. K. Leung, "Link residual-time estimation for VANET cross-layer design," in *Proc. International Workshop on Cross Layer Design (IWCLD)*, Jun. 2009, pp. 1–5.

[210] J. P. Singh, N. Bambos, B. Srinivasan, and D. Clawin, "Cross-layer multi-hop wireless routing for inter-vehicle communication," in *Proc. International Conference on Testbeds and Research Infrastructures for the Development of Networks and Communities (TRIDENTCOM)*, Barcelona, Mar. 2006.

[211] H. Menouar, M. Lenardi, and F. Filali, "Movement prediction-based routing (MOPR) concept for position-based routing in vehicular networks," in *Proc. IEEE Vehicular Technology Conference (VTC) Fall*, Sep.–Oct. 2007, pp. 2101–2105.

[212] G. Korkmaz, E. Ekici, and F. Ozguner, "A cross-layer multihop data delivery protocol with fairness guarantees for vehicular networks," *IEEE Trans. Vehicular Technol.*, vol. 55, no. 3, pp. 865–875, May 2006.

[213] R. Schmilz, A. Leiggener, A. Festag, L. Eggert, and W. Effelsberg, "Analysis of path characteristics and transport protocol design in vehicular ad hoc networks," in *Proc. IEEE Vehicular Technology Conference (VTC) Spring*, vol. 2, May 2006, pp. 528–532.

[214] L. Zhou, B. Zheng, B. Geller *et al.*, "Cross-layer rate control, medium access control and routing design in cooperative VANET," *Computer Commun.*, vol. 31, no. 12, pp. 2870–2882, Jul. 2008.

[215] M. Drigo, W. Zhang, R. Baldessari *et al.*, "Distributed rate control algorithm for VANETS (DRCV)," in *Proc. ACM International Workshop on VehiculAr InterNETworking (VANET)*, Sept. 2009, pp. 119–120.

[216] A. Chen, B. Khorashadi, D. Ghosal, and C. Chuah, "Impact of transmission power on TCP performance in vehicular ad hoc networks," in *Proc. IEEE/IFIP Wireless On-demand Networks and Services (WONS)*, Jan. 2007, pp. 65–71.

[217] B. Khorashadi, A. Chen, D. Ghosal, C. Chuah, and M. Zhang, "Impact of transmission power on the performance of UDP in vehicular ad hoc networks," in *Proc. IEEE International Conference on Communications (ICC)*, Jun. 2007, pp. 3698–3703.

[218] J. Eriksson, H. Balakrishnan, and S. Madden, "Cabernet: Vehicular content delivery using WiFi," in *Proc. ACM International Conference on Mobile Computing and Networking (MobiCom)*, Sept. 2008, pp. 199–210.

[219] X. Zhu, S. Wen, C. Wang *et al.*, "A cross-layer study: Information correlation based scheduling scheme for device-to-device radio underlaying cellular networks," in *Proc. International Conference on Telecommunications (ICT)*, Apr. 2012.

[220] Y. Zeng, N. Xiong, L. T. Yang, and Y. Zhang, "Cross-layer routing in wireless sensor networks for machine-to-machine intelligent hazard monitoring applications," in *Proc. IEEE Conference on Computer Communications Workshops (INFOCOM WKSHPS)*, Apr. 2011, pp. 206–211.

[221] Y. Zeng, C. J. Sreenan, and L. Sitanayah, "A real-time and robust routing protocol for building fire emergency applications using wireless sensor networks," in *Proc. IEEE International Conference on Pervasive Computing and Communications Workshops (PERCOM Workshops)*, Mar.–Apr. 2010, pp. 358–363.

[222] O. Chipara, Z. He, G. Xing *et al.*, "Real-time power-aware routing in sensor networks," in *Proc. IEEE International Workshop on Quality of Service (IWQoS)*, Jun. 2006, pp. 83–92.

[223] H. Luo, S. Ci, and D. Wu, "A cross-layer optimized distributed scheduling algorithm for peer-to-peer video streaming over multi-hop wireless mesh networks," in *Proc. IEEE Communications Society Conference on Sensor, Mesh and Ad Hoc Communications and Networks (SECON)*, Jun. 2009, pp. 1–9.

[224] X. Zhang, J. Liu, B. Li, and T. P. Yum, "Coolstreaming/donet: A data-driven overlay network for peer-to-peer live media streaming," in *Proc. INFOCOM*, vol. 3, Mar. 2005, pp. 2102–2111.

[225] FCC, "Connecting America: The national broadband plan," Technical Report, Mar. 2010.

[226] T. E. Humphreys, B. M. Ledvina, M. L. Psiaki, B. W. O'Hanlon, and P. M. Kintner, "Assessing the spoofing threat: Development of a portable GPS civilian spoofer," in *Proc. 21st International Technical Meeting of the Satellite Division of the Institute of Navigation, ION GNSS*, Savannah, GA, Sept. 2008, pp. 2314–2325.

[227] N. O. Tippenhauer, C. Popper, K. B. Rasmussen, and S. Capkun, "On the requirements for successful GPS spoofing attacks," in *Proc. 18th ACM Conference on Computer and Communications Security, CCS*, Chicago, IL, Oct. 2011, pp. 75–86.

[228] E. Mills, "Drones can be hijacked via GPS spoofing attack," June 29, 2012. http://news.cnet.com/8301-1009_3-57464271-83/drones-can-be-hijacked-via-gps-spoofing-attack.

[229] A. Rawnsley, "Iran's alleged drone hack: Tough, but possible," *Wired*, Dec 2011. http://www.wired.com/dangerroom/2011/12/iran-drone-hack-gps/?utm_source=Contextly&utm_medium=RelatedLinks&utm_campaign=Previous.

[230] S. Lawson, "FCC to move on sharing scheme that could free up 100 MHz of wireless spectrum," *PC World*, Sept. 13, 2012. http://www.pcworld.com/article/262301/fcc_to_move_on_sharing_scheme_that_could_free_up_100mhz_of_wireless_spectrum.html.

[231] S. Kim, H. Jeon, and J. Ma, "Robust localization with unknown transmission power for cognitive radio," in *Proc. IEEE MILCOM*, Orlando, FL, Oct. 2007, pp. 1–6.

[232] M. Robinson and I. Psaromiligkos, "Received signal strength based location estimation of a wireless LAN client," in *Proc. IEEE WCNC*, New Orleans, LA, Mar. 2005, pp. 2350–2354.

[233] J. Yang and Y. Chen, "Indoor localization using improved RSS-based lateration methods," in *Proc. IEEE GLOBECOM*, Honolulu, HI, Dec. 2009, pp. 1–6.

[234] X. Cheng, A. Thaeler, G. Xue, and D. Chen, "TPS: A time-based positioning scheme for outdoor wireless sensor networks," *Proc. IEEE INFOCOM*, vol. 4, pp. 2685–2696, Mar. 2004.

[235] S. A. Golden and S. S. Bateman, "Sensor measurements for Wi-Fi location with emphasis on time-of-arrival ranging," *IEEE Trans. Mobile Computing*, vol. 6, no. 10, pp. 1185–1198, Oct. 2007.

[236] N. B. Priyantha, A. Chakraborty, and H. Balakrishnan, "The cricket location-support system," in *Proc. 6th Annual International Conference on Mobile Computing and Networking, MobiCom*, Boston, MA, Aug. 2000, pp. 32–43.

[237] D. Niculescu and B. Nath, "Ad hoc positioning system (APS) using AOA," in *Proc. IEEE INFOCOM*, San Francisco, CA, Apr. 2003, pp. 1734–1743.

[238] P. Rong and M. Sichitiu, "Angle of arrival localization for wireless sensor networks," in *Proc. 3rd Annual IEEE Communications Society on Sensor and Ad Hoc Communications and Networks (SECON)*, Reston, VA, Sept. 2006, pp. 374–382.

[239] P. Bahl and V. N. Padmanabhan, "Radar: An in-building RF-based user location and tracking system," in *Proc. IEEE INFOCOM*, Tel Aviv, Mar. 2000, pp. 775–784.

[240] P. Bahl and V. N. Padmanabhan, "Enhancements to the radar user location and tracking system," Microsoft Research, Technical Report, Feb. 2000.

[241] C. Feng, W. Au, S. Valaee, and Z. Tan, "Compressive sensing based positioning using RSS of WLAN access points," in *Proc. IEEE INFOCOM*, San Diego, CA, Mar. 2010, pp. 1–9.

[242] K. Kaemarungsi and P. Krishnamurthy, "Modeling of indoor positioning systems based on location fingerprinting," in *Proc. IEEE INFOCOM*, Hongkong, Mar. 2004, pp. 1012–1022.

[243] S. Sen, B. Radunovic, R. Choudhury, and T. Minka, "Spot localization using PHY layer information," in *Proc. ACM MOBISYS*, Low Wood Bay, Lake District, Jun. 2012, pp. 183–196.

[244] S. Sen, B. Radunovic, R. R. Choudhury, and T. Minka, "Precise indoor localization using PHY information," in *Proc. 9th International Conference on Mobile Systems, Applications, and Services, MobiSys*, Washington, DC, Jun. 2011, pp. 413–414.

[245] Y. Chen, D. Lymberopoulos, J. Liu, and B. Priyantha, "FM-based indoor localization," in *Proc. 10th International Conference on Mobile Systems, Applications, and Services, MobiSys*, Low Wood Bay, Lake District, Jun. 2012, pp. 169–182.

[246] M. Azizyan, I. Constandache, and R. R. Choudhury, "Surroundsense: Mobile phone localization via ambience fingerprinting," in *Proc. 15th Annual International Conference on Mobile Computing and Networking, MobiCom*, Beijing, Sept. 2009, pp. 261–272.

[247] N. Bulusu, J. Heidemann, and D. Estrin, "GPS-less low-cost outdoor localization for very small devices," *IEEE Personal Commun.*, vol. 7, no. 5, pp. 28–34, Oct. 2000.

[248] T. He, C. Huang, B. M. Blum, J. A. Stankovic, and T. Abdelzaher, "Range-free localization schemes for large scale sensor networks," in *Proc. 9th Annual International Conference on Mobile Computing and Networking, MobiCom*, San Diego, CA, Sept. 2003, pp. 81–95.

[249] Y. Shang, W. Ruml, Y. Zhang, and M. Fromherz, "Localization from connectivity in sensor networks," *IEEE Trans. Parallel Distributed Systems*, vol. 15, no. 11, pp. 961–974, Nov. 2004.

[250] Y. Shang, W. Ruml, Y. Zhang, and M. P. J. Fromherz, "Localization from mere connectivity," in *Proc. 4th ACM International Symposium on Mobile Ad Hoc Networking & Computing, MobiHoc*, Annapolis, MD, Jun. 2003, pp. 201–212.

[251] I. Constandache, X. Bao, M. Azizyan, and R. R. Choudhury, "Did you see Bob?: Human localization using mobile phones," in *Proc. 16th Annual International Conference on Mobile Computing and Networking, MobiCom*, Chicago, IL, Sept. 2010, pp. 149–160.

[252] I. Constandache, R. R. Choudhury, and I. Rhee, "Towards mobile phone localization without war-driving," in *Proc. IEEE INFOCOM*, San Diego, CA, Mar. 2010, pp. 1–9.

[253] B. Zhang, J. Teng, J. Zhu *et al.*, "Ev-loc: Integrating electronic and visual signals for accurate localization," in *Proc. 13th ACM International Symposium on Mobile Ad Hoc Networking and Computing, MobiHoc*, Hilton Head Island, CA, Jun. 2012, pp. 25–34.

[254] H. Liu, Y. Gan, J. Yang *et al.*, "Push the limit of WiFi based localization for smartphones," in *Proc. 18th Annual International Conference on Mobile Computing and Networking, MobiCom*, Istanbul, Aug. 2012, pp. 305–316.

[255] J. G. Manweiler, P. Jain, and R. R. Choudhury, "Satellites in our pockets: An object positioning system using smartphones," in *Proc. 10th International Conference on Mobile Systems, Applications, and Services, MobiSys*, Low Wood Bay, Lake District, Jun. 2012, pp. 211–224.

[256] S. Sen, R. R. Choudhury, and S. Nelakuditi, "Spinloc: Spin once to know your location," in *Proc. Twelfth Workshop on Mobile Computing Systems & Applications, HotMobile*, San Diego, CA, Feb. 2012, p. 12.

[257] H. Wang, S. Sen, A. Elgohary *et al.*, "No need to war-drive: Unsupervised indoor localization," in *Proc. 10th International Conference on Mobile Systems, Applications, and Services, MobiSys*, Low Wood Bay, Lake District, Jun. 2012, pp. 197–210.

[258] Y. Chen, W. Trappe, and R. P. Martin, "Attack detection in wireless localization," in *Proc. IEEE INFOCOM*, Anchorage, AK, May 2007, pp. 1964–1972.

[259] K. Bauer, D. McCoy, E. Anderson *et al.*, "The directional attack on wireless localization: How to spoof your location with a tin can," in *Proc. IEEE GLOBECOM*, Honolulu, HI, Dec. 2009, pp. 1–6.

[260] N. O. Tippenhauer, C. Popper, K. B. Rasmussen, and S. Capkun, "On the requirements for successful GPS spoofing attacks," in *Proc. 18th ACM Conference on Computer and Communications Security (CCS)*, Chicago, IL, Oct. 2011, pp. 75–86.

[261] L. Hu and D. Evans, "Using directional antennas to prevent wormhole attacks," in *Network and Distributed System Security Symposium*, San Diego, CA, Feb. 2004, pp. 131–141.

[262] L. Lazos and R. Poovendran, "Serloc: Secure range-independent localization for wireless sensor networks," in *Wireless Security*, Philadelphia, PA, Oct. 2004, pp. 21–30.

[263] S. Capkun, M. Cagalj, and M. Srivastava, "Secure localization with hidden and mobile base stations," in *Proc. 25th IEEE International Conference on Computer Communications, INFOCOM*, Barcelona, Apr. 2006, p. 110.

[264] L. Lazos and R. P. Hirloc, "High-resolution robust localization for wireless sensor networks," *IEEE J. Selected Areas Commun.*, vol. 24, no. 2, p. 233–246, Feb. 2006.

[265] N. Sastry, U. Shankar, and D. Wagner, "Secure verification of location claims," in *Proc. 2nd ACM Workshop on Wireless Security*, San Diego, CA, Sept. 2003, p. 110.

[266] S.-H. Fang, C.-C. Chuang, and C. Wang, "Attack-resistant wireless localization using an inclusive disjunction model," *IEEE Trans. Commun.*, vol. 60, no. 5, pp. 1209–1214, May 2012.

[267] Y. Hu, A. Perrig, and D. Johnson, "Packet leashes: A defense against wormhole attacks in wireless networks," *Twenty-Second Annual Joint Conference of the IEEE Computer and Communications, INFOCOM*, vol. 3, pp. 1976–1986, Apr. 2003.

[268] J. H. Lee and R. Buehrer, "Location spoofing attack detection in wireless networks," in *Proc. IEEE INFOCOM*, Miami, FL, Dec. 2010, p. 16.

[269] X. Li, Y. Chen, J. Yang, and X. Zheng, "Designing localization algorithms robust to signal strength attacks," in *Proc. IEEE INFOCOM*, Shanghai, Apr. 2011, pp. 341–345.

[270] Z. Li, W. Trappe, Y. Zhang, and B. Nath, "Robust statistical methods for securing wireless localization in sensor networks," in *Fourth International Symposium on Information*

Processing in Sensor Networks, IPSN, Los Angeles, CA, Apr. 2005, pp. 91–98.

[271] D. Liu, P. Ning, and W. Du, "Attack-resistant location estimation in sensor networks," in *Fourth International Symposium on Information Processing in Sensor Networks, IPSN*, Los Angeles, CA, Apr. 2005, pp. 99–106.

[272] J. S. Warner and R. G. Johnston, "GPS spoofing countermeasures," *Homeland Security Journal*, Dec. 2003.

[273] Y. Zhang, W. Liu, Y. Fang, and D. Wu, "Secure localization and authentication in ultra-wideband sensor networks," *IEEE J. Selected Areas Commun.*, vol. 24, no. 4, pp. 829–835, Apr. 2006.

[274] P. Bao and M. Liang, "A security localization method based on threshold and vote for wireless sensor networks," *Procedia Engineering*, vol. 15, no. 12, pp. 2783–2787, Dec. 2011.

[275] Q. Mi, J. A. Stankovic, and R. Stoleru, "Secure walking GPS: A secure localization and key distribution scheme for wireless sensor networks," in *Proc. Third ACM Conference on Wireless Network Security, WiSec*, Hoboken, NJ, Mar. 2010, pp. 163–168.

[276] S. K. Leung-Yan-Cheong and M. E. Hellman, "The Gaussian wiretap channel," *IEEE Trans. Information Theory*, vol. 24, no. 4, pp. 451–456, Jul. 1978.

[277] A. D. Wyner, "The wire-tap channel," *Bell. Syst. Tech. J.*, vol. 54, no. 8, pp. 1355–1387, Oct. 1975.

[278] P. C. Pinto, J. Barros, and M. Z. Win, "Physical-layer security in stochastic wireless networks," in *11th IEEE Singapore International Conference on Communication Systems*, Singapore, Nov. 2008.

[279] Z. Shu, Y. Yang, Y. Qian, and R. Q. Hu, "Impact of interference on secrecy capacity in a cognitive radio network," in *Global Telecommunications Conference (GLOBECOM 2011)*, Houston, TX, Dec. 2011.

[280] G. Karagiannis, O. Altintas, E. Ekici *et al.*, "Vehicular networking: A survey and tutorial on requirements, architectures, challenges, standards and solutions," *Commun. Surveys Tutorials*, vol. 13, no. 4, pp. 584–616, Oct.–Dec. 2011.

[281] ETSI, "Intelligent transport system (ITS); vehicular communications; basic set of applications; definition," Technical Report, Jun. 2009, ETSI Std. ETSI ITS Specification TR 102 638 version 1.1.1.

[282] J. Misic, G. Badawy, and V. B. Misic, "Performance characterization for IEEE 802.11p network with single channel devices," *IEEE Trans. Vehicular Technol.*, vol. 60, no. 4, pp. 1775–1787, 2011.

[283] X. Chen and D. Yao, "An empirically comparative analysis of 802.11n and 802.11p performances in CVIS," in *Proc. International Conference on ITS Telecommunications (ITST)*, Taipei, Taiwan, Nov. 2012, pp. 848–851.

[284] C.-S. Lin, B.-C. Chen, and J.-C. Lin, "Field test and performance improvement in IEEE 802.11p v2r/r2v environments," in *Proc. IEEE International Conference on Communications Workshops (ICC)*, Cape Town, May 2010, pp. 1–5.

[285] H. Guo, S. T. Goh, N. C. S. Foo, Q. Zhang, and W.-C. Wong, "Performance evaluation of 802.11p device for secure vehicular communication," in *Proc. International Wireless Communications and Mobile Computing Conference (IWCMC)*, Jul. 2011, pp. 1170–1175.

[286] J. A. Fernandez, K. Borries, L. Cheng *et al.*, "Performance of the 802.11p physical layer in vehicle-to-vehicle environments," *IEEE Trans. Vehicular Technol.*, vol. 61, no. 1, pp. 3–14, 2012.

[287] C. Han, M. Dianati, R. Tafazolli, R. Kernchen, and X. Shen, "Analytical study of the IEEE 802.11p MAC sublayer in vehicular networks," *IEEE Trans. Intelligent Transportation Systems*, vol. 13, no. 2, pp. 873–886, 2012.

[288] J.-C. Lin, C.-S. Lin, C.-N. Liang, and B.-C. Chen, "Wireless communication performance based on IEEE 802.11p r2v field trials," *IEEE Commun. Mag.*, vol. 50, no. 5, pp. 184–191, 2012.

[289] T. Sukuvaara, R. Ylitalo, and M. Katz, "IEEE 802.11p based vehicular networking operational pilot field measurement," *IEEE J. Selected Areas Commun.*, vol. 31, no. 9, pp. 409–417, Sept. 2013.

[290] S. Cespedes, N. Lu, and X. Shen, "VIP-wave: On the feasibility of IP communications in 802.11p vehicular networks," *IEEE Trans. Intelligent Transportation Systems*, vol. 14, no. 1, pp. 82–97, Mar. 2013.

[291] F. Li and Y. Wang, "Routing in vehicular ad hoc networks: A survey," *IEEE Vehicular Technol. Mag.*, vol. 2, no. 2, pp. 12–22, Jun. 2007.

[292] C. E. Perkins and E. M. Royer, "Ad-hoc on demand distance vector routing," in *Proc. IEEE Workshop on Mobile Computing Systems and Applications (WMCSA)*, Feb. 1999, pp. 90–100.

[293] D. B. Johnson and D. A. Maltz, *Mobile Computing*. Springer, 1996, ch. Dynamic source routing in ad hoc wireless networks, pp. 153–181.

[294] V. Namboodiri, M. Agarwal, and L. Gao, "A study on the feasibility of mobile gateways for vehicular ad-hoc networks," in *Proc. First International Workshop on Vehicular Ad Hoc Networks*, Philadelphia, PA, Oct. 2004, pp. 66–75.

[295] S. Y. Wang, C. C. Lin, Y. W. Hwang, K. C. Tao, and C. L. Chou, "A practical routing protocol for vehicle-formed mobile ad hoc networks on the roads," in *Proc. IEEE International Conference on Intelligent Transportation Systems*, Vienna, Sept. 2005, pp. 161–165.

[296] V. Namboodiri and L. Gao, "Prediction-based routing for vehicular ad hoc networks," *IEEE Trans. Vehicular Technol.*, vol. 56, no. 4, pp. 2332–2345, Jul. 2007.

[297] B. Karp and H. T. Kung, "GPSR: Greedy perimeter stateless routing for wireless networks," in *Proc. ACM/IEEE International Conference on Mobile Computing and Networking (MobiCom)*, Boston, MA, Aug. 2000, pp. 243–254.

[298] H. Fubler, M. Mauve, H. Hartenstein, M. Kasemann, and D. Vollmer, "Location-based routing for vehicular ad-hoc networks," *ACM SIGMOBILE Mobile Computing and Communications Review (MC2R)*, vol. 7, no. 1, pp. 47–49, Jan. 2003.

[299] E. H. Wu, P. K. Sahu, and J. Sahoo, "Destination discovery oriented position based routing in VANET," in *Proc. IEEE Asia–Pacific Services Computing Conference (APSCC)*, Dec. 2008, pp. 1606–1610.

[300] Y. Ohta, T. Ohta, and Y. Kakuda, "An autonomous clustering-based data transfer scheme using positions and moving direction of vehicles for VANETS," in *Proc. IEEE Wireless Communications and Networking Conference (WCNC)*, Apr. 2012, pp. 2900–2904.

[301] M. Durresi, A. Durresi, and L. Barolli, "Emergency broadcast protocol for intervehicle communications," in *Proc. International Conference on Parallel and Distributed Systems Workshops (ICPADS)*, Fukuoka, Jul. 2005, pp. 402–406.

[302] G. K. E. Ekici, F. Ozguner, and U. Ozguner, "Urban multi-hop broadcast protocol for inter-vehicle communication systems," in *ACM International Workshop on Vehicular Ad Hoc Networks*, Philadelphia, PA, Oct. 2004, pp. 76–85.

[303] M. Sun, W. Feng, T.-H. Lai *et al.*, "GPS-based message broadcasting for inter-vehicle communication," in *Proc. International Conference on Parallel Processing (ICPP)*, Toronto, Aug. 2000, pp. 279–286.

[304] S. Panichpapiboon and W. Pattara-Atikom, "A review of information dissemination protocols for vehicular ad hoc networks," *Commun. Surveys Tutorials*, vol. 14, no. 3, pp. 784–798, Oct.–Dec. 2012.

[305] T. Zhong, B. Xu, and O. Wolfson, "Disseminating real-time traffic information in vehicular ad-hoc networks," in *Proc. IEEE Intelligent Vehicles Symposium (IV)*, Jan. 2008, pp. 1056–1061.

[306] T. Fujiki, M. Kirimura, T. Umedu, and T. Higashino, "Efficient acquisition of local traffic information using inter-vehicle communication with queries," in *Proc. IEEE Intelligent Transportation Systems Conference (ITSC)*, Sept. 2007, pp. 241–246.

[307] D. Li, H. Huang, X. Li, M. Li, and F. Tang, "A distance-based directional broadcast protocol for urban vehicular ad hoc network," in *Proc. International Conference on Wireless Communications, Networking and Mobile Computing (WiCom)*, Sept. 2007, pp. 1520–1523.

[308] N. Wisitpongphan, O. K. Tonguz, J. S. Parikh *et al.*, "Broadcast storm mitigation techniques in vehicular ad hoc networks," *IEEE Wireless Commun.*, vol. 14, no. 6, pp. 84–94, Dec. 2007.

[309] L. Li, R. Ramjee, M. Buddhikot, and S. Miller, "Network coding-based broadcast in mobile ad-hoc networks," in *Proc. IEEE International Conference on Computer Communications (INFOCOM)*, May 2007, pp. 1739–1747.

[310] Y.-S. Chen, Y.-W. Lin, and S.-L. Lee, "A mobicast routing protocol in vehicular ad-hoc networks," in *Proc. IEEE Global Telecommunications Conference (GLOBECOM)*, Nov.–Dec. 2009, pp. 1–6.

[311] B. Zhou, H. Hu, S.-Q. Huang, and H.-H. Chen, "Intracluster device-to-device relay algorithm with optimal resource utilization," *IEEE Trans. Vehicular Technol.*, vol. 62, no. 5, pp. 2315–2326, Jun. 2013.

[312] B. Shrestha, D. Niyato, Z. Han, and E. Hossain, "Wireless access in vehicular environments using BitTorrent and bargaining," in *Proc. IEEE Global Telecommunications Conference (GLOBECOM)*, Nov.–Dec. 2008, pp. 1–5.

[313] D. Qiu and R. Srikant, "Modeling and performance analysis of BitTorrentlike peer–peer networks," *SIGCOMM Computer Commun. Rev.*, vol. 34, no. 4, pp. 367–378, Oct. 2004.

[314] T. S. Rappaport, *Wireless Communications: Principles and Practice*, 2nd edn. Prentice Hall, 2002.

[315] M. H. Ahmed, H. Yanikomeroglu, and S. Mahmoud, "Fairness enhancement of link adaptation techniques in wireless networks," in *Proc. IEEE Vehicular Technology Conference (VTC)*, vol. 4, Oct. 2003, pp. 1554–1557.

[316] D. Niyato, E. Hossain, and P. Wang, "Optimal channel access management with QoS support for cognitive vehicular networks," *IEEE Trans. Mobile Computing*, vol. 10, no. 4, pp. 573–591, Feb. 2011.

[317] M. M. Buddhikot, "Understanding dynamic spectrum access: Models, taxonomy and challenges," in *Proc. IEEE International Symposium on New Frontiers in Dynamic Spectrum Access Networks (DySPAN)*, Apr. 2007, pp. 649–663.

[318] L. Le and E. Hossain, "A MAC protocol for opportunistic spectrum access in cognitive radio networks," in *Proc. IEEE Wireless Communications and Networking Conference (WCNC)*, Mar.–Apr. 2008, pp. 1426–1430.

[319] Q. Liu, S. Zhou, and G. B. Giannakis, "Cross-layer combining of adaptive modulation and coding with truncated ARQ over wireless links," *IEEE Trans. Wireless Commun.*, vol. 3, no. 5, pp. 1746–1755, Sept. 2004.

[320] M. L. Puterman, *Markov Decision Processes: Discrete Stochastic Dynamic Programming*. Wiley-Interscience, 1994.

[321] N. Kayastha, D. Niyato, P. Wang, and E. Hossain, "Applications, architectures, and protocol design issues for mobile social networks: A survey," *Proc. IEEE*, vol. 99, no. 12, pp. 2130–2158, 2011.

[322] N. Vastardis and K. Yang, "Mobile social networks: Architectures, social properties, and key research challenges," *IEEE Commun. Surveys Tutorials*, vol. 15, no. 3, pp. 1355–1371, Oct.–Dec. 2013.

[323] D. J. Watts and S. H. Strogatz, "Collective dynamics of 'small-world' networks," *Nature*, vol. 393, pp. 440–442, 1998.

[324] Y. Zhu, B. Xu, X. Shi, and Y. Wang, "A survey of social-based routing in delay tolerant networks: Positive and negative social effects," *IEEE Commun. Surveys Tutorials*, vol. 15, no. 1, pp. 387–401, Oct.–Dec. 2013.

[325] K. Wei, X. Liang, and K. Xu, "A survey of social-aware routing protocols in delay tolerant networks: Applications, taxonomy and design-related issues," *IEEE Commun. Surveys Tutorials*, vol. 16, no. 1, pp. 556–578, Jan.–Mar. 2014.

[326] C.-M. Huang, K. C. Lan, and C.-Z. Tsai, "A survey of opportunistic networks," in *Proc. International Conference on Advanced Information Networking and Applications – Workshops (AINAW)*, Okinawa, Mar. 2008, pp. 1672–1677.

[327] J. G. Scott, *Social Network Analysis: A Handbook*. SAGE Publications, 2012.

[328] D. Knoke and S. Yang, *Social Network Analysis (Quantitative Applications in the Social Sciences)*. SAGE Publications, 2007.

[329] T. Hossmann, F. Legendre, and T. Spyropoulos, "From contacts to graphs: Pitfalls in using complex network analysis for DTN routing," in *Proc. INFOCOM Workshops*, Rio de Janeiro, Apr. 2009, pp. 1–6.

[330] M. E. J. Newman, "Detecting community structure in networks," *Eur. Phys. J. B – Condensed Matter Complex Systems*, vol. 38, no. 2, pp. 321–330, Mar. 2004.

[331] L. Danon, J. Duch, A. Diaz-Guilera, and A. Arenas, "Comparing community structure identification," *J. Statist. Mech.: Theory Exp.*, p. 09008, 2005.

[332] G. Bigwood, D. Rehunathan, M. Bateman, T. Henderson, and S. Bhatti, "Exploiting self-reported social networks for routing in ubiquitous computing environments," in *Proc. IEEE International Conference on Wireless and Mobile Computing, Networking and Communication (WiMob)*, Avignon, Oct. 2008, pp. 484–489.

[333] K. Jahanbakhsh, G. C. Shoja, and V. King, "Social-greedy: A socially-based greedy routing algorithm for delay tolerant networks," in *Proc. Second International Workshop on Mobile Opportunistic Networking*, Pisa, Feb. 2010, pp. 159–162.

[334] M. E. J. Newman, "Fast algorithm for detecting community structure in networks," *Phys. Rev. E*, vol. 63, no. 6, p. 066133, Jun. 2004.

[335] M. Girvan and M. E. J. Newman, "Community structure in social and biological networks," *Proc. Nat. Acad. Sci. USA*, vol. 99, no. 12, pp. 7821–7826, Jun. 2002.

[336] N. P. Nguyen, Y. X. T. N. Dinh, and M. T. Thai, "Adaptive algorithms for detecting community structure in dynamic social networks," in *Proc. IEEE INFOCOM*, Shanghai, Apr. 2011, pp. 2282–2290.

[337] V. D. Blondel, J. Guillaume, R. Lambiotte, and E. Lefebvre, "Fast unfolding of communities in large networks," *J. Statist. Mech.: Theory Exp.*, p. 10008, Oct. 2008.

[338] Z. Ye, S. Hu, and J. Yu, "Adaptive clustering algorithm for community detection in complex networks," *Phys. Rev. E*, vol. 78, no. 4, p. 046115, 2008.

[339] G. Palla, P. Pollner, A. Barabasi, and T. Vicsek, *Adaptive Networks*. Springer, 2009, ch. Social group dynamics in networks, pp. 11–38.

[340] A. Chaintreau, J. C. P. Hui, C. Diot, R. Gass, and J. Scot, "Impact of human mobility on opportunistic forwarding algorithms," *IEEE Trans. Mobile Computing*, vol. 6, no. 6, pp. 606–620, Jun. 2007.

[341] P. Hui and J. Crowcroft, "How small labels create big improvements," in *Proc. IEEE International Conference on Pervasive Computing and Communications Workshops (PerCom Workshops)*, White Plains, NY, Mar. 2007, pp. 65–70.

[342] T. N. Dinh, Y. Xuan, and M. T. Thai, "Towards social-aware routing in dynamic communication networks," in *Proc. IEEE International Performance Computing and Communications Conference (IPCCC)*, Phoenix, AZ, Dec. 2009, pp. 161–168.

[343] P. Hui, E. Yoneki, S.-Y. Chan, and J. Crowcroft, "Distributed community detection in delay tolerant networks," in *Proc. ACM International Workshop on Mobility in the Evolving Internet Architecture (MobiArch)*, no. 7, Kyoto, Aug. 2007.

[344] Haggle project, 2004. http://www.haggleproject.org.

[345] N. Eagle and A. Pentland, "Reality mining: Sensing complex social systems," *Personal and Ubiquitous Computing*, vol. 10, no. 4, pp. 255–268, May 2006.

[346] M. McNett and G. M. Voelker, "Access and mobility of wireless PDA users," *SIGMOBILE Mobile Computing Commun. Rev.*, vol. 9, no. 2, pp. 40–55, Apr. 2005.

[347] D. Kempe, J. Kleinberg, and E. Tardos, "Influential nodes in a diffusion model for social networks," in *International Colloquium on Automata, Languages and Programming*, no. 32, Lisbon, Jul. 2005, pp. 1127–1138.

[348] P. Domingos and M. Richardson, "Mining the network value of customers," in *Proc. 7th ACM SIGKDD International Conference on Knowledge Discovery and Data Mining*, San Francisco, CA, Aug. 2001, pp. 57–66.

[349] D. Kempe, J. Kleinberg, and E. Tardos, "Maximizing the spread of influence through a social network," in *Proc. 9th ACM SIGKDD International Conference on Knowledge Discovery and Data Mining*, Washington, DC, Aug. 2003, pp. 137–146.

[350] J. Leskovec, A. Krause, C. Guestrin *et al.*, "Cost-effective outbreak detection in networks," in *Proc. 13th ACM SIGKDD International Conference on Knowledge Discovery and Data Mining*, San Jose, CA, Aug. 2007, pp. 420–429.

[351] W. Chen, Y. Wang, and S. Yang, "Efficient influence maximization in social networks," in *Proc. 15th ACM SIGKDD International Conference on Knowledge Discovery and Data Mining*, Paris, Jun. 2009, pp. 199–208.

[352] Y. Wang, G. Cong, G. Song, and K. Xie, "Community-based greedy algorithm for mining top-*k* influential nodes in mobile social networks," in *Proc. 16th ACM SIGKDD International Conference on Knowledge Discovery and Data Mining*, Washington, DC, Jul. 2010, pp. 25–28.

[353] E. M. Daly and M. Haahr, "Social network analysis for routing in disconnected delay-tolerant MANETS," in *Proc. ACM International Symposium on Mobile Ad Hoc Networking and Computing (MobiHoc)*, Montreal, QC, Sept. 2007, pp. 32–40.

[354] P. Hui, J. Crowcroft, and E. Yoneki, "Bubble rap: Social-based forwarding in delay tolerant networks," in *Proc. ACM International Symposium on Mobile Ad Hoc Networking and Computing (MobiHoc)*, Hongkong, May 2008, pp. 241–250.

[355] G. Palla, I. Derenyi, I. Farkas, and T. Vicsek, "Uncovering the overlapping community structure of complex networks in nature and society," *Nature*, vol. 435, no. 7043, pp. 814–818, Jun. 2005.

[356] M. E. J. Newman, "Analysis of weighted networks," *Phys. Rev. E*, vol. 70, no. 5, p. 056131, Nov. 2004.

[357] A. Lindgren, A. Doria, and O. Schelen, "Probabilistic routing in intermittently connected networks," *ACM SIGMOBILE Mobile Computing Commun. Rev.*, vol. 7, no. 3, pp. 19–20, Jul. 2003.

[358] E. Bulut and B. K. Szymanski, "Exploiting friendship relations for efficient routing in mobile social networks," *IEEE Trans. Parallel Distributed Systems*, vol. 23, no. 12, pp. 2254–2265, Dec. 2012.

[359] J. Fan, J. Chen, Y. Du *et al.*, "Geocommunity-based broadcasting for data dissemination in mobile social networks," *IEEE Trans. Parallel Distributed Systems*, vol. 24, no. 4, pp. 734–743, Apr. 2013.

[360] D. Niyato, P. Wang, W. Saad, and A. Hjorungnes, "Controlled coalitional games for cooperative mobile social networks," *IEEE Trans. Vehicular Technol.*, vol. 60, no. 4, pp. 1812–1824, May 2011.

[361] R. Nelson, *Probability, Stochastic Processes, and Queueing Theory: The Mathematics of Computer Performance Modeling*. Springer, 2010.

[362] Y.-K. Ip, W.-C. Lau, and O.-C. Yue, "Performance modeling of epidemic routing with heterogeneous node types," in *Proc. IEEE International Conference on Communications (ICC)*, Beijing, May 2008, pp. 219–224.

[363] D. Uckelmann, M. Harrison, and F. Michahelles, *Architecting the Internet of Things*. Springer, 2011.

[364] 3GPP, "Service requirements for machine-type communications," Technical Report, 2012.

[365] 3GPP, "Evolved universal terrestrial radio access (E-UTRA) and evolved universal terrestrial radio access network (E-UTRAN), overall description," Technical Report, Jun. 2012.

[366] Alcatel-Lucent, "The LTE network architecture," Alcatel-Lucent, Technical Report, 2009.

[367] K. Zheng, F. Hu, W. Wang, W. Xiang, and M. Dohler, "Radio resource allocation in LTE-advanced cellular networks with M2M communications," *IEEE Commun. Mag.*, vol. 50, no. 7, pp. 184–192, Jul. 2012.

[368] S. Sesia, I. Toufik, and M. Baker, *LTE, The UMTS Long Term Evolution: From Theory to Practice*. Wiley Publishing, 2009, ch. 19.

[369] 3GPP, "Medium access control (MAC) protocol specification," Technical Report, Mar. 2012.

[370] 3GPP, "Study on RAN improvements for machine-type communications," Technical Report, Sept. 2011.

[371] M.-Y. Cheng, G.-Y. Lin, H.-Y. Wei, and A.-C. Hsu, "Overload control for machine-type-communications in LTE-advanced system," *IEEE Commun. Mag.*, vol. 50, no. 6, pp. 38–45, Jun. 2012.

[372] S.-Y. Lien, K.-C. Chen, and Y. Lin, "Toward ubiquitous massive accesses in 3GPP machine-to-machine communications," *IEEE Commun. Mag.*, vol. 49, no. 4, pp. 66–74, Apr. 2011.

[373] C.-Y. Tu, C.-Y. Ho, and C.-Y. Huang, "Energy-efficient algorithms and evaluations for massive access management in cellular based machine to machine communications," in *Proc. Vehicular Technology Conference (VTC Fall)*, Sept. 2011, pp. 1–5.

[374] S.-Y. Lien, T.-H. Liau, C.-Y. Kao, and K.-C. Chen, "Cooperative access class barring for machine-to-machine communications," *IEEE Trans. Wireless Commun.*, vol. 11, no. 1, pp. 27–32, Jan. 2012.

[375] J.-P. Cheng, C.-H. Lee, and T.-M. Lin, "Prioritized random access with dynamic access barring for RAN overload in 3GPP LTE-A networks," in *Proc. IEEE GLOBECOM Workshops*, Dec. 2011, pp. 368–372.

[376] K.-D. Lee, S. Kim, and B. Yi, "Throughput comparison of random access methods for M2M service over LTE networks," in *Proc. IEEE GLOBECOM Workshops*, Dec. 2011, pp. 373–377.

[377] S. Choi, W. Lee, D. Kim *et al.*, "Automatic configuration of random access channel parameters in LTE systems," in *Proc. IFIP Wireless Days (WD)*, Oct. 2011, pp. 1–6.

[378] A. Lo, Y. W. Law, and M. Jacobsson, "Enhanced LTE-advanced random-access mechanism for massive machine-to-machine (M2M) communications," in *Proc. 27th Meeting of Wireless World Research Form (WWRF)*, Oct. 2011, pp. 1–5.

[379] S.-Y. Lien, K.-C. Chen, and Y. Lin, "Toward ubiquitous massive accesses in 3GPP machine-to-machine communications," *IEEE Commun. Mag.*, vol. 49, no. 4, pp. 66–74, Apr. 2011.

[380] M.-S. Lee and Y.-M. Choi, "An efficient receiver for preamble detection in LTE SC-FDMA systems with an antenna array," *IEEE Commun. Lett.*, vol. 14, no. 12, pp. 1167–1169, Dec. 2010.

[381] 3GPP, "Feasibility study for proximity services (ProSe)," Technical Report, Jun. 2013.

Index